Universitat de Girona

VALORISATION OF INDUSTRIAL WASTES FOR THE REMOVAL OF METALS AND ARSENIC FROM AQUEOUS EFFLUENTS

Carlos ESCUDERO OÑATE

ISBN: 978-84-692-3178-4
Dipòsit legal: GI-546-2009
http://hdl.handle.net/10803/7802

Universitat de Girona

Departament d'Enginyeria Química, Agrària i Tecnologia Agroalimentària

Tesis Doctoral

Valorisation of industrial wastes for the removal of metals and arsenic from aqueous effluents

Carlos Escudero Oñate

Girona, Febrero de 2009

MARIA ISABEL VILLAESCUSA i GIL, professora del Departament d'Enginyeria Química Agrària i Tecnologia Agroalimentària de la Universitat de Girona,

CERTIFICA: que el llicenciat Carlos Escudero Oñate ha dut a terme, sota la meva direcció, el treball que, amb el títol "**Valorisation of industrial wastes for the removal of metals and arsenic from aqueous effluents**", presenta en aquesta memòria, la qual constitueix la seva Tesi per optar a grau de Doctor.

I perquè així consti i tingui els efectes oportuns davant del departament d'Enginyeria Química, Agrària i Tecnologia Agroalimentària, signo la present certificació a Girona, 1 de Febrer de 2009.

Maria Isabel Villaescusa i Gil

A mis padres, hermanos
y sobrinos.
A Laura.

Agradecimientos

A Isabel, por haberme dado la oportunidad de realizar el Doctorado en sus laboratorios, por haberme seguido, orientado y motivado durante estos años. Su enorme entusiasmo por la investigación siempre ha sido un referente. Agradecer de igual modo la paciencia, dedicación y esfuerzo adicional que ha supuesto la corrección de una Tesis escrita íntegramente en inglés. También agradecer a Núria Fiol su ayuda en las fases iniciales de investigación, cuando todo esto era nuevo para mí y su soporte durante este tiempo. A ambas, agradecerles sus consejos y ayuda constante en la elaboración de todas las comunicaciones realizadas. Cuatro años han pasado muy rápido.

A mis padres, hacia los que siento la más profunda admiración por el enorme esfuerzo que en su momento hicieron y que a día de hoy siguen haciendo. Muchas gracias por vuestra dedicación constante hacia mí y mis hermanos. Siempre habéis sido un modelo a seguir y gracias a vosotros, yo he llegado hasta aquí. Nunca os estaré lo suficientemente agradecido.

A Víctor, Trini y Javi, mis hermanos, por su apoyo y por haber estado a mi lado hasta la culminación de mi objetivo. A mis sobrinos, Paula, Irune, Yoel, Pablo y Hugo; porque sin darse cuenta, con sus juegos, dibujos y constantes preguntas me han motivado como nadie para continuar investigando en el camino de las tecnologías limpias y sostenibles.

A Laura. Tú has sufrido y disfrutado junto a mí desde el comienzo hasta la culminación de este proyecto. Sólo tú has sabido comprender como nadie lo que esto representaba. Por tu paciencia para soportar mis continuas ausencias y la separación, sólo en distancia, que implicó venir aquí. Hacia ti va dirigida mi gratitud, pero aún más, mi admiración.

A Laura, José María y Victor, por los grandes momentos vividos y por las risas compartidas en tantas ocasiones.

A Amparo, Eduardo y Jordi, por entender en todo momento la peculiaridad de este trabajo, escucharme pacientemente y aconsejarme.

Especialmente mi agradecimiento va también dirigido a Benjamín y Chelo, por su interés hacia el proyecto que desarrollaba, por su apoyo y ánimo constante para la consecución de este objetivo. Gracias por entender la dedicación que implica este camino y por vuestros consejos y palabras de aliento.

A Xisca, agradecerle los buenos momentos vividos en el corto periodo en el que nuestras vidas se cruzaron en el laboratorio de MMA, pero, por encima de todo, agradecerle su apoyo constante hacia la finalización de este proyecto y lo que es más valioso, su sincera amistad. A Jaume, por su inestimable ayuda en la creación de la portada. Como el mismo pudo comprobar, el diseño gráfico no se encontraba en mi lista de virtudes.

A mis compañeros de piso, Albert, Gina, Gilbert, Carla, Javi, David y Raúl. Aquellas tardes delante de varios cafés y aquellas noches eternas debatiendo sobre nada en particular fueron de los mejores momentos pasados durante mi estancia en Girona.

A Paula Marzal y Carmen Gabaldón, mis directoras durante la estancia en la Universitat de València. Mi más sincero agradecimiento por recibirme y acogerme como a uno más de su grupo, así como por su continuo soporte y atención. También agradecer su acogida a Marta, Javi y Vero. Gracias a todos vosotros por los buenos momentos pasados.

A Jean-Claude Bollinger y a todo el grupo del GRESE en Limoges, por su cálidez y cercanía durante los meses de estancia en Francia. Fue una experiencia muy enriquecedora, no sólo a nivel científico, sino también personal.

A Elena, Núria, Gemma, Olga y Anna Maria. Siempre era una alegría encontraros en los pasillos o en cualquier laboratorio. Ha sido para mi un auténtico privilegio conocer y compartir una parte de mi vida con personas tan entusiastas y maravillosas como vosotras. Gracias por vuestro ánimo continuo y por vuestro apoyo en todo momento. Os voy a echar mucho de menos.

También agradecer a Carme, Montse, Josep, Jaume, Farners y Pere su acogida en los comienzos, así como por su interés y apoyo durante estos cuatro años.

Agradecer también a Carme, Lluisa y Dani, de los Servicios Técnicos de Investigación por su gran ayuda en el disparo e interpretación de fotos electrónicas y con los diferentes análisis. Vuestra enorme calidad profesional es sólo superada por vuestra calidad humana. Gracias por vuestra calidez y proximidad.

A Florencio de la Torre, Joan Serarols y al grupo de la UPC: Antonio Florio, Núria Miralles, María Martínez e Ignasi Casas. Muchas gracias por valorarme y hacerme sentir siempre como una pieza importante del Proyecto. Vuestro interés en los progresos de mi tesis y vuestras palabras de ánimo han sido siempre un punto de apoyo que, en múltiples ocasiones, me ha animado a seguir adelante con los trabajos de investigación.

A Jordi Poch. Por perder tiempo conmigo ayudándome a vislumbrar la enorme utilidad y capacidad descriptiva de los modelos matemáticos. Gracias, Jordi, por enseñarme a ver procesos donde, en origen (a t=0), sólo veía números.

Finalmente me gustaría expresar mi gratitud a Salah-Eddine Stiriba. Si bien hace ya años que nuestros caminos de investigación se separaron, jamás olvidaré que él fue quien me enseñó la belleza de la investigación y me dio el impulso necesario para la realización del Doctorado. Muchas gracias Salah.

Agraïments

A Isabel, per haver-me donat l'oportunitat de realitzar el Doctorat en els seus laboratoris, per haver-me seguit, orientat i motivat durant aquests anys. El seu enorme entusiasme per la recerca sempre ha estat un referent. Agrair d'igual manera la paciència, dedicació i esforç addicional que ha suposat la correcció d'una Tesi escrita íntegrament en anglès. També agrair a Núria Fiol la seva ajuda en les fases inicials d'investigació, quan tot això era nou per a mi i el seu suport durant aquest temps. A ambdues, agrair-los els seus consells i ajuda constant en l'elaboració de totes les comunicacions realitzades. Quatre anys han passat molt ràpid.

Als meus pares, cap als quals assec la més profunda admiració per l'enorme esforç que en el seu moment van fer i que a dia d'avui segueixen fent. Moltes gràcies per la vostra dedicació constant cap a mi i els meus germans. Sempre heu estat un model a seguir i gràcies a vosaltres, jo he arribat fins a aquí. Mai no us estaré prou agraït.

A Víctor, Trini i Javi, els meus germans, pel seu suport i per haver estat al meu costat fins a la culminació del meu objectiu. Als meus nebots, Paula, Irune, Yoel, Pablo i Hugo; perquè sense adonar-se, amb els seus jocs, dibuixos i constants preguntes m'han motivat com ningú per a continuar investigant en el camí de les tecnologies netes i sostenibles.

A Laura. Tu has sofert i gaudit al meu costat des del començament fins a la culminació d'aquest projecte. Només tu has sabut comprendre com ningú el que això representava. Per la teva paciència per a suportar les meves contínues absències i la separació, només en distància, que va implicar venir aquí. Cap a tu va dirigida la meva gratitud, però encara més, la meva admiració.

A Laura, José María i Victor, pels grans moments viscuts i pels riures compartits en tantes ocasions.

A Amparo, Eduardo i Jordi, per entendre en tot moment la peculiaritat d'aquest treball, escoltar-me pacientment i aconsellar-me.

Especialment el meu agraïment va també dirigit a Benjamí i Chelo, pel seu interès cap al projecte que desenvolupava, pel seu suport i ànim constant per a la consecució d'aquest objectiu. Gràcies per entendre la dedicació que implica aquest camí i pels vostres consells i paraules d'alè.

A Xisca, agrair-li els bons moments viscuts en el curt període en el qual les nostres vides es van creuar en el laboratori de MMA, però sobre de tot, agrair-li el seu suport constant cap a la finalització d'aquest projecte i el que és més valuós, la seva sincera amistat. A Jaume, per la seva inestimable ajuda en la creació de la portada. Com ell mateix va poder comprovar, el disseny gràfic no es trobava en la meva llista de virtuts.

Als meus companys de pis, Albert, Gina, Gilbert, Carla, Javi, David i Raúl. Aquelles tardes davant de diversos cafès i aquelles nits eternes debatent sobre no-res en particular han estat dels millors moments passats durant la meva estada a Girona.

A Paula Marzal i Carmen Gabaldón, les meves directores durant l'estada a la Universitat de València. El més sincer agraïment per rebre'm i acollir-me com a un més del seu grup, així com pel seu continu suport i atenció. També agrair la seva acollida a Marta, Javi i Vero. Gràcies a tots vosaltres pels bons moments passats.

A Jean-Claude Bollinger i a tot el grup del GRESE en Limoges, per la seva calidesa i proximitat durant els mesos d'estada a França. Va ser una experiència molt enriquidora, no només a nivell científic, sinó també personal.

A Elena, Núria, Gemma, Olga i Anna Maria. Sempre era una alegria trobar-vos en els passadissos o en qualsevol laboratori. Ha estat per mi un autèntic privilegi conèixer i compartir una part de la meva vida amb persones tan entusiastes i meravelloses com vosaltres. Gràcies pel vostre ànim continu i pel vostre recolzament en tot moment. Us trobaré molt a faltar.

També agrair a Carme, Montse, Josep, Jaume, Farners i Pere la seva acollida en els començaments, així com el seu interès i suport durant aquests quatre anys. Agrair també a Carme, Lluïsa i Dani, dels Serveis Tècnics d'Investigació, la seva gran ajuda en el tret i interpretació de fotos electròniques i amb les diferents anàlisis. La vostra enorme qualitat professional és només superada per la vostra qualitat humana. Gràcies a tots per la vostra calidesa i proximitat.

A Florencio de la Torre, Joan Serarols i al grup de la UPC: Antonio Florio, Núria Miralles, María Martínez i Ignasi Casas. Moltes gràcies per valorar-me i fer-me sentir sempre com una peça important del Projecte. El vostre interès en els progressos de la meva tesi i les vostres paraules d'ànim han estat sempre un punt de suport que, en múltiples ocasions, m'ha animat a seguir endavant amb els treballs d'investigació.

A Jordi Poch. Per perdre temps amb mi ajudant-me a entreveure l'enorme utilitat i capacitat descriptiva dels models matemàtics. Gràcies, Jordi, per ensenyar-me a veure processos on, en origen (a t=0), només veia numeros.

Finalment voldria expressar la meva gratitud a Salah-Eddine Stiriba. Si be fa anys que els nostres camins de recerca es van separar, mai oblidaré que ell va ser qui em va ensenyar la bellesa de la recerca i em va donar l’espenta necessària per la realització d’un Doctorat. Moltes gràcies Salah.

Chapter 0. Introduction.

Chapter 1. Cr(III) and Cr(VI) sorption onto grape stalk entrapped in calcium alginate.

Chapter 2. Detoxification of a Cr(VI) polluted effluent by a combined sorption-reduction process using grape stalk.

Chapter 3. Effect of EDTA on divalent metal adsorption onto grape stalk and exhausted coffee wastes.

Chapter 4. Cu(II), Ni(II), Pb(II) and Cd(II) sorption onto grape stalk in single and multimetal mixtures.

Chapter 5. Arsenic removal by a metal (hydr)oxide waste entrapped in calcium alginate gel beads.

Chapter 6. Conclusions.

Chapter 0. INTRODUCTION

1. General introduction to heavy metal pollution……...1

2. Occurrence and toxicity of heavy metals……..…1

2.1. Chromium……...2

2.2. Copper…….3

2.3. Nickel……..4

2.4. Lead……....…4

2.5. Cadmium…….6

2.6. Arsenic……....7

3. Treatment technologies for the removal of heavy metals.....8

3.1. Chemical precipitation……8

3.2. Reverse osmosis and ultrafiltration……9

3.3. Electrodialysis……...10

3.4. Ion exchange…….……10

3.5. Solvent extraction…….11

3.6. Adsorption……12

4. Description of the sorption process……12

4.1. Chemisorptive mechanisms……..14

4.1.1. Complexation……...14

4.1.2. Chelation……..15

4.1.3. Ion exchange……17

4.2. Physisorptive mechanisms……18

4.2.1. Physical adsorption……...……18

4.2.2. Inorganic microprecipitation……18

5. Industrial liquid effluents in the plating industry……19

5.1. Problems associated with this industry…….19

6. The particular polluting frame of the electroplating industries: pollutants and treatment processes……21

7. Low-cost materials as sorbents……...……28

7.1. General overview……..28

7.2. Industrial by-products as sorbents: the particular use of grape stalk, exhausted coffee and of industrial electroplating (hydr)oxide industrial wastes……..……29

8. Advantages of low-cost sorption technology for metal-polluted water treatment and real industrial applications……..33

9. Thesis project frame: valorisation of industrial by-products for metals and arsenic removal from aqueous solutions……...37

10. Objectives…….41

11. References…….……...……43

Chapter 1. Cr(III) AND Cr(VI) SORPTION ONTO GRAPE STALK ENTRAPPED IN CALCIUM ALGINATE

1. Introduction……..…51

2. Objectives……..…53

3. Materials and methods……54

3.1. Reagents…….....54

3.2. Material…….....55

3.3. Equipment…….55

4. Methodology…….56

4.1. Grape stalk preparation…….56

4.2. Calcium Alginate (CA) and Calcium Alginate containing a 2% (w/v) of Grape Stalk (2% GS-CA) gel beads preparation……...56

4.3. General Cr(III) and Cr(VI) sorption procedure……57

4.4. Initial pH effect on Cr(III) and Cr(VI) sorption……...57

4.5. Sorption kinetics study…….58

4.6. Sorption equilibrium study……...58

4.7. Cr(VI) to Cr(III) reduction study…….….59

4.7.1. Cr(VI) determination in solution……..59

4.7.2. Cr(III) determination in solution…….….60

4.8. Spectroscopic analysis of the material…….….60

5. Results and discussion.....61

5.1. Initial pH effect in Cr(III) and Cr(VI) sorption…….…...61

5.2. Cr(III) and Cr(VI) sorption kinetics onto CA and 2% GS-CA gel beads……....65

5.2.1. Cr(III) sorption kinetics ……...66

5.2.2. Cr(VI) sorption kinetics……....68

5.2.3. Comparison between Cr(III) and Cr(VI) sorption onto CA and 2% GS-CA……..71

5.3. pH evolution…….……...…….73

5.4. Sorption kinetic modeling……79
5.4.1. Pseudo-first order kinetic model……..……80
5.4.2. Pseudo-second order model……..82
5.4.3. Intraparticle diffusion rate analysis……..87
5.4.4. General discussion……89
5.5. Cr(III) and Cr(VI) sorption equilibrium study onto CA and 2% GS-CA…….……92
5.5.1. Mathematical modeling of equilibrium results……95
5.5.1.1. Langmuir model……...…….95
5.5.1.2. Freundlich model……..……97
5.6. Ion exchange mechanism in Cr(III) sorption onto CA and 2% GS-CA gel beads……..……101
5.6.1. Calcium ions release during the sorption kinetics…….102
5.6.2. Calcium ions release in the sorption equilibrium……..……105
5.7. Spectroscopic analysis of the material and of the sorption mechanism….107
5.7.1. Fourier Transform Infrared-Attenuated Total Reflectance Spectroscopy (FTIR-ATR)…….107
5.7.2. Electron Paramagnetic Resonance (EPR)…….....110
5.7.3. Scanning Electron Microscopy-Energy Dispersive X-Ray analysis and Backscattered Electrons Microscopy study (SEM-EDX, BSE)…….114
5.7.3.1. Morphological and compositional study of the calcium alginate……115
5.7.3.2. Study of the zone distribution of Cr(III) and Cr(VI) on 2% GS-CA gel beads……. 116
5.7.3.2.1. Cr(III) zone distribution study on 2% GS-CA gel beads…….116
5.7.3.2.2. Cr(VI) zone distribution study on 2% GS-CA gel beads…… 121
6. Conclusions……....127
7. References……..129

Chapter 2. DETOXIFICATION OF A Cr(VI) POLLUTED EFFLUENT BY A COMBINED SORPTION-REDUCTION PROCESS USING GRAPE STALK

1. Introduction…….....133

2. Objectives…….....135

3. Materials and methods…….....136

3.1. Reagents……..136

3.2. Material……...…137

3.3. Equipment……...138

4. Methodology…….....139

4.1. Development and description of the installation……139

4.1.1. Installation scheme……..…….139

4.1.2. Description of the control elements…….....140

4.1.2.1. Programmable Logic Controller (PLC) and pH electrode……..140

4.1.2.2. Peristaltic pumps…….....140

4.1.2.3. Sampling……...140

4.2. General operation procedure……...141

4.2.1. PLC programming……141

4.2.2. Reactor building……...……141

4.2.3. Preparation and conditioning of the collection tube…….……142

4.2.4. Solution introduction and conditioning……143

4.2.5. Draining and cleaning of the reactor and tubes……....144

4.3. Sorbent preparation…….……144

4.4. Sorption experiments……..……144

4.4.1. Temperature effect on Cr(VI) sorption/reduction kinetics at constant pH……..……145

4.4.2. Effect of pH readjustment on Cr(VI) sorption/reduction kinetics …..……145

4.4.3. Effect of initial Cr(VI) concentration in sorption/reduction kinetics at constant pH and temperature……...……145

4.5. Chromium analysis……..…145

4.6. Residual Cr(III) removal assays……146
4.6.1. Precipitation assays……146
4.6.2. Continuous bed up-flow sorption experiments……146

5. Results and discussion……148
5.1. Temperature effect on chromium sorption/reduction kinetics at constant pH……148
5.1.1. Total chromium removal……148
5.1.2. Hexavalent chromium removal……152
5.1.3. Trivalent chromium formation and removal……154
5.2. Effect of temperature and pH readjustment on Cr(VI) sorption/reduction kinetics……156
5.2.1. Total chromium removal……157
5.2.2. Hexavalent chromium removal……160
5.2.3. Trivalent chromium formation and removal……163
5.3. Effect of initial Cr(VI) concentration in sorption/reduction kinetics at constant pH and temperature……167
5.3.1. Total chromium removal……167
5.3.2. Hexavalent chromium removal……171
5.3.3. Trivalent chromium formation and removal……173
5.4. Kinetic modeling of Cr(VI) sorption/reduction process……175
5.4.1. Effect of temperature at constant pH……177
5.4.2. Effect of pH at constant temperature……181
5.5. Residual Cr(III) removal assays……185
5.5.1. Precipitation assays……185
5.5.2. Continuous bed up-flow sorption experiments……187
6. Conclusions.....191
7. References……193

Chapter 3. EFFECT OF EDTA ON DIVALENT METAL ADSORPTION ONTO GRAPE STALK AND EXHAUSTED COFFEE WASTES

1. Introduction……...…197

2. Objectives…….....201

3. Materials and methods……..…202

3.1. Reagents…….....202

3.2. Material……...202

3.3. Equipment……...203

4. Methodology……...204

4.1. Sorbent preparation…….....204

4.2. pH and EDTA effect in Cu(II) and Ni(II) sorption onto GS and EC…….204

4.3. Sorption kinetics…….……205

4.4. Sorption isotherms…….….205

4.5. Column adsorption experiments…….……205

4.5.1. Effect of feeding metal concentration……207

4.5.2. Effect of EDTA in Cu(II) and Ni(II) sorption ……...……207

4.5.3. Effect of EDTA in binary equimolar Cu(II)/Ni(II) solutions…….……207

4.6. Column desorption experiments…….……208

5. Results and discussion……...209

5.1. pH and EDTA effect in Cu(II) and Ni(II) sorption onto GS and EC…209

5.2. Cu(II) and Ni(II) sorption kinetics onto GS and EC: effect of complexing agent EDTA……...…….215

5.2.1. Cu(II) sorption kinetics onto GS and EC……...……215

5.2.2. Ni(II) sorption kinetics onto GS and EC……..……..……220

5.3. Sorption kinetics modeling……..…...……224

5.4. Cu(II) and Ni(II) sorption equilibrium study onto GS and EC: effect of complexing agent EDTA……...…….....229

5.4.1. Mathematical modeling of equilibrium results……..…....233

5.4.1.1. Langmuir model……..…....233

5.4.1.2. Freundlich model…….....235

5.5. Column experiments…….....…239
5.5.1. Effect of feeding metal concentration ……...……239
5.5.2. Desorption experiments……...…246
5.5.3. Effect of EDTA in Cu(II) and Ni(II) sorption ……...…249
5.5.4. Effect of EDTA in binary equimolar Cu(II)/Ni(II) mixtures……..…251
6. Conclusions…….259
7. References……..…….261

Chapter 4. Cu(II), Ni(II), Pb(II) AND Cd(II) SORPTION ONTO GRAPE STALK IN SINGLE AND MULTIMETAL MIXTURES

1. Introduction……267

2. Objectives……269

3. Materials and methods……270

3.1. Reagents……270

3.2. Material……270

3.3. Equipment……271

4. Methodology……272

4.1. Grape stalk preparation……272

4.2. Column experiments……272

4.2.1. Single metal uptake ……273

4.2.2. Binary mixtures uptake……273

4.2.3. Ternary mixtures uptake……273

4.2.4. Quaternary mixtures uptake……274

4.2.4.1. Sorption experiments……274

4.2.4.2. Multiple sorption/desorption cycles……274

4.3. Thermodynamic study……275

5. Results and discussion……276

5.1. Cu(II), Ni(II), Pb(II) and Cd(II) sorption from single solutions……276

5.2. Cu(II), Ni(II), Pb(II) and Cd(II) sorption from binary mixtures……278

5.3. Cu(II), Ni(II), Pb(II) and Cd(II) sorption from ternary mixtures……286

5.4. Cu(II), Ni(II), Pb(II) and Cd(II) sorption/desorption from quaternary mixtures……293

5.4.1. Sorption/desorption experiments……293

5.5. Effect of temperature on Cu(II), Ni(II), Pb(II) and Cd(II) equilibrium…..306

5.5.1. Sorption isotherms……..…307
5.5.2. Calculation of equilibrium parameters of adsorption…….311
5.5.3. Calculation of thermodynamics parameters of adsorption…….321
6. Conclusions……327
7. References……..……329

Chapter 5. ARSENIC REMOVAL BY A METAL (HYDR)OXIDE WASTE ENTRAPPED IN CALCIUM ALGINATE GEL BEADS

1. Introduction……...…333

2. Objectives……...……335

3. Materials and methods……..336

3.1. Reagents……..336

3.2. Material……...……337

3.3. Equipment……...…337

4. Methodology……...…338

4.1. (Hydr)oxide preparation…….……338

4.2. (Hydr)oxide characterization……...…338

4.3. Sorbent gel beads synthesis……339

4.4. General uptake procedure……...……340

4.5. Effect of (hydr)oxide concentration in the beads in As(III) and As(V) removal…….……341

4.6. pH effect on As(III) and As(V) sorption and sorbent solubilization…..…341

4.7. Sorption kinetics study…….....341

4.8. Sorption equilibrium study…….…342

4.9. Solid state analysis…….….342

4.10. Hazard classification of the spent sorbent……..…343

5. Results and discussion……...…344

5.1. (Hydr)oxide characterization……..……344

5.2. Effect of (hydr)oxide concentration in the beads in As(III) and As(V) removal…….…346

5.3. pH effect on As(III) and As(V) sorption and sorbent solubilization……..348

5.4. As(III) and As(V) sorption kinetics onto O and 10% O-CA……..……355

5.4.1. Sorption kinetics modelling……357

5.4.2. Arsenic diffusion vs external mass transport modeling onto O and 10% O-A……...……359

5.5. Arsenic sorption equilibrium study onto O and 10% O-CA…….....361
5.5.1. Sorption equilibrium modelling.…….……363
5.6. Solid state analysis and sorption mechanistic approach…….368
5.6.1. Solid state analysis…….……368
5.6.2. As(III) and As(V) sorption mechanistic approach…….……372
5.7. Hazard classification of the spent sorbent……..……375
6. Conclusions……376
7. References……..……378

Chapter 6. CONCLUSIONS

1. Conclusions……383

Chapter 0. INTRODUCTION

INTRODUCTION

1. GENERAL INTRODUCTION TO HEAVY METAL POLLUTION

Modern industry is, to a large degree, responsible for contamination of the environment. Lakes, rivers and oceans are being overwhelmed with bacteria and waste matter. Among toxic ubiquitous substances reaching hazardous levels we find heavy metals and metalloids. Anthropogenic release of metals creates public health problems due to their toxicity and persistence in the environment. They occur naturally as ions, compounds and complexes and -to an increasingly relevant degree- in the anthroposphere in a variety of forms and their presence poses environmental–disposal problems due to their non-degradable and persistence nature.

There are many industrial sources of metal pollution including manufacturing processes such as smelting and refining, electricity generation and nuclear power, agricultural fertilization, wastewater treatment, fuel combustion but also natural; running water erodes soil and rock, dissolving and transporting some metals thousands of kilometres before being redeposited.

2. OCCURRENCE AND TOXICITY OF HEAVY METALS

With the rapid development of various industries as mining and smelting of metalliferous, surface finishing, energy and fuel production, fertilizers and pesticides, metallurgy, electroplating, electrolysis, leatherworking, photography, metal surface treating, aerospace and atomic energy installations, wastes containing metals are directly or indirectly discharged into the environment, having brought serious environmental pollution and threatened biolife (Bishop, 2002; Wang and Chen, 2006; Volesky, 1990).

The toxic characteristics of heavy metals can be displayed as follows: (1) the toxicity can last for a long time in the environment; (2) some heavy metals even could be transformed from relevant low toxic species into more toxic forms in a certain environment (as the case of methylation of mercury to form methyl-mercury cation); (3) the bioaccumulation and bioaugmentation of heavy metal by food chain could damage normal physiological activity

and endanger human life; (4) metals can only be transformed and changed in valence and species, but cannot be degraded by any methods including biotreatment; (5) the toxicity of heavy metals occurs even in lower concentration of 0.001-0.1 $mg \cdot L^{-1}$ (Alkorta *et al*., 2004; Volesky, 1990).

Due to their increasing application and its immutable nature, heavy metal pollution has become one of the most serious environmental problems today. As they are no degradable, they can accumulate in the components of the environment where their toxicity is expressed being its ultimate sink the soils and sediments.

In the ranking of the most toxic metals emitted to environmental systems it can be found Cr(VI), Cu(II), Ni(II), Pb(II) and Cd(II) and from the metalloids, one of the most abundant and relevant by its toxicity is arsenic, both As(III) and As(V) forms. The sources, properties, applications and toxicological effects of these pollutants are detailed next.

2.1. Chromium

Chromium is a silvery, shiny, malleable metal with a density of 7.2 $g \cdot cm^{-3}$ that melts at 1860 ºC and boils at about 2670 ºC. Its surface and alloys (chrome steel) can be passivated by treatment with a strong oxidative agent such as nitric acid, which makes it largely corrosion resistant. It is a relative common element with an average concentration of 100 $mg \cdot kg^{-1}$. Chromium can exist mainly in three oxidation states: Cr(II), Cr(III) and Cr(VI). The chromous state is unstable and rapidly suffers oxidation to the chromic state, that is the most stable. The chromium on its hexavalent oxidation state is the most widely used in industry due to its acidic and oxidant properties and also due to the formation of very coloured and insoluble salts with cations as Ag^{+}.

Natural chromium ores are mainly chromite ($FeCr_2O_4$) and less frequently krokoite ($PbCrO_4$). For the production of chromium, only chromite is used.

This metal is widely employed in industry. Among the most important applications can be remarked the chrome plating in galvanizing industry, preparation of dyes, pigments and catalysers, oxidative agent of organic compounds, use in tanning, wood and leather treatment, and use in printing industries and in oil industries as anticorrosive.

The toxicity of this metal is strongly dependent on the oxidation state. While Cr(VI) can easily cross the cell-membranes, where the phosphate-sulphate carrier also transports the chromate anions, Cr(III) does not use any specific mechanisms and its entrance into the cell occurs by a less efficient mechanisms as simple diffusion or endocytosis (in animal cells). Cr(VI) is rapidly reduced to Cr(III) inside the cells and its biological activity depends on both, the process of its reduction and the subsequent trapping of Cr(III) in the different cell compartments.

Chromium has both beneficial and detrimental properties. Cr(III) is an essential trace element in mammalian metabolism. In addition to insulin, it is responsible for reducing blood glucose levels and is used in certain cases of diabetes. It has also been found to reduce blood cholesterol levels by diminishing the concentration of "bad" low density lipoproteins "LDLs" in the blood (Mohan and Pittman, 2006). On the other hand, acute exposure to Cr(VI) causes liver and kidney damage, dermatitis, internal haemorrhage and respiratory problems (Mohan and Singh, 2006).

In last term, it can be considered that hexavalent chromium is about 100 to 1000 times more toxic than the trivalent chromium.

2.2. Copper

Copper has been known for about 10000 years and occurs in both, metallic form or in compounds as Cu(I) and Cu(II). The red metal has a density of 8.93 $g \cdot mL^{-1}$, a melting point of 1083 ºC and a boiling point of about 2590 ºC. Copper is easily manufactured from ores in underground or open-pit mines. The most important ores contain, besides small amounts of metallic copper, Cu_2S, CuS, $CuFeS_2$, CuO and $Cu_2CO_3(OH)_2$. The main copper oxidation states are the Cu(I) and Cu(II).

Its uses are mainly derived from its excellent electrical conduction property, but this metal is also widely used in alloys, as an algaecide, for the preparation of pigments, as supplement in pastures and for the preparation of catalysers. The metal enters to the hydrological system, either groundwater or surface water, from dissolution of rocks and soils, from biological cycles, atmospheric fallout and, specially, from industrial processes and waste disposal (Merian, 1991).

Copper is biologically available as Cu(I) and Cu(II) in inorganic salts and in organic complexes. In high dose, this metal can cause dermatitis in contact with skin and hepatic and kidney damage, if ingestion is produced.

2.3. Nickel

Nickel is widely distributed in the environment and its bioavailability and biological effects strongly depend of the type of compounds. The metal is a silver-white, hard, malleable, ductile ferromagnetic metal that maintains a high lustre and is relatively resistant to corrosion. This material has a density of 8.9 $g \cdot mL^{-1}$, a melting point of 1453 ºC and a boiling point of 2732 ºC. The oxidation states of nickel include -1, +1, +2, +3 and +4, being the Ni(II) the most stable. The main minerals containing nickel are formed mainly by oxides containing mixed nickel iron and also sulphides as the pentlandite, $Ni(Fe)_9S_8$.

Among its main uses it can be remarked the formation of alloys like Ni-Cr-Fe, Ni-Cu and Ni-Al. The metal is also widely used in electroplating industries, in the manufacture of Ni-Cd batteries, as catalyser forming the structure of organometallic compounds for petroleum refining and other organic processes (Merian, 1991).

The different dysfunctions and diseases promoted by nickel can be classified in three categories: (1) Allergic processes, (2) Respiratory system diseases and (3) Tumoral and cancerous processes (OIT, 2001).

2.4. Lead

Metallic lead is a bluish-white, soft metal with a density of 11.34 $g \cdot mL^{-1}$, a melting point of 327.5 ºC and a boiling point of about 740 ºC. The main oxidation state of lead is +2 and its minerals can be found in many regions worldwide. The richest lead mineral is the galene (PbS), being the most important source for the commercial production of this metal. Other minerals containing lead are the cerussite ($PbCO_3$) and anglesite ($PbSO_4$). In many cases, minerals containing lead can contain also other toxic heavy metals.

In nature lead is a ubiquitous, non-essential element that can be found in all environmental media (air, soil, rocks, sediments and water) and in all components of the biosphere. Lead and its compounds may enter the environment at any point during mining, smelting, processing, use, recycling or disposal. Estimates of the dispersal lead emissions into the environment indicate that the atmosphere is the major initial recipient. Mobile and stationary sources of lead emissions tend to be concentrated in areas of high population density and near smelters. From these emission sources, lead moves through the atmosphere to various components of the environment. It is deposited on soil, surface waters and plants and thus is incorporated into the food chain of animals and man.

The commercial use of lead includes the lead-batteries production, alloys, glassware and ceramics. Extended uses in the past were also the preparation of lead based pigments and methyl/ethyl derivatives added as antiknock agents in gasoline. These processes were prohibited years ago in many countries (Merian, 1991).

Lead natural concentrations are not very high, however, in the last sixty years, great amounts of lead have been extracted, concentrated, used and re-emitted into the environment. Lead concentrations are now locally and regionally much higher that they used to be. Animals and humans are thus exposed to new health risks and their body, tissues and fluids may contain more lead than normal.

Once in blood, lead is distributed in three ways: blood, soft tissues (kidney, bone-marrow, liver and brain) and in mineralized tissues (bones and teeth). The mineralized tissue contains, in adults, approximately the 95% of the total lead. Lead inhibits organism's capacity to produce haemoglobin, due to the interference with several enzymatic steps in the metabolism of hemo group. This metal is associated also to cardiotoxic effects, hypertension, inhibition of teeth and bones growing and also, appearance of neurological disorders (OIT, 2001).

2.5. Cadmium

Cadmium is a relatively volatile non-essential element for plants, animals and humans. Because cadmium occurs together with zinc, from which it must be separated, cadmium production depends on the production of zinc. Cadmium is a silver-white, lustrous and ductile metal with a density of 8.64 $g \cdot mL^{-1}$, a melting point of 320.9 ºC and a boiling point of 767 ºC. The main Cd oxidation state is +2, and it's present in this form in rare minerals as greenockite (hexagonal CdS), hawleyte (cubic CdS), otavite ($CdCO_3$), and cadmoselite (CdSe). Cadmium mostly occurs in isomorphic form in zinc minerals such as zinc blende (ZnS) with cadmium contents ranging from 0.1 to 0.5% and smithsonite ($ZnCO_3$) with cadmium contents up to a maximum of 5%.

Cadmium has been emitted in minor amounts into the environment from the rise of industrialization, but in greatly increased quantities after World War II, in the form of dusts and aerosols to the atmosphere, effluents into rivers and lakes and as solid from point sources (waste, slag, incineration, coal combustion and sewage sludge).

Cadmium is very corrosion-resistant and the electrodeposited cadmium shows excellent properties for protecting iron and steel. The metal has been employed widely also in rechargeable nickel-cadmium batteries, but the development of new accumulator materials and the need of lower weight in the final products is progressively replacing cadmium in this application. One of its main applications is the production of cadmium soaps made with saturated and unsaturated fatty acids that play an important role as temperature and light stabilizers mainly for PVC. The metal is also used in nuclear reactors as a neutron absorber and in various alloys with such metals as tin, copper and aluminium (Merian, 1991).

After cadmium absorption, either digestive or by the respiratory tract, cadmium is transported to the liver, where the production of low molecular weight and high sulphur content proteins, named metallothioneins production begins. These proteins avoid cadmium to exert its toxic activity when present in free form. When the amount of cadmium ingested overpass the metallothioneins production capacity of the organism, the consequence is a renal failure. Moreover cadmium strongly accumulates in kidney and liver, and its rate of elimination is very slow, increasing its concentration with the age and

the exposition period. Cadmium has been associated also to the appearance of tumoral and cancerous processes (OIT, 2001).

2.6. Arsenic

Elemental arsenic exists at room temperature as metallic or grey and yellow arsenic. Grey arsenic represents the common stable form. Its density is 5.73 $g \cdot mL^{-1}$ and its melting and boiling points are 613 and 817 ºC respectively. Arsenic displays variable valences, -3, +3 and +5 and has both cationic and anionic forms. It is extracted mainly from arsenopyrite (FeAsS), the most abundant ore of this element, but also from arsenolite (As_2O_3) and mimetite ($Pb_5Cl(AsO_4)_3$). Arsenic oxide is usually produced as a by-product of copper, lead and nickel smelting and the metalloid can be obtained by hydrogen reduction of As_2O_3 (Merian, 1991).

The pollution by arsenic can be caused by either human activities such as mining, pesticides use, smelting of non-ferrous metals, burning of fossil fuels and timber treatment, but usually the main source of arsenic is geogenic: the Earth's crust is an abundant natural source of arsenic, being present in more than 200 different minerals.

When discussing arsenic toxicity, speciation plays a special important role: hydrides, halogenides, oxides, sulphides, arsenites, arsenates and organic arsenic compounds all exhibit very different properties. In the case of toxicological effect appearance by inhalation of gaseous arsenic compounds, one of the most frequently observed is the intoxication by arsine (AsH_3). This kind of poisoning involves a high degree of mortality due to the intense haemolytic activity of this gas (OIT, 2001).

Long term drinking water exposure to inorganic arsenic compounds can cause different dysfunctions and diseases as, loss of appetite and nausea, muscular weakness, neurological disorders, and cancers (Kapaj *et al.*, 2006).

3. TREATMENT TECHNOLOGIES FOR THE REMOVAL OF HEAVY METALS

Over the past 50 years, a wide variety of treatment technologies for the decontamination of metal-polluted effluents have been investigated and developed being, among others the based on chemical precipitation, ion exchange, adsorption, solvent extraction, membrane processes and electrochemical techniques. The basis and applicability of the different techniques are presented next.

3.1. Chemical precipitation

By this technique the acidic effluent is firstly neutralized and heavy metals are then precipitated in the form of metal (hydr)oxides. For this process, one of the most widely used reagents is lime according to the reaction:

$$Ca(OH)_2 + M^{2+}/M^{3+} + H_2SO_4 \longrightarrow M(OH)_2/M(OH)_3 + CaSO_4 + H_2O$$

The mixture of gypsum ($CaSO_4$) and metal hydroxides is called sludge.
In effluents containing iron, air is frequently used to oxide ferrous to ferric iron during precipitation, because ferric iron sludge is chemically more stable than ferrous iron sludge.
The sludge produced is allowed to settle in clarifiers/thickeners. When the solid content of the waste-water is less than 1 $mg \cdot L^{-1}$, sand-bed filters are employed for polishing, to meet the required level of suspended solids in the final effluent. The supernatant is then discharged to the receiving stream and the settled sludge is disposed of in specifically designed ponds.
Many small treatment plants have a total daily volume of waste less than 115 m^3 and the most economical system for such plants is a batch treatment in which two tanks are provided, each with a capacity of one day's flow. One tank undergoes treatment while the other is filling. When the daily volume exceeds 115-150 m^3, batch treatment is usually non feasible because of the large tankage required. Hence, a continuous treatment plant is used requiring a tank for acidification and reduction, then a mixing tank, for lime addition and

finally a settling tank. The sludge densities vary from 1-30% solids, depending on the metal concentration of the water and the sophistication of the treatment process (Cox *et al*., 2006).

Treatment with lime (CaO) requires a short reaction period, however, this process may have some drawbacks such as poor quality of the final effluent and the need to dispose of a large volume of sludge. As the driving force of the precipitation process is the concentration of metal in solution, this method is not very favourable specially when dealing with large volumes of solution which contains heavy metal ions in low concentration. The pH of minimum solubility of hydroxides is different for the various metals presenting thus a problem with multi-element waste-waters. Also the resulting effluent has a high salinity and so limited possibilities for reuse.

Precipitation may be accompanied by flocculation or coagulation and one major problem is the formation of large amounts of sediments containing heavy metal ions.

Alternatives to the use of lime as reagent is the use of calcium carbonate ($CaCO_3$), whose main advantage is its lower price and the production of a denser sludge; sulphides, as Na_2S, NaHS, FeS, that are more effective for the treatment of wastewaters containing highly toxic heavy metals or caustic soda (NaOH), that is very soluble in water, disperses rapidly and raises the pH of the water quickly, but presents high cost and danger in handling.

3.2. Reverse osmosis and ultrafiltration

There's no a sharp distinction between reverse osmosis and ultrafiltration. In ultrafiltration the separation is based primarily on the size of the solute which, depending on the particular membrane porosity, can range from about 2 to 10000 nm. In the reverse osmosis process, the size of the solute is not the unique basis for the degree of removal because the ability of the membranes to reject electrolytes increases with an increase of the element oxidation state.

Reverse osmosis is based on the principle of osmosis, where diffusion of the solvent or osmotic flow, will continue until the difference of concentration on both sides of the membrane creates pressure enough to counteract the net solvent flow. This natural

tendency for osmosis can be stopped and reversed by applying a hydraulic pressure to the solution side and so as the solvent is forced to flow from the solution. In order to obtain reasonable flow rates through the membranes, reverse osmosis systems operate at pressures ranging from 2 to 10 MPa while ultrafiltration systems operate between 70-700 KPa.

3.3. Electrodialysis

Dissolved inorganic substances in wastewater can be removed by electrodialysis. When an inorganic salt is dissolved in water it ionizes to produce cations and anions. When an electrical potential is then passed through the solution, the cations migrate to the negative electrode and the anions to the positive electrode. Semi-permeable membranes are commercially available and they allow the passage of ions of only one charge: cation-exchange membranes are permeable only to positive ions and anion-exchange membranes are permeable only to negative ions. When series of these membranes are placed alternatively in a solution and a voltage is applied, the solution between one pair of electrodes becomes clarified as the ions concentrate in the solution in the adjacent compartments (Harrison, 1996).

3.4. Ion exchange

As discussed previously, precipitation processes lose their advantage at low solute feed concentrations and an alternative technology is required. Among the possible alternatives, one of the most widely used is ion exchange.

Ion exchange is the reversible exchange of ions between a solid phase (ion exchanger) and a polar solution phase containing ions, the ion exchanger being insoluble in the medium in which exchange takes place. Currently the majority of commercial exchangers are based on styrene or acrylic polymers containing various functional groups substituted onto the polymer backbone to provide the ion exchange sites, copolymerised with divinyl benzene to promote crosslinking. The nature of the functional group determines the primary exchange properties of the resin, i.e. cationic or anionic exchange, with the ion selectivity modified by the group acidity/basicity.

The volume of adsorbent material increases proportionately with the solute load, so that at higher solute concentrations, equipment size makes such processes economically unfeasible. Applications of ion exchange are thus limited to levels of contaminants in the ppm range. Synthetic ion-exchange resins have long been used in commercial scale applications for the softening or demineralisation of water. While these materials are effective in reducing ionic contaminants to a low level, such resins have traditionally suffered from a lack of selectivity. Moreover, the matrix degrades with time and with the long term contact with certain materials such as radioactive or oxidizing agents.

3.5. Solvent extraction

The overall process consists on the extraction of the metal/s by contacting an organic solvent phase with the aqueous waste stream, followed by separation of the loaded organic phase from the aqueous raffinate. This loaded phase is then further contacted with a second aqueous phase to back-extract or strip the metal, and allow the organic phase to recycle to treat more wastewater. The metal ions released in the aqueous stripping solution can be recovered for reuse or sale.

This technology is well established for metal recovery and employed in large-scale operations, where the concentration of contaminants is quite high.

As discussed previously, heavy metals can be present in wastewater as either cations or anions. Cations are usually extracted into an organic diluent by simple or chelating organic acidic extractants. Metal anions can be extracted by ion-pair formation with long chain alkylamines or quaternary ammonium compounds in an organic diluent. When the metals are present as ion pairs in the aqueous phase, then organic compound, e.g. ketones, organo-phosphates or organo-phosphine oxides, capables of solvating these complexes can be used.

The capital outlay for such equipment can be expensive, due to the large volumes of organic extractants and performance is often limited by hydrodynamic constraints such as flooding and entrainment. There is also the potential for cross-contamination of the aqueous stream with the organic solution.

3.6. Adsorption

Adsorption is a process that occurs when a gas or liquid solute accumulates on the surface of a solid or a liquid (adsorbent), forming a molecular or atomic film (adsorbate). It is different from absorption, in which a substance diffuses into a liquid or solid to form a solution. The term sorption encompasses both processes, while desorption is the reverse process.

Many substances can be used as sorbents for the removal of a variety of metal ions from aqueous solutions. These include activated carbon, alumina and silica gel, being the first one the most widely employed for sorption (Chen *et al*., 2003; Chen and Wang, 2000; Seco *et a*l., 1999; Gabaldón *et al*., 1996; Ouki and Heufeld, 1996; Aksu and Kabasakal, 2004; Banat *et al.* 2003; Hamadi *et al.* 2004; Malik, 2004; Krishnan and Anirudhan, 2003; Basso *et al.*, 2002; Kardivelu *et al.* 2004; Demirbas, 2003; Abdulkarim and Abu Al-Rub, 2004). Commercial activated carbons can be obtained from waste plant materials such as coconut wastes (Selomuya *et al*., 1999), *Arundo donax* canne (Basso *et al*., 2002), sugarcane (Mohan and Singh, 2002) and nuts bark (Demirbas *et al*., 2004) among others.

The theory and the possible mechanisms involved in this process will be explored and discussed in more extension in the next section.

4. DESCRIPTION OF THE SORPTION PROCESS

The process of accumulation in an interface of substances that initially are in solution is known as sorption. The adsorbate is the substance that is being removed from the fluid and the adsorbent is the solid, liquid or gas phase in which the sorbent is being accumulated.

In the general sorption term, two basic terms can be distinguished: adsorption and absorption. The adsorption involves the accumulation or concentration of the sorbed substance in the surface, while the absorption involves the concentration of the absorbate in the whole volume of the sorbent.

The adsorption, first time observed by C.W. Scheele in 1773 for gases and subsequently for solution by Lowitz in 1785, is currently recognized as a very important phenomena in

many physical, chemical and biological processes. In the next figure, the different steps involved in the sorption process of a substance in a porous solid sorbent are presented.

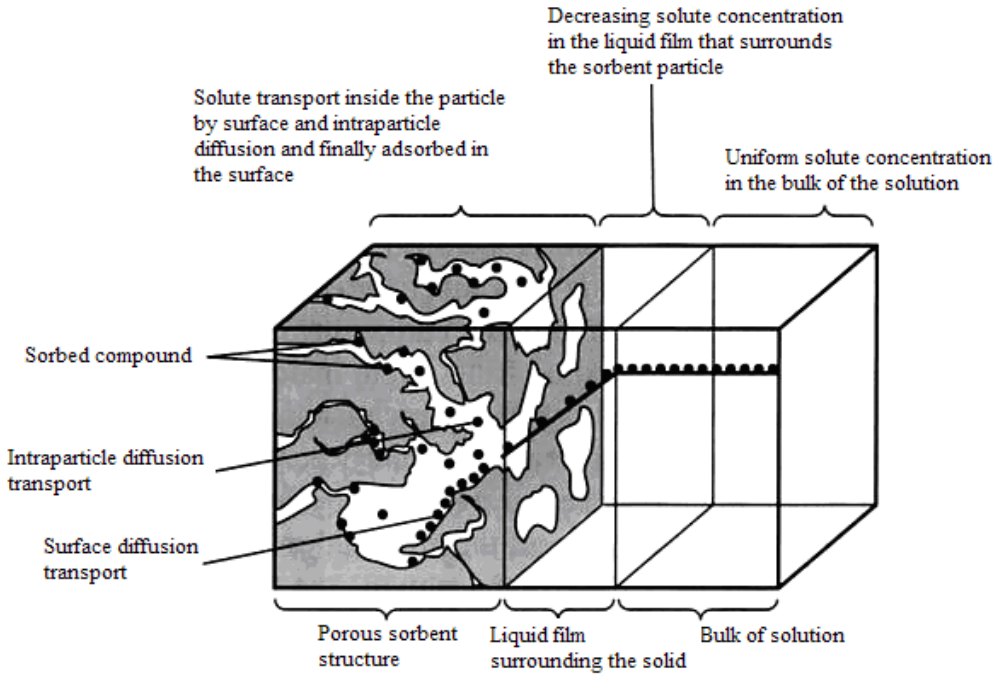

Figure 1: Sorption steps in a porous solid sorbent (Tchobanoglous *et al*., 2003).

As it can be observed in the figure, sorption takes place in four steps: (1) solute transport from the bulk of the solution, (2) diffusion through the fluid film that surrounds the particle to the surface, (3) intraparticle diffusion and (4) adsorption.

The transport from the bulk of the solution involves the movement of the substance that is going to be adsorbed until the liquid film that surrounds the particle. The external film diffusion involves diffusional transport through this liquid film, until reaching the pores entrance on the adsorbent material. Finally in the intraparticle diffusion stage, the sorbate migrates throughout pores by a mechanism based on the molecular diffusion through the fluid contained in the pore and/or diffusion throughout the surface of the sorbent. The final step of this process is the adsorption itself, when formation of sorbent-sorbate bonds takes place.

Among the different forces responsible of sorption, the most remarkable are:

· Coulombic interactions
· Punctual charge-dipole
· Dipole-dipole interactions
· Punctual charge-neutral species
· London or Van der Waals forces
· Covalent bond formed after chemical reaction
· Hydrogen bridges

As the sorption process takes place in several steps, the slower in considered as the rate limiting step. In a general way, if the main sorption mechanism is of physic nature, some of the diffusion steps is the rate limiting step, because physical sorption takes place fast. If a chemical mechanism is the main responsible of sorption, it has been frequently observed as rate limiting step the formation of the bond sorbent-sorbate (Tchobanoglous *et al*., 2003).

According to the strength of the interaction sorbent-sorbate, it can be distinguished between chemisorptive and physisorptive mechanisms. While chemisorption involves the net formation of chemical bonds sorbent-sorbate, in physisorption the sorbate is only retained by weak interactions, as London or Van Der Waals forces. The most common mechanisms for both sorption types are presented next. It has to be remarked also that due to the structural complexity that might be reflected in the presence of different types of sorption sites in the sorbents, it is possible that various mechanisms would participate in different extension in the total sorbate uptake (Volesky, 2003).

4.1. Chemisorptive mechanisms

4.1.1. Complexation

Complexation is defined as the formation of a new species by the association of two or more species. When one of the species is a metal ion, the resulting entity is known as a metal complex. Mononuclear complexes are formed by the interaction of a metal cation and a number of anions, or ligands. As a general rule, the metal ion occupies a central

position in a complex, as exemplified in the next structure, corresponding to the Heme group.

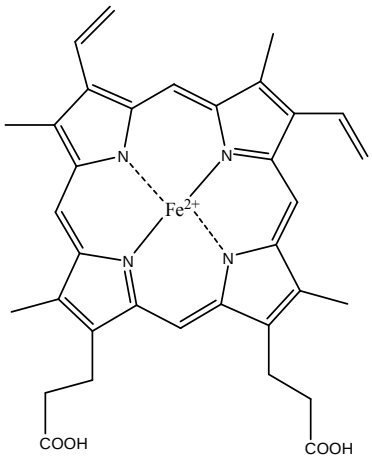

Figure 2: Heme group

However, there are complexes, known as polynuclear complexes, which may contain more than one metal atom center. According to the number of metals and ligands and their respective charges, the complex can show different net charge. It has been proposed that in microbian walls, oxygenated, phosporilated and nitrogenated ligands contribute to the complexation of transition metals (Volesky, 2003; Wase and Forster, 1997).

4.1.2. Chelation

The term ligand has been used in two different senses. It is sometimes applied to the particular atom in a molecule by means of which the molecule is attached to a central metal atom, e.g. the nitrogen atom in ammonia, or it may be applied to the molecule as a whole. Where there is any risk of ambiguity, it may be avoided by using the term ligand atom or donor atom to denote the atom attached to a metal. In the next figure, an example of chelate is shown.

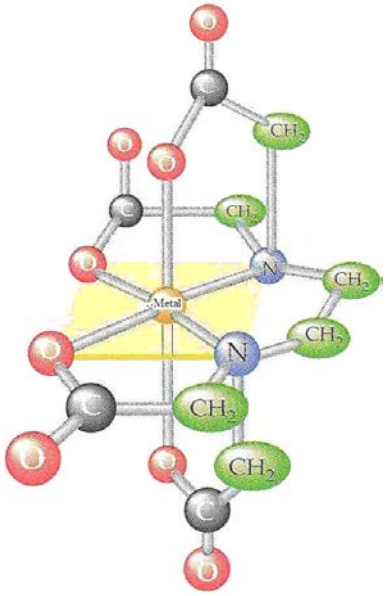

Figure 3: Metal-EDTA chelate (Cox *et al*., 2006)

Some ligands are attached to a metal atom by more than one donor atom in such a manner as to form a heterocyclic ring of the kind found in the copper-EDTA complex presented in **Figure 3**. The process of forming a chelate ring is known as chelation.

The most common metal complexes occurring in aqueous solutions are aquated metal ions or aquocomplexes. It is mainly from these kind of complexes that metal chelates are formed by the replacement of water molecules.

If a molecule is going to act as a chelating agent, it must fulfil at least two conditions. First, it must possess at least two appropriate functional groups, the donor atoms which are capable of combining with a metal atom by donating a pair of electrons. These electrons may be given by basic groups or groups functionating as acids by losing a proton. Second, the donor atoms must be so situated in the molecule as to permit the formation of a ring with a metal atom as the closing member.

In solution, chelating anions are proton acceptors, and so, protons compete with metal ions for these anions (Volesky, 2003). If HL represents a protonated ligand, this overall equilibrium with divalent metal ion may be represented as:

$$Me^{2+} + 2\ HL \leftrightarrow [MeL_2] + 2\ H^+$$

4.1.3. Ion exchange

The ion exchange properties of many organic and inorganic based materials has been reported. It's well known that divalent cations of metals from the transition serie can be exchanged by light metals as Na^+, K^+ or Ca^{2+} or by H^+ firstly coordinated to the basic sites of the sorbents, according to the scheme presented next.

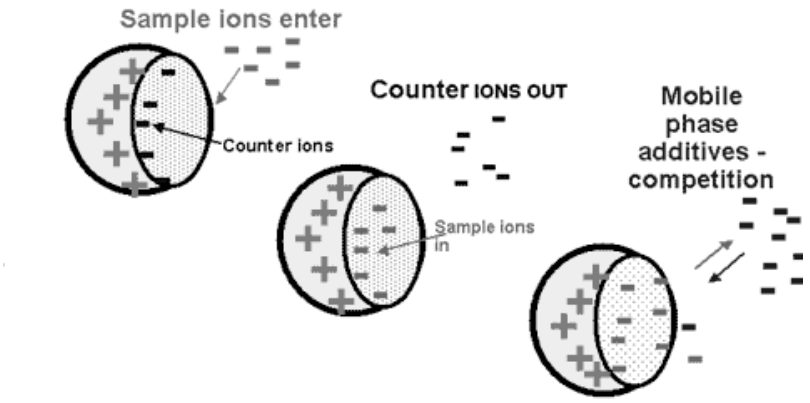

Figure 4: Ion exchange steps (Volesky, 2003)

Studies carried out with microbial (Pagnanelli *et al*., 2000), marine (Schiewer and Volesky, 1996; Schiewer and Volesky, 1997) and vegetable (Martínez *et al*., 2006; Villaescusa *et al*., 2004) biomass has put into evidence the important role of this mechanism in the sorption of different heavy metal cations. The nature of the active sites varies widely according to the sorbent used, however, common examples of functional groups that provide the material with its ion exchange capacity are carboxyl, sulphate and phosphate.

4.2. Physisorptive mechanisms

4.2.1. Physical adsorption

Physical adsorption is a non specific process where the interactions that attract the solute molecules through the solid surface are relatively weak as, for instance, Van der Waals forces. The weakness of these interactions makes the extension of physical sorption dramatically dependent on the temperature.

4.2.2. Inorganic microprecipitation

Metals microprecipitation takes place when the solubility of the sorbate reaches its limit. This may happen even due to local conditions, e.g. on or inside of the sorbent, and not necessarily in the bulk of the solution. These favourable conditions for microprecipitation may be created by local deviations in physical conditions such as pH or by the presence of materials released from the sorbent itself.

When sorption is studied, special attention has to be paid that the solubility limits are not exceeded even locally because the consequence would be that the metal is not removed from the solution by sorption but by precipitation. On the other hand, microprecipitation in any sorption process could contribute to the overall metal removal efficiency a great deal whereby the metal microprecipitate becomes collected by the solid phase and thus immobilized and separated from the solution itself (Volesky, 2003). This is the case of gold and silver uptake by nanoprecipitation on calcium alginate beads (Torres *et al*., 2005) and lead and cadmium removal by *Pynus silvestris* (Taty-Costodes *et al*., 2003).

5. INDUSTRIAL LIQUID EFFLUENTS IN THE PLATING INDUSTRY

5.1. Problems associated with this industry

The surface treatment industry uses large quantities of chemical products, many of which are toxic to man and the environment. Such chemicals provide the major components in the gaseous, liquid and solid effluents from the industry and represent 40% of the total aqueous metallic pollution. Globally the industry produces 20% of the total aqueous pollution of which the surface treatment sector contributes with around 6 to 8%. This amount has been consistently reduced for some years, thanks to the introduction of strict regulations concerning discharge levels and to the introduction of techniques to purify aqueous effluents. These kind of industries use large quantities of water in its processes that do not only feature in the composition of processing baths such as: degreasing, etching or plating, but specially in the rinsing of the pieces between the different processes an in the final washing stage. During these different phases water is polluted by heavy metals and their salts must be treated before disposal into the natural habitat according to very strict and specific standards in every country of the EU (Cox *et al*., 2006).

In these industries, the different sources of potential pollution can be classified as follows:

- bath to bath transfer of the work piece
- spillages, accidents, etc.
- overflow, droplets falling from work-pieces
- draining of the exhausted processing and rinsing baths
- evaporation

On the other hand, the types of wastes in surface treatment industry can be classified in four categories:

- solid wastes from decontaminating processes (mostly hydroxide muds), representing around 47%.
- wastes from preparation and coatings, being around 36%.
- solvents, with a contribution around 7.6%
- liquid mineral wastes, in around 9.4%

The nature of the pollutants contained in the surface treatment industry effluents includes several types of substances as detailed next.

· *Cations*. Generally ions of heavy metals such as aluminium, chromium, copper, iron, lead, magnesium, nickel and zinc are the most frequently rejected. Depending on the process, it can be also found smaller quantities of precious metals as gold, palladium, rhodium and silver, as well as the less common metals: molybdenum, titanium or zirconium.

· *Anions*. The largest proportion comes from the metallic salts contained in the processing and etching baths. These are chlorides, fluorides, cyanides, nitrates and nitrites, phosphates, sulphates and hexavalent chromium as either, chromate or dichromate.

· *Organic compounds.* The surface treatment industry use a growing number of organic chemical products to enhance the quality of coatings (brighteners) or complexing agents such as tertiary amines, quaternary ammonium salts, ethylenediaminetetraacetate salts (EDTA), etc. to promote deposition, specially in the case of co-deposits. These chemicals have negative effects on the environment because they significantly increase the chemical oxygen demand (COD) of the effluent and are difficult to eliminate. Moreover, some of them, specially molecules like EDTA, citrate and gluconate show strong complexing properties through different heavy metals affecting dramatically the performance of the water treatment.

6. THE PARTICULAR POLLUTING FRAME OF THE ELECTROPLATING INDUSTRIES: POLLUTANTS AND WATER TREATMENT PROCESSES

Most surface treatment workshops use physico-chemical techniques to purify liquid effluents. These consist of a combination of a physical techniques, e.g. precipitation, decantation, filtration, etc. and chemical processes of oxidation-reduction to eliminate the polluting metals in solution.

During the construction of plating workshops, several networks for the collection of waste-water streams are constructed to separate incompatible flows and to facilitate subsequent purification. Such networks would include pipework for:

- basic solutions and those containing cyanide
- acidic and chromic solutions
- acid/basic stream

Next, the different treatment of these representative effluent streams will be described.

In a physico-chemical purification scheme, three basic steps can be observed:

(1) Initially, the alkaline cyanide stream is oxidized in the alkaline environment to convert cyanides to cyanates, and the acidic chromic stream is reduced by bisulphite to transform Cr(VI) to Cr(III).

(2) Then, the above purified streams are mixed with the mixed acid/basic stream, and the resulting effluent is treated with sulphuric acid or soda (or lime) to adjust the pH to 6.5-9 to precipitate heavy metals as hydroxides.

(3) Finally, the precipitated hydroxides are decanted, filtered and dewatered in a press to separate water from hydroxide mud; the hydroxide mud is sent to an agreed centre for treatment or disposal and the water from the decantation and the filter press, conforming to discharge limits, is sent to sewage for disposal.

In the next figure, a scheme of a real electroplating industry is presented. In it, the different steps can be clearly observed.

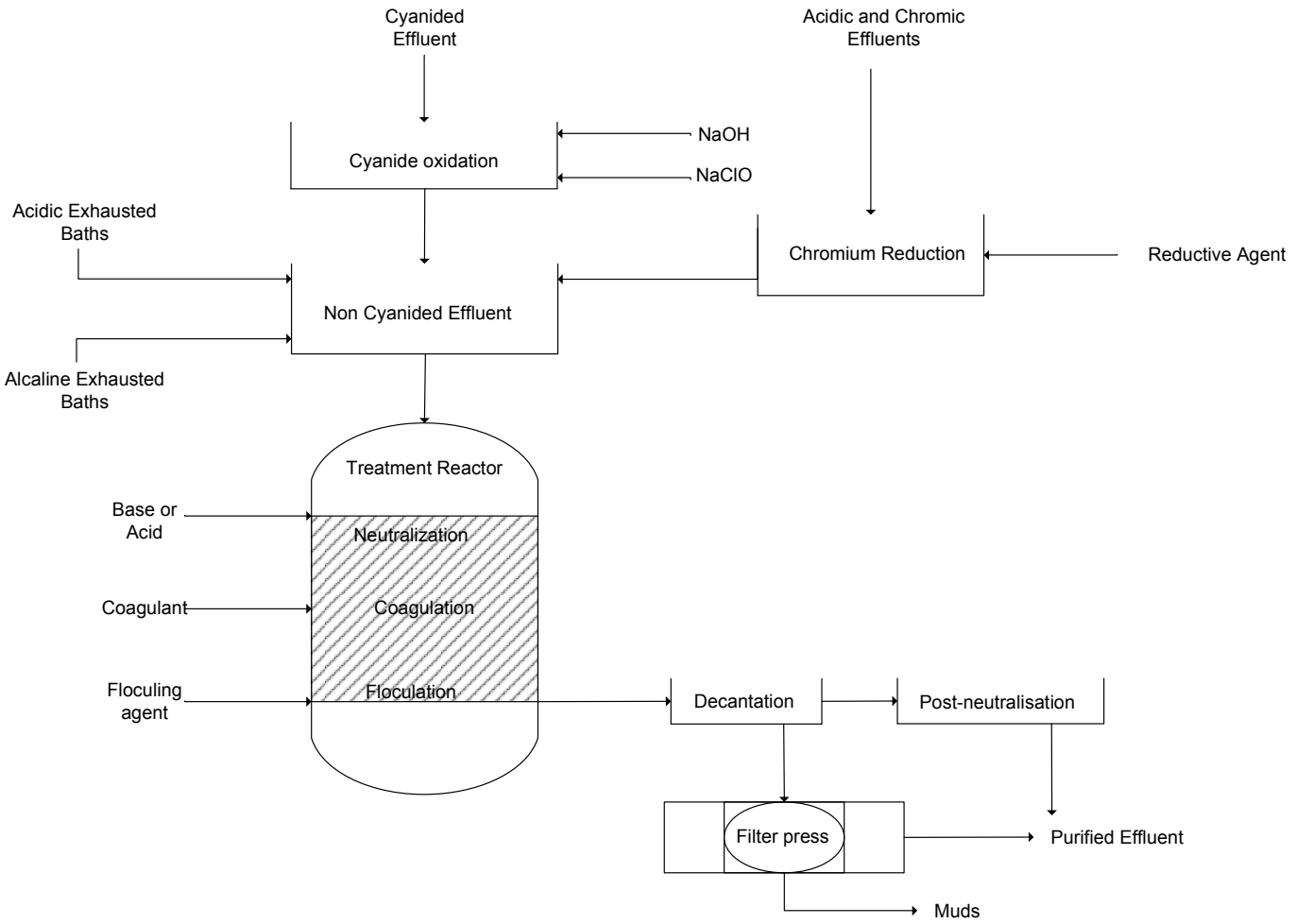

Figure 5: Electroplating industry scheme.

As it can be seen in the figure, the detoxification of the effluent is carried out in different phases by means of different techniques, involving both chemical and physical processes. These different steps are summarized in detail next.

1) First step: pre-treatment of effluents

a. Dechromisation

The chromic acid effluents, whose frequently found characteristics are presented in **Table 1**, are treated in a dechromisation reactor with sodium bisulphite ($NaHSO_3$) under acidic conditions, normally managed with H_2SO_4 and mechanical agitation, to reduce hexavalent to trivalent chromium according to the reactions presented next:

$$H_2Cr_2O_7 + 3\ NaHSO_3 + 3\ H_2SO_4 \longrightarrow Cr_2(SO_4)_3 + 3\ NaHSO_4 + 4\ H_2O$$

or

$$4\ H_2CrO_4 + 6\ NaHSO_3 + 3\ H_2SO_4 \longrightarrow 2\ Cr_2(SO_4)_3 + 3\ Na_2SO_4 + 10\ H_2O$$

Table 1: Typical composition of a chromium/acid effluent from a surface processing workshop before dechromisation. Concentrations are expressed in $mg \cdot L^{-1}$ and conductivity, in $mS \cdot cm^{-1}$.

Polluting agents	Chromium acid effluent
pH	2.6
Total suspended solids	140
Chromium(VI)	490
Fluorides	5
Chlorides	520
Total cyanide	0.02
COD	177
Conductivity	7.2
Dry residue (105 ºC)	4930
Total metal content	730

A pH value lower than 2.5 is required because the Cr(VI) to Cr(III) reduction kinetics decreases quickly if the pH rises, the critical limit being pH 3.5 at which the reaction rate becomes zero. The reduction is continuously controlled by monitoring the pH and redox potential of the reaction. This technique has been extensively used and provides good results, with residual hexavalent chromium concentration lower than 0.1 $mg \cdot L^{-1}$. Like in

any application, this detoxification technique has advantages and drawbacks, both presented next.

Advantages:

- easy supply and storage of chemicals
- automatic control of mechanic operations, pumps, stirrers, etc.,
- automatic process control by measurement of pH and redox potential
- proven efficiency
- relatively low operation cost

Drawbacks:

- increase of effluent salinity due to added reagents
- ventilation of storage area and reactors needed because of the release of SO_2 from the $NaHSO_3$ in acidic media.
- reagent consumption; in practice an excess of expensive reducing reagents is used as part of them reduces any organic matter in the effluents.

Other dechromisation processes involve the use of alternative reagents to sodium bisulphite to reduce Cr(VI) to Cr(III). These alternative reagents include SO_2, Na_2SO_3, $Na_2S_2O_4$, $Na_2S_2O_5$ and it can also be undertaken with the help of iron(II) salts as $FeSO_4$. This practice of using ferrous salts is not very common but interesting for workshops that practice sulphuric etching of steel on a big scale as, in this case, it is sufficient to mix the etching residues with the chromium acid effluent to reduce Cr(VI) much more easily whatever the pH (between 1 and 8.5) (Cox *et al*., 2006).

Drawbacks of this process are the formation of huge quantities of mud from iron hydroxide precipitation because $FeSO_4$ is added in large quantities for practical reasons.

· Implementation:

Cr(VI) to Cr(III) reduction reaction requires a minimum reagent contact time of 20 minutes. This should be determined during the design of the dechromisation reactor and measurements should be calculated for a contact time of 30 minutes to ensure the total reduction of the effluent. The reduction reaction does not produce any toxic fumes provided that there's not an excess of bisulphite; if there's an excess, SO_2 fumes are produced. SO_2 will also be released at pH<1.5, hence the need to regulate the pH.

b. Decyanidation

The alkaline effluents containing cyanide are treated in a decyanidation reactor under mechanical agitation with added bleach (sodium hypochlorite, NaClO) and soda (NaOH) at pH>11.5 to prevent the emission of very toxic fumes of cyanogen chloride. The chemical oxidation of cyanides (CN^-) in cyanates (CNO^-) occurs in two steps:

$$CN^- + ClO^- + H_2O \longrightarrow CNCl + 2\ OH^-$$

$$CNCl + 2\ OH^- \longrightarrow Cl^- + CNO^- + H_2O$$

Being the overall reaction:

$$NaCN + NaClO \longrightarrow NaCNO + NaCl$$

The oxidation reaction is continuously controlled by measurement of pH and redox potential. This technique has been used for many years and provides good results with residual cyanide concentration lower than 0.1 $mg \cdot L^{-1}$.

Advantages:

- easy supply and storage of chemicals
- automatic control of mechanic operations, pumps, stirrers, etc.,
- automatic process control by measurement of pH and redox potential
- proven efficiency
- relatively low operation cost
- low COD

Drawbacks:

- increase of effluent salinity due to added reagents
- ventilation of storage area and reactors needed due to the risk of emissions of organo-chlorine compounds
- not suitable for cyanide concentration >2 $g \cdot L^{-1}$
- chlorine must be eliminated from the treated effluents
- unstability of bleach solutions
- reagent consumption; in practice an excess of reactive needed

Other decyanidation processes, not so extended as the described previously, include the use of persulfuric acid (H_2SO_5) instead of bleach as oxidant, the advantage being the direct formation of cyanate CNO^-, without the intermediate step of cyanogen chloride formation.

$$NaCN + H_2SO_5 \longrightarrow NaCNO + H_2SO_4$$

After this process, a hydrolytic step is carried out to produce from the CNO^- directly CO_2, according to the next reaction.

$$NaCNO + 2\ H_2O \longrightarrow CO_2 + NH_3 + NaOH$$

To destroy small amounts of cyanide it is also possible to use hydrogen peroxide, as oxidant in presence of copper as catalyst. This technique can be enhanced by the use of ultrasound, when the reaction becomes instantaneous.

The total destruction of cyanide in metallurgic effluents is needed, not only because of the high toxicity to environmental systems, but also because of its strong complexing capacity through heavy metals. The cyanide complexation can also reduce the efficiency of the subsequent processes for the removal of these metals.

2) Second step: Neutralisation and precipitation

a. Neutralisation

The effluents following destruction of hexavalent chromium and cyanides are mixed with the acid/basic effluents in a reactor controlled at pH between 6.5-9 by the addition of sulphuric acid or soda as appropriate. Such neutralisation has the following goals:

- to obtain an effluent pH without danger for the environment
- to precipitate the heavy metals as insoluble hydroxides
- to eliminate some anions such as phosphates, fluorides and sulphates

b. Ensurance of insolubility of metal hydroxides

This is a difficult problem with effluents from surface processing specially in workshops that deposit many different metals. Indeed, according to the nature of the metal and the pH value, the extent of hydroxide solubility can vary considerably. Cadmium, for example, has a minimum solubility at pH 11, but if the effluents also contain chromium, zinc or nickel, these can redissolve at this pH due to the formation of anionic complexes.

Therefore, the pH value is of primary importance, and on its value is going to depend the solubility of the metallic hydroxides and, consequently, the amount of heavy metals remaining in the effluent after treatment. The best solution, when effluents contain

cadmium, is to treat this metal independently of the others by electrolysis, ion exchange, evaporation, etc.

c. Precipitation

The precipitation of the metal hydroxides takes place during neutralisation. As the pH achieves the appropriate value for precipitation of the metal, some microflocs appear in the solution, and it is important to increase the size of these flocs to facilitate decantation. To increase floc size, anionic organic flocculating agents are added to the effluents. The choice of such flocculating agents is undertaken from the representative trials on the effluents.

3) Third step: precipitate treatment

a. Decantation

After precipitation of the hydroxides, the effluents are generally decanted in a conical decanter, where the feed enters at the centre of the cylinder and the removal of water takes place at the periphery toward the throat.

b. Pressing of the muds

After decantation the hydroxide muds are pumped from the base of the decanter and fed to a filter press to separate the residual water. After the dewatering, the solid cakes of mud are transported to the agreed centres for treatment or disposal. Nowadays, this physico-chemical decontamination system is used in more then 80% of the surface processing workshops in Europe. Despite of the broad application of this water detoxification process, several drawbacks include:

- consumption of chemicals and water
- high salinity of the decontaminated effluent
- non-possible water re-use without prior treatment due to its high salinity
- limitation in extent of decontamination

7. LOW COST MATERIALS AS SORBENTS

7.1. General overview

In an attempt to reduce the high operation costs of the metal removal process from liquid effluents, from the beginning of the 90s, a new scientific area appeared: the biosorption. First works carried out in this area promisingly showed that some materials of biological origin presented extracting properties for some heavy metals at low concentration level (Vieira and Volesky, 1990). Among the most employed sorbents from biological origin, it can be remarked the use of biomass, as fungi (Kapoor and Viraraghavan, 1997; Pal *et al*., 2006), yeast (Volesky and May-Phillips, 1995; Wang and Chen, 2006; Padmavathy, 2008) or bacteria (Churchill and Walters, 1995; Green-Ruiz, 2006) marine seaweed and algae (Vilar *et al*., 2008; Onyancha *et al*., 2008; Matheickal *et al*., 1999; Kratochvil *et al.*, 1998; Gupta *et al*., 2001; Apiratikul and Pavasant, 2008) vegetable wastes either natural as coniferous leaves (Cho *et al*., 1999), or industrial as lignocellulosic substrate (Dupont and Guillon, 2003), grape stalk (Villaescusa *et al.*, 2004; Fiol *et al*., 2004; Fiol *et al*., 2005) cork and yohimbe bark (Villaescusa *et al*., 2000), exhausted coffee (Fiol *et al*., 2008) citrus peel (Schiewer and Patil, 2008) and wine processing waste sludge (Yuan-Shen *et al*., 2004).

But the property of effective sequestration of heavy metals from aqueous effluents has not been demonstrated by only organic-based materials; many other inorganic materials such as some minerals abundantly available in nature or some industrial by-products, have been successfully used for the detoxification of different metal-polluted effluents. Among the mineral-base materials, it can be remarked the use of ferrihydrite (Raven *et al*., 1998), iron phosphate, either crystalline or amorphous (Lenoble *et al*., 2005) and goethite (Ladeira and Ciminelli, 2004) all these, useful for the removal of arsenic, but also zeolites and clays have been successfully used for the removal of different heavy metals such as nickel(II) (Carvalho *et al*., 2007), lead(II) and cadmium(II) (Wingenfelder *et al*., 2005) and chromium(III), nickel(II), zinc(II), copper(II) and cadmium(II) (Álvarez-Ayuso *et al*., 2003).

Among the industrial by-products, its noteworthy the use of red mud for the removal also of arsenic (Altundogan *et al*., 2002), activated red mud for the removal of nickel(II) (Zouboulis and Kydros, 1993), iron(III)/chromium(III) hydroxide for the removal of chromium(VI) (Namasivayam and Ranganathan, 1993), and blast furnace slag for the removal of lead(II) and chromium(VI) (Nehrenheim and Gustafsson, 2008).
The wide variety of potential low-cost sorbent materials and metals that can be adsorbed makes this process a promising technique for the treatment and recovery of metals from different polluted effluents.

7.2. Industrial by-products as sorbents: the particular use of grape stalk, exhausted coffee and industrial electroplating (hydr)oxide industrial wastes

As it had been described, a wide variety of materials fully available have been employed as sorbents as natural, agricultural or industrial by-products. These materials can be used either on its raw form or after a previous treatment to enhance their sorption capacity or to improve their mechanical or mass transfer properties. Some authors processed chemically low-cost materials such as coconout shell, (Kirubakaran *et al*., 1991), pistachio shell (Abe *et al*., 1990), tropical wood (Maniatis and Nurmala, 1992), almond shell (Hayashi *et al*., 2000) and rice bran (Suzuki *et al*., 2007) to produce activated carbon, but these processes are normally time consuming and expensive due to the use of chemical reagents and high temperatures. That's why if the material shows good sorption properties on its raw form and not very important improvement is achieved after the treatment, this modification is not feasible.
The importance of the agroalimentary sector in Spain as one of the main economic motors leads to the production of many industrial vegetable by-products. Among these, wine industry has to be remarked as a producer of a huge amount of a particular waste, the grape stalk (GS). These materials are the branches that connect the grape grains making a compact structure, the grape bunch. In the vinification industries, it can be admitted that, in average, from each 100 kg of material, 5 to 6 kg are GS and 94-95 is grape (Boulton *et al.*, 2002). Despite 5-6% of waste material doesn't seem an excessive amount, it has to be taken into account that a small vinification industry can process about 16.000.000 kg of

grape bunches, involving thus the need of management of approximately 880.000 kg of grape stalk wastes. The immense production of this material after the fruit recollection and industrial processing is currently dispersed in the fields or incinerated.

The grape stalk can get the industry in green or ligneous state. The composition, in average, for each form is summarized next:

1. The green contains from 70 to 80% water, 1.3 to 4% tannins, 0.5 to 1.3% of tartaric and malic acid, 0.3 % of nitrogenated substances, chlorophile, potassium bitartrate and mineral salts.
2. Ligneous grape stalk contains a lower water content, from 35 to 60%, less free acids, more potassium bitartrate and less tannins (Aleixandre, 1999).

In the next figure, the shape of GS after its separation from the grape is shown:

Figure 6: Grape stalk detail.

The use of this material as sorbent for divalent metal cations as Cu(II) and Ni(II) (Villaescusa *et al*., 2004), Pb(II) and Cd(II) (Martínez *el al*., 2006) and for hexavalent chromium (Fiol *et al*., 2003) has been previously reported.

Among the vegetable wastes available in big quantities it can be found also the exhausted ground coffee waste (EC), from the manufacture of soluble instant coffee. At present this waste is mainly used to prepare compost and in some biological waste water treatment plants to adjust to optimal levels the amount of Carbon and Nitrogen. This material, structurally similar to GS, is based in a lignin and cellulose structure. The lignin provides polyhydroxy and polyphenol functional groups that are potentially good metal binding groups (Lima *et al.,* 1998). In the next figure, a picture of the raw EC is presented.

Figure 7: Exhausted coffee detail.

Studies on metal removal by using exhausted coffee residues are scarce. Among these studies, Cr(VI), Cd(II), and Al(III) sorption by Turkish coffee and exhausted coffee has been investigated by Orhan and Buyukgungor (1993) and Utomo and Hunter (2006) studied Cu(II), Zn (II), Cd(II), and Pb(II) sorption onto used exhausted coffee grounds. The use of the raw material to adsorb and reduce hexavalent chromium has been also reported by Fiol *et al*. (2008). Results obtained in those studies, indicate that coffee waste offers considerable promise as low cost sorbent for waste water treatment.

On the other hand, some inorganic wastes are widely produced in many industrial processes such as electroplating ((hydr)oxide mud), Bayer process of alumina production (red mud), steel plants (blast furnace slag) and coal combustion for power production (coal fly ash). These materials, as it had been discussed previously, represent an important extra management cost for the industries to guarantee their adequate management and disposal. That's why increasing attention is currently being paid by these industries to researcher's advances in the development of low-cost alternatives for the management of these wastes.

As it had been described in the previous section, one of the most common activities generating either an important amount of polluted effluents and solid wastes, is the electroplating of metallic pieces. In a medium size electroplating industry, the activity generates several tones of mud yearly. These muds are potential toxic materials, because ions can be mobilized to the liquid phase by solubilization of the material and they can create a serious pollution hazard. It becomes thus necessary the improvement of disposal techniques or the valorisation of this material as a prime material for other industries, processes or applications. Some proposals have appeared for the mud utilization. Currently red muds derived from the alumina production are being used for the manufacture of

building materials and ceramics, as filler in road asphalt and as a source of iron and various minerals (Mohan and Pittman, 2006).

A preliminary analysis of the composition of a real electroplating waste mud revealed a high content of both iron(III) and nickel(II) ions and a residual content of chromium(III), copper(II) and calcium. Despite no available information about the use of this specific type of waste as sorbent was found, the use of similar materials as Fe(III)/Cr(III) hydroxide coming from a petrochemical industry for the removal of Pb(II), Ni(II) and Cd(II) (Namasivayam and Ranganathan, 1997), red mud from an aluminium industry for the removal of Pb(II) and Cr(VI) (Gupta *et al.*, 2001) have been reported. Besides, it has been reported that iron-rich materials are effective sorbents for the removal of one of the most important water pollutants, the arsenic, either as As(III) or As(V) (Shao *et al*., 2008; Deschamps *et al*., 2005; Banerjee *et al*., 2007; Mondal *et al*., 2008; Guo *et al*., 2007; Giménez *et al*., 2007). The important iron content of the material leads us to think in a possible valorisation of this waste as sorbent for arsenic from aqueous solutions.

8. ADVANTAGES OF LOW-COST SORPTION TECHNOLOGY FOR METAL-POLLUTED WATER TREATMENT AND REAL INDUSTRIAL APPLICATIONS

As it had been discussed previously, a wide variety of materials with different origin and available in huge amounts have been proposed as sorbents for the removal of different metals from aqueous solutions. These materials are mainly natural or agricultural wastes but also industrial wastes or process by-products. The main attractive of the use of this kind of technology is based on two aspects. The first one is the intrinsic low cost of the materials, because they are either natural widely available materials or by-products of industrial processes (Bailey *et al*., 1999). The second is that in the case of reuse of industrial by-products, an added value is conferred to these materials. Otherwise, they would be considered as wastes, raising the costs in the industry, because they have to be transported to the agreed centres for treatment, management or disposal.

Pilot installations and few commercial scale units were constructed in the USA and Canada in the 80s and 90s and some of them are presented in **Table 2**. These pilot plants confirmed the applicability of biosorption as a basis for metal sequestering/recovery processes specially in the case of uranium.

In order to stabilize and enhance mechanical properties and even the chemical resistance of raw biomass for potential technological use, immobilization is sometimes required. Immobilisation of the biomass in solid structures creates a material with the rightsize, mechanical strength, rigidity and porosity necessary for use in unit operations typical of chemical engineering. Various techniques are used for the biomass immobilisation. The principal immobilisation techniques found in the literature are based in entrapment in a polymeric matrix, encapsulation or in cross-linking reactions. A brief description of the different immobilization techniques is presented next.

· *Entrapment in polymeric matrices*: The technique is based in the use of another material to hold the active micro-particles together. There are well developed gel entrapment techniques used for enzyme and whole microbial cell immobilization. The polymers used are mainly calcium alginate (Chhikara and Dhankhar, 2008, Arica *et al*, 2001; Pandey *et*

al, 2002; Seki *et al*, 1990), polyacrylamide (Wong and Kwok, 1992.), polysulfone (Kapoor and Viraraghavan, 1998) and polyhydroxoethylmethacrylate (Veglió *et al.,* 1997). Immobilization in calcium alginate of grape stalk powder has demonstrated excellent sorption behaviour for hexavalent chromium removal (Fiol et al., 2004; Fiol et al., 2005). Nevertheless, the entrapment matrix (usually a gel) may cause some mass transfer problems for metal ions. When too much active biosorbent material is entrapped in the particle, it might lose its mechanical properties and easily disintegrates as it does under pressure in larger sorption columns or due to the shear forces in mixed reactors (Volesky, 2003).

· *Encapsulation*: Another method of entrapment whereby a permeable membrane envelope holds the granule of biosorbent together. This technique exhibits some drawbacks as the difficulties of preparation of a suitable membrane envelope with mechanical properties required for the relatively large optimal granule size required in the sorption process applications (1 to 3 mm). The thin membrane envelopes may be fragile and disintegrate easily.

· *Cross-linking*: The objective of this technique is the reinforcing of the active micro-particles by bridging-binding of their own molecules. The addition of a cross-linker leads to the formation of stable aggregates. The most common cross-linkers are: formaldehyde, glutaric dialdehyde, divinylsulfone and formaldehyde-urea mixtures. This technique was successfully applied to immobilise algae and the obtained sorbent was used in the removal of cadmium ions (Holan *et al*., 1993). This technique is not suitable for making macro-particle granules. Furthermore, the crosslinking chemical agent will waste or make inaccessible a portion of sorption active sites. There is always a danger that the chemical treatment procedures may damage the sorption activity of the biomaterial processed. Moreover, these chemicals add an important cost and may generate some additional chemical waste.

Table 2: Biological based sorbent particles developed for metal bearing waste-water treatment (Cox *et al*., 2006).

Name	Material	Immobilization matrix	Particle size (mm)
Bio-fix U.S. Bureau of Mines, (Golden, Colorado)	Cyanobacteria (*Spirulina*); Yeast, Algae; Plants *(Lemma sp., Sphagnum sp*.,)	polyethylene or polypropylene or polysulfone in dimethylformamide	0.5-2.5
AMT-Bioclaim	Bacillus subtilis		
AlgaSORB™ Bio-recovery System Inc. (Las Cruces, New Mexico)	*Chlorella vulgaris*	silica or polyacrylamide gels	
B.V. Sorbex Inc. (Montreal, Canada)	*Sargassum natans; Ascophyllum nodosum; Halimeda opuntia; Palmyra pamata; Chondrus crispus; Chlorella vulgaris*		
Tsezos (Greece)	*Rhizopus arrhizus Activated sludge P. chrysogenum*	polymer coating	0.5-1.0

These pilot plants helped researchers to realize the limitations associated to the use of biosorption with inactive microbial biomass in an industrial application, mainly due to the cost of formulating the biomass into an appropriate biosorbent material. Furthermore, the negative effect of co-ions in the solution on the uptake of the targeted metals by the immobilized microbial biomass, and the reduced resilience of the biological material, made recycling and reuse of the biosorbent even more difficult (Tsezos *et al*., 1997).

Biosorption however is a process with some unique characteristics. It can effectively sequester dissolved metals from very dilute complex solutions with high efficiency. This makes biosorption an ideal candidate for the treatment of high volume low metal concentration effluents.

The management of the solid waste produced after the sorption process should be considered according to the characteristics of the treatment procedure and the metal sorbed. A possible scheme of sorbent use and processing of the metal-laden material to convert into a re-usable form is proposed in the next figure.

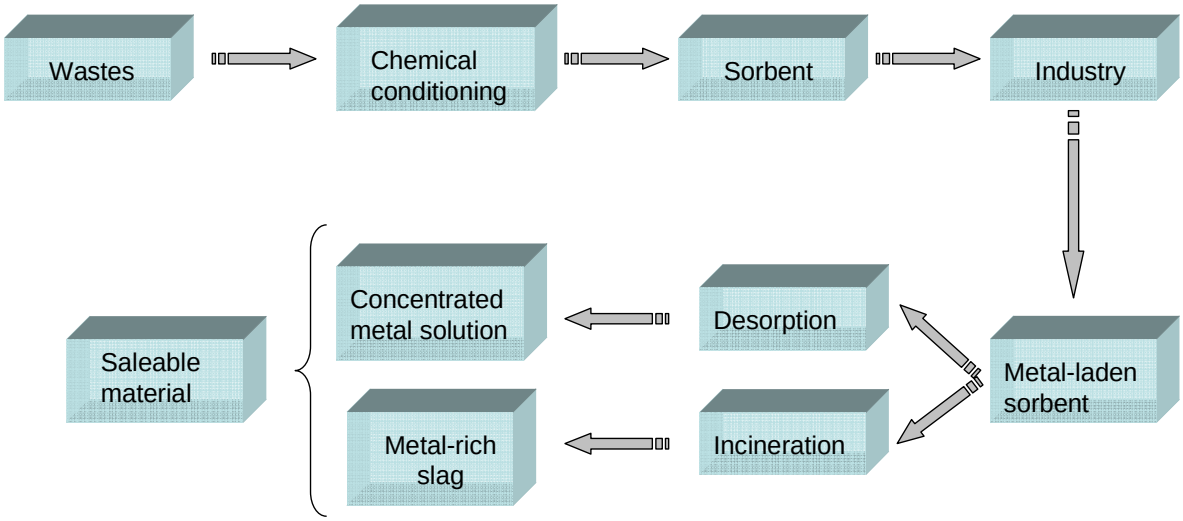

Figure 8: Schematic diagram illustrating the use and re-use of the sorbents (Wase and Forster, 1997).

The processing of sorbents which have been used to treat wastewaters containing a single metal might not pose any significant problem. The use of acids to regenerate sorbents (Philip *et al.*, 1995; Aldor *et al.*, 1995; Stanley and Ogden, 2003; Aldor *et al.*, 1995; Gabaldón *et al.*, 2006) as well as the use of electrochemical techniques to recover metals from solutions (Campell *et al.*, 1994) is well established. Alternatively, if the original sorbent had been based on a waste product and could be viewed as "disposable", incineration could be used to produce a metal-rich slag and use it as a secondary source for metallic elements with a high value. If the metal-loaded material is going to be disposed in a landfill, its potential hazard, associated to the mobility of the ions sorbed on it, should be previously evaluated.

9. THESIS PROJECT FRAME: VALORISATION OF INDUSTRIAL BY-PRODUCTS FOR METALS AND ARSENIC REMOVAL FROM AQUEOUS SOLUTIONS

The present thesis is framed in the projects "Aprovechamiento de residuos vegetales procedentes de procesos industriales para la separación y concentración de iones metálicos" from Ministerio de Educación y Ciencia; project PPQ2002-04131-C02-02 followed by "Valorización de residuos vegetales procedentes de procesos industriales como adsorbentes para la eliminación de iones metálicos de efluentes acuosos"; project CTM2005-07342-C02-01 and finally, in a broader view by "Utilización de residuos industriales para la depuración de efluentes contaminados con metales pesados" (CTM2008-06776-C02-01/TECNO). The first two projects are centered in the development of metal polluted water detoxification techniques by the use of industrial vegetable wastes, while the last one would cover a broader area, because the search of high-performance and low-cost sorbent materials would not be restricted to only vegetable-based industrial by-products.

This thesis project was born in views of reaching a double goal: to develop the basis of a technology for the detoxification of metal-polluted effluents by using non-expensive and oil-independent environmentally friendly materials and to provide a possible solution to industrial complex and expensive management by-products problem, by giving an added value to this huge industrial wastes quantities that are produced in different processes.

In the first beginning of this project, a material of proved efficiency for hexavalent chromium removal based on calcium alginate gel spheres containing grape stalks wastes, was evaluated for the removal of either Cr(VI) and Cr(III) from aqueous solutions. Due to the important toxicity of chromium in waters, particularly when it is on its hexavalent oxidation state, optimization of the detoxification process would include the obtention of mechanistical information about the chemistry of the interaction of either Cr(VI) and Cr(III) with the sorbents.

These studies clearly demonstrated the role of GS as sorbent by mechanisms involving either coordination of hexavalent chromium to the material or reduction of hexavalent to the less toxic trivalent oxidation state. The predominance of the sorption or the reduction

mechanism was strongly affected by the pH of the medium, being the sorptive mechanism favourable under low acidity and the reductive, under high acidity conditions. The obtained results opened a possible broader horizon in the development of a process where the raw non-expensive and abundantly available GS, would take the protagonism for being used as technique for detoxification of Cr(VI) polluted effluents, based on the reductive potential exhibited by this material under acidic conditions. A process with these characteristics would be directly facing the important economical cost associated to the strong consumption of expensive reducing reagents in the dechromisation step.

This idea was reflected in the implementation of a reactor that, in a first approach, would operate in batch mode, in the same way as many electroplating industries operate when carrying out the Cr(VI) to Cr(III) reduction process, according to the techniques described previously. In order to optimize the reductive process, an internal sensor controlled by an external device would be used to monitor acid consumption when reaction progressed and to automatically compensate this consumption by addition of acid from an external source. On the other hand, as it is well known, many reactions are thermally activated and its progress rate and extension can be strongly affected by the temperature. This fact leads us to think that reduction could not be only activated by proton addition, but also by an extra heat apportation to the reactive medium. With these expectations, evaluation of temperature on Cr(VI) to Cr(III) detoxification process mediated by GS was also considered.

Despite of the high toxicity of Cr(VI) and its occurrence in polluted effluents, a global view of the processes of many electroplating industries lead us to see that the Cr(VI) occurrence and its reductive treatment to accomplish environmental pollution criteria is only the “tip of the iceberg”. As it had been exposed in previous sections, the effluents produced in many industries usually contain different organic chemical products that are added to enhance quality of coatings (brighteners) or complexing agents, such as the ethylenediaminetetraacetate, an aminecarboxylic derivative commonly known as EDTA, to promote metal deposition. These compounds can dramatically affect the performance of the treatment to remove the metals from the solution due to the formation of soluble complexes. So that, one chapter was devoted to the study of the presence of complexing agent EDTA in the sorption of two of the most frequently found in wastewater heavy

metals; Cu(II) and Ni(II). With this purpose, GS was evaluated as sorbent and compared with another waste fully available also, the exhausted coffee (EC).

On the other hand, the problems concerning the presence of heavy metals in most of the cases is not reduced to the presence of possible potential sorption inhibitors in single or in binary metal mixtures, as previously discussed with the case of EDTA, but also to the frequent presence of multimetal mixtures, facing thus a much more complex multimetal polluting scenario where the competition of the different metals to be sorbed onto a limited number of active sites can play a decisive role in the performance of the biosorptive system. Among the most common metals present in aqueous industrial effluents, it can be found Cu(II) and Ni(II), as discussed previously, but it cannot be neglected the possible presence of other metals whose environmental toxicity or bioaccumulation potential is of special concern, like Pb(II) and Cd(II). With this basis, sorption behaviour of GS when facing complex mixtures of all the possible single, binary, ternary and quaternary combinations of Cu(II), Ni(II), Pb(II) and Cd(II) will be evaluated in a continuous bed up-flow process. The possible competition for sorption will be studied and discussed in basis of the thermodynamic calculated parameters related to the sorption process.

Until the present moment, the ability of vegetable wastes as grape stalk and the exhausted coffee had been evaluated for different metal polluted waters detoxification scenarios. But when looking at the general operational scheme of a common electroplating industry, a clear evidence appears: metal polluted fluid effluents are the primary decontamination objective to face with the technology proposed until this point but, what about the solid waste (muds) these industries produce as well? Many times, these industries and institutions working with them transmit us their interest in all the processes and scenarios here proposed, studied and discussed. They show an enormous interest through the inexpensive dechromisation process and through the toxic metal removal from the liquid phase that takes place promoted by the GS, but, always a final inquiry comes: might we find ourselves in the shoes of the vegetable industries you work with? Is there any low-cost alternative for the valorisation of the huge amount of muds that are yearly produced after the primary precipitation treatment of the effluent?

Our response: a firstly dubitative “maybe” that, after some preliminary studies finally turned into a strong, “yes, there is”. The last chapter of the present thesis is devoted to this

solid waste. The by-product of precipitation of the metals on the liquid effluent coming from an electroplating industry based on Fe(III), Ni(II), Cu(II) and Cr(III) (hydr)oxides will be valorised and investigated for As(III) and As(V) removal from aqueous solutions. The problems associated to the dusty shape and potential increase of toxicity of the effluent because of the possible mobilization of the toxic ions that form the material will be solved by entrapment of the dust into calcium alginate. After this modification, a double goal is pursuit: the improvement of mechanical properties of the sorbent and the introduction of a reactive medium that avoid the release of toxic heavy metals from the inert solid phase to the liquid.

10. OBJECTIVES

The objective of the present thesis project is to evaluate the performance of widely available industrial by-products, for the detoxification of heavy metal and arsenic polluted effluents.

The present document is structured in three sections, with a total of five different chapters where, after a general introduction, each one pursuits the achievement of different objectives. In a first section, the detoxification of chromium containing effluents by grape stalks is studied. In the second section, the removal of heavy metal divalent cations is studied in different industrial representative conditions; in presence of complexing agents and in multimetal mixtures. In the last section the solid waste produced in electroplating industries after the detoxification treatment of the effluent, will be explored as a possible arsenic sorbent.

The general objectives of each chapter are presented next.

- To study the sorption behaviour of grape stalk wastes entrapped in a calcium alginate gel matrix to remove trivalent and hexavalent chromium from aqueous solutions. To analyze the role of both, alginate and grape stalk in the sorption of each chromium oxidation state and obtain mechanistical information about the sorption process.

- To investigate the detoxification of a Cr(VI) polluted effluent in a stirred batch reactor operating in batch mode by using grape stalk as a sorption-reduction agent. To evaluate the effect of temperature, pH compensation and initial hexavalent chromium concentration on the kinetics of Cr(VI) removal. To develop a mathematical model to explain the dynamics of the process.

- To evaluate and compare sorptive activity of grape stalk with the sorptive behaviour of exhausted coffee, industrial by-product of the preparation of soluble coffee, for the removal of Cu(II) and Ni(II) from aqueous effluents. To evaluate the effect of the complexing agent EDTA in Cu(II) and Ni(II) removal by grape stalk and exhausted coffee.

- To investigate the uptake of Cu(II), Ni(II), Pb(II) and Cd(II) by grape stalk in a continuous bed up-flow process in single, binary, ternary and quaternary mixtures. To evaluate the sorption competitive effects by studying the sorption thermodynamics of each metal onto grape stalk.

- To study the possible valorisation of one of the most problematic by-products of electroplating industries, the metal hydroxide precipitation waste, as a potential sorbent for the removal of As(III) and As(V) from aqueous solutions.

11. REFERENCES

· Abe, I., Tatsumoto, H., Ikuta, N., Kawafune, I., Preparation of activated carbon from pisthachio nut shell. Chem. Exp. 5 (1990) 177–180.

· Abdulkarim, M., Abu Al-Rub, F.A., Adsorption of lead ions from aqueous solution onto activated carbon and chemically-modified activated carbon prepared from date pits, Adsorpt. Sci. Technol. 22 (2004) 119-134.

· Aksu, Z., Kabasakal, E., Batch adsorption of 2,4-dichlorophenoxy-acetic acid (2,4-D) from aqueous solutions by granular activated carbon, Sep. Purif. Technol. 35 (2004) 223-240.

· Aldor, I., Fourest, E., Volesky, B., Desorption of cadmium from algal biosorbent, Can. J. Chem. Eng. 73 (1995) 516-522.

· Alkorta I., Hernández-Allica Becerril J.M., Amezaga I., Albizu I., Garbisu C., Recent findings on the phytoremediation of soils contaminated with environmentally toxic heavy metals and metalloids such as zinc, cadmium, lead, and arsenic. Rev. Environ. Sci. Biotechnol. 3 (2004) 71–90.

· Aleixandre J.L., Vinos y bebidas alcohólicas,. Universidad Politécnica de Valencia, (1999), Valencia, España.

· Altundogan, H.S., Altundogan, S., Tumen, F., Bildik, M., Arsenic adsorption from aqueous solutions by activated red mud, Waste Manage. 22 (2002) 357–363.

· Álvarez-Ayuso, E., García-Sánchez, A., Querol, X., Purification of metal electroplating waste waters using zeolites Water Res. 37 (2003) 4855–4862.

· Apiratikul, R., Pavasant, P., Batch and column studies of biosorption of heavy metals by *Caulerpa lentillifera*, Bioresource Technol. 99 (2008) 2766–2777.

· Arıca, MY., Kaçar, Y., Genç, Ö., Entrapment of white-rot fungus Trametes versicolor in Ca-alginate beads: preparation and biosorption kinetic analysis for cadmium removal from an aqueous solution Bioresource Technology.80 (2001): 121-12.

· Bailey, S.E, Olin, T.J., Bricka, R.M., Adrian, D.D. A review of potentially low-cost sorbents for heavy metals. Water Res. 33(11) (1999) 2469-2479.

· Banat, F., Al-Asheh, S., Makhadmeh, L., Preparation and examination of activated carbons from date pits impregnated with potassium hydroxide for the removal of Methylene blue from aqueous solutions, Adsorpt. Sci. Technol. 21 (2003) 597-606.

· Banerjee, A., Nayak, D., Lahiri, S., Speciation-dependent studies on removal of arsenic by iron-doped calcium alginate beads. Appl. Radiat. Isot. 65 (2007) 769-775

· Basso, M.N., Cerrella, E.G., Cukierman, A.L. Activated carbons developed from a rapidly renewable biosource for removal od cadmium (II) and nickel (II) ions from dilute aqueous solutions. Ind. Eng. Chem. Res. 41 (2002) 180-189.

· Bishop P.L., Pollution prevention: fundamentals and practice. Beijing: Tsinghua University Press; 2002.

· Boulton R.B., V.L. Singleton, L.F. Bisson, R.E. Kunkee, Teoría y práctica de la elaboración del vino, (2002). Acribia, S.A. Zaragoza. España.

· Campbell, D.A., Dalrymple, I.M., Sunderland, J.G., Tilston, D., The electrochemical recovery of metals from effluent and process streams. Resource, conservation and recycling. 10 (1994) 25-33.

· Carvalho, W.A., Vignado, C., Fontana, J., Ni(II) removal from aqueous effluents by silylated clays, J. Hazard. Mater. (2007), doi:10.1016/j.jhazmat.2007.09.083

· Chen, J.P., Yoon, J.T., Yiacoumi, S., Effects of chemical and physical properties of influent on copper sorption onto activated carbon fixed-bed columns, Carbon 41 (2003) 1635-1644.

· Chen, J.P., Wang, X., Removing copper, zinc and lead ion by granular activated carbon in pretreated fixed-bed columns, Sep. Purif. Technol. 19 (2000) 157-167.

·Chhikara, S., Dhankhar, R., Biosorption of Cr(VI) ions from electroplating industrial effluent using immobilized *Aspergillus niger* biomass, J. Environ. Biol. 29 (2008) 773-778.

· Cho, N.S., Aoyama M., Seki, K., Hayashi, N., Doi, S., Adsorption by coniferous leaves of chromium ions from effluent, J. Wood Sci. 45 (1999) 266-270.

· Churchill, S.A, Walters, J.V., Churchill, P.F., Sorption of heavy metals by prepared bacterial cell surfaces, J Environ Eng. 121 (1995) 706-711.

· Cox, M., Négré, P., Yurramendi, L., A guide book on the treatment of effluents for the mining/metallurgy, paper, plating and textile industries. Inasmet-Tecnalia, San Sebastián (España), 2006.

· Demirbas, E., Kobya, M., Senturk, E., Ozkan K., Adsorption kinetics for the removal of chromium (VI) from aqueous solutions on the activated carbons prepared from agricultural wastes. Water SA. 30(4) (2004) 533-539.

· Demirbas, E., Adsorption of cobalt(II) ions from aqueous solution onto activated carbon prepared from hazelnut shells, Adsorpt. Sci. Technol. 21 (2003) 951-963.

· Deschamps, E., Ciminelli, V.S.T., Höll, W.H. Removal of As(III) and As(V) from water using a natural Fe and Mn enriched sample. Water Res. 39 (2005) 5212-5220.

· Dupont, L.I., Guillon, E., Removal of hexavalent chromium with a lignocellulosic substrate extracted from wheat bran, Environ. Sci. Technol. 37 (2003) 4235-4241.

· Fiol, N., Villaescusa, I., Martínez, M., Miralles, N., Poch, J., Serarols, J., Biosorption of Cr(VI) using low cost sorbents. Environ. Chem. Lett. 1 (2003) 135-139.

· Fiol N., Poch J., Villaescusa I., Chromium(VI) uptake by grape stalks wastes encapsulated in calcium alginate beads: equilibrium and kinetics studies, Chem. Spec. Bioavailab. 16 (2004) 25-33

· Fiol N., Poch J., Villaescusa I., Grape stalks wastes encapsulated in calcium alginate for Cr(VI) removal from aqueous solutions, Sep. Sci. Technol. 40 (2005) 1013-1028.

· Fiol, N., Escudero, C., Villaescusa, I., Re-use of exhausted ground coffee waste for Cr(VI) sorption. Sep. Sci. Technol. 43 (2008) 582-596.

· Gabaldón, C., Marzal, P., Álvarez-Hornos, F.J., Modelling Cd(II) removal from aqueous solutions by adsorption on a highly mineralized peat. Batch and fixed-bed column experiments, J. Chem. Technol. Biotechnol. 81 (2006) 1107-1112.

· Gabaldón, C., Marzal, P., Ferrer, J., Seco, A., Single and competitive adsorption of Cd and Zn onto a granular activated carbon, Water Res. 30 (1996) 3050-3060.

· Giménez, J., Martínez, M., de Pablo, J., Rovira, M., Duro, L., Arsenic sorption onto natural hematite, magnetite and goethite. J. Hazard. Mater. 141 (2007) 575–580.

· Green-Ruiz, C., Mercury(II) removal from aqueous solutions by nonviable Bacillus sp. from a tropical estuary, Bioresource Technol. 97 (2006) 1907–1911

· Guo, H., Stüben, D., Berner, Z., Removal of arsenic from aqueous solution by natural siderite and hematite. Appl. Geochem. 22 (2007) 1039-1051.

· Gupta, V.K., Shrivastava, A.K., Jain, N., Biosorption of chromium(VI) from aqueous solutions by green algae Spirogyra species, Water Res. 35 (2001) 4079-4085.

· Gupta, V. K., Gupta, M., Sharma, S., Process development for the removal of lead and chromium from aqueous solutions using red mud- an aluminium industry waste. Water Res. 35 (2001) 1125-1134.

· Hamadi, N.K., Swaminathan, S., Chen, X.D., Adsorption of Paraquat dichloride from aqueous solutions by activated carbon derived from used tires, J. Hazard. Mater. 112 (2004) 133-141.

· Harrison, R.M., Pollution, causes, effects and control, 3rd edition (1996), The Royal Society of Chemistry, Cambridge. UK.

· Hayashi, J., Horikawa, T., Muroyama, K., Gomes, V.G., Activated carbon from chickpea husk by chemical activation with K_2CO_3: preparation and characterization. Micropor. Mesopor. Mater. 55 (2002) 63–68.

· Holan, Z.R., Volesky, B., Prasetyo, I., Biosorption of cadmium by biomass of marine algae. Biotechnol. Bioeng., 41 (1993) 819-825.

· Kapaj, S., Peterson, H., Liber, K., Bhattacharya, P., Human health effects from chronic arsenic poisoning – A review. J. Environ. Sci. Health. 41A (2006) 2399-2428.

· Kapoor, A., Viraraghavan, T., Heavy metal biosorption sites in *Aspergillus niger*. Biores. Technol. 61 (1997) 221-227.

· Kapoor, A., Viraraghavan, T., Removal of heavy metals from aqueous solutions using immobilized fungal biomass in continuous mode. Water Res., 32 (1998) 1968-1977.

· Kardivelu, K., Kanmani, P., Senthilkumar, P., Subburam, V., Separation of mercury(II) from aqueous solution by adsorption onto an activated carbon prepared *from Eichornia crassipes,* Adsorpt. Sci. Technol. 22 (2004) 207-222.

· Kirubakaran, C.J., Krishnaiah, Seshadri, S.K., 1991. Experimental study of the production of activated carbon from coconut shells in fluidized bed reactor. Ind. Eng. Chem. Res 27, 2411–2416.

· Kratochvil, D., Pimentel, P., Volesky, B., Removal of trivalent and hexavalent chromium by seaweed biosorbent, Environ. Sci. Technol. 32 (1998) 2693-2698.

· Krishnan, K.A., Anirudhan, T.S., Removal of cadmium(II) from aqueous solutions by steam-activated sulphurised carbon prepared from sugar-cane bagasse pith: kinetics and equilibrium studies, Water SA 29 (2003) 147-156.

· Ladeira, A.C.Q., Ciminelli, V.S.T, Adsorption and desorption of arsenic on an oxisol and its constituents, Water Res. 38 (2004) 2087–2094.

· Lenoble, V., Bouras, O., Deluchat, V., Serpaud, B., Bollinger, J.C., Arsenic adsorption onto pillared clays and iron oxides, J. Colloid Interface Sci. 255 (2002) 52-58.

· Lima, L., Olivares, S., Martínez, F., Torres, J., de la Rosa, D., and Sepúlveda, C., Use of immobilized tannin adsorbent for removal of Cr(VI) from water. J. Radioanal. Nucl. Chem., 231 (1998) 35-40.

· Malik, P.K., Dye removal from wastewater using activated carbon developed from sawdust: adsorption equilibrium and kinetics, J. Hazard. Mater. 113 (2004) 81-88.

· Maniatis, K., Nurmala, M., Activated carbon production from biomass. Biomass Energy Ind. Environ. 274 (1992) 1034–1308.

· Martínez, M., Miralles, N., Hidalgo, S., Fiol, N., Villaescusa, I., Poch, J., Removal of lead(II) and cadmium(II) from aqueous solutions using grape stalk waste J. Hazard. Mater. B133 (2006) 203–211.

· Matheickal, J.T., Yu, Q., Woodburn, G.M., Biosorption of cadmium from aqueous solutions by preatreated biomass of marine algae *Durvillaea potatorum*, Water Res. 33 (1999) 335-342.

· Merian, E., (editor) Metals and their compounds in the environment, occurrence, analysis and biological relevance. VCH publishers, Inc., New York, 1991.

· Mohan, D., Singh, K.P. Single and multi-component adsorption of cadmium and zinc using activated carbon derived from bagasse-an agricultural waste. Water Res. 36 (2002) 2304-2318.

· Mohan D., Pittman Jr. C.U., Activated carbons as low cost adsorbents for remediation of tri- and hexavalent chromium from water. J. Hazard. Mater. B137 (2006) 762-811.

· Mohan, D., Singh, K.P., Singh, V.K., Trivalent chromium removal from wastewater using low cost activated carbon derived from agricultural waste material and activated carbon fabric cloth, J. Hazard. Mater. 135 (2006) 280-295.

· Mondal, P., Majumder, C.B., Mohanty, B., Effects of adsorbent dose, its particle size and initial arsenic concentration on the removal of arsenic, iron and manganese from simulated ground water by Fe^{3+} impregnated activated carbon. J. Hazard. Mater. 150 (2008) 695–702.

· Namasivayam, C., Ranganathan, K., Waste Fe(III)/Cr(III) hydroxide as adsorbent for the removal of Cr(VI) from aqueous solution and chromium plating industry wastewater. Environ. Pollut. 82 (1993) 255-261.

· Namasivayam, C., Ranganathan, K., Effect of organic ligands on the removal of Pb(II), Ni(II) and Cd(II) by "waste" Fe(III)/Cr(III) hydroxide, Water Res. 32 (1998) 969-971.

· Nehrenheim, E., Gustafsson, J.P., Kinetic sorption modelling of Cu, Ni, Zn, Pb and Cr ions to pine bark and blast furnace slag by using batch experiments, Bioresource Technol. 99 (2008) 1571–1577.

· Onyancha, D., Mavura, W., Ngila, J.C., Ongoma, P., Chacha, J., Studies of chromium removal from tannery wastewaters by algae biosorbents, *Spirogyra condensata* and *Rhizoclonium hieroglyphicum,* J. Hazard. Mater. (2008) doi:10.1016/j.hazmat.2008.02.043.

· Orhan, Y. and Buyukgungor, H., The removal of heavy-metals by using agricultural wastes. Water Sci. Technol., 28 (1993) 247.

· Organización Internacional del Trabajo (OIT). Ministerio de Trabajo y Asuntos Sociales. Enciclopedia de Salud y Seguridad en el Trabajo. Capítulo 63. Metales: propiedades químicas y toxicidad. 3ª Ed. (2001).

· Ouki, S.K., Neufeld, R.D., Use of activated carbon for the recovery of chromium from industrial wastewaters, J. Chem. Technol. Biotechnol. 70 (1997) 3-8.

· Padmavathy, V., Biosorption of nickel(II) ions by baker's yeast: Kinetic, thermodynamic and desorption studies. Bioresource Technol. 99 (2008) 3100–3109.

· Pagnanelli, F., Petrangeli Papini, M., Toro, L., Trifoni, M., Vegliò, F., Biosorption of metal ions on Arthrobacter sp.: biomass characterization and biosorption modelling. Environ. Sci. Technol. 34 (2000) 2773-2778.

· Pal, A., Ghosh, S., Paul A.K., Biosorption of cobalt by fungi from serpentine soil of Andaman, Bioresource Technol. 97 (2006) 1253–1258.

· Pandey, K., Pandey, SD., Misra, V., Removal of toxic metals from leachates from hazardous solid wastes and reduction of toxicity to Microtox by the use of calcium alginate beads containing humic acid. Ecotoxicol. Environ. Saf. 52 (2002) 92-96.

· Philip, L., Iyengar, L., Venkobachar, C., Biosorption of copper(II) by *Pseudomonas aeruginosa*, Int. J. Environ. Pollut. 5 (1995) 92-99.

· Raven, K.P., Jain, A., Loeppert, R.H., Arsenite and arsenate adsorption on ferrihydrite: kinetics, equilibrium and adsorption envelopes, Environ. Sci. Technol. 32 (1998) 344-349.

· Schiewer, S., Patil, S.B., Modeling the effect of pH on biosorption of heavy metals by citrus peels, J. Hazard. Mater. 157 (2008) 8–17

· Schiewer, S., Volesky, B., Ionic strength and electrostatic effects in biosorption of divalent metal ions and protons. Environ. Sci. Technol. 31 (1997) 2478-2485.

· Schiewer, S., Volesky, B., Modeling multi-metal ion exchange in biosorption. Environ. Sci. Technol. 30 (1996) 2921-2927.

· Seco, A., Gabaldón, C., Marzal, P., Aucejo, A., Effect of pH, cation concentration and sorbent concentration on cadmium and copper removal by a granular activated carbon, J. Chem. Technol. Biotechnol. 74 (1999) 911-918.

· Seki, AS., Kashiky, I., Adsorption of lead ions on immobilized humic acid. J. Colloid. Interf. Sci. 134 (1990) 59-65.

· Selomuya, C., Meeyo, V.I., Amal, R. (1999). Mechanismes of Cr(VI) removal from water by variuos types of activated carbons. J. Chem. Technol. Biotechnol. 74 (1999) 111-122.

· Shao, W., Li, X., Cao, Q., Luo, F., Li, J., Du, Y., Adsorption of arsenate and arsenite anions from aqueous medium by using metal(III)-loaded amberlite resins. Hydrometallurgy 91 (2008) 138-143.

· Stanley, L.C., Ogden, K.L., Biosorption of copper (II) from chemical mechanical planarization wastewaters. J. Environ. Manage. 69 (2003) 289–297.

· Suzuki, R.M., Andrade, A.D., Sousa, J.C., Rollemberg, M.C., Preparation and characterization of activated carbon from rice bran. Bioresource Technol. 98 (2007) 1985–1991

· Taty-Costodes, V.C., Fauduet, H., Porte, C., Delacroix, A., Removal of Cd(II) and Pb(II) ions, from aqueous solutions, by adsorption onto sawdust of *Pinus sylvestris*. J. Hazard. Mater. B121 (2003) 121-142.

· Tchobanoglous G., Burton F.L., Stensel H.D., Wastewater engineering: treatment and reuse/ Metcalf & Eddy, Inc. 4th Edition (2003). Mc. Graw Hill. Boston.

· Torres, E., Mata, Y.N., Blázquez, M.L., Muñoz, J.A., González, F., Ballester, A., Gold and silver uptake and nanoprecipitation on calcium alginate beads, Langmuir. 21 (2005) 7951-7958.

· Tsezos, M., Georgousis, Z., Remoundaki, E., Ionic competition effects in a continuous uranium biosorptive recovery process, J. Chem. Technol. Biotechnol. 70 (1998) 198-206.

· Utomo, H.D. and Hunter, K.A., Adsorption of heavy metals by exhausted coffee grounds as a potential treatment method for waste waters, J. Surf. Sci. Nanotech. 4 (2006) 504-506-

· Veglió, F., Beolchini, F., Gasbarro, A., Lora, S., Corain, B. and Toro, L., Polyhydroxoethilmethacrylate- trimethylolpropanetrimethacrilate as a support for metal biosorption with *Arthrobacter sp.* 44 (1997) 317-320.

· Vieira, R., Volesky, B., Biosorption: a solution to pollution? Int. Microbiol. 3 (2000)17-24.

· Vilar, V.J.P., Botelho, C.M.S., Loureiro J.M., Boaventura, R.A.R., Biosorption of copper by marine algae Gelidium and algal composite material in a packed bed column Biores. Technol. 99 (2008) 5830–5838

· Villaescusa, I., Fiol, N., Martínez, M., Miralles, N., Poch, J., Serarols, J., Removal of copper and nickel ions from aqueous solutions by grape stalks wastes, Water Res. 38 (2004) 992–1002

· Villaescusa, I., Martínez, M., Miralles, N., Heavy metal uptake from aqueous solution by cork and yohimbe bark wastes. J. Chem. Technol. Biotechnol. 75 (2000) 1-5.

· Volesky B., Biosorption and biosorbents. In: Volesky B, editor. Biosorption of heavy metals. Florida: CRC press; 1990.

· Volesky, B., Biosorption and me, Water Res. 41 (2007) 4017-4029.

· Volesky, B., May-Phillips, HA., Biosorption of heavy metals by *Saccharomyces cerevisiae*. Biotechnol. Bioeng. 41 (1995) 826-829.

· Volesky B., Sorption and biosorption, (2003) BV Sorbex Inc. St Lambert – Montreal, Quebec. Canada.

· Yuan-Shen L., Cheng-chung L., and Chyow-san C., Adsorption of Cr (III) from wastewater by wine processing waste sludge, J. Colloid. Interf. Sci. 273 (2004) 95-101.

· Wang, J., Chen, C., Biosorption of heavy metals by *Saccharomyces cerevisiae*: A review, Biotechnol. Adv. 24 (2006) 427-451.

· Wase J., Forster C., Biosorbents for metal ions (1997). Taylor & Francis, London, UK.

· Wingenfelder, U., Bernd Nowack, B., Gerhard Furrer, G., Rainer Schulin, R., Adsorption of Pb and Cd by amine-modified zeolite, Water Res. 39 (2005) 3287–3297.

· Wong, P.K., Kwok, S.C., Accumulation of nickel ion (Ni 2+) by immobilized cells of *Enterobacter* species. Biotechnol. Lett., 14 (1992) 629-634.

· Zouboulis, A.I., Kydros, K.A., Use of red mud for toxic metal removal: The case of nickel, J. Chem. Technol. Biotechnol. 58 (1993) 95-101.

Chapter 1. Cr(III) AND Cr(VI) SORPTION ONTO GRAPE STALK ENTRAPPED IN CALCIUM ALGINATE

1. INTRODUCTION

Chromium occurs in wastewaters in both trivalent and hexavalent forms as a result of its use in many industries such as electroplating, mining, leather tanning, paints and pigments, fungicides, wood preservatives, etc. The metal occurs in 2+, 3+ and 6+ oxidation states but Cr^{2+} is unstable and very little is known about its hydrolysis. Cr(III) in solution produces mononuclear species such as $CrOH^{2+}$, $Cr(OH)_2^{+}$, $Cr(OH)_4^{-}$, polinuclear species as $Cr_3(OH)_4^{5+}$ and neutral species, $Cr(OH)_3$. Cr(VI) hydrolysis produces only neutral (H_2CrO_4) and anionic species, predominantely CrO_4^{2-}, $HCrO_4^{-}$ and $Cr_2O_7^{2-}$ (Mohan and Pittman, 2006).

Due to its great oxidant activity, Cr(VI) compounds are considered as human carcinogen and mutagenic agents. On the other hand, Cr(III) is an essential bioelement for humans and it seems to take place in lipids and carbohydrates metabolism, despite at high concentrations this chromium oxidation state is toxic as well, specially for plants and fungi. Because of the particular great toxicity of Cr(VI), a large number of biosorption studies have been devoted to its removal from wastewater (Mohan and Pittman, 2006; Onyancha *et al*., 2008; Fiol *et al*., 2004; Sari and Tuzen, 2008;) while studies on Cr(III) are scarce (Gürü *et al*., 2008; Lazaridis and Charalambous, 2005; Mohan *et al*., 2006; Wu *et al*., 2008). In spite of not being particularly toxic, the release of great amounts of Cr(III) as effluents in natural waters or the disposal of sludge in soils must be also of a special concern, as the potential oxidation to its hexavalent form represents a potential source of toxicity. Therefore, most of the processes to remove chromium from wastewater should ensure the removal of both, Cr(VI) and Cr(III). Currently, one of the most employed method to remove hexavalent chromium from aqueous solutions involves, in a first step, its reduction to the trivalent form by addition of reducing agents (as metabisulfite or Fe(II) salts) followed by precipitation of the formed Cr(III) as $Cr(OH)_3$ by basification of the media to a pH≈9. After this process, flocculating agents are added and solids are removed by filtration. The addition of these reagents to the wastewater involves an increase of economical cost of the process and a sludge generation, whose management uses to be also expensive, as it has to be considered as a toxic waste. Removal of chromium directly on its hexavalent form, without the reduction step, could involve an important reduction of the economical cost of the detoxification process. So that, sorption onto raw materials appears

as a potential low-cost technology for the removal of these toxic species. Many times, the raw material shows low mechanical properties that make difficult its application in sorption systems, particularly in fixed bed operations. A methodology that had been successfully applied for the improvement of hydrodinamical and mechanical properties of sorbents is based on the entrapment of these materials in a biopolymeric gel matrix of calcium alginate. In this context, the removal of trivalent and hexavalent chromium has been studied by using composite alginate-goethite beads (Lazaridis and Charalambous, 2005) and humic acids encapsulated in calcium alginate beads (Pandey, 2003). This procedure may facilitate the application of the sorbents in industrial continuous operations.

Alginates, exopolymers extracted mainly from brown seaweeds, are salts of unbranched copolymers with 1-4 links, of β-D-mannuronic and α-L-guluronic acids (Usov, 1999) and they are well known for their ability to form gels with divalent cations such as Ca^{2+}. While alginate salts with monovalent cations are generally soluble in water, in presence of many divalent cations the linear alginate chains are crosslinked and water insoluble gel is formed (Fang *et al.*, 2007). Those gels are commonly used in the food industry as matrices for colorants, flavours or for fruit or vegetable reconstitution. A further application is the immobilization of spores, cells or bacteria as bioindicators for evaluation of the efficiency of sterilization processes (Hanlon and Hodges, 1993). Calcium alginate is one of the most widely used carriers for the immobilization of several materials as enzymes, proteins and microorganisms as well as an efficient sorbent for metal cations due to its Ca^{2+} exchange capacity (Bai and Abraham, 2003; Sahin *et al.*, 2005; Chang and Huang, 1998). Calcium alginate beads are easy and rapidly formed when dropping a sodium alginate solution into a calcium chloride one due to the crosslinking of the alginate chains by the presence of multivalent cations. Recently, Cr(VI) uptake by grape stalk encapsulated in calcium alginate beads has been studied (Fiol *et al*., 2005). In the above mentioned study, the entrapment of grape stalk in calcium alginate beads was proved to enhance Cr(VI) sorption yield and to provide the sorbent with an appropriate shape and a greater mechanical strength for its possible use in continuous sorption processes, but no information about Cr(III) sorption by this novel sorbent had been obtained. In this first chapter, the potential activity of grape stalk entrapped in a calcium alginate gel matrix as a sorbent for Cr(VI) and Cr(III) in the same experimental conditions will be evaluated.

2. OBJECTIVES

The objective of the present work is to investigate the ability of grape stalk encapsulated into calcium alginate beads to adsorb Cr(III) and Cr(VI) so as to fulfil with an unique process the objective of the removal of both trivalent and hexavalent chromium.

For this purpose, Cr(VI) and Cr(III) sorption studies were carried out in the same experimental conditions in order to compare sorption performance of the sorbent for both chromium forms. Results will be compared to these obtained with pure calcium alginate beads to understand the mechanisms that govern chromium uptake.

In order to determine the potential rate controlling steps such as mass transport and chemical reaction processes, kinetic data will be treated by using two different kinetic models, the pseudo-first order and the pseudo-second order equation. Rate parameters will be determined and the effectiveness of each model to describe the sorption process will be assessed.

Release of calcium ions while sorbing trivalent chromium will be also investigated in order to know if an ion exchange mechanism describes Cr(III) sorption onto the sorbents.

Cr(VI) to Cr(III) reduction will be also investigated in both, liquid and solid phase.

Micro- and spectroscopic analysis on the solid phase of the sorbent will be also carried out in order to obtain information about the chemistry of the interaction between Cr(VI) and Cr(III) ions and the sorbent materials; the calcium alginate gel matrix and the grape stalk surface.

3. MATERIALS AND METHODS

3.1. Reagents

To prepare trivalent and hexavalent chromium solutions:

- $K_2Cr_2O_7$ 99% Panreac
- $Cr(NO_3)_3 \cdot 3H_2O$ 98% min. Panreac
- Milli-Q water

To prepare the calcium alginate and calcium alginate containing 2% (w/v) of grape stalk:

- Brown algae sodium alginate Fluka
- $CaCl_2 \cdot 2H_2O$ 99-105% Panreac
- Powdered grape stalk (< 500 μm) coming from a wine producer from Castilla La Mancha region

For pH adjustment:

- HCl (37%) Panreac
- NaOH in pellets Panreac

Standard solutions for Flame Atomic/Emission Spectroscopy:

- $Cr(NO)_3 \cdot 9H_2O$ in HNO_3 0.5 N (1000 $mg \cdot L^{-1}$) Panreac
- $Ca(NO_3)_2 \cdot 4H_2O$ in HNO_3 0.5 N (1000 $mg \cdot L^{-1}$) Panreac

For Cr(VI) analysis by the colorimetric method of diphenylcarbazide:

- 1,5-Diphenylcarbazide Aldrich
- Ethanol 96% v/v Panreac
- Sulphuric acid 96% Panreac

3.2. Material

General laboratory material
25 mL capacity glass tubs with cap
Cellulose filters
Oven (P Selecta)
Rotary shaker (Stuart Stientific)
Peristaltic pump (Gilson Minipuls 3)
Peristaltic pump tubes Tygon R-3603
Chronometers (Berlabo, SA)
Vortex (Velp Scientifica $2x^3$)
pHmeter (Crison pH – meter Basic 20)
Analytical balance (Cobos precision, J. Touron, SA)
Coffee grinder (Taurus MS 50)
Sieves (Sulab, S.A.)

3.3. Equipment

· Flame Atomic Absorption/Emission Spectrophotometer Varian SpectrAA 220FS with automatic dilutor Varian SIPS and autosampler Varian SPS3.
· Flame Emission Photometer Sherwood Scientific A410
· UV-Vis Absorption Spectrophotometer Cecil CE2021
· Electron Microscope Zeiss DSM 960 A, with Energy Dispersive X-Ray analyser Link Isis Pentafet (Oxford). For the treatment of the electronic images, Quartz PCI and Picture Gear software was used.
· Fourier transform infrared spectrometer Mattson Satellite, with MKII golden gate reflection ATR system.

4. METHODOLOGY

4.1. Grape stalk preparation

Grape stalk wastes generated in a wine manufacturer from Castilla La Mancha region was washed three times with distilled water and dried in an oven at 80 ºC until constant weight. Afterwards, it was cut in small pieces, grinded and sieved to obtain a powder (< 500 μm particle size).

4.2. Calcium Alginate (CA) and Calcium Alginate containing a 2% (w/v) of Grape Stalk (2% GS-CA) gel beads preparation.

Calcium Alginate containing 2% (w/v) of Grape Stalk were prepared. A 2% (w/v) proportion was chosen because it had been found as optimal in previous studies (Fiol *et al.*, 2004). For this purpose, a 1% (w/v) sodium alginate solution was prepared by solving 0.5 g of this compound in 50 mL of MilliQ water. Once alginate was dissolved, 1 g of grape stalk powder (<500 μm) was added, keeping an intense agitation in order to produce the suspension of the powder in the dense solution of alginate.

The solution obtained so was added dropwise to 200 mL solution of calcium chloride 0.1 M in Ca^{2+}. At the end of the tube, a yellow type micropipette tip was fixed. Calcium alginate beads (CA) where also prepared according to the same procedure as described, but without addition of grape stalk to the sodium alginate solution. Those beads where used as a blank for comparative sake.

The gel beads preparation scheme is summarized in the next figure:

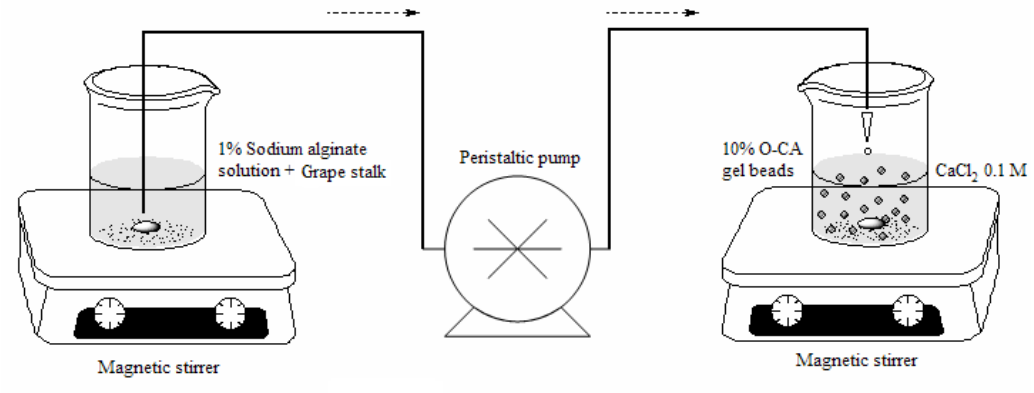

Figure 1: Sorbent preparation scheme (Fiol *et al.*, 2004).

While CA solution or 2% GS-CA suspension was added, the calcium chloride solution was kept in soft agitation. The control of the agitation speed is important in order to avoid the deviation from the sphericity of the alginate drops when contact with a solution in movement. Another important consideration that has to be taken into account is that the micropipette tip that dispenses the alginate solution has not to be very far away from the surface of the calcium solution, because the beads could lose sphericity if they fall from an excessive height. An optimal distance tip-$CaCl_2$ solution surface was found in around 10 mm.

Rotation speed of the peristaltic pump was fixed to 7.65 rpm. By doing this, a continuous flow of around 75 drops per minute, who gave spheres with uniform shape and with GS homogeneously distributed in the internal volume of the spheres, was obtained.

After addition of the alginate solution, the beads were allowed to harden in the calcium chloride solution for 24 hours. After this period, 3 washings with 300 mL of MilliQ water each time were carried out to remove the Ca^{2+} ions that don't form part of the hydrogel. After this, the obtained beads were covered with abundant MilliQ water and stored in the fridge at around 4 ºC.

To carry on the Cr(III) and Cr(VI) sorption assays, the sorbent units with non-spherical shape were discarded.

4.3. General Cr(III) and Cr(VI) sorption procedure

Experiments were carried out in batch mode, using stoppered glass tubes. For these purpose, 40 beads of either CA or 2% GS-CA were added to 15 mL of metal solution. Agitation was carried out in a rotary shaker. After agitation, gel beads were separated from the metal solution by filtration onto cellulose paper and metal concentration in the liquid phase was analysed.

4.4. Initial pH effect on Cr(III) and Cr(VI) sorption

Before beginning with kinetics and equilibrium experiments, initial pH effect on Cr(III) and Cr(VI) sorption onto CA or 2% GS-CA gel beads was studied.

pH variation after contact of the sorbents with the metal solutions was followed in order to obtain information of the H^+ role in Cr(III) and Cr(VI) sorption.
For these experiments, initial pH range studied was from 1 to 6 and initial metal concentration was around 15 $mg \cdot L^{-1}$. Contact time was fixed at 48 hours.

4.5. Sorption kinetics study

Sorption kinetics was studied for three different initial concentrations of Cr(III) (48.85, 93.95, 204.77 $mg \cdot L^{-1}$) and Cr(VI) (45.70, 93.21, 207.86 $mg \cdot L^{-1}$). Metal solutions were prepared in HCl 10^{-3} M to get a pH around 3, found as optimal for Cr(III) and Cr(VI) sorption (section 5.1).
For each contact time, stirring was briefly interrupted and a tube was removed. The content of the tube was filtered and chromium concentration in solution was analysed. The studied time range was varied in the range 0-2880 minutes.

4.6. Sorption equilibrium study

Sorption experiments for different initial metal concentration in the range 27.5 to 3107.6 in the case of Cr(III) and 26.2 to 1259.4 $mg \cdot L^{-1}$ for Cr(VI) were carried out. Despite the contact time to reach equilibrium from the kinetic experiments was estimated in around 2000 minutes, experiments were carried out for a contact time of 2880 minutes, to ensure that the system reaches equilibrium until at low initial metal concentrations. After this contact time, agitation was interrupted, solution was filtered and metal analysis in the liquid phase was carried out.
The metal concentration in the solid, q_e ($mg \cdot bead^{-1}$) was calculated from the difference between the initial, C_i and equilibrium, C_e metal concentration in solution ($mg \cdot L^{-1}$). The uptake of the sorbent was calculated according to the next equation:

$$q_e = (C_i - C_e)\frac{V}{N} \qquad (1)$$

where V (L) is the solution volume and N is the amount of gel beads.

4.7. Cr(VI) to Cr(III) reduction study

Previous studies have shown that grape stalk is able to reduce hexavalent to trivalent chromium in some extension (Fiol *et al.*, 2007). This reduction process takes place when several materials with lignocellulosic basis are used as sorbents and it has been reported previously by several authors (Dupont and Guillon, 2003; Daneshvar *et al.*, 2002; Mel Lytle *et al.*, 1998).

According to these previously reported data, in the filtrates obtained in the kinetics study of Cr(VI) removal, total and hexavalent chromium concentration were measured and Cr(III) concentration was calculated by difference.

4.7.1. Cr(VI) determination in solution

Cr(VI) determination in solution was carried out by the colorimetric method of the 1,5-diphenylcarbazide, adapted from Standard Methods book. The procedure of reagent preparation and of operation was as follows.

First place, the next solutions are prepared:

1. 0.4 g of 1,5-diphenylcarbazide in 200 mL ethanol 96 %
2. 80 mL sulphuric acid (96%) in 720 mL of Milli-Q water

After sulphuric acid addition on water, an important increase on the temperature of the solution takes place. As 1,5-diphenylcarbazide can suffer degradative reactions as such a high temperature, the acidic solution has to be allowed to get cold. Once the sulphuric solution has reached room temperature, the ethanolic solution containing the diphenylcarbazide is added and the mixture is strongly shaken. The solution obtained so is transferred to a topace colour bottle and stored in the fridge.

Standards Cr(VI) solutions in the range from 0.25 to 1.5 $mg \cdot L^{-1}$ are prepared from anhydrous $K_2Cr_2O_7$. The calibration curve is obtained by adding 1 mL of diphenylcarbazide solution to 20 mL of each one of the different Cr(VI) standards and waiting 30 minutes to ensure the fully development of the colour. After this reaction time, absorbance of the solutions at 540 nm is measured. In the case of samples, the same procedure is carried out, taking into account that dilution to the range 0.25-1.5 $mg \cdot L^{-1}$ of Cr(VI) is necessary if samples have concentrations higher than the top value of this range.

4.7.2. Cr(III) determination in solution

In order to check if either CA or 2% GS-CA can reduce Cr(VI) to Cr(III), the presence of Cr(III) in the filtrates obtained in the kinetic experiments of Cr(VI) sorption was analysed. Trivalent chromium concentration in solution was quantified by means of the difference in between total chromium concentration (obtained by FAAS) and hexavalent chromium concentration (obtained by the colorimetric method of 1,5-diphenylcarbazide).

4.8. Spectroscopic analysis of the material

Different spectroscopic and microscopic analysis on the solid sorbent phase were carried out to obtain information about Cr(III) and Cr(VI) sorption mechanism onto 2% GS-CA. Scanning electron microscopy with energy-dispersive X-ray analysis (SEM-EDX) was used to detect the location of accumulated chromium in the sorbents. Chromium loaded samples were prepared by contacting the sorbents for 48 hours with either Cr(III) or Cr(VI) solutions containing an initial concentration of 800 $mg \cdot L^{-1}$. Samples were then rinsed in deionized water and dried at 50 ºC for 24 hours. Materials were mounted in a stub, carbon-coated and analyzed.

FTIR-ATR and RPE measurements were carried out directly on the chromium-loaded material according to the protocol described before.

5. RESULTS AND DISCUSSION

5.1. Initial pH effect in Cr(III) and Cr(VI) sorption

Cr(III) and Cr(VI) sorption results onto spheres of either CA or 2% GS-CA are presented in **Figures 2** and **3**. In these graphics it has been plotted the percentage of sorption as a function of the initial pH of the metal solution. In the case of Cr(VI) solutions, the percentage of chromium removed is expressed as total chromium.

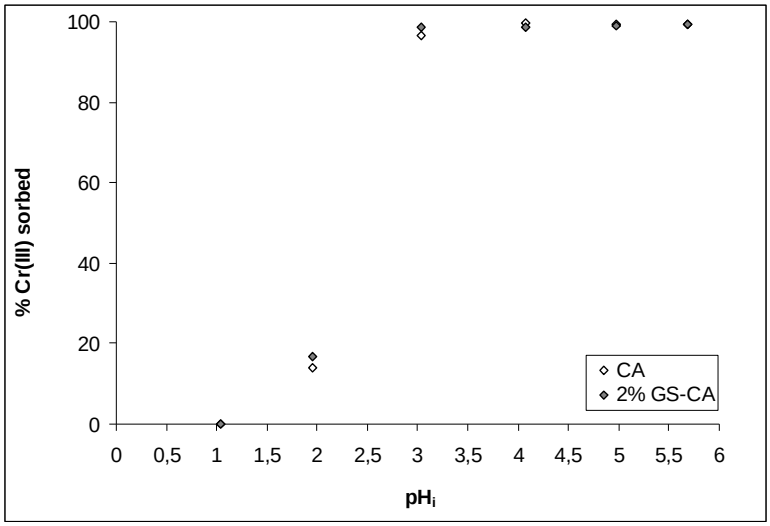

Figure 2: Cr(III) removal percentage by CA and 2% GS-CA gel beads as a function of initial solution pH. $[Cr(III)]_0$ = 15.0 mg·L^{-1}, 40 beads, V_{sol} = 15 mL, agitation time = 72 h.

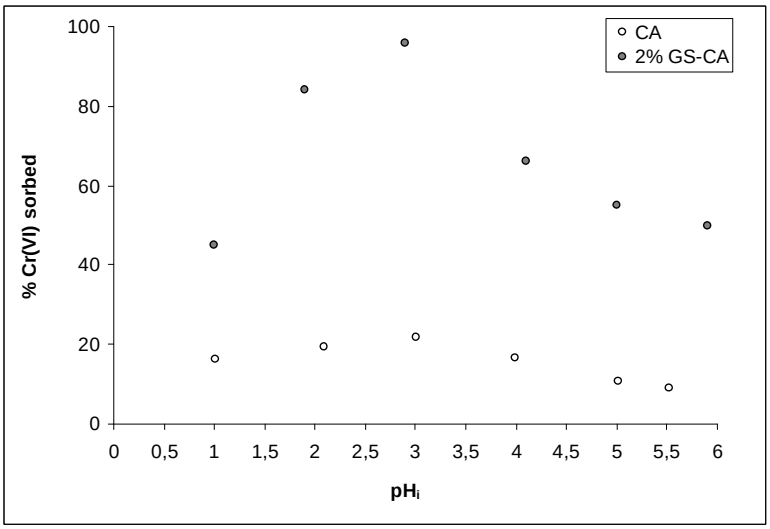

Figure 3: Cr(VI) removal percentage by CA and 2% GS-CA gel beads as a function of initial solution pH. $[Cr(VI)]_0$ = 15.0 mg·L^{-1}, 40 beads, V_{sol} = 15 mL, agitation time = 72 h.

As it can be seen in **Figure 2**, Cr(III) sorption is almost negligible (< 20%) for initial pHs 1 and 2, and is at pHs higher than 4 when total removal is achieved, for an initial concentration of 15 $mg \cdot L^{-1}$. Sorption results for both types of beads are very similar, therefore almost no influence of grape stalk is observed in Cr(III) sorption.

In the case of Cr(VI) (**Figure 3**), it was observed an increase on chromium removal percentage when increasing initial pH, until a maximum is reached for both types of sorbents at around pH 3. A very important difference in Cr(VI) sorption percentage was observed when comparing both sorbents; while beads containing GS are able to remove 100% of the initial Cr(VI) present in a 15 $mg \cdot L^{-1}$ solution at pH 3, these of pure CA were not able to remove more than 20 % of the initial chromium amount. This fact seems to indicate that GS plays a very important role in Cr(VI) uptake.

If Cr(III) and Cr(VI) sorption results are compared, it can be observed that removal percentage as a function of initial solution pH tendency is clearly different. While at low pHs (less than 2.5) there's almost no Cr(III) sorption neither in CA nor in 2% GS-CA gel beads, Cr(VI) at pHs around 2 is uptaken with high efficiency (around 80% removed). These data seem to indicate that high proton concentration in solution exerts a higher inhibition influence on Cr(III) sorption than on Cr(VI). In order to properly discuss these results, it becomes necessary to know about the hydrochemical speciation as a function of pH of both, Cr(III) and Cr(VI), in the experimental conditions of the study.

Speciation diagrams were simulated by means of MEDUSA computer program (Puigdomènech, 2004) and are presented in **Figures 4** and **5**. The hydrochemical constants presented in the MEDUSA database have been uncritically employed.

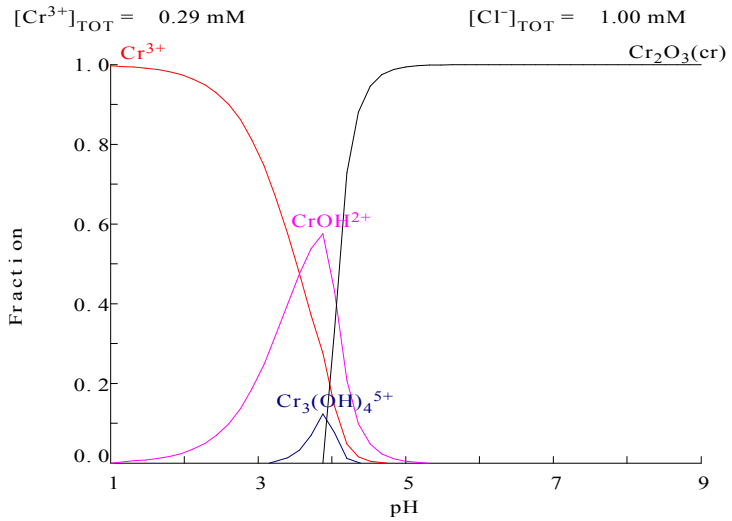

Figure 4: Cr(III) speciation diagram as a function of pH. [Cr(III)]=15.0 mg·L^{-1}; [Cl$^-$]= 0.001 M.

From the speciation diagram, several important facts can be concluded. First place, it can be observed that Cr(III) speciation is strongly dependent on solution pH. While at pH 2 almost all the Cr(III) is present on its free form, Cr^{3+}, this species concentration decreases dramatically when pH of solution increases. At pH 3, species distribution is approximately 70% Cr^{3+} and 30% $CrOH^{2+}$.

In the next figure, the Cr(VI) speciation diagram is shown:

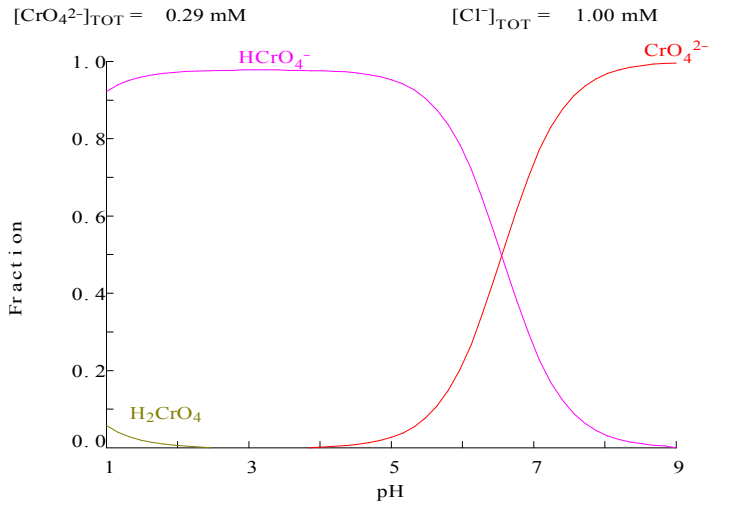

Figure 5: Cr(VI) speciation diagram as a function of pH. [Cr(VI)]=15.0 mg·L^{-1}; [Cl$^-$]= 0.001 M.

As it can be seen in the species distribution diagram of Cr(VI), this oxidation state would be in solution, independently of pH, as an anion. In the interval from 3 to 5 pH units, the anion $HCrO_4^-$ would represent almost 100% of the species, and it's only at pHs higher than 5 when CrO_4^{-2} appears in a significant concentration.

According to the speciation diagrams, it can be concluded that, in the experimental conditions of this study, Cr(III) is found as a cation, while Cr(VI) is in anionic form. In the bibliography it has been reported that solution pH is a very important parameter for cationic and anionic sorption. While in the first case, pHs higher than 4.5 are required, in the case of anions, the maximum capacity is obtained for a pH range within 1.5 to 4 (Volesky, 2003). Results obtained in this work are in agreement with this previously reported information.

The low Cr(III) sorption observed at acidic pH, can be due to the high H^+ concentration in the media, that fully protonates the active sites of the material, of basic nature. According to this, a competition for the active sites of the material takes place between protons and cationic Cr(III) species.

In order to ascertain the role of H^+, final pHs obtained after contact of the sorbents with different HCl initial concentrations (blanks) and for the Cr(III) and Cr(VI) solutions at different initial pHs have been presented in **Table 3**.

Table 3: Initial and final pH for Cr(III) and Cr(VI) solutions alter contact with CA and 2% GS-CA gel beads. $[Metal]_0$=15 mg·L^{-1}, 40 beads, V_{sol}=15 mL, agitation time=72 h.

	Blank		**Cr(III)**		**Cr(VI)**	
	CA	**2% GS-CA**	**CA**	**2% GS-CA**	**CA**	**2% GS-CA**
pH_i	**pH_f**	**pH_f**	**pH_f**	**pH_f**	**pH_f**	**pH_f**
1.04	1.06	1.07	1.06	1.20	1.18	1.32
1.99	2.19	2.24	2.11	2.15	2.16	2.82
3.03	4.66	6.18	3.66	3.90	4.70	6.63
3.99	6.36	6.46	5.55	5.84	5.60	7.10
4.99	6.61	6.71	6.55	6.30	5.82	7.01
5.61	6.67	6.66	6.27	6.50	5.90	7.01

As it can be seen in the table, final pH of blank solutions is always higher than pH of these containing Cr(III), indicating thus, that Cr(III) cationic species (Cr^{3+} and $CrOH^{2+}$) block coordinative positions that, in absence of metal, would be coordinated to H^{+}. Additionally, it was observed that final solution pH was always higher in the case of beads containing GS, indicating that this material had to contain additional basic groups.

In the case of Cr(VI), as presented in **Figure 3**, the maximum adsorption takes place for an initial pH around 3. This results are in agreement with those reported by several authors, when studying Cr(VI) sorption onto different materials as green algae *Spirogyra* (Gupta *et al*., 2001), *Avena monida* (Gardea-Torresdey *et al*., 2000), grape stalk (Fiol *et al*., 2003), cork (Fiol *et al*., 2003), yohimbe bark (Fiol *et al*., 2003) and tannins (Nakano *et al.*, 2001). In all these studies, optimum pH values for sorption around 2-3 were reported.

In the same figure, it could be observed that there was a very big difference in the sorption behaviour of beads containing only calcium alginate and those containing grape stalk. Beads containing grape stalk are able to remove almost all the Cr(VI) present in the solution, while those formed only by calcium alginate still leave in solution a very important concentration of Cr(VI). Results seem to indicate that the main sorption of Cr(VI), as opposed to Cr(III), is due to the grape stalk.

According to these results, an initial pH of 3 was chosen to carry out further Cr(III) and Cr(VI) sorption experiments onto both types of gel beads. Despite this pH was not exactly the optimal for Cr(III) removal, it was chosen to compare sorption behaviour in the same conditions.

5.2. Cr(III) and Cr(VI) sorption kinetics onto CA and 2% GS-CA gel beads

In this section trivalent and hexavalent chromium sorption for three different initial metal concentrations and an initial pH 3 is studied. Kinetics results will be mathematically treated according to pseudo-first, pseudo-second and intraparticle diffusion model. From the fitting of these models, information related to the contribution of each one of the stages in the total sorption rate will be obtained and discussed.

5.2.1. Cr(III) sorption kinetics

In the next table, Cr(III) concentration in solution for each contact time with either CA or 2% GS-CA and for the three initial metal concentrations is presented.

Table 4: Evolution of total chromium concentration with time when contacting different initial Cr(VI) concentrations with either CA or 2% GS-CA gel beads. 40 gel beads, V_{sol}= 15 mL, pH_i=2.98.

	$[Cr(III)]_i$ (mg·L^{-1})					
	48.85 mg·L^{-1}		93.95 mg ·L^{-1}		204.77 mg·L^{-1}	
t (min)	CA	2% GS-CA	CA	2% GS-CA	CA	2% GS-CA
0	48.85	48.85	93.95	93.95	204.77	204.77
5	40.88	35.60	80.55	70.42	140.84	127.20
10	36.65	33.15	79.43	71.25	128.88	107.60
15	32.35	28.91	77.66	70.32	110.90	109.97
20	31.59	27.61	72.82	68.57	116.05	107.71
30	30.55	25.28	71.97	65.03	113.35	107.52
60	26.54	21.86	67.97	59.34	112.33	108.80
120	23.63	17.93	67.32	56.62	111.69	108.01
300	20.70	15.78	62.78	55.22	110.23	103.13
420	21.33	15.64	63.55	56.67	110.30	105.80
720	20.85	15.29	67.02	57.80	110.89	105.64
1440	19.22	14.08	60.53	52.79	104.25	101.14
1860	17.73	12.28	58.93	52.94	108.20	102.10
2880	17.14	11.08	57.89	50.81	106.73	102.42

Results presented in this table indicate that trivalent chromium concentration in solution progressively decreases until an equilibrium concentration value is reached. The equilibrium concentration in solution is higher as higher is the initial metal concentration. It has to be remarked that despite both beads lead to a similar equilibrium concentration concentration, those beads containing GS are always slightly more effective for the removal of trivalent chromium.

For and easier comparison of the evolution of metal concentration in solution as a function of time, the results presented in this table have been presented in graphic form in the next figure.

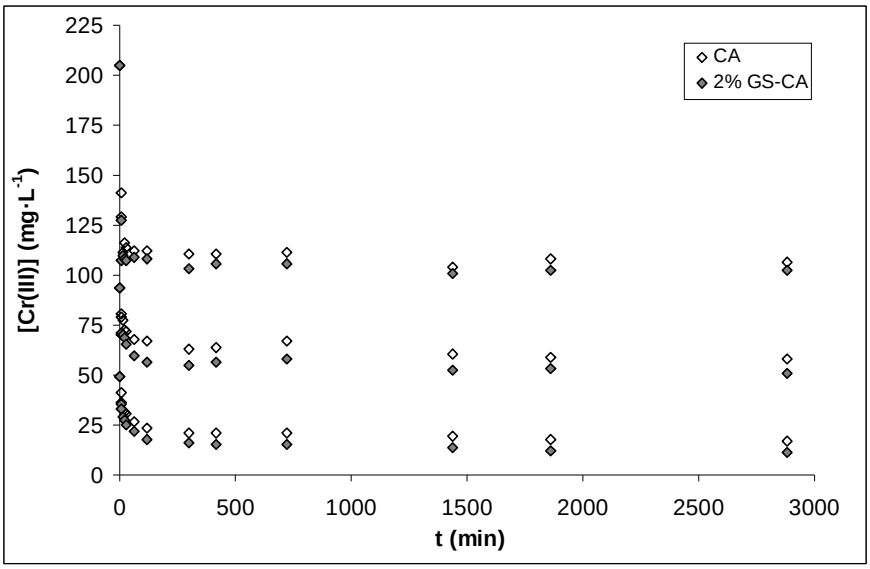

Figure 6: Cr(III) sorption kinetics for three different initial metal concentration (48.85, 93.95, 204.77 $mg \cdot L^{-1}$) on CA and 2% GS-CA gel beads.

From the data shown in **Figure 6**, it can be seen that metal sorption is fast. As an example, remark that, to reach a 50% of removal from an initial metal concentration of 48.85 $mg \cdot L^{-1}$, it is necessary a contact time of only 60 minutes for the spheres of CA while only 30 minutes in the case of 2% GS-CA would be required.

As seen in the figure, the kinetic sorption behaviour of Cr(III) is the same for beads of CA and for 2% GS-CA ones, however an additional adsorption is observed for all the contact times in the case of beads containing grape stalk. The very similar results observed seem to indicate that the main active material for Cr removal is the calcium alginate gel matrix.

5.2.2. Cr(VI) sorption kinetics

Table 5 shows the total chromium concentration in solution for each contact time with either CA or 2% GS-CA and for the three initial metal concentrations.

Table 5: Evolution of total chromium concentration with time when contacting different initial Cr(VI) concentrations with either CA or 2% GS-CA gel beads. 40 gel beads, V_{sol}= 15 mL, pH_i=2.98.

	$[Cr(VI)]_i$ (mg·L^{-1})					
	45.70 mg·L^{-1}		93.21 mg·L^{-1}		207.86 mg·L^{-1}	
t (min)	CA	2% GS-CA	CA	2% GS-CA	CA	2% GS-CA
0	45.70	45.70	93.21	93.21	207.86	207.86
5	45.21	40.46	77.57	71.11	160.48	160.59
10	43.96	39.55	74.46	69.84	158.40	150.12
15	45.72	38.65	71.35	64.42	148.45	130.35
20	46.13	36.11	72.91	65.39	153.50	135.27
30	45.82	35.34	74.66	63.63	155.02	128.27
60	45.68	31.20	72.49	56.38	154.13	123.56
120	45.89	25.35	71.88	50.27	147.15	111.96
300	44.10	17.85	72.27	41.13	143.71	10553
420	44.89	14.98	71.46	40.15	142.25	101.94
720	44.47	11.22	73.51	35.86	149.67	96.01
1440	43.88	6.48	70.63	30.33	149.10	77.32
1860	43.29	4.42	72.68	27.50	154.71	79.84
2880	41.20	3.44	71.82	24.21	147.48	71.43

The results of the present table put into evidence a decrease in chromium concentration in solution when contacting the hexavalent chromium solutions with both, CA and 2% GS-CA. From this results it is noteworthy the different sorption behaviour of beads of pure calcium alginate and these containing grape stalk; while the first seem to adsorb only a small fraction of the initial Cr(VI), these containing GS are able to produce a higher chromium content reduction in the solution.

As in the case of Cr(III), for and easier comparison, results of metal concentration in solution as a function of contact time with the sorbents are presented on its graphic form in **Figure 7(a)**.

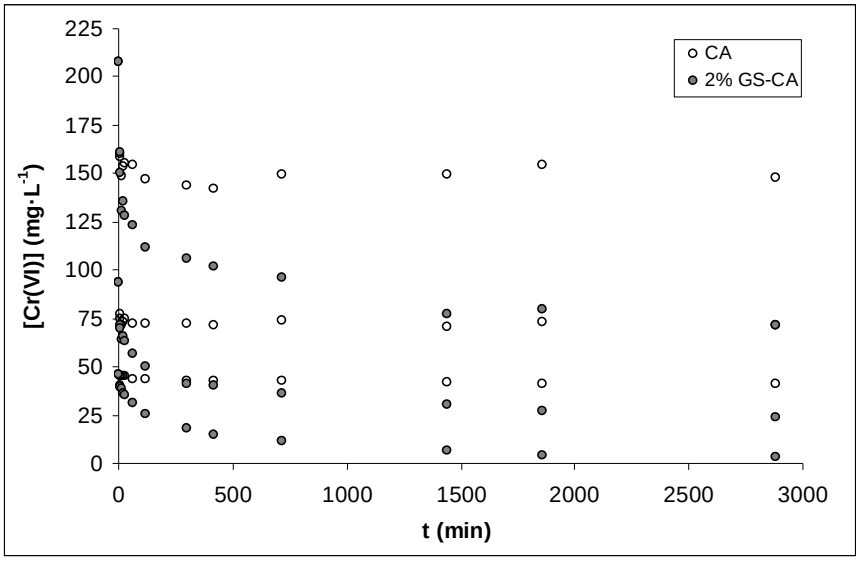

Figure 7(a): Cr(VI) sorption kinetics for three different initial metal concentration (45.70, 93.21, 207.86 $mg \cdot L^{-1}$) on CA and 2% GS-CA gel beads.

As it can be seen, despite in the first minutes of contact time there's a decrease in chromium concentration in solution, this decrease is not so pronounced as it was in the case of Cr(III) sorption. As an example, it is remarkable that, to achieve a reduction to half the initial concentration from a solution of 45.70 $mg \cdot L^{-1}$ of Cr(VI), a contact time of around 210 minutes is needed, in the case of 2% GS-CA gel beads, and in the case of beads of only CA, not even in 2880 minutes this adsorption is achieved, as observed in **Table 5**.

A very important difference in the kinetic behaviour of both gel beads was observed for Cr(VI) sorption. While CA beads adsorb a small amount of Cr(VI) and achieve equilibrium very fast, those containing grape stalk, follow a much more slow kinetics but they adsorb a higher chromium amount.

Slow kinetics, as the observed for Cr(VI) removal by 2% GS-CA could be indicative of diffusion processes as limiting of the sorption process (Ho *et al*., 2000), that's why, diffusion has to be considered as a possible rate limiting step for the sorption or Cr(VI) onto beads containing grape stalk.

These two experimental observations, the low adsorption of the gel beads of only CA compared with that containing GS, and the slow sorption kinetic of Cr(VI) sorption onto

2% GS-CA beads, suggest that the main responsible of Cr(VI) sorption would be the grape stalk powder.

Previous studies carried out in our laboratory, demonstrated that the native grape stalk, without entrapment in calcium alginate, were able to adsorb Cr(VI) (Fiol *et al.*, 2003). In these studies, it was verified that part of the Cr(VI) was reduced by the material to Cr(III), and this trivalent chromium was distributed between the solid and the liquid phase (Fiol *et al.*, 2007).

In order to know if this reductive process took place in our system, the presence of Cr(III) in solution was analysed in the kinetic series, by difference between the total Cr concentration (obtained by FAAS) and the Cr(VI) concentration (obtained according to the 1,5-diphenylcarbazide method). As an example, total chromium and Cr(VI) kinetics for an initial concentration of 207.86 $mg \cdot L^{-1}$ have been plotted together and shown in **Figure 7(b)**.

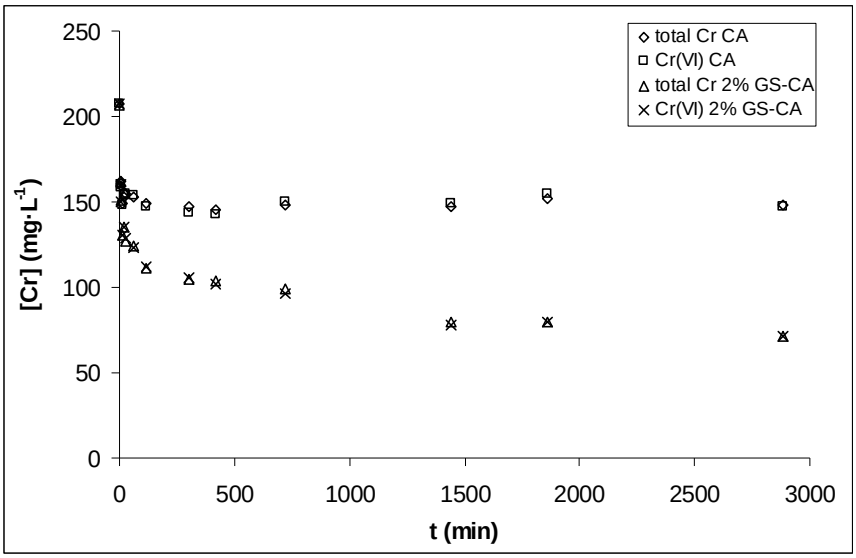

Figure 7(b): Total and Cr(VI) sorption kinetics for an initial concentration of Cr(VI) of 207.86 $mg \cdot L^{-1}$ onto CA and 2% GS-CA.

As it can be seen in this figure, for all the contact time sorbent-solution and for both types of beads, the total concentration of chromium in solution is equal to the concentration of Cr(VI), indicating this fact that there's no Cr(III) in the aqueous phase. However, its possible that the reduction reaction takes place and the Cr(III) sorbed remains adsorbed in

the solid phase of the adsorbent. The possible presence of Cr(III) in the solid phase will be investigated and discussed later by using different spectro- and microscopic techniques.

5.2.3. Comparison between Cr(III) and Cr(VI) sorption onto CA and 2% GS-CA

In order to compare the amount of metal adsorbed for each oxidation state on either CA and 2% GS-CA, the percentage of metal adsorbed at equilibrium time on both types of sorbents has been calculated for the different initial metal concentrations. The obtained results are shown in the next table:

Table 6: Cr(III) and Cr(VI) sorbed percentage at equilibrium time for different initial metal concentrations. pH_i=3.0.

	$[Cr(III)_0]$ ($mg \cdot L^{-1}$)			**$[Cr(VI)_0]$ ($mg \cdot L^{-1}$)**		
	48.85	**93.95**	**204.77**	**45.70**	**93.21**	**207.86**
CA	64.92 %	38.38 %	47.88 %	9.84 %	22.95 %	29.05 %
2% GS-CA	77.31 %	45.92 %	49.98 %	92.45 %	74.03 %	65.64 %

As can be seen in **Table 6**, both types of beads exhibit a similar sorption equilibrium for Cr(III), however, those containing grape stalk adsorbed a little additional amount. In the case of Cr(VI), the beads containing grape stalk show a very different behaviour than those formed by only CA. For the three initial metal concentrations studied, the beads of 2% GS-CA show always higher removal percentages than these of pure CA.

The table demonstrates that, from the four studied systems (Cr(III) and Cr(VI) sorption onto CA and 2% GS-CA beads), is Cr(VI) sorption onto 2% GS-CA the one that achieves the highest performance at equilibrium, reaching a 92.45% of removal from an initial metal concentration of 45.70 $mg \cdot L^{-1}$.

For an easier comparison between the dynamics of trivalent and hexavalent chromium removal, in the next figure, sorption kinetics onto CA and 2% GS-CA for an initial metal concentration around 45 $mg \cdot L^{-1}$ have been plotted together.

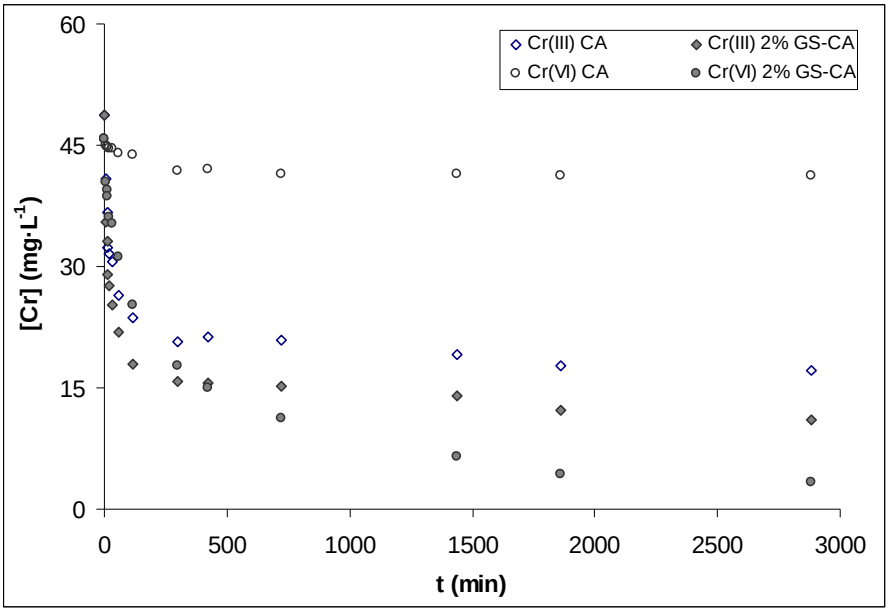

Figure 8: Cr(III) and Cr(VI) sorption kinetics onto CA and 2% GS-CA gel beads. Initial metal concentration≈45 $mg \cdot L^{-1}$.

As can be seen in this figure, while in the case of the trivalent oxidation state the sorption in both types of beads is very fast, in the case of Cr(VI) sorption onto 2% GS-CA beads, the variation of concentration in solution with contact time is not so pronounced. However, metal concentration in solution attained at equilibrium is lower in the case of Cr(VI) than in the case of Cr(III) onto 2% GS-CA. In the case of beads of only CA, Cr(VI) sorption takes place in very low extension and equilibrium is rapidly reached. These results confirm that while in Cr(III) sorption, calcium alginate is the main sorbent material, in the case of Cr(VI), conversely, grape stalk would be the main responsible.

As it had been discussed in section 5.1, protons seem to play a different role in Cr(III) than in Cr(VI) sorption. Dealing with this, in the next section, the pH variation that takes place in the kinetics series will be studied and discussed, in an attempt to go further in the understanding of the different mechanisms governing chromium sorption.

5.3. pH evolution

In **Tables 8** to **10**, results of pH evolution as a function contact time is shown for Cr(III) and Cr(VI) sorption onto CA and 2% GS-CA for the three initial metal concentrations studied. Additionally, on each of the tables, the pH variation for the blank solution in contact with CA and 2% GS-CA is also shown.

Table 8: pH evolution of Cr(III) and Cr(VI) solutions as a function of contact time with the beads of either CA and 2% GS-CA. $[Cr(III)]_0$=48.85 mg·L^{-1}, $[Cr(VI)]_0$=45.70 mg·L^{-1}, $pH_o \approx 3$.

	Blank		**Cr(III) 48.85 mg·L^{-1}**		**Cr(VI) 45.70 mg·L^{-1}**	
t (min)	**CA**	**2% GS-CA**	**CA**	**2% GS-CA**	**CA**	**2% GS-CA**
0	2.96	2.96	2.96	2.96	2.99	2.99
5	3.81	3.98	3.69	3.53	4.01	4.21
10	3.97	4.27	3.58	3.55	4.17	4.90
15	3.93	4.42	3.61	3.91	4.70	5.63
20	4.13	4.68	3.65	3.88	5.12	5.33
30	4.32	4.64	3.71	3.75	4.90	5.78
60	4.75	4.70	3.71	3.95	5.36	5.94
120	4.75	4.90	3.78	4.12	5.09	6.22
300	5.16	5.62	3.67	4.04	5.04	6.21
420	5.22	5.63	3.62	4.04	4.92	6.51
720	5.32	5.60	3.63	3.96	4.99	6.52
1440	5.60	5.94	3.66	4.01	4.97	6.54
1860	5.84	6.06	3.67	3.95	5.03	6.80
2880	5.90	6.20	3.54	3.87	4.98	7.05

Table 9: pH evolution of Cr(III) and Cr(VI) solutions as a function of contact time with the beads of either CA or 2% GS-CA. $[Cr(III)]_0$=93.95 mg·L^{-1}, $[Cr(VI)]_0$=93.21 mg·L^{-1}, pH_o≈3.

	Blank		Cr(III) 93.95 mg·L^{-1}		Cr(VI) 93.21 mg·L^{-1}	
t (min)	**CA**	**2% GS-CA**	**CA**	**2% GS-CA**	**CA**	**2% GS-CA**
0	2.96	2.96	2.95	2.95	2.97	2.97
5	3.81	3.98	3.35	3.35	4.17	4.09
10	3.97	4.27	3.37	3.39	4.53	4.57
15	3.93	4.42	3.43	3.46	5.21	5.17
20	4.13	4.68	3.34	3.48	4.42	5.11
30	4.32	4.64	3.36	3.49	4.88	5.32
60	4.75	4.70	3.38	3.48	5.09	5.43
120	4.75	4.91	3.34	3.49	5.20	5.58
300	5.16	5.62	3.39	3.55	5.08	5.86
420	5.22	5.63	3.40	3.47	5.08	5.94
720	5.32	5.60	3.41	3.41	5.05	6.02
1440	5.60	5.94	3.40	3.40	4.86	6.16
1860	5.84	6.06	3.37	3.43	4.85	6.23
2880	5.90	6.20	3.36	3.41	4.97	6.33

Table 10: pH evolution of Cr(III) and Cr(VI) solutions as a function of contact time with the beads of either CA or 2% GS-CA. $[Cr(III)]_0$=204.77 mg·L^{-1}, $[Cr(VI)]_0$=207.86 mg·L^{-1} pH_o≈3.

	Blank		Cr(III) 204.77 mg·L^{-1}		Cr(VI) 207.86 mg·L^{-1}	
t (min)	**CA**	**2% GS-CA**	**CA**	**2% GS-CA**	**CA**	**2% GS-CA**
0	2.96	2.96	2.95	2.95	2.96	2.96
5	3.81	3.98	3.28	3.02	4.46	4.09
10	3.97	4.27	3.26	3.36	4.62	4.93
15	3.93	4.42	3.35	3.39	4.89	5.11
20	4.13	4.68	3.32	3.46	4.68	5.03
30	4.32	4.64	3.27	3.43	4.65	5.17
60	4.75	4.70	3.29	3.28	4.95	5.45
120	4.75	4.90	3.27	3.30	4.92	5.47
300	5.16	5.62	3.38	3.43	4.93	5.64
420	5.22	5.63	3.37	3.32	4.84	5.78
720	5.32	5.61	3.37	3.36	5.03	5.90
1440	5.60	5.94	3.20	3.34	4.91	6.04
1860	5.84	6.06	3.19	3.36	4.61	6.16
2880	5.90	6.20	3.18	3.35	4.78	6.35

Results presented in the tables are shown in graphical form for an easier comparison of the different behaviour in front of H^+ of Cr(III) and Cr(VI) while adsorption is taking place.

In the next figure, pH variation as a function of contact time for Cr(III) and Cr(VI) solutions contacted with CA and 2% GS-CA are presented. For comparison sake, results obtained for the blanks are also shown.

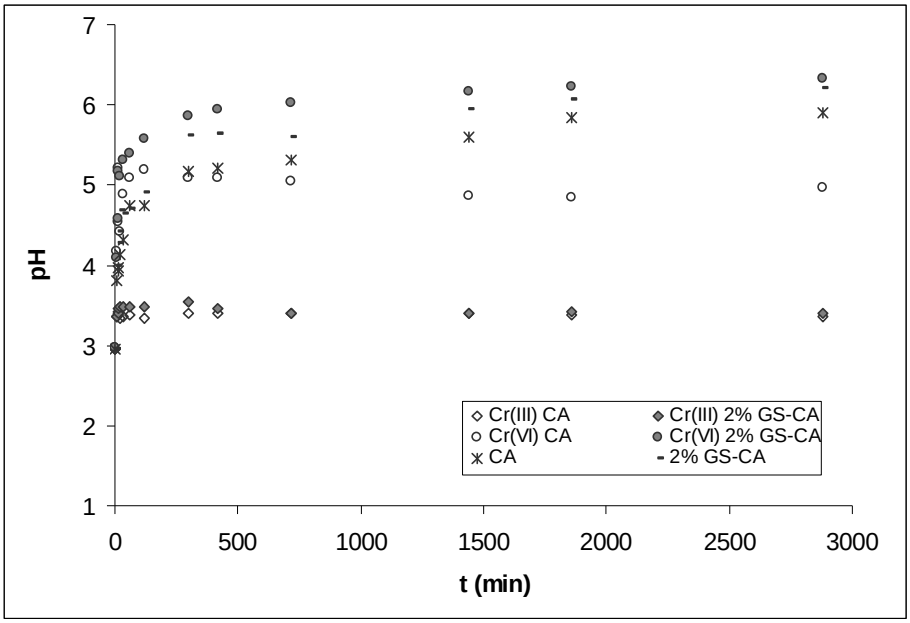

Figure 9: pH variation as a function of sorbent-solution contact time for the different Cr(III) and Cr(VI) solutions and the blank. $[Cr]_0 \approx 93.5$ mg·L^{-1}, 40 gel beads, V_{sol}=15 mL, pH_i=2.98.

As the main pH variation occurs in the beginning of the process, a magnification of the region between 0 and 140 minutes of contact time has been included (**Figure 10**).

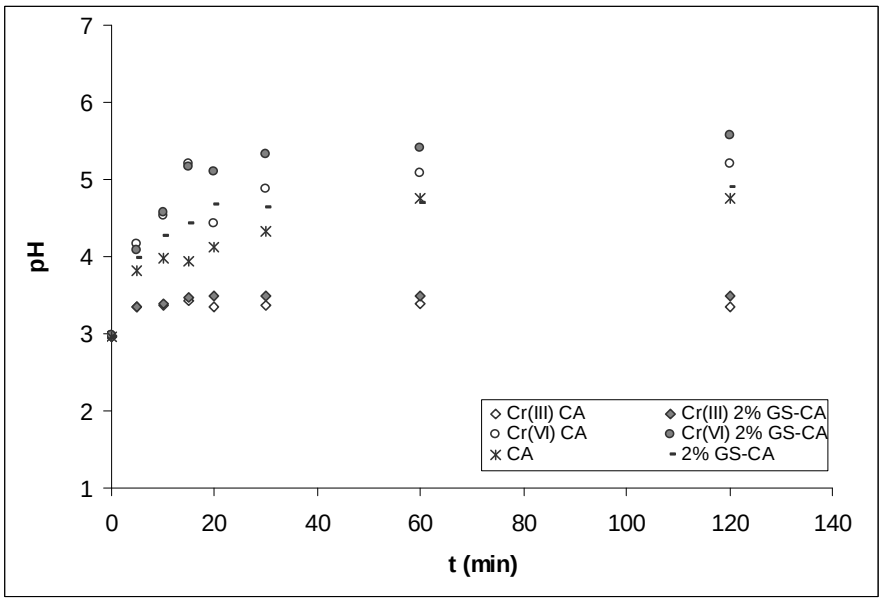

Figure 10: pH evolution as a function of contact time for the Cr(III), Cr(VI) solutions and the blank. $[Cr]_0 \approx 93.5\ mg \cdot L^{-1}$, 40 gel beads, V_{sol}=15 mL, pH_i=2.98.

As can be seen in **Figure 10**, blank solutions in contact with both kind of sorbents exhibit a rapid pH increase (from 2.98 to 3.98 in 5 minutes), reaching in the equilibrium a pH close to neutrality. The important H^+ consumption observed indicates that the sorbent has to contain an important amount of basic groups. In alginate structure, the main basicity comes from the presence of unprotonated carboxylate groups. These groups would be protonated at low pHs, while at high pHs, would be in an anionic form. These carboxylate coming from the alginate structures are the main responsible of the basification of the media, due to hydrolytic reactions as shown:

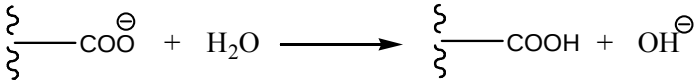

In the case of the beads containing grape stalk, the final solution pH is slightly higher than the one obtained for the calcium alginate beads. This fact is indicative of the existence of additional basic groups. According to Sharma and Forster, vegetal biomass contains oxo-groups with basic properties (represented as C_xO y C_xO_2).

These groups can provoke hydrolytic reactions according to the next equation (Sharma and Forster, 1993):

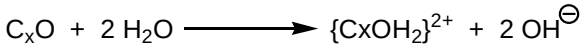

This reaction provokes the development of positive surface charge on the material and the release of OH^- and, in consequence, an increase of solution pH. Once explained the reason of the natural tendency of the sorbents to raise up the solutions pH, the differences between the pH increase when Cr(III) and Cr(VI) are present in the medium can be explored.
In the next table, the pH increase observed for the three different initial Cr(III) and Cr(VI) concentrations after contact with the adsorbents at equilibrium time is presented. Additionally, for comparative sake, pH increase for the corresponding blanks has also been included.

Table 11: pH increase for the three different initial metal concentrations at equilibrium time after contact with the CA and 2% GS-CA beads.

	ΔpH			**ΔpH**	
$[Cr(III)]_0$ ($mg \cdot L^{-1}$)	**CA**	**2% GS-CA**	**$[Cr(VI)]_0$ ($mg \cdot L^{-1}$)**	**CA**	**2% GS-CA**
48.85	0.58	0.91	45.70	1.99	4.06
93.95	0.41	0.46	93.21	2.00	3.36
204.77	0.23	0.40	207.86	1.82	3.39
Blank	2.94	3.24	**Blank**	2.94	3.24

In this table, it can be observed that the pH increase of solutions containing Cr(III) is always lower than the corresponding to the blanks. Furthermore, it can be observed that this is lower as higher is the initial Cr(III) concentration in solution. These facts are indicative of some kind of competition between H^+ and Cr(III)cationic species, so that, the coordination of the metal cations to the active sites of the sorbent, inhibits protonation in some extension. This process impedes the natural tendency of the sorbents to move solution initial pH from about 3 to a final pH close to neutrality.
Results shown in **Table 11** indicate that, when 2% GS-CA beads are contacted with solutions containing Cr(VI), an additional proton consumption respect to the corresponding blank takes place. This fact indicates that Cr(VI) sorption is related, in some extension, to a H^+ consumption that is not linked to the sorbent protonation.
Previous studies carried out in our laboratory indicated that some biomaterials with lignocellulosic base, as the grape stalk and the yohimbe bark, were able to reduce Cr(VI) to Cr(III). This reaction has associated 7 mol of H^+ consumption per mol of Cr(VI) reduced, as it can be seen in the next redox semireaction:

$$HCrO_4^- + 7\ H^+ + 3\ e^- \longrightarrow Cr(III) + 4\ H_2O$$

If Cr(VI) sorption onto 2% GS-CA gel beads involves Cr(VI) to Cr(III) reduction, the concentration of protons in the medium can be a critical limiting factor. In order to check whether H^+ acts as a limiting reagent of Cr(VI) sorption onto 2% GS-CA, a kinetic experiment with pH readjustment to the initial 3.0 value was carried out. For this purpose, 4 L of Cr(VI) solution with an initial concentration of 92.3 mg L^{-1} and initial pH 3.0 was introduced in a stirred reactor of 5 L capacity. Then, a concentration of 2.5 beads·mL^{-1} of 2% GS-CA beads were added to the vessel under continuous stirring and the variation of metal concentration and pH as a function of time was followed. When pH achieved almost a constant value, it was manually readjusted to the initial value (pH 3.0) by addition of negligible amounts of hydrochloric acid.

Results of chromium concentration in solution and pH evolution as a function of contact time are plotted in **Figure 11**. In the same figure it has been indicated with arrows the times at wich the reacidifications were carried out.

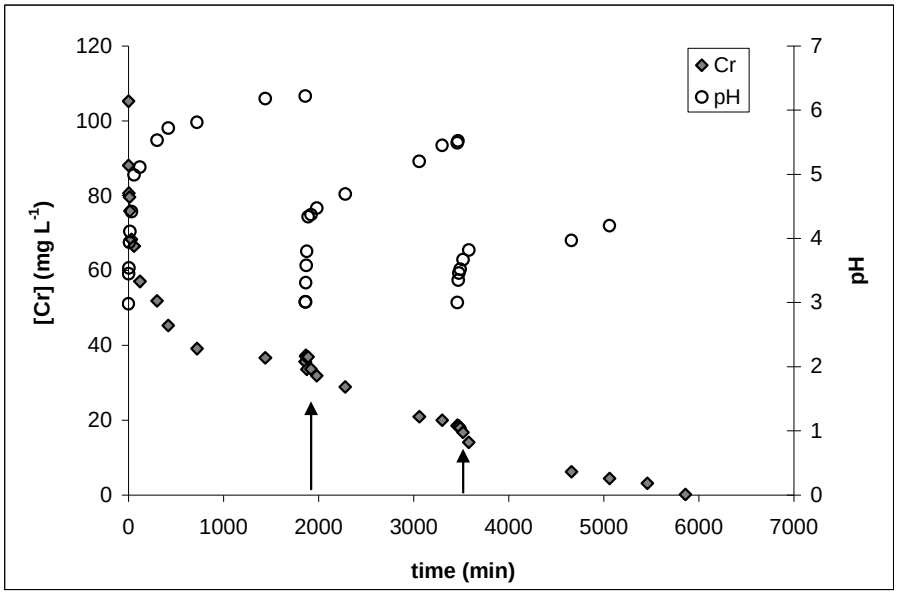

Figure 11: Chromium concentration in solution and pH variation as a function of contact time of Cr(VI) with 2% GS-CA gel beads. Initial Cr(VI) concentration: 92.3 mg·L^{-1}, sorbent dose: 2.5 beads·mL^{-1}. The arrows indicate the times at which pH readjustment was carried out.

This figure shows that in a first step, after 1500 minutes, pH rapidly increases to an equilibrium value around 6 and chromium concentration also reaches an equilibrium with

around 38 $mg \cdot L^{-1}$. In this point, a pH readjustment to the initial 3.0 value was carried out, as it can be seen in the figure. After this, chromium sorption was reactivated and again pH increased while chromium concentration decreased. A new equilibrium was achieved with a chromium concentration of about 20 $mg \cdot L^{-1}$ and pH, 5.5.

Then, a second pH readjustment was carried out monitoring again the chromium content in the effluent and the pH as a function of time. After readjustment, chromium totally disappeared leading to a solution with a final pH around 4.0. These results put into evidence the role of H^+ as a limiting reagent in Cr(VI) sorption onto 2% GS-CA gel beads. From this experiment, it is worth mentioning the total dissapearence of the initial hexavalent chromium in solution. In order to know if the sorbent material could act as a Cr(VI) reducing agent, the possible presence of Cr(III) in the solid phase will be studied, in order to check if the sorption process takes place involving a reductive-sorption step.

5.4. Sorption kinetic modeling

Kinetic data obtained for the three initial chromium concentrations were submitted to different models. From the fitting of the different kinetic models, information about the contribution of the sorption steps will be obtained. The chosen models were three widely applied for the description of biosorption phenomena: the pseudo-first and pseudo-second order kinetic models and the intraparticular diffusion one.

Fitting of the different models to the experimental results obtained are shown next, beginning from the pseudo-first order model.

5.4.1. Pseudo-first order kinetic model

The first-order rate expression of Lagergren, based on solid capacity is generally expressed as follows (Ho *et al*., 2000):

$$\frac{dq_t}{dt} = k_1(q_e - q_t) \qquad (2)$$

where q_e and q_t are the sorption capacity at equilibrium and at time t, respectively (mg bead^{-1}) and k_1 is the rate constant of pseudo-first order sorption (min^{-1}). After integration and applying the initial condition $t=0$ and $q_t=0$, the integrated form of equation (2) becomes:

$$\ln(q_e - q_t) = \ln q_e - k_1 t \qquad (3)$$

According to this expression, if kinetics can be described by a pseudo-first order model, the plot of $ln\ (q_e - q_t)$ versus t, should provide a straight line from whom slope and origin intercept, k_1 and q_e parameters could be determined.

In **Figures 12** to **14** the fitting of the pseudo-first order kinetic model on its linear form to the experimental sorption data is shown. In symbols experimental data have been represented while the solid line indicates the model fitting.

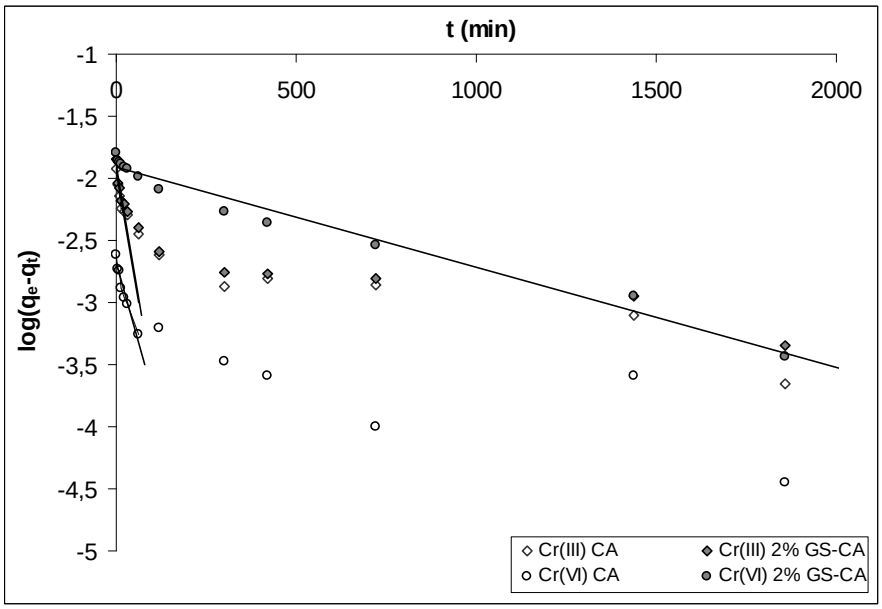

Figure 12: Pseudo-first order model fitting on its linear form to the experimental results for Cr(III) and Cr(VI) sorption onto CA and 2% GS-CA gel beads. $[Cr]_0 \approx 45$ mg·L^{-1}.

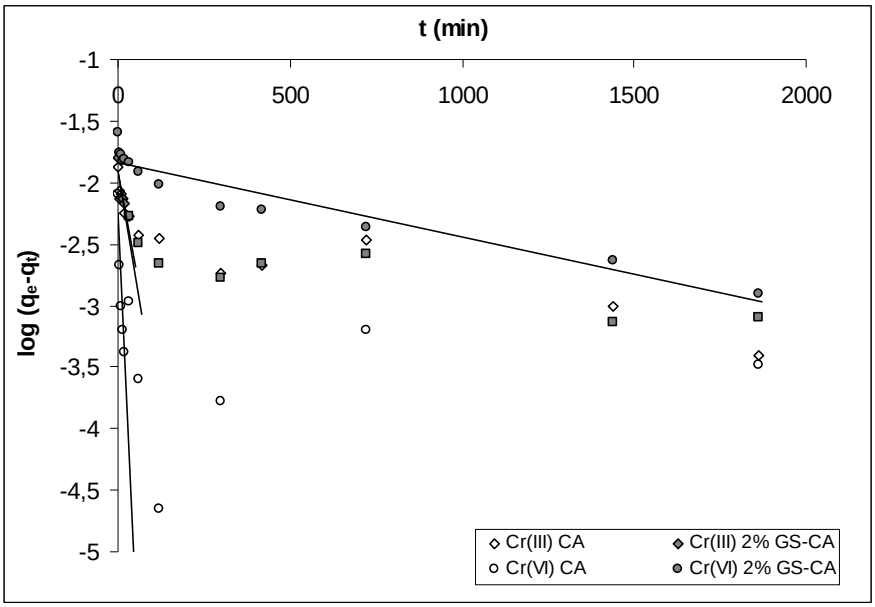

Figure 13: Pseudo-first order model fitting on its linear form to the experimental results for Cr(III) and Cr(VI) sorption onto CA and 2% GS-CA gel beads. $[Cr]_0 \approx 93$ mg·L^{-1}.

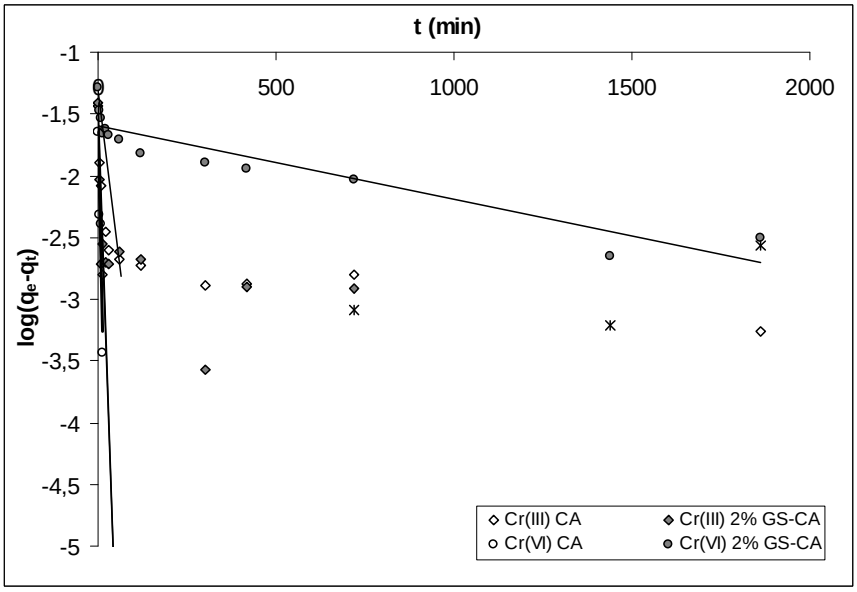

Figure 14: Pseudo-first order model fitting on its linear form to the experimental results for Cr(III) and Cr(VI) sorption onto CA and 2% GS-CA gel beads. $[Cr]_0 \approx 205$ mg·L^{-1}.

From this model fitting, the pseudo-first order kinetic constant k_1 (min^{-1}) for each sorption scenario can be obtained. Results, together with the time range adjusted, are presented in **Table 12**.

Table 12: Pseudo-first order kinetic model parameters for Cr(III) and Cr(VI) sorption onto CA and 2% GS-CA gel beads.

$[Cr]_0$ (mg·L^{-1})	System	t (min)	k_1 (min^{-1})	R^2
45	Cr(III) CA	20	0.043	0.962
	Cr(III) 2% GS-CA	20	0.039	0.915
	Cr(VI) CA	60	0.024	0.945
	Cr(VI) 2% GS-CA	2880	0.002	0.975
93	Cr(III) CA	20	0.038	0.887
	Cr(III) 2% GS-CA	20	0.036	0.807
	Cr(VI) CA	20	0.134	0.938
	Cr(VI) 2% GS-CA	2880	0.001	0.913
205	Cr(III) CA	20	0.198	0.948
	Cr(III) 2% GS-CA	20	0.188	0.811
	Cr(VI) CA	20	0.251	0.903
	Cr(VI) 2% GS-CA	2880	0.052	0.958

As it can be seen in the table, while pseudo-first order model is able to provide a reasonably good fitting for Cr(VI) sorption onto CA and 2% GS-CA gel beads for the whole studied contact time range (2880 minutes), in the case of Cr(III), this model is only able to fit the kinetic results obtained during the 20 first minutes of contact time.

In the next section, kinetic data will be treated according to the pseudo-second order model.

5.4.2. Pseudo-second order model

If the rate of sorption is related to a second order equation based on the sorbent uptake, the kinetics of the process will follow the pseudo-second order kinetic equation expressed as (Ho *et al*., 1996):

$$\frac{dq_t}{dt} = k_2 (q_e - q_t)^2 \qquad (4)$$

where q_e and q_t are the sorption capacity at equilibrium and at time t, respectively (mg·bead^{-1}) and k_2 is the rate constant of pseudo-second order sorption (bead mg^{-1} min^{-1}). For the initial condition $t = 0$ and $q_t = 0$, the integrated form of equation (4) becomes:

$$\frac{1}{(q_e - q_t)} = \frac{1}{q_e} + k_2 t \qquad (5)$$

which is the integrated rate law for a pseudo-second order reaction. Equation (5) can be rearranged to obtain the linear form:

$$\frac{t}{q_t} = \frac{1}{k_2 q_e^2} + \frac{1}{q_e} t \qquad (6)$$

If pseudo-second order kinetics is applicable to the pollutant-biosorbent system, the plot of t/q_t against of t should provide a linear relationship, from which equation slope and origin intercept the characteristic parameters of the model could be obtained. If the sorbent-sorbate system can be described by this model, initial sorption rate defined as $h=k_2 q_e^2$ can be obtained.

In **Figures 15** to **17** the fitting of the pseudo-second order kinetic model on its linear form to the experimental sorption data is shown. Symbols represent the experimental data and solid line, the model fitting.

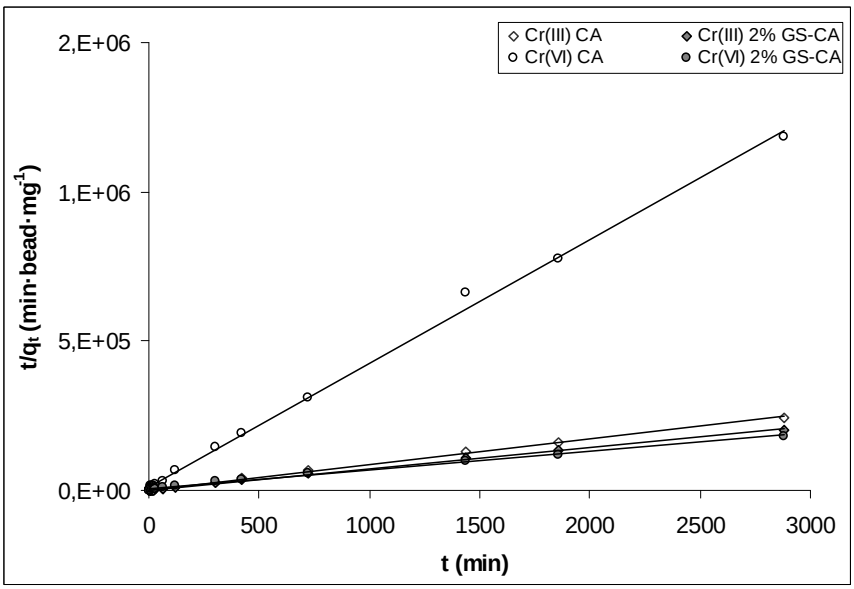

Figure 15: Pseudo-second order model fitting on its linear form to the experimental results (symbols) for Cr(III) and Cr(VI) sorption onto CA and 2% GS-CA gel beads. $[Cr]_0 \approx 45$ $mg \cdot L^{-1}$.

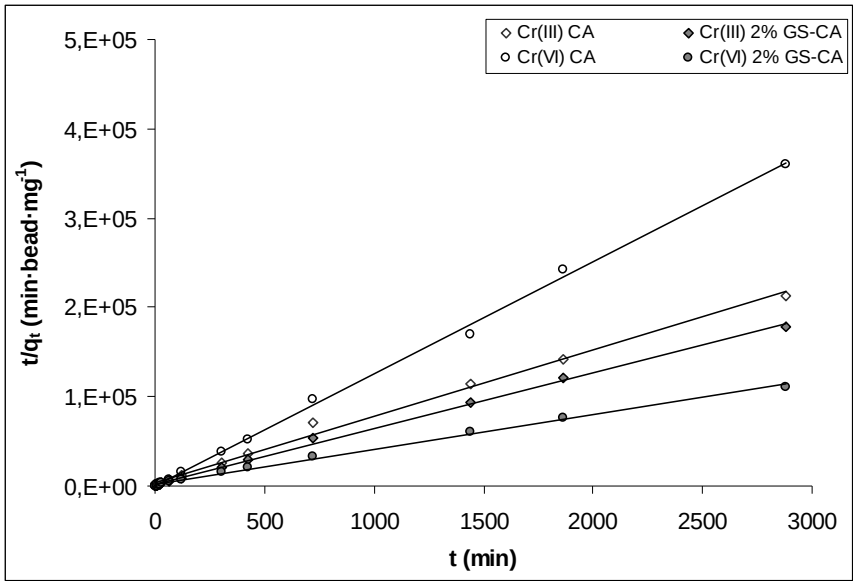

Figure 16: Pseudo-second order model fitting on its linear form to the experimental results (symbols) for Cr(III) and Cr(VI) sorption onto CA and 2% GS-CA gel beads. $[Cr]_0 \approx 93$ $mg \cdot L^{-1}$.

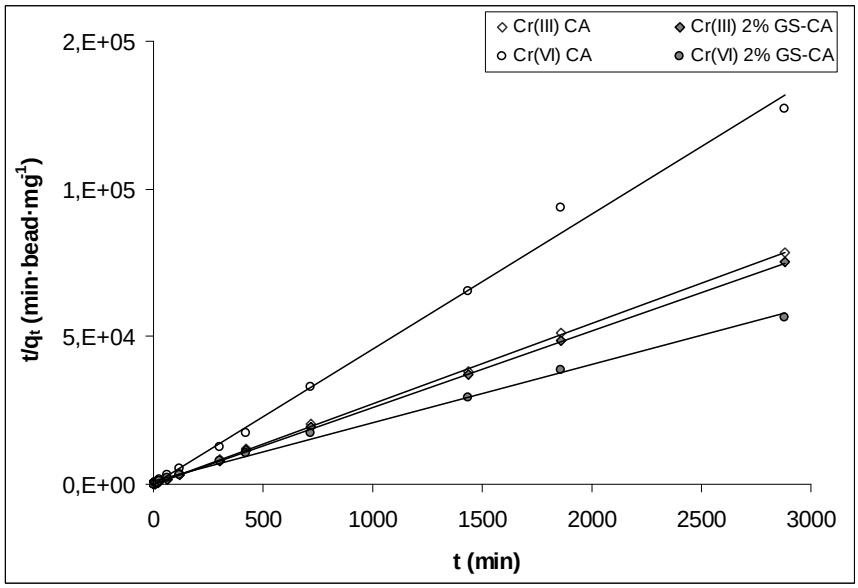

Figure 17: Pseudo-second order model fitting on its linear form to the experimental results (symbols) for Cr(III) and Cr(VI) sorption onto CA and 2% GS-CA gel beads. $[Cr]_0 \approx 205$ $mg \cdot L^{-1}$.

As it can be seen in the **Figures 15** to **17**, pseudo-second order model is able to provide a successful description of the sorption kinetics of both, Cr(III) and cr(VI) onto CA and 2% GS-CA gel beads.

From the slope and the intercept of these plots, the characteristic parameters were calculated and are presented in the next table.

Table 13: Pseudo-second order kinetic model parameters for Cr(III) and Cr(VI) sorption onto CA and 2% GS-CA gel beads.

$[Cr]_0$ (mg·L^{-1})	System	$q_e \cdot 10^2$ (mg·bead^{-1})	$h \cdot 10^3$ (mg·bead^{-1}· min^{-1})	R^2
45	Cr(III) CA	1.2	0.32	0.999
	Cr(III) 2% GS-CA	1.4	0.49	0.999
	Cr(VI) CA	0.2	0.08	0.998
	Cr(VI) 2% GS-CA	1.6	0.17	0.996
93	Cr(III) CA	1.3	0.39	0.999
	Cr(III) 2% GS-CA	1.6	0.59	0.999
	Cr(VI) CA	0.8	2.37	0.999
	Cr(VI) 2% GS-CA	2.6	0.47	0.997
205	Cr(III) CA	3.7	6.77	0.995
	Cr(III) 2% GS-CA	3.9	9.45	0.998
	Cr(VI) CA	2.2	178.60	0.996
	Cr(VI) 2% GS-CA	5.1	1.10	0.997

From the q_e and h parameters obtained from the pseudo-second order model, the theoretical sorption kinetics for each one of the systems under study can be calculated.

The results of the fitting of the pseudo-second order model to the experimental data are shown in the next figures:

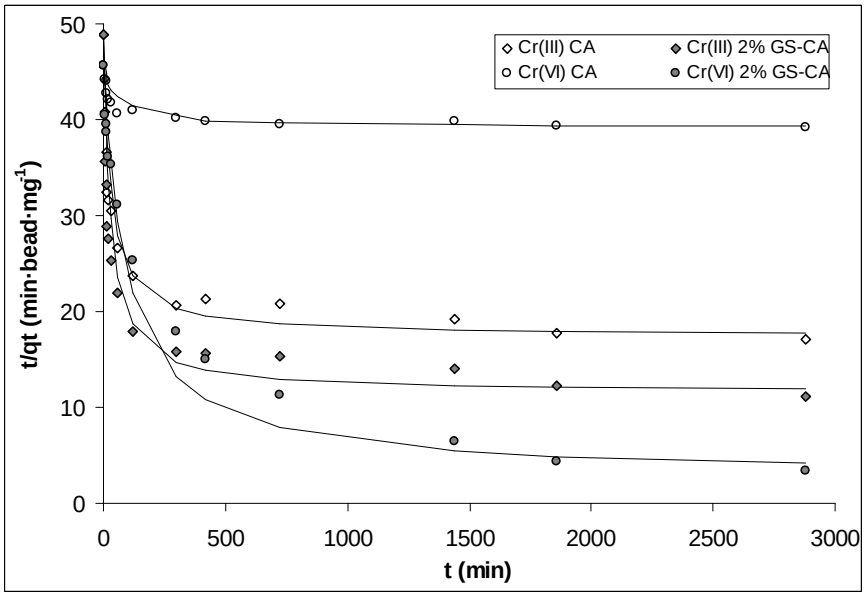

Figure 18: Pseudo-second order model fitting (solid line) to the experimental kinetic results (symbols) for Cr(III) and Cr(VI) sorption onto CA and 2% GS-CA gel beads. $[Cr]_0 \approx 45$ mg·L^{-1}.

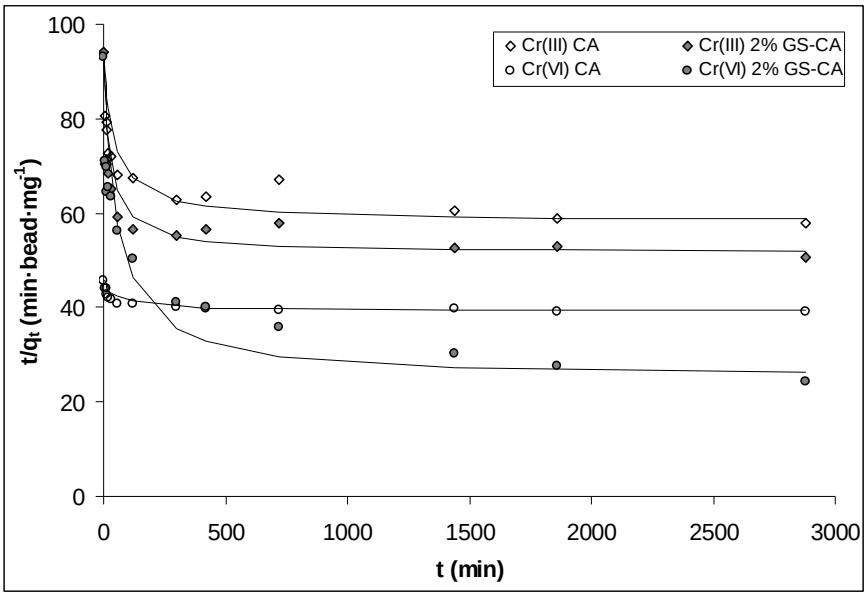

Figure 19: Pseudo-second order model fitting (solid line) to the experimental kinetic results (symbols) for Cr(III) and Cr(VI) sorption onto CA and 2% GS-CA gel beads. $[Cr]_0 \approx 93$ mg·L^{-1}.

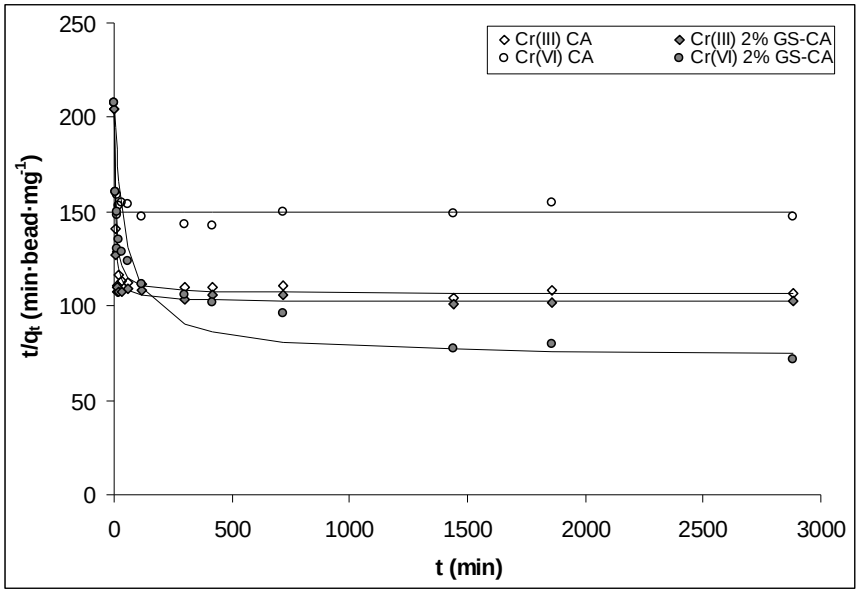

Figure 20: Pseudo-second order model fitting (solid line) to the experimental kinetic results (symbols) for Cr(III) and Cr(VI) sorption onto CA and 2% GS-CA gel beads. $[Cr]_0 \approx 205$ mg·L^{-1}.

As can be seen in these figures, for the three initial concentrations studied, the pseudo-second order model is able to describe the Cr(III) and Cr(VI) kinetic behaviour for the sorption onto CA and 2% GS-CA gel beads.

5.4.3. Intraparticle diffusion rate analysis

Despite the good performance to describe the sorption kinetics of the pseudo-second order model, this cannot provide any diffusional information; therefore, in order to investigate if the sorption rate limiting step is the solute transport from the sorbent surface to the intraparticle active sites, the model proposed by Weber and Morris (Weber and Morris, 1963) was applied. The equation of this model can be expressed as:

$$q_t = k_{id} t^{1/2} + C \qquad (7)$$

where q_t is the amount of metal adsorbed per bead at time t (mg·bead^{-1}), C is the intercept and k_{id}, the intraparticle diffusion rate constant (mg·bead^{-1}·min^{-1}). According to this model, the plot of uptake, q_t, as a function of the square root of time, $t^{1/2}$, should be linear if an intraparticle diffusion process is involved as rate limiting step. When the straight line passes through the origin then intraparticle diffusion is the rate-controlling step. This model has been applied for several authors studying kinetics of different sorbate-sorbent

systems (Kannan and Sundaram, 2001; Li *et al*, 2004; Özcan *et al*., 2005; Cochrane *et al*., 2006).

Results obtained for Cr(III) and Cr(VI) sorption onto CA and 2% GS-CA gel beads for the different initial metal concentrations are shown in next figures.

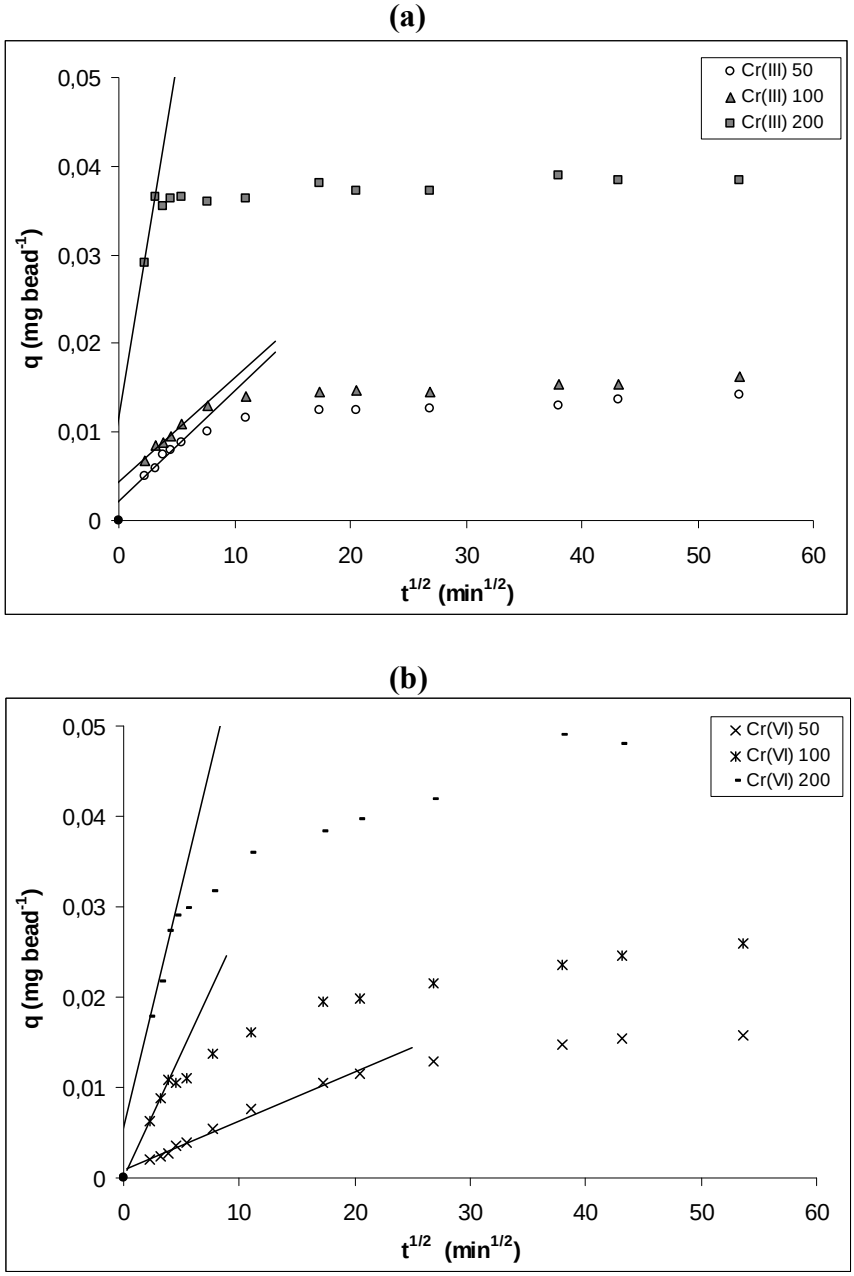

Figure 21. Intraparticle diffusion plots for (a) Cr(III) and (b) Cr(VI) sorption onto 2% GS-CA for different initial metal concentration.

From the linear plots of this model, intraparticle diffusion constant, k_{id} can be calculated and results are shown in the next table.

Table 14: Intraparticle diffusion constants for Cr(III) and Cr(VI) sorption onto CA and 2% GS-CA gel beads.

	$k_{id} \cdot 10^4$ (mg·bead^{-1}·min$^{-1/2}$)			$k_{id} \cdot 10^4$ (mg·bead^{-1}·min$^{-1/2}$)	
$[Cr(III)]_0$ (mg·L^{-1})	**CA**	**2% GS-CA**	**$[Cr(VI)]_0$ (mg·L^{-1})**	**CA**	**2% GS-CA**
48.85	1.2	1.3	45.05	0.5	0.5
93.95	1.3	1.6	93.21	0.9	2.8
204.77	5.2	7.9	207.86	2.7	5.6

Results presented in this table demonstrate an increase of k_{id} when increasing initial metal concentration in solution. On the other hand, the intraparticle diffusion constant seems to be higher in the case of beads containing grape stalk particles. The possible explanation for these facts will be discussed in the next section.

5.4.4. General discussion

As it can be seen in **Figures 12** to **14**, corresponding to the mathematical treatment of experimental data according to pseudo-first order model, this model would provide a suitable fitting for the 20 first minutes of the sorption process in the case of Cr(III) sorption onto CA and 2% GS-CA gel beads. However, in the case of Cr(VI) sorption onto 2% GS-CA gel beads, this model is able to successfully describe the sorption process in the whole studied time range. Pseudo first order model fitting is indicative of a possible diffusion process as the rate limiting sorption step, being the constant k_1 an indicative parameter of the initial external film diffusion. According to this, the higher the k_1 value, the faster the external film diffusion is. The obtained results for the different sorption experiments would indicate that external film diffusion could be the limiting sorption step for the first minutes in the case of Cr(III) sorption onto CA and 2% GS-CA gel beads and in the case of Cr(VI) sorption onto spheres of CA. In the case of Cr(VI) sorption onto beads containing GS, external film diffusion seems to be a sorption rate limiting step, due to the high determination coefficients derived from pseudo-first order fitting to the experimental kinetics observed.

Several authors have reported that, in general, sorption processes that reach equilibrium after contact times lower than 3 hours, use to be kinetically controlled, while processes whose equilibrium is reached in contact times higher than 24 hours, are usually diffusionally rate controlled. In the range between 3 and 24 hours, it is possible the existence of either kinetics or difusional control (Li *et al.,* 2004).

If Cr(III) and Cr(VI) kinetic as a function of the initial metal concentrations are observed (**Figures 6** and **7** respectively), it can be seen that, while Cr(III) sorption onto both types of beads reaches equilibrium in around 120 minutes of contact time, in the case of Cr(VI) sorption onto gel beads containing GS, a contact time of 1440 minutes is needed. These facts, together with the different time ranges in which pseudo-first order can be applied, are indicative of a greater external film transport resistance in the case of Cr(VI) sorption onto beads containing GS than in the case of Cr(III) sorption onto both types of sorbents.

On the other hand, when experimental Cr(III) and Cr(VI) sorption results onto CA and 2% GS-CA beads were submitted to pseudo-second order model an excellent fitting, with determination coefficients higher than 0.995 was obtained. According to these results, it can be concluded that Cr(III) and Cr(VI) sorption kinetics onto CA and 2% GS-CA gel beads follows a pseudo-second order kinetics, based on the sorbent capacity. From the fitting of this model, initial sorption rate parameter, h, was also obtained and presented, for the different sorption scenarios, in **Table 13**. Results put into evidence an increase of initial sorption rate when increasing the initial metal concentration in solution for all the situations studied. This is consistent with the fact that as higher the initial metal concentration in solution is, the highest the mass transfer from the solution to the solid phase per time unit.

The intraparticle diffusion plot of q_t as a function of $t^{1/2}$ for three different initial metal concentrations had been presented in **Figure 21** for **(a)** Cr(III) and **(b)** Cr(VI) sorption onto 2% GS-CA. As can be seen in **Figure 21 (a)**, intraparticle diffusion seems not to be the rate limiting step for Cr(III) sorption onto CA and 2% GS-CA gel beads, as any of the lines had a zero intercept value. In the case of Cr(VI) sorption onto 2% GS-CA, the lines corresponding to the two lowest Cr(VI) initial concentrations passed through the origin, indicating that at low concentrations, intraparticle diffusion is the rate limiting step of Cr(VI) sorption onto beads containing grape stalk. The plots corresponding to Cr(III) and

Cr(VI) sorption onto CA showed a linear regression but the lines did not pass through the origin. It has been reported that slow kinetics as the observed in this study are indicative of sorbate diffusion through the sorbent pores as a possible sorption rate limiting step (Ho *et al.*, 2000).

On the other hand, in **Table 14** the values of intraparticle diffusion constant, k_{id}, had been presented. In that table it can be observed that this parameter increases in all the cases when increasing the initial metal concentration in solution. For both, Cr(VI) and Cr(III), and a given initial metal concentration, k_{id} values obtained for beads containing grape stalk were higher than those obtained for CA beads. This fact might be due to the channelling produced in the calcium alginate gel due to the presence of the grape stalk particles that could make easier the diffusion of the metal through the internal volume of the bead.

When comparing Cr(III) and Cr(VI) intraparticle diffusion on 2% GS-CA gel beads for a given initial metal concentration, it can be observed that Cr(III) k_{id} values are always higher than the obtained for Cr(VI). This observation is consistent with the important role that GS plays in hexavalent chromium sorption. As Cr(VI) sorption occurs mainly onto the grape stalk particles, in a first step it has to cross the internal volume of the hydrogel, reach the particle surface and, after this, diffuse again to the internal volume of the grape stalk particle. All these steps make the global Cr(VI) sorption process slower than Cr(III) sorption, where the same CA hydrogel was able to fix the cationic Cr^{3+} and $Cr(OH)^{2+}$ species on its structure.

The high pseudo-first order constants and the intraparticle diffusivity obtained in the case of Cr(VI) sorption onto 2% GS-CA seem to indicate that, in fact, the main resistance would not come from the Cr(VI) diffusion into the bead, formed by around 95% of water (Fiol *et al.*, 2005), but from the mass transfer of chromium from the bead to the grape stalk particles, that is likely to be the material responsible of the major Cr(VI) sorption.

Once analysed the kinetics of both trivalent and hexavalent chromium sorption onto the sorbents and evaluated the contact time required by the different systems to reach equilibrium, in the next section, the distribution of the sorbates between the liquid and the solid phase will be studied and discussed.

5.5. Cr(III) and Cr(VI) sorption equilibrium study onto CA and 2% GS-CA

In the next section, Cr(III) and Cr(VI) sorption equilibrium onto both, CA and 2% GS-CA gel beads will be studied and discussed. Experimental data will be submitted to Langmuir and Freundlich sorption equilibrium models, which are widely employed in many sorbent-sorbate systems.

In **Tables 15(a)** Cr(III) and Cr(VI) initial and final metal concentration in solution after contact with CA and 2% GS-CA gel beads are presented.

Table 15 (a): Cr(III) and Cr(VI) initial and equilibrium concentration in solution after contact with CA and 2% GS-CA gel beads. Initial pH = 2.98, contact time 2880 minutes.

Cr(III)			Cr(VI)		
	CA	2% GS-CA		CA	2% GS-CA
C_i(mg·L^{-1})	C_e(mg·L^{-1})	C_e(mg·L^{-1})	C_i(mg·L^{-1})	C_e(mg·L^{-1})	C_e(mg·L^{-1})
27.51	2.36	0.64	26.21	19.79	0.55
53.01	14.13	6.32	51.31	41.23	4.40
76.52	32.03	20.24	73.91	66.83	14.22
102.38	45.92	34.20	97.71	72.99	20.00
155.52	68.86	64.58	150.83	114.90	46.18
206.08	89.70	87.95	183.80	155.08	70.87
296.99	152.13	132.09	267.08	212.98	139.75
667.27	464.17	412.77	494.60	437.15	339.50
853.27	645.82	592.12	560.00	502.12	390.85
1103.28	887.45	825.60	888.50	828.06	699.09
1570.20	1352.60	1279.87	1259.42	1197.90	1071.88
3107.60	2883.92	2734.60			

Amount of metal sorbed per bead for each initial metal concentration have been calculated according to the equation: $q = (C_i - C_{eq})V/40$ beads. The results are presented in **Table 15(b)**.

Table 15 (b): Metal concentration on CA and 2% GS-CA gel beads at equilibrium time for the different initial metal concentrations studied. pH_0=2.98, agitation time: 2880 minutes.

Cr(III)			Cr(VI)		
	CA	2% GS-CA		CA	2% GS-CA
C_i(mg·L^{-1})	q_e(mg·bead^{-1})	q_e(mg·bead^{-1})	C_i(mg·L^{-1})	q_e(mg·bead^{-1})	q_e(mg·bead^{-1})
27.51	0.0094	0.0101	26.21	0.0024	0.0096
53.01	0.0146	0.0175	51.31	0.0038	0.0176
76.52	0.0167	0.0211	73.91	0.0045	0.0224
102.38	0.0212	0.0256	97.71	0.0093	0.0290
155.52	0.0325	0.0341	150.83	0.0135	0.0392
206.08	0.0436	0.0443	183.80	0.0108	0.0423
296.99	0.0543	0.0618	267.08	0.0203	0.0477
667.27	0.0762	0.0954	494.60	0.0215	0.0582
853.27	0.0778	0.0979	560.00	0.0218	0.0634
1103.28	0.0809	0.1041	888.50	0.0227	0.0710
1570.20	0.0816	0.1089	1259.42	0.0231	0.0703
3107.60	0.0839	0.1399			

If metal concentration in the solid phase is plotted as a function of metal concentration in solution at equilibrium, sorption isotherms are obtained. The experimental Cr(III) and Cr(VI) sorption isotherms onto CA and 2% GS-CA are presented in the next figure.

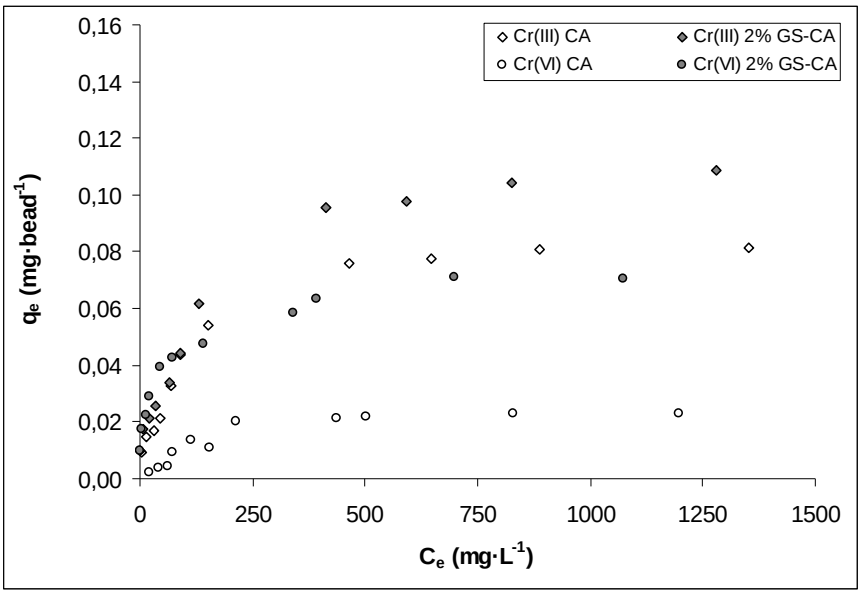

Figure 22: Cr(III) and Cr(VI) sorption isotherms onto CA and 2% GS-CA gel beads. pH_o=2.98, agitation time: 2880 minutes.

In the figure it can be seen that the amount of metal sorbed, Cr(III) or Cr(VI), increases until a maximum value is achieved. From this point, the increase in the solution concentration is not associated to an increase in the metal on the solid phase.

As it can be observed in the figure, in the case of Cr(III), a similar sorption capacity is achieved with either CA or 2% GS-CA beads for equilibrium concentrations lower than 250 $mg \cdot L^{-1}$. For concentrations higher than this value, a significative higher sorption capacity is observed for gel beads containing grape stalks. In the extreme of this last situation, if experimental maximum sorption capacity is evaluated and a comparison is established between both sorbents, it's observed that while CA beads become saturated with about 0.08 $mg \cdot bead^{-1}$, 2% GS-CA beads, load around 0.13 $mg \cdot bead^{-1}$. The isotherm of Cr(III) sorption onto CA and 2% GS-CA gel beads put into evidence that calcium alginate matrix would be the main responsible of Cr(III) sorption at low concentrations, while at higher metal concentrations, once the alginate gel matrix is saturated, grape stalk powder would begin to play an important role in sorption. Similar results had been previously reported when studying trivalent chromium sorption onto calcium alginate (Araújo and Teixeira, 1997)

In the same figure, it can be observed a very different behaviour of both sorbents in the adsorption of Cr(VI) for both, low and high metal concentrations in solution. While the beads containing grape stalk show an important capacity, around 0.07 $mg \cdot bead^{-1}$, those beads formed by pure calcium alginate, show an experimental maximum capacity value about 0.02 $mg \cdot bead^{-1}$. This experimental evidence is indicative of the important role of the grape stalk powder entrapped in the polymeric matrix in the sorption of Cr(VI).

5.5.1. Mathematical modeling of equilibrium results

5.5.1.1. Langmuir model

Langmuir model assumes that adsorption occurs at specific homogenous sites within the adsorbent and has found successful application in many monolayer adsorption processes. Langmuir treatment is based on the assumption that a maximum adsorption corresponds to a saturated monolayer of solute molecules on the adsorbent surfaces, that the energy of adsorption is constant and that there is no transmigration of adsorbate in the plane of the surface. Langmuir model is represented by the next equation

$$q = \frac{K_L q_{\max} C_{eq}}{(1 + K_L C_{eq})} \qquad (8)$$

that on its linear form is:

$$\frac{C_f}{q} = \frac{1}{(q_{\max} \cdot K_L)} + \frac{C_f}{q_{\max}} \qquad (9)$$

where $q_{max.}$ is the maximum uptake ($mol \cdot g^{-1}$) and K_L ($L \cdot mol^{-1}$) is a constant related to energy of adsorption which quantitatively reflects the affinity between the sorbent and the sorbate.

In the next figure the fitting of experimental Cr(III) and Cr(VI) sorption results onto CA and 2% GS-CA beads data to the linearized Langmuir equation is shown:. Experimental data and model fitting have been plotted in symbols and in solid line respectively.

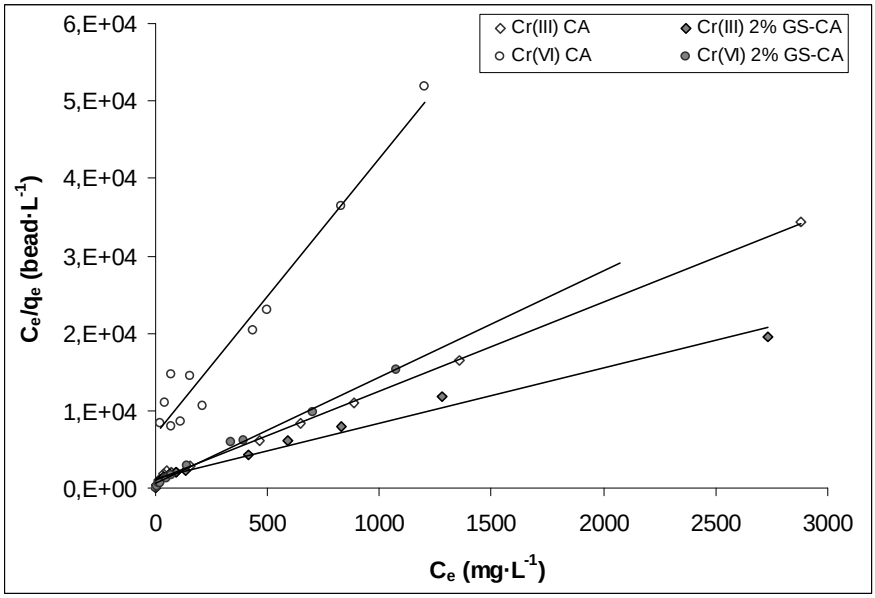

Figure 23: Langmuir fitting to the experimental Cr(III) and Cr(VI) sorption data onto CA and 2% GS-CA gel beads.

From these plots, parameters of maximum sorption capacity (q_{max}) and Langmuir constant (K_L) related to the affinity sorbent-sorbate for each sorption scenario can be obtained. Results are presented in **Table 16**. From these parameters, the isotherm simulation can be obtained and the fitting of the predicted results to the experimental sorption data is shown in the next figure.

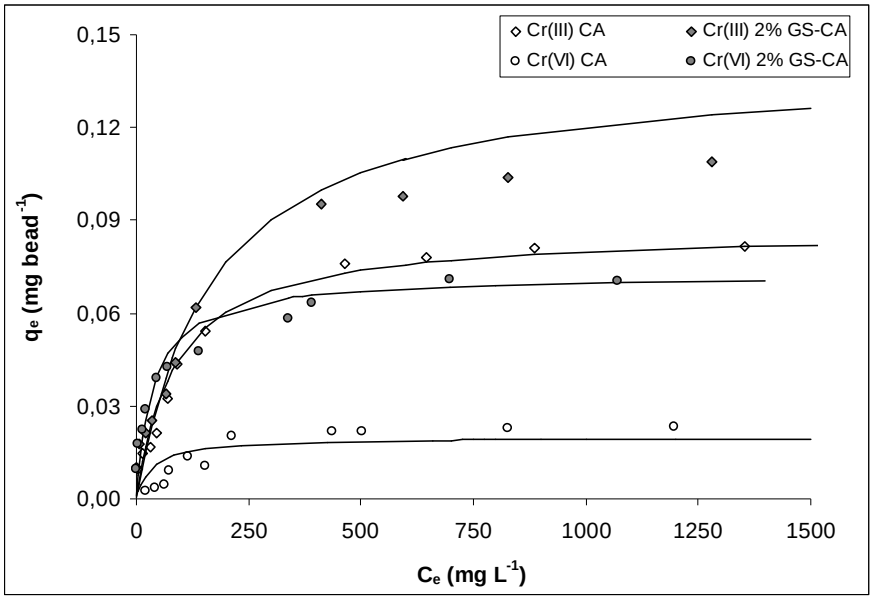

Figure 24: Langmuir model fitting to Cr(III) and Cr(VI) equilibrium data. In symbols and in solid line, experimental results and model prediction are plotted respectively.

5.5.1.2. Freundlich model

The Freundlich isotherm is an empirical equation based on sorption on a heterogeneous surface and assumes that different sites with different adsorption energies are involved. This equation is commonly presented as:

$$q_e = K_F C_e^{1/n} \qquad (10)$$

that on its linear form is:

$$\log q_e = \log K_F + \frac{1}{n} \log C_e \qquad (11)$$

where K_F and n are empirical constants that indicate the relative sorption capacity and sorption intensity respectively.

In the next figure, the fitting of experimental data to the linearized form of Freundlich model is presented. Experimental data and model fitting have been plotted in symbols and in solid line respectively.

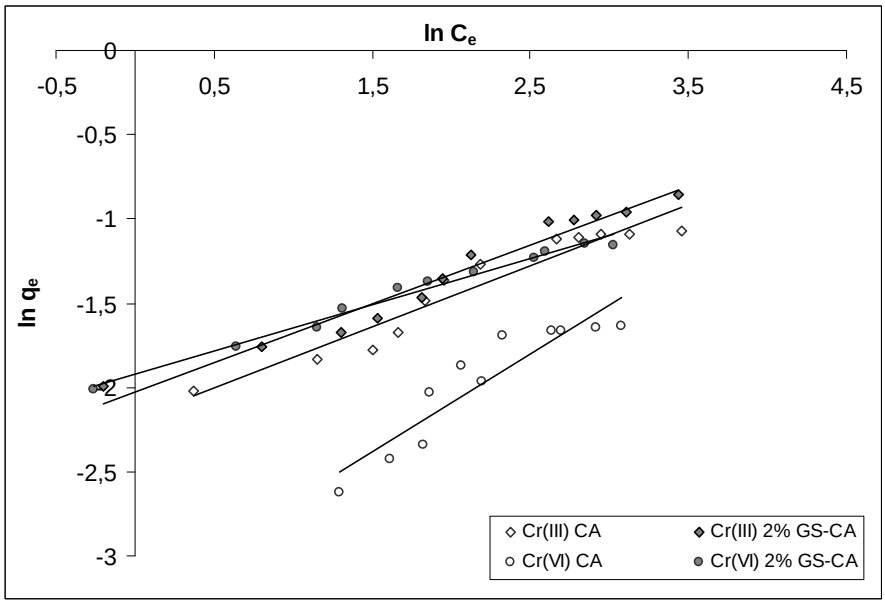

Figure 25: Freundlich fitting to the experimental Cr(III) and Cr(VI) sorption data onto CA and 2% GS-CA gel beads.

From the fitting of experimental data to Freundlich model, characteristic parameters K and n, related to the intensity of sorption, can be calculated for each sorption systems. Results

are presented in **Table 16**. From these parameters, sorption isotherms can be simulated. Model prediction and experimental data are presented in the next figure.

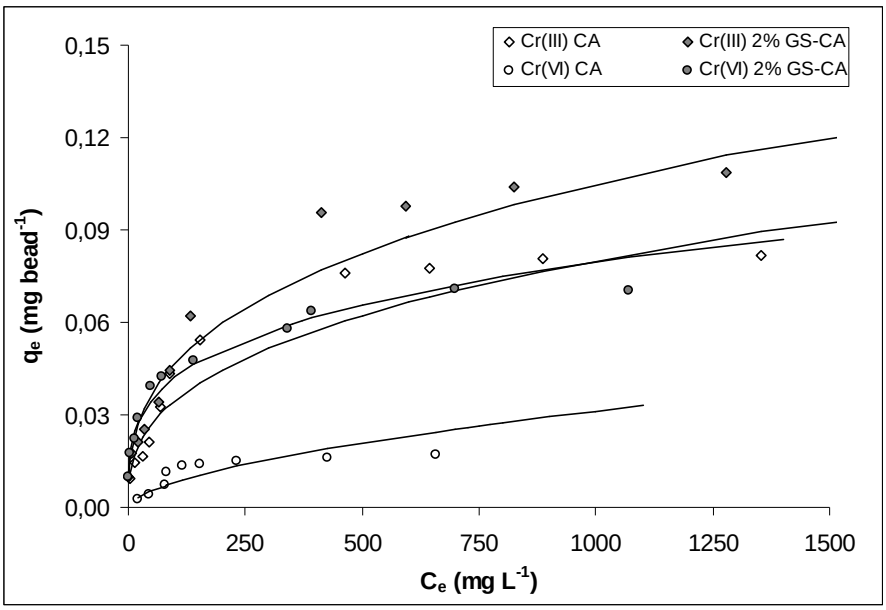

Figure 26: Freundlich model fitting to Cr(III) and Cr(VI) equilibrium data. In symbols and in solid line, experimental results and model prediction are plotted respectively.

In **Table 16**, parameters obtained after submission of experimental data to Langmuir and Freundlich model are shown. Additionally, Langmuir constant (K_L) was used to calculate the variation of Gibbs free energy of sorption process according to the equation: $\Delta G = -RT \cdot \ln K_L$ (Li *et al.*, 2004).With this parameter, thermodynamic spontaneity of Cr(III) and Cr(VI) sorption onto both, CA and 2% GS-CA can be compared.

Table 16: Langmuir and Freundlich parameters for Cr(III) and Cr(VI) sorption onto CA and 2% GS-CA.

	Langmuir model				**Freundlich model**		
	q_{max} (mg·bead^{-1})	**K_L (L·mg^{-1})**	**ΔG^0 (kJ·mol^{-1})**	**R^2**	**K**	**n**	**R^2**
Cr(III)-CA	0.0874	0.0114	-15.57	0.999	0.112	2.749	0.922
Cr(III)-2% GS-CA	0.1404	0.0059	-13.99	0.982	0.132	2.868	0.964
Cr(VI)-CA	0.0467	0.0026	-11.96	0.921	0.032	1.710	0.938
Cr(VI)-2% GS-CA	0.0722	0.0264	-17.61	0.995	0.146	3.606	0.983

The good determination coefficients obtained when submitting experimental data to Langmuir and Freundlich models demonstrates a good predictive capacity of both models, as it can be observed in **Figures 24** and **26**, respectively. However, Langmuir model seems to fail only in the case of Cr(VI) sorption onto spheres whose component is only calcium alginate.

From the fitting of Langmuir model, maximum sorption capacity of each sorbent for each chromium oxidation state, Q_{max}, as well as Langmuir constant, K_L (related to the affinity sorbent-sorbate) can be calculated. Additionally, if sorption process follows a Langmuirian sorption behaviour, variation of Gibbs free energy can be also calculated according to the equation $\Delta G = -RT \cdot \ln K_L$ (Li *et al.*, 2004). As it can be deduced from this expression, higher Langmuir constants would indicate a ΔG smaller and so, a higher spontaneity of the sorption process. Results shown in **Table 16** allow us to stablish the next spontaneity ranking of Cr(III) and Cr(VI) sorption onto the different sorbents.

Cr(VI)-2% GS-CA > Cr(III)-CA > Cr(III)-2% GS-CA > Cr(VI)-CA

While sorption spontaneity is quite similar for Cr(III) sorption onto both CA and 2% GS-CA, it is noteworthy the important difference between Cr(VI) sorption onto both materials. The minimum ΔG is the related to Cr(VI) sorption onto 2% GS-CA spheres.

As shown in **Table 16**, the highest sorption capacity is attained for Cr(III) sorption onto spheres containing GS (0.1404 $mg \cdot bead^{-1}$). Nevertheless, it can not be neglected the good sorption performance of pure CA beads through Cr(III) sorption (0.0874 $mg \cdot bead^{-1}$). This fact would confirm that CA is the main responsible of Cr(III) sorption, and that GS can adsorb only an additional amount when calcium alginate is close to saturation. Efficient Cr(III) removal by alginate had been also previously reported by several authors (Araújo and Teixeira, 1997).

In the case of Cr(VI) sorption onto gel beads of 2% GS-CA, q_{max} obtained (0.0722 $mg \cdot bead^{-1}$) is almost double than the corresponding to beads of only CA (0.0467 $mg \cdot bead^{-1}$). This indicates that, in contrast to Cr(III), GS is the main responsible of Cr(VI) sorption.

Despite for all the sorption systems, the determination coefficient was higher than 0.92, the Freundlich model did not provide as good determination coefficients as the Langmuir one. However, Freundlich model was used to calculate K and n, being this last parameter

associated to the sorption intensity (Karthikeyan *et al*., 2004). Treybal (1980) proposed that n values between 1 and 10 were indicative of a favourable sorption process. As it had been presented in **Table 16**, n value for all the sorption systems studied are in this range, indicating thus that chromium sorption onto the studied sorbents is favourable.

In order to compare Cr(III) and Cr(VI) sorption capacity of the developed sorbents with the reported in literature, in the next table a summary including maximum sorption capacities of CA and 2% GS-CA obtained in the present work, is presented with the results obtained by other authors. To establish this comparison, the results of q_{max} obtained in this study must be expressed in terms of dry sorbent. The dry mass of the different beads was calculated and the results obtained were 0.3 and 1.08 $mg \cdot bead^{-1}$ for CA and 2% GS-CA spheres respectively. Taking into account these values, maximum sorption capacities in terms of dry sorbent mass were: 291.3 and 130.0 $mg \cdot g^{-1}$ for Cr(III) and 155.7 and 66.8 $mg \cdot g^{-1}$ for Cr(VI) sorption onto CA and 2% GS-CA respectively. The higher capacity of Cr(III) and Cr(VI) observed onto CA than onto 2% GS-CA when the dry sorbent mass is used instead of the number of beads comes from the fact that a dry 2% GS-CA bead is about 3.6 times heavier than a CA one.

Table 17: Maximum uptake (q_{max}) of Cr(III) and Cr(VI) for diferent biosorbent materials

	Adsorbent capacity ($mg \cdot g^{-1}$)		
Sorbent	**Cr(III)**	**Cr(VI)**	**Reference**
CA	291.3	130.0	This work
2% GS-CA	155.7	66.8	This work
Grape stalk		59.8	Fiol *et al*., 2003
Yohimbe bark		42.5	Fiol *et al*., 2003
Cork		17.0	Fiol *et al*., 2003
Olive stones		9.0	Fiol *et al*., 2003
Exhausted coffee		10.2	Fiol *et al*., 2008
Sugar cane bagasse		13.4	Sun *et al*., 2004
Seaweed *Ecklonia* sp.		233.5	Park *et al.*, 2004
Aeromonas caviae biomass		284.4	Loukidou *et al.*, 2004
Brown seaweed (*Turbinaria* spp.)	31.0		Aravindhan *et al*., 2004
Tannin gel (77% water)	50.0	287.0	Nakano *et al.*, 2001
Aspergillus biomass	15.6	23.6	Sekhar *et al*., 1998
Peat	14.0	30.7	Dean and Tobin, 1999

Despite many efforts have been devoted to the study of hexavalent chromium sorption and many are thus the examples that can be found in literature, fewer is the number of studies

concerning trivalent chromium sorption. This special focusing of authors in Cr(VI) removal is due to its higher toxicity and difficulty of removal compared with Cr(III).
As it can be seen in the table the sorbent materials of this study exhibit high capacities for both chromium oxidation states. In the case of Cr(III), it must be pointed out that the sorbents have demonstrated a particularly great efficiency compared to other biosorbents. In the case of Cr(VI), the entrapment of the GS in the calcium alginate gel provokes an improvement in sorption capacity of the native GS (Fiol *et al*., 2003). Nevertheless, notably higher capacity values of Cr(VI) adsorption have been reported for Seaweed *Ecklonia* sp. (Park *et al*., 2004), *Aeromonas caviae* (Loukidou *et al.*, 2004) and Tannin gel (Nakano, 2001).

5.6. Ion exchange mechanism in Cr(III) sorption onto CA and 2% GS-CA gel beads

The alginate gel used in this study is formed by the calcium salt of this biopolymer. In the crosslinking process of the polymeric alginate chains, two mols of Na^+ are replaced by one mol of Ca^{2+} that remains bonded to the carboxylate groups of the alginate. These groups, which could act as active sites for the coordination of the cationic trivalent chromium species, would be coordinated to calcium cations. So that, it might be possible that Cr(III) sorption would be associated, in some extension, to a Ca^{2+} release from the solid material.
In literature, different studies of metal sorption onto calcium alginate gels can be found. Many authors propose Ca^{2+} ions exchange as the main mechanism for the sorption of cationic species of different metallic ions (Jodra and Mijangos, 2001; Araujo and Teixeira, 1997). Additionally, studies carried out previously in our laboratory, pointed out that some divalent heavy metal cations as copper and nickel were adsorbed onto the raw grape stalk, partially, by an ionic exchange mechanism (Villaescusa *et al*., 2004).
According to this background, a possible ion exchange process taking place between cationic Cr(III) species and Ca^{2+} was investigated. This possible mechanism was checked by analysing calcium released in the filtrates of both, kinetics and equilibrium sorption experiments. Results of calcium ion exchange in the Cr(III) sorption kinetics experiments onto CA and 2% GS-CA for three initial metal concentrations are presented and discussed in the next section.

5.6.1. Calcium ions release during the sorption kinetics

The results of Ca^{2+} released as a function of time for both CA and 2% GS-CA beads and for the three initial Cr(III) concentrations are presented in the next table.

Table 18: Calcium released by CA and 2% GS-CA gel beads as a function of contact time for three initial Cr(III) concentrations.

	Ca^{2+} released ($mg \cdot L^{-1}$)					
[Cr(III)]($mg \cdot L^{-1}$)	**48.85 $mg \cdot L^{-1}$**		**93.95 $mg \cdot L^{-1}$**		**204.77 $mg \cdot L^{-1}$**	
t (min)	**CA**	**2% GS-CA**	**CA**	**2% GS-CA**	**CA**	**2% GS-CA**
0	0	0	0	0	0	0
5	31.55	30.05	29.38	31.03	30.33	3528
10	32.23	32.56	36.15	37.13	35.25	45.52
15	40.68	42.75	43.49	43.81	45.58	53.79
20	40.51	41.51	40.05	43.85	46.15	62.78
30	45.47	40.25	44.85	48.35	51.70	63.39
60	49.76	47.17	48.41	53.70	60.17	64.17
120	52.00	50.76	48.33	57.87	60.93	69.54
300	54.40	50.02	52.91	56.25	64.83	71.84
420	50.52	50.30	51.44	56.78	60.80	70.64
720	50.55	49.26	54.33	55.80	63.33	67.54
1440	51.88	53.15	54.49	63.60	63.87	71.46
1860	51.68	53.53	56.56	61.02	61.94	76.20
2880	48.50	52.42	54.96	60.77	62.69	86.64

As it can be seen in the table, Ca^{2+} concentration in solution rapidly increases in the first minutes of sorbent-solution contact. After this, the increase is slower until a maximum Ca^{2+} concentration is achieved and it remains almost constant. From these results and the obtained for the Cr(III) sorption kinetics (**Table 4**), molar ratio between Ca^{2+} released and Cr(III) adsorbed for each contact time has been calculated and results are presented in the next table.

Table 19: Ratio mmol Ca^{2+} released/mmol Cr(III) adsorbed per either, CA or 2% GS-CA bead, as a function of time for the three initial Cr(III) concentrations studied.

	Ca^{2+} rel./Cr(III) ads.					
[Cr(III)] ($mg \cdot L^{-1}$)	**48.85 $mg \cdot L^{-1}$**		**93.95 $mg \cdot L^{-1}$**		**204.77 $mg \cdot L^{-1}$**	
t (min)	**CA**	**2% GS-CA**	**CA**	**2% GS-CA**	**CA**	**2% GS-CA**
0	/	/	/	/	/	/
5	2.04	1.08	1.00	0.66	0.23	0.27
10	1.41	1.12	1.53	1.03	0.28	0.35
15	1.71	1.54	1.95	1.36	0.37	0.48
20	1.62	1.37	1.29	1.27	0.39	0.58
30	1.87	1.16	1.52	1.31	0.46	0.59
60	1.78	1.35	1.46	1.30	0.58	0.61
120	1.69	1.33	1.43	1.35	0.58	0.68
300	1.63	1.21	1.41	1.24	0.63	0.67
420	1.48	1.22	1.38	1.31	0.57	0.68
720	1.46	1.17	1.70	1.32	0.61	0.64
1440	1.44	1.27	1.38	1.40	0.58	0.66
1860	1.36	1.22	1.39	1.32	0.58	0.72
2880	1.21	1.15	1.29	1.25	0.57	0.86

To evaluate if calcium ion exchange can explain trivalent chromium sorption, the information about the hydrochemical speciation of this metal in our experimental conditions is required. In the next figure, Cr(III) speciation diagram for an initial metal concentration of 100 $mg \cdot L^{-1}$ and a Cl^- concentration of 1.00 mM is presented. Introduction of Cl^- anion is needed because HCl was added to the media to achieve a solution pH of 3. The added chloride could provoke the formation of chloroclomplexes with charge different than +3. Cr(III) speciation for the three different initial metal concentrations was simulated but, as the proportion of the different species was almost equal, in the next figure has been only presented the speciation for the intermediate concentration, about 100 $mg \cdot L^{-1}$.

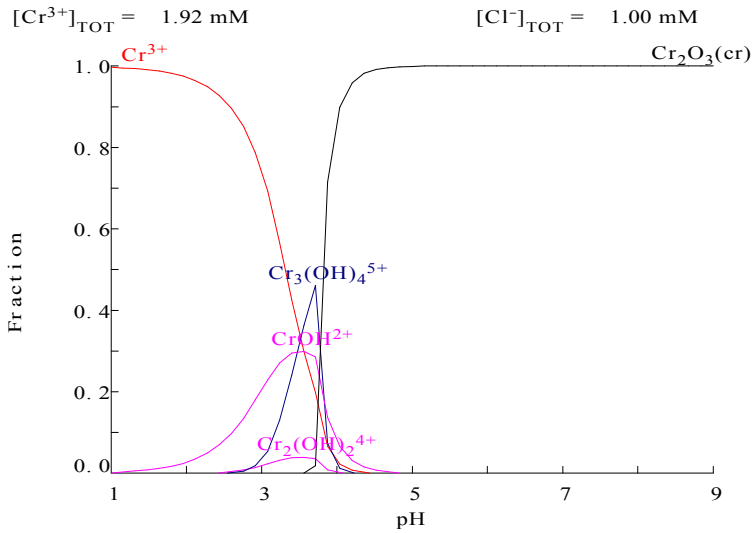

Figure 27: Cr(III) speciation diagram as a function of solution pH. [Cr(III)]=100.0 mg·L^{-1}. [Cl$^-$]=0,001 M.

As it can be seen in **Figure 27**, in the pH range studied, the main Cr(III) species in solution are Cr^{3+} and $Cr(OH)^{2+}$. According to this speciation, if Cr(III) sorption is due to a Ca^{2+} ion exchange, the next reactions, where the brackets indicate the solid alginate phase, could summarize the sorption process:

$$3\ \{COO\}_2\text{-}Ca + 2\ Cr^{3+} \leftrightarrow 2\ \{COO\}_3\text{-}Cr + 3\ Ca^{2+}$$

$$\{COO\}_2\text{-}Ca + CrOH^{2+} \leftrightarrow \{COO\}_2\text{-}CrOH + Ca^{2+}$$

These reactions indicate that the quotient between Ca^{2+} released and Cr(III) sorbed for each contact time would have to be between 1 (corresponding to the exchange of 1 Ca^{2+} atom by 1 molecule of monohydroxocomplex $Cr(OH)^{2+}$, $1Ca^{+2}/1Cr(OH)^{+2}$) and 1.5 (corresponding to the exchange of 3 atoms of Ca^{2+} by 2 atoms of Cr^{3+}, $3Ca^{+2}/2Cr^{+3}$)

As it can be observed in **Table 18**, the amount of Ca^{2+} released by gel bead is approximately 1-1.5 folds the amount of Cr(III) adsorbed for initial Cr(III) concentrations about 50 and 100 mg·L^{-1}. Nevertheless, this relation fails when initial metal concentration is 200 mg·L^{-1}. In this last case, the amount of Ca^{2+} released per bead is lower than the corresponding of Cr(III) sorbed. This fact suggests an ion exchange mechanism as main responsible of Cr(III) cationic species sorption onto both, CA and 2% GS-CA gel beads.

This mechanism provides a reasonably explanation for the sorption kinetics when initial metal concentrations are 50 and 100 mg·L^{-1}, but it fails when trying to explain the sorption

mechanism for an initial concentration of 200 mg·L^{-1}. In this last case, another mechanism different than Ca^{2+} ion exhange has to be the responsible of the extra Cr(III) sorption observed. Similar results were obtained by authors (Araujo and Teixeira, 1997) who reported that, at low Cr(III) concentrations, Ca^{2+} ion exchange was the dominant sorption mechanism but at high initial metal concentrations, other mechanism different than ion exhange, like surface complexation or microprecipitation could take place.

5.6.2. Calcium ions release in the sorption equilibrium

In the previous section it was observed that calcium ion exchange was able to explain trivalent chromium sorption for initial metal concentrations about 50 and 100 mg·L^{-1}. Nevertheless, it was observed that this mechanism failed to explain the sorption of the highest of the initial metal concentrations of the kinetics study, about 200 mg·L^{-1}. Thus, in order to determine the Cr(III) concentration range in which ion exchange describes sorption, equilibrium was studied for different initial Cr(III) concentrations in the range from 27.51 to 1580.20 mg·L^{-1}. The amount of Cr(III) sorbed and the amount of Ca^{2+} released was analysed and the quotient Ca^{2+} released/Cr(III) adsorbed (both per bead) was calculated. The results obtained for CA and 2% GS-CA beads are presented in **Tables 20** and **21** respectively.

Table 20: Cr(III) adsorbed and Ca^{2+} released per CA bead for different initial Cr(III) concentrations. pH_o=3.0, agitation time: 2880 minutes.

C_o (mg·L^{-1})	q_e Cr(III)·10^4 (mmol·bead^{-1})	Ca rel.·10^4 (mmol·bead^{-1})	Ca rel./Cr(III) sorb.
27.51	1.81	3.47	1.91
53.01	2.80	3.75	1.34
76.52	3.21	4.41	1.37
102.38	4.07	4.22	1.04
155.52	6.25	4.31	0.69
206.08	8.39	4.59	0.55
296.99	10.45	3.75	0.36
667.27	14.65	3.00	0.20
853.27	14.96	2.81	0.19
1103.27	15.56	3.19	0.21
1570.20	15.69	3.38	0.22

Table 21: Cr(III) adsorbed and Ca^{2+} released per 2% GS-CA bead for different initial Cr(III) concentrations. pH_o=3.00, agitation time: 2880 minutes.

C_o ($mg \cdot L^{-1}$)	q_e Cr(III)·10^4 ($mmol \cdot bead^{-1}$)	Ca rel.·10^4 ($mmol \cdot bead^{-1}$)	Ca rel./Cr(III) sorb.
27.51	1.94	3.75	1.94
53.01	3.37	4.69	1.39
76.52	4.06	5.06	1.25
102.38	4.92	6.28	1.28
155.52	6.56	6.28	0.96
206.08	8.52	6.39	0.75
296.99	11.89	6.28	0.53
667.27	18.35	4.88	0.27
853.27	18.83	3.94	0.21
1103.27	20.03	3.66	0.18
1570.20	20.94	4.31	0.21

The results obtained in this section put into evidence that ion exchange would successfully describe Cr(III) sorption in the initial concentration range from 27.51 to 102.38 $mg \cdot L^{-1}$ in the case of CA and from 27.51 to 155.52 in the case of 2% GS-CA gel beads. It is noteworthy the broader applicability range of the ion exchange mechanism in the case of beads containing grape stalk than in these of pure calcium alginate. This fact indicates that grapes stalk might contain basic groups binded to Ca^{2+} available for Cr(III) cations coordination.

For initial metal concentrations higher than about 100 $mg \cdot L^{-1}$ in the case of CA and 150 in the case of 2% GS-CA, the participation of mechanisms other than ion exchange such as surface complexation, chelation or microprecipitation of Cr(III) hydroxides have to be taken into account in the net metal removal.

5.7. Spectroscopic analysis of the material and of the sorption mechanism

5.7.1. Fourier Transform Infrared-Attenuated Total Reflectance Spectroscopy (FTIR-ATR).

In order to obtain information about the contribution of the different functional groups of grape stalks and calcium alginate in the removal of either Cr(III) and Cr(VI) by CA and 2% GS-CA gel beads, FTIR-ATR analysis in the solid phase were carried out before and after loading the material with chromium.

The samples for these analyses were prepared according to the protocol described in section 4.3. Initial metal concentration was 800 $mg \cdot L^{-1}$ and initial pH was 3.0.

The spectra of the beads containing GS is not shown due to the overlap of the bands of CA with these of vegetal material. In **Figures 25** and **26**, the infrared spectra of grape stalk and of calcium alginate before and after Cr(III) and Cr(VI) sorption are presented, respectively. In the spectra, the position of the main bands that suffer position modifications after metal sorption have been indicated with arrows.

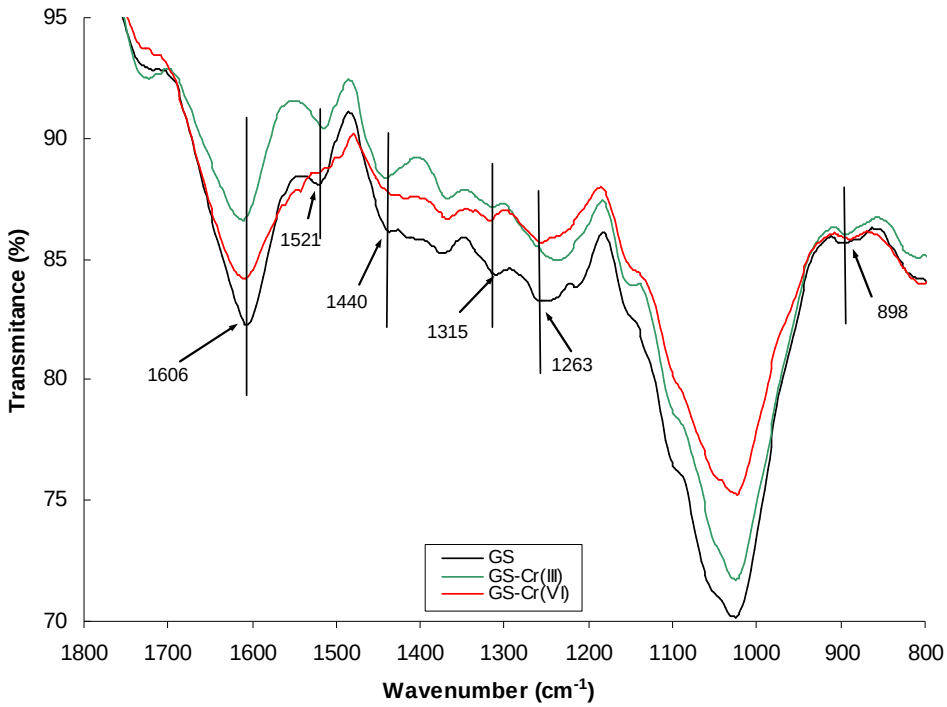

Figure 28: Grape stalk FTIR-ATR spectra before and after treatment with Cr(III) and Cr(VI) solutions. Initial metal concentration: 800 $mg \cdot L^{-1}$. Agitation time: 24 h. pH_o= 3.

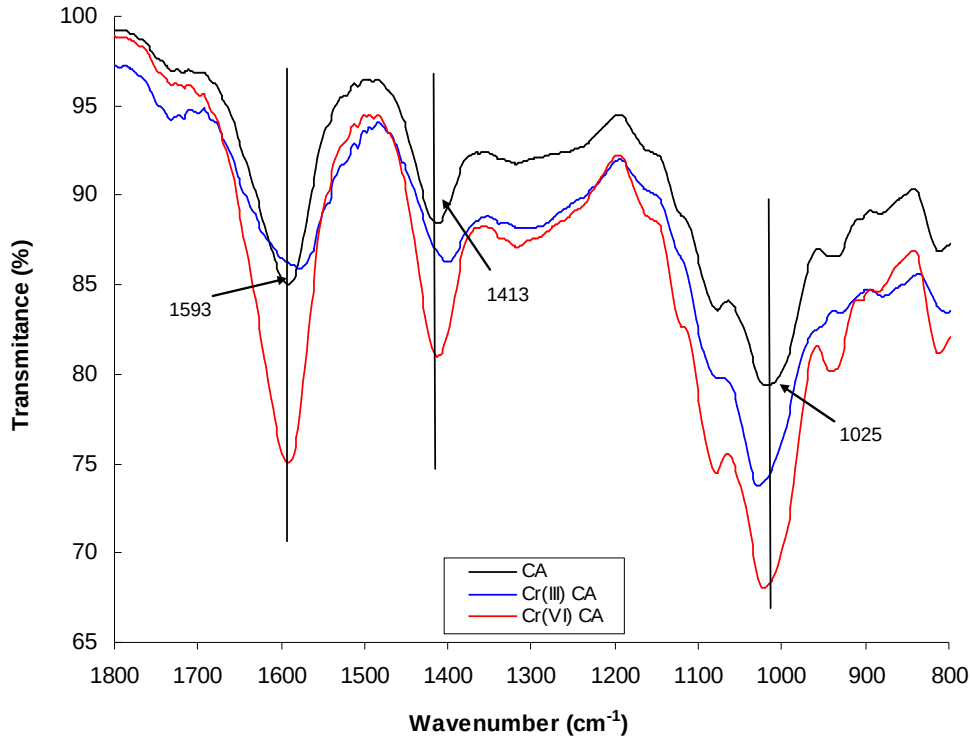

Figure 29: Calcium alginate FTIR-ATR spectra before and after treatment with Cr(III) and Cr(VI) solutions. Initial metal concentration: 800 mg·L^{-1}; Agitation time: 24 h; pH_o= 3.

For an easier visualization of the effect of chromium loading on the materials, the initial and final position of the modified bands has been presented in the next table as well as the possible assignation of the bands to the corresponding functional groups involved in Cr(III) and Cr(VI) sorption is shown.

Table 22: Observed frequencies and assignation.

Frequency (cm^{-1})			Assignation
CA	**CA-Cr(III)**	**CA-Cr(VI)**	
1020	1028	1022	Undetermined
1415	1398	1413	COO^- stretching symmetric (Sartori *et al*., 1997)
1594	1581	1592	COO^- stretching asymmetric (Sun *et al*., 2004)
GS	**GS-Cr(III)**	**GS-Cr(VI)**	
898	897	898	Carbohydrates (unaltered) (Dupont and Guillon, 2003)
1263	1238	1247	Guayacyl/C-O phenolic (Twadowska and Kyziol, 2003)
1315	1319	1321	Syringyl (Dupont and Guillon, 2003)
1440	1444	1421	Metoxi deformation (Dupont and Guillon, 2003)
1521	1515	1511	Aromatic skeleton vibration (Dupont and Guillon, 2003)
1606	1614	1612	C=C Aromatic vibration (Dupont and Guillon, 2003)

As it can be seen in the infrared spectra of calcium alginate, after Cr(III) treatment, the main modifications are based in the displacement of the bands related to asymmetric and symmetric vibration of the carboxylate function (1594 and 1415 cm^{-1} respectively). This fact is indicative of the binding of Cr(III) to this functional group. On the other hand almost no modifications of calcium alginate bands was noticed after contact of this material with solutions containing Cr(VI). This result is consistent with the low sorption of this oxidation state onto the pure calcium alginate gel.

In the case of grape stalk treated with Cr(III) and Cr(VI) solutions, the main modifications observed are the corresponding to the characteristic bands of Syringyl and Guayacyl units of the lignin (1263 and 1315 cm^{-1} respectively), the methoxy deformation (1440 cm^{-1}), the aromatic skeleton vibration (1521 cm^{-1}) and the aromatic ring vibration (1606 cm^{-1}). All these bands, characteristic of the lignin macromolecule, indicate that both, Cr(III) and Cr(VI) are adsorbed onto this component of the sorbent, remaining the cellulose almost unaltered during the sorption process. The important role of lignin in sorption of copper and nickel onto cork had been previously noticed by results of ^{13}CP-MAS NMR on the solid phase of the sorbent (Villaescusa *et al*., 2002).

5.7.2. Electron Paramagnetic Resonance (EPR).

In previous studies on Cr(VI) sorption carried out in our laboratory, it was noticed that raw grape stalk was able to reduce Cr(VI) to Cr(III). In fact, several authors had found Cr(VI) sorption mechanism partially based on its reduction to trivalent chromium, and that the Cr(III) formed could remain fixed to the surface (Nakano *et al.,* 2001) or being partially released to the solution (Gardea-Torresdey *et al*., 2000; Fiol *et al*., 2008; Park *et al*., 2004; Park *et al*., 2005; Dupont and Guillon, 2003).

In our case, despite no Cr(III) in solution was detected in Cr(VI) sorption kinetics on either CA or 2% GS-CA, the strong proton consumption while hexavalent chromium was being sorbed suggests that reduction might take place, but the chromium formed is not released to the fluid. So, the evaluation of the oxidation state of the sorbed chromium would provide us of useful mechanistical information and also of the potential toxicity of the chromium-laden material. As it was discussed in the introductory section, it's evident that the toxicity of a solid Cr(VI)-laden material would be greater than the corresponding to the Cr(III) one. That's why, the possible presence of sorbed Cr(III) on the solid phase was studied in this section. To carry out this study, the Cr(III) permanent magnetism (because of its d^3 electronic configuration) was useful for its detection in the solid phase by means of the Electron Paramagnetic Resonance technique (EPR).

In order to obtain information about the effect of initial solution pH and initial Cr(VI) concentration on the reducing capacity of CA and 2% GS-CA gel beads, experiments at two different initial pHs (1 and 3) and two different initial metal concentrations (100 and 800 $mg \cdot L^{-1}$) were carried out. EPR spectra obtained in the different scenarios are presented in the next figure:

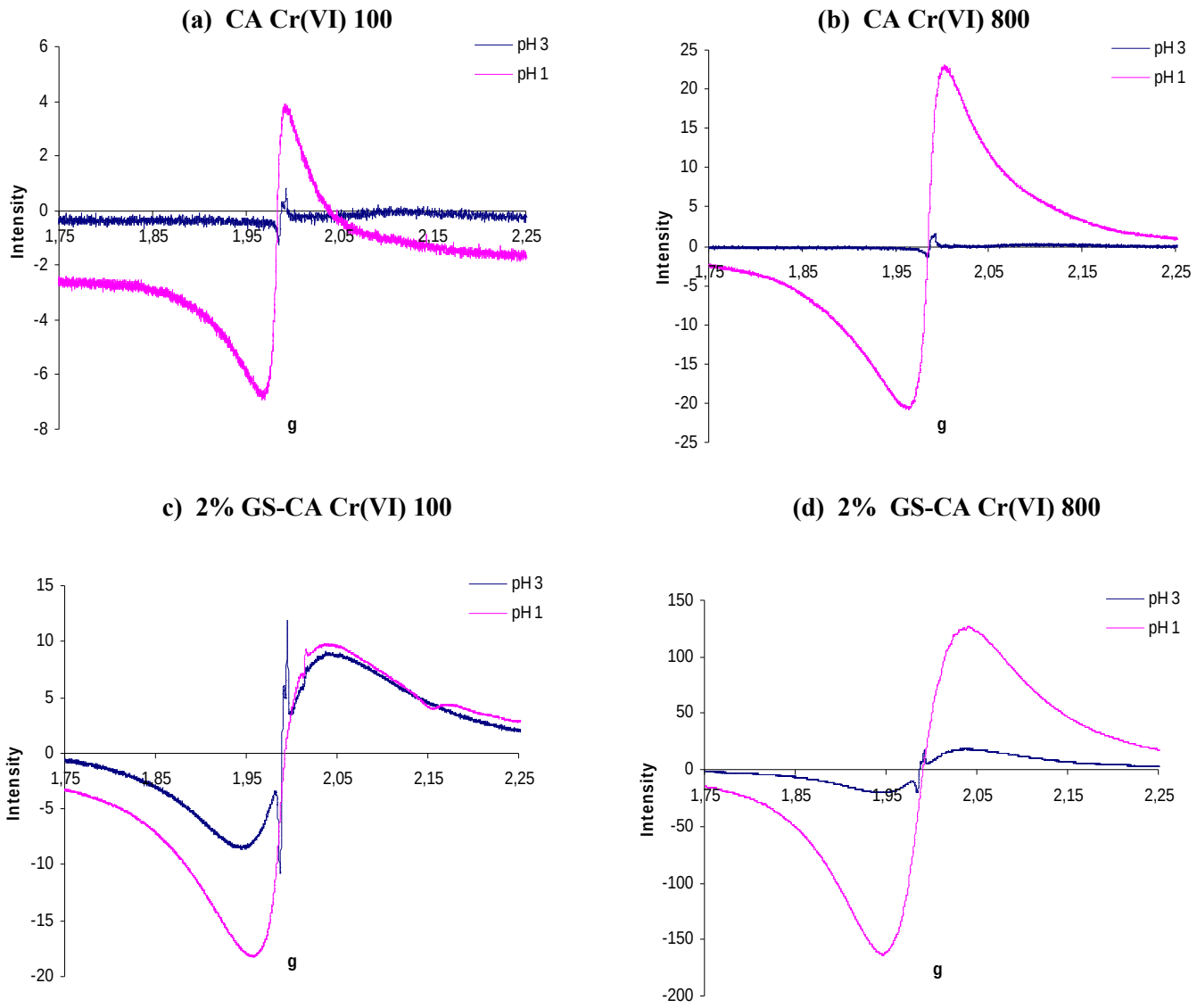

Figure 30: Paramagnetic Electron Resonance spectra of CA and 2% GS-CA beads contacted with Cr(VI) solutions. Initial metal concentration: 100 or 800 $mg \cdot L^{-1}$; Agitation time: 24 h; Initial pH: 1 or 3.

(e) *Magnification spectra (d)

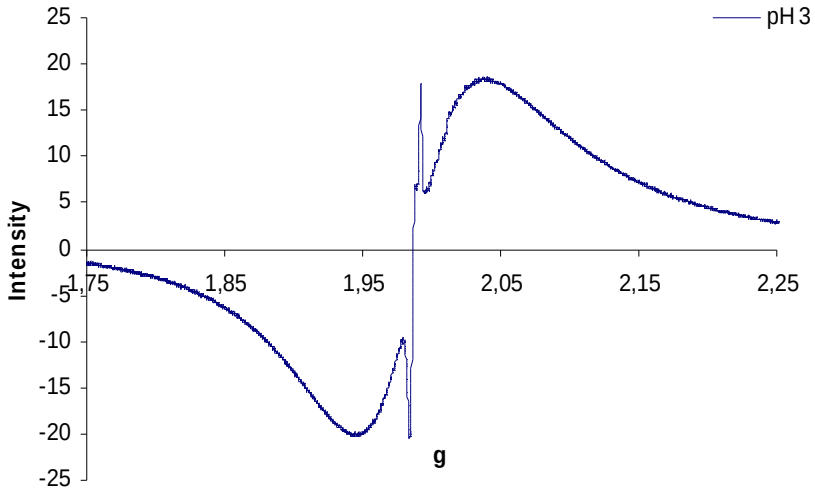

In the first of the spectra (**Figure 30 (a)**), reducing capacity as a function of the initial solution pH was studied for an initial Cr(VI) concentration of 100 $mg \cdot L^{-1}$. The intensity of the EPR signal is indicative of the Cr(III) concentration in the solid phase. In the spectra it can be observed the appearance of a very broad band centered at g=1.982, that might be attributed to Cr(III). As it can be evidenced by the low intensity of the EPR signal corresponding to pH 3 treatment, the extension of Cr(VI) to Cr(III) reduction is very low, however, when for the same initial Cr(VI) concentration the sorption experiment is carried out at pH 1, a higher EPR intensity signal is observed. These facts put into evidence that CA is able to reduce Cr(VI) to Cr(III), but only under strong acidic conditions.

If Cr(VI) to Cr(III) reduction by CA is studied for a higher initial metal concentration as a function of the initial solution pH, an analogous result is observed (**Figure 30 (b)**). A higher Cr(III) amount remains sorbed on the solid phase, as indicates the higher intensity of the EPR signal, as lower is the initial solution pH. These results support the experimental observation of **Figure 30 (a)**; calcium alginate can act as a Cr(VI) to Cr(III) reducing agent, and the extension of the reduction reaction increases when it does the initial H^+ concentration in solution.

In the same way as in the case of pure CA beads, reductive power of 2% GS-CA as a function of pH and Cr(VI) metal concentration was evaluated. **Figure 30 (c)** corresponds to the Cr(VI) treatment of 2% GS-CA gel beads with an initial metal concentration of 100 $mg \cdot L^{-1}$ at pH 3 and 1. In the spectra corresponding to the treatment at pH 3, a very narrow

signal centered at a g value of 1.970, is observed. The appearance of this signal, attributed to Cr(V), has been previously reported by authors when studying Cr(VI) to Cr(III) reduction by plant roots (Micera and Dessi, 1988) and when studying the formation of paramagnetic intermediates when treating wood with Cr(VI) solutions (Humar *et al.,* 2004). As it can be observed in **Figure 30 (c)**, the presence of Cr(V) was only observed in the case of the treatment of 2% GS-CA sorbents with hexavalent chromium solutions of initial pH 3.0. In the case of the treatment of the same sorbent with Cr(VI) solution at initial pH 1, only the broad signal corresponding to Cr(III) was observed. The absence of the Cr(V) signal at pH 1, could be explained by the total Cr(VI) to Cr(III) reduction that would take place in excess of H^+ in the media (conditions of strong acidity).

Figure 30 (d) corresponds to the treatment of 2% GS-CA beads with a solution containing 800 $mg \cdot L^{-1}$ of Cr(VI) at initial pHs 3 and 1. As it can be observed by the intensity of the EPR signal, the treatment in the most acidic conditions leads to the formation of a very important amount of Cr(III) in the solid phase. The high scale needed to completely observe the EPR band when material is contacted with the Cr(VI) solution at pH 1 makes difficult the observation of the details of the treatment at pH 3. So that, a magnification of this spectra has been presented in **Figure 30 (e)**. In this figure, it can be observed that the shape of this spectra is similar to the obtained after treatment with the 100 $mg \cdot L^{-1}$ Cr(VI) solution at initial pH 3; presence of a broad band corresponding to Cr(III) and a very narrow one, corresponding to Cr(V). Despite initial Cr(VI) concentration of the spectra of **Figure 30 (e)** is 8 folds higher than in the experiment corresponding to **Figure 30 (c)**, the EPR intensity of Cr(III) signal is not much higher. These results support the fact that, in presence of an excess of Cr(VI), H^+ can act as a limiting reagent in the extension of the reduction.

5.7.3. Scanning Electron Microscopy-Energy Dispersive X-Ray analysis and Backscattered Electrons Microscopy study (SEM-EDX, BSE)

In order to obtain morphologic and local chemical information of the gel beads before and after Cr(III) and Cr(VI) sorption, Scanning Electron Microscopy (SEM) coupled to Energy Dispersive X-Ray analysis (EDX) was carried out. Furthermore, micrographs in the Backscattered Electron mode (BSE) were also taken. This technique was employed in an attempt to detect high electronic density regions that could be attributed to the presence of metallic deposits in the solid surfaces under study. Backscattered electrons consist of high-energy electrons originated in the electron beam that are reflected or back-scattered out of the specimen interaction volume. These electrons may be used to detect contrast between areas with different chemical compositions, specially when the average atomic number of the various regions is different, since the brightness of the BSE image tends to increase with the atomic number (Goldstein *et al*., 1981). These regions, of high electronic density, are known to produce a special bright, that can be clearly differenced in a surface mainly formed by light atoms (C, O and H), as is the case of the organic material used as sorbent.

Chromium loading of the samples was carried out according to the procedure described in section 4.3. Initial metal concentration was about 800 $mg \cdot L^{-1}$ and initial pH was adjusted to 3.0. Prior to the analysis, samples were carbon-coated to improve its electrical conductivity and immersed in a colloidal silver gel.

Each figure is formed by the next elements: (a) micrograph in Electronic Scanning mode (SEM), (b) micrograph in the Backscattered Electrons mode (BSE) and (c) X-Ray Energy Dispersive (EDX) spectra with the local chemical composition summarized in a table.

5.7.3.1. Morphological and compositional study of the calcium alginate

In **Figure 31**, SEM-EDX, BSE analysis of the dry spheres of calcium alginate is shown.

(a) (b)

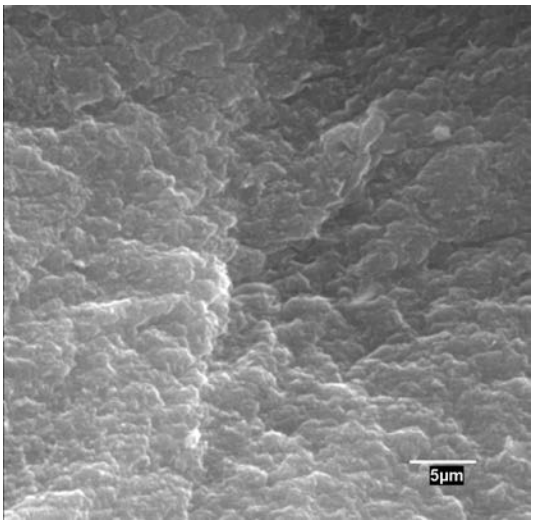

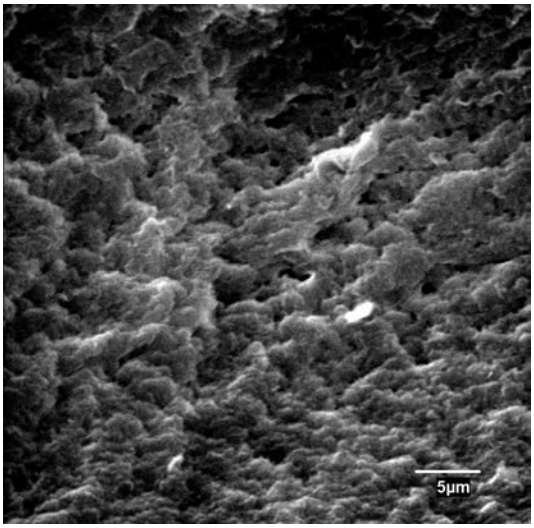

(c)

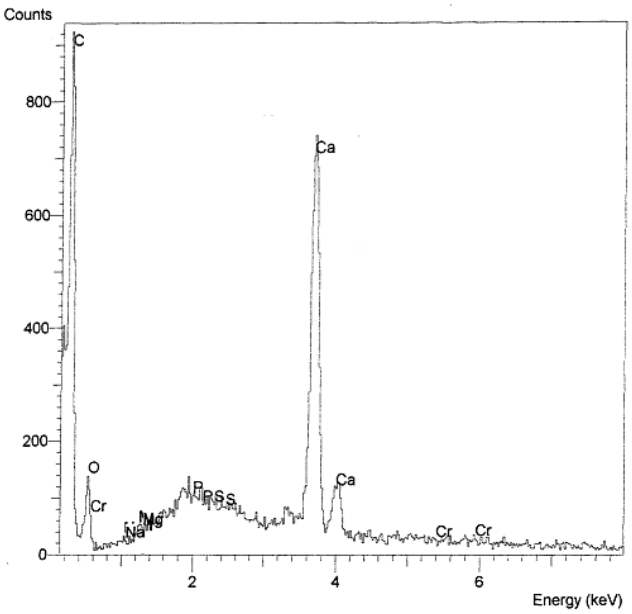

Element	Percentage
C	54.11
O	23.18
Na	N.D.
Ca	22.63
Cr	N.D.

Figure 31: SEM-BSE, EDX analysis of calcium alginate. Electronic micrograph in (a) Scanning mode (b) Backscattered mode and (c) EDX analysis.

In the Scanning Electron micrograph the heterogeneous external topology of the calcium alginate beads can be evidenced. The BSE micrograph, shows no special brightness regions, so that, no metallic deposits are on the surface of this material. The local composition evaluated by the EDX spectra, indicates that this material is mainly formed by C, O and Ca. Despite this material also contains H, this atom doesn't appear in this kind of spectroscopy. As can be seen in the table, calcium represents a very important part of the calcium alginate, around 23% of the dry mass.

5.7.3.2. Study of the zone distribution of Cr(III) and Cr(VI) on 2% GS-CA gel beads.

In this study, information about Cr(III) and Cr(VI) distribution onto 2% GS-CA gel beads was tried to be obtain. To reach this goal, SEM-BSE, EDX analysis on the different regions of the sorbent were carried out. The regions under study were, thus, the calcium alginate matrix itself, the grape stalk particle and the interface alginate-grape stalk region.

5.7.3.2.1. Cr(III) zone distribution study on 2% GS-CA gel beads

Next figure shows the alginate region of the 2% GS-CA beads after treatment with the Cr(III) solution.

(a) (b)

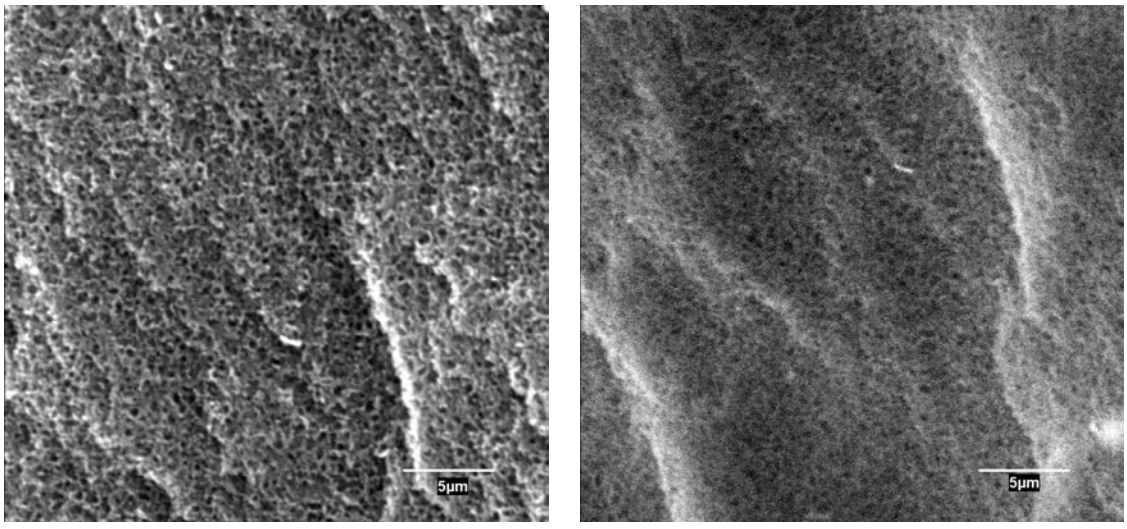

(c)

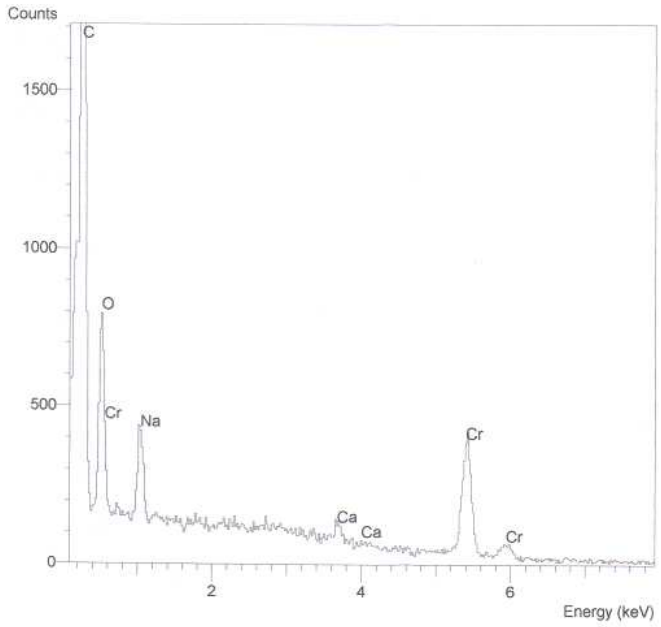

Element	Percentage
C	59.92
O	25.91
Na	4.61
Ca	0.49
Cr	7.27

Figure 32: SEM-BSE, EDX analysis of 2% GS-CA gel beads after treatment with Cr(III) solution. Electronic micrograph in (a) Scanning mode (b) Backscattered mode and (c) EDX analysis.

As it can be seen, the alginate surface after contacting with the Cr(III) solution, appears as a denser and more porous structure if is compared to the SEM picture of only CA (**Figure 31**). In section 5.5, where the ion exchange Ca^{2+}-Cr(III) was discussed, it was found that this mechanism was the main responsible of Cr(III) sorption. Its possible that Ca^{2+} substitution in the hydrogel structure by either Cr^{3+} or $Cr(OH)^{2+}$ species, modifies the structural characteristics of the polymer and this might be reflected in a morphology change. By the BSE microscopy, the absence of metallic deposits on the surface was checked, indicating thus, that Cr(III), under the experimental conditions of this study, is not removed by microprecipitation on CA hydrogel. After the contact of the material with the Cr(III) solution, the EDX analysis showed a very important Cr amount (7.27 %) in the alginate region of the sorbent and an important Ca^{2+} decrease (from 22.63 % to 0.49 %), if compared to the amount existing in the non-treated material. This observation confirms the fact that Cr(III) is mainly removed by ion exchange, and that this ion exchange takes place mainly by the Ca^{2+} present on the calcium alginate hydrogel structure.

The next region under analysis was the interface that is formed in the contact region between alginate and grape stalk particles. Surface topology and local compositional analysis of this region are shown next.

(a) (b)

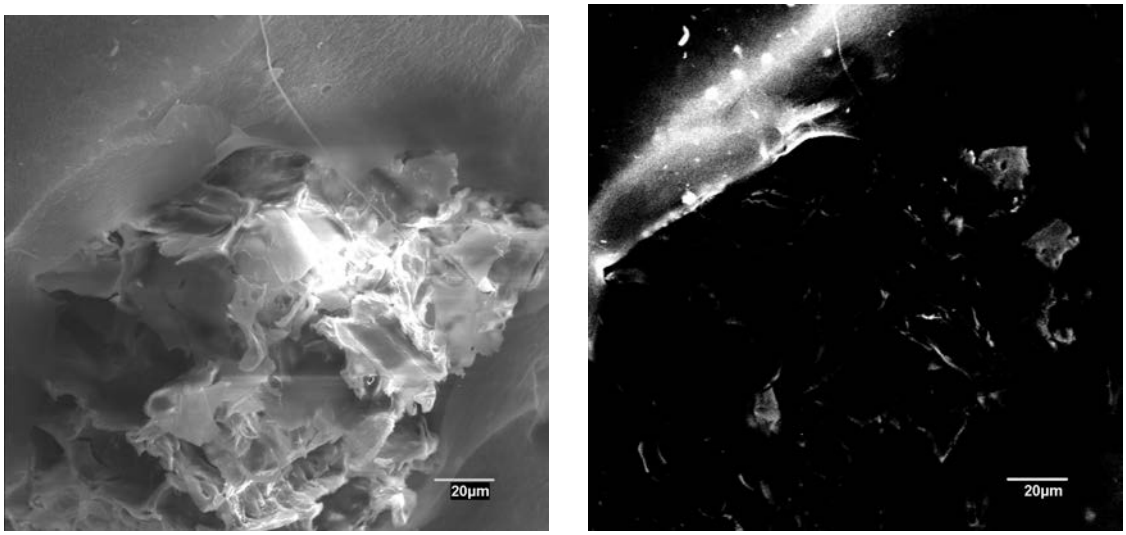

(c)

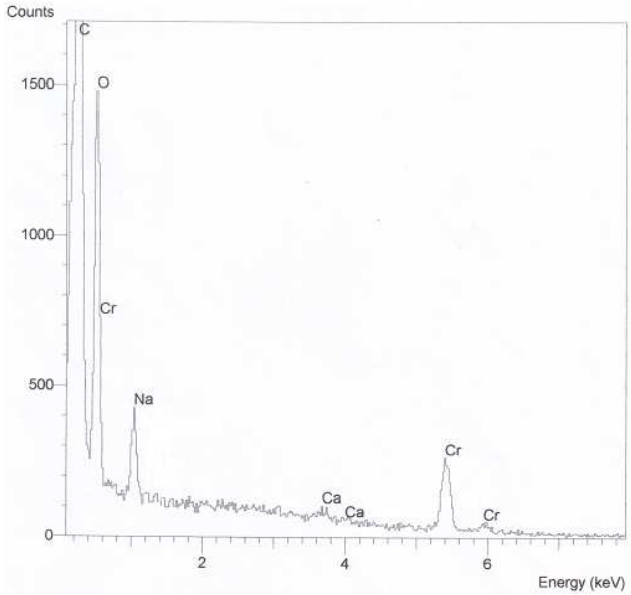

Element	Percentage
C	55.80
O	36.04
Na	3.24
Ca	N.D.
Cr	3.67

Figure 33: SEM-BSE, EDX analysis in an interface alginate-grape stalk particle region, after treatment with Cr(III) solution. Electronic micrograph in (a) Scanning mode (b) Backscattered mode and (c) EDX analysis.

Figure 33(a) shows the more heterogeneous morphology of grape stalk particle than of than calcium alginate. On the other hand, no deposits that could indicate the formation of local metal deposition due to a Cr(III) microprecipitation process, appear on the surface of the material. In order to further confirm this last affirmation, an electronic picture in the backscattered electrons mode was taken in this same region. As it can be seen, no special brightness regions that could be attributed to metallic deposits appear on the surface under study, discarding thus a Cr(III) local precipitation in the interface alginate-grape stalks.

If local chemical composition in this sorbent area is compared with that of calcium alginate after treatment with Cr(III) solution, almost no differences are evidenced, despite Cr(III) percentage in this interface region (3.67 %) is much lower than the observed in the alginic region (7.27 %). This fact is indicative of the higher affinity of CA for the trivalent chromium than the GS. Finally, and to confirm this last hypothesis, the surface of the grape stalk after Cr(III) treatment, was analysed too and results are presented in **Figure 34**.

(a) (b)

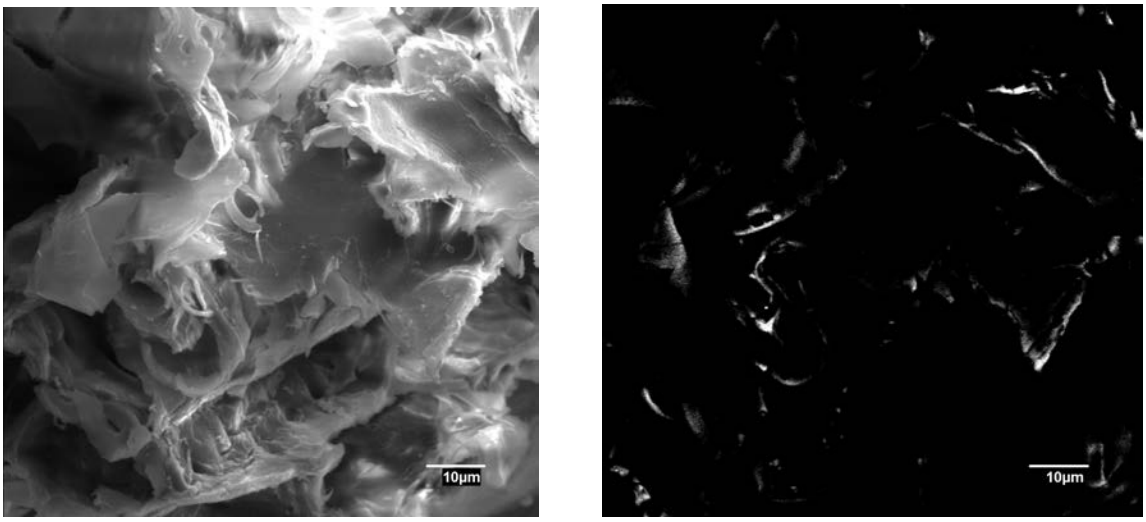

(c)

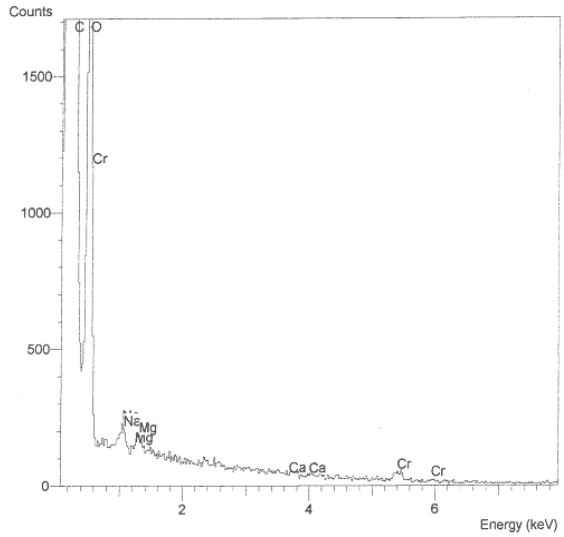

Element	Percentage
C	58.48
O	40.47
Na	0.59
Ca	N.D.
Cr	0.30

Figure 34: SEM-BSE, EDX analysis of 2% GS-CA in the region corresponding to a GS particle, after treatment with Cr(III) solution. Electronic micrograph in (a) Scanning mode (b) Backscattered mode and (c) EDX analysis.

As it can be seen in the SEM and BSE picture, neither surface deposit nor specially bright areas, respectively, were observed, indicating thus that local microprecipitation onto the surface of GS would not be take place in our experimental conditions.

If the GS surface chemical composition is analysed and it is compared with the composition of the regions studied in **Figures 32** and **33**, valuable information about the affinity of Cr(III) for the different materials of the sorbent can be extracted. As it can be seen, the EDX analysis of the GS surface shows a very low metal concentration (around 0.3 %) when it's compared with the concentration in the interface alginate-grape stalk particle (3.67 %) or still more, when it's compared with the metal concentration in the alginic region (7.27 %). These results strongly support the role of calcium alginate as main responsible of trivalent chromium sorption, while only a small amount of Cr(III) would be uptaken by the grape stalk particles.

The same methodology employed until this moment to explore the Cr(III) distribution in the different 2% GS-CA regions, was employed to analyse Cr(VI) distribution. The obtained results are presented in the next section.

5.7.3.2.2. Cr(VI) zone distribution study on 2% GS-CA gel beads

Calcium alginate beads after contacting with the Cr(VI) solution were analysed and results are shown in next figure.

(a) (b)

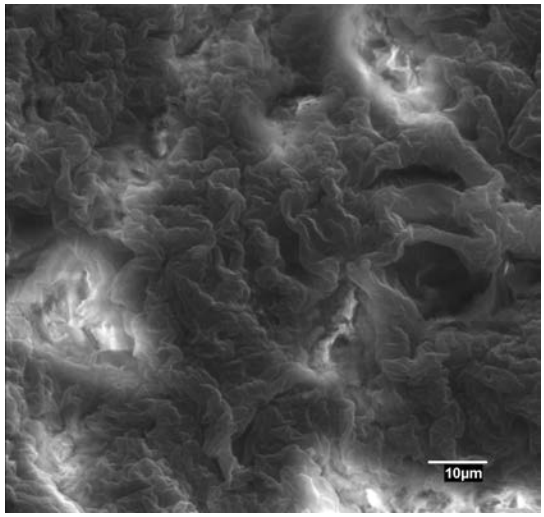

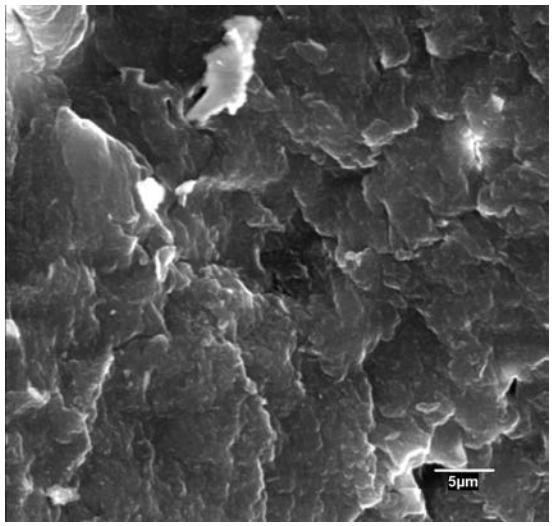

(c)

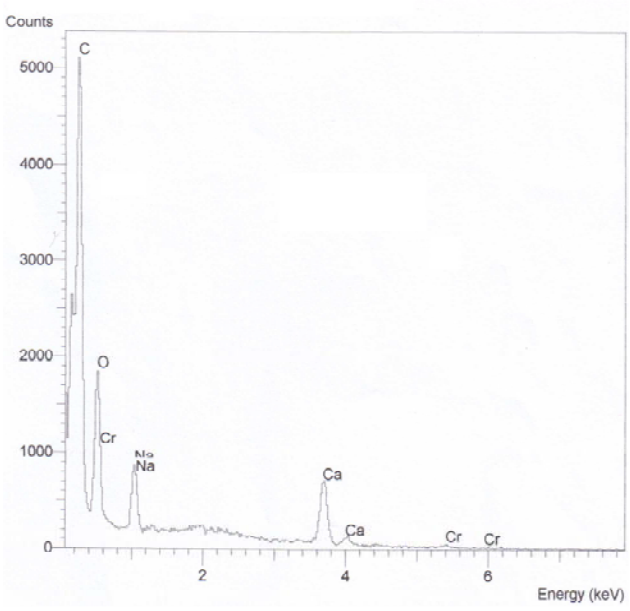

Element	Percentage
C	55.79
O	34.93
Na	4.97
Ca	3.78
Cr	N.D.

Figure 35: SEM-BSE, EDX analysis of CA gel beads after treatment with Cr(VI) solution. Electronic micrograph in (a) Scanning mode (b) Backscattered mode and (c) EDX analysis.

In the pictures carried out in Scanning and in Backscattered mode of the CA gel beads after treatment with Cr(VI), it can be observed that the topology is quite similar to the obtained for the untreated material (**Figure 31**), indicating thus that alginate structure suffers almost no modification after the contact with hexavalent chromium. On the other hand, kinetic and equilibrium studies demonstrated that the main responsible of Cr(VI) sorption in 2% GS-CA was the grape stalk. If EDX spectra and quantitative chemical analysis of the surface of CA is observed, it can be seen that there is no Cr in the calcium alginate gel. The obtained microscopical and spectroscopical data strongly support the low Cr(VI) sorption observed in both, kinetic and equilibrium experiments.

Conversely, it had been demonstrated with the kinetic and equilibrium experiments that 2% GS-CA was able to remove a very important amount of Cr when it was contacted with Cr(VI) solutions. In order to clarify wether this chromium is fixed in the composite grape stalks-calcium alginate sorbent and ascertain the role of both materials in Cr(VI) sorption, an analysis on different regions of these beads was carried out. The obtained results are presented in **Figures 36** and **37**.

(a) (b)

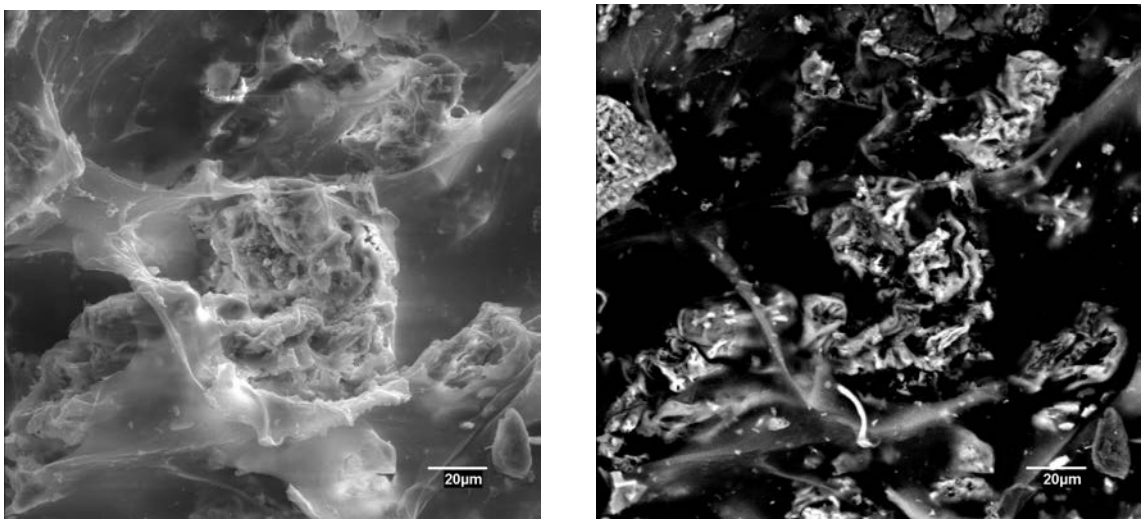

(c)

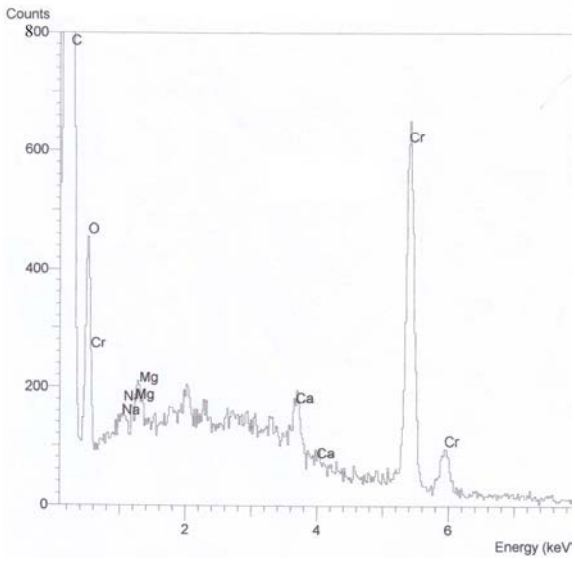

Element	Percentage
C	52.90
O	39.50
Na	1.01
Ca	2.24
Cr	5.35

Figure 36: SEM-BSE, EDX analysis of 2% GS-CA gel beads after treatment with Cr(VI) solution. Electronic micrograph in (a) Scanning mode (b) Backscattered mode and (c) EDX analysis.

As it can be observed in SEM micrography, **36(a)**, GS particles are surrounded by the calcium alginate matrix. In this picture, some pellets on the surface of the grape stalk particle seem to appear. In order to check if these nodules are electronic-rich regions, the micrographs of the same region in BSE mode were taken. BSE pictures demonstrated that GS region appeared with a particular brightness, indicating thus that it could be a chromium enriched region. If the same region of the sorbent is further analised by EDX, its local chemical composition can be obtained. The EDX spectra indicates an intense chromium line that, when quantified, reveals a high chromium content (5.35%) on the surface of the grape stalk particle. These results indicate that treatment of the alginate beads containing grape stalk particles with Cr(VI) solutions lead to the selective concentration of chromium mainly on the surface of the grape stalk. In order to check this observation, a further surface analysis at greater magnification and focusing only on the GS surface was carried out. SEM and BSE micrographs are presented in the next figures.

(a) (b)

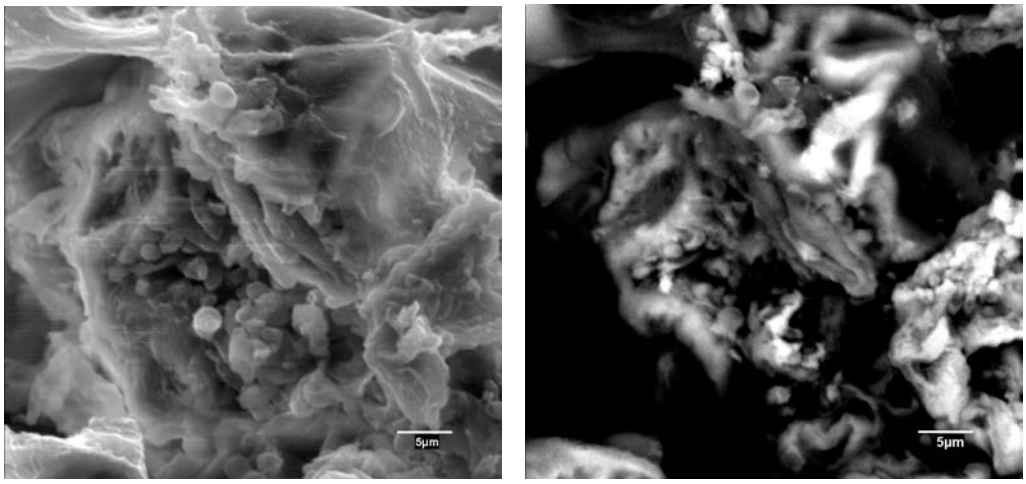

As it can be seen, scanning electron micrograph show important nodule coverage of the GS surface. In order to check the nature of these pellets, micrograph in the backscattered electrons mode of this region was taken, and picture labelled as (b) was obtained. In this picture it can be clearly observed the brightness of either GS surface and, in particular, of the pellets covering its surface, indicating thus that those are electronically high density regions. This fact could be indicative of some kind of surface precipitation or deposition of any chromium species.

Additionally, two more pictures focusing on the presence of surface nodules and its brightness in BSE are shown next. EDX spectra and chemical percentage composition of this region is also shown in **Figure 37**.

(a) (b)

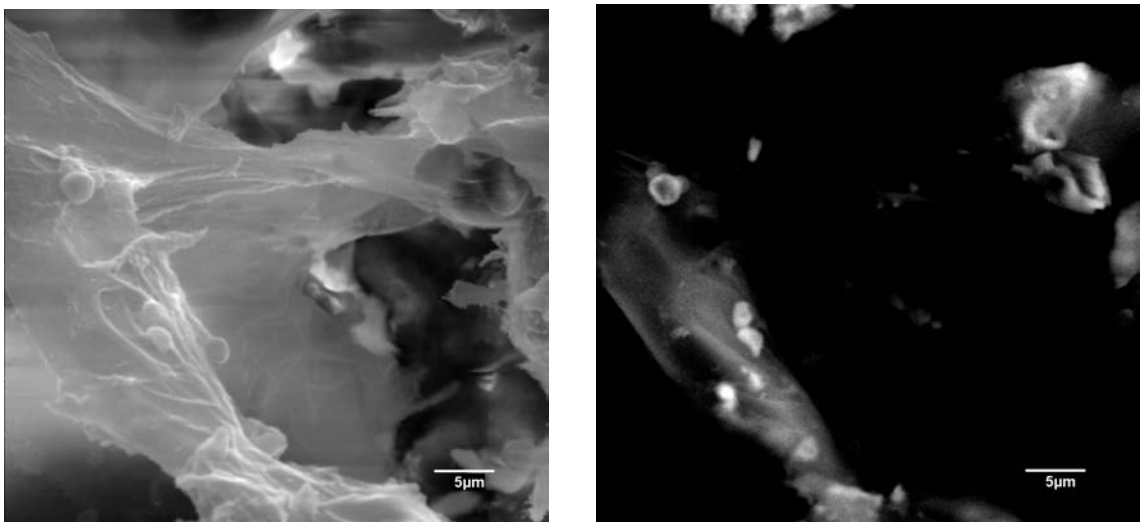

(c)

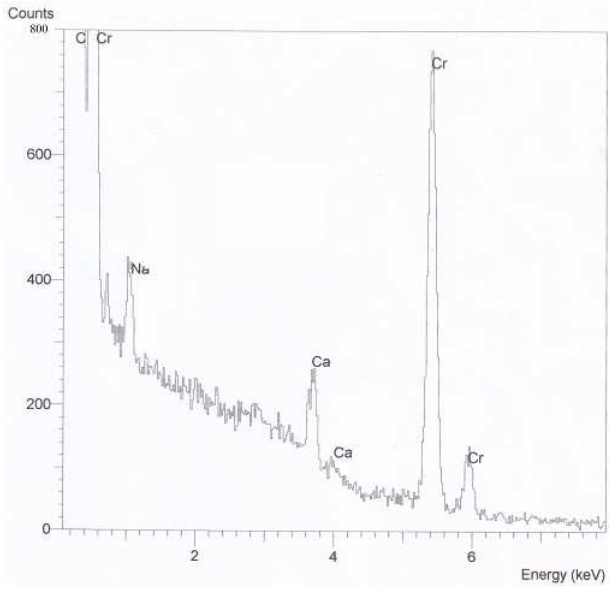

Element	Percentage
C	60.49
O	20.36
Na	0.82
Ca	1.20
Cr	16.40

Figure 37: SEM-BSE, EDX analysis of 2% GS-CA gel beads after treatment with Cr(VI) solution. Electronic micrograph in (a) Scanning mode (b) Backscattered mode and (c) EDX analysis.

As can be seen, the pellets on the surface of the grape stalk contain a important Cr content, 16.4%, indicating thus, that are formations of some type of chromium precipitate. Although SEM-EDX technique allows the obtention of valuable information about the surface topology and local chemical composition and by means of the BSE technique, information about the presence of metallic deposits can be derived, any of them is capable to provide us of information related to the oxidation state of the metal deposits found in the surface.

However, by means of the Electron Paramagnetic Resonance (EPR) technique, it had been previously checked the presence of Cr(III) sorbed onto 2% GS-CA, coming from Cr(VI) reduction.

It's possible that, after reduction process, where 7 mols of H^+ are consumed per mol of Cr(VI) reduced and, in such a basic pH as the produced after this H^+ consumption, the Cr(III) formed could precipitate as some kind of hydroxide or oxide, onto the surface that suffered the reduction. Indeed, this Cr(VI) to Cr(III) reduction with subsequent precipitation of the Cr(III) formed onto the surface has been previously reported by several authors (Kratochvil *et al*., 1998; Mel Lytle *et al*., 1998; Micera and Dessi, 1988).

6. CONCLUSIONS

The results derived from the present chapter lead us to the obtention of different conclusions.

Grape stalk wastes entrapped in calcium alginate efficiently remove both, trivalent and hexavalent chromium from aqueous solutions. The sorption is strongly pH-dependent; while in the case of Cr(III) initial pHs higher than 3 are optimal, in the case of Cr(VI), an initial pH about 3 shows the best performance.

Cr(III) sorption onto 2% GS-CA takes place mainly by a Ca^{2+} ionic exchange mechanism on the calcium alginate gel matrix and proton acts as a competing agent. In contrast, Cr(VI) sorption occurs mainly in the grape stalk particles due to a combined sorption/reduction mechanism. In the case of Cr(VI), the H^{+} plays an important role in the chemistry of both, coordination to the solid surface and on its reduction to Cr(III).

Cr(III) sorption onto 2% GS-CA is faster than Cr(VI) sorption. While the calcium alginate gel matrix is the main active component for Cr(III) sorption, Cr(VI) sorption occurs mainly on the grape stalk particles. In last term, while Cr(III) is directly adsorbed by the permeable alginate gel, Cr(VI) has to diffuse through the bulk of the alginate gel to reach the solid GS particles, being this fact reflected in an overall slowing down of the Cr(VI) removal rate.

The instrumental analysis of the solid samples before and after Cr(III) and Cr(VI) sorption provides useful information about the sorption mechanism. FTIR-ATR analysis indicate that carboxylates of calcium alginate are the main active group for Cr(III) sorption. In the case of Cr(VI), lignin is the main responsible of sorption. Cr(VI) sorption mechanism by 2% GS-CA gel beads is partially based in a reduction to Cr(III) promoted by GS. The extension of this reduction is strongly pH dependent and it seems to occur by formation of paramagnetic Cr(V) intermediates. At pH 3, the Cr(III) formed by reduction of the Cr(VI) in the GS particles is not transferred to the solution because CA acts as a barrier to its release.

Mycroscopic analysis of the solid surfaces confirms that calcium alginate is the main responsible of Cr(III) sorption, contributing this material only in slight extension to Cr(VI) sorption. On the other hand, grape stalk was found to be the main responsible for Cr(VI) sorption. Formation of high chromium content pellets on the GS surface after treatment with Cr(VI) solutions indicated a possible proton consuming reduction to Cr(III) followed by microprecipitation of $Cr(OH)_3$.

7. REFERENCES

· Araujo M., Teixeira J.A., Trivalent chromium sorption on alginate beads, Int. Biodeter. Biodegr. 40 (1997) 63-74.

· Aravindhan, R., Madhan, B., Rao, J.R., Nair, B.U., Recovery and reuse of chromium from tannery wastewaters using *Turbinaria ornata* seaweed, J. Chem. Techol. Biotechnol. 79 (11) (2004) 1251-1258.

· Bai, R.S., Abraham, T.E., Studies on chromium(VI) adsorption-desorption using immobilized fungal biomass. Bioresource Technol. 87 (2003) 17-26.

· Chang, J.S., Huang, J.C., Selective adsorption/recovery of Pb, Cu and Cd with multiple fixed beds containing immobilized bacterial biomass. Biotechnol. Prog. 14 (1998) 735-741.

· Cochrane, E.L., Lu, S., Gibbs, S.W., Villaescusa, I., A comparison of low-cost biosorbents and commercial sorbents for the removal of copper from aqueous media, J. Hazard. Mater. B137 (2006) 198-206.

· Daneshvar, N., Salari, D., Aber, S., Chromium adsorption and Cr(VI) reduction to trivalent chromium in aqueous solutions by soya cake, J. Hazard. Mater. B94: (2002) 49-61.

· Dean, S.A., Tobin, J.M., Uptake of chromium cations and anions by milled peat, Resour. Conserv. Recycl. 27 (1999) 151–156.

· Dupont, L., Guillon, E., Removal of hexavalent chromium with a lignocellulosic substrate extracted from wheat bran, Environ. Sci. Technol. 37 (2003) 4235-4241.

· Fang, Y., Al-Assaf, S., Phillips, G.O., Nishinari, K., Funami, T., Williams, P.A., Li, L., Multiple steps and critical behaviors of the binding of calcium to alginate. J. Phys. B111 (2007) 2456-2462.

· Fiol, N., Villaescusa, I., Martínez, M., Miralles, N., Poch, J., Serarols, J., Biosorption of Cr(VI) using low cost sorbents, Environ. Chem. Lett. 1 (2003) 135-139.

· Fiol, N., Poch, J., Villaescusa, I., Chromium(VI) uptake by grape stalks wastes encapsulated in calcium alginate beads: equilibrium and kinetics studies, Chem. Spec. Bioavailab. 16 (2004) 25-33.

· Fiol, N., Poch, J., Villaescusa, I., Grape stalks wastes encapsulated in calcium alginate beads for Cr(VI) removal from aqueous solutions, Sep. Sci. Technol. 40 (2005) 1013-1028.

· Gardea-Torresdey, J.L., Tiemann, K.J., Armendariz, V., Bess-Oberto, L., Chianelli, R.R., Rios, J., Parsons, J.G., Gamez, G., Characterization of Cr(VI) binding and reduction to

Cr(III) by the agricultural byproducts of *Avena monida* (Oat) biomass, J. Hazard. Mater. B80 (2000) 175-188.

· Goldstein G.I., Newbury D.E., Echlin, P., Joy D.C., Fiori, C.Lifshin E (1981) Scanning electron microscopy and x-ray microanalysis. Plenum Press, New York

· Gupta, V.K., Shrivastava, A.K., Jain, N., Biosorption of chromium(VI) from aqueous solutions by green algae *Spirogyra* species, Water Res. 17 (2001) 4079-4085.

· Gürü, M., Venedik, D., Murathan, A., Removal of trivalent chromium from water using low-cost natural diatomite, (2008) doi:10.1016/j.jhazmat.2008.03.002

· Hanlon, G.W., Hodges, N.A., Quantitative assessment of sterilization efficientcy using lyophilized calcium alginate biological indicators, Lett. Appl. Microbiol. 17 (1993) 171-173.

· Ho, Y.S., Wase, D.A.J., Forster, C.F., Kinetic studies of competitive heavy metal adsorption by Sphagnum moss peat. Environ. Technol. 17(1) (1996) 71-76.

· Ho, Y.S., Ng, J.C.Y., McKay, G., Kinetics of pollutant sorption by biosorbents: review, Sep. Purif. Methods. 29 (2000) 189-232.

· Humar, M., Bokan, M., Amartey, S.A., Sentjurc, M., Kalan, P., Pohleven, F., Fungal bioremediation of copper, chromium and boron treated wood as studied by electron paramagnetic resonance, Int. Biodeter. Biodegr. 53 (2004) 25-32.

· Jodra,Y., Mijangos, F., Ion Exchange selectivities of calcium alginate gels for heavy metals, Water Sci. Technol., 43 (2001) 237-244.

· Kannan, N., Sundaram, M.M., Kinetics and mechanism of removal of methylene blue by adsorption on various carbons-a comparative study, Dyes Pigments. 51(1) (2001) 25-40.

· Karthikeyan G., Anbalagan K., Muthulakshmi N., Adsorption dynamics and equilibrium studies of Zn(II) onto chitosan. J. Chem. Sci., 116 (2004) (2): 119–127.

· Kratochvil, D., Pimentel, P., Volesky, B., Removal of trivalent and hexavalent chromium by seaweed biosorbent, Environ. Sci. Technol. 32 (1998) 2693-2698.

· Lazaridis, N.K., Charalambous, C., Sorption removal of trivalent and hexavalent chromium from binary aqueous solutions by composite alginate-goethite beads, Water Res. 39 (2005) 4385-4396.

· Li, Y.S., Liu, C.C., Chiou, C.S., Adsorption of Cr(III) from wastewater by wine processing waste sludge. J. Colloid. Interf. Sci. 273 (2004) 95-101.

· Loukidou, M.X., Karapantsios, T.D., Zouboulis, A.I., Matis, K.A., Diffusion kinetic study of chromium(VI) biosorption by *Aeromonas caviae*, Ind. Eng. Chem. Res. 43 (2004) 1748–1755.

· Mel Lytle, C., Lytle, F., Yang, N., Qian, J.-H., Hansen, D., Zayed, A., Terry, N., Reduction of Cr(VI) to Cr(III) by wetland plants: potential for in situ heavy metal detoxification. Environ. Sci. Technol., 32 (1998) 3087-3093.

· Micera, G., Dessi, A., Chromium adsorption by plant roots and formation of long-lived Cr(V) species: An ecological hazard?, J. Inorg. Biochem. 34 (1988) 157-166.

· Mohan, D., Singh, K.P., Singh, V.K., Trivalent chromium removal from wastewater using low cost activated carbon derived from agricultural waste material and activated carbon fabric cloth, J. Hazard. Mater. B135 (2006) 280–295.

· Mohan, D., Pittman, C.U., Activated carbons and low cost adsorbents for remediation of tri- and hexavalent chromium from water. Review, J. Hazard. Mater. B137 (2006) 762-811.

· Nakano, Y., Takeshita, K., Tsutsumi, T., Adsorption mechanism of hexavalent chromium by redox within condensed-tannin gel, Water Res. 35 (2001) 496-500.

· Onyancha, D., Mavura, W., Ngila, J.C., Ongoma, P.,Chacha, J., Studies of chromium removal from tannery wastewaters by algae biosorbents, *Spirogyra condensata* and *Rhizoclonium hieroglyphicum,* J. Hazard. Mater. (2008) doi:10.1016/j.hazmat.2008.02.043.

· Özcan A., Özcan, A.S., Tunali, S., Akar, T., Kiran, I., Determination of the equilibrium, kinetics and thermodynamic parameters of adsorption of copper(II) ions onto seeds of *Capsicum annuum*, J. Hazard. Mater. B124 (2005) 200-208.

· Pandey, A.K., Pandey, S.D., Misra, V., Devi, S., Role of humic acid entrapped calcium alginate beads in removal of heavy metals, J. Hazard. Mater. B98 (2003) 177-181.

· Park, D., Yun, Y.S., Park, J.M., Studies on hexavalent chromium biosorption by chemically-treated biomass of *Ecklonia* s.p., Chemosphere. 60 (2005) 1356-1364.

· Park, D., Yun, Y.S., Park, J.M., Reduction of hexavalent chromium with the brown seaweed *Ecklonia* biomass. Environ. Sci. Technol. 38 (2004) 4860-4864.

· Puigdomènech, I., Make Equilibrium Diagrams Using Sophisticated Algorithms (MEDUSA), software version 18 February 2004. Inorganic Chemistry Department, Royal Institute of Technology, Stockholm, Sweden.

· Sahin, F., Demirel, G., Tümtürk, H., A novel matrix for the immobilization of acetylcholinesterase. Int. J. Biol. Macromol. 37 (2005) 148-153.

· Sari, A., Tuzen, M., Biosorption of total chromium from aqueous solution by red algae (*Ceramium virgatum*): Equilibrium, kinetic and thermodynamic studies, J. Hazard. Mater. (2008), doi:10.1016/j.jhazmat.2008.03.005

· Sartori, C., Finch, D.S., Ralph, B., Determination of the cation content of alginate thin films by FTIR spectroscopy, Polymer, 38 (1997) 43-51.

· Sekhar, K.C., Subramanian, S., Modak, J.M., Natarajan, K.A., Removal of metal ions using an industrial biomass with reference to environmental control, Int. J. Min. Process. 53 (1998) 107–120.

· Sharma, D.C., Forster, C.F., Removal of hexavalent chromium using sphagnum moss peat, Water Res. 27 (1993) 1202-1208.

· Sun J.X., Sun, X.F., Zhao, H., Sun, R.C., Isolation and characterization of cellulose from sugarcane bagasse, Polym. Degrad. Stabil. 84 (2004) 331-339.

· Treybal R.E., Mass transfer operations, McGraw Hill, New York, (1980).

· Twadowska, I., Kyziol, J., Sorption of metals onto natural organic matter as a function of complexation and adsorbent-adsorbate contact mode, Environ. Int. 28 (2003) 783-791.

· Usov, A.I., Alginic acids and alginates: analytical methods used for their estimation and characterisation of composition and primary structure, Russ. Chem. Rev. 68 (1999) 957-966.

· Villaescusa, I., Fiol, N., Martínez, M., Miralles, N., Poch, J., Serarols, J., Removal of copper and nickel ions from aqueous solutions by grape stalks wastes, Water Res. 38 (2004) 992-1002.

· Villaescusa, I., Fiol, N., Cristiani, F., Floris, C., Lai, S., Nurchi, V.M., Copper(II) and nickel(II) uptake from aqueous solutions by cork wastes: a NMR and potentiometric study.Polyhedron 21 (2002) 1363-1367.

· Volesky, B., Sorption and Biosorption, BV Sorbex, Inc. Montreal, Canada (2003).

· Weber, W.J., Morris, J.C., Kinetics of adsorption on carbon from solution, J. Sanitary Eng. Div. Am. Soc. Civ. Eng. 89 (1963) 31-60.

· Wu, D., Sui, Y., He, S., Wang, X., Li, C., Kong, H., Removal of trivalent chromium from aqueous solution by zeolite synthesized from coal fly ash, J. Hazard. Mater. 155 (2008) 415-423.

Chapter 2. DETOXIFICATION OF A Cr(VI) POLLUTED EFFLUENT BY A COMBINED SORPTION-REDUCTION PROCESS USING GRAPE STALK.

1. INTRODUCTION

In the previous chapter, chromium removal from aqueous solutions by using grape stalk wastes entrapped in a biopolymeric gel matrix had been studied and discussed. The results obtained put into evidence the important role of the gel matrix in the removal of trivalent chromium while for the removal of the hexavalent, the grape stalk was the main sorption-active material.

In most of the industries using chromium in their processes, this metal is present mainly as Cr(VI) and the detoxification of the effluent passes, in a first step, by its reduction to Cr(III) according to the methods described in the introductory chapter (section 6). As it had been exposed in the introduction chapter, the dechromisation step involved a very important economical cost due to the great consumption of expensive reducing agents such as $NaHSO_3$, SO_2, Na_2SO_3, $Na_2S_2O_4$, $Na_2S_2O_5$ or by addition of iron(II) salts. From these agents, sodium bisulphite ($NaHSO_3$) and Fe(II) salts are nowadays the most widely employed. In the case of Cr(VI) reduction with $NaHSO_3$, while a theoretical amount of reagent of 5.7 mL of 40% solution and 0.95 g of H_2SO_4 are needed per gram of Cr(VI), in the practice, 7 mL and 1.2 g of bisulphite and sulphuric acid solutions respectively must be added. In the case of reduction by $FeSO_4 \cdot 7H_2O$, despite theoretically 16 g of reagent and 1.9 g of H_2SO_4 would be enough to reduce 1 gram of Cr(VI), in the practice, amounts ranging from 60 to 90 grams of iron salt and 2.5 g of concentrated sulphuric acid are required (Cox *et al*., 2006).

Moreover, these chromium reduction techniques exhibit also some other drawbacks. When reduction is carried out with sodium metabisulphite, an important increase of salinity of the effluent occurs, due to important sodium addition and also constant ventilation of storage area and reactors is needed because of the release of toxic sulphurous gases from $NaHSO_3$ in acidic media. In the case of reduction by iron(II) salts, the main drawback is the formation of huge quantities of mud from iron hydroxide precipitation because of the large addition of $FeSO_4$. This mud has to be managed as a hazardous waste by agreed organisms, involving thus an increase of the overall economical cost.

The hexavalent chromium reduction in the industry is usually carried out in batch mode by means of two deposits: one for treatment and the other for filling with the solutions to treat while reduction is taking place in the first one. To simulate the industrial conditions of the reduction, in this chapter, a reactor operating in batch mode will be evaluated for the detoxification of a hexavalent chromium polluted effluent.

Many plating operations involving chromium are normally carried out at temperatures between 40 to 60 ºC (Cox *et al*., 2006), so that temperature of the effluent could be an important parameter to take into account when studying Cr(VI) sorption. Some authors have reported that hexavalent chromium sorption is a temperature-dependent process. In many low-cost sorbents of lignocellulosic base such as pomace, an olive oil industry waste (Malkoc *et al*., 2006), *Pynus sylvestris* (Ucun *et al*., 2007), *Agave lechuguilla* biomass (Romero-González *et al*., 2005), pine sawdust (Uysal and Ar, 2007) and maize bran (Hasan *et al*., 2007), Cr(VI) sorption has been demonstrated to be and endothermic process. The endothermic nature of the Cr(VI) sorption is reflected in a positive effect of the increase of temperature in chromium removal rate and efficiency. Some of these authors reported also the presence of Cr(III) either in solution or in the solid phase, coming from the reduction of Cr(VI) (Hasan *et al*., 2007; Romero-González *et al*., 2005). The reduction of hexavalent to trivalent chromium promoted by low-cost materials could be of economical interest for many industries working with Cr(VI), due to the important saving in the consumption of reducing reagents in the dechromisation step.

In chapter 1 of the present work and in previous experiments carried out in our laboratory, it was demonstrated that grape stalk particles played a key role in hexavalent chromium removal through sorptive/reductive processes (Fiol *et al*., 2008). In that same chapter it was also ascertained the role of H^+ as a limiting reagent in the extension of hexavalent chromium removal by 2% GS-CA. Despite of the proven good sorption performance of these beads for the removal of Cr(III) and Cr(VI), it is well known that stirred tank reactors exert a shearing effect on the material contained within them. This shear forces acting on the soft calcium alginate matrix could provoke its damage and the final disintegration of the gel, being the grape stalk particles released to the media. With this basis, in a first approach, the reactor proposed in this chapter to carry out the detoxification of a Cr(VI)-polluted effluent will be fed with raw grape stalks.

2. OBJECTIVES

The objective of this chapter is to study the effect of solution pH and temperature on the detoxification process of Cr(VI) solutions by grape stalk. To carry out this study, a jacketed stirred batch reactor with auxiliary equipment to keep the pH of the media constant will be implemented.

In a first step, the effect of temperature on Cr(VI) sorption/reduction kinetics at constant pH of 3 will be carried out. Role of proton will be ascertained and discussed by performing complementary experiments at fixed temperature but allowing the free evolution of pH.

As in real industrial effluents it is possible to face different initial Cr(VI) concentrations in the feeding effluent of the dechromisation reactor, this study will include the evaluation of the sorption/reduction behaviour of GS when is submitted to different initial metal concentrations at a fixed pH and for a temperature of 20 ºC.

Chemical sorption/reduction process, as revealed from the kinetic experiments for the different Cr species, will be described by combination of sorption-reaction steps and a mathematical expression that describe the dynamics of the process will be obtained.

It can be advanced that in the Cr(VI) detoxification promoted by GS, a relatively small remaining concentration of non-adsorbed Cr(III) is formed at equilibrium. In the last section of this chapter, in an attempt to remove this Cr(III), different methods will be proposed and their efficiency will be discussed. This complementary study will allow the obtention of valuable information about the chemical environment of this reduction-formed trivalent chromium.

3. MATERIALS AND METHODS

3.1. Reagents

Sorbent material:

- Powdered grape stalk (250≤ø≤560μm) coming from a wine producer from Castilla La Mancha.

To prepare trivalent and hexavalent chromium solutions:

- $K_2Cr_2O_7$ 99% Panreac
- $Cr(NO_3)_3 \cdot 9H_2O$ 98% min. Panreac
- Milli-Q water

For pH adjustment in the reactor:

- HCl 37% Panreac
- NaOH 96% Panreac

For pH adjustment in the Cr(III) sorption experiments:

- HCl 1 and 0.01 M Panreac
- NaOH 1 and 0.01 M Panreac

Standard solutions for Flame Atomic/Emission Spectroscopy calibration:

- $Cr(NO_3)_3 \cdot 9H_2O$ in HNO_3 0.5 N (1000 $mg \cdot L^{-1}$) Panreac

For pH adjustment:

- HCl (37%) Panreac
- NaOH in pellets Panreac

For Cr(VI) analysis by the colorimetric method of diphenylcarbazide:

- 1,5-Diphenylcarbazide Aldrich
- Ethanol 96% v/v Panreac

- Sulphuric acid 96% Panreac

3.2. Material

General laboratory material

pH indicator paper (Panreac)

25 mL capacity glass tubs with cap

Cellulose filters

Nylon 45µm pore size membrane filters (VWR international)

Chronometers (Berlabo, SA)

Vortex (Velp Scientifica $2x^3$)

pHmeter (Crison pH – meter Basic 20)

pHmeter (Easyferm plus, Hamilton S.A.)

Analytical balance (Cobos precision, J. Touron, SA)

Coffee grinder (Taurus MS 50)

Siever and sieves (Sulab, S.A.)

Oven (P Selecta)

Peristaltic pump (Gilson Minipuls 3)

Peristaltic pump tubes Tygon R-3603

Dispenser pump (Seko)

Reactor stirrer (Stuart Stirrer SS20)

Rotary shaker (Stuart Stientific)

Orbital Shaker (SSL1, Stuart Stientific)

Flocculator (Flocumatic, JP-Selecta)

Cryostatic device, “cold finger” (JP-Selecta)

Balance (AND HF-300G)

5 L jacketed reactor vessel (V-62825, Afora)

Programmable logic controller, PLC (Eutech Instruments, αlpha-pH2000W)

Thermostated bath (JP-Selecta)

Bath thermometer (Digiterm 3000S42 JP-Selecta)

Stirring blade (Afora)

Fraction collector (Gilson, FC203B)

Three way valve (Gilson)
Column 100x10 mm (Omnifit)

3.3. Equipment

· Flame Atomic Absorption/Emission Spectrophotometer Varian SpectrAA 220FS.
· UV-Vis Absorption Spectrophotometer Cecil CE2021.

4. METHODOLOGY

4.1. Development and description of the installation

In this study, the detoxification of Cr(VI) solutions by a combined sorption/reduction process with grape stalk is proposed. The scheme of the installation implemented to carry out this process is presented in the next section.

4.1.1. Installation scheme

In the next figure the installation scheme is presented. Detailed description of the individual elements is presented below.

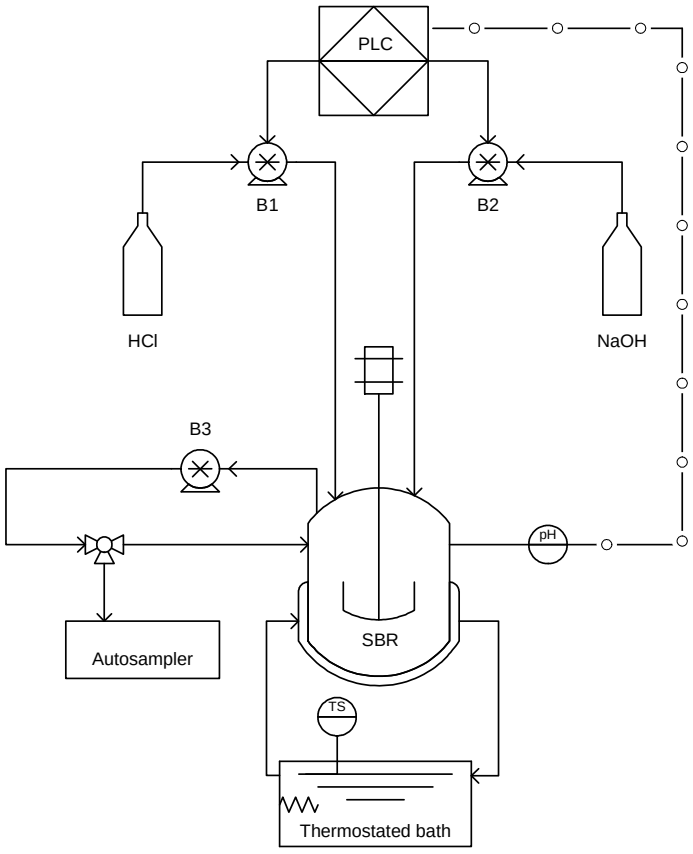

Figure 1. Installation scheme

4.1.2. Description of the control elements

4.1.2.1. Programmable Logic Controller (PLC) and pH electrode

A PLC (Programmable Logic Controller) and a pH electrode were used for correction and monitoring of solution pH while Cr(VI) sorption/reduction process was taking place. The function of the PLC is to continuously measure, by means of the electrode, the pH of the reactor solution and to apply the corrective measures by activation of the pumps that add either acid or base to the reaction vessel.

Experiments will be conducted for different temperatures in the range 5 to 60 ºC. As the signal provided by pH sensors is slightly temperature-dependent, the PLC was programmed to operate in ATC mode (Automatic Temperature Compensation). Thus, the pH dependence on the temperature of the solution will be automatically corrected by the controller.

4.1.2.2. Peristaltic pumps

Two peristaltic pumps (B1 and B2), one for acid and the other for base dossification, act as final control elements. They are the responsible of the addition of the required volume of a 1.5% HCl or NaOH solution to keep the pH constant. The movement of these pumps depends of the pH value registered by the pH electrode and processed by the PLC.

The peristaltic pump labelled as B3 is responsible of automatic sampling by carrying out a recirculation of the solution passing through the three ways valve of the sample collector.

4.1.2.3. Sampling

During the first hour, sampling was performed manually by taking 5 mL samples in order to get as much information as possible about the rate sorption at the beginning of the process. After this time, a peristaltic pump (Minipuls 3, Gilson) pumped 0.85 $L \cdot h^{-1}$ solution from the reactor to a fraction collector (FC203B, Gilson), recirculating the effluent by means of a three way valve. At programmed times, the collection arm of the autosampler moved, the sampling head was positioned on the tube and the valve was opened for 30

seconds taking an aliquot of approximately 7 mL. This recirculation system was adapted to return the effluent to the reactor vessel when the autosampler was in waiting mode.

4.2. General operation procedure

4.2.1. PLC programming

In a first step, the PLC was programmed. A pH of 3.0 and a variation of ±0.1 units were chosen. As studies at different solution temperatures were going to be carried out, the PLC was programmed in the ATC mode. By doing so, values of pH transmitted by the electrode were automatically corrected by the PLC depending on the temperature values.

4.2.2. Reactor building

The experiments have been carried out in a 5 L capacity stirred glass reactor in batch mode. The reactor is equipped with a glass jacket surrounding the vessel, and the heating and cooling of the reactor content is carried out by a water recirculation from a thermostatic bath. The reactor is provided also of a valve in the bottom for its draining.
For the understanding of the installation, the description of the reactor plumbing is needed. As the sampling and acid or base addition for pH correction is carried out through the glass cap of the reactor, a picture of this element with the additional elements is presented in **Figure 2**.

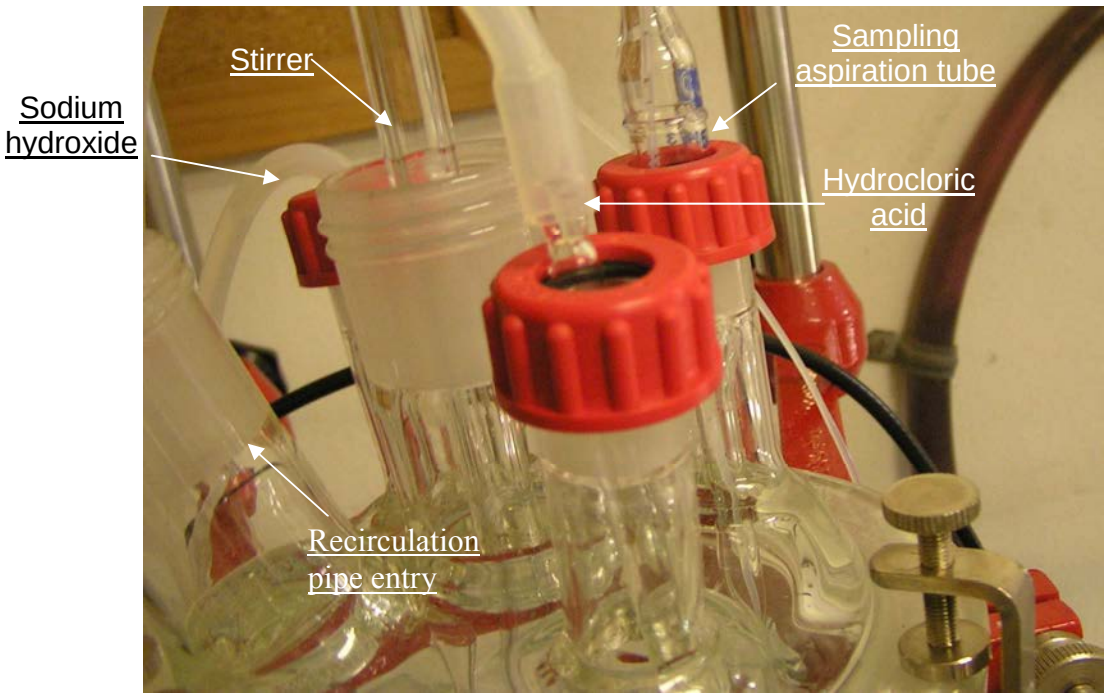

Figure 2. Reactor cover and plumbing detail.

By the central hole on the top of the glass cover, the stirrer blade is introduced and positioned approximately 5 cm from the bottom of the vessel. This cap is provided also of four equidiametral holes forming approximately a 90º angle between them. Two of these entries were used for the introduction of the hydrochloric acid and sodium hydroxide solutions needed for pH adjustment of the solution in the reactor. The other two entries were used to introduce the aspiration pipe device and the tube for the returned effluent, both needed for the automatic sample collection. The setup of the aspiration pipe device is detailed in the next section.

4.2.3. Preparation and conditioning of the collection tube

For the sampling, the capillary plastic tube was placed on the bottom of a glass hollow tube partially filled with glass beads. This capillary was connected to the peristaltic tube and after the pump, it was connected to the three way valve of a fraction collector. In order to avoid the obstruction of the small diameter channels of the three way valve, the bottom of the glass tube was covered with a piece of cloth, that would act as a filtering media avoiding the pass of small size particles released from the grape stalk.

This device is presented in the next figure.

Figure 3. Collection tube and filtering media

4.2.4. Solution introduction and conditioning

In a first step, the pH electrode was washed with MilliQ water and introduced on its position. After, and for all the studied scenarios, 4L of a Cr(VI) solution with a pH about 3 were introduced in the reactor, and both agitation and thermostated bath were switched on. The temperature of the chromium solution was monitored by suspending on the reactor a mercury thermometer. When the solution reached thermal steady state at the desired temperature, the PLC was turned on and it was allowed to automatically correct pH providing a solution pH 3.

When the solution in the reactor had reached the required temperature and pH, the first sample, corresponding to contact time 0 was taken. Once extracted the first aliquot the sampling and recirculation tubes were introduced in the reactor and the recirculation pump was switched on. After this, and with the stirring speed fixed to 250 rpm, the grape stalk was added by using a solids funnel and the chronometer was started.

4.2.5. Draining and cleaning of the reactor and tubes

When the process finished, the reaction vessel and all the plumbing were drained and cleaned. In a first step, the reactor content was drained by the bottom valve of the vessel and filtered by a cellulose filter to separate the grape stalk particles and the liquid. The reactor walls and the stirrer blade were washed also with deionized water. Once drained and cleaned the reactor vessel, the pH electrode was removed from its fixed position, washed with MilliQ water and stored in a 3M KCl solution.

The glass hollow sampling tube was removed and the filtering media was disassembled and washed with deionized water to remove all the material retained and that would difficult the sampling in a subsequent reaction cycle.

Finally all the plumbing of the recirculation device for the autosampling was washed in continuous by pumping through the tubes and the valve 500 mL of MilliQ water.

4.3. Sorbent preparation

Grape stalk wastes generated in a wine manufacturer from Castilla La Mancha region was washed three times with distilled water and dried in an oven at 80 ºC until constant weight. Afterwards, it was cut in small pieces, grinded and sieved. For this study, the particle size range employed was $250 \leq ø \leq 560 \mu m$.

4.4. Sorption experiments

Sorption experiments under different conditions were conducted to ascertain the effect of temperature, pH readjustment and initial Cr(VI) concentration in the performance of the equipment proposed in the present chapter as possible low-cost dechromisation installation.

4.4.1. Temperature effect on Cr(VI) sorption/reduction kinetics at constant pH

Effect of temperature in the sorption/reduction process was studied by contacting 4 L of a 10 $mg \cdot L^{-1}$ Cr(VI) solution with 10 g of GS under continuous pH readjustment to the original pH 3 value. For the different studies, the temperature was varied within 5 to 60 ºC.

4.4.2. Effect of pH readjustment on Cr(VI) sorption/reduction kinetics

Cr(VI) sorption/reduction without pH compensation was studied by carrying out experiments at three different temperatures 5, 20 and 50 ºC in the same conditions as described in section 4.4.1. In order to ascertain the effect that pH compensation exerts on the removal process of Cr(VI), these results were compared with the obtained, at the same temperatures, with automatic pH correction to the initial 3.0 value.

4.4.3. Effect of initial Cr(VI) concentration in sorption/reduction kinetics at constant pH and temperature

Cr(VI) concentration effect on kinetics and equilibrium of sorption/reduction was studied for three feeding concentrations: 5.52, 10.68 and 19.65 $mg \cdot L^{-1}$ and for a sorbent dose of 2.5 $g \cdot L^{-1}$. For these experiments the Cr(VI) solutions were directly prepared in the reactor by adding the required amount of potassium dichromate to 4 L of MilliQ water under continuous stirring and allowing the PLC to autoadjust the pH to the initial value 3.0. All the experiments were carried out at a fixed temperature of 20±0.1 ºC.

4.5. Chromium analysis

The total concentration of chromium, i.e., Cr(VI) + Cr(III), was determined by flame atomic emission spectroscopy (FAES) (Varian SpectrAA 220FS). Hexavalent chromium was analysed by the standard colorimetric 1,5-diphenylcarbazide method according to the protocol described in chapter 1, section 4.7.1. The concentration of trivalent chromium was determined as the difference between total chromium and hexavalent chromium concentration, respectively. For comparison sake, the Cr(VI) standard used in

diphenylcarbazide method was analysed by FAES. Analytical measurements made by the two techniques were comparable within 5%.

4.6. Residual Cr(III) removal assays

After the treatment of the different Cr(VI) solutions with GS in the reactor, always the presence of a non-adsorbed Cr(III) fraction at equilibrium time was observed. In an attempt to remove this residual metal concentration, different assays, the first based in batch basic precipitation and the second in continuous bed-up flow sorption were proposed and their methodology is presented next.

4.6.1. Precipitation assays

To carry out this experiment, the effluent produced in the experiments carried out in the reactor at 20 and 30 ºC with pH adjustment were mixed, obtaining a solution with an initial Cr(III) concentration of 2.85 $mg \cdot L^{-1}$. 500 mL from this solution were taken for each experiment, placed in a 1L glass and mounted in flocculation equipment under continuous stirring. Basification of the media to give final pH values in the range 4 to 11.5 was carried out by dropwise addition of 1M NaOH. When pH of each solution was adjusted, they were still stirred for 30 minutes to allow the formation of any precipitate. Then 20 mL of effluent were taken, filtered by a 0.45 μm membrane, acidified and analysed by FAES.

4.6.2. Continuous bed up-flow sorption experiments

Fixed bed sorption on the same effluent produced after the treatment of the Cr(VI) solution in the reactor were carried out in glass columns of 10 cm length and 1.0 cm inner diameter. As feeding solution for this experiment, the effluent produced in the sorption assays carried out in the reactor at 50 and 60 ºC with pH adjustment were mixed, obtaining a solution with an initial Cr(III) concentration around 2.5 $mg \cdot L^{-1}$.

The experimental device to carry out the continuous Cr(III) sorption experiments is presented in the next figure.

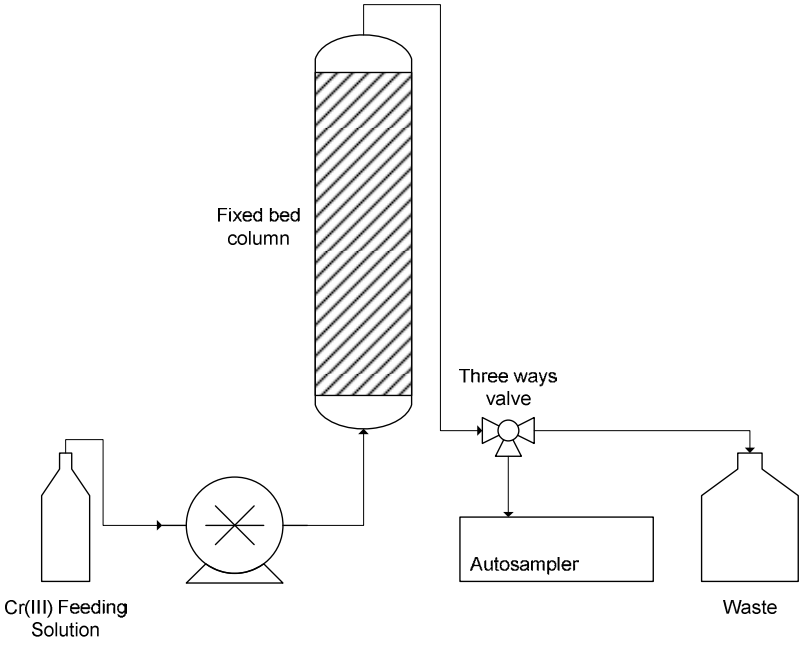

Figure 4: Cr(III) continuous bed up-flow sorption device.

The Cr(III) solution was pumped at room temperature (20±1ºC) upwards the column by a peristaltic pump at a flow rate of 32 $mL \cdot h^{-1}$. The columns were fully packed with the sorbent giving a bed height of around 70mm. The operation was carried out in the up-flow mode to avoid possible short-circuiting by clogging and channelling. By using an automatic fraction collector, samples of 5 mL were collected each hour, acidified and metal concentration in solution was determined by FAAS. The non-collected effluent was collected in a waste bottle for safe management.

The studies were performed by using two materials, the raw grape stalk and an activated carbon obtained from the same. To prepare an activated carbon from GS, the protocol described by Suzuki *et al*. for activated carbon preparation from rice bran was followed (Suzuki *et al*., 2007). In this procedure acid treated grape stalk (AGS) was obtained by treating GS with concentrated sulphuric acid (weight:ratio 1:1) for 24 h at 150 °C in an oven. After cooling, the excess of acid present on the material was leached out by washing with a sodium bicarbonate solution (1% w/v) until neutrality (tested with pH indicator paper) and finally washed with MilliQ water. The material obtained so was then dried at 50 ºC for 24 hours and used on its present form.

5. RESULTS AND DISCUSSION

The effect of temperature of the Cr(VI) solution in the sorption/reduction process that takes place when contacting with GS has been studied under conditions of constant pH 3.0±0.1. Results obtained are presented in the next section.

5.1. Temperature effect on chromium sorption/reduction kinetics at constant pH

This study was conducted by monitoring total, hexavalent and trivalent chromium in solution. In a first step, the effect of temperature in chromium removal rate, expressed as total chromium concentration in solution as a function of contact time, was studied under conditions of constant pH 3.

5.1.1. Total chromium removal

In the next table, total chromium concentration in solution for each contact time is presented.

Table 1: Total chromium concentration in solution ($mg \cdot L^{-1}$) as a function of contact time for the different studied temperatures. $[Cr(VI)]_0 \approx 10.5\ mg \cdot L^{-1}$; pH: 3.0±0.1; sorbent dose: $2.5\ g \cdot L^{-1}$.

	5 ºC	**20 ºC**	**30 ºC**	**50 ºC**	**60 ºC**
t(min)	**$[Cr]_t$**	**$[Cr]_t$**	**$[Cr]_t$**	**$[Cr]_t$**	**$[Cr]_t$**
0	10.64	10.68	10.31	10.87	10.13
1	10.08	9.42	9.58	9.86	8.72
2	9.8	8.65	9.03	8.8	8.26
3	9.41	8.09	8.28	7.55	7.50
5	8.79	7.87	7.41	6.82	6.90
7	8.47	7.15	7.04	6.14	6.32
8	8.43	6.56	6.51	6,10	6.16
10	8.09	6.22	5.59	5.46	5.23
12	7.82	5.98	5.03	4.69	5.06
15	7.55	5.73	4.87	4.35	4.75
20	6.87	5.29	4.13	3.95	4.08
25	6.41	4.75	3.82	3.63	3.72
30	6.08	4.47	3.62	3.43	3.48
45	5.29	3.82	3.38	3.22	3.25
60	4.63	3.43	3.36	3.07	3.19
90	4.04	3.05	3.34	3.05	3.17
120	3.44	2.65	3.32	3.02	3.16
150	3.11	2.62	3.26	3.01	3.17
180	2.93	2.58	3.26	3.02	3.15
210	2.75	2.55	3.26	3.02	3.15
240	2.71	2.55	3.26	3.02	3.15

As it can be seen in this table, a reduction of chromium content in solution takes place when contacting the solution with GS. To ascertain the effect of the increase of the temperature on the total chromium removal kinetics, a comparison of the time to reach half the reduction of the initial chromium concentration ($t_{1/2}$) has been carried out. In the table it has been indicated, underlined, half the initial chromium concentration for each temperature. As it can be observed in **Table 1**, $t_{1/2}$ is strongly dependent on the temperature at which experiments are conducted. Results varied from about 45 minutes in the case of 5 ºC to only 10 minutes of contact time for the two highest temperatures, 50 and 60 ºC.

If results of chromium concentration in solution are plotted as a function of time for the five temperatures studied, the next figure is obtained:

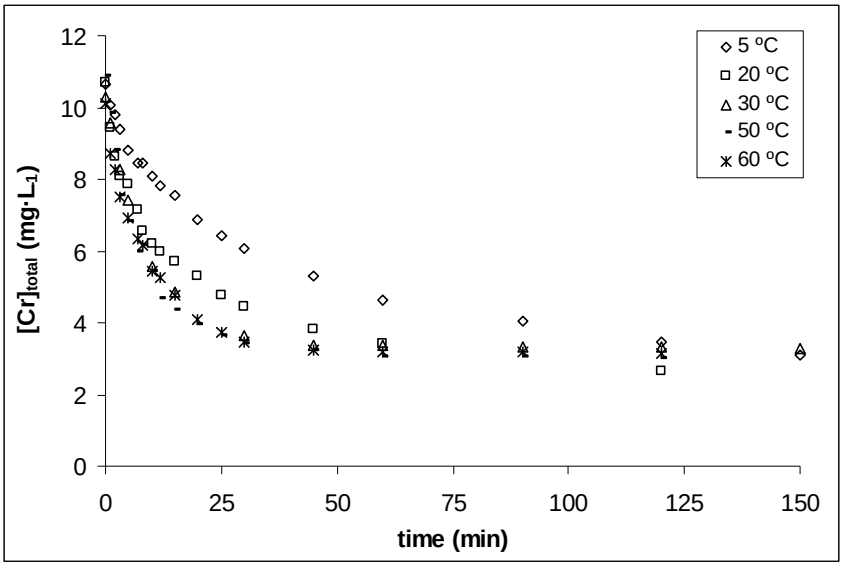

Figure 5: Total chromium concentration in solution as a function of time for the different process temperatures. $[Cr(VI)]_0 \approx 10.5$ mg·L^{-1}; pH: 3.0±0.1 ; T: 5-60 ºC; sorbent dose: 2.5 g·L^{-1} .

As it can be observed in **Figure 5**, for the initial concentration of around 10.5 mg·L^{-1}, the rate of metal removal seems to be strongly affected by the temperature of the media. The experimental results clearly demonstrates an increase of metal sorption rate when increasing temperature, finding the highest difference between kinetic data at 5 and 20 ºC. In cases where the interaction between metal ions and biomass surface is favourable at higher temperatures, binding is said to be endothermic. The endothermic nature of hexavalent chromium adsorption has also been reported previously for different biomaterials (Romero-González *et al*. 2005; Hasan *et al*., 2007; Uysal and Ar, 2007; Ucun *et al*., 2007). It has to be also remarked that from a temperature of 30 ºC, the chromium concentration decay as a function of time becomes almost equal.

Also, time to reach equilibrium seems to be affected by the temperature at which the process takes place due to the slowing down of the total chromium removal rate at low temperatures. While for the two lowest of the temperatures, 5 and 20 ºC, a contact time of 150 and 90 minutes is required respectively, for 30 ºC and higher temperatures, equilibrium is reached in only 60 minutes. These results demonstrate that, if we focus on the total chromium concentration in solution, with continuous reacidification of the media, the heating of the industrial effluent would become unnecessary if the solution to treat is

present at a quite common temperature of around 20 ºC or higher. The effect of the temperature can be explained in basis to the thermal kinetic energies of the sorbate molecules. Kinetic energies of chromium ions would be low at low temperatures and an increase of temperature provokes an increase in the mobility of the ions. Therefore, it would be a much more difficult and a time-consuming process for ions to reach the sorbent active sites at low than at high temperatures (Malkoc and Nuhoglu, 2007; Gasser *et al*., 2007; Sharma and Weng, 2007; Juang *et al*., 1997; Dönmez *et al*., 1999).

On the other hand, when equilibrium concentration in solution is compared for the different series, it can be observed that despite the different thermic conditions of the reaction, the final chromium concentration seems not to be dependent of the temperature. The process reaches a residual chromium concentration at equilibrium about 3 $mg \cdot L^{-1}$.

All these data put into evidence a positive and almost neutral effect of temperature in total chromium sorption kinetics and in equilibrium respectively: while an increase on temperature of the solution involves an important increase on metal sorption rate in the range 5 to 30 ºC, the equilibrium concentration in solution is not strongly modified by the temperature of the media.

Despite chromium in the feeding effluent was present on its hexavalent form, it's known that the biomaterial employed in this study has the potential to reduce this Cr(VI) to the less toxic Cr(III) oxidation state (Fiol *et al*., 2008). So that it becomes necessary to obtain the information concerning the evolution of both, trivalent and hexavalent concentration in solution as a function of contact time in the different thermic series, in order to ascertain the effect that temperature exerts in the sorption/reduction process at constant pH. In the next two sections, the total chromium sorption kinetics will be separated in two: the corresponding to the hexavalent and to the trivalent.

5.1.2. Hexavalent chromium removal

In this section the variation of Cr(VI) concentration in solution as a function of contact time for the different thermic series is analyzed and discussed. In the next table, results of Cr(VI) concentration in solution as a function of contact time with the GS for the experiments carried out at different temperatures under constant pH 3.0±0.1 conditions are presented.

Table 2: Cr(VI) concentration in solution ($mg \cdot L^{-1}$) as a function of time for the different studied temperatures. $[Cr(VI)]_0 \approx 10.5\ mg \cdot L^{-1}$; T: 5-60 ºC; pH=3.0±0.1; sorbent dose: 2.5 $g \cdot L^{-1}$.

	5 ºC	20 ºC	30 ºC	50 ºC	60 ºC
t(min)	[Cr(VI]	[Cr(VI]	[Cr(VI]	[Cr(VI]	[Cr(VI]
0	10.64	10.68	10.31	10.87	10.13
1	4.19	5.57	3.40	4.31	0.89
2	2.89	4.29	2.23	1.37	0.79
3	2.62	2.24	0.71	0.68	0.79
5	1.96	1.35	0.70	0.64	0.77
7	1.80	1.24	0.54	0.61	0.79
8	1.64	1.11	0.42	0.61	0.74
10	1.60	0.77	0.34	0.61	0.37
12	1.51	0.61	0.31	0.40	0.37
15	1.31	0.61	0.33	0.00	0.00
20	1.02	0.61	0.33	0.00	0.00
25	0.99	0.61	0.36	0.00	0.00
30	0.95	0.31	0.33	0.00	0.00
45	0.99	0.31	0.22	0.00	0.00
60	0.47	0.31	0.00	0.00	0.00
90	0.47	0.27	0.00	0.00	0.00
120	0.47	0.22	0.00	0.00	0.00
150	0.25	0.00	0.00	0.00	0.00
180	0.13	0.00	0.00	0.00	0.00
210	0.00	0.00	0.00	0.00	0.00
240	0.00	0.00	0.00	0.00	0.00

As it can be seen in this table, hexavalent chromium concentration in solution follows the same trend as total chromium; reduction of metal content in solution with time when contacting the solution with GS. In this table it has been underlined the point at which hexavalent chromium disappears from solution at the different temperatures.

As it can be observed, the time to reach total Cr(VI) disappearance is reduced when temperature of the media increases, varying from 210 minutes in the case of 5 ºC to only 15 minutes of contact time for the two highest temperatures, 50 and 60 ºC.

When hexavalent chromium concentration in solution is plotted as a function of time for the five temperatures studied, the next figure is obtained:

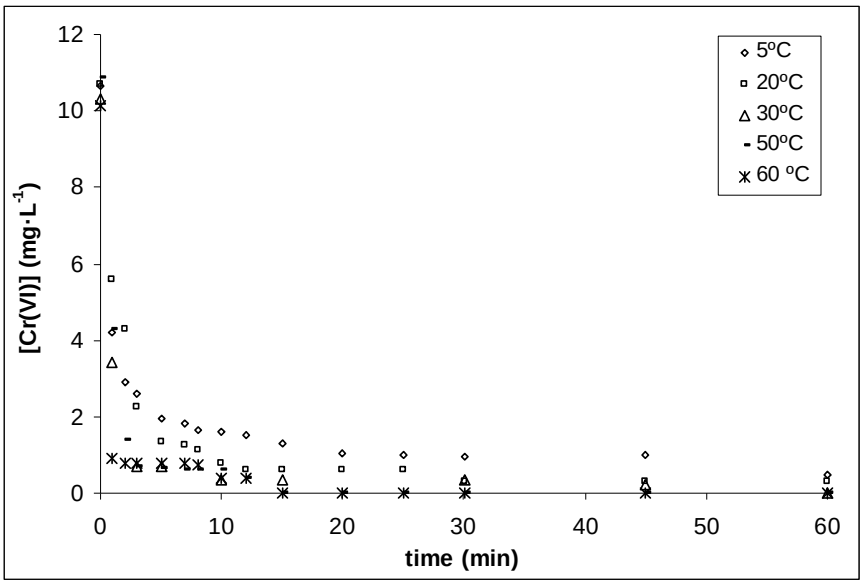

Figure 6: Hexavalent chromium concentration in solution as a function of time for the different process temperatures. $[Cr(VI)]_0 \approx 10.5$ mg·L^{-1}; T: 5-60 ºC; pH: 3.0±0.1; sorbent dose: 2.5 g·L^{-1}.

This figure allows an easy visualization of the effect that temperature provokes in the Cr(VI) disappearance kinetics. The general trend observed is that an increase of temperature is related to an increase of the initial slope of the process. This increase on the rate of disappearance of Cr(VI) in solution can be due to either, increase of sorption rate onto the GS, keeping its hexavalent oxidation state or increase on the reduction rate to its trivalent form and release of this oxidation state again to the solution. The relative relevance of these two processes will be further discussed when modeling the process.

By subtracting the hexavalent concentration from the total chromium, the trivalent chromium concentration in solution can be obtained for each contact time and for each thermal experiment. Results obtained are presented in the next section.

5.1.3. Trivalent chromium formation and removal

In this section, the evolution of Cr(III) concentration in solution as a function of contact time for the different thermic series is analyzed and discussed. In the next table, results of Cr(III) concentration in solution as a function of contact time with the GS for the experiments carried out at different temperatures under constant pH 3.0±0.1 conditions are presented.

Table 3: Cr(III) concentration in solution ($mg \cdot L^{-1}$) as a function of time for the different studied temperatures. $[Cr(VI)]_0 \approx 10.5\ mg \cdot L^{-1}$; pH=3.0±0.1; sorbent dose: $2.5\ g \cdot L^{-1}$.

	5 ºC	20 ºC	30 ºC	50 ºC	60 ºC
t(min)	[Cr(III)]	[Cr(III)]	[Cr(III)]	[Cr(III)]	[Cr(III)]
0	0.00	0.00	0.00	0.00	0.00
1	5.89	3.85	6.18	5.55	7.83
2	6.91	4.36	7.09	7.43	7.47
3	6.79	5.85	7.57	6.87	6.71
5	6.83	6.52	6.71	6.18	6.13
7	6.67	5.91	6.11	5.39	5.53
8	6.79	5.45	5.86	5.53	5.42
10	6.49	5.45	5.25	4.85	5.06
12	6.31	5.37	4.94	4.08	4.89
15	6.24	5.12	4.54	4.35	4.75
20	5.85	4.68	4.09	3.95	4.08
25	5.42	4.14	3.61	3.63	3.72
30	5.13	4.16	3.29	3.43	3.48
45	4.30	3.51	3.16	3.22	3.25
60	4.16	3.12	3.36	3.07	3.19
90	3.57	2.72	3.34	3.05	3.17
120	2.97	2.43	3.32	3.02	3.16
150	2.86	2.51	3.26	3.02	3.16
180	2.80	2.58	3.26	3.02	3.16
210	2.75	2.55	3.26	3.02	3.16
240	2.71	2.55	3.26	3.02	3.16

This table clearly demonstrates a contrast with the trends observed for both, total and hexavalent chromium removal. Dynamics of Cr(III) in the reactor passes by two different steps. The first step is characterized by the appearance of Cr(III) coming from the reduction of Cr(VI) and the achievement of a maximum trivalent chromium concentration in solution. This maximum represents and inflexion point from whom, in a second step, Cr(III) in solution decreases by adsorption onto the GS until an equilibrium concentration

is reached. In this table can be also observed that the equilibrium Cr(III) concentration in solution is a parameter that seems not to be very affected by the temperature at which the process take place.

When trivalent chromium concentration in solution is plotted as a function of time for the five temperatures studied, the next figure is obtained:

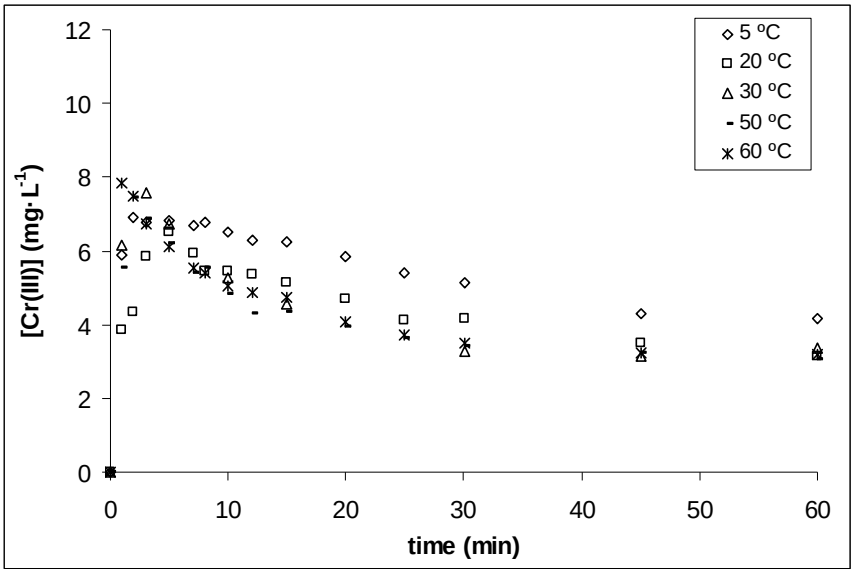

Figure 7: Trivalent chromium concentration in solution as a function of time for the different process temperatures. $[Cr(VI)]_0 \approx 10.5$ mg·L^{-1}; T: 5-60 ºC; pH: 3.0±0.1; sorbent dose: 2.5 g·L^{-1}.

This plot allows both, an easy visualization of the dynamics of Cr(III) appearance/disappearance in the reactor and comparison of the effect of temperature on this process. **Figure 7** indicates that an increase of Cr(III) production rate occurs when temperature is increased. The maximum concentration of Cr(III) produced seems not to be strongly dependent on the temperature, despite a slightly higher production of Cr(III) is observed in the case of the experiment carried out at the highest temperature (7.83 mg·L^{-1} for the 60 ºC experiment) when compared with the lowest temperature (6.90 mg·L^{-1} for the 5 ºC experiment). After maximum Cr(III) concentration is reached, the system tends to adsorb a fraction of this Cr(III) provoking thus the consequent decrease on the concentration of this oxidation state in solution. This disappearing kinetics seems to have a

clear tendency with the temperature, being faster when higher is the temperature of the media. This effect is much clearly observed when comparing the kinetics at 20 ºC or higher with the 5 ºC one, being the highest difference the established between these two series. When the process is carried out at a temperature of 30 ºC or higher, the kinetics of Cr(III) disappearance after the Cr(III) production step, becomes almost equal.

5.2. Effect of temperature and pH readjustment on Cr(VI) sorption/reduction kinetics

In the previous section, the effect of temperature in the sorption /reduction kinetics of Cr(VI) under conditions of constant pH 3.0 has been studied and discussed, reporting that an increase on temperature of the media increased both, sorption and reduction rates. To complete this study, it was needed to ascertain the role that protons played in the combined sorption/reduction process, so that, evaluation of the sorptive/reductive system under conditions of free pH evolution was required.

So that, and summarizing, the aim of the study presented in this section was to ascertain the combined role of temperature and H^+ concentration in the Cr(VI) sorption and reduction processes provoked by GS. To reach this objective, experiments of Cr(VI) sorption/reduction without pH readjustment were carried out for three different temperatures and compared with the results obtained with pH correction to the initial 3.0±0.1 value. As in the other sections, kinetic results expressing total, hexavalent and trivalent chromium concentration in solution will be presented and discussed.

In a first step, kinetics of total chromium removal was studied and it's presented in the next section.

5.2.1. Total chromium removal

In the next table chromium concentration in solution, expressed as total chromium, for each contact time is presented.

Table 4: Total chromium concentration in solution ($mg \cdot L^{-1}$) as a function of time for the experiments with and without pH readjustment. $[Cr(VI)]_0 \approx 10.5\ mg \cdot L^{-1}$; sorbent dose: 2.5 $g \cdot L^{-1}$; T: 5, 20 and 50 ºC. Initial pH: 3.0±0.1.

	5 ºC		20 ºC		50 ºC	
t(min)	**pH adj.**	**Free evol.**	**pH adj.**	**Free evol.**	**pH adj.**	**Free evol.**
0	10.64	11.05	10.68	10.38	10.87	9.82
1	10.08	10.93	9.42	10.31	9.86	8.07
2	9.8	10.54	8.65	10.12	8.8	6.90
3	9.41	10.50	8.09	9.73	7.55	6.38
5	8.79	10.39	7.87	9.60	6.82	5.48
7	8.47	9.99	7.15	9.46	6.14	4.89
8	8.43	9.86	6.56	9.10	6,10	4.80
10	8.09	9.47	6.22	9.10	5.46	4.33
12	7.82	9.37	5.98	8.86	4.69	3.97
15	7.55	9.16	5.73	8.55	4.35	3.58
20	6.87	8.87	5.29	8.31	3.95	3.26
25	6.41	8.33	4.75	7.46	3.63	2.90
30	6.08	7.92	4.47	7.19	3.43	2.71
45	5.29	7.31	3.82	6.36	3.22	2.46
60	4.63	6.42	3.43	5.52	3.07	2.35
90	4.04	--	3.05	3.77	3.05	--
120	3.44	5.63	2.65	2.86	3.02	2.33
150	3.11	--	2.62	2.32	3.01	--
180	2.93	3.77	2.58	--	3.02	2.34
210	2.75	--	2.55	--	--	--
240	2.71	2.84	2.55	1.94	--	2.35

* -- not determined

The concentration profile with time for total chromium is analogous to the observed in previous section: a general decreasing trend when contacting the solution with the agrowaste.

As in the previous section, half the initial chromium concentration for each temperature in experiments with and without pH control has been underlined. Thus, the time to reach half the reduction of the initial chromium content ($t_{1/2}$) can be compared in the different conditions.

As it can be observed in **Table 4**, $t_{1/2}$ is, for the temperatures of 5 and 20 ºC, lower in the case of the process under reacidification conditions. While in the experiments without pH readjustment, $t_{1/2}$ of 120 and 60 minutes were observed for 5 and 20 ºC respectively, with pH readjustment, $t_{1/2}$ time varies from 45 to 20 minutes respectively. So that, the pH compensation involves a $t_{1/2}$ reduction of 75 and 40 minutes for 5 ºC and 20 ºC respectively.

In the case of the higher temperature (50 ºC), under conditions of free pH evolution $t_{1/2}$ is only 10 minutes, while 7 minutes are required with pH readjustment. In this case, the effect of pH compensation seems not to have a clear effect on the rapid chromium removal rate, probably due to the fact that the sorption/reduction reaction is enough activated with high temperatures (50 and 60 ºC).

To establish an easier comparison and ascertain the effect of pH compensation in the total chromium removal rate for the different temperatures, the experimental chromium concentration in solution has been plotted as a function of contact time for the different studied temperatures with and without pH readjustment. The results obtained for the three temperatures are presented in the next figure:

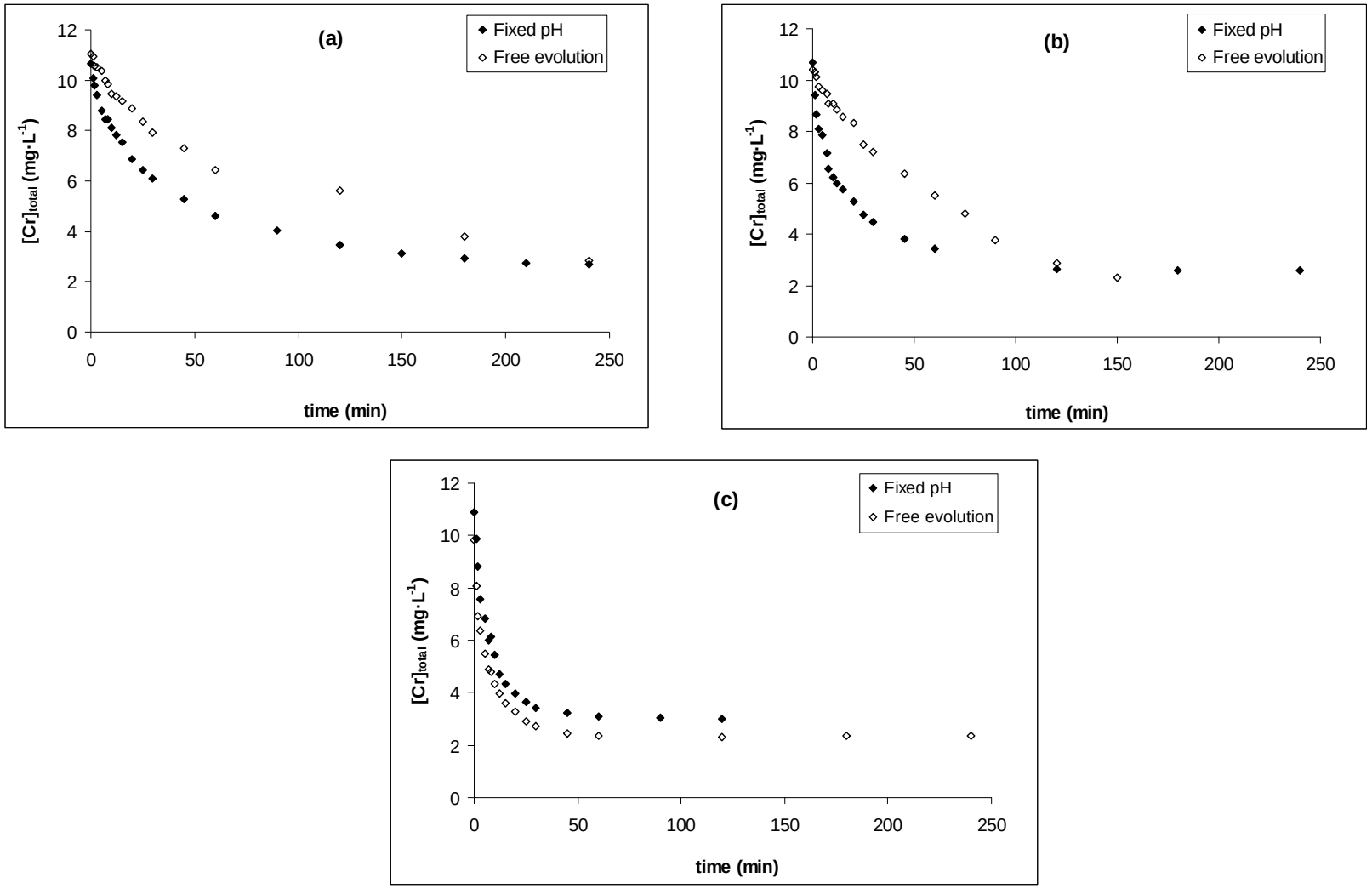

Figure 8: Total chromium concentration in solution as a function of contact time for the different thermic series with and without pH readjustment to the initial 3.0±0.1 value. (a) 5 ºC, (b) 20 ºC and (c) 50 ºC. $[Cr(VI)]_0 \approx 10.5$ mg·L^{-1}; sorbent dose: 2.5 g·L^{-1}.

As it can be observed in **Figure 8**, for the lowest and intermediate temperatures, the metal removal rate is strongly affected by the acidification conditions under which the kinetics is conducted. For the experiments at 5 and 20 ºC, total chromium removal rate is strongly increased under continuous pH compensation. In the case of 50 ºC, the total chromium concentration temporal profile for experiments performed under condition of readjusted and non-readjusted pH becomes almost equal.

On the other hand, it seems that the residual chromium concentration at equilibrium is not affected by the particular conditions of acidity under which the experiments have been conducted.

The results obtained in this section indicate that, if we focus in the pollution of an industrial effluent expressed as total chromium concentration in solution, two options would present: carry out the process under continuous reacidification conditions to reduce the reaction time or to extend the reaction time, avoiding the addition of acid to the media.

As it was discussed in a previous section, despite chromium in the feeding effluent is on hexavalent form, the material exhibits strong reducing properties, becoming thus necessary for a total description of the dynamics of the process, the quantification of both, trivalent and hexavalent chromium concentration in solution as a function of contact time. In the next two sections, the total chromium sorption kinetics will be divided in two: the corresponding to the hexavalent and to the trivalent.

5.2.2. Hexavalent chromium removal

In this section, Cr(VI) concentration in solution as a function of contact time with GS for the three different temperatures, 5, 20 and 50 ºC, in experiments with and without pH readjustment to the initial 3.0 value will be monitored and results, discussed.

The experimental hexavalent chromium concentration in solution as a function of time is presented in the next table.

Table 5: Hexavalent chromium concentration in solution ($mg \cdot L^{-1}$) as a function of time for the experiments with and without pH readjustment. $[Cr(VI)]_0 \approx 10.5\ mg \cdot L^{-1}$; sorbent dose: $2.5\ g \cdot L^{-1}$; T: 5, 20 and 50 ºC. Initial pH: 3.0±0.1.

	5 ºC		20 ºC		50 ºC	
t(min)	**pH adj.**	**Free evol.**	**pH adj.**	**Free evol.**	**pH adj.**	**Free evol.**
0	10.64	11.05	10.68	10.80	10.87	9.82
1	4.19	8.52	5.57	9.82	4.31	2.39
2	2.89	8.36	4.29	8.35	1.37	1.03
3	2.62	8.01	2.24	8.32	0.68	0.92
5	1.96	7.91	1.35	7.77	0.64	0.54
7	1.80	7.20	1.24	7.75	0.61	0.45
8	1.64	6.67	1.11	7.29	0.61	0.45
10	1.60	6.08	0.77	6.97	0.61	0.45
12	1.51	5.80	0.61	6.95	0.40	0.45
15	1.31	5.35	0.61	6.67	0.00	0.00
20	1.02	4.87	0.61	6.14	0.00	0.00
25	0.99	4.04	0.61	5.93	0.00	0.00
30	0.95	3.85	0.31	5.92	0.00	0.00
45	0.99	2.57	0.31	4.45	0.00	0.00
60	0.47	1.62	0.31	1.53	0.00	0.00
90	0.47	--	0.27	1.09	0.00	--
120	0.47	0.39	0.22	0.83	0.00	0.00
150	0.25	--	0.00	0.64	0.00	--
180	0.13	0.37	0.00	--	0.00	0.00
210	0.00	--	0.00	--	0.00	--
240	0.00	0.12	0.00	0.00	0.00	0.00

* -- not determined

The results presented in the table indicate that hexavalent chromium concentration in solution follows, for the series with and without pH readjustment, a similar trend to the observed for total chromium; a progressive decay of metal concentration when contacting the chromium polluted effluent with GS. Nevertheless, the main difference between total and hexavalent chromium series would be that, while in the first case a non-negligible chromium concentration remains in solution, in the case of the hexavalent chromium, its total removal is observed at equilibrium time, except in the case of the lowest temperature, 5 ºC, without pH readjustment. In this experiment, a residual Cr(VI) concentration of 0.12 $mg \cdot L^{-1}$ remained in solution after 4 hours of contact time with the grape stalk.

If hexavalent chromium concentration in solution is plotted as a function of time for the three temperatures with and without pH compensation, the next figure is obtained:

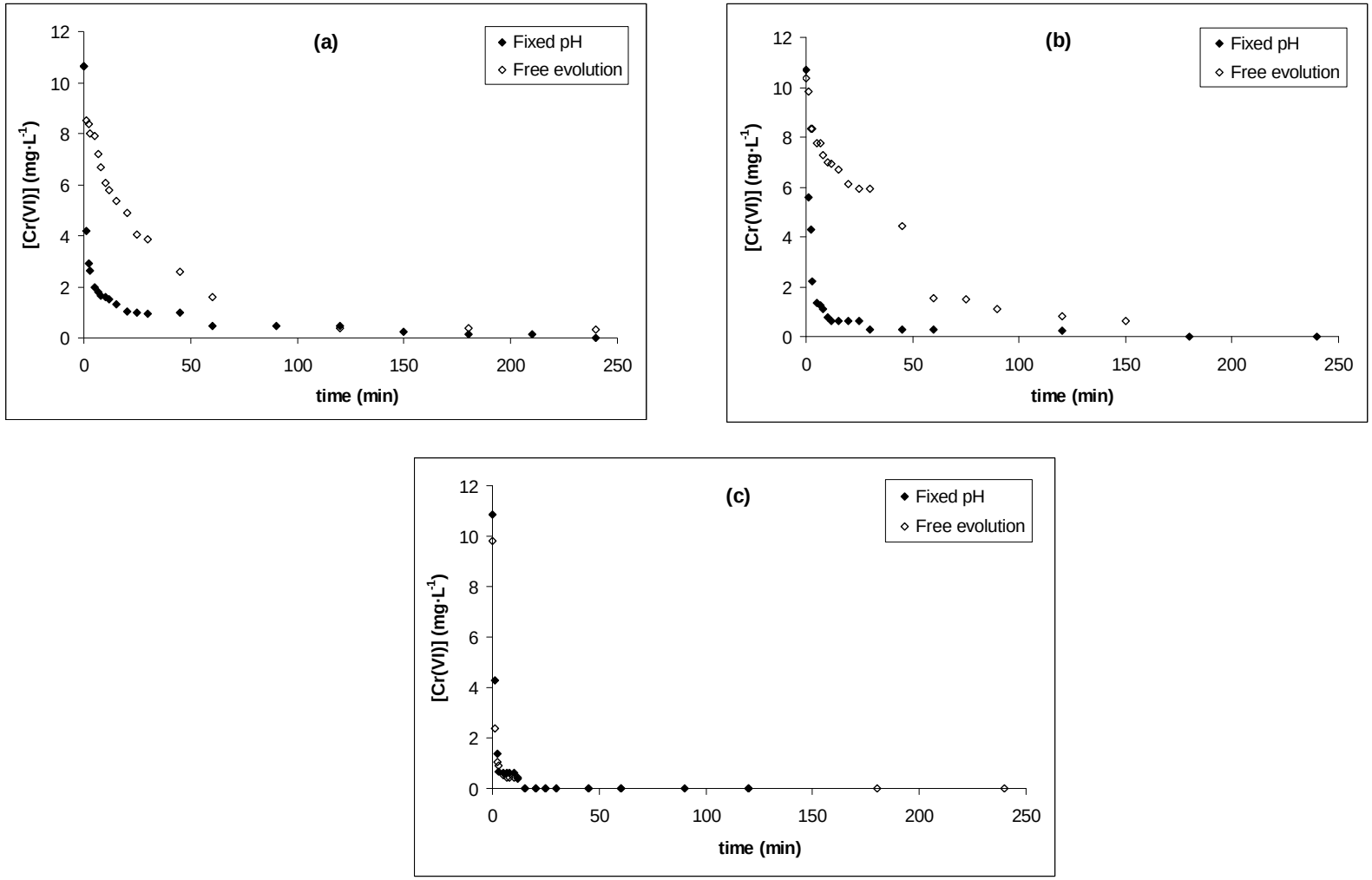

Figure 9: Hexavalent chromium concentration in solution as a function of contact time for the different thermic series with and without pH readjustment to the initial 3.0±0.1 value. (a) 5 ºC, (b) 20 ºC and (c) 50 ºC. $[Cr(VI)]_0 \approx 10.5$ mg·L^{-1}; sorbent dose: 2.5 g·L^{-1}.

The figure presented in this section clearly demonstrates the effect that reacidification exerts in the hexavalent chromium removal kinetics at a given temperature. As it can be seen, for the kinetic experiments carried out at 5 and 20 ºC, the constant pH compensation strongly enhances the rate of disappearance of chromium in this oxidation state and makes the process much faster than the performed under conditions of free pH evolution. A continuous H^+ addition to the media while it is being consumed accelerates the redox reaction since protons take part on it. Strong proton concentration dependency in hexavalent chromium sorption due to partial reduction to trivalent by a wide range o natural sorbents has been previously reported in the literature (Fiol *et al*., 2008; Park *et al*., 2005; Park *et al*., 2007; Park *et al*., 2008; Lytle *et al*., 1998; Cabatingan *et al*., 2001).

When the experiments were performed at the highest temperature, 50 ºC, no differences between the reacidified and the non-acidified series were observed. This fact is corroborating thus that Cr(VI) sorption/reduction process by GS can be enhanced by either, H^+ addition to the media or increasing of thermal energy to the reaction volume.

Nevertheless, as it had been discussed previously, the remaining hexavalent chromium concentration in solution at equilibrium does not depend on the temperature of the media, since almost complete hexavalent chromium removal is achieved for all the experiments.

With the data of total and hexavalent chromium concentration evolution in the liquid phase as a function of contact time, trivalent chromium temporal profile can be easily calculated by subtracting to the total chromium concentration, the corresponding to the hexavalent. Results obtained are presented in the next section.

5.2.3. Trivalent chromium formation and removal

In this last section of the study of combined effect of temperature and pH on the detoxification of a Cr(VI) polluted effluent by using grape stalk wastes, Cr(III) concentration in solution as a function of contact time profile for the different thermic series is presented and discussed.

In the next table, results of Cr(III) concentration in solution as a function of contact time for experiments performed at 5, 20 and 50 ºC under conditions of constant pH 3.0 and pH allowed to free evolve are presented.

Table 6: Trivalent chromium concentration in solution ($mg \cdot L^{-1}$) as a function of time for the experiments with and without pH readjustment. $[Cr(VI)]_0 \approx 10.5\ mg \cdot L^{-1}$; sorbent dose: $2.5\ g \cdot L^{-1}$; T: 5, 20 and 50 ºC; Initial pH: 3.0±0.1.

	5 ºC		20 ºC		50 ºC	
t(min)	**pH adj.**	**Free evol.**	**pH adj.**	**Free evol.**	**pH adj.**	**Free evol.**
0	0.00	0.00	0.00	0.00	0.00	0.00
1	5.89	2.41	3.85	0.49	5.55	5.68
2	6.91	2.18	4.36	1.77	7.43	5.87
3	6.79	2.49	5.85	1.41	6.87	5.46
5	6.83	2.48	6.52	1.83	6.18	4.94
7	6.67	2.79	5.91	1.82	5.39	4.44
8	6.79	3.19	5.45	1.93	5.53	4.35
10	6.49	3.39	5.45	213	4.85	3.88
12	6.31	3.57	5.37	1.91	4.08	3.52
15	6.24	3.81	5.12	1.88	4.35	3.58
20	5.85	4.00	4.68	2.17	3.95	3.26
25	5.42	4.29	4.14	2.27	3.63	2.90
30	5.13	4.07	4.16	2.53	3.43	2.71
45	4.30	4.74	3.51	2.91	3.22	2.46
60	4.16	4.80	3.12	3.99	3.07	2.35
90	3.57	--	2.72	2.68	3.05	--
120	2.97	5.24	2.43	2.03	3.02	2.33
150	2.86	--	2.51	1.68	3.02	--
180	2.80	3.40	2.58	--	3.02	2.34
210	2.75	--	2.55	--	--	--
240	2.71	2.51	2.55	1.94	--	2.35

* -- not determined

This table demonstrates again the contrast between the dynamics of total and hexavalent chromium and the corresponding to the trivalent chromium: while the first two follow a continuous decreasing profile with time, in the case of the trivalent chromium, the equilibrium is reached after two different processes, involving the first one the production of Cr(III) from reduction of Cr(VI) and the subsequent progressive decay of this reduction-formed Cr(III) by sorption onto GS, reaching an equilibrium value. For comparison sake, experiments with and without pH readjustment for a given temperature have been plotted and presented in the next figure.

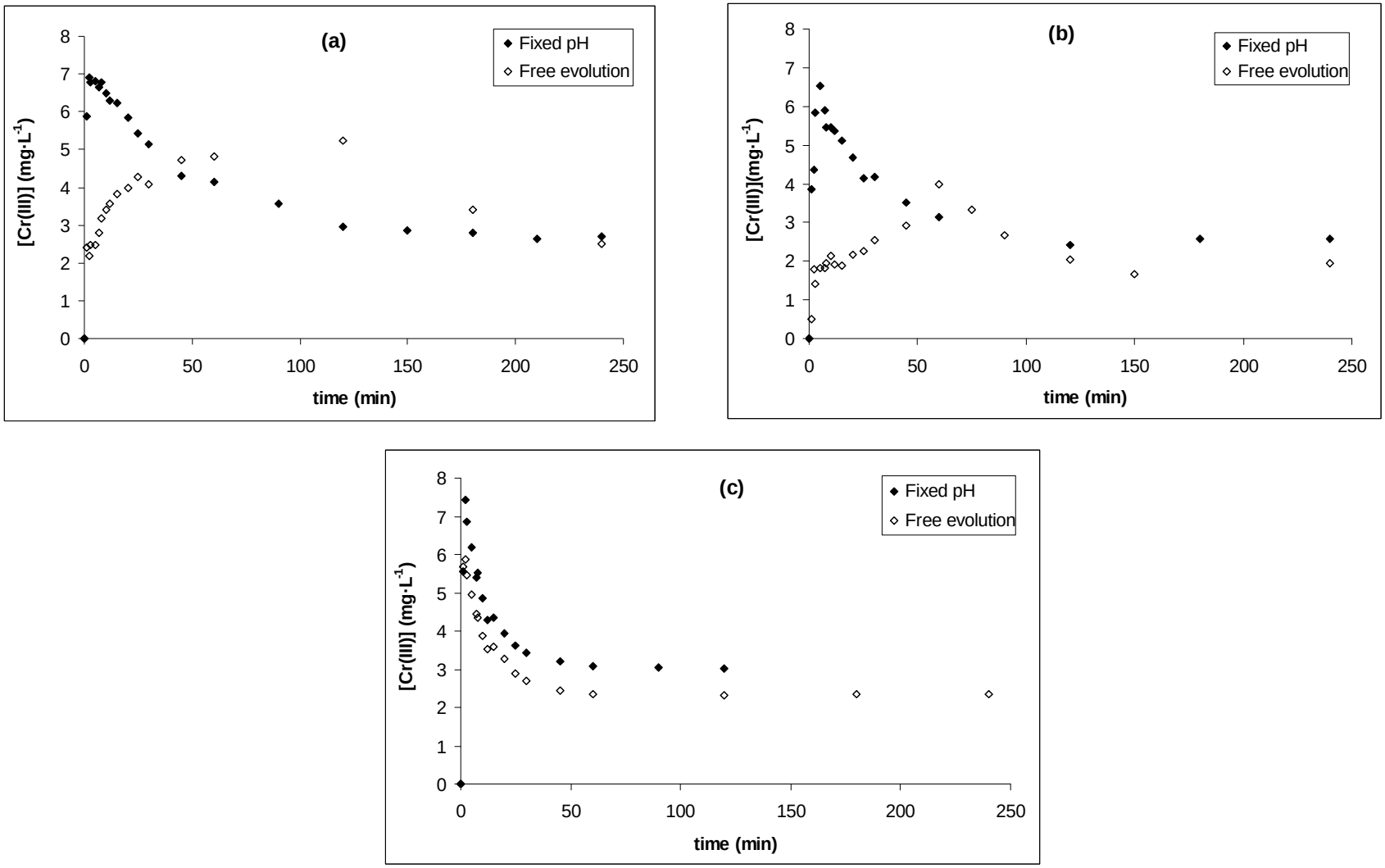

Figure 10: Trivalent chromium concentration in solution as a function of contact time for the different thermic series with and without pH readjustment to the initial 3.0±0.1 value. (a) 5 ºC, (b) 20 ºC and (c) 50 ºC. $[Cr(VI)]_0 \approx 10.5$ mg·L^{-1};sorbent dose: 2.5 g·L^{-1}.

As it can be seen in the figure, for the temperatures of 5 and 20 ºC, the Cr(III) production rate is strongly dependent on the acidity conditions under which the process takes place. For these two temperatures, under continuous pH compensation the ascendant slope corresponding to the Cr(III) production per time unit is much higher than in the case of the experiments carried out under non-corrected pH conditions. This fact is reflected also in the time to reach the maximum Cr(III) concentration in solution. For experiments at 5 ºC, this time varies, from 2 minutes (reaching a concentration of 6.91 $mg \cdot L^{-1}$) in the case of corrected pH, to 120 minutes (reaching a concentration of 5.24 $mg \cdot L^{-1}$) without pH compensation. For the temperature of 20 ºC, the maximum Cr(III) concentration in solution is reached after 3 minutes (with a concentration of 5.85 $mg \cdot L^{-1}$) in the experiments carried out with pH compensation and in 60 minutes (with a lower concentration, 3.99 $mg \cdot L^{-1}$) without pH control. In the case of the highest temperature, 50 ºC, both, the reacidified and the allowed to free evolve scenarios become almost equal kinetically, reaching a maximum Cr(III) concentration of 7.43 and 5.87 $mg \cdot L^{-1}$ respectively in only 2 minutes.

These data point out that trivalent chromium maximum production is strongly dependent on the acidity conditions; for a given temperature, the experiments carried out under constant reacidification conditions lead always to a higher maximum Cr(III) concentration in solution.

As the temporal profile of trivalent chromium is not continuous; the reaching of the maximum Cr(III) concentration in solution marks an inflexion point in the increasing tendency and, from this point, the concentration progressively decreases by sorption n equilibrium value. When the rate of this decrease is compared for a given temperature under conditions of pH control and allowed to free evolve, it can be observed that, for all the temperatures, the negative slopes that would be derived from this process would exhibit a quite good parallelism, indicating thus that Cr(III) sorption rate would not be influenced by the extra presence of H^+ of the reacidified scenario.

On the other hand, the equilibrium Cr(III) concentration in solution is, for the three temperatures, higher in the case of the process carried out under pH readjustment. The extra H^+ concentration of the reacidified series respect to the allowed to free evolve provokes an extra competition with cationic Cr^{3+} and $CrOH^{2+}$ species of Cr(III). This leads to a partial replacement of Cr(III) by H^+ from the sorption active sites of the material and release of trivalent chromium to the solution.

5.3. Effect of initial Cr(VI) concentration in sorption/reduction kinetics at constant pH and temperature

In order to check the feasibility of this process to adapt to different conditions of Cr(VI) concentration in the effluent, the effect of initial metal content was studied under conditions of constant pH 3.0±0.1. Three initial Cr(VI) concentrations around 5, 10 and 20 $mg \cdot L^{-1}$ were chosen, and a temperature of 20.0±0.1 ºC. As in previous sections, the chromium removal rate will be evaluated in all its possible ways; expressed as total, hexavalent and trivalent concentration in solution. In the next section the results obtained for total chromium removal as a function of time are presented and discussed.

5.3.1. Total chromium removal

In the next table, total chromium concentration in solution for each contact time is presented for the three different initial hexavalent chromium concentrations.

Table 7: Total chromium concentration in solution ($mg \cdot L^{-1}$) as a function of contact time for the different initial Cr(VI) concentrations. $[Cr(VI)]_0$: 5.52, 10.68 and 19.65 $mg \cdot L^{-1}$; pH : 3.0±0.1; sorbent dose: 2.5 $g \cdot L^{-1}$; T: 20.0±0.1 ºC.

	Initial Cr(VI) concentration		
	5.52 $mg \cdot L^{-1}$	**10.68 $mg \cdot L^{-1}$**	**19.65 $mg \cdot L^{-1}$**
t(min)	**$[Cr]_t$**	**$[Cr]_t$**	**$[Cr]_t$**
0	5.52	10.68	19.65
1	5.39	9.42	19.10
2	5.14	8.65	18.20
3	4.92	8.09	17.01
5	4.86	7.87	16.79
7	4.79	7.15	15.73
8	4.61	6.56	14.72
10	4.60	6.22	13.68
12	4.44	5.98	12.00
15	4.28	5.73	10.60
20	3.98	5.29	9.95
25	3.72	4.75	7.88
30	3.67	4.47	6.31
45	3.04	3.82	4.68
60	2.59	3.43	4.72
120	1.60	2.65	4.70
180	1.17	2.58	4.71
240	0.90	2.58	4.65
300	0.86	2.55	4.74
360	0.83	2.54	4.73

The table shows a decrease of total chromium content when contacting the solution with GS wastes. As it was expected, the remaining concentration in solution at equilibrium time increases when it does the feeding metal concentration. The chromium equilibrium concentrations vary from 0.83 $mg \cdot L^{-1}$ in the case of the lowest initial Cr(VI) concentration, to 2.54 in the case of the intermediate one and to 4.73 $mg \cdot L^{-1}$ when the material is submitted to an initial Cr(VI) concentration of 19.65 $mg \cdot L^{-1}$. This reduction in total metal content in solution can be expressed also as percentage obtaining values of 85% for the lowest initial metal concentration and around 76% for both, the intermediate and highest one.

From this table it is also interesting to compare the time to reach the 50% of removal of the initial metal content ($t_{1/2}$) for the different initial concentrations. In the table it has been underlined half the feeding metal concentration for each series. As it can be observed, while in the case of the lowest concentration this reduction of the total chromium content in the

effluent is achieved after approximately 60 minutes of contact time, in the case of the other two concentrations, only 20 minutes are required. In the same way, when comparing the contact time needed to reach sorption equilibrium, a decrease from around 300 minutes in the case of the lowest concentration, to 180 for the intermediate and to only 45 minutes in the case of the highest concentration was observed

The decrease of needed time to reach equilibrium when increasing metal content in solution is common in sorption due to the strong relevance of this parameter as driving force of the liquid to solid mass transfer rate.

When the variation of metal content in solution as a function of time is plotted for the different initial Cr(VI) concentrations, the next figure is obtained.

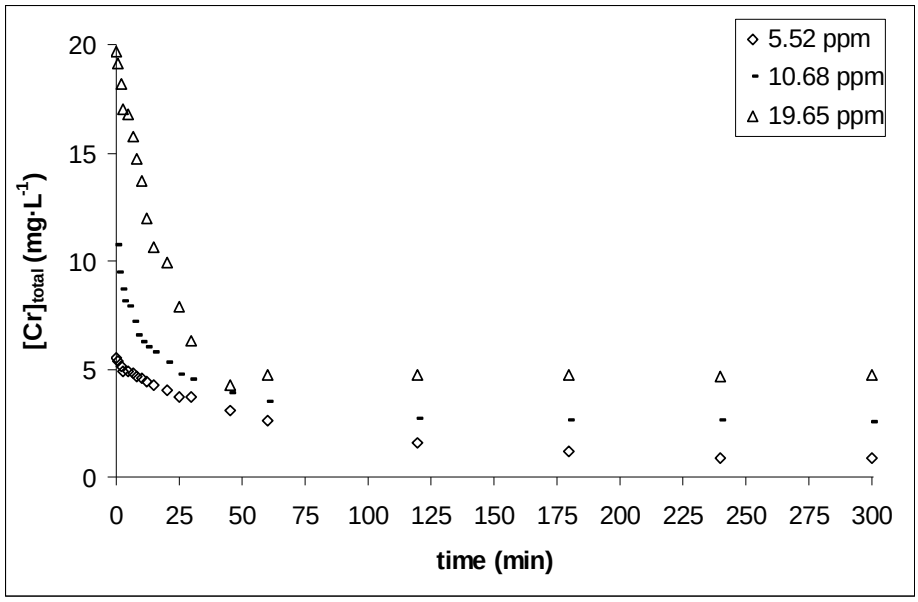

Figure 11: Total chromium concentration in solution as a function of time for the different initial hexavalent chromium concentrations. $[Cr(VI)]_0$: 5.52, 10.68 and 19.65 $mg \cdot L^{-1}$; T: 20.0±0.1 ºC; pH: 3.0±0.1; sorbent dose: 2.5 $g \cdot L^{-1}$.

As it can be observed in the figure, total chromium removal for the two highest Cr(VI) concentrations exhibit a two-phase profile. First phase, from 0 to approximately 25 minutes, involves a fast removal of the pollutant and the second one, related to a lower removal rate slowly drives the system to the equilibrium. In the case of the lowest initial chromium concentration, the temporal concentration profile does not exhibit such a pronouncing change fast-slow as the observed for the 10.68 and 19.65 $mg \cdot L^{-1}$ series.

It is noteworthy also the increase of the slope related to the decrease of metal concentration as a function of time when increasing the initial Cr(VI) concentration in solution. This behaviour can be explained by the fact that, higher initial adsorbate concentration would provide a higher driving force to overcome all mass transfer resistances of the metal ions from the aqueous to the solid phase resulting in higher probability of a collision leading to sorption between Cr(VI) ions and active sites (Baral *et al*., 2006).

As it had been discussed in previous sections, in order to obtain information about the performance of the detoxification process, it becomes necessary to know exactly the profile with time of chromium oxidation states in solution for the different initial Cr(VI) concentrations. In the next two sections Cr(VI) and Cr(III) temporal concentration profiles respectively, will be presented and discussed.

5.3.2. Hexavalent chromium removal

In the next table, experimental hexavalent chromium concentration in solution for each contact time is presented for the three different initial hexavalent chromium concentrations.

Table 8: Hexavalent chromium concentration in solution ($mg \cdot L^{-1}$) as a function of contact time for the different initial Cr(VI) concentrations. $[Cr(VI)]_0$: 5.52, 10.68 and 19.65 $mg \cdot L^{-1}$; pH : 3.0±0.1; sorbent dose: 2.5 $g \cdot L^{-1}$; T: 20.0±0.1 ºC.

	Initial Cr(VI) concentration		
	5.52 $mg \cdot L^{-1}$	**10.68 $mg \cdot L^{-1}$**	**19.65 $mg \cdot L^{-1}$**
t(min)	**[Cr(VI)]**	**[Cr(VI)]**	**[Cr(VI)]**
0	5.52	10.68	19.65
1	4.78	5.57	13.90
2	4.55	4.29	13.01
3	4.10	2.24	12.17
5	4.00	1.35	11.39
7	3.93	1.24	11.23
8	3.69	1.11	10.27
10	3.37	0.77	9.61
12	3.16	0.61	8.39
15	2.15	0.61	6.83
20	2.12	0.61	5.73
25	1.59	0.61	4.54
30	1.16	0.31	4.00
45	0.50	0.31	1.08
60	0.39	0.31	0.48
120	0.25	0.22	0.00
180	0.21	0.00	0.00
240	0.21	0.00	0.00
300	0.00	0.00	0.00
360	0.00	0.00	0.00

The results presented in the table indicate that hexavalent chromium concentration as a function of contact time exhibits an analogous trend as total chromium removal; decrease of Cr(VI) content when contacting the solution with GS wastes. When only hexavalent chromium is considered, equilibrium is reached when this specie completely disappears in the liquid phase, independently of the total concentration considered. It has to be mentioned also that the time to reach equilibrium for the different Cr(VI) initial concentrations is reduced

from 300 minutes in the case of the lowest to 180 for the intermediate and to 120 minutes in the case of the highest.

For and easier comparison of Cr(VI) evolution profile, its concentration in solution as a function of contact time with GS has been plotted in the next figure for the different initial Cr(VI) concentrations.

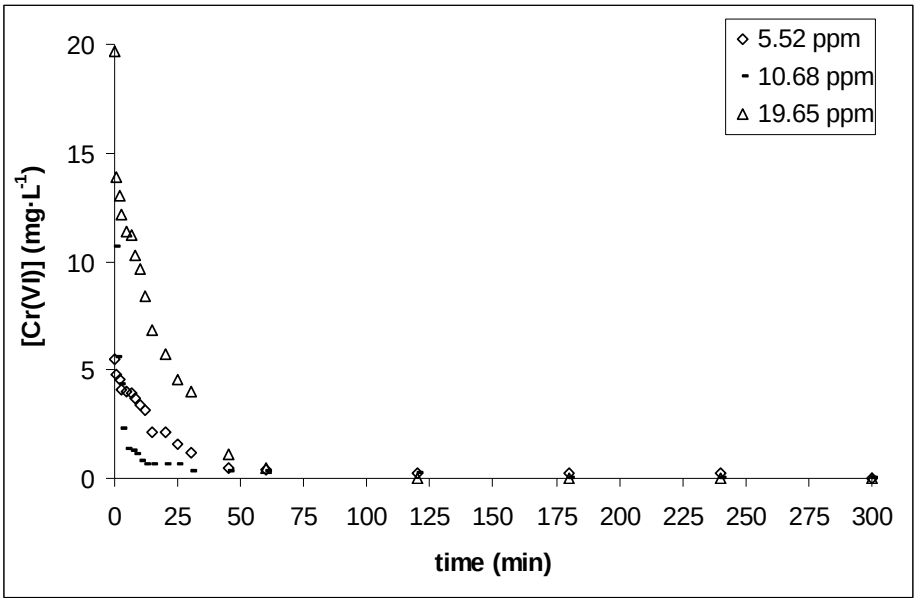

Figure 12: Hexavalent chromium concentration in solution as a function of time for the different initial hexavalent concentrations. $[Cr(VI)]_0$: 5.52, 10.68 and 19.65 $mg \cdot L^{-1}$; T: 20.0±0.1 ºC; pH: 3.0±0.1; sorbent dose: 2.5 $g \cdot L^{-1}$.

This figure clearly demonstrates the excellent detoxification performance of the process for the three initial metal concentrations due to the total removal of the most toxic hexavalent chromium concentration in solution in the first minutes of contact with GS. When comparing this graphic with the obtained for total chromium, it can be observed that, for all the initial hexavalent chromium concentrations, the initial slopes for Cr(VI) removal are higher than the observed for total chromium removal. So that, to fulfil the chromium mass balance in solution, it is clear that Cr(III) has to appear in solution. In the next section, the evolution of Cr(III) concentration in solution for the different Cr(VI) feeding concentrations is presented and discussed.

5.3.3. Trivalent chromium formation and removal

In the next table, experimental trivalent chromium concentration in solution for each contact time is presented for the three different initial hexavalent chromium concentrations.

Table 9: Trivalent chromium concentration in solution ($mg \cdot L^{-1}$) as a function of contact time for the different initial Cr(VI) concentrations. $[Cr(VI)]_0$: 5.52, 10.68 and 19.65 $mg \cdot L^{-1}$; pH : 3.0±0.1; sorbent dose: 2.5 $g \cdot L^{-1}$; T: 20.0±0.1 ºC.

	Initial Cr(VI) concentration		
	5.52 $mg \cdot L^{-1}$	**10.68 $mg \cdot L^{-1}$**	**19.65 $mg \cdot L^{-1}$**
t(min)	**[Cr(III)]**	**[Cr(III)]**	**[Cr(III)]**
0	0.00	0.00	0.00
1	0.61	3.85	5.20
2	0.59	4.36	5.19
3	0.82	5.85	4.84
5	0.86	6.52	5.40
7	0.86	5.91	4.50
8	0.92	5.45	4.45
10	1.23	5.45	4.07
12	1.28	5.37	3.61
15	2.13	5.12	3.77
20	1.86	4.68	4.22
25	2.13	4.14	3.34
30	2.51	4.16	2.31
45	2.54	3.51	3.20
60	2.20	3.12	4.24
120	1.35	2.43	4.70
180	0.96	2.58	4.71
240	0.69	2.58	4.65
300	0.86	2.55	4.74
360	0.83	2.54	4.73

This table puts into evidence an important Cr(III) production by the system from the beginning of the process, followed by a decrease in the Cr(III) concentration in solution by adsorption onto the GS particles. As it was expected, this Cr(III) production is higher as higher is the initial Cr(VI) content. It is noteworthy the formation of 5.20 $mg \cdot L^{-1}$ of trivalent chromium in only 1 minute of contact time for the highest Cr(VI) concentration. It's interesting also to compare the extension of the Cr(VI) to Cr(III) reduction reaction for the different initial metal concentrations for the lowest of the studied contact time, 1 minute, in

order to make an idea of the detoxification rate in the very first beginning of the process. If a comparison by percentage of reduction respect to the feeding Cr(VI) concentration is carried out for this first minute of contact GS-solution, values of 11.1% for the lowest Cr(VI) initial concentration, 36.1% for the intermediate and 26.5% for the highest one are obtained. On the other hand, if maximum Cr(III) production percentage respect to the feeding Cr(VI) concentration is calculated, values of 46.0 % for the lowest, 61.1% for the intermediate and 27.5 % for the highest Cr(VI) concentration are obtained. It is also interesting also to make the comparison of the time to reach the maximum Cr(III) production for each feeding Cr(VI) concentration. As it can be seen in **Table 9**, the maximum Cr(III) production is very fast for the two highest initial metal concentrations, taking place in only 5 minutes with a Cr(III) concentration of 6.52 and 5.40 for the feeding Cr(VI) concentrations of 10.68 and 19.65 respectively. For the lowest initial Cr(VI) concentration, 5.52 $mg \cdot L^{-1}$, maximum is reached with 2.54 $mg \cdot L^{-1}$ of Cr(III) in 50 minutes. All these results clearly put into evidence the strong reductive potential of the material in the conditions of constant 3.0 pH.

For easier comparison of trivalent chromium concentration profile for the different initial Cr(VI) concentrations, Cr(III) concentration in solution as a function of contact time with GS has been plotted in **Figure 13**.

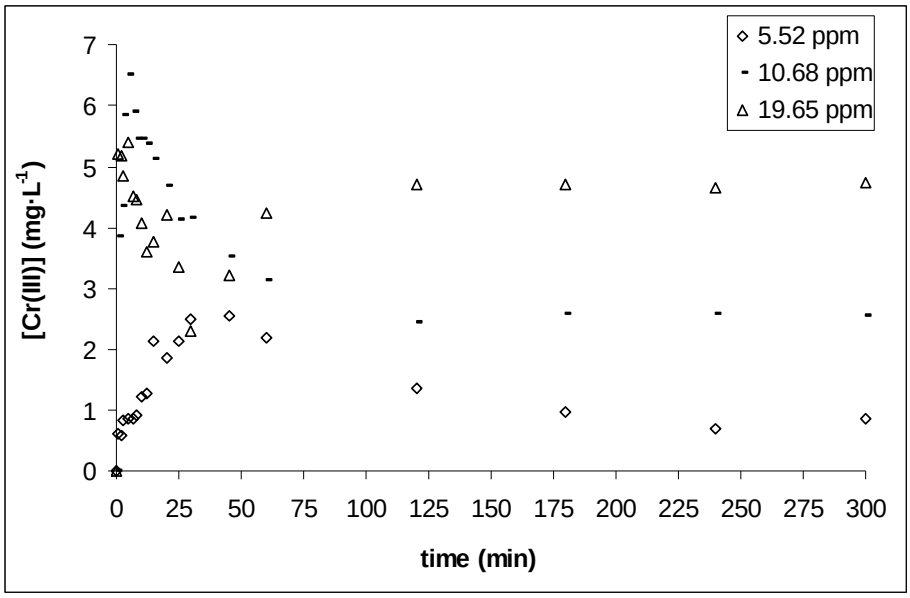

Figure 13: Trivalent chromium concentration in solution as a function of time for the different initial hexavalent concentrations. $[Cr(VI)]_0$: 5.52, 10.68 and 19.65 $mg \cdot L^{-1}$; T: 20.0±0.1 ºC; pH: 3.0±0.1; sorbent dose: 2.5 $g \cdot L^{-1}$.

In this figure it can be clearly observed the dynamics of Cr(III) in the reactor: (i) a fast Cr(III) production due to Cr(VI) reduction, (ii) the reach of a maximum concentration and (iii) the progressive decrease of Cr(III) concentration to reach an equilibrium concentration.
As it was expected and shown also in **Table 9**, the higher the initial hexavalent chromium concentration in the feeding effluent, the higher the Cr(III) remaining concentration in solution at equilibrium time.

5.4. Kinetic modeling of Cr(VI) sorption/reduction process

Dynamic simulation can be considered as an essential part of any hazard or operability study. It is of capital importance in both, large scale continuous process operations and other inherently dynamic operations such as batch, semi-batch and cyclic manufacturing processes. Dynamic simulation also aids in a very positive sense in gaining a better understanding of process performance and is a powerful tool for plant optimisation, both at the operational and at the design stage. As presented in the introduction section, the overall liquid-solid sorption process can be described by combination of different steps:

- Solute transport from the bulk of the solution
- Diffusion through the fluid film that surrounds the particle to the surface
- Intraparticle diffusion
- Adsorption by chemical reaction or physical weak interactions

In this section, a batch dynamic model that integrates the hexavalent to trivalent reaction process and the sorption/desorption of both oxidation states onto grape stalk will be developed. Its predictive power to successfully explain the dynamics of chromium disappearing, in the case of total and hexavalent, and appearing/disappearing in the case of the trivalent will be evaluated and discussed. The model has been proposed in basis to: (i) irreversible reduction of Cr(VI) to Cr(III) reaction, whose reaction rate is assumed to be proportional to the Cr(VI) concentration in solution and (ii) adsorption and desorption of Cr(VI) and Cr(III) formed assuming that all the processes follow a Langmuir kinetics (Suen, 1996). A scheme of the different steps is depicted in **Figure 14**.

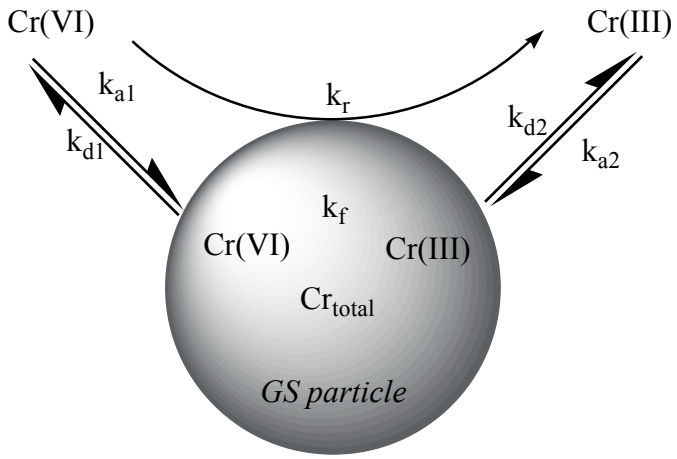

Figure 14: Scheme of the mechanistical approach proposed for hexavalent chromium sorption/reduction process promoted by grape stalk.

The process has been represented by the equilibrium corresponding to the sorption/desorption of trivalent and hexavalent chromium on the grape stalk particle and a reaction that irreversibly transforms the hexavalent to trivalent chromium.

The reaction constant corresponding to the Cr(VI) to Cr(III) reduction has been labelled as k_r. On the other hand, the constants related to sorption and desorption have been labelled as k_a and k_d respectively. In the same way, the constants that present the subindex 1 make reference to the hexavalent chromium and these containing the subindex 2, to trivalent. The constant k_f makes reference to the relative proportion of the chromium sorbed keeping its hexavalent oxidation state, to the total chromium sorbed.

The different phenomena can be included in a series of dimensionless equations, leading to the system:

$$\frac{du_1}{dt} = -k_r u_1 - k_{a1} u_1 (1 - k_f u_3) + k_{d1} k_f u_3 \quad (1)$$

$$\frac{du_2}{dt} = k_r u_1 - k_{a2} u_2 (1 - (1 - k_f) u_3) + k_{d2} (1 - k_f) u_3 \quad (2)$$

$$\frac{du_3}{dt} = k_{a1} u_1 (1 - k_f u_3) - k_{d1} k_f u_3 + k_{a2} (u_2 (1 - (1 - k_f) u_3) - k_{d2} (1 - k_f u_3) \quad (3)$$

where u_1 is defined as the ratio between Cr(VI) concentration in solution at time t and initial Cr(VI) concentration in $mg \cdot L^{-1}$ ($C_{Cr(VI)t}/C_{Cr(VI)0}$); u_2 as the ratio between Cr(III) concentration at time t and initial Cr(VI) concentration in $mg \cdot L^{-1}$ ($C_{Cr(III)t}/C_{Cr(VI)0}$) and u_3, as q_t/q_e where q_t

and q_e are the amount of total chromium sorbed ($mg \cdot g^{-1}$) at time t and at equilibrium, respectively.

In the differential equations system, k_f has been defined as the ratio of the amount of hexavalent chromium ($q_{Cr(VI)}$) to total chromium sorbed (q_{Tot}) ($k_f = q_{Cr(VI)}/q_{Tot}$).

The results of the model have been calculated by integration of the differential equations system by means of the function Ode 45 of Matlab v. 7.1 (R-14), which applies Runge-Kutta method of 4-5 order.

The constants of the model were determined by minimizing the Sum of Squared Error (SSE). The function is described as the sum of the relative square errors for Cr(VI) and Cr(III), according to the next equation:

$$SSE = \sum_{i=1}^{n} \left(\frac{C_{Cr(VI)\exp}(t_i) - C_{Cr(VI)calc}(t_i)}{C_0} \right)^2 + \left(\frac{C_{Cr(III)\exp}(t_i) - C_{Cr(III)calc}(t_i)}{C_0} \right)^2 \quad (4)$$

Minimization of the function was carried out by using the method of Generalized Reduced Gradient (GRG).

5.4.1. Effect of temperature at constant pH

Experimental data obtained in the study of the effect of temperature in the sorption/reduction process by grape stalk were submitted to the model and the characteristic constants were calculated. In the next table, the numerical values of these constants as well as the square error derived from the calculations are presented in the next table.

Table 10. Constants of the sorption/reduction process by GS calculated by means of the model for the different temperatures in the range 5 to 60 ºC under conditions of constant pH 3.0±0.1.

T (ºC)	k_r	k_{a1}	k_{d1}	k_{a2}	k_{d2}	k_f	SSE
5	23.75	9.84	0.21	1.23	0.91	0.80	0.30
20	25.77	9.79	0.57	3.23	0.65	0.45	0.07
30	50.57	6.49	1.42	5.33	2.33	0.60	0.02
50	60.73	6.18	1.49	8.83	2.14	0.30	0.03
60	110.33	6.10	1.51	8.90	1.98	0.10	0.05

From the results presented in the table, different evidences can be pointed out. Firstly, it can be observed that the constant related to the irreversible transformation of hexavalent to trivalent chromium, k_r, shows an increasing tendency with the temperature, ranging from a value of 23.75 at 5ºC to 110.33 at 60 ºC. These fact is indicative of the enhancement of the Cr(VI) to Cr(III) transformation rate when temperature is raised. This positive effect of temperature is consistent with the results reported in literature, where authors observed an increase of Cr(VI) removal and reduction rate when increasing the temperature at wich the process took place (Park *et al*., 2004; Gardea-Torresdey *et al*., 2000, Sharma and Forster, 1993).

The table shows a decreasing trend of the Cr(VI) sorption constant, (k_{a1}), when increasing the temperature from values ranging from 9.84 at 5 ºC to 6.10 at 60 ºC. These results would indicate that hexavalent chromium sorption rate slightly decreases when increasing the temperature. But in this discussion it has to be also taken into account that the hexavalent to trivalent chromium transformation rate is strongly enhanced by an increase of the temperature, as reflected the k_r values. This enhancement of the reduction reaction would involve a decrease on the hexavalent chromium in solution. Taking into account the relevance of the sorbate concentration in solution as driving force of the sorption process, the decrease in the Cr(VI) concentration would contribute to decrease the numerical values or the adsorption rate constants k_{a1}.

On the contrary, the constant that reflects the Cr(III) adsorption rate, k_{a2}, shows a clear increasing trend with the temperature from values ranging from 1.23 at 5 ºC to 8.90 at 60 ºC. These results indicate that the increase of temperature increases the trivalent chromium removal rate. In a similar way as discussed previously for Cr(VI), the adsorption rate constant of Cr(III) is expected to be also influenced by the k_r values. As indicated previously, k_r strongly increases with temperature, indicating that the Cr(III) production rate would be higher as higher is the temperature. As the trivalent chromium concentration for a given time is expected to be higher as higher is the temperature, it would be expected also the increase of the Cr(III) sorption rate, due to its higher concentration in solution.

Concerning the desorption rate, while constants obtained for Cr(VI) (k_{d1}) exhibited a clear increasing trend with temperature, the Cr(III) desorption rate constants (k_{d2}) did not exhibit such a clear tendency. The results put into evidence that an increase of temperature would negatively affect the sorption of the hexavalent chromium, due to the enhancement of the desorption, while not a clear effect could be ascertained for the trivalent.

From this model it is also of remarkable interest, the obtention of a measure of the extension in which chromium is sorbed on the grape stalk as either, Cr(VI) or Cr(III). This extension is expressed by means of the constant k_f that, as discussed previously, quantitatively reflects the contribution of the hexavalent chromium fraction on the solid phase to the total chromium sorbed amount ($k_f=q_{Cr(VI)}/q_{total\ Cr}$). As it can be seen in the table, the k_f constant exhibits a fair decreasing tendency when increasing the temperature. The calculated values varied from 0.80 (80% of the total chromium as Cr(VI) and 20% as Cr(III)) at 5ºC to 0.10 (10% of Cr(VI) and 90% of Cr(III)) at 60 ºC. These results indicate that an increase of the temperature leads to an increase of the sorption of the trivalent oxidation state, in detriment of the sorption in the hexavalent form. This observation is in agreement with the results pointed out by the Cr(VI) to Cr(III) transformation rate constant, k_r, that demonstrated that the higher the temperature was, the higher the rate of the hexavalent reduction process and thus, the higher the trivalent chromium concentration in solution to be sorbed.

The constants presented in the table were introduced in the model and used to calculate the theoretical chromium concentration in solution expressed as total, hexavalent and trivalent for each contact time. Experimental results and those predicted by the model for the different temperatures under conditions of constant 3.0±0.1 pH are presented in the next figure in terms of normalized chromium concentration.

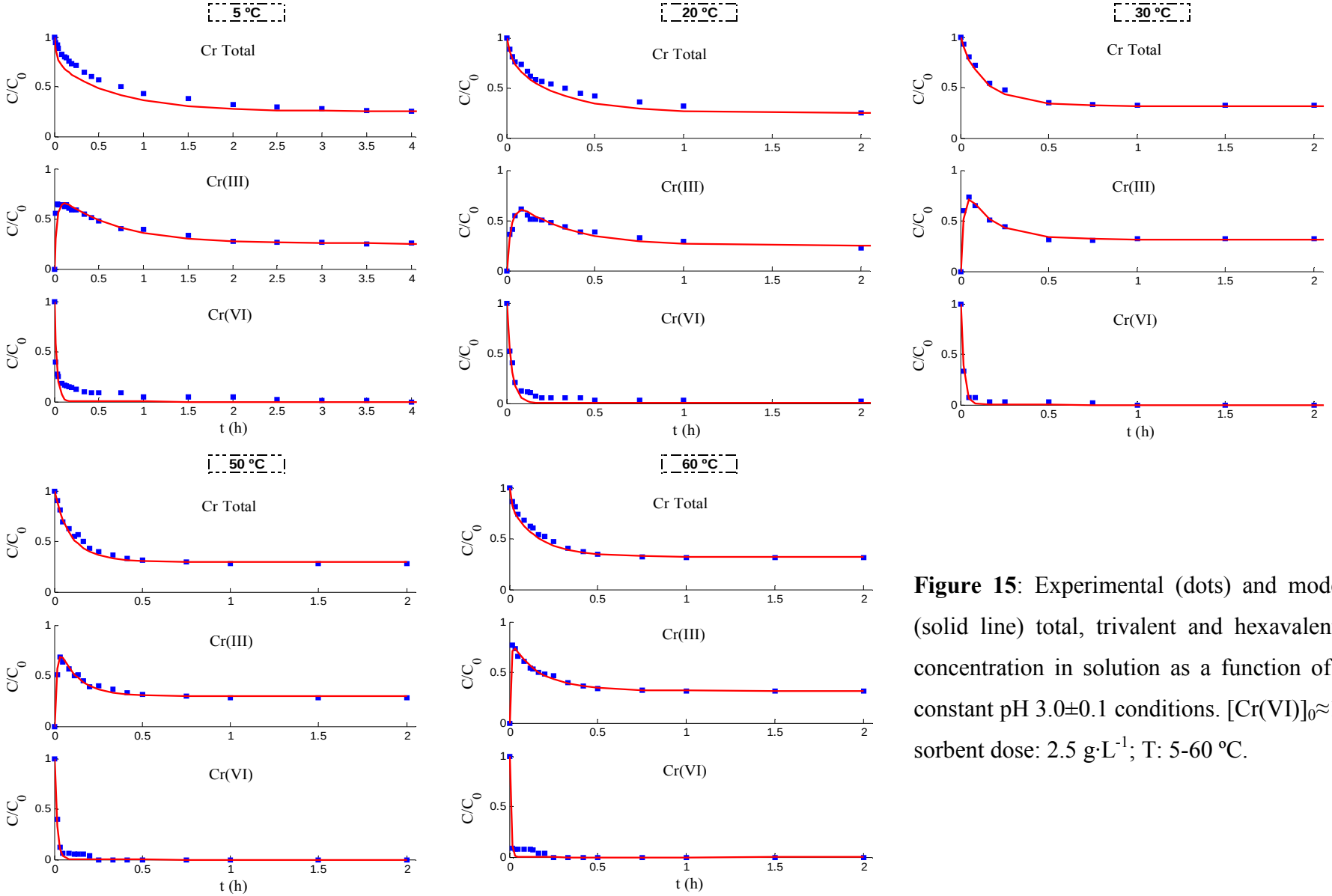

Figure 15: Experimental (dots) and model predicted (solid line) total, trivalent and hexavalent chromium concentration in solution as a function of time under constant pH 3.0±0.1 conditions. $[Cr(VI)]_0 \approx 10.5$ mg·L^{-1}; sorbent dose: 2.5 g·L^{-1}; T: 5-60 ºC.

In the figure, experimental results have been presented in blue dots, and model prediction in red solid line. The figure demonstrates the excellent correlation between the model predicted concentration values and those obtained through experimentation for both, hexavalent and trivalent chromium concentration and also, when the dynamics of the process is expressed in terms of total chromium.

5.4.2. Effect of pH at constant temperature

Kinetics of total, hexavalent and trivalent chromium concentration for three temperatures, 5, 20 and 50 ºC without pH readjustment were also submitted to the model proposed in this section and the characteristic constants were calculated. In the next table, the constants and the square error obtained on its calculations are presented. For comparison sake, the rate constants obtained for the same temperatures in experiments with pH adjustment have been also included.

Table 11. Constants of the sorption/reduction process by GS calculated by means of the model for different temperatures, 5, 20 and 50 ºC under conditions of constant pH 3.0±0.1 and allowed to free evolve.

T (ºC)	pH adjustment (Y/N)	k_r	k_{a1}	k_{d1}	k_{a2}	k_{d2}	k_f	SSE
5	Y	23.75	9.84	0.21	1.23	0.91	0.80	0.30
	N	1.35	1.62	0.05	0.27	0.23	0.90	0.33
20	Y	25.77	9.79	0.57	3.23	0.65	0.45	0.07
	N	1.37	0.29	0.04	1.74	0.48	0.69	0.20
50	Y	60.73	6.18	1.49	8.83	2.14	0.30	0.03
	N	59.54	0.18	0.02	8.3	0.97	0.10	0.03

In the table it can be observed how the numerical values of the constant related to the irreversible transformation of hexavalent to trivalent chromium (k_r) clearly reflects the experimental observed trend. As discussed in section 5.2, the reduction of the hexavalent chromium to its trivalent form was strongly influenced by both, the temperature and the acidity conditions of the process. The reduction rate had been proven to be, for the temperatures of 5 and 20 ºC, higher when the detoxification process was carried out under conditions of continuous pH compensation. On the other hand, it had been demonstrated

also that for the highest of the temperatures of this study, 50 ºC, the reduction rate under conditions of continuous pH compensation became almost equal. This fact demonstrates thus that the activation of the reduction could be carried out by either addition of thermic energy or by proton addition to the content of the reaction vessel. All these evidences are successfully described by the numerical values of the k_r constant of **Table 11**. As it can be seen in the table, for the temperatures of 5 and 20 ºC, the k_r is always higher for the experiments performed under conditions of pH compensation while for the temperature of 50 ºC, the constants obtained for the two acidity scenarios, become almost equal.

If the constants k_a and k_d, related to the sorption and desorption rate respectively, are compared for a given temperature with and without pH readjustment, it can be observed that both constants are always higher in the case of the experiments carried out under pH readjustment. On the other hand, the results presented in the table point out that hexavalent chromium sorption/desorption is more sensitive to the acidity conditions than trivalent chromium, as it can be concluded from the higher differences between the pair k_{a1} and k_{d1} than k_{a2} and k_{d2}.

The higher hexavalent chromium sorption rate (k_{a1}) in conditions of constant pH 3.0 could be explained by the higher number of positively charged sites. By constant addition of H^+ to the media the natural capacity of the GS to raise the pH of acidic solutions (buffering capacity) is avoided, and the development of a greater positive charge density on the surface is possible. These protonated sites can be available for the sorption of $HCrO_4^-$ anion through weak coulombic interactions.

In the case of the trivalent chromium, also higher sorption and desorption rate constants, (k_{a2}) and (k_{d2}) respectively, are obtained when experiments are carried out under constant pH readjustment conditions. The higher Cr(III) sorption rate constant (k_{a2}) observed under conditions of pH readjustment could be explained by the enhancement of the Cr(VI) reduction rate, that leads to the faster formation of a higher Cr(III) concentration in solution, increasing thus its sorption driving force. On the other hand, the higher Cr(III) desorption rate constant (k_{d2}) obtained under conditions of pH readjustment indicates that desorption is also more favourable under conditions of constant H^+ addition to keep the pH at 3.0. This fact could be explained by the competition that the extra H^+ addition creates with Cr^{3+} and $CrOH^{2+}$ species for the sorption active sites and that leads to a partial Cr(III) release from the sorbent.

On the other hand, it's interesting the comparison that can be established, by means of the constant k_f, between the fraction of hexavalent and trivalent chromium in the solid phase. As it can be seen in **Table 11**, for the temperatures of 5 and 20 ºC, the fraction of Cr(VI) sorbed is always higher in the case of the experiments performed without pH correction and decreases when increasing the temperature. In the case of the highest temperature, 50 ºC, the Cr(VI) fraction is higher than in the case of constant pH (30% Cr(VI) and 70% Cr(III)) than in the case of the non-compensated pH (10% Cr(III) and 90% Cr(VI)). In any case, it has to be remarked that in such a high temperature, the system has, as discussed previously, thermic energy enough to evolve to almost total conversion of hexavalent to trivalent chromium on the solid phase.

The constants of **Table 11** were introduced in the model to simulate the theoretical profile of chromium concentration in solution expressed as total, hexavalent and trivalent as a function of time. The experimental and model-predicted results for the different temperatures under conditions of constant pH and allowed to free evolve, are presented in the next figure in terms of normalized chromium concentration.

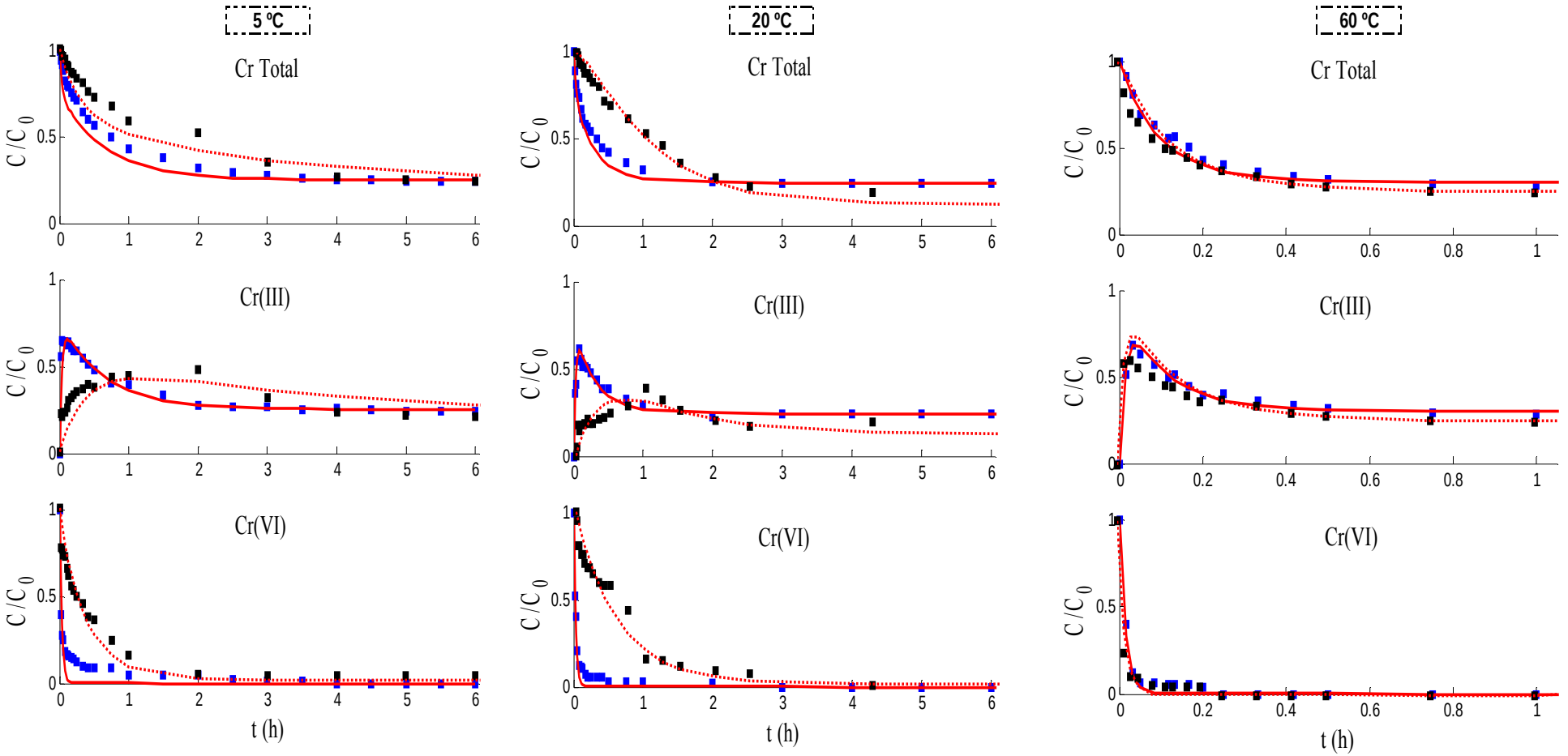

Figure 16: Experimental and model predicted total, trivalent and hexavalent chromium concentration in solution as a function of time. (■) Constant pH 3.0±0.1; (■) Non-readjusted pH; (−) Model prediction under constant pH 3.0±0.1 conditions; (·····) Model prediction under initial and non-readjusted pH 3.0 conditions. $[Cr(VI)]_0 \approx 10.5$ mg·L^{-1}; sorbent dose: ○2.5 g·L^{-1}; T: 5, 20 and 50 ºC.

In the figure the experimental results obtained under conditions of continuous pH readjustment and pH allowed to free evolve have been presented in blue and black dots respectively. On the other hand, the model prediction has been presented in red solid and dotted line for the scenarios of pH readjustment and free evolution respectively.
When looking at the figure, again, the excellent predictive power on the dynamics of the system for all the proposed scenarios is clearly demonstrated.

5.5. Residual Cr(III) removal assays

In previous sections, the presence of Cr(III) coming from the contact of solutions containing Cr(VI) with grape stalk particles has been reported and the dynamics of the process modelled and discussed. If it's true that a very important reduction of the polluting charge of the primary effluent has been achieved with the treatment in the reactor, the presence of this small concentration of Cr(III) should not be neglected and further treatment of the effluent would be required to reduce this concentration under acceptable discharge levels.
In an attempt to remove the residual Cr(III) produced after the treatment in the reactor of the Cr(VI) effluent, two different techniques were employed: (i) batch precipitation in basic media and (ii) continuous bed up-flow sorption with two different sorbent materials. The obtained results are presented and discussed in the next sections.

5.5.1. Precipitation assays

Precipitation assays in basic medium were carried out according to the methodology described in section 4.6.1. Results of Cr(III) concentration in solution for the different studied pHs are presented in the next table.

Table 12. Cr(III) concentration in solution for the different pHs. $[Cr(III)]_0$=2.85 mg·L^{-1}.

pH	$[Cr(III)]_f$ (mg·L^{-1})
3.9	2.82
5.0	2.71
5.9	2.50
7.1	2.58
8.0	2.60
9.0	2.70
10.0	2.50
11.0	2.63
11.5	2.43

The results presented in the table indicate that there's almost no variation of Cr(III) concentration is solution when varying the pH of the media from 4 to 11.5 units. These results are in disagreement with the expected according to the Cr(III) speciation diagram as a function of pH presented in **Figure 17**.

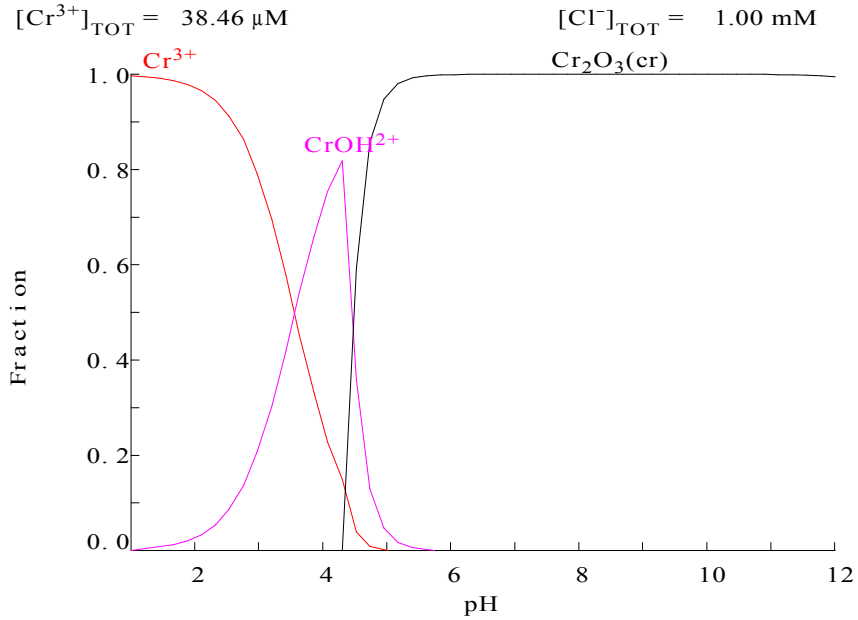

Figure 17: Cr(III) speciation diagram as a function of solution pH. [Cr(III)]= 2.5 mg·L^{-1}; [Cl$^-$] = 0.001 M.

As shown in this figure, MEDUSA simulation under our experimental conditions indicates that total precipitation of Cr(III) has to take place for pHs higher than 5. Under this pH value, the speciation varies between Cr^{3+} and $CrOH^{2+}$, but always Cr(III) leads to cationic species distribution. For an accurate simulation of the Cr(III) speciation possible formation

of chromium(III) chlorocomplexes has been also taken into account by including the chlorides coming from the addition of HCl to the reaction media.

The observed inefficiency in the basic precipitation process, lead us to think that the Cr(III) could not be available for precipitation with hydroxyls due to its complexation with some substance directly released from the grape stalk wastes or some by-product released after the oxidation of the organic structure of the sorbent by Cr(VI) under acidic conditions.

As basic precipitation of the residual fraction of Cr(III) was not efficient for the removal of this pollutant in the effluent of the reactor, another alternative, based in the sorption of Cr(III) from this solution in a continuous fixed bed up-flow process was evaluated.

5.5.2. Continuous bed up-flow sorption experiments

Two different sorbents were evaluated for the removal of the Cr(III) remaining fraction present in the Cr(VI) effluent after the primary treatment in the reactor. It had been previously reported that GS had the ability of successfully remove heavy metal cations from aqueous solutions as Cu(II) and Ni(II) (Villaescusa *et al*., 2004) and also Pb(II) and Cd(II) (Martínez *et al*., 2006). According to these antecedents, the ability of GS to remove Cr(III) from the Cr(VI) solution treated in the reactor was evaluated. On the other hand, the inefficiency of the precipitation process for the removal of the Cr(III) coming from reduction of Cr(VI) in the reactor lead us to think that this cation could be inactivated because of its complexation with some substance released from the biomaterial. As it will be discussed in chapter 3, in the literature some activated carbons have been successfully tested in the removal of different metallic ions in presence of complexing agents. According to these results, and taking in mind the possible complexation of the trivalent chromium, it was decided to prepare also an activated carbon from the raw GS and to evaluate it as well, according to the procedure described in section 4.6.2.

As sorption of Cr(III) onto raw GS and onto its derived activated carbon (AGS) had not been previously studied, it was needed to obtain the optimal solution pH to carry out sorption experiments before starting with column experiments. The study of effect of pH on Cr(III) sorption onto GS was carried out in batch by contacting for 48 hours, 15 mL of a 10 $mg \cdot L^{-1}$ Cr(III) solutions adjusted at different pHs in the range 1.5 to 10 units with 0.1 g

of GS. Cr(III) source for this experiment was $Cr(NO_3)_3 \cdot 9H_2O$. Results of metal concentration in solution for the different pHs are presented in **Table 13**.

Table 13: Initial and final pHs and Cr(III) concentration in solution ($mg \cdot L^{-1}$) before and after contact with either GS or AGS. $[Cr(III)]_0 \approx 10$ mg/L; V = 15 mL; sorbent mass = 0.1 g; agitation time: 48 h.

pH_i	pH_f (GS)	pH_f (AGS)	$[Cr(III)]_i$	$[Cr(III)]_f$ (GS)	$[Cr(III)]_f$ (AGS)
1.50	1.62	1.67	10.29	9.45	5.91
2.00	2.28	2.47	9.76	8.77	1.00
3.01	3.82	4.74	10.74	1.32	0.21
4.00	4.32	4.98	10.40	1.32	0.24
5.01	4.47	5.09	10.06	1.30	1.33
6.03	4.61	5.16	3.29	4.77	1.58
6.99	4.85	5.15	0.11	1.78	2.01
7.98	4.88	5.17	0.10	3.66	2.37
9.04	5.06	5.17	0.11	4.94	2.81
10.51	5.97	5.41	0.15	2.44	1.16

From this table two evidences are remarkable. The first one is that an increase of initial pH of the solution in the range 1.5 to 5 positively affects sorption by GS and AGS, as it demonstrates the decrease of Cr(III) residual concentration in solution. The second would be the possible inconsistence that seems to take place for initial pHs 6 and higher: an increase of Cr(III) concentration in solution when contacting with either GS or AGS. To explain this phenomena it has to be remarked first place that the initial Cr(III) concentration in solution is, in all these cases, lower than in the situations of lower pHs, despite the same mother solution (around 10 $mg \cdot L^{-1}$) was employed. These results put into evidence the strong reduction of metal concentration in solution due to precipitation of $Cr(OH)_3$ taking place at initial pHs≥6. When this solution containing both, dissolved and precipitated Cr(III), is contacted with GS or AGS a decrease of solution pH to values around 5 takes place, as it can be observed in the **Table 13**. This partial acidification of the media is due to the acidic properties of both materials, grape stalk and its derived activated carbon, and provokes a partial redissolution of the chromium hydroxide formed in the basic conditions of the original solutions. The reactions can be summarized as follows:

$$Cr(III) + 3OH^- \leftrightarrow Cr(OH)_3 \downarrow$$

$$R\text{-}OH \leftrightarrow R\text{-}O^- + H^+$$

where R-OH represents the acidic groups present in the raw and carbonaceous biomaterial. To avoid the phenomena of precipitation-redissolution in the search of the optimal pH for continuous sorption experiments, removal efficiency of GS and AGS is presented as a function of the initial pH in the next figure, avoiding pHs≥6, where the precipitation of $Cr(OH)_3$ strongly interferes in the discussion of sorption results.

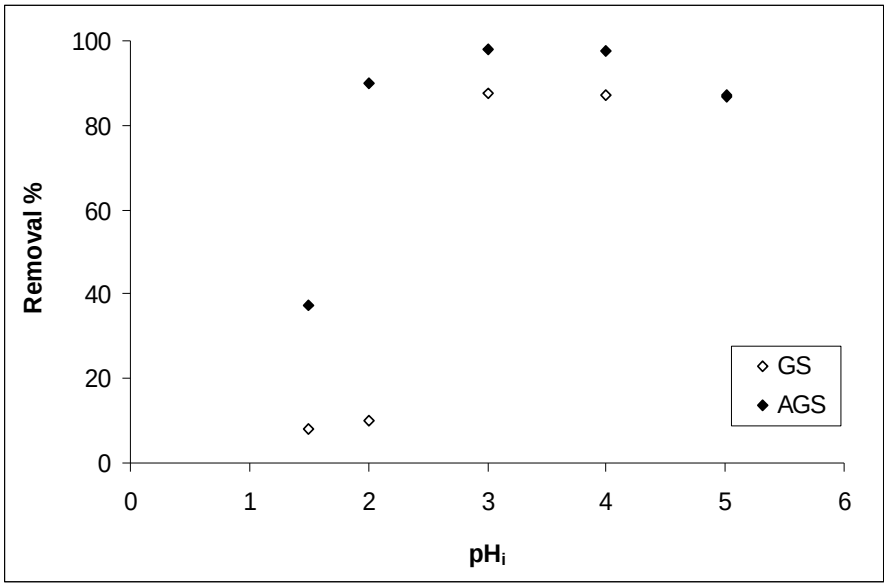

Figure 18: Initial pH effect in Cr(III) sorption onto GS and AGS.

As it can be seen in the figure, Cr(III) sorption trend observed for GS is analogous to the discussed in chapter 1 when Cr(III) sorption onto grape stalk entrapped in calcium alginate was studied. In that chapter it was demonstrated and discussed the low Cr(III) sorption onto 2% GS-CA at acidic pHs in the basis of the competition established between H^+ and the cationic species Cr^{3+} and $CrOH^{2+}$ for the sorption active sites of the material. In the case of Cr(III) sorption onto AGS, despite the sorption trend is quite similar to the observed for the raw GS, the carbonaceous materials exhibits a higher removal efficiency. This enhancement on the sorption capacity of the carbonaceous respect to the raw GS is particularly higher in the lower pH range; while for initial pHs 2 and 3, GS shows a percentage of removal of approximately 8 and 10% respectively, the carbonaceous material, AGS, exhibits removal efficiencies of 35 and 90% respectively.

Summarizing the results obtained in this study, it can be concluded that trivalent chromium coming from a synthetic Cr(III) solution is efficiently removed by both GS and AGS at

initial pHs 3 and 4. For pHs≥6, a very important decrease of Cr(III) concentration in solution takes place because of the precipitation of $Cr(OH)_3$. This experimental observation, in agreement with the hydrochemical predictions of Cr(III) speciation, is further confirming the possible complexation of the Cr(III) formed in the reactor, due to the lack of removal when batch precipitation experiments in basic media were carried out. According to these results, an initial pH of 3 for the Cr(III) feeding solution was chosen as optimal to carry out the continuous sorption experiments onto both, GS and AGS. As the set point of the reactor was fixed to 3.0, the same effluent obtained after the treatment of the Cr(VI) effluent, with addition of neither acid nor base was used to feed the column

Results of eluted chromium concentration as a function of time (data not shown) indicated that, from the beginning of the process, the same Cr(III) concentration in the feeding effluent was eluted from both GS or AGS filled columns.

These results strongly contrast with the obtained for Cr(III) sorption from synthetic chromium nitrate solutions in batch, where it was demonstrated that this metal could be successfully removed by the two materials in the pH conditions of the column. As in the case of the basic precipitation assays, the results obtained in continuous corroborate the presence of some kind of complexing agent in solution or some special coordination of Cr(III) that inactivates the cation for sorption onto the two studied materials. To face this problem, maybe other alternatives can be proposed. For instance the employment of different nature commercial activated carbons or materials of proven performance for the removal of complexed metallic species (Chen and Wu, 2000; Chu and Hashim, 2000; Gyliene *et al*., 2002), the use of oxidative techniques such as advanced photodegradation in solution by UV-Vis irradiation (Metsärinne *et al*., 2001) or by ozone treatment of the effluent in a attempt to oxidize the organic structure and allow thus the release of Cr(III).

6. CONCLUSIONS

A rapid and efficient Cr(VI) detoxification of an aqueous effluent by a combined sorption/reduction process can be carried out by using raw grape stalk wastes under fixed pH 3.0±0.1 conditions. The process can be automatized by constant pH monitorization and correction by means of a Programmable Logic Controller (PLC). The dynamics of hexavalent chromium removal reveal that grape stalk biomass sorbs Cr(VI) but, some of this, is electrochemically reduced, thereby resulting in the appearance of Cr(III) in solution. Sorption and reduction of monohydrogenchromate ions are parallel processes.

The sorption/reduction process is strongly dependent on temperature. Both hexavalent and trivalent chromium removal and production/removal rate respectively increase when the temperature is increased under both conditions, constant 3.0 pH and allowed to free evolve.

The dynamics of the hexavalent and trivalent concentration in solution in the experiments carried out in the stirred tank reactor show completely different profiles; while Cr(VI) concentration continuously decreases to reach its almost total removal (for initial hexavalent chromium concentrations within 5 to 20 $mg \cdot L^{-1}$), Cr(III) appears in solution, evolves to a maximum concentration and then decreases to reach an equilibrium non-adsorbed concentration.

Continuous pH readjustment strongly increases the rate at which the sorption and reduction processes occur at low temperatures. At high temperatures there are almost no differences between sorption scenarios with continuous reacidification and without acid addition. This fact indicates that hexavalent chromium sorption/reduction process by grape stalk can be enhanced by either, H^+ addition to the media or by an addition of thermal energy to the reaction volume.

The detoxification process proposed in the present chapter was found to be robust enough to completely remove hexavalent chromium from feeding concentrations of approximately 5 to 20 $mg \cdot L^{-1}$.

A batch model integrating the irreversible conversion of hexavalent chromium to trivalent and the sorption/desorption of both oxidation states onto grape stalk, successfully describes the dynamics of chromium disappearing (in the case of total and hexavalent) and appearing/disappearing (in the case of the trivalent). The analysis of the sets of

experimental data demonstrated that the model successfully described the dynamics of the sorption/reduction process for the temperatures studied with and without pH readjustment.

The constants obtained from the model provide useful information about the contribution of both, temperature and acidity to the sorption/reduction process. The model quantitatively reflects, by means of a constant labelled as k_r, the enhancement of sorption and reduction rate when the process is either thermally (by increasing the temperature) or chemically (by continuous addition of H^+ to the media) activated. The proposed model provides also information of the extension in which chromium is fixed in the grape stalk as either, Cr(VI) or Cr(III) by means of a constant labelled as k_f. Under conditions of constant 3.0 pH, the distribution of both chromium oxidation states in the solid phase is strongly dependent on the temperature. The values vary from 80% of the total chromium sorbed as Cr(VI) and 20% as Cr(III) at 5ºC to 10% of Cr(VI) and 90% of Cr(III) at 60 ºC. An increase of the temperature leads to an increase of the sorption of the trivalent oxidation state, in detriment of the sorption in the hexavalent form. Thus, for a given temperature, hexavalent chromium sorption and desorption is more affected by the reacidification of the media than trivalent chromium, as it reflected the higher difference between k_a and k_d constants corresponding to sorption of Cr(VI) and Cr(III).

The Cr(III) produced by reduction of the hexavalent chromium in the reactor and released to the liquide phase is in a non-cationic form. During the sorption/reduction process, it might occur the release from the grape stalk of natural soluble organic molecules, that could exhibit complexing activity through Cr(III) cations.

7. REFERENCES

· Baral, S.S., Das, S.N., Rath, P., Hexavalent chromium removal from aqueous solution by adsorption on treated sawdust. Biochem. Eng. J. 31 (2006) 216–222.

· Cabatingan, L.K., Ramelito, C.A., Johannes, L.L.R., Ottens, M., van der Wielen, A.M., Potential of biosorption for the recovery of chromate in industrial wastewaters. Ind. Eng. Chem. Res. 40 (2001) 2302-2309.

· Chen, J.P., Wu, S., Study on EDTA-chelated copper adsorption by granular activated carbon, J. Chem. Technol. Biotechnol. 75 (2000) 791-797.

· Chu, K.H., Hashim, M.A., Adsorption of copper(II) and EDTA-chelated copper(II) onto granular activated carbons, J. Chem. Technol. Biotechnol. 75 (2000) 1054-1060.

· Cox, M., Négré, P., Yurramendi, L., A guide book on the treatment of effluents for the mining/metallurgy, paper, plating and textile industries. Inasmet-Tecnalia, San Sebastián (España), 2006.

· Dönmez, G.C., Aksu, Z., Ozturk, A., Kutsal, T., A comparative study on heavy metal biosorption characteristics some algae, Process Biochem. 34 (1999) 885–892.

·Fiol, N., Escudero, C., Villaescusa, I., Chromium sorption and Cr(VI) reduction to Cr(III) by grape stalks and yohimbe bark. Biores. Technol. 99 (2008) 5030-5036

· Gardea-Torresdey, J.L., Tiemann, K.J., Armendariz, V., Bess-Oberto, J., Chianelli, R.R., Rios, J., Parsons, J.G., Gamez, G., Characterization of Cr(VI) binding and reduction to Cr(III) by the agricultural byproducts of *Avena monida* (oat) biomass. J. Hazard. Mater. B80 (2000) 175-188.

· Gasser, M.S., Morad, G.H., Aly, H.F., Batch kinetics and thermodynamics of chromium ions removal from waste solutions using synthetic adsorbents. J. Hazard. Mater. 142 (2007) 118–129.

· Gyliene, O., Rekertas, R., Salkauskas, M., Removal of free and complexed heavy-meta ions by sorbents produced from fly (*Musca domestica*) larva shells, Water Res. 36 (2002) 4128-4136.

· Hasan, S.H., Singh, K.K., Prakash, O., Talat, M, Ho, Y.S., Removal of Cr(VI) from aqueous solutions using agricultural waste ‘maize bran’, J. Hazard. Mater. (2007), doi:10.1016/j.jhazmat.2007.07.006.

· Juang R.S., Wu, F.C., Tseng, R.L., The ability of activated clay for the adsorption of dyes from aqueous solutions, Environ. Technol. 18 (1997) 525–531.

· Lytle, C.M., Lytle, F.W., Yang, N., Quian, J.-H., Hansen, D., Zayed, A., Terry, N., Reduction of Cr(VI) to Cr(III) by wetland plants: potential for in situ heavy metal detoxification Environ. Sci. Technol. 32 (1998) 3087-3093.

· Malkoc, E., Nuhoglu, Y., Potential of tea factory waste for chromium(VI) removal from aqueous solutions: thermodynamic and kinetic studies. Sep. Purif. Technol. 54 (3) (2007) 291–298.

· Malkoc, E., Nuhoglu, Y., Dundar, M., Adsorption of chromium(VI) on pomace-An olive oil industry waste:Batch and column studies. J. Hazard. Mater. B138 (2006) 142–151.

· Martínez, M., Miralles, N., Hidalgo, S., Fiol, N., Villaescusa, I., Poch, J., Removal of lead(II) and cadmium(II) from aqueous solutions using grape stalks waste. J. Hazard. Mater. B133 (2006) 203–211.

· Metsärinne, S., Tuhkanen, T., Aksela, R., Photodegradation of ethylenediaminetetraacetic acid (EDTA) and ethylenediamine disuccinic acid (EDDS) within natural UV radiation range. Chemosphere 45 (2001) 949-955.

· Park, D., Yun, Y.S., Park, J.M., XAS and XPS studies on chromium-binding groups of biomaterial during Cr(VI) biosorption. Journal of Colloid and Interface Science 317 (2008) 54–61.

· Park, D., Lim, S.R., Yun, Y.S., Park, J.M., Reliable evidences that the removal mechanism of hexavalent chromium by natural biomaterials is adsorption-coupled reduction. Chemosphere 70 (2007) 298–305

· Park, D., Yun, Y.S., Park, J.M., Reduction of hexavalent chromium with the brown seaweed *Ecklonia* biomass. Environ. Sci. Technol. 38 (2004) 4860-4864.

· Romero-González, J., Peralta-Videa, J.R., Rodríguez, E., Ramirez S.L., Gardea-Torresdey, J.L., Determination of thermodynamic parameters of Cr(VI) adsorption from aqueous solution onto *Agave lechuguilla* biomass. J. Chem. Thermodynamics 37 (2005) 343–347.

· Sharma, Y.C., Weng, C.H., Removal of chromium(VI) from water and wastewater by using riverbed sand: kinetic and equilibrium studies. J. Hazard. Mater. 142 (2007) 449–454.

· Sharma, D.C., Forster, C.F., Removal of hexavalent chromium using sphagnum moss peat.Water Res. 27 (1993) 1201-1208.

· Suen, S.Y., A comparison of isotherm and kinetic models for binary-solute adsorption to affinity membranes. J. Chem. Tech. Biotechnol. 65 (1996) 249-257

· Suzuki, R.M., Andrade, A.D., Sousa, J.C., M.C. Rollemberg, M.C., Preparation and characterization of activated carbon from rice bran. Bioresource Technol. 98 (2007) 1985–1991.

· Ucun, H., Bayhan, Y.K., Kaya, Y., Kinetic and thermodynamic studies of the biosorption of Cr(VI) by Pinus sylvestris Linn. J. Hazard. Mater. doi:10.1016/j.jhazmat.2007.08.018.

· Uysal, M., Ar, I., Removal of Cr(VI) from industrial wastewaters by adsorption Part I: Determination of optimum conditions. J. Hazard. Mater. 149 (2007) 482–491.

Chapter 3. EFFECT OF EDTA ON DIVALENT METAL ADSORPTION ONTO GRAPE STALK AND EXHAUSTED COFFEE WASTES

1. INTRODUCTION

In previous chapters, dechromisation of polluted effluents by using grape stalk wastes, either entrapped or on its raw form, had been evaluated and discussed. Despite of its great toxicity, it has to be taken into account that hexavalent chromium, either as $HCrO_4^-$ or CrO_4^{2-} anions, is only one of the metallic pollutants that plating and electroplating industries may generate. The presence of heavy metal cations in these liquid effluents cannot be neglected. Among others, Cu and Ni are present in many of these operations and are considered in the European Union regulations as substances which have a deleterious effect on the aquatic environment and should be subject to authorization with specification of emission standards prior to discharge (Directive 2006/11/EC); the emission standards must be calculated in terms of environmental quality standards for water. Spanish environmental quality standards are fixed in 5 to 120 μg/L range for Cu and in 50 to 200 $\mu g \cdot L^{-1}$ range for Ni (Real Decreto 995/2000). European Union health standard in drinking water is 2 $mg \cdot L^{-1}$ for Cu and 20 $\mu g \cdot L^{-1}$ for Ni (Directive 98/83/EC).

In addition to metallic ions, effluents produced in several industries as those of metal finishing, electroplating, painting, dying, printed circuit board manufacturing, photography, or surface treatment usually contain different complexing agents, being frequently found the aminecarboxylic derivatives.

The industrial complexing agents are chemically and thermally very stable and used for a wide variety of, e.g. for controlling the oxidation potential of metal ions, for adjusting metal concentration, for masking free metal ions to avoid metal-catalyzed spoilage or the precipitation of poorly soluble salts, and for cleansing processes where precipitates of salts in tubes, bottles, and on membranes must be removed. In **Figure 1**, the structure of some commonly used industrial complexing agents is presented (Nörtemann, 1999).

Of the aminopolycarboxylic acids, ethylenediaminetetraacetate (EDTA) is technically the most important and is used in large quantities (sales quantities in Europe 1997: EDTA, 32550 tons; nitrilotriacetate (NTA), 18600 tons; diethylenetriaminepentaacetate (DTPA), 14000 tons) (Nörtemann, 1999).

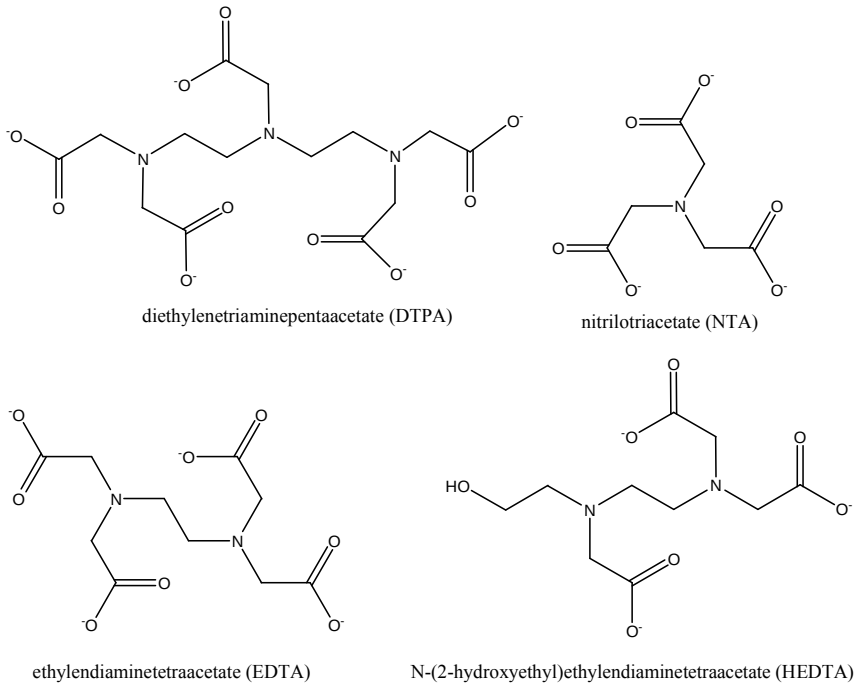

Figure 1: Aminopolycarboxylates of technical importance for use as chelating agents

Many divalent and trivalent metal cations are strongly complexed by ethylenediaminetetraacetate, being the order of the stability constants (Stumm, 1990; Nowack *et al*., 2001; Nowack *et al*., 1996)

$$Na^{+}<Mg^{2+}<Ca^{2+}<Fe^{2+}<Al^{3+}<Zn^{2+}<Cd^{2+}<Pb^{2+}<Ni^{2+}<Cu^{2+}<Hg^{2+}<Fe^{3+}$$

It is well known that, in presence of chelating agents, the performance of metal removal can be adversely affected due to the formation of soluble complexes that can be removed neither by conventional ion-exchange based sorbents nor by precipitation in basic media. When chelating agents become an important interference in the metal removal process, the destruction of the ligand is needed, and this process normally involves the addition of several chemicals, the use of oxidative or biological techniques that, in last term, contribute to increase the economical cost of the wastewater treatment.

Conventional removal of complexing agents would involve ex-situ advanced oxidation processes as those involving oxidation by Fenton processes (Walling *et al*., 1970), by Fe(III) with and without O_2, at temperatures above 100 ºC or until with iron, in absence of H_2O_2 but in aerated conditions at ambient temperature (Englehardt *et al.*, 2007), treatment with ozone (Gilbert and Hoffmann-Glewe, 1990) or specialized biological treatment (Klüner *et al*., 1998; Kaluza *et al*., 1998). Despite for a long time, EDTA was thought to be

resistant to biodegradation (Madsen and Alexander 1985; Alder *et al*. 1990; Bolton *et al*. 1993), in recent years, the biodegradability of EDTA has been increasingly recognized and investigated (Nörtemann, 1999).

Another possibility to reduce the problem that EDTA generates in the removal of toxic metals from aqueous effluents, would pass by the substitution of this compound by more readily degradable complexing agents such as tartrate, citrate, alaninediacetate, methylglycinediacetate, and NTA. By doing so, metal removal could be carried out by conventional techniques, after a previous ligand destruction step. However, the thermodynamic stabilities of the corresponding metal complexes are relatively low compared to metal-EDTA chelates. They are thus not suited for many industrial processes or products where strong chelating properties are required. In addition, technically applicable complexing agents must often be very resistant to chemical and thermal effects as well as to biodegradation (e.g., cleansing processes, process baths). For these technical processes, EDTA is still the best compound known because it is cheap to produce and to apply and is not toxic to mammals. In contrast, other compounds with chelating properties comparable to those of EDTA are usually more expensive, and have been less intensively investigated with regard to their toxic or ecotoxic behaviour (Nörtemann, 1999).

When EDTA is present in solution and the complexation of the metal is unavoidable, an alternative to the destruction of the ligand would be the removal of the metal chelate itself, by i.e., sorption. Unfortunately, despite sorption of different heavy metal ions on its free form on low cost sorbents has been widely studied (Babel and Kurniawan, 2003; Wang and Chen, 2006; Ho *et al*., 2000; Palma *et al*., 2003; Brown *et al*., 2000; Ma and Tobin, 2003; Gabaldón *et al*., 2006; Villaescusa *et al*., 2004; Low *et al*., 2000; Holan and Volesky, 1994; Sun and Shi, 1998; Bertocchi *et al*., 2006; Gupta and Sharma, 2002; Gupta *et al*., 2003; Singh *et al*., 2008), fewer effort has been devoted to the study of the effect of organic complexing agents on metal ions removal.

From the scarce studies of metal sorption in presence of complexing agents, some materials have demonstrated good sorptive capacity for metal chelates. Among these studies, can be remarked the use of commercial and low-cost activated carbons for the removal of Pb(II) in presence of NTA and EDTA (Krishnan *et al.*, 2003); Cu(II), Fe(III), Pb(II), Zn(II), Ni(II) and Mn(II) removal by fly (*Musca domestica*) larva shells in presence

of glycine and EDTA (Gyliene *et al.*, 2002); Ni and Cu removal by activated carbon in presence of EDTA (Gabaldón *et al*., 2008; Gabaldón *et al*., 2007), Cu(II) sorption onto chitosan in presence of EDTA (Gyliene *et al*., 2006); Cu(II) removal by chitosan in presence of citrate (Guzman *et al*., 2003); Cu(II) sorption onto granular activated carbons in presence of EDTA (Chu and Hashim, 2000; Chen and Wu, 2000) and Pb(II), Cd(II) and Ni(II) removal by waste Fe(III)/Cr(III) hydroxide in presence of EDTA, citrate and acetate (Namasivayam and Ranganathan, 1998).

Despite promising results had been reported in our laboratory for Cu(II) and Ni(II) removal by sorption onto grape stalk (Villaescusa *et al*., 2004), the potential sorptive ability of exhausted coffee and the effect of complexing agent EDTA on sorption on these materials had not been previously evaluated.

2. OBJECTIVES

The main objective of this chapter is to evaluate the behaviour of two food industry vegetable wastes, grape stalk and exhausted coffee, as sorbents of two of the main metals present in wastewaters coming from metallurgic industries, Cu(II) and Ni(II) in presence of one of the most strong complexing agents, the ethylenediaminetetraacetate anion (EDTA).

Effect of pH on sorption, kinetics and maximum capacity in presence/absence of complexing agent will be evaluated and comparisons between both sorbents performance will be established.

Once optimized sorption operational parameters in batch, column studies will be carried out by using the sorbent that provides the best sorption feature, in order to obtain information in views of a possible continuous process scale-up. Dealing with this, the effect of complexing agent in column sorption performance for both, single and binary Cu(II) and Ni(II) mixtures will be studied. The possibility of metal recovering by desorption in mild acidic conditions will be also analysed.

3. MATERIALS AND METHODS

3.1. Reagents

To prepare copper, nickel and EDTA solutions:

- $CuCl_2.2H_2O$ Panreac
- $NiCl_2.2H_2O$ Panreac
- Na_2EDTA Panreac
- Milli-Q water

Sorbents:

- Exhausted coffee coming from a soluble coffee production industry of Girona.
- Grape stalk coming from a wine producer from Castilla La Mancha region.

For pH adjustment:

- HCl (37%) Panreac
- NaOH in pellets Panreac

Standard solutions for Flame Atomic Spectroscopy:

- $Cu(NO_3)_2 \cdot 2H_2O$ in HNO_3 0.5 N (1000 mg/L) Panreac
- $Ni(NO_3)_2 \cdot 2H_2O$ in HNO_3 0.5 N (1000 mg/L) Panreac

3.2. Material

General laboratory material

100 mL Erlenmeyer flasks with cap

Cellulose acetate filters and holders (Millipore)

Orbital shaker (New Brunswick Scientific Model G25KC)

Peristaltic pump (Watson-Marlow model 101 U/R) and tubes

Chronometers (Berlabo, SA)

pH meter (Crison pH – meter Basic 20)

Analytical balance (Cobos precision, J. Touron, SA)

Coffee grinder (Taurus MS 50)

Sieves

Glass columns (350 x 10 mm)

Glass beads

3.3. Equipment

· Flame Atomic Absorption Spectrophotometer Unicam Model 939.

· Automatic fraction collector.

4. METHODOLOGY

4.1. Sorbent preparation

Grape stalk and exhausted coffee wastes generated in wine and soluble coffee production, were kindly supplied by a wine manufacturer (Cuenca, Spain) and a soluble coffee production industry (Girona, Spain), respectively. Grape stalk wastes (GS) were washed with distilled water, cut in small pieces, dried and ground. Exhausted coffee wastes (EC) were dried and used without any previous treatment. Both materials were sieved for a particle size of 0.25-0.50 mm.

4.2. pH and EDTA effect in Cu(II) and Ni(II) sorption onto GS and EC

Batch experiments at different pHs within the range 1-7 were carried out at 20 ± 1 ^{o}C in 100 cm^3 glass flasks covered with a cap. A fixed mass of 0.1 g of dry sorbent with 20 mL of metal or EDTA-chelated metal solutions were shaken in an orbital shaker for 24 hours. The initial Cu(II) and Ni(II) concentration was fixed at 0.4 mM and the EDTA concentration was varied in order to get metal-EDTA molar ratios of 1:0, 1:0.5 and 1:1. In these experiments, pH was periodically readjusted to the initial value by addition of negligible volumes of either HCl or NaOH.

After agitation the solid was removed by filtration through a Millipore filter with filter holders (25 mm diameter, 1.2 μm pore size). The initial and final metal concentration in the filtrates after sorption, previously acidified, were determined by Flame Atomic Absorption Spectrometry (FAAS) (Unicam Model 939).

The metal concentration in the solid phase, q_e (mg·g^{-1}) was calculated from the difference between the initial, C_i and equilibrium, C_e metal concentration in solution (mg·L^{-1}). The following equation was used to compute the specific uptake of the sorbent:

$$q_e = (C_i - C_e)\frac{V}{w} \qquad (1)$$

where V (expressed in L) is the solution volume and w (in g) is the amount of dry sorbent.

4.3. Sorption kinetics

Batch kinetic experiments were carried out at 20 ± 1 ^{o}C in 1000 cm^3 flasks by mixing, at 200 rpm, 750 cm^3 of Cu(II), Ni(II), Cu(II)-EDTA and Ni(II)-EDTA solutions with three different GS or EC masses (1.87, 3.75 or 7.50 g). Metal initial concentration was fixed at 0.4 mM. For metal-EDTA solutions, 0.2 mM EDTA concentration was used (Metal:EDTA ratio 1:0.5). Initial pH was adjusted to 5.2.

5 mL samples were withdrawn at suitable time intervals within the range 0-250 minutes. Samples were filtered, pH was measured and metal concentration was determined by FAAS.

4.4. Sorption isotherms

Equilibrium isotherms were obtained by contacting, as described previously, 0.1 g of GS or EC with 20 mL of different Cu(II) and Ni(II) solutions within the initial concentration range 5-300 mg L^{-1} in absence of EDTA and in presence of appropriate EDTA amounts to provide 1:0.5 and 1:1 metal:EDTA molar ratios. Initial pH was adjusted to 5.2 and readjusted if necessary after each 24 hours in order to reach sorption equilibrium at this pH. The pH adjustment was performed by addition of negligible volumes of concentrated solutions of either HCl or NaOH. After equilibration, for at least 24 hours from the last pH adjustment, the samples were filtered, acidified and metal concentration in solution was determined by FAAS. Metal sorbed amount per mass unit was calculated according to Eq. (1).

4.5. Column adsorption experiments

From the two sorbent materials studied, grape stalk exhibited the best sorption performance, so that column experiments were carried out with this material. Fixed bed sorption experiments were performed in glass columns of 35 cm length and 1.0 cm inner diameter. To pack the column, glass beads were introduced at the bottom up to around 25 cm length. Then, 0.7 g of grape stalk of 0.25-0.5 mm particle size were packed to a bed height of around 8.5 cm. Finally, some glass beads were added at the top in order to fill up the column. The operation was carried out in the up-flow mode to avoid possible short-

circuiting by clogging and channelling according to the experimental set up is presented in the next figure.

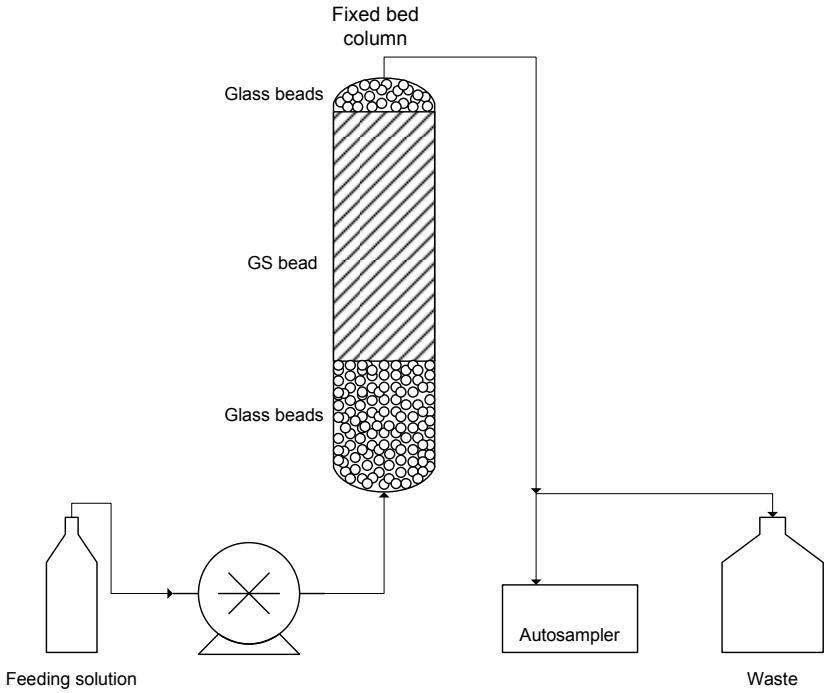

Figure 2: Experimental set up of the operating continuous flow sorption column.

The solutions were pumped at room temperature (20±1 ºC) upwards the grape stalk packed column by a peristaltic pump (Watson-Marlow model 101 U/R) at a flow rate of 30 $mL \cdot h^{-1}$. By using an automatic fraction collector, samples of 7 mL were collected each two hours, the pH was measured and metal concentration in solution was determined by FAAS.

From the difference between the feeding and the eluted metal concentration for each time, metal sorbed amount can be calculated. Metal concentration in the sorbent, C_s is calculated as the difference between the feeding (C_0) and eluted (C_t) concentrations, according to Eq. (2).

$$C_s = (C_0 - C_t) \qquad (2)$$

the amount of metal sorbed per mass unit can be calculated according to the next equation:

$$q_t = \sum (dV \cdot C_{av}) \qquad (3)$$

were dV and C_{av} are the differential of volume treated in the time interval $i\text{-}1 \leq t \leq i$ and the average metal concentration of the interval respectively.

$$dV = V_i - V_{i-1} \quad (4)$$

$$C_{av} = (C_s + C_{s,i-1}) / 2 \quad (5)$$

4.5.1. Effect of feeding metal concentration

Effect of feeding metal concentration in GS sorption performance in a fixed bed column was evaluated in absence of complexing agent. Experiments were carried out as described in section 4.5. Cu(II) initial concentration was varied in the range 1.40 to 38.90 mg·L^{-1} and Ni(II) from 2.19 to 59.10 mg·L^{-1}. Initial pH for all the series was adjusted to 5.20.

4.5.2. Effect of EDTA in Cu(II) and Ni(II) sorption

Effect of the presence of complexing agent in Cu(II) and Ni(II) sorption onto GS in single metal solutions was evaluated according to the general column studies procedure described in section 4.5.

The feeding single metal and metal-EDTA solutions was 0.2 mM in metal, corresponding to approximately 12.50 mg·L^{-1} of Cu(II) and 11.75 mg·L^{-1} of Ni(II). In the case of metal-EDTA solutions, the ligand concentrations used were: 6.25 and 12.50 mg·L^{-1} for the copper experiments; 5.87 and 11.74 mg·L^{-1} for the nickel assays. Initial pH was adjusted to 5.20.

4.5.3. Effect of EDTA in binary equimolar Cu(II)/Ni(II) solutions

Grape stalk sorption behaviour in a binary equimolar Cu(II)/Ni(II) solution in absence and in presence of complexing agent EDTA was evaluated. The feeding single metal and metal-EDTA solutions contained a 0.1 mM concentration of each one the two metals (corresponding to a concentration around 6 mg·L^{-1} for both Cu(II) and Ni(II)). In the case of binary mixtures containing EDTA, complexing agent concentrations used were: 6.00 and 12.00 mg·L^{-1}. Initial pH for all the binary mixtures, in presence and in absence of EDTA, was adjusted to 5.20.

4.6. Column desorption experiments

Continuous wastewater treatment requires a reversible sorption-desorption process in order to reuse the adsorbent and to recover the metals in a concentrated form. Desorption experiments were carried out by feeding the column containing the metal loaded sorbent, with 0.05 M HCl at a flow rate of 30 $mL \cdot h^{-1}$, same flow rate used for sorption experiments. For these assays, the whole eluted effluent was collected in fractions of about 7mL, pH was measured and metal concentration was determined by FAAS. Metal desorption ratio was calculated by a mass balance.

5. RESULTS AND DISCUSSION

5.1. pH and EDTA effect in Cu(II) and Ni(II) sorption onto GS and EC

pH of the solution can affect the extent of the adsorption because it strongly influences the metal speciation, metal precipitation and the protonation degree both of the ligand (EDTA) and of the sorbent surface. Concentration of EDTA influences on the degree of metal complexation and subsequently the concentration of free metal in solution. Results of Cu(II) and Ni(II) sorption onto grape stalk (GS) and exhausted coffee wastes (EC) in presence and in absence of complexing agent EDTA as a function of final solution pH are shown in **Tables 1** to **4**.

Table 1: Final pH and metal concentration in solution after contact with GS and EC in absence of EDTA. Initial metal concentration≈0.4 mM.

	GS			**EC**	
pH_f	**[Cu(II)] ($mg \cdot L^{-1}$)**	**% removal**	**pH_f**	**[Cu(II)] ($mg \cdot L^{-1}$)**	**% removal**
1.14	24.95	0.00	1.09	24.95	0.00
2.03	20.18	19.12	2.07	24.58	1.48
2.80	13.11	47.45	3.08	16.14	35.31
4.06	9.72	61.04	4.08	5.12	79.48
5.02	7.78	68.82	5.03	2.86	88.54
6.05	3.81	84.73	6.10	0.66	97.35
7.20	4.94	80.20	7.09	0.42	98.32
pH_f	**[Ni(II)] ($mg \cdot L^{-1}$)**	**% removal**	**pH_f**	**[Ni(II)] ($mg \cdot L^{-1}$)**	**% removal**
1.29	32.30	1.52	1.32	34.15	0.00
1.95	31.06	5.30	2.00	34.06	0.00
3.10	23.89	27.16	3.20	27.75	15.40
3.97	18.93	42.29	4.20	19.89	39.36
5.21	18.54	43.48	4.92	16.24	50.49
5.97	18.33	44.12	6.20	4.29	86.92
6.96	15.17	53.75	6.96	4.81	85.34

Table 2: Final pH and metal concentration in solution after contact with GS and EC. Initial metal concentration≈0.4 mM; [EDTA]=0.2 mM.

	GS			EC	
pH_f	**[Cu(II)] ($mg \cdot L^{-1}$)**	**% removal**	**pH_f**	**[Cu(II)] ($mg \cdot L^{-1}$)**	**% removal**
1.10	24.95	0.00	1.05	24.95	0.00
1.96	24.56	1.56	2.08	24.65	0.00
2.75	18.97	23.97	3.09	20.34	18.48
4.02	18.63	25.33	4.03	16.24	34.91
4.94	14.61	41.44	4.96	12.89	48.34
6.11	13.09	47.54	6.05	11.59	53.55
7.22	13.01	47.86	7.08	11.56	53.67
pH_f	**[Ni(II)] ($mg \cdot L^{-1}$)**	**% removal**	**pH_f**	**[Ni(II)] ($mg \cdot L^{-1}$)**	**% removal**
1.27	31.25	4.73	1.30	33.79	0.00
2.04	30.58	6.77	1.96	31.36	4.39
2.96	27.55	16.01	3.09	30.14	8.11
3.92	24.51	25.27	4.21	24.75	24.54
4.97	24.22	26.16	4.90	19.47	40.64
5.90	24.20	26.22	6.17	19.93	39.24
6.98	24.29	25.95	6.82	17.25	47.41

Table 3: Final pH and metal concentration in solution after contact with GS and EC. Initial metal concentration≈0.4 mM; [EDTA]=0.4 mM.

	GS			EC	
pH_f	**[Cu(II)] ($mg \cdot L^{-1}$)**	**% removal**	**pH_f**	**[Cu(II)] ($mg \cdot L^{-1}$)**	**% removal**
1.12	24.95	0.00	1.05	24.95	0.00
1.97	24.95	0.00	2.02	24.94	0.04
2.73	24.83	0.48	3.07	24.64	1.24
4.06	23.83	4.49	4.05	22.74	8.86
4.95	23.75	4.81	5.05	22.84	8.46
6.12	23.33	6.49	6.07	22.97	7.94
7.28	23.27	6.73	7.15	23.02	7.74
pH_f	**[Ni(II)] ($mg \cdot L^{-1}$)**	**% removal**	**pH_f**	**[Ni(II)] ($mg \cdot L^{-1}$)**	**% removal**
1.27	31.60	3.66	1.29	31.06	5.30
2.07	31.76	3.17	2.04	31.04	5.37
3.17	31.59	3.69	3.29	31.65	3.51
4.18	29.56	9.88	4.18	29.30	10.67
5.03	31.64	3.54	5.03	32.79	0.03
5.93	32.08	2.20	6.12	33.20	0.00
6.90	31.86	2.87	7.12	32.97	0.00

Table 4: Final pH and metal concentration in solution after contact with GS and EC. Initial metal concentration≈0.4 mM; [EDTA]=0.8 mM.

	GS			**EC**	
pH_f	**[Cu(II)] ($mg \cdot L^{-1}$)**	**% removal**	**pH_f**	**[Cu(II)] ($mg \cdot L^{-1}$)**	**% removal**
1.09	25.10	0.00	1.14	25.62	0.00
2.10	25.16	0.00	2.14	25.87	0.00
2.96	24.92	0.00	2.92	25.21	0.00
4.08	25.32	0.00	4.01	24.96	0.00
4.96	25.69	0.00	5.07	25.20	0.00
6.14	25.46	0.00	6.04	24.85	0.00
7.20	25.54	0.00	7.04	25.33	0.00
pH_f	**[Ni(II)] ($mg \cdot L^{-1}$)**	**% removal**	**pH_f**	**[Ni(II)] ($mg \cdot L^{-1}$)**	**% removal**
1.20	32.8	0.00	1.12	32.8	0.00
2.01	32.8	0.00	2.09	32.8	0.00
3.08	32.8	0.00	3.05	32.8	0.00
4.15	32.8	0.00	4.25	32.8	0.00
5.10	32.8	0.00	5.04	32.8	0.00
6.06	32.8	0.00	6.15	32.8	0.00
7.10	32.8	0.00	7.14	32.8	0.00

For an easier visualization of the effect of pH and presence of complexing agent in Cu(II) and Ni(II) sorption, in the next figure the amount of metal removed by both materials in absence of EDTA and for two different metal-EDTA molar ratios, as a function of final pH has been presented.

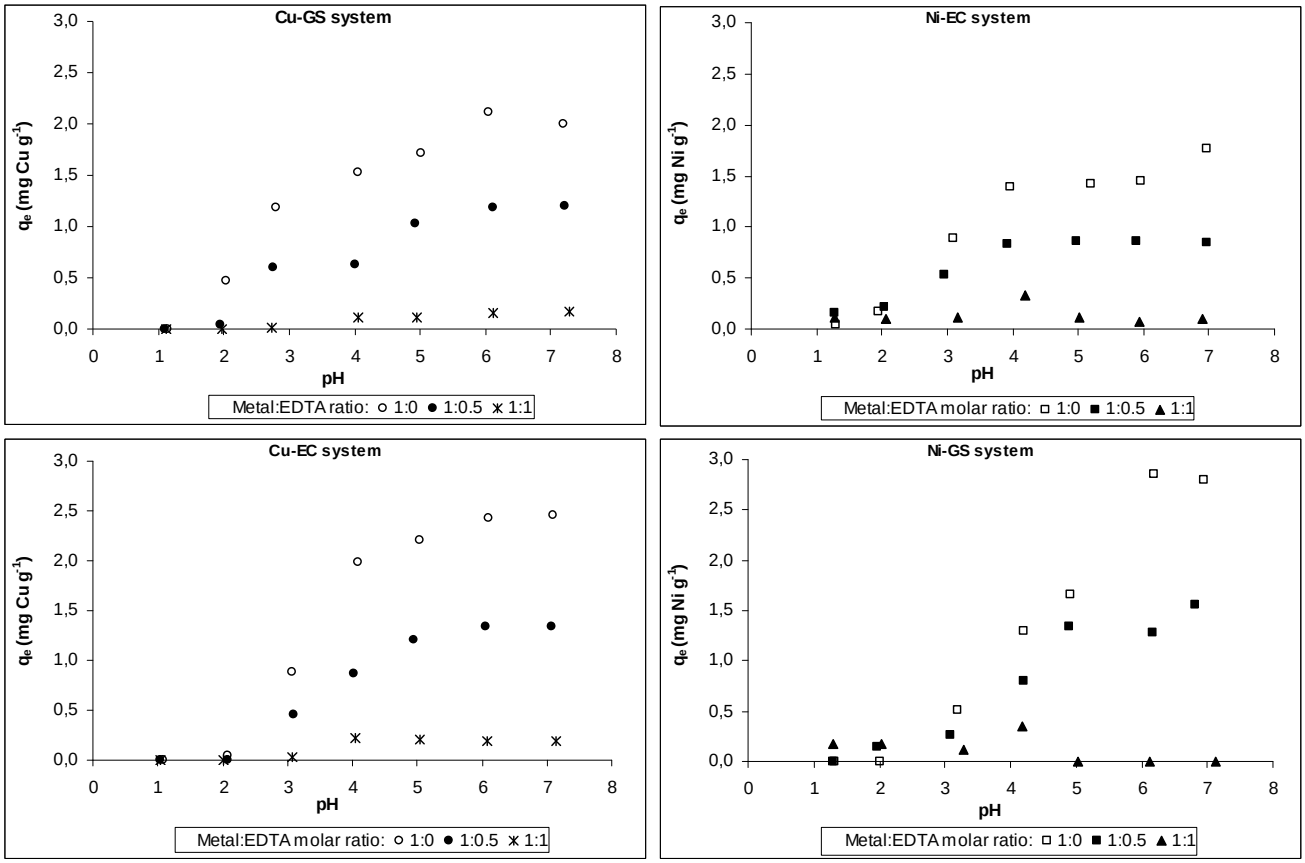

Figure 3: Effect of pH on the adsorption of Cu(II) and Ni(II) on (a,b) Grape Stalk (GS) and (c,d) Exhausted Coffee (EC) in presence and in absence of EDTA. Initial metal concentration: 0.4 mM.

As can be seen, in all the cases the amount of metal removed increased when increasing the pH of the solution. In particular, there was an abrupt increase of metal uptake when the pH varied from 3 to 5 and maximum removal value was achieved from a pH around 5.5. Further increase in the pH didn't improve significantly the metals uptake. These results point out that the optimum pH for the removal of both metals was not affected by the presence of the complexing agent. Similar results have been reported for Cu(II) sorption onto activated carbon in presence of EDTA (Chen and Wu, 2000) and onto chitosan in presence of citrate ions (Guzmán *et al.* 2003). To understand the effect that complexing agent provokes in divalent metal sorption, the information about the metal speciation would be of capital importance. In **Figure 4** Cu(II) and Ni(II) species distribution diagram as a function of pH in presence and in absence of EDTA is presented.

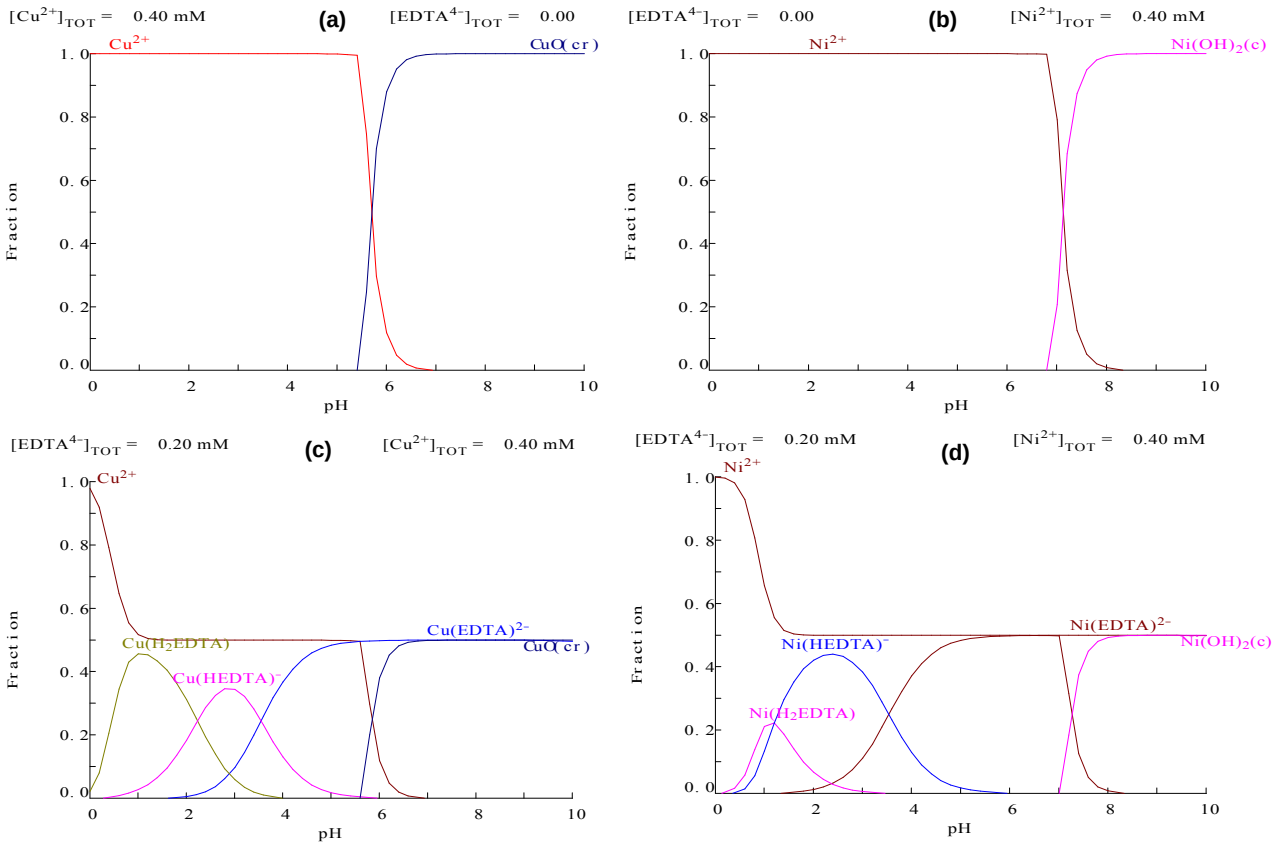

Figure 4: Speciation diagrams as a function of pH for (a) Cu(II), (b) Ni(II), (c) Cu:EDTA 1:0.5 molar ratio and (d) Ni:EDTA 1:0.5 molar ratio. Initial metal concentration: 0.4 mM.

As it can be observed, in absence of ligand, both metals are 100% as divalent free metal cation until reaching precipitation pH around 6.0 in the case of Cu(II) and around 7.0 in the case of Ni(II). When EDTA is present in solution at 1:0.5 metal:ligand molar ratio, free metal cation concentration dramatically decreases due to the formation of neutral or anionic metal:EDTA species. Nevertheless, free Cu^{2+} and Ni^{2+} cations are still the predominant species at pH<5.5 and pH<7.0, respectively. Therefore, the adsorption observed in the pH range 1-6 may be basically attributed to the interaction of free metal cations, and the sorbent surface. The low adsorption observed at low pH values can be explained by the fact that at high H^+ concentration in solution, protons compete with the metal cations for the coordination sites of basic nature of the sorbent. Conversely, as the pH of the solution increases, the decrease in H^+ concentration in solution favours the binding of the heavy metal to the sorbent surface.

On the other hand, the surface charge of the sorbents is characterised by a point of zero charge or pH_{zpc}. The surface of the sorbent is positively charged at pH< pH_{zpc}, and negatively charged at pH>pH_{zpc}. The pH_{zpc} of GS and EC determined by potentiometric mass titration by Fiol (Fiol and Villaescusa, 2008), according to the procedure described by Bourika *et al.*, 2003, resulted to be 5.1 and 3.9, for GS and EC, respectively. Therefore, the increase of pH towards higher pH than the sorbents pH_{zpc} can be related to a decrease of the positive surface charge, which results in a lower electrostatic repulsion between the surface and the positively charged metal ion.

In **Figure 3**, it can also be observed an important decrease of metal sorption in the experiments performed with 1:0.5 Cu(II)-EDTA and Ni(II)-EDTA molar ratio at pH values within 3.0 and 7.0 in comparison with the results obtained in absence of EDTA. The species distribution diagrams of **Figure 4** show that at pH >2 copper and nickel are 50% complexed with the subsequent decrease to half of free cations predominance and the appearance in solution of the neutral CuH_2EDTA and the negative $CuHEDTA^-$ and $CuEDTA^{2-}$ species. These anionic species are not likely to be electrostatically bound at pH> pH_{zpc} when the sorbent is partially or totally negatively charged. Therefore, it seems that only free Cu^{2+} and Ni^{2+} cations would be adsorbed.

The species distribution diagram corresponding to solutions of 1:1 Cu(II)-EDTA and Ni(II)-EDTA molar ratio (figure not shown), indicates that 100% of metals are complexed as neutral or anionic metal-EDTA species. Therefore, the almost total absence of free metal cations in equimolar metal-EDTA solutions would explain the low metal adsorption observed. An adverse effect of complexing agents like citrate (Namasivayam and Ranganathan, 1998; Guzmán *et al.*, 2003), acetate and EDTA (Namasivayam and Ranganathan, 1998) on metal sorption on different sorbents has been previously reported.

Taking into account the obtained results further experiments were carried out at pH around 5.2 in order to avoid metal hydroxides precipitation.

5.2. Cu(II) and Ni(II) sorption kinetics onto GS and EC: effect of complexing agent EDTA

In this section, Cu(II) and Ni(II) sorption behaviour onto both GS and EC for three different sorbent concentrations and the effect of complexing agent EDTA is evaluated. Kinetics data will be modelled according to pseudo-second order model.

5.2.1. Cu(II) sorption kinetics onto GS and EC

In **Tables 5** and **6** Cu(II) concentration in solution as a function of contact time is shown for different sorbent concentrations in the range 2.5 to 10 $g \cdot L^{-1}$ in absence of EDTA and in presence of a Metal/EDTA ratio 1:0.5. Results for higher complexing agent concentration are not shown in these tables due to the negligible metal sorption observed.

Table 5: Cu(II) concentration in solution ($mg \cdot L^{-1}$) as a function of time for three initial GS concentrations. $[Cu(II)]_0 \approx 25\ mg \cdot L^{-1}$; $pH_0=5.20$.

Sorbent dose:	**2.5 $g \cdot L^{-1}$**		**5 $g \cdot L^{-1}$**		**10 $g \cdot L^{-1}$**	
t (min)	**Cu**	**Cu/EDTA 1:0.5**	**Cu**	**Cu/EDTA 1:0.5**	**Cu**	**Cu/EDTA 1:0.5**
0	24.08	24.09	24.44	24.31	25.02	25.15
1	23.86	23.81	21.79	23.10	13.94	19.71
2	21.45	22.69	19.85	22.36	13.89	19.32
3	21.50	22.27	18.36	21.06	12.41	18.59
5	20.39	20.89	16.37	20.64	11.70	18.04
10	18.16	20.25	14.56	19.04	10.20	17.08
15	17.43	19.49	13.46	18.36	9.04	16.72
30	15.33	18.98	12.04	18.23	7.78	16.26
60	14.48	17.59	10.69	17.41	7.71	15.97
120	14.33	17.25	10.56	17.36	7.42	15.87
180	14.27	17.13	10.02	17.30	7.50	16.01
240	14.10	17.20	9.97	17.24	7.64	16.15
300	13.98	17.21	9.90	17.24	7.61	16.15
360	13.70	17.21	9.90	17.24	7.58	16.17
420	13.70	17.21	9.90	17.24	7.27	16.10

Table 6: Cu(II) concentration in solution ($mg \cdot L^{-1}$) as a function of time for three initial EC concentrations. $[Cu(II)]_0 \approx 25\ mg \cdot L^{-1}$; $pH_0=5.2$.

Sorbent dose:	**2.5 g·L^{-1}**		**5 g·L^{-1}**		**10 g·L^{-1}**	
t (min)	**Cu**	**Cu/EDTA 1:0.5**	**Cu**	**Cu/EDTA 1:0.5**	**Cu**	**Cu/EDTA 1:0.5**
0	24.20	24.37	24.80	24.99	24.80	24.80
1	20.31	23.03	17.37	23.19	9.27	16.00
2	20.04	23.07	16.16	22.37	8.55	16.05
3	19.57	22.81	16.54	21.52	8.38	16.04
5	19.60	22.08	15.02	20.05	7.93	16.04
10	18.85	23.11	14.47	19.82	7.08	16.04
15	18.22	22.08	13.68	19.55	7.29	16.04
30	17.48	21.53	13.09	18.73	6.76	15.76
60	16.01	21.06	12.76	18.43	6.91	15.80
120	15.51	20.67	12.43	18.42	6.80	15.74
180	15.21	19.96	12.40	18.40	6.81	15.76
240	15.11	19.84	12.38	18.42	6.87	15.74
300	15.31	19.76	12.38	18.42	6.72	15.67
360	15.01	19.48	12.36	18.42	6.71	15.60
420	15.01	19.36	12.34	18.42	6.70	15.60

In the tables it can be observed how, in all the cases, the amount of metal in solution progressively decreases when increasing contact time until the achievement of an equilibrium concentration. Results for both materials put into evidence the positive effect of the increase of sorbent dose in both, the kinetics of the process and the equilibrium. It can be observed that, independently of the presence/absence of EDTA, sorption rate increases when increasing sorbent concentration and a lower metal concentration at equilibrium is achieved. As it had been indicated in the previous section, EDTA has a negative effect on copper sorption onto both materials, as demonstrates the higher metal concentrations in solution at equilibrium time when free and Metal:EDTA systems are compared.

To compare the effect of complexing agent in the rate at which the metal is concentrated in the solid phase and in the equilibrium for the different sorbent doses, copper accumulation as a function of contact time has been ploted for GS and EC in **Figures 5** and **6** respectively.

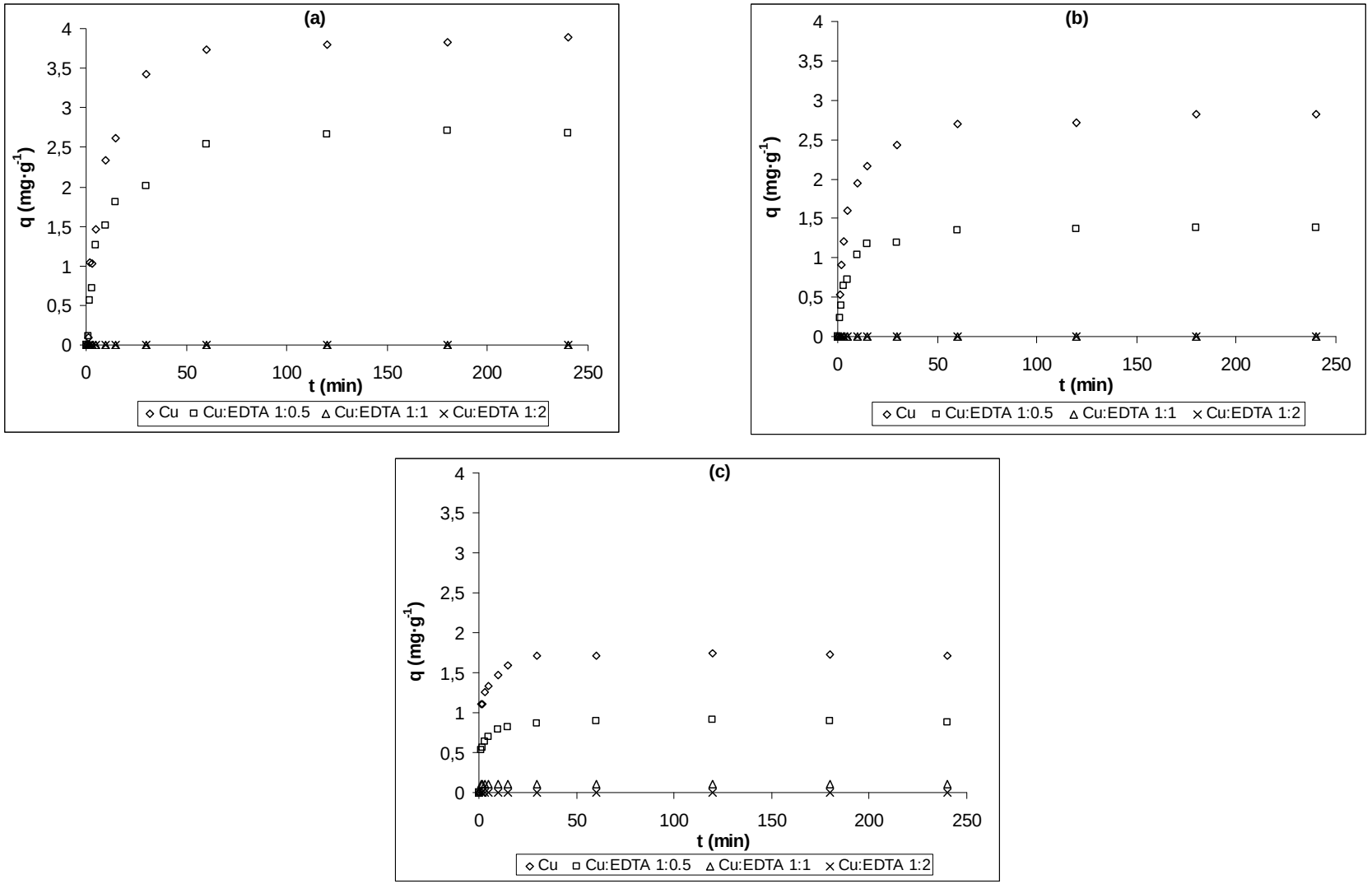

Figure 5: Effect of contact time on Cu(II) sorption onto GS for three different Metal:EDTA ratios. Sorbent dose: (a) 2.5 $g \cdot L^{-1}$; (b) 5 $g \cdot L^{-1}$ and (c) 10 $g \cdot L^{-1}$; $[Cu(II)]_0 \approx 25\ mg \cdot L^{-1}$; pH_0=5.2.

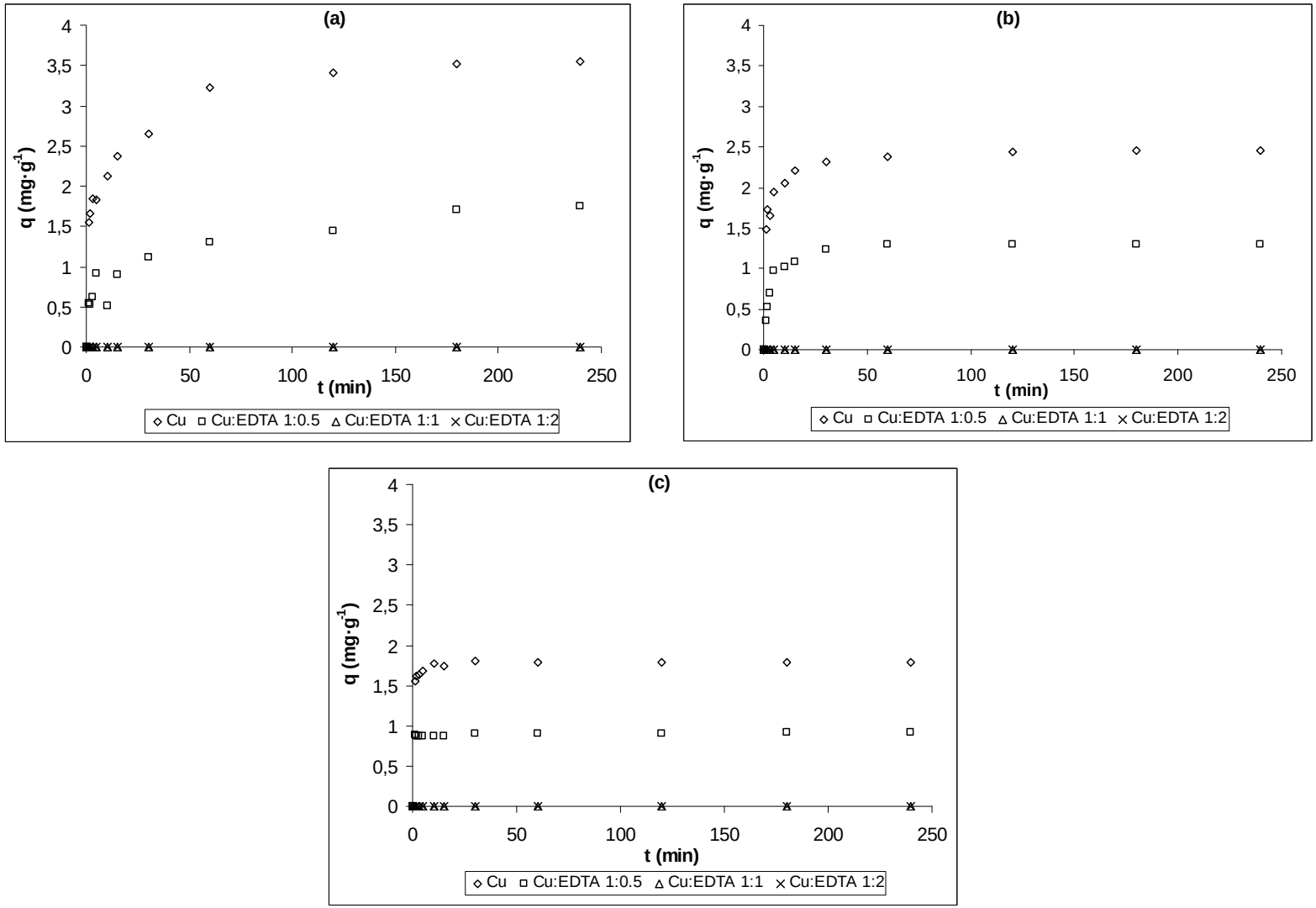

Figure 6: Effect of contact time on Cu(II) sorption onto EC for three different Metal:EDTA ratios. Sorbent dose: (a) 2.5 $g \cdot L^{-1}$; (b) 5 $g \cdot L^{-1}$ and (c) 10 $g \cdot L^{-1}$; $[Cu(II)]_0 \approx 25\ mg \cdot L^{-1}$; $pH_0=5.2$.

As it can be observed in both figures, metal removal seems to occur in two steps involving the first step rapid copper uptake within the first 20 minutes, followed by a subsequent removal of metal until equilibrium was reached, at around 60 minutes for all the studied sorbent doses except for the lowest one, that needs a contact time about 170 minutes. The rapid step is probably due to the abundant availability of active sites on the material, and with the gradual occupancy of these sites, sorption becomes less efficient leading to the slowering down of the removal rate that originates the slow step. The results presented here indicate that the presence of the ligand EDTA did not influence on metal sorption equilibrium achievement, but, as discussed previously, strongly influences the metal sorbed amount.

It can also be observed that from the two sorbents, GS is the one that shows the best performance, expressed as total sorbed amount, for copper sorption in presence and in absence of complexing agent. Nevertheless, it is noteworthy that EC sorption capacity is not so affected by the presence of EDTA as GS capacity.

In the figures, results for Metal:EDTA molar ratios 1:1 and 1:2 have been also included to demonstrate that the total complexation of the metal leads to the total absence of copper in the solid phase.

5.2.2. Ni(II) sorption kinetics onto GS and EC

In **Tables 7** and **8** Ni(II) concentration in solution as a function of contact time is shown for different sorbent concentrations in the range 2.5 to 10 $g \cdot L^{-1}$ in absence of EDTA and in presence of a Metal/EDTA ratio 1:0.5. As iin the case of Cu(II) sorption, results for higher complexing agent concentration are not presented in the table due to the negligible metal sorption observed.

Table 7: Ni(II) concentration in solution ($mg \cdot L^{-1}$) as a function of time for three initial GS concentrations. $[Ni(II)]_0 \approx 25\ mg \cdot L^{-1}$; $pH_0=5.2$.

	Sorbent concentration					
	2.5 $g \cdot L^{-1}$		5 $g \cdot L^{-1}$		10 $g \cdot L^{-1}$	
t (min)	Ni	Ni/EDTA 1:0.5	Ni	Ni/EDTA 1:0.5	Ni	Ni/EDTA 1:0.5
0	23.27	24.96	23.27	25.31	23.27	25.66
1	21.73	23.52	21.08	22.97	19.02	23.59
2	20.98	22.74	19.52	22.11	17.84	21.91
3	19.68	21.66	18.22	21.78	16.88	20.55
5	19.89	20.92	17.60	20.34	16.31	19.77
10	18.07	20.78	16.67	20.07	15.68	18.98
15	18.22	20.29	16.53	19.15	15.09	18.70
30	18.04	20.04	15.78	18.76	15.10	18.57
60	18.04	20.02	15.90	18.74	15.08	18.64
120	18.04	20.02	15.90	18.74	15.08	18.64
180	18.04	20.02	15.90	18.74	15.08	18.64
240	18.04	20.02	15.90	18.74	15.08	18.64
300	18.04	20.02	15.90	18.74	15.08	18.64
360	18.04	20.02	15.90	18.74	15.08	18.64
420	18.04	20.02	15.90	18.74	15.08	18.64

Table 8: Ni(II) concentration in solution ($mg \cdot L^{-1}$) as a function of time for three initial EC concentrations. $[Ni(II)]_0 \approx 25\ mg \cdot L^{-1}$; $pH_0=5.2$.

	Sorbent concentration					
	2.5 g·L^{-1}		5 g·L^{-1}		10 g·L^{-1}	
t (min)	Ni	Ni/EDTA 1:0.5	Ni	Ni/EDTA 1:0.5	Ni	Ni/EDTA 1:0.5
0	23.02	25.85	23.02	25.85	23.02	25.85
1	22.99	25.72	22.73	25.61	22.07	25.25
2	22.79	25.57	22.56	25.57	21.76	25.18
3	22.75	25.43	22.35	25.31	21.37	25.12
5	22.70	25.41	21.71	25.21	21.06	25.13
10	22.45	25.39	21.45	25.09	20.16	25.14
15	22.35	25.26	21.25	24.94	20.08	25.11
30	22.15	25.06	21.13	24.64	20.07	25.06
60	21.95	25.01	21.12	24.65	20.07	25.00
120	21.75	25.01	21.08	24.54	20.07	25.00
180	21.75	25.01	21.08	24.54	20.07	25.00
240	21.75	25.01	21.08	24.54	20.07	25.00
300	21.75	25.01	21.08	24.54	20.07	25.00
360	21.75	25.01	21.08	24.54	20.07	25.00
420	21.75	25.01	21.08	24.54	20.07	25.00

As it had been reported in the previous section for copper, nickel concentration in solution progressively decays when contact time advances until the achievement of an equilibrium concentration. Also for this metal, as it was expected, an increase of sorbent dose provokes an acceleration on the sorption rate and the achievement of a lower equilibrium metal concentration in solution in scenarios with and without EDTA.

The presence of complexing agent provokes, at equilibrium, an inhibition effect on nickel sorption onto both, grape stalk and exhausted coffee. As in the case of copper, the effect of complexing agent in the solid phase accumulation rate and in the equilibrium for the different sorbent doses was compared. Results for GS and EC are presented in **Figures 7** and **8** respectively.

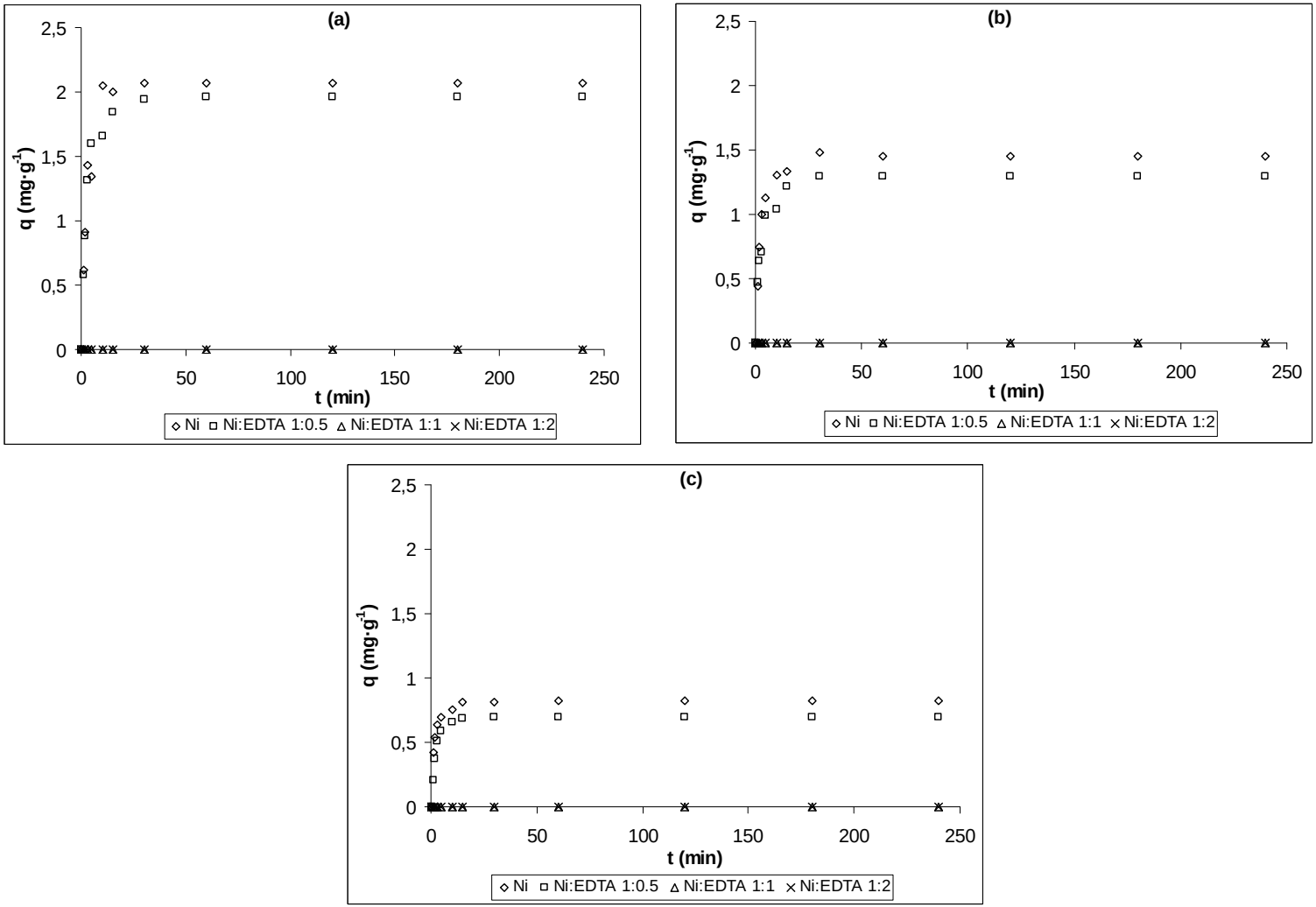

Figure 7: Effect of contact time on Ni(II) sorption onto GS for three different Metal:EDTA ratios. Sorbent dose: (a) 2.5 $g \cdot L^{-1}$; (b) 5 $g \cdot L^{-1}$ and (c) 10 $g \cdot L^{-1}$; $[Ni(II)]_0 \approx 25\ mg \cdot L^{-1}$; $pH_0=5.2$.

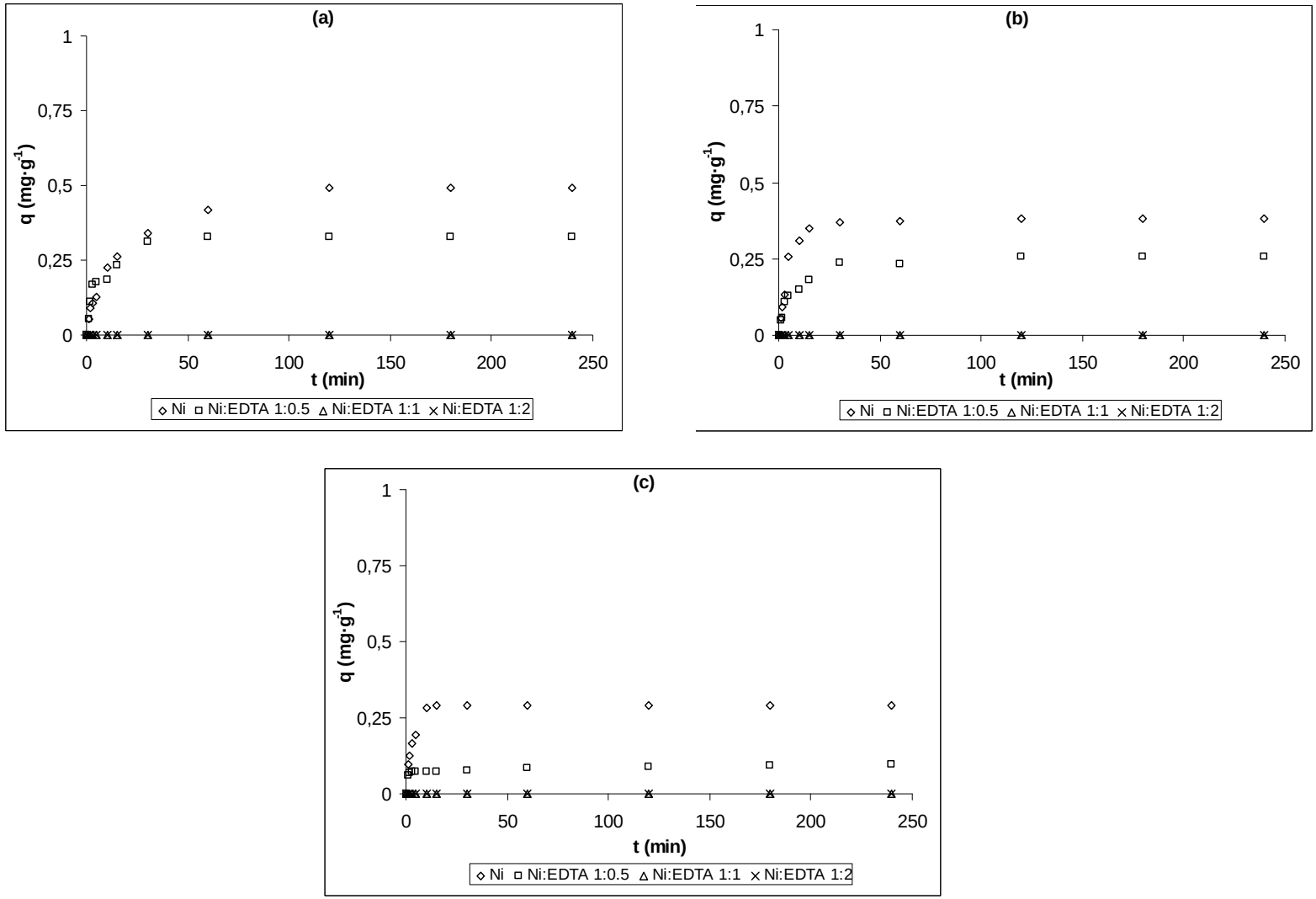

Figure 8: Effect of contact time on Ni(II) sorption onto EC for three different Metal:EDTA ratios. Sorbent dose: (a) 2.5 $g \cdot L^{-1}$; (b) 5 $g \cdot L^{-1}$ and (c) 10 $g \cdot L^{-1}$; $[Ni(II)]_0 \approx 25\ mg \cdot L^{-1}$; $pH_0=5.2$.

As in the case of copper sorption kinetics, nickel removal occurs in two steps; a fast accumulation on the solid phase followed by a slower process that drives the material to equilibrium. Kinetics of nickel sorption is also fast and saturation is achieved in about 30 minutes for both materials and the three sorbent doses studied. The presence of the ligand EDTA seemed not to influence the time to achieve sorption equilibrium, but, as in the case of copper, strongly diminished the metal sorbed amount.

It can also be observed that from the two evaluated sorbents, GS shows the best performance for nickel sorption in presence and in absence of complexing agent. Nevertheless, when sorption capacity was compared, EC seemed not to be as much affected by the presence of EDTA than GS. In the figures, also results for Metal:EDTA molar ratios 1:1 and 1:2 have been included. As it can be observed, under total nickel complexation conditions (ratios metal:EDTA 1:1 or higher), nickel removal by sorption onto GS and EC is absolutely inefficient.

Finally, when copper and nickel capacity onto both sorbents is compared, it has to be remarked that copper is always the most efficiently sorbed.

For a deeper understanding of the copper and nickel sorption kinetics onto GS and EC in presence and in absence of complexing agent, the results obtained in this section were modelled according to the pseudo-second order equation. The obtained results are presented in the next section.

5.3. Sorption kinetics modeling

In order to investigate the sorption rate law of metal sorption the obtained kinetic data were analysed using the pseudo-second order equation proposed by Ho (Ho *et al.*, 2000):

$$\frac{dq_t}{dt} = k_2 (q_e - q_t)^2 \qquad (6)$$

where q_e and q_t are the sorption capacity at equilibrium and at time t, respectively ($mg \cdot g^{-1}$) and k_2 is the rate constant of pseudo-second order sorption ($g \cdot mg^{-1} \cdot min^{-1}$). For the initial condition $t = 0$ and $q_t = 0$, the integrated form of equation (6) becomes:

$$\frac{1}{(q_e - q_t)} = \frac{1}{q_e} + k_2 t \qquad (7)$$

which is the integrated rate law for a pseudo-second order reaction. Equation (7) can be rearranged to obtain the linear form:

$$\frac{t}{q_t} = \frac{1}{k_2 q_e^2} + \frac{1}{q_e} t \qquad (8)$$

When the experimental data were introduced into the Eq. (8), straight lines for all cases were obtained by plotting t/q_t versus t, indicating that the processes follow the pseudo-second order rate equation. As an example, **Figures 9** and **10** show the pseudo-second order plot for the sorption of Cu(II) and Ni(II) onto GS and EC for a sorbent concentration of 5 $g \cdot L^{-1}$. Symbols represent the experimental data and solid line, the model fitting.

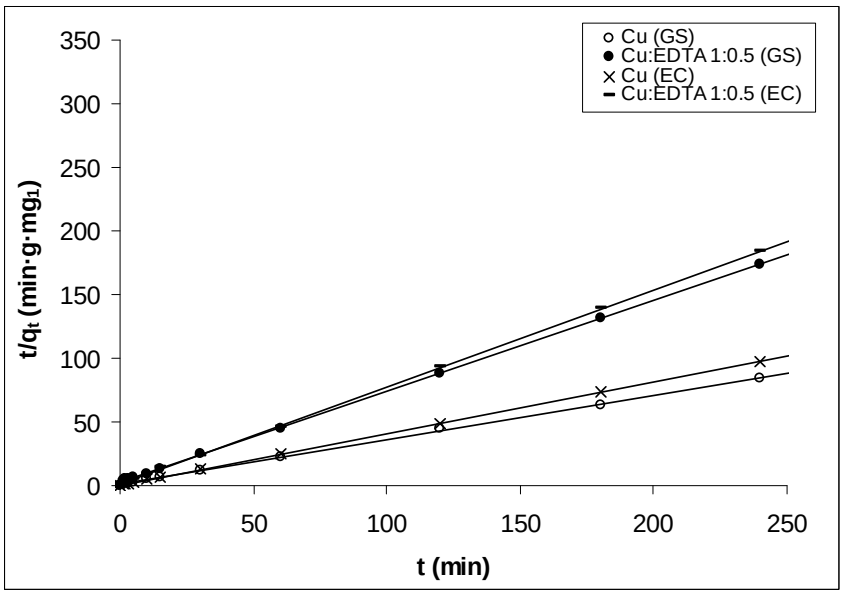

Figure 9: Pseudo-second order plot for the adsorption of Cu(II) onto GS and EC. pH_0=5.2; sorbent dose: 5 $g \cdot L^{-1}$; initial metal concentration: 0.4 mM.

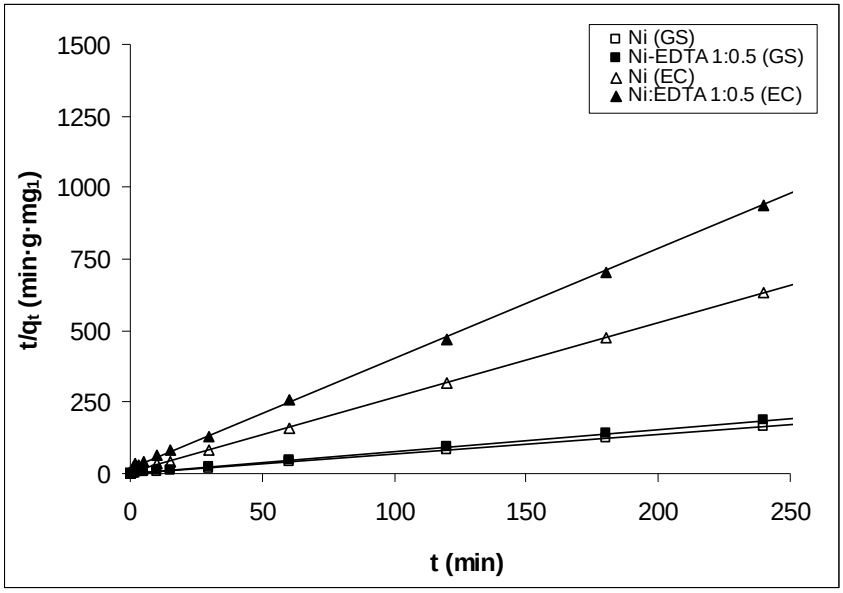

Figure 10: Pseudo-second order plot for the adsorption of Ni(II) onto GS and EC. pH_0= 5.2; sorbent dose: 5 $g \cdot L^{-1}$; initial metal concentration: 0.4 mM.

The pseudo-second order rate constant k_2 and the equilibrium metal sorption capacity, q_e, were calculated from the linear regressions plots, and results are presented in **Tables 9** and **10** for copper and nickel, respectively, along with the determination coefficient, R^2.

Table 9: Pseudo-second order kinetic parameters for Cu(II) adsorption on GS and EC in presence and in absence of EDTA.

Sorbent	Sorbent dose ($g \cdot L^{-1}$)	EDTA conc. (mM)	Pseudo-second order model		
			k_2 ($g \cdot mg^{-1} \cdot min^{-1}$)	q_e ($mg \cdot g^{-1}$)	R^2
GS	2.5	---	0.022	4.09	0.9906
		0.2	0.039	2.82	0.9996
	5	---	0.086	2.87	0.9999
		0.2	0.198	1.40	0.9952
	10	---	0.651	1.73	0.9999
		0.2	1.766	0.89	0.9998
EC	2.5	---	0.058	3.60	0.9985
		0.2	0.051	1.77	0.9919
	5	---	0.313	2.47	0.9999
		0.2	0.373	1.30	0.9999
	10	---	3.612	1.79	1.0000
		0.2	2.100	0.92	0.9999

Table 10: Pseudo-second order kinetic parameters for Ni(II) adsorption on GS and EC in presence and in absence of EDTA.

Sorbent	Sorbent dose ($g \cdot L^{-1}$)	EDTA conc. (mM)	Pseudo-second order model		
			k_2 ($g \cdot mg^{-1} \cdot min^{-1}$)	q_e ($mg \cdot g^{-1}$)	R^2
GS	2.5	---	0.410	2.08	1.0000
		0.2	0.399	1.97	1.0000
	5	---	0.609	1.46	1.0000
		0.2	0.546	1.31	0.9999
	10	---	1.956	0.82	1.0000
		0.2	1.778	0.70	1.0000
EC	2.5	---	0.177	0.52	0.9962
		0.2	0.749	0.34	0.9998
	5	---	0.829	0.39	0.9998
		0.2	0.777	0.26	0.9998
	10	---	2.788	0.29	0.9994
		0.2	3.185	0.10	0.9990

In all the studied scenarios, R^2 values higher than 0.99 were obtained, indicating the good compliance of the experimental data with the pseudo-second order model. The k_2 values for copper sorption show that the pseudo-second order constant rate increase in the presence of complexing agent in the case of grape stalk while complexation seemed to have a fairly influence on k_2 when EC was the sorbent. Complexation seems also not to have a clear influence on nickel sorption constant rate onto both GS and EC sorbents. When the sorption rate constant values are compared, it can be seen that, independently of the presence/absence of complexing agent, k_2 increases with the increase of sorbent dose. When sorption of both metals onto both materials was compared, it was observed that, in general, nickel sorption was faster than copper sorption, as indicate the higher values of the pseudo-second order rate constant.

For all the studied systems, the amount of metal sorbed at equilibrium (q_e) decreased when increasing the sorbent concentration. This observation is consistent with the fact that the addition of a higher sorbent mass to the media leads to a higher distribution of the sorbates. As it had been discussed previously, the presence of EDTA provokes a decrease on metal sorbed amount, and this is reflected in a decrease in the q_e values predicted by the pseudo-second order model. In the case of copper, the presence of EDTA in a 1:0.5 molar concentration ratio provoked around a 50% decrease in the amount of metal sorbed on both

GS and EC. In the same conditions the sorption of nickel was only fairly decreased. The results provided by the model, clearly put into evidence that copper sorption is more affected by the presence of complexing agent than nickel sorption.

From the q_e and k_2 parameters obtained from the linear fitting of the pseudo-second order equation, the theoretical sorption kinetics for each studied system be simulated. As an example of the prediction of the pseudo-second order model, calculated curves corresponding to metal uptake by both biomaterials for a sorbent concentration of 5 $g \cdot L^{-1}$ have been plotted together with the experimental data in **Figure 11** and **12** for Cu(II) and Ni(II) respectively. The figures put into evidence the good agreement between the pseudo-second order model predicted results and the obtained experimentally, either in presence or in absence of EDTA.

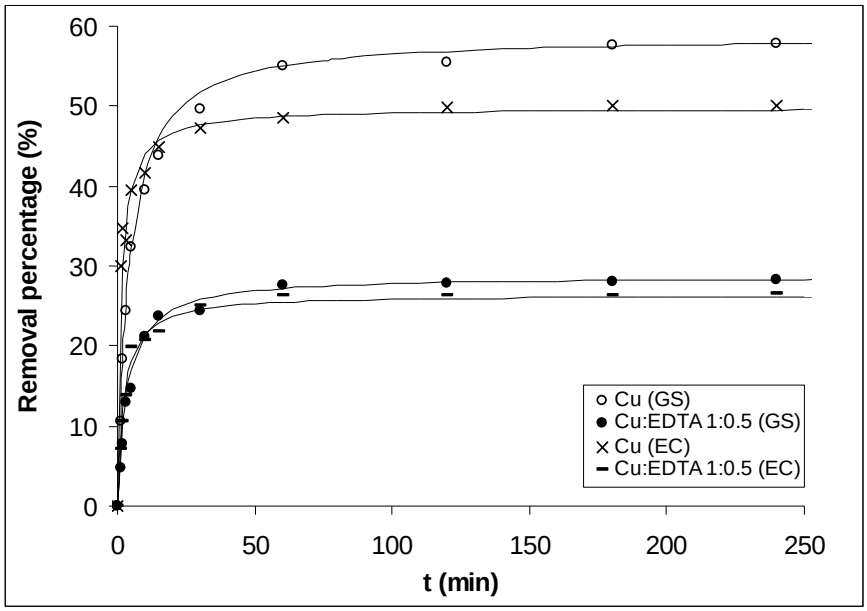

Figure 11: Effect of contact time on the removal of Cu(II) onto GS and EC in presence and in absence of EDTA. pH_0 =5.2; sorbent dose, 5 g/L; initial metal concentration: 0.4 mM. In symbols are shown the experimental results, in solid line, the model prediction.

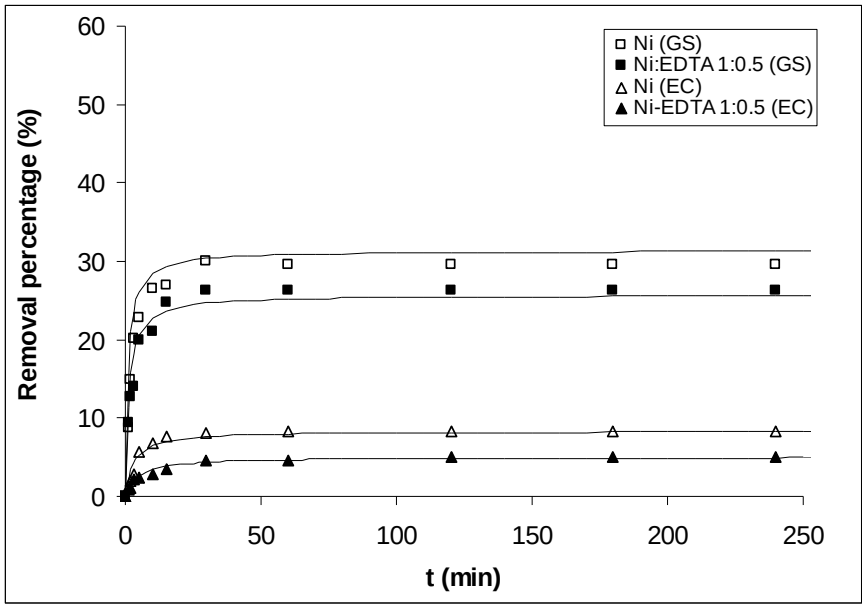

Figure 12: Effect of contact time on the removal of Ni(II) onto GS and EC in presence and in absence of EDTA. pH_0 =5.2; sorbent dose: 5 g/L; initial metal concentration: 0.4 mM. In symbols are shown the experimental results, in solid line, the model prediction.

5.4. Cu(II) and Ni(II) sorption equilibrium study onto GS and EC: effect of complexing agent EDTA.

In this section the effect of initial metal concentration in solution and of the presence of complexing agent in the sorption capacity of GS and EC is explored and discussed.

In **Tables 11** and **12** Cu(II) and Ni(II) initial and final metal concentration after sorption onto both, GS and EC, in absence of EDTA and for a molar ratio 1:0.5 are presented. Results for higher complexing agent ratios are not presented due to the almost complete metal sorption inhibition that EDTA provokes.

Table 11: Cu(II) initial and equilibrium concentration in solution after contact with GS and EC in absence of EDTA and in presence of complexing agent (1:0.5 molar ratio). pH_0=5.2; agitation time: 72h.

Cu			Cu:EDTA 1:0.5		
	GS	EC		GS	EC
C_i(mg·L^{-1})	C_e(mg·L^{-1})	C_e(mg·L^{-1})	C_i(mg·L^{-1})	C_e(mg·L^{-1})	C_e(mg·L^{-1})
4.71	0.79	0.94	4.22	2.69	2.09
8.67	1.29	1.89	8.81	5.36	5.20
18.17	2.18	2.45	18.09	9.88	10.62
27.6	3.57	7.01	27.69	14.83	15.30
37.23	5.96	15.11	36.72	20.43	20.10
46.18	5.84	19.45	47.65	26.04	28.54
67.75	15.16	40.27	67.76	37.82	44.80
94.09	22.08	58.25	93.96	55.37	65.48
14.58	37.19	103.67	142.32	90.00	108.57
196.57	59.25	149.75	195.94	135.40	152.82
253.02	94.25	202.21			

Table 12: Ni(II) initial and equilibrium concentration in solution after contact with GS and EC in absence of EDTA and in presence of complexing agent (1:0.5 molar ratio). Initial pH = 5.2; Agitation time: 72h.

Ni			Ni:EDTA 1:0.5		
	GS	EC		GS	EC
C_i(mg·L^{-1})	C_e(mg·L^{-1})	C_e(mg·L^{-1})	C_i(mg·L^{-1})	C_e(mg·L^{-1})	C_e(mg·L^{-1})
5.05	0.99	1.04	5.03	3.19	2.90
12.84	2.29	2.03	10.94	4.06	6.05
20.57	3.18	4.03	21.83	8.33	12.49
29.19	4.57	8.32	32.08	12.28	19.42
40.47	6.96	17.94	40.74	17.03	27.51
49.09	7.84	25.07	59.39	27.28	41.43
75.47	13.16	49.15	72.41	37.30	56.24
102.10	20.08	70.15	89.47	49.29	70.18
132.28	34.19	98.36	151.22	99.29	126.24
206.50	75.25	171.27	209.76	155.12	183.06
267.73	119.25	232.74			

As it can be seen in **Tables 11** and **12**, for initial metal concentrations lower than about 20 mg·L^{-1} in absence of complexing agent, equilibrium concentration in solution after contact with either GS or EC is quite similar for both, Cu(II) and Ni(II). These results point out that in the low concentration range and in absence of complexing agent, both sorbents would be effective for the removal of both metals. From inital metal concentrations in

solution higher than 20 $mg \cdot L^{-1}$, GS is much more efficient for divalent metal removal than EC.

If metal concentration on the solid phase is plotted as a function of metal concentration in solution at equilibrium, sorption isotherms are obtained. Results are presented in **Figures 13** and **14** for copper and nickel respectively.

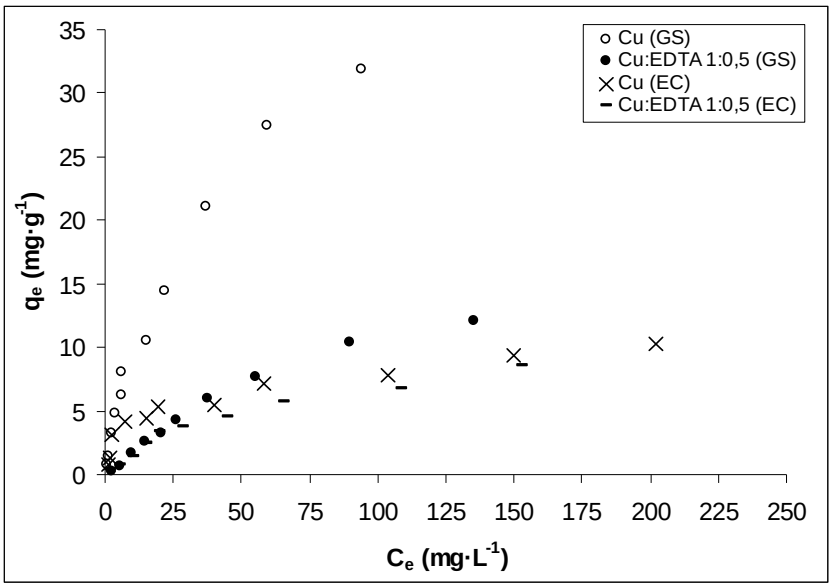

Figure 13: Sorption isotherms of Cu(II) onto GS and EC in presence and in absence of EDTA.

The different sorption behaviour between GS and EC is evidenced in **Figure 12**. In this figure it can be observed that while for an equilibrium copper concentration in solution of approximately 40 $mg \cdot L^{-1}$ EC has almost reached saturation with a capacity about 5 $mg \cdot g^{-1}$, GS seems not to be still saturated when equilibrium metal concentration in solution is close to 95 $mg \cdot L^{-1}$.

As it can be observed in **Figure 13**, the presence of EDTA dramatically affects copper sorption onto both materials, but it is noteworthy that the sorption decrease that the complexing agent provokes is higher for GS than for EC. Despite GS shows a higher sorption capacity for all the initial Cu(II) concentrations than EC, EC is less affected by the presence of complexing agent than GS.

In the next figure, Ni(II) sorption onto both, GS and EC in absence and in presence of a Ni(II):EDTA molar ratio 1:0.5 are presented.

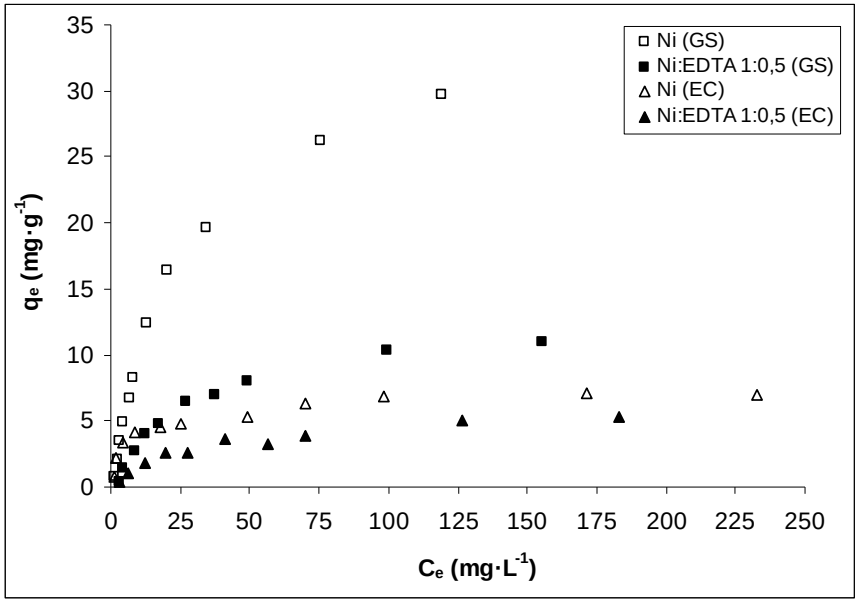

Figure 14: Sorption isotherms of Ni(II) onto GS and EC in presence and in absence of EDTA.

A similar discussion as in the case of Cu(II) sorption onto both materials can be made in the case of Ni(II) sorption. Again, a similar capacity is observed for both GS and EC in absence of complexing agent in the initial concentration range within 5.1 to 20.6 $mg \cdot L^{-1}$, showing both materials a similar removal efficiency for this low initial metal concentrations. For higher concentrations, GS is again the material that shows the best sorption performance for the non-complexed Ni(II).

Figure 14 indicates that, as in the case of Cu(II), the presence of complexing agent EDTA strongly decreases Ni(II) sorption onto both materials and this sorption decrease is higher in the case of GS than in the case of EC.

In order to obtain additional information on the effect of complexing agent in maximum sorbent capacity and of sorbent-sorbate affinity, experimental Cu(II) and Ni(II) equilibrium results onto both materialswere modelled according to Langmuir and Freundlich equations. Results obtained are presented and discussed in the next section.

5.4.1. Mathematical modeling of equilibrium results

5.4.1.1. Langmuir model

As it had been presented in chapter 1, section 5.5.1.1, Langmuir model assumed the formation of a homogeneous surface and, at saturation, the formation of a monolayer of adsorbate was formed. This model was characterized by the parameters $q_{max.}$, corresponding to the maximum metal uptake ($mg \cdot g^{-1}$) and K_L ($L \cdot mg^{-1}$), a constant related to the affinity between the sorbent and the sorbate.

In **Figure 15**, the fitting of the experimental Cu(II) and Ni(II) sorption data in absence of EDTA and for a metal:EDTA molar ratio 1:0.5 onto GS and EC to the linearised form of Langmuir model is shown: $\frac{C_f}{q} = \frac{1}{(q_{max} \cdot K_L)} + \frac{C_f}{q_{max}}$.

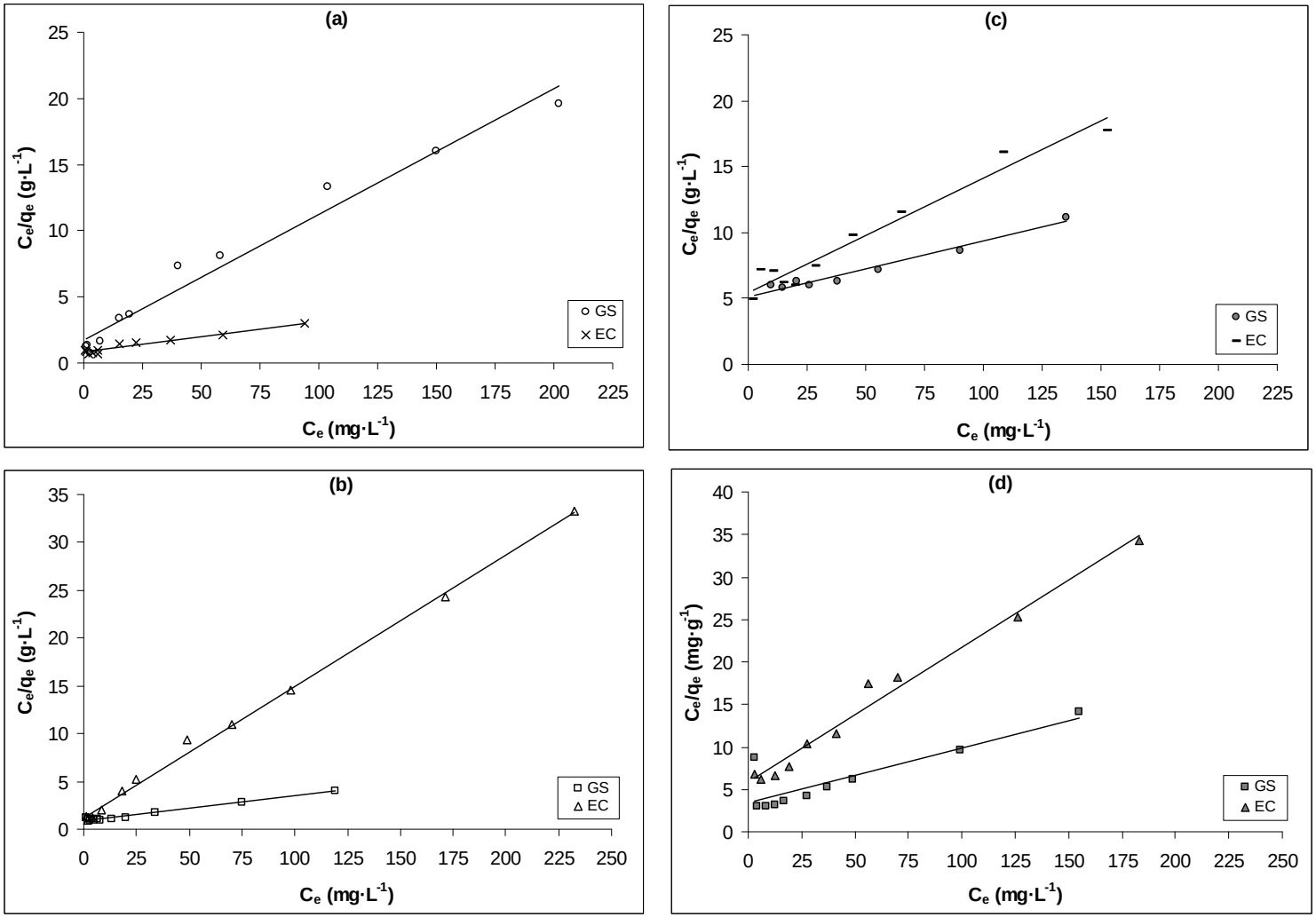

Figure 15: Langmuir model fitting of the experimental sorption equilibrium results for free Cu(II) and Ni(II) (**(a)** and **(b)** respectively) and in presence of complexing agent (**(c)** and **(d)** for Cu(II) and Ni(II) respectively).

From the fit of the experimental data obtained for both sorbents in presence and in absence of complexing agent to the linearized equation of Langmuir equation, parameters related to maximum capacity of the sorbents (q_{max}) and to the affinity sorbent-sorbate (K_L) can be calculated. Results are presented in **Table 13**.

5.4.1.2. Freundlich model

The Freundlich isotherm, in contrast to the Langmuir model, was based on sorption on a heterogeneous surface and assumed that different sites with different adsorption energies were involved. This model was characterized by the empirical constants K_F and n are that indicate the relative sorption capacity and sorption intensity respectively.

In **Figure 16**, the fitting of the experimental Cu(II) and Ni(II) sorption data in absence of EDTA and for a metal:EDTA molar ratio 1:0.5 onto GS and EC to the linearised form of Freundlich model is presented: $\log q_e = \log K_F + \frac{1}{n} \log C_e$.

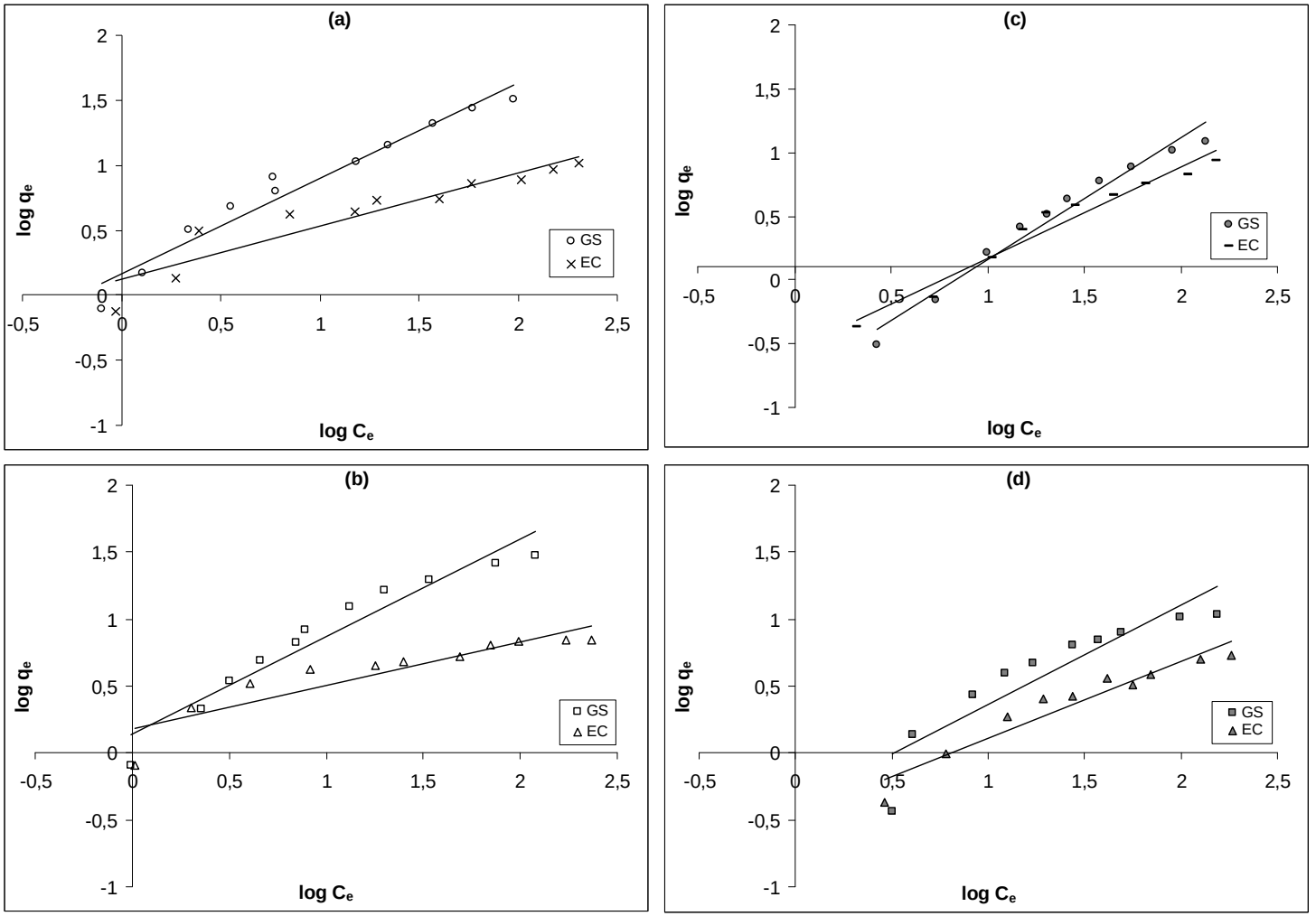

Figure 16: Freundlich model fitting of the experimental sorption equilibrium results for free Cu(II) and Ni(II) (**(a)** and **(b)** respectively) and in presence of complexing agent (**(c)** and **(d)** for Cu(II) and Ni(II) respectively).

As in the case of Langmuir equation, from the fitting of the experimental data obtained for both sorbents in presence and in absence of complexing agent to the linearized equation of Freundlich sorption model, the characteristic parameters, K_F and 1/n, can be calculated and are presented in **Table 13**.

Table 13: Langmuir and Freundlich parameters for the adsorption of Cu(II) and Ni(II) in presence and in absence of EDTA on GS and EC.

Sorbent	Metal	[EDTA] (mM)	Langmuir model			Freundlich model		
			$q_{max.}$ ($mg \cdot g^{-1}$)	K_L ($L \cdot mg^{-1}$)	R^2	K_F	1/n	R^2
GS	Cu	---	42.92	0.0283	0.948	1.48	0.73	0.957
		0.2	23.86	0.0082	0.967	0.16	0.95	0.970
	Ni	---	38.31	0.0302	0.979	1.38	0.73	0.932
		0.2	15.48	0.0189	0.746	0.42	0.74	0.828
EC	Cu	---	11.60	0.0541	0.974	1.31	0.41	0.878
		0.2	10.52	0.0160	0.957	0.28	0.72	0.962
	Ni	---	7.25	0.1227	0.997	1.55	0.32	0.804
		0.2	6.30	0.0275	0.983	0.35	0.57	0.920

As it can be seen in the table, both models provided quite good determination coefficients for all the studied systems. As it was expected, q_{max} predicted from the Langmuir model for the systems Cu(II):EDTA and Ni(II):EDTA was lower than the corresponding to non-complexed metal systems. When GS was used as sorbent, q_{max} is reduced in a 50% for both metals when EDTA is present in the media. This fact was predictable if we take into account that in the 1:0.5 Metal:EDTA solution approximately a 50% of the metal is complexed, indicating that the free metal cation seems to be the most sorbed species on GS. In experiments performed with EC, lower maximum sorption capacities than for GS were achieved in uncomplexing media and the effect of the presence of EDTA was less noticeable (10-20% of reduction of the maximum sorbent capacity). In an attempt to provide an explanation to the different intensity in which the complexing agent affects divalent metal sorption onto GS and EC, the parameters related to the affinity of the interaction sorbent-sorbate, K_L and 1/n of the Langmuir and Freundlich models, respectively, will be explored later.

It is well known that while in the case of K_L, higher numerical values indicate a more favourable adsorption, in the case of 1/n, lower values are related to a stronger bond

adsorbate-surface. From the fitting of the experimental data, the introduction of the complexing agent resulted in a decrease in the K_L values and an increase of 1/n. It was also observed that, for both metals in presence and in absence of complexing agent, the parameters K_L and 1/n indicate that the sorption onto EC is more favourable than onto GS. This data suggest the more favourable interaction of both, Cu(II) and Ni(II) with EC than with GS and it could explain the lower sensitivity to the presence of EDTA of EC compared to GS in of both metals sorption. Whatever case, in presence and in absence of EDTA, grape stalk showed a higher capacity than exhausted coffee for copper and nickel uptake.

This reduction of metal ions uptake when EDTA is present in solution has already been reported. Gyliene *et al.* (2006) found around 45% decrease on copper sorption onto chitosan at pH 3 and 1:0.5 metal-EDTA molar ratio; Chu and Hashim (2000) reported that copper removal efficiency at pH 6 decreases from 80% to 30 % and to 40% when using as sorbent coal-based and coconut shell-based activated carbons, respectively, at 1:1 metal-EDTA molar ratio.

In the next table, sorption results in absence of complexing agent are compared to other results obtained by authors studying copper and nickel sorption at pH 5–5.5 using different biosorbents.

Table 14: Maximum uptake (q_{max}) of Cu(II) and Ni(II) for selected biosorbent materials

	Adsorbent capacity ($mg \cdot g^{-1}$)		
Sorbent	**Cu(II)**	**Ni(II)**	**Reference**
GS	42.92	38.31	This work
EC	11.6	7.25	This work
Papaya wood	19.85		Saed *et al*., 2005
Sugar beet pulp (native)	21.16	11.85	Reddad *et al*., 2002
Seeds of *Capsicum annuum*	16.71		Özcan *et al*., 2005
Crop milling waste (black gram husk)	27.97	20.15	Saeed *et al*., 2005
Activated carbon from almond husk		30.8-37.2	Hasar, 2003
Brown algae *Fucus vesiculosus*	61.6	46.9	Rincón *et al*., 2005
Olive stone waste	2.02	2.13	Fiol *et al*., 2006
Green algae *Spirogyra*	133.3		Gupta *et al*., 2006
Algae *Chlorella vulgaris*		59.7	Aksu, 2002
Olive mill residues	13.5		Veglió *et al*., 2003
Deactivated protonated yeast		9.01	Padmavathy, 2008

As seen in the table, the maximum sorption values obtained for Cu and Ni when using GS are greater than those reported in literature for other sorbents except for the algaes (*Fucus vesiculosus*, *Spirogyra* and *Chorella vulgaris*).
The uptake capacity of EC for both metals is greater than those found for olive stones but lower compared to the capacities of the other sorbents listed in **Table 14**.

5.5. Column experiments

5.5.1. Effect of feeding metal concentration

Adsorption experiments in packed bed-up flow columns using GS as adsorbent were carried out to evaluate the performance of this biomaterial in a continuous process. GS was chosen because from the two materials studied, showed the highest removal capacity for copper and nickel from free and EDTA-complexed metal solutions.
In order to obtain both, the temporal profile of metal concentration in the eluted flow and in the solid phase in absence of complexing agent, in **Figures 17** and **18,** Cu(II) and Ni(II) concentration respectively has been presented in terms of normalized concentration (liquid phase) and accumulation (solid phase).

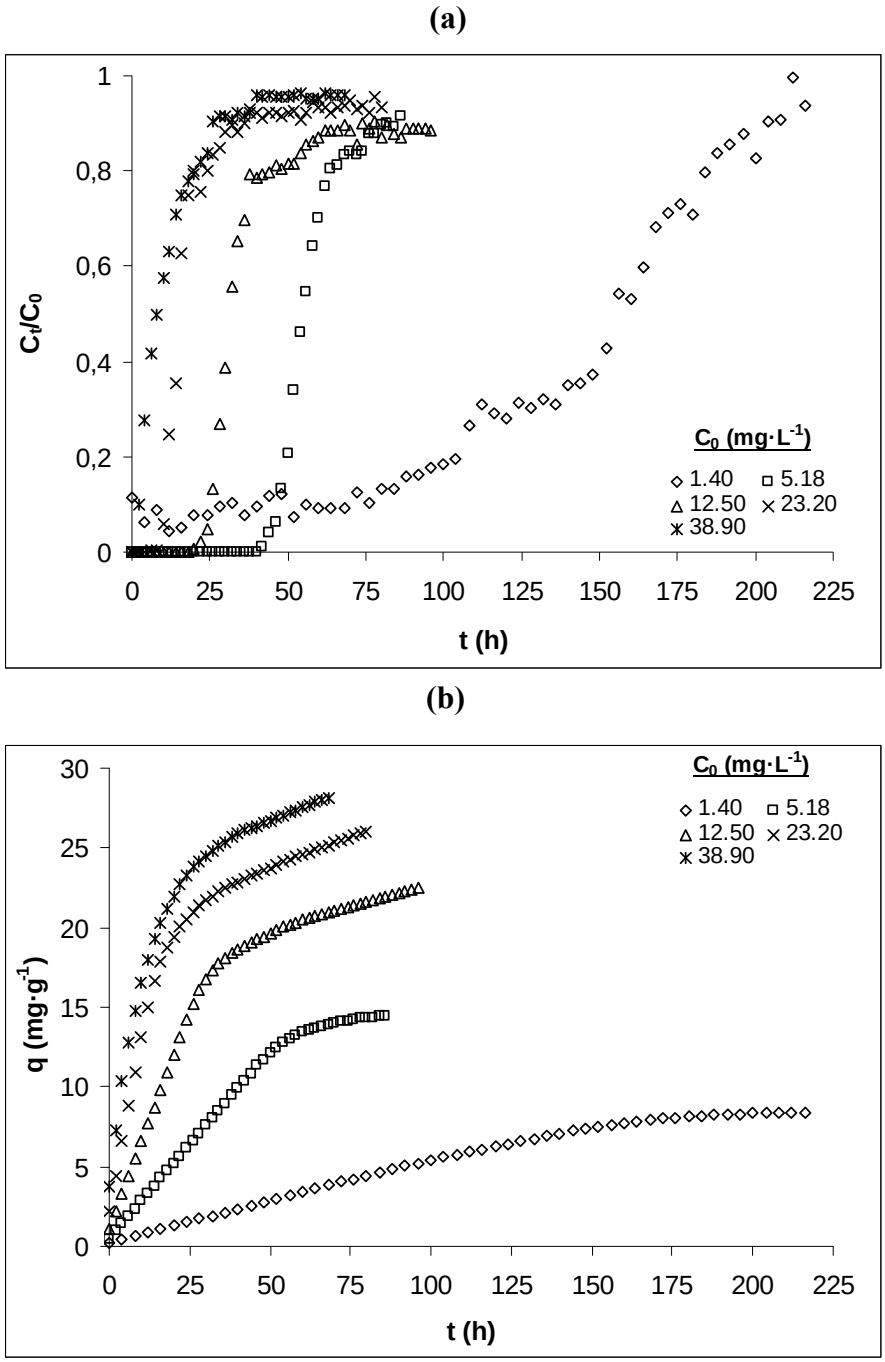

Figure 17: (a) Normalized breakthrough curves and (b) capacity evolution as a function of time for the adsorption of Cu(II) onto GS in a packed bed up-flow column in absence of EDTA for different feeding metal concentrations ($mg \cdot L^{-1}$). Feeding solution concentration range: 1.40-38.90 $mg \cdot L^{-1}$.

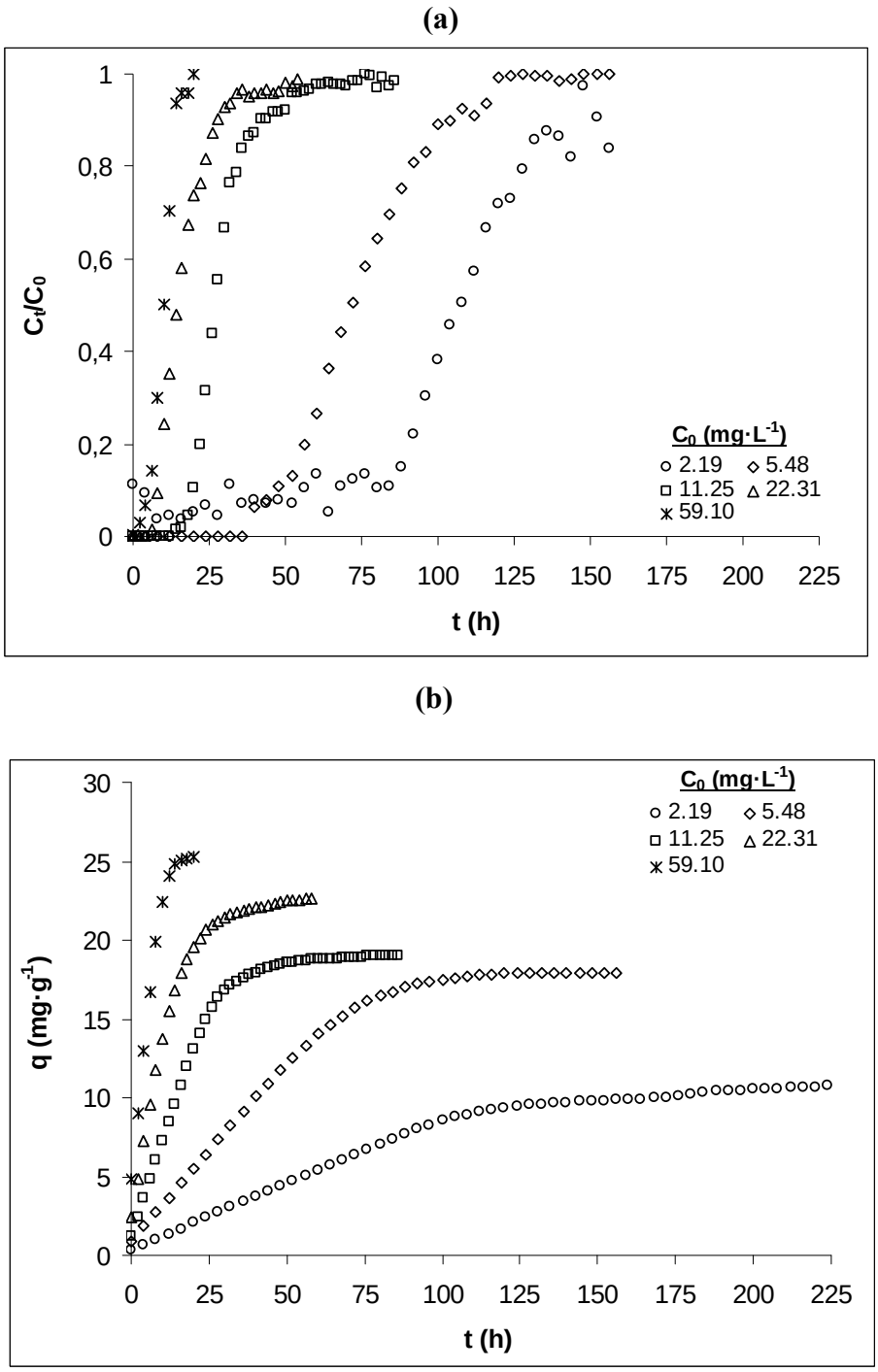

Figure 18: (a) Normalized breakthrough curves and (b) capacity evolution as a function of time for the adsorption of Ni(II) onto GS in a packed bed up-flow column in absence of EDTA for different feeding metal concentrations ($mg \cdot L^{-1}$). Feeding solution concentration range: 2.19-59.10 $mg \cdot L^{-1}$.

As it can be seen in both, **Figures 17** and **18**, a similar sorption trend is observed when feeding Cu(II) and Ni(II) GS-packed columns. In the case of the lowest concentration, for both metals and in average, only a 8% of the feeding concentration was observed in the outlet flow during the first 80 hours of process (corresponding to 0.11 $mg \cdot L^{-1}$ of Cu(II) and 0.18 $mg \cdot L^{-1}$ in the case of Ni(II)). In the experimental conditions of these assays, a volume of 2.4 L of polluted effluent has been treated with only 775.50 mg of dry grape stalk, accomplishing the Spanish environmental quality standards (Real Decreto 995/2000), indicating an excelent sorption performance of this sorption system for the removal of relatively low metal concentrations. As it would be expected, the higher the metal concentration in the feeding effluent, the higher the liquid-solid mass transfer rate, as it can be observed by the higher slopes of the plots time-solid phase metal concentration, and the lower time to reach solid phase saturation.

It has to be remarked that the sorption process took place with only a slight pH variation (data not shown), indicating thus that H^+ are not strongly involved in Cu(II) and Ni(II) sorption process in a first sorption cycle onto raw GS.

From these same plots, maximum capacity of the sorbent for the different feeding metal concentrations can be calculated, obtaining thus valuable information about the capacity of the sorbent for different equilibrium concentrations in the continuous flow process. If sorbed amount concentration is plotted as a function of feeding metal concentration, column sorption isotherms can be obtained. The results are presented in **Figures 19** and **20** for Cu(II) and Ni(II) respectively. As in the case of batch isotherms, experimental equilibrium results obtained in continuous were submitted to Langmuir and Freundlich models and its characteristic parameters were calculated. The parameters previously obtained in batch and those obtained in continuous are presented in **Table 14**. The predictive power of both models was evaluated by superimposing the predicted equilibriums to the experimental results.

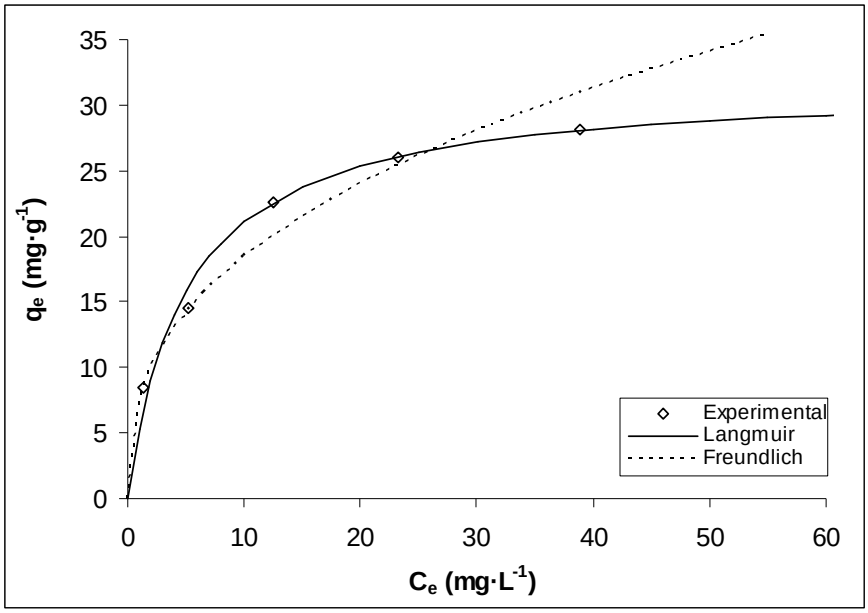

Figure 19: Copper sorption isotherm in continuous. Symbols represent the experimental results and in lines, the prediction of Langmuir and Freundlich models.

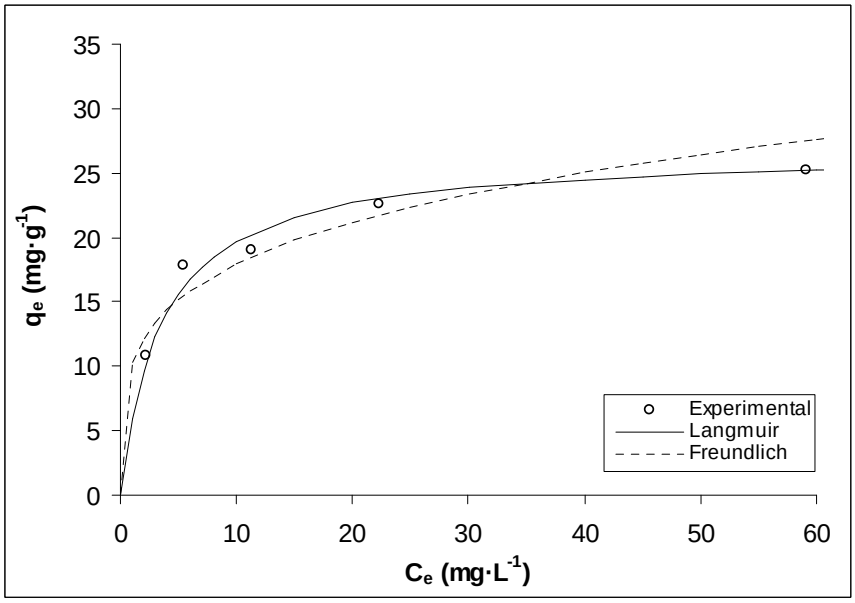

Figure 20: Nickel sorption isotherm in continuous. Symbols represent the experimental results and in lines, the prediction of Langmuir and Freundlich models.

As it can be seen in these figures, a better description of the experimental continuous bed up-flow equilibrium sorption results is obtained by means of the Langmuir model.

Table 15: Comparison of Langmuir and Freundlich parameters for the adsorption of Cu(II) and Ni(II) in batch and in continuous mode. B: Batch; C: Continuous.

		Langmuir model			Freundlich model		
Metal	**Operation**	$q_{max.}$ (mg·g^{-1})	K_L (L·mg^{-1})	R^2	K_F	1/n	R^2
Cu	B	42.92	0.0283	0.9477	1.48	0.73	0.9570
	C	31.70	0.1993	0.9972	7,68	0.38	0,9760
Ni	B	38.31	0.0302	0.9793	1.38	0.73	0.9319
	C	26.65	0.2845	0.9991	10.27	0.24	0.8851

As it can be seen in this table, for a given metal, higher K_L and lower 1/n values were obtained when comparing the batch and continuous operation, indicating that, for both metals, the continuous flow process is more favourable than the batch one. Despite of this, the prediction of Langmuir model provides a higher capacity in the case of batch than in continuous operation. This can be explained if experimental isotherms obtained in both operation modes are compared. In the next figures, experimental batch and column isotherms for Cu(II) and Ni(II) sorption onto GS have been presented.

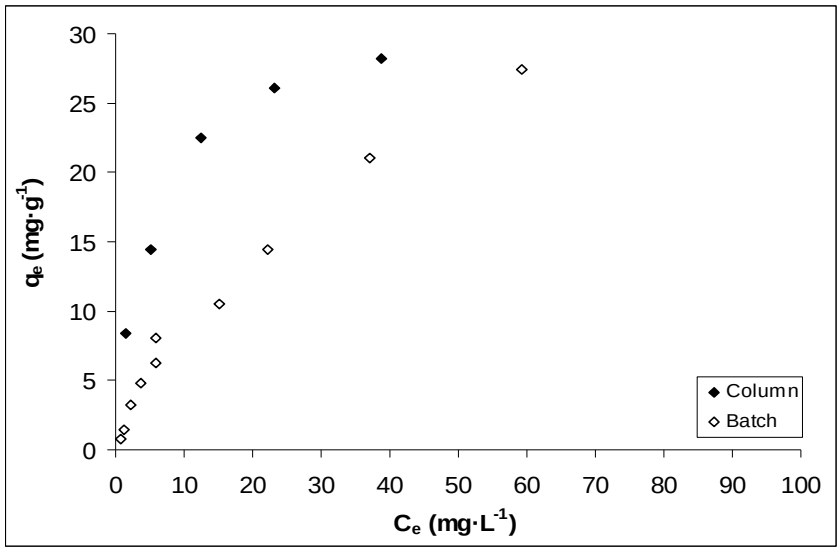

Figure 21: Column and batch experimental Cu(II) sorption isotherm onto GS.

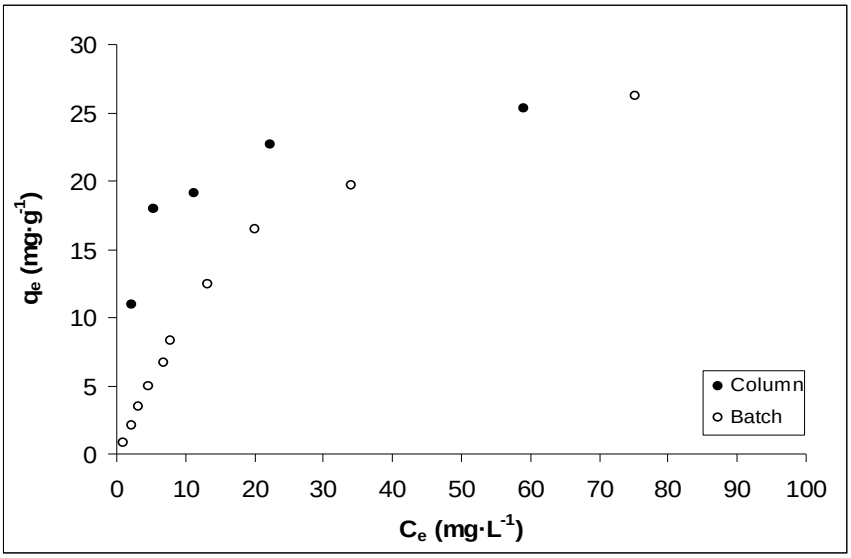

Figure 22: Column and batch experimental Ni(II) sorption isotherm onto GS.

As it can be seen in **Figures 21** and **22**, while column sorption isotherms seem to reach plateau for both Cu(II) and Ni(II) at the higher equilibrium metal concentrations, in the case of batch isotherms, the equilibrium seems not to have been reached, and when Langmuir model extrapolates to obtain maximum sorption capacity, this parameter is overestimated. On the other hand, these plots allow us to compare the different sorption capacities achieved for a given equilibrium concentration in the liquid phase for both, batch and contiuous operation. As it can be observed in the figures, for both metals at the lowest concentrations, always the capacity observed in the continuous bed up-flow operation is higher than the obtained in batch, so that, for the low concentration range, column process appears as much more efficient than batch. This phenomena of higher adsorption in continuous flow processes than in batch has been previously reported for different sorbents such as: *Pinus radiata* bark (Palma *et al.* 2003), peat (Gabaldón *et al.* 2006), activated carbon (Gabaldón *et al.* 2000), and Sasafras soils (Clancy and Jennings, 1988). Clancy and Jennings reported that "sorption parameters measured under static conditions underestimated the attenuation capacities observed during dynamic transport". At the high sorbent-to-solution ratios of column environments, specific interactions between solutes and sorbent result in higher removal capacities than those obtained in batch tests.

5.5.2. Desorption experiments

In order to apply the sorption process to real wastewater, regeneration of the sorbent is important for economic reasons. The overall recovery depends on the efficiency of the metal elution.

In the literature several different types of eluent agents have been reported (Atdor *et al.*, 1995; Ahuja *et al*., 1999; Zhou *et al*., 1998; Hammaini *et al*., 2007), mainly organic and inorganic acids solutions and complexing agents (Gong *et al*., 2005; Hashim *et al*., 2000). Despite many author use EDTA as eluting agent, its strong complexation capacity on divalent metallic ions would make difficult its subsequent recovery, as it has been demonstrated in the present chapter. So that, in this section, hydrochloric acid was chosen because it would provide the H^+ needed to replace the heavy metal from the basic-nature coordingation position of the sorbent. Also, the Cl^- added as counterion of the acid does not provoke precipitation of neither Cu(II) nor Ni(II), and also provides a weak complexation of them that facilitates its elution.

In **Figures 23** and **24**, desorption profile for Cu(II) and Ni(II) for the different initial feeding metal concentrations is presented.

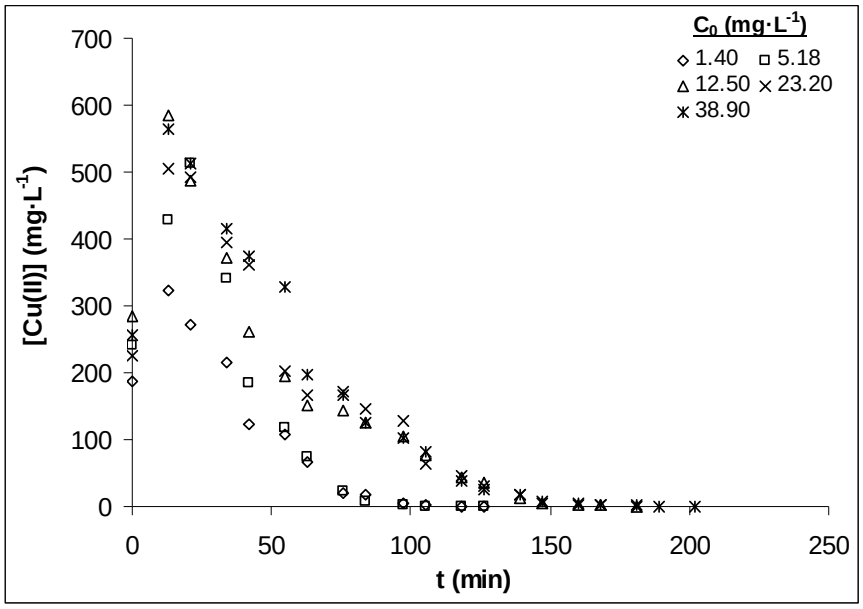

Figure 23: Desorption profile of Cu(II) from a GS packed bed up-flow column by feeding 0.05 M HCl.

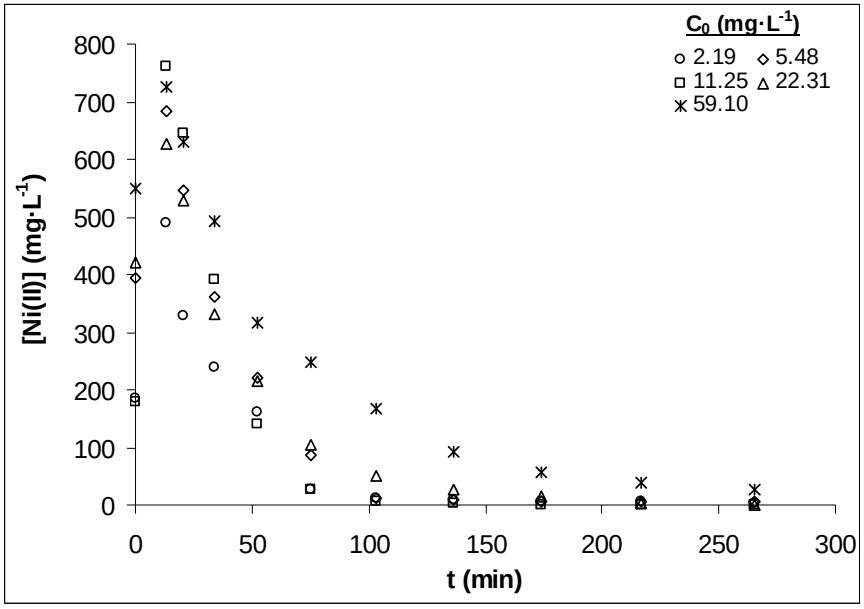

Figure 24: Desorption profile of Ni(II) from a GS packed bed up-flow column by feeding 0.05 M HCl.

As it can be seen in these figures, metal desorption profiles exhibited a sharp increase of metal concentration in solution, reaching a maximum in all the cases after approximately 13 minutes. The maximum concentration values ranged from 583.6 to 323.4 $mg \cdot L^{-1}$ for Cu(II) and from 761.8 to 489.5 $mg \cdot L^{-1}$ for Ni(II); the lowest values corresponding to desorption from the sorbent loaded with the lowest feeding metal concentration.

The total amount of eluted metal during desorption was calculated and compared to the capacitiy values obtained in the sorption process and so, recovery efficiencies could be calculated. The obtained results are presented in **Table 16**.

Table 16: Cu(II) and Ni(II) sorbed and desorbed amount and recuperation percentage obtained for the different feeding metal concentrations.

Metal	C_0 (mg·L^{-1})	Sorbed amount (mg)	Desorbed amount (mg)	Recuperation %
Cu(II)	1.40	6.47	7.05	108.90
	5.18	9.87	10.83	109.70
	12.50	15.83	15.15	95.69
	23.20	16.42	15.52	94.49
	38.90	17.27	16.58	95.97
Ni(II)	2.19	7.71	7.54	97.87
	5.48	12.81	12.24	95.58
	11.25	11.13	11.75	103.14
	22.31	12.91	12.58	97.34
	59.10	15.31	14.83	96.89

The table demonstrates an excellent desorption performance. For the whole experimental set, metal recovery efficiency has been higher than 97%.

On the other hand, it has to be remarked that by application of this technology, great values of preconcentration factors can be achieved for the lowest feeding metal concentrations. In the case of both, Cu(II) and Ni(II), a volume of approximately 2.4 L could be treated under discharge limit, as seen above. As shown in desorption figures, for this feeding metal concentration, desorption is finished after 100 minutes of process, when only 50 mL have been eluted from the column. According to these values, a preconcentration ratio about 50 can be obtained by this process for the lowest feeding metal concentration.

Once analysed the effect of initial metal concentration in column sorption behaviour, in a further step, the effect of different EDTA concentration in single Cu(II) and Ni(II) sorption in a continuous bed up-flow system was evaluated. The results obtained are presented in the next section.

5.5.3. Effect of EDTA in Cu(II) and Ni(II) sorption

In order to evaluate metal sorption behaviour of GS in a continuous flow process in presence of complexing agent EDTA, column experiments at different Metal:EDTA mass ratio were carried out. Breakthrough curves obtained in absence of complexing agent and in presence of two different Metal:EDTA ratios for Cu(II) and Ni(II) sorption onto GS are presented in **Figures 25** and **26** respectively.

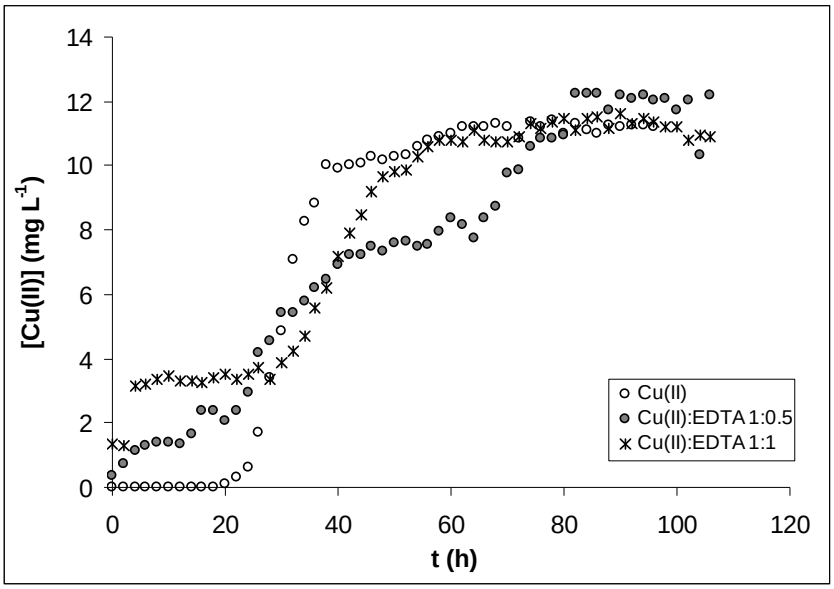

Figure 25: Breakthrough curves for the adsorption of Cu(II) onto GS in a packed bed up-flow column in absence and in presence of EDTA. Feeding Cu(II) solution concentration: 12.50 mg·L^{-1}.

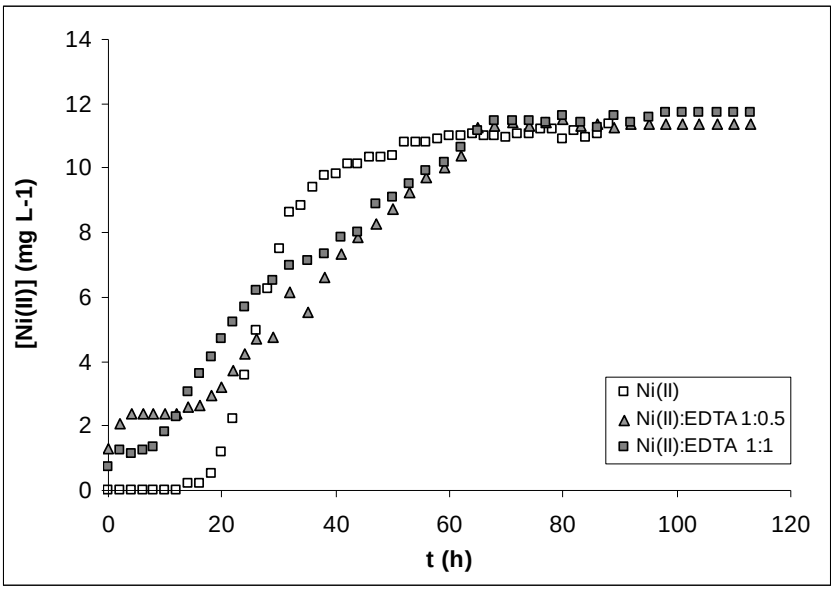

Figure 26: Breakthrough curves for the adsorption of Ni(II) onto GS in a packed bed up-flow column in absence and in presence of EDTA. Feeding Ni(II) solution concentration: 11.74 $mg \cdot L^{-1}$.

In these two figures it can be observed that when feeding the column with single copper or nickel solutions, no metal was detected in the outlet effluent during the first 22 h in the case of Cu(II), and 18 h in the case of Ni(II). By applying the mass balances to the breakthrough curves, capacity values of 22.52 and 19.05 $mg \cdot g^{-1}$ were obtained for copper and nickel, respectively, being these results almost two folds higher than the sorption capacities obtained at equilibrium in batch experiments (11.94 and 10.03 $mg \cdot g^{-1}$).

When metals were in presence of complexing agent EDTA, a constant metal concentration in the effluent was detected during approximately the first 18 and 10 h for copper and nickel, respectively. As can be seen, this initial eluted metal concentration increased when increasing the EDTA concentration. This fact suggests that this eluted metal concentration could correspond to the complexed metal fraction, not adsorbed on the GS.

The experimental values along with the theoretical concentration of the complexed metal calculated by using the MEDUSA computer program are summarized in **Table 17**.

Table 17: Theoretical and eluted experimental concentration in the initial zone of the breakthrough curves for Cu(II) and Ni(II) adsorption onto GS in presence of EDTA. Feeding Cu(II) solution concentration: 12.50 $mg \cdot L^{-1}$. Feeding Ni(II) solution concentration: 11.74 $mg \cdot L^{-1}$.

Metal	[EDTA] ($mg \cdot L^{-1}$)	Theoretical complexed metal concentration ($mg \cdot L^{-1}$)	Effluent concentration in the first hours of operation ($mg \cdot L^{-1}$)
Cu	6.25	1.37	1.38
	12.50	2.87	3.15
Ni	5.87	1.12	1.16
	11.74	2.46	2.40

The good agreement between experimental and theoretical concentration values suggests that species derived from metal complexation were not adsorbed on the GS. These results, confirm that only free metal cation of Cu(II) and Ni(II) were adsorbed onto GS.

During the development of this section, devoted to the study of Cu(II) and Ni(II) sorption in a continuous bed up-flow process, valuable information about the effect of feeding metal concentration and of presence of complexing agent in single monometallic solutions had been obtained and discussed. Nevertheless, no information about the possible interactions in the simultaneous sorption of these two metals and the effect that the complexing agent could provoke on it was obtained. To obtain this information, in the next section, metal sorption from a binary Cu(II)/Ni(II) mixture and the effect of EDTA on the simultaneous sorption of these two metals will be studied.

5.5.4. Effect of EDTA in binary equimolar Cu(II)/Ni(II) mixtures

In real wastewater effluents, i.e. from different electroplating operations, it is possible the coexistence of more than one metal in presence also of complexing agent. That's why in this section, attention will be paid to the effect of complexing agent EDTA in the simultaneous Cu(II) and Ni(II) sorption from binary mixtures onto GS.

In the next figures, metal concentration in solution and in the solid phase as a function of time is shown for Cu(II) (**Figure 27**) and Ni(II) (**Figure 28**). Experiments were carried out in absence of complexing agent and in presence of two different concentrations of EDTA.

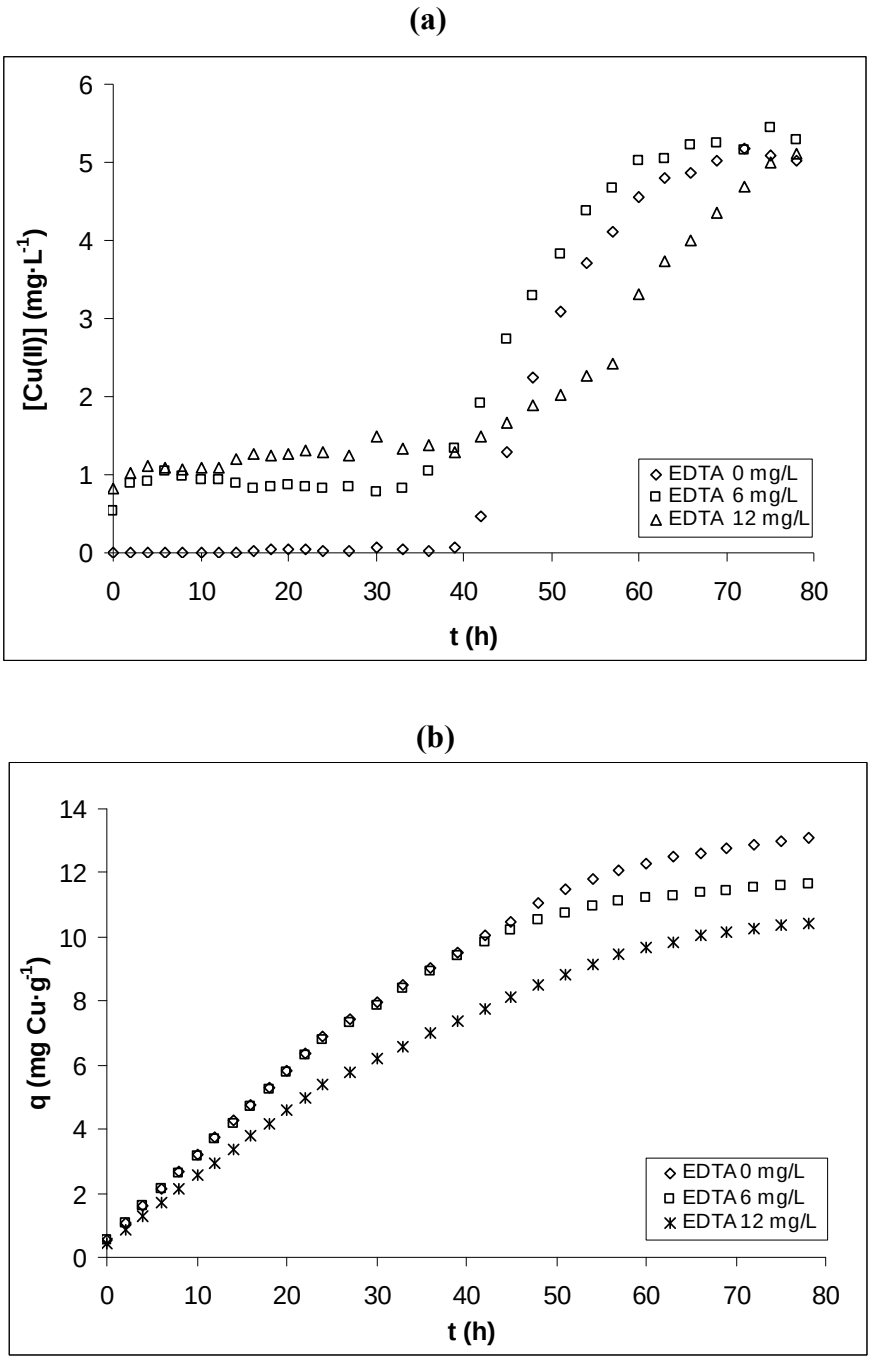

Figure 27: Breakthrough curves (a) and capacity evolution as a function of time (b) for the adsorption of Cu(II) onto GS in a packed bed up-flow column in a binary equimolar Cu(II)/Ni(II) mixture in absence and in presence of EDTA. Feeding Cu(II) concentration: 6 $mg \cdot L^{-1}$. Feeding Ni(II) concentration: 6 $mg \cdot L^{-1}$.

As shown in this figure, the same trend as in the case of single Cu(II) solution in presence of EDTA is observed. From the beginning of the process, an eluted metal concentration corresponding to the complexed metal fraction is observed.

When a mass balance is applied to the sorption process, Cu(II) sorbed amount as a function of time can be obtained and results are presented in **Figure 27 (b)**. As it demonstrates this figure, when increasing EDTA concentration in solution the slope of this plot decreases, indicating thus a slower Cu(II) mass transfer rate from the liquid to the solid phase. As a very important driving force of the sorption process is the effective sorbate concentration in solution, the mass transfer rate decrease observed can be explained by the lower concentration of Cu(II) cationic species in solution when increasing EDTA concentration. Furthermore, from this plots, equilibrium capacity for each sorption scenario can be obtained. In the case of Cu(II), the capacity of the material for the fixed initial metal concentration of 6 ppm decreases from 13.09 to 10.42 $mg \cdot g^{-1}$ respectively for solutions without EDTA and for the highest complexing agent concentration (12 $mg \cdot L^{-1}$).

In the solutions eluted from the column, Ni(II) concentration was also analysed and results of metal concentration in liquid and in solid phase as a function of time are presented in **Figure 28 (a)** and **(b)** respectively.

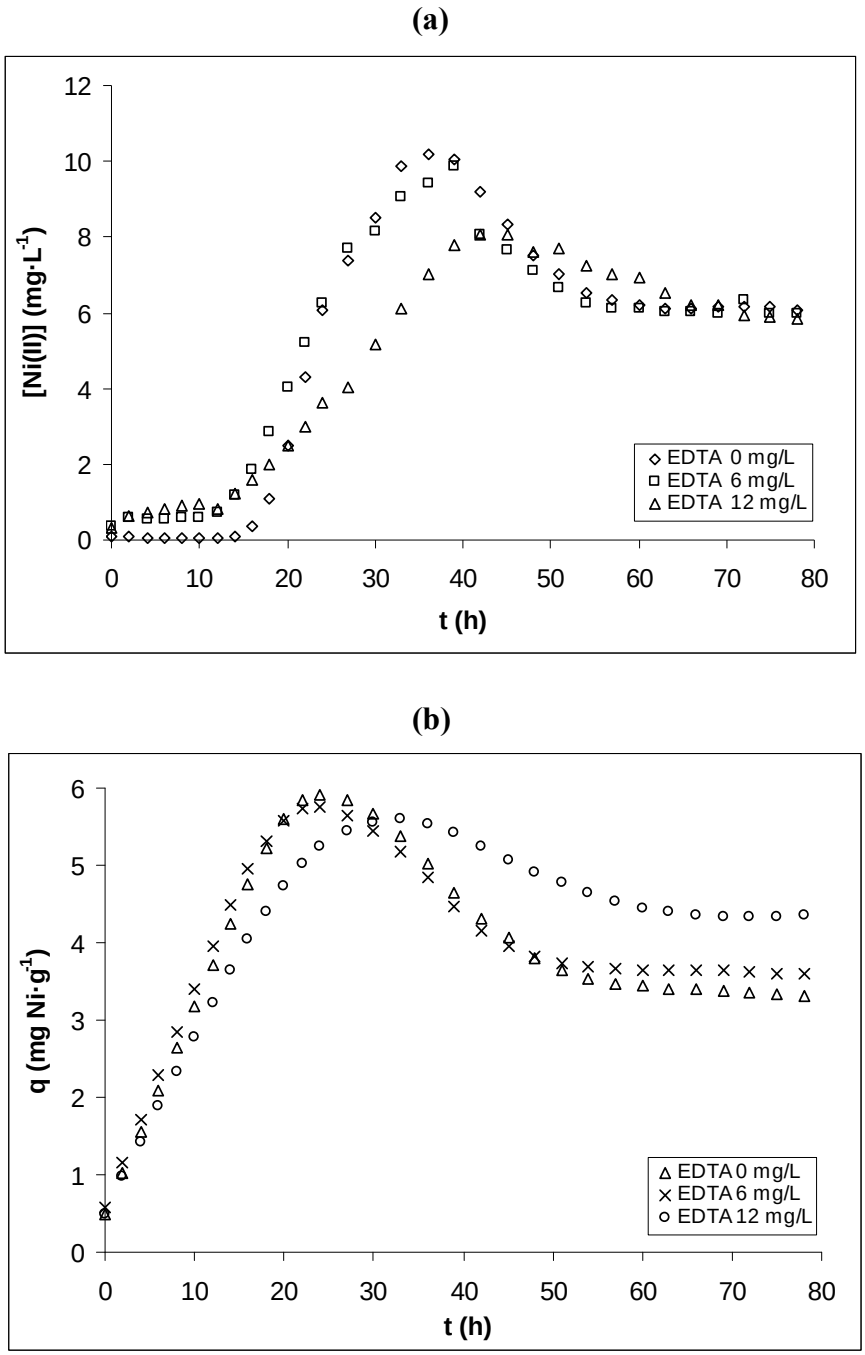

Figure 28: Breakthrough curves (a) and capacity evolution as a function of time (b) for the adsorption of Ni(II) onto GS in a packed bed up-flow column in a binary equimolar Cu(II)/Ni(II) mixture in absence and in presence of EDTA. Feeding Cu(II) solution concentration: 6 $mg \cdot L^{-1}$. Feeding Ni(II) solution concentration: 6 $mg \cdot L^{-1}$.

In **Figures 27** and **28** two important observations must be pointed out: first, the observation of an overconcentration in the outlet flow (overshoot) and second, the decrease of this overconcentration when EDTA concentration is increased in the feeding effluent of the binary metal mixture.

As in the case of Cu(II), in solutions containing EDTA, from the beginning of the process, a non-adsorbed Ni(II) concentration, higher as higher was the complexing agent concentration in the feeding solution, was observed. As discussed previously, this sorption-inert fraction can be attributed to the presence of complex Ni(II)-EDTA species with neutral or anionic charge that are not efficiently adsorbed by GS.

The presence of overshoots when studying metal sorption on multimetal solutions has been previously reported by several authors. An overshoot occurs when the concentration of a species in a downstream plateau is higher than in the adjacent upstream plateau. The condition under which overshoots takes place can be formulated as follows: low-affinity species present in the feed overshoot in the column effluent only if the species with the highest affinity in the feed is bound to the biosorbent more strongly than the species with which the biosorbent had been presaturated (Volesky, 2003).

The compounds may mutually enhance sorption, act relatively independently or may interfere with one another. The degree of mutual inhibition of competing sorbates should be related to the relative size of the molecules being adsorbed, to the relative affinities and to the concentration of the sorbates (Volesky, 2003).

In our case, as Cu(II) and Ni(II) concentrations in the inlet flow is equal, no effects due to higher concentration of one of the compounds would explain this fact. The concentration overshoot that Cu(II) produces on Ni(II) sorption in solutions without complexing agent must be due to a higher affinity of the sorbent through Cu(II). In a first step both metals would fix to the sorbent surface, but on its advance through the column Cu(II) would displace Ni(II) from its coordination position. This desorbed Ni(II) would increase feeding solution concentration leading to the increase of around 4 $mg \cdot L^{-1}$ on the outlet effluent observed in the maximum of the overshoot produced by Cu(II) in absence of complexing agent EDTA.

This hypothesis will be further studied and discussed in the chapter of multimetal sorption by checking the energies and affinities of the sorption process of different metals onto GS.

In any case, it's clear that an increase of EDTA concentration in the bimetal mixture produces a decrease of the Ni(II) overshoot as observed in the plot of both, Ni(II) concentration in solution and in solid phase as a function of time and a increase of the equilibrium sorbed concentration, as shown in the plot of solid phase concentration as a function of time.

In the case of Ni(II), in contrast with Cu(II), maximum capacity in the binary mixture is positively affected by the presence of complexing agent EDTA. Ni(II), capacity of the material for a fixed initial metal concentration of 6 ppm increases from 3.31 to 4.35 $mg \cdot g^{-1}$ for solutions without EDTA and with a complexing agent concentration of 12 $mg \cdot L^{-1}$ respectively.

To discuss this effect, information about Cu(II) and Ni(II) EDTA complex formation becomes necessary. So that, simulation of Cu(II) and Ni(II) speciation in the binary equimolar solution in absence of EDTA and in presence of the two complexing agent concentrations studied was carried out by means of MEDUSA computer program. Speciation diagrams for Cu(II) and Ni(II) are shown respectively in **Figures 29** and **30**.

Figure 29: Cu(II) speciation as a function of pH and EDTA concentration. [Cu(II)]= 6 mg·L^{-1}. [EDTA] varied within 0 to 12 mg·L^{-1}.

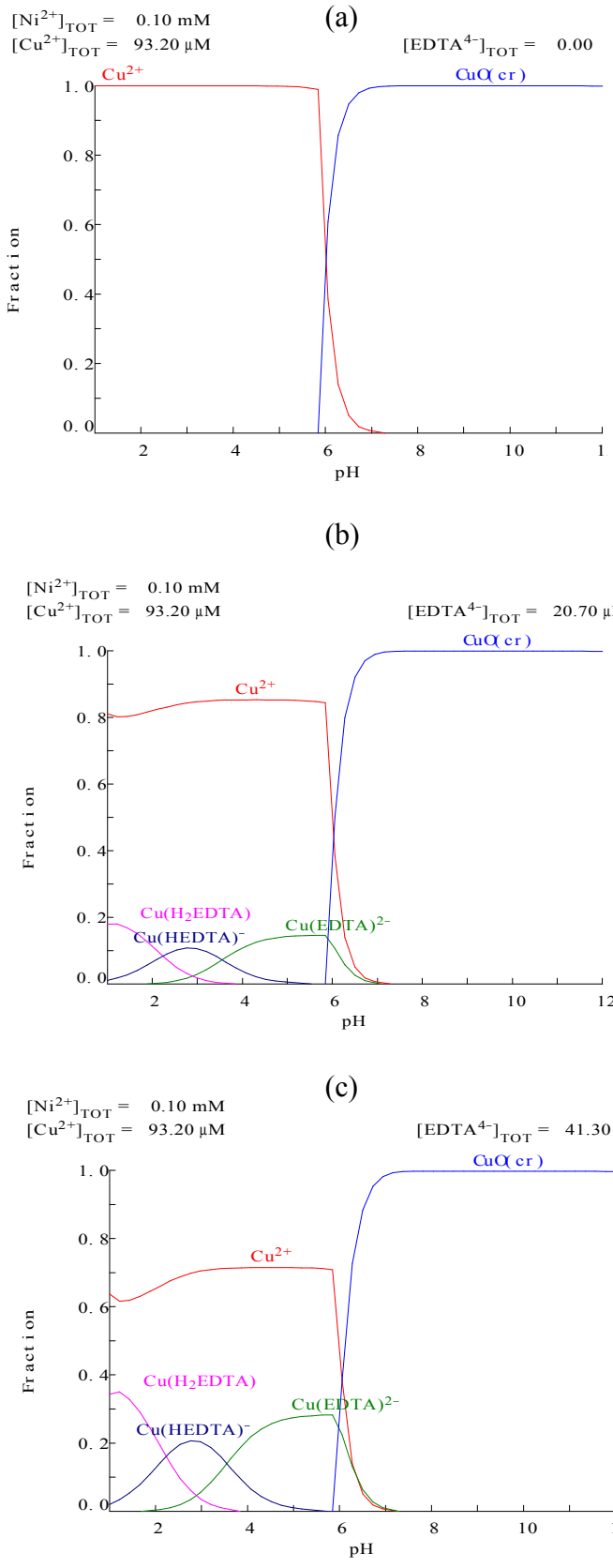

Figure 30: Ni(II) speciation as a function of pH and EDTA concentration. [Ni(II)]= 6 mg·L^{-1}. [EDTA] varied within 0 to 12 mg·L^{-1}.

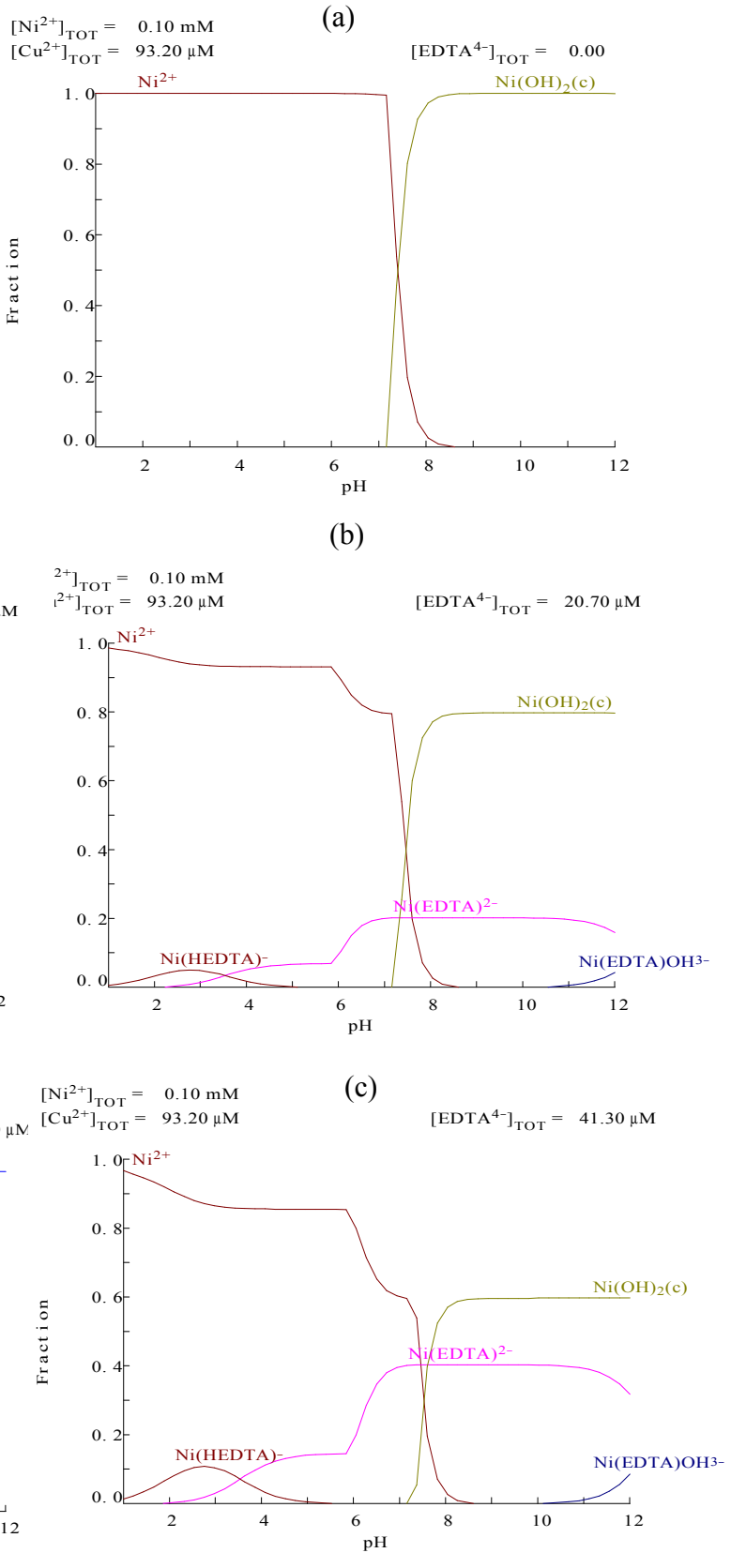

As it can be seen in the figures, when metals are present in solution without EDTA, at pH< 6 in the case of Cu and pH< 7.2 in the case of Ni, both metals are present as divalent free cations Cu^{2+} and Ni^{2+}. No formation of hydroxocomplexes is observed in the experimental conditions of this study. From these pHs, precipitation of metal hydroxides takes place.

When EDTA is present in solution, complex Metal:EDTA species are formed, decreasing thus the concentration of the free cation. The charge of the complex species is strongly pH dependent, varying from neutral to mono- and dianionic, but, in any case, non-cationic complexes with EDTA are formed. As it had been discussed previously, only positively charged copper and nickel species are effectively sorbed onto GS, so that the complex species of these metals would be not adsorbed onto the material. When comparing Cu(II) and Ni(II) complexed metal fraction in the bimetal mixture, it can be observed that, for a given EDTA concentration in solution, always free Cu^{2+} concentration in solution is much more affected that Ni^{2+}, as expected by the higher formation constants of EDTA complexes with copper than with nickel. While in the case, for instance, of EDTA concentration of around 21 μM and a pH around 5 the 95% of nickel is present on its free divalent form, only a 85% of copper is present as Cu^{2+} (**Figures 29(b)** and **30(b)**). If Cu^{2+} showed a higher affinity for GS than Ni^{2+}, and this would be the explanation of the Ni(II) concentration overshoot observed, a decrease in the free copper concentration in solution, joined to a preferably coordination of EDTA with Cu(II) than with Ni(II) would explain the increase of nickel sorption in presence of increasing concentrations of complexing agent.

6. CONCLUSIONS

Cu(II) and Ni(II) sorption onto grape stalk and exhausted coffee wastes is strongly pH dependent and maximum sorption capacity is achieved for pHs higher than 5.5 onto both sorbents. Complexing agent EDTA negatively affects the sorption capacity of both sorbents because of the formation of neutral or anionic complexes (according to the solution pH) with both, Cu(II) and Ni(II). In presence of complexing agent, only the cationic free metal (non-complexed fraction) remains as a sorption-active form. Total sorption inhibition for both sorbents is observed when EDTA is present in the media at equimolar or higher EDTA:Metal ratios.

Despite the capacity of both sorbents materials is dramatically affected by the presence of complexing agent, the rate at which the sorbent-sorbate systems reach equilibrium is not so affected. Cu(II) and Ni(II) sorption kinetics onto GS and EC is extremely fast, reaching equilibrium in about 1 hour. In general, nickel sorption is faster than copper.

Cu(II) and Ni(II) sorption kinetics onto both GS and EC can be successfully described with a pseudo-second order expression. The values of the pseudo-second order constants pointed out that sorption rate is not strongly affected by the presence of EDTA but increases when increasing the sorbent dose.

Both Langmuir and Freundlich sorption equilibrium models provide a successful description of the batch equilibrium data. Grape stalk shows a higher uptake capacity for copper and nickel than exhausted coffee in absence and presence of EDTA. Nevetheless, exhausted coffee capacity is less affected by the presence of the complexing agent. Exhausted coffee shows a higher affinity than grape stalk for Cu(II) and Ni(II) ions in presence and in absence of complexing agent EDTA.

Column experiments carried out in single metal solutions in presence and in absence of EDTA indicate that grape stalk is an efficient sorbent of the free Cu^{2+} and Ni^{2+} species. Column experiments carried out with five different feeding metal concentrations allowed to generate the continuous sorption isotherms and compare it with the obtained in batch. Results indicated that for the lowest feeding concentrations, sorption capacities in continuous mode are higher than the observed in batch.

The sorption equilibrium results obtained in continuous can be successfully modelled according to Langmuir and Freundlich equations. For a given metal, higher K_L and lower

1/n values are obtained in continuous mode than in batch indicating thus that, for both metals, the continuous flow process is more favourable than the batch one. Despite of this, the prediction of Langmuir model provides a higher capacity in the case of batch than in the case of column operation.

In presence of EDTA, the column effluent presented metal leakage from the beginning of the operation. The metal eluted from the beginning of the process corresponds to the complexed fraction. In column also, only the free metal cation is adsorbed onto grape stalk.

Cu(II) and Ni(II) sorption onto grape stalk in a continuous flow process in a binary equimolar mixture and in absence of EDTA demonstrates that these two metal compete in sorption. While Cu(II) is continuously sorbed, Ni(II) is partially replaced from its original coordinating positions by Cu(II), leading to an overconcentration of Ni(II) in the outlet effluent of the column (overshoot). In presence of EDTA, the magnitude of nickel overconcentration in the outlet effluent decreases and a higher amount of this metal is adsorbed at equilibrium, in detrimental of the copper sorbed amount. The stronger EDTA complexation towards Cu(II) reduces its free cation concentration and so, less nickel is replaced from the sorbent.

After the continuous bed up-flow sorption process, the metal sorbed can be rapid and quantitatively recovered in a very concentrated form by treating the biomaterial in mild acidic conditions (HCl 0.05M).

7. REFERENCES

· Ahuja, P., Gupta, R., Saxena, R.X., Sorption and desorption of cobalt by *Oscilatoria anguistissima*. Current Microbiol. 39 (1999) 49–52.

· Aksu, Z., Determination of the equilibrium, kinetic and thermodynamic parameters of the batch biosorption of nickel(II) ions onto Chlorella vulgaris. Process Biochem. 38 (2002) 89-99.

· Alder AC, Siegrist H, Gujer W, Giger W Behaviour of NTA and EDTA in biological wastewater treatment. Water Res. 24 (1990) 733-742

· Atdor, I., Fourest, E., Volesky, B., Desorption of cadmium from algal biosorbent. Can. J. Chem. Eng., 73 (1995) 516–522.

· Babel, S., Kurniawan, T.A., Low-cost adsorbents for heavy metals uptake from contaminated water: a review, J. Hazard. Mater. 97 (2003) 219-243.

· Bertocchi, A.F., Ghiani, M., Peretti, R., Zucca, A., Red mud and fly ash for remediation of mine sites contaminated with As, Cd, Cu, Pb and Zn, J. Hazard. Mater. 134 (2006) 112-119.

· Bolton, H., Li, S.W., Workman, D.J., Girvin, D.C., Biodegradation of synthetic chelates in subsurface sediments from the southeast coastal plain. J. Environ. Qual. 22 (1993) 125-132

· Bourika, K., Vakros, J., Kordulis, C., Lycourghiotis, A., Potentiometric mass titrations: experimental and theoretical establishment of a new technique for determining the point of zero charge (PZC) of metal hydroxides, J. Phys. Chem. B, 107 (2003) 9441-9451.

· Brown, P.A., Gill, S.A., Allen, J., Metal removal from wastewater using peat, Water Res. 34 (2000) 3907-3916.

· Chen, J.P., Wu, S., Study on EDTA-chelated copper adsorption by granular activated carbon, J. Chem. Technol. Biotechnol. 75 (2000) 791-797.

· Chu, K.H., Hashim, M.A., Adsorption of copper(II) and EDTA-chelated copper(II) onto granular activated carbons, J. Chem. Technol. Biotechnol. 75 (2000) 1054-1060.

· Clancy, K.M., Jennings, A.A., Experimental verification of multicomponent groundwater contamination predictions, Water Resour. Bull. 24 (1988) 307-316.

· Directive 2006/11/EC of the European Parliament and of the Council of 15 February 2006 on pollution caused by certain dangerous substances discharged into the aquatic environment of the Community. Official Journal of the European Union, 4.3.2006.

· Directive 98/83/EC of 3 November 1998 on the quality of water intended for human consumption. Official Journal of the European Union, 5.12.98.

· Englehardt, J.D., Meeroff, D.E., Echegoyen, L., Deng, Y., Raymo, F.R., Shibata, T., Oxidation of aqueous EDTA and associated organics and coprecipitation of inorganics by ambient iron-mediated aeration, Environ. Sci. Technol. 41 (2007) 270-276.

· Fiol, N., Villaescusa, I., Martínez, M., Miralles, N., Poch, J., Serasols, J., Sorption of Pb(II), Ni(II), Cu(II) and Cd(II) from aqueous solution by olive stone waste, Sep. Purif. Technol. 50 (2006) 132-140.

· Fiol, N., Villaescusa, I., Determination of sorbent point zero charge: usefulness in sorption studies, Environ. Chem. Lett. DOI 10.1007/s10311-008-0139-0.

· Gabaldón, C., Izquierdo, M., Martin, M., Marzal, P., Fixed-bed removal of free and complexed Ni from synthetic and industrial aqueous solutions, Sep. Sci. Technol. 43 (2008) 1157-1173.

· Gabaldón, C., Izquierdo, M., Marzal, P., Sempere, F., Evaluation of biosorbents for Cu removal from wastewater in the presence of EDTA, J. Chem. Technol. Biotechnol. 82 (2007) 888-897.

· Gabaldón, C., Marzal, P., Alvarez-Hornos, J., Modelling Cd(II) removal from aqueous solutions by adsorption on a highly mineralized peat. Batch and fixed-bed column experiments, J. Chem. Technol. Biotechnol. 81 (2006) 1107-1112.

· Gabaldón, C., Marzal, P., Seco, A., Gonzalez J.A., Cadmium and copper removal by a granular activated carbon in laboratory column systems, Sep. Sci. Technol. 35 (2000) 1039-1053.

· Gilbert, E.; Hoffmann-Glewe, S. Ozonation of ethylenediaminetetraacetic acid (EDTA) in aqueous-solution, influence of pH value and metal-ions. Water Res. 1990, 24, 39-44.

· Gong, R., Ding, Y., Lui, H., Chem, Q., Liu, Z., Lead biosorption and desorption by intact and pretreated *Spirula maxima* biomass. Chemosphere 58, (2005) 125–130.

· Gupta, V.K., Jain, C.K., Ali, I., Sharma, M., Saini, V.K., Removal of cadmium and nickel from wastewater using bagasse fly ash – a sugar industry waste, Water Res. 37 (2003) 4038-4044.

· Gupta, V.K., Rastogi, A., Saini, V.K., Jain, N., Biosorption of copper(II) from aqueous solutions by *Spirogyra* species, J. Colloid Interface Sci. 296 (2006) 59-63.

· Gupta, V.K., Sharma, S., Removal of cadmium and zinc from aqueous solutions using red mud, Environ. Sci. Technol. 36 (2002) 3612-3617.

· Guzmán, J., Saucedo, I., Revilla, J., Navarro, R., Guibal, E., Copper sorption by chitosan in presence of citrate ions: influence of metal speciation on sorption mechanism and uptake capacities, Int. J. Biol. Macromol. 33 (2003) 57-65.

· Gyliene, O., Nivinskiene, O., Razmute, I., Copper(II)-EDTA sorption onto chitosan and its regeneration applying electrolysis, J. Hazard. Mater. B137 (2006) 1430-1437.

· Gyliene, O., Rekertas, R., Salkauskas, M., Removal of free and complexed heavy-meta ions by sorbents produced from fly (*Musca domestica*) larva shells, Water Res. 36 (2002) 4128-4136.

· Hammaini, A., González, F., Ballester, A., Blazquez, M.L., Muñoz, J.A., Biosorption of heavy metals by activated sludge and their desorption characteristics, J. Environ. Manage. 84 (2007) 419-426.

· Hasar, H., Adsorption of nickel(II) from aqueous solution onto activated carbon prepared from almond husk, J. Hazard. Mater. B97 (2003) 49-57.

· Hashim, M.A., Tan, H.N., Chu, K.H., Immobiliced marine algal biomass for multiple cycles of copper adsorption and desorption. Sep. Purif. Technol. 19 (2000) 39–42.

· Ho, Y.S., Ng, J.C.Y., McKay, G., Kinetic of pollutant sorption by biosorbents: Review, Sep. Purif. Meth. 29 (2000) 189-232.

· Holan, Z.R., Volesky, B., Biosorption of lead and nickel by biomass of marine algae, Biotechnol. Bioeng. 43 (1994) 1001-1009.

· Kaluza, U., Klingelhöfer, P., Taeger, K., Microbial degradation of EDTA in an industrial wastewater treatment plant. Water Res. 32 2843 (1998) 2845

· Klüner, T., Hempel D.C., Nörtemann, B., Metabolism of EDTA and its metal chelates by whole cells and cell-free extracts of strain BNC1. Appl. Microbiol. Biotechnol. 49 (1998) 194-201.

· Krishnan, K.A., Sheela, A., Anirudhan, T.S., Kinetic and equilibrium modelling of liquid-phase adsorption of lead and lead chelates on activated carbons. J. Chem. Technol. Biotechnol. 78 (2003) 642-653.

· Low, K.S., Lee, C.K., Liew, S.C., Sorption of cadmium and lead from aqueous solutions by spent grain, Process. Biochem. 36 (2000) 59-64.

· Ma, W., Tobin, J.M., Development of multimetal binding model and application to binary metal biosorption onto peat biomass, Water Res. 37 (2003) 3967-3977.

· Madsen, E.L., Alexander, M., Effects of chemical speciation on the mineralization of organic compounds by microorganisms. Appl Environ Microbiol 50 (1985) 342-349

· Namasivayam, C., Ranganathan, K., Effect of organic ligands on the removal of Pb(II), Ni(II) and Cd(II) by 'waste' Fe(III)/Cr(III) hydroxide, Water Res. 32 (1998) 969-971.

· Nörtemann, B., Biodegradation of EDTA. Appl. Microbiol. Biotechnol. 51 (1999) 751-759

· Nowack, B., Kari, F.G., Kruger, H.G., The remobilization of metals from iron oxides and sediments by metal-EDTA complexes, Water, Air, Soil Pollut. 125 (2001) 243-257.

· Nowack, B., Lutzenkirchen, T., Behra, P., Sigg, L., Modeling the adsorption of metal-EDTA complexes onto oxides. Environ. Sci. Technol. 30 (1996) 2397-2405.

· Özcan, A., Özcan, A.S., Tunali, S., Akar, T., Kiran, I., Determination of the equilibrium, kinetic and thermodynamic parameters of adsorption of copper(II) ions onto seeds of *Capsicum annuum*, J. Hazard. Mater. B124 (2005) 200-208.

· Padmavathy, V., Biosorption of nickel(II) ions by baker's yeast: Kinetic, thermodynamic and desorption studies Bioresource Technol. 99 (2008) 3100–3109

· Palma, G., Freer, J., Baeza, J., Removal of heavy metal ions by modified *Pinus radiata* bark and tannins from water solutions, Water Res. 37 (2003) 4974-4980.

· Puigdomènech, I., Make Equilibrium Diagrams Using Sophisticated Algorithms (MEDUSA), software version 18 February 2004. Inorganic Chemistry Department, Royal Institute of Technology, Stockholm, Sweden.

· Real Decreto 995/2000, de 2 de junio, por el que se fijan objetivos de calidad para determinadas sustancias contaminantes y se modifica el Reglamento de Dominio Público Hidráulico, aprobado por el Real Decreto 849/1986, de 11 de abril. (Spain) Boletin Oficial del Estado Nº 189, de 09-08-1995.

· Reddad, Z., Gérente, C., Andrès, Y., Ralet, M.C., Thibault, J.P., Le Cloirec, P., Ni(II) and Cu(II) binding properties of native and modified sugar beet pulp, Carbohyd. Polym. 49 (2002) 23-31.

· Rincón, J., González, F., Ballester, A., Blázquez, M.L., Muñoz, J.A., Biosorption of heavy metals by chemically-activated alga *Fucus vesiculosus*, J. Chem. Technol. Biotechnol. 80 (2005) 1403-1407.

· Saeed, A., Akhter, M.W., Iqbal, M., Removal and recovery of heavy metals from aqueous solution using papaya wood as a new biosorbent, Sep. Purif. Technol. 45 (2005) 25-31.

· Saeed, A., Iqbal, M., Akhtar, M.W., Removal and recovery of lead(II) from single and multimetal (Cd, Cu, Ni, Zn) solutions by crop milling waste (black gram husk), J. Hazard. Mater. B117 (2005) 65-73.

· Seco, A., Gabaldón, C., Marzal, P., Aucejo, A., Effect of pH, cation concentration and sorbent concentration on cadmium and copper removal by a granular activated carbon, J. Chem. Techol. Biotechnol. 74 (1999) 911-918.

· Singh, A., Kumar, D., Gaur, J.P., Removal of Cu(II) and Pb(II) by *Pithophora edogonia*: Sorption, desorption and repeated use of the biomass, J. Hazard. Mater. 152 (2008) 1011–1019

· Stumm, W., Aquatic Chemical Kinetics; John Wiley & Sons: NewYork, 1990.

· Sun, G., Shi, W.X., Sunflower stalk as adsorbents for the removal of metal ions from wastewater, Ind. Eng. Chem. Res. 37 (1998) 1324-1328.

· Veglió, F., Beolchini, F., Prisciandaro, M., Sorption of copper by olive mill residues Water Res. 37 (2003) 4895–4903.

· Villaescusa, I., Fiol, N., Martínez, M., Miralles, N., Poch, J., Serarols, J., Removal of copper and nickel ions from aqueous solutions by grape stalk waste, Water Res. 38 (2004) 992-1002.

· Volesky, B., Sorption and Biosorption, BV Sorbex, Inc. Montreal, Canada (2003).

· Walling, C.; Kurz, M.; Schugar, H. The iron(III)-ethylenediaminetetraacetic acid peroxide system. Inorg. Chem. 9 (1970) 931-937.

· Wang, J., Chen, C., Biosorption of heavy metals by *Saccharomyces cerevisiae*: A review, Biotechnol. Adv. 24 (2006) 427-451.

· Zhou, J.L., Huang, P.L., Lin., R.G., Sorption and desorption of Cu and Cd by macroalgae and microalgae. Environ. Pollut. 101 (1998) 67–75.

Chapter 4. Cu(II), Ni(II), Pb(II) AND Cd(II) SORPTION ONTO GRAPE STALK IN SINGLE AND MULTIMETAL MIXTURES.

1. INTRODUCTION

In previous chapters, sorption onto grape stalk and exhausted coffee wastes of two of the most commonly polluting metals present in industrial wastewaters, Cu(II) and Ni(II), was studied. The effect of complexing agent EDTA in metal sorption performance was evaluated and discussed in batch and continuous mode. In literature numerous studies reporting the biosorption of metals by materials of diverse biological origin can be found, as it was discussed in chapter 3. Nevertheless most of these studies have remained limited to sorption of single species of heavy metal ions and fewer is the information concerning sorption from multimetal solutions. It has to be also taken into account that the problem of heavy metals does not only reside in the presence of themselves in single metal solutions or in presence of potential sorption inhibitors such as complexing agents, tensioactives or dewaxing agents. In most cases, more than one metal are found in water, leading to the formation of multimetal polluting effluents.

Among the few studies on multimetal biosorption, different materials of diverse origin such as algae, bacteria or different agrowastes can be found. In the first group it can be found the use of algae Gelidium for metal removal from Pb(II)/Cd(II) mixtures, (Vilar *et al*., 2007), *Sargassum* algal biosorbent (Kratochvil and Volesky, 2000; Volesky et al., 2003). Studies of multimetal sorption by bacteria biomass have been carried out by using *Pseudomonas putida* to carry out metal removal from binary Pb(II)/Cu(II), Pb(II)/Cd(II) and Pb(II)/Cu(II) mixtures, *Sphaerotilus natans* for the removal of Cu(II), Ni(II), Pb(II) and Cd(II) mixtures (Pagnanelli *et al*., 2003). Despite of the good sorption performance of these biological materials its use inevitably adds cost and complexity to the biosorption procedures, due to the drawback of the biomass culture.

The use of agrowastes for metal removal from multimetal mixtures has been also reported. In literature it can be found the use of grape stalk to remove Cu(II) and Ni(II) from binary mixtures (Villaescusa *et al*., 2004), crop milling waste for the removal of Cd(II), Cu(II), Ni(II) and Zn(II) from binary and ternary mixtures (Saeed *et al*., 2005).

The use of non-biological materials for the removal of heavy metals from multimetal mixtures has also been reported. This is the case of Cu(II), Ni(II), Cd(II) and Zn(II) sorption from binary Cu/Ni, Cu/Cd and Ni/Cd mixtures by activated carbon (Seco *et al*.,

1997) and the use of inorganic materials such as hydroxyapatite for the removal of Cd(II) Pb(II), Zn(II) and Cu(II) and soils for the removal of Cd(II), Ni(II) and Zn(II) (Antoniadis and Tsadilas, 2007). Most of the multimetal sorption studies reported in the literature were performed in batch, which cannot be extrapolated for designing an operational technology, for which the data obtained from a continuous flow system becomes absolutely necessary.

In wastewaters containing multiple metals, interactive effects appear depending on the number of metals competing for binding sites, the combination of these, the initial concentrations, the equilibrium steady state concentration of different metal ion species, limitations presented by the binding sites as well as the nature and quantity of the sorbent. In multimetal mixtures, the different nature of the metals to be adsorbed can lead thus to kinetic competition or replacement at equilibrium. This phenomenon can be explained considering a reversible reaction between metals and adsorbent sites so that, when the adsorbent in near saturation, heavy metal ions sorbed with lower affinity can be replaced by those that exhibit a higher affinity by the sorbent. When this occurs in a continuous flow process, an overconcentration in the outlet flow (overshoot) respect to the feeding solution of the metal/s uptaken with less affinity takes place (Kratochvil and Volesky, 2000). Despite column assays provide useful information about the dynamics of metal sorption in a continuous flow process and about the possible sorption competence in multimetal polluted effluents, no information about the energetic change that could give an explanation to the sorption competence between metals can be derived from these experiments. It becomes necessary thus, the obtention of parameters that could quantitatively reflect the different tendency of the metals to remain sorbed. The knowledge of sorption thermodynamics appears thus as an important tool to understand the uptake mechanism/s. In last term and since the evaluation of the heat change of the sorption process is considered as a very important parameter for reactor design, the thermodynamics of the sorption process is also of special concern, as it demonstrates the large number of studies concerning sorption thermodynamics (Özcan *et al*., 2005; Uslu and Tanyol, 2006; Ucun *et al*., 2007; Ho and Ofomaja, 2006; Aksu, 2002; Sari *et al*., 2007; Dursun, 2006; Romero-González *et al*., 2005). The study of the thermodynamic of the sorption process could be useful for the comprehension of the interactive effects of the different metals in a continuos bed up flow.

2. OBJECTIVES

The objective of this work is to investigate Cu(II), Ni(II) Pb(II) and Cd(II) uptake by grape stalk wastes in a continuous bed up-flow process. In a first step, sorption performance of the process when feeding the column with single Cu(II), Ni(II), Pb(II) and Cd(II) solutions will be studied. As it had been discussed in the introduction of the present chapter, metals can be frequently found in mixtures, leading to multimetal polluted effluents where sorption competitive effects can appear. As these sorption incompatibilities depend on the nature of the metals forming the mixture, in a second step of this study, uptake and competition effects of these metals will be evaluated in all the binary and ternary possible combinations of these four metals. In a final step, sorption and desorption performance of grape stalk when facing a quaternary Cu(II), Ni(II), Pb(II) and Cd(II) mixture will be evaluated. By means of this study, the possible sorption incompatibilities of the metals will be ascertained.

To give an explanation to sorption competition observed in multimetal mixtures, affinity and strength of the interaction between the grape stalk and the different metals will be evaluated. To obtain this information, sorption equilibrium experiments at different temperatures will be carried out and modeled to obtain the characteristic thermodynamic parameters of the different sorptive systems. The evaluation of the characteristic sorption parameters and its thermal variation for the individual metal-sorbent systems will provide us of useful information of both, the kind and strength of the interaction and also of the global spontaneity of the sorption process. In last term, this study will also allow us to ascertain the effect of temperature on the capacity of the material for the different metals.

3. MATERIALS AND METHODS

3.1. Reagents

To prepare copper, nickel, lead and cadmium solutions:

- $CuCl_2 \cdot 2H_2O$ Panreac
- $NiCl_2 \cdot 6H_2O$ Panreac
- $PbCl_2$ Panreac
- $CdCl_2 \cdot 2 \cdot 1/2H_2O$ Panreac
- Milli-Q water

Sorbents:

- Grape stalk coming from a wine producer from Castilla La Mancha region.

For pH adjustment:

- HNO_3 (67%) Panreac
- NaOH in pellets Panreac

Standard solutions for Flame Atomic/Emission Spectroscopy calibration:

- $Cu(NO_3)_2 \cdot 3H_2O$ in HNO_3 0.5 N (1000 mg/L) Panreac
- $Ni(NO_3)_2 \cdot 6H_2O$ in HNO_3 0.5 N (1000 mg/L) Panreac
- $Pb(NO_3)_2$ in HNO_3 0.5 N (1000 mg/L) Panreac
- $Cd(NO_3)_2 \cdot 4H_2O$ in HNO_3 0.5 N (1000 mg/L) Panreac

3.2. Material

General laboratory material

25 mL volume glass tubs with cap

Cellulose filters

Oven (P Selecta)

Rotary shaker (Stuart Stientific)

Peristaltic pump (Gilson Minipuls 3)

Peristaltic pump tubes Tygon R-3603
Chronometers (Berlabo, SA)
pHmeter PHM 250 (Meterlab)
Analytical balance (Cobos precision, J. Touron, SA)
Sieves
Cooled incubator-compressor type (ICP-500, Memmert)
Thermometers
Vortex (Velp Scientifica $2x^3$)
Coffee grinder (Taurus MS 50)
Fraction collector (Gilson, FC203B)
Column 100x10 mm (Omnifit)
Multicolumn head adapter (Omnifit)

3.3. Equipment

· Flame Atomic Absorption/Emission Spectrophotometer Varian SpectrAA 220FS with automatic dilutor Varian SIPS and autosampler Varian SPS3.

4. METHODOLOGY

4.1. Grape stalk preparation

Grape stalk wastes generated in a wine production industry were kindly supplied by a wine manufacturer (Cuenca, Spain). The material was washed with distilled water, cut in small pieces, dried and ground. Then, it was sieved for a particle size of 0.25-0.50 mm.

4.2. Column experiments

Fixed bed sorption experiments were carried out in glass columns of 10 cm length and 1.0 cm inner diameter.

Columns were packed with approximately 0.5 g of 0.25-0.5 mm particle size grape stalk, providing a bed height about 6.7 cm. The sorbent was previously rinsed with water until no leaching of coloured compounds was observed. The sorption operation was carried out in the up-flow mode to avoid possible short-circuiting by clogging and channelling.

The solutions were pumped at room temperature (20±1ºC) upwards the grape stalk packed column by a peristaltic pump at a flow rate of approximately 30 $mL \cdot h^{-1}$. By using an automatic fraction collector (Gilson FC 203B), samples of approximately 5.5 mL were collected at different times. The experimental set-up is presented in the **Figure 1**.

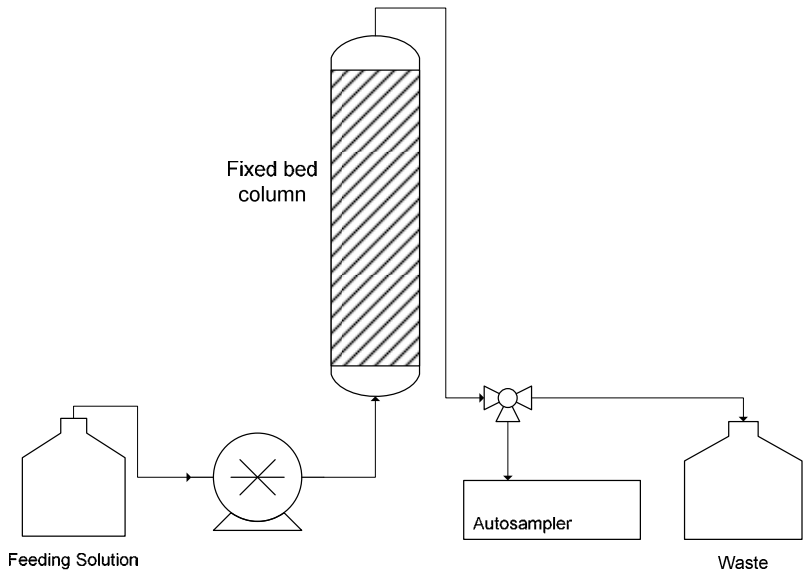

Figure 1: Experimental set up of the operating continuous flow sorption column.

Once the samples were collected, they were acidified and metal concentration in solution was determined by FAAS. The amount of metal sorbed was calculated according to the methodology described in section 4.5 of chapter 3.

4.2.1. Single metal uptake

Grape stalk sorption behaviour in single Cu(II), Ni(II), Pb(II) and Cd(II) solutions was evaluated. The feeding metal solutions concentration was around 0.2 mM. Initial pH was adjusted to 5.20 and the automatic fraction collector was programmed to carry out the sampling each hour.

4.2.2. Binary mixtures uptake

Grape stalk sorption behaviour in binary equimolar Cu(II)/Ni(II), Cu(II)/Cd(II), Cu(II)/Pb(II), Ni(II)/Pb(II), Ni(II)/Cd(II), Pb(II)/Cd(II) solutions was evaluated. The metal solutions contained an approximated 0.2 mM concentration of each one of the two metals. Initial pH of the feeding solutions for all the binary mixtures, was adjusted to 5.20 and the automatic fraction collector was programmed to carry out the sampling each 30 minutes.

4.2.3. Ternary mixtures uptake

Grape stalk sorption behaviour in ternary equimolar Cu(II)/Ni(II)/Cd(II), Cu(II)/Pb(II)/Cd(II), Pb(II)/Ni(II)/Cd(II) and Cu(II)/Pb(II)/Ni(II) solutions was evaluated. Concentration in solution was around 0.2 mM for each metal. Initial pH of the feeding solutions for all the binary mixtures, was adjusted to 5.20 and the automatic fraction collector was programmed to carry out the sampling each 30 minutes.

4.2.4. Quaternary mixtures uptake

4.2.4.1. Sorption experiments

Grape stalk sorption behaviour in a quaternary equimolar Cu(II)/Ni(II)/Pb(II)/Cd(II) mixture was evaluated. Concentration of each metal in solution was around 0.2 mM. Initial pH of the feeding solutions for all the binary mixtures, was adjusted to 5.20 and the automatic fraction collector was programmed to carry out the sampling each 30 minutes.

4.2.4.2. Multiple sorption/desorption cycles

Continuous wastewater treatment requires a reversible sorption-desorption process in order to reuse the adsorbent and to recover the metals in a concentrated form. Four sorption and desorption cycles were carried out in a column filled with GS. Sorption experiments were carried out according to the procedure described previously.

Desorption was carried out by feeding the column containing the four metals-loaded sorbent with 0.05 M HCl at the same flow rate as in sorption experiments, about 30 $mL \cdot h^{-1}$. Despite many authors use EDTA as desorbing agent, its strong complexation capacity on divalent heavy metals would make difficult its subsequent recovery. In the present work, hydrochloric acid has been chosen as desorbing agent due to the demonstrated good performance for both, Cu(II) and Ni(II) recovery from a fixed GS bed (chapter 3). In this acid, also the Cl^- added as counterion does not provoke precipitation of any of the metals and provides also a weak complexation capacity that would be expected to make easier its elution. From the other possible mineral acids that could be employed such as HNO_3 or $HClO_4$, in such a concentrated form as the required to elute the metals from the solid phase, these acids could exhibit oxidizing properties, being possible the chemical degradation of the sorbent. H_2SO_4 was also discarded, not because of its oxidizing properties, but because of the insolubility of lead sulphates (pKs $PbSO_4$=7.80).

As it was reported in chapter 3, divalent metal desorption in mild acidic conditions is a fast process. Due to this fast metal elution, the whole volume eluted by the top of the column was collected in separated tubes during 10 minutes, without draining, obtaining fractions of approximately 5 mL. In these samples, pH was measured and Cu(II), Ni(II), Pb(II) and

Cd(II) concentration was determined by FAAS. Metal desorption ratio was calculated by a mass balance.

The ability of the material to recover its sorption capacity after suffering the acidic desorption treatment was evaluated in the quaternary mixture. When acidic desorption treatment was finished, the columns were fed with MilliQ water adjusted to an initial pH value of 5.2. This solution was pumped upwards the column until pH in the outlet and inlet flow were equal. Once reached this point, pumping was briefly interrupted and the MilliQ solution was replaced by the solution containing the four metals to begin a new sorption cycle. According to this protocol sorption/desorption was evaluated in four cycles.

4.3. Thermodynamic study

Equilibrium isotherms were obtained in batch by contacting 0.1 g of GS with 15 mL of different Cu(II), Ni(II), Pb(II) and Cd(II) solutions within the initial concentration range 5-1000 mg· L^{-1}. Initial pH was adjusted to 5.2 and temperature was varied within the range 5-60 ºC. After equilibration for at least 24 hours, the samples were filtered, acidified and metal concentration in solution was determined by FAAS.

5. RESULTS AND DISCUSSION

5.1. Cu(II), Ni(II), Pb(II) and Cd(II) sorption from single solutions

The breakthrough curves for single metal sorption were measured for Cu(II), Ni(II), Pb(II) and Cd(II). The results are given in terms of metal concentration in solution and in the solid phase as a function of time in **Figures 2 (a)** and **(b)** respectively.

(a)

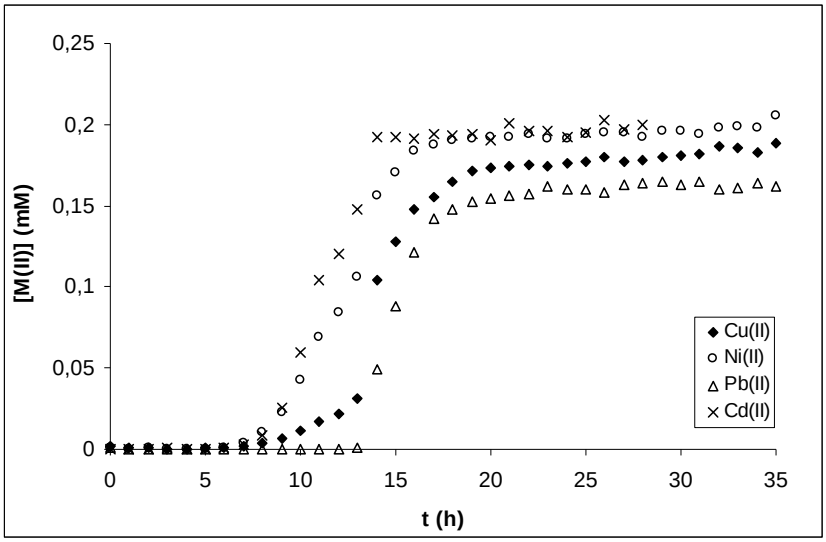

(b)

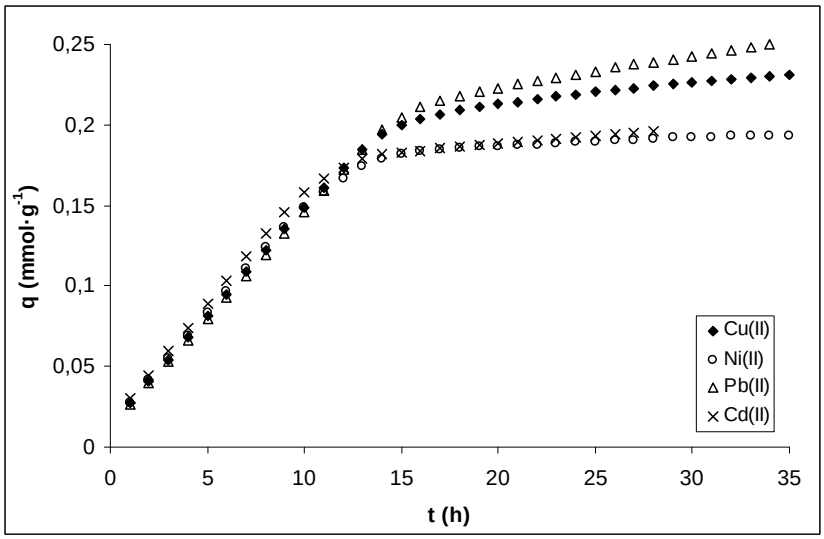

Figure 2: (a) Breakthrough curves and (b) capacity evolution as a function of time for the adsorption of Cu(II), Ni(II), Pb(II) and Cd(II) in single solutions onto GS in a packed bed up-flow column. pH_0: 5.2; $[M(II)]_0 \approx 0.2$ mM; Flow rate≈30 ml·h^{-1}; Sorbent mass≈0.5 g.

The figures of either metal concentration in solution or in the solid phase show a similar profile when Cu(II), Ni(II), Pb(II) and Cd(II) sorption in the GS-packed columns. When breakthrough curves are compared for the four metals, it can be observed a time range in which metal is not found in the eluted effluent, being the amplitude of this interval dependent on the metal. If time of operation under which the system elutes a metal concentration ≤ 0.1 mg·L^{-1} is compared for the different metals, values of 7, 6, 13 and 6 hours, corresponding to eluted volumes about 210, 180, 390 and 180 mL are obtained for Cu(II), Ni(II), Pb(II) and Cd(II) respectively. It has to be also remarked that this important detoxification has been reached with such a small sorbent mass of approximately 0.5 g of dry waste.

The shape of the breakthrough curves obtained when plotting the normalized metal concentration in solution as a function of time provides also useful information about the possible sorption-controlling step. According to the classification proposed by Hand *et al*. (1984), the shape of the breakthrough curves obtained in this study, with an initial time range of very low metal concentration in the outlet flow followed by a fast increase to reach the feeding concentration, is indicative of a liquid-phase mass transfer step as the controlling step.

On the other hand, it seems that the nature of the metal does not affect liquid-solid mass transfer, as it can be concluded from the almost equal initial slopes of the plots time-solid phase metal concentration (**Figure 2** (**b**)). The same chart provides also valuable information about the maximum capacity of the sorbent for the different metals. Results of maximum capacity expressed in mmol·g^{-1} were in the range 0.19-0.25 for all the divalent metals.

The results obtained in this section indicate that neither the liquid to solid mass transfer rate nor the sorbed amount at equilibrium are strongly influenced by the nature of the divalent cation.

Once analyzed the sorption of Cu(II), Ni(II), Pb(II) and Cd(II) from single solutions, in the next section, GS sorption behaviour in binary mixtures will be studied and discussed.

5.2. Cu(II), Ni(II), Pb(II) and Cd(II) sorption from binary mixtures

The breakthrough curves for metal biosorption from the binary solution are presented in the **Figure 3**.

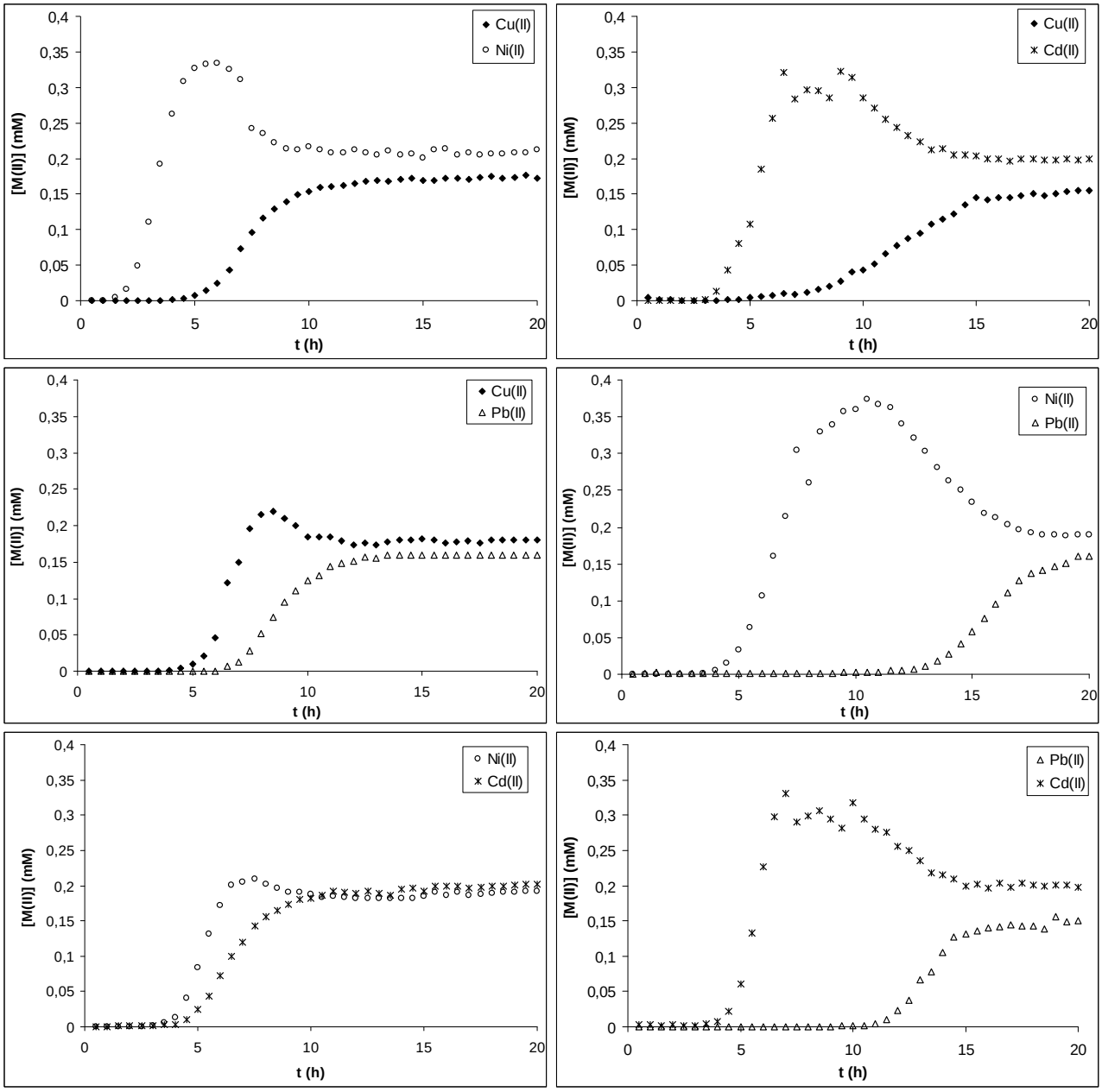

Figure 3: Cu(II), Ni(II), Pb(II) and Cd(II) concentration in solution as a function of time in the different binary mixtures. pH_0: 5.2; $[M(II)]_0 \approx 0.2$ mM; Flow rate≈30 ml·h^{-1}; Sorbent mass≈0.5 g.

Also profile of evolution of metal accumulation in the solid phase of the sorbent is an interesting parameter, so that capacity has been calculated as a function of time for the different binary mixtures and results have been plotted in the next figure.

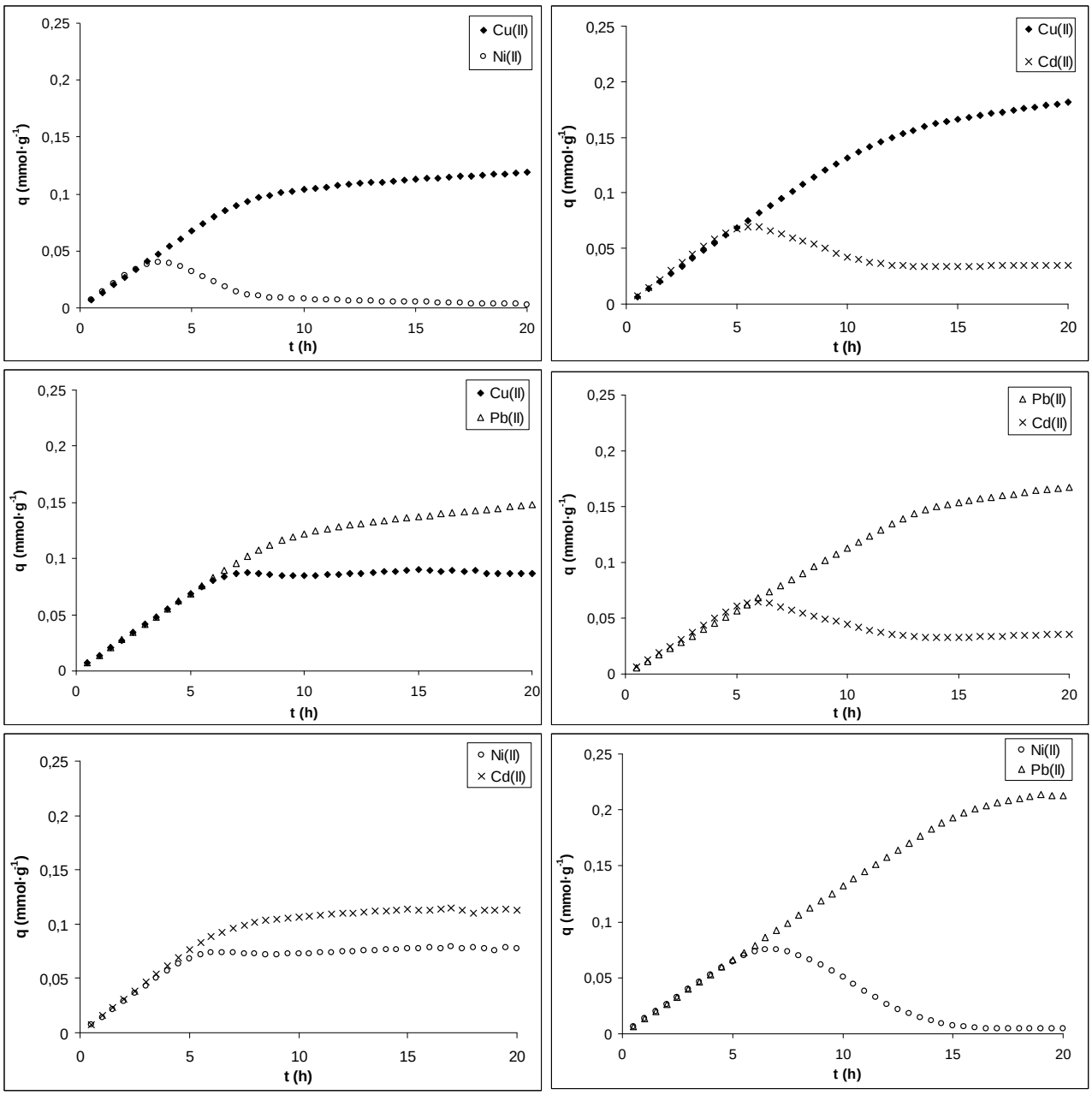

Figure 4: Capacity evolution as a function of time for the adsorption of Cu(II), Ni(II), Pb(II) and Cd(II) in the different binary mixtures. pH_0: 5.2; $[M(II)]_0 \approx 0.2$ mM; Flow rate≈30 ml·h^{-1}; Sorbent mass≈0.5 g.

Results of both, metal concentration in solution and in the solid phase as a function of time show quite differenced trends when metal sorption from the different binary mixtures is compared. When metal concentration in the liquid phase is monitored in the outlet flow, in all the binary mixtures, an overconcentration respect to the feeding metal concentration is observed (**Figure 3**). On the other hand, when metal accumulation in the solid phase is calculated and plotted as a function of time for each metal of the binary mixture (**Figure 4**) it can be observed how the continuous increasing tendency is broken and an inflexion point appears for one of the metals. From this inflexion point, the concentration in the solid phase progressively decreases with time from the maximum (q_{max}) to an equilibrium value (q_{eq}). According to the decrease from the maximum to the equilibrium sorption capacity, overshoots magnitude will be classified later as slight, medium and intense.

These observations strongly contrast with the results obtained in single solutions, where there is a continuous increasing tendency on metal accumulation in the solid phase with time until saturation of the material is achieved.

The origin of the overshoots observed in multimetal polluted effluents, is based on the nature of sorption itself. As said in previous chapters, divalent metal sorption occurs mainly via ion exchange, therefore, metal sorption from multimetal mixtures in column would involve competitive ion exchange. In this case, toxic metallic ions compete for a limited number of binding sites. When the column capacity is approached, species with a lower affinity are pushed off by others with higher affinity and displacement of the first species occurs (Trujillo *et al*., 1991; Kratochvil and Volesky, 1998).

From the figures presented in this section it can be observed that, from the four metallic ions studied, only Pb(II) does not suffer overconcentration in the outlet flow in any of the binary mixtures. This fact suggests that the affinity of GS for Pb(II) has to be greater than for the other three metals. But that's not the only information that can be obtained; it can be observed also that Cu(II) is only overshot in binary mixtures when the solution contains Pb(II), so that, affinity Cu(II)-GS should be lower than Pb(II)-GS but higher than Ni(II)-GS and Cd(II)-GS. Of course its clear that Ni(II) and Cd(II) would be overshot in presence of Pb(II). Finally, to determine which of these two metals, Ni(II) or Cd(II) would exhibit the weakest interaction with GS, its sorption behaviour in the binary mixture Ni(II)-Cd(II) has to be analyzed. As it can be seen, in both **Figures 3** and **4**, Ni(II) suffers a slight

overshoot, indicating thus that, despite the affinity of GS for Ni(II) would be lower than for Cd(II), the difference has not to be so high.

According to the results obtained and discussed in this section, an affinity ranking for the sorption of the different divalent cations onto GS can be proposed. This ranking would be, from higher to lower sorbent affinity:

Pb>Cu>Cd>Ni

where the metals with higher affinity are expected to replace those with lower position in the ranking provoking, in last term, an overconcentration of the weaker-bonded metal in the outlet flow of the column.

Several authors have reported that the affinity sorbent-sorbate reflects the hydrolytic properties of metals (Pagnanelli *et al*., 2003; Vegliò *et al*., 2002). These authors propose that the affinity series is in agreement with the first hydrolysis constant value so that, the more acidic the ion is, the higher the adsorbent affinity. The same authors proposed that the correlation between metal acidity property and the affinity sorbent-sorbate is even more important than the specific functional groups present on the adsorbent surface; in other words, metal speciation predominates on adsorbent characteristics (Pagnanelli *et al*., 2003). The explanation provided by authors is based on the tendency of the metals to form hydrolysed species $Me(OH)^+$ according to the next reaction:

$$H_2O + Me^{2+} \longrightarrow Me(OH)^+ + H^+$$

The sorption affinity that the different metals exhibit in a given multimetal solution is interpreted by supposing that the affinity of the sorbent for the hydrolysed metal species Me(OH) is significantly greater than for the unhydrolysed ones (Spark *et al*., 1995; Pagnanelli *et al*., 2003). It is also considered that in the usual pH range (above 5) $[Me(OH)^+] << [Me^{2+}]$.

This observation is enforced by many studies using both, biological and inorganic sorbents, as it can be seen in **Table 1**.

Table 1: Affinity series for different natural adsorbents

Sorbent	Affinity order	Reference
Microcystis and *Spirogyra*	Pb>Cu>Zn>Cd	Rai, 2000
Streptoverticillium and *Penicillium*	Pb>Cu>Zn>Cd>Ni>Co	Puranik and Paknikar, 1999
Activated sludge	Pb>Cu>Zn=Cd>Ni	Hammaini *et al*., 1999
Pseudomonas aeruginosa PU21	Pb>Cu>Cd	Chang and Chen, 1999
Fungal biomasses	Pb>Cu>Cd>Zn	Yin *et al*., 1999
Sphaerolitus natans	Pb>Cu>Zn>Cd	Pagnanelli *et al*., 2003
Hydrous ferric oxide	Pb>Cu>Zn>Cd	Benjamín *et al*., 1981
Humic umbrisols	Pb>Cr>Cu>Cd≈Ni≈Zn	Covelo *et al*., 2004
Soils	Zn>Ni>Cd	Antoniadis and Tsadilas, 2007

As it can be seen in the table, Pb(II) always occupies the first position in the affinity ranking, followed (when present) by Cu(II). On the other hand, Ni(II) and Cd(II) are always in the range of lower affinity and its relative order depends on the sorbent.

In our case, considering the logarithmic values of the metal's first hydrolysis constant, the next affinity ranking would be expected: log $K_{Pb(II)}$=-7.71>log $K_{Cu(II)}$=-8.00>log $K_{Ni(II)}$= -9.9>log $K_{Cd(II)}$=-10.8 (Smith and Martell, 1976). The ranking successfully describes the observed first position of Pb(II), followed by Cu(II). Nevertheless, this theory fails to describe the relative position Ni(II) to Cd(II). These results put into evidence that the description of the interaction of the different metals and the sorbent might be a more complex process that could not be only described through the tendency of the metals to form hydrolysed species.

The magnitude of the overshoots has been evaluated by comparing the maximum capacity (q_{max}) and the observed at equilibrium (q_{eq}) for the metal that is displaced. The effect of metal replacement can be visualized easier if the decrease in sorption capacity for the metal that suffers the overshoot is expressed as percentage of capacity loose. In this chapter, we have defined as CLO the percentage of Capacity Loose from the maximum to the equilibrium value for the Overshot metal, according to the next equation:

$$CLO = ((q_{\max} - q_{eq}) / q_{\max}) \cdot 100 \qquad (1)$$

According to CLO values, overshoots have been classified in three categories:

(i) Slight, if CLO (%) ≤35

(ii) Medium, if 35≤CLO (%)≤70

(iii) Intense, if 70≤CLO (%)≤100

In **Table 2** it is presented a summary indicating presence/absence (Y/N) and magnitude of overshoots (Slight: S; Medium: M; Intense: I), maximum (q_{max}) and equilibrium (q_{eq}) sorption capacities, percentage of capacity loose from the maximum to the equilibrium value for the overshot metal (CLO) and total metal sorbed amount ($q_{eq\ (M1+M2)}$).

If evaluation of the water detoxification performance on the different binary mixtures is carried out according to the European Union quality standards for human consumption, the maximum allowed concentration is dependent on the nature of the metal (Council Directive 98/83/EC). According these standards, the maximum allowed concentration values for the different metals are: Cu(II) 2 $mg \cdot L^{-1}$; Ni(II): 20 $\mu g \cdot L^{-1}$; Pb(II): 10 $\mu g \cdot L^{-1}$ and Cd(II): 5 $\mu g \cdot L^{-1}$. This relative permissiveness in the concentration level of copper, in the range of ppm, remarkably contrasts with the low allowed values for nickel, lead and cadmium, for which the European Union accepts only few ppb.

The application of this sorption technology for the different binary mixtures would be restricted thus to the time from which the concentration in the outlet flow overpass the maximum allowed concentration for one of the metals. The times of operation of the continuous bed-up flow system, according to the E.U. discharge limits for each individual metal on each binary mixture are presented in the **Table 2**. Underlined is indicated the maximum time of applicability that would accomplish the discharge limits for both metals in each binary mixture.

As the maximum allowed concentrations according to the E.U. criteria are metal-dependent in the table it has been also included the time under which the column can operate eluting a concentration lower than 0.1 $mg \cdot L^{-1}$ for each metal of the mixture. This concentration value has been arbitrarily fixed to allow an easy comparison of the different sorption behaviour of the different divalent cations.

Table 2: Breakthrough parameters for divalent metal sorption in the binary mixtures.

System	Metal	Overshoot/magnitude	$t_{[M(II)]<0.1\ ppm}$ (h)	$t_{[M(II)]>EU}$ (h)	t_{qmax} (h)	q_{max} (mmol·g^{-1})	q_{eq} (mmol·g^{-1})	CLO (%)	$q_{eq\ (M1+M2)}$ (mmol·g^{-1})
Cu/Ni	Cu	N	4	6	--	--	0.1244	--	0.1262
	Ni	Y/Intense	1.5	1	3.5	0.0403	0.0018	95.5	
Cu/Cd	Cu	N	4.5	9	--	--	0.1866	--	0.2217
	Cd	Y/Medium	3	3	5.5	0.0696	0.0351	49.6	
Cu/Pb	Cu	Y/Slight	4	5.5	7.5	0.0884	0.0871	1.5	0.2389
	Pb	N	6	5.5	--	--	0.1527	--	
Ni/Pb	Ni	Y/Intense	3.5	3	7	0.0755	0.0047	93.8	0.2184
	Pb	N	5.5	0.5	--	--	0.2137	--	
Pb/Cd	Pb	N	9	3.5	--	--	0.1738	--	0.2110
	Cd	Y/Medium	0	0	6	0.0649	0.0372	42.7	
Ni/Cd	Ni	Y/Slight	3	3	6.5	0.0736	0.0770	0.01	0.1904
	Cd	N	3	1	--	--	0.1134	--	

* $t_{[M(II)]<0.1\ ppm}$: time from which metal concentration in the outlet flow is >0.1 mg·L^{-1}.
* $t_{[M(II)]>EU}$: time from which metal rises the maximum allowed concentration for drinking water (according to EU criteria).
* t_{qmax}: time to reach maximum capacity for the overshot metal (h).
* q_{max}: maximum metal sorbed amount for the overshot metal (mmol·g^{-1}).
* q_{eq}: metal sorbed amount at equilibrium (mmol·g^{-1}).
* **CLO**: percentage of Capacity Loose from the maximum to the equilibrium value for the Overshot metal (%).
* $q_{eq\ (M1+M2)}$**:** total divalent metal sorbed amount (mmol·g^{-1}).

As it can be seen in the table, while in the case of the Cu(II)/Pb(II) mixture the column can operate under the specified concentration limits for both metals for around 5.5 hours, in the case of Pb(II)/Cd(II) mixture an initial eluted Cd(II) concentration higher than the acceptable limit was observed from the beginning of the process.

For a given metal, its concentration in the solid phase depends on the other metal of the binary mixture. As it had been previously exposed, the extension of metal replacement in the different mixtures can be computed by means of the parameter previously defined as CLO. Values of CLO from 95.5, involving almost total replacement, as it happens for Ni(II) in the binary Cu(II)/Ni(II) mixture, to approximately 0, indicating almost no replacement, as in the case of Ni(II) in the binary Ni(II)/Cd(II) mixture were observed. If the affinity ranking proposed from the analysis of the overshoots is taken into account, it can be observed how the longer the distance between the metals in the ranking, the higher the capacity loose for the metal uptaken with lower affinity.

This phenomena has to be strongly related to the affinity of GS for the different metals or to the energy variation in the global sorption process, involving metal transferring from the liquid to the solid surface and formation of M(II)-GS bonds. In an attempt to give an explanation to these phenomena, information about sorbent-sorbate affinity and energetic aspects of the sorption process is required. In a later section of this chapter, thermodynamics of divalent metal sorption onto GS will be studied and discussed.

Also total divalent metal sorption capacity at equilibrium, $q_{eq\ (M1+M2)}$ ($mmol \cdot g^{-1}$), has been calculated for the different binary mixtures and presented in **Table 2**. As it can be observed this parameter depends also on the nature of the binary mixtures and varies from 0.1262 $mmol \cdot g^{-1}$ in the case of the Cu(II)/Ni(II) mixture to 0.2389 $mmol \cdot g^{-1}$ in the case of the Cu(II)/Pb(II). Except in the case of the Cu(II)/Ni(II) mixture, where the total capacity value is quite low, in all the other binary mixtures, independently of the metals involved, $q_{eq\ (M1+M2)}$ is close to 0.2 $mmol \cdot g^{-1}$.

After this study concerning metal sorption from binary mixtures, in a further step, GS sorptive performance when facing different ternary metal mixtures will be studied.

5.3. Cu(II), Ni(II), Pb(II) and Cd(II) sorption from ternary mixtures

In this section, copper, nickel, lead and cadmium sorption was studied in all the possible ternary combinations. The breakthrough curves obtained for each metal in the different ternary mixtures, as well as the amount of metal sorbed as a function of time, are presented in **Figures 5** and **6** respectively.

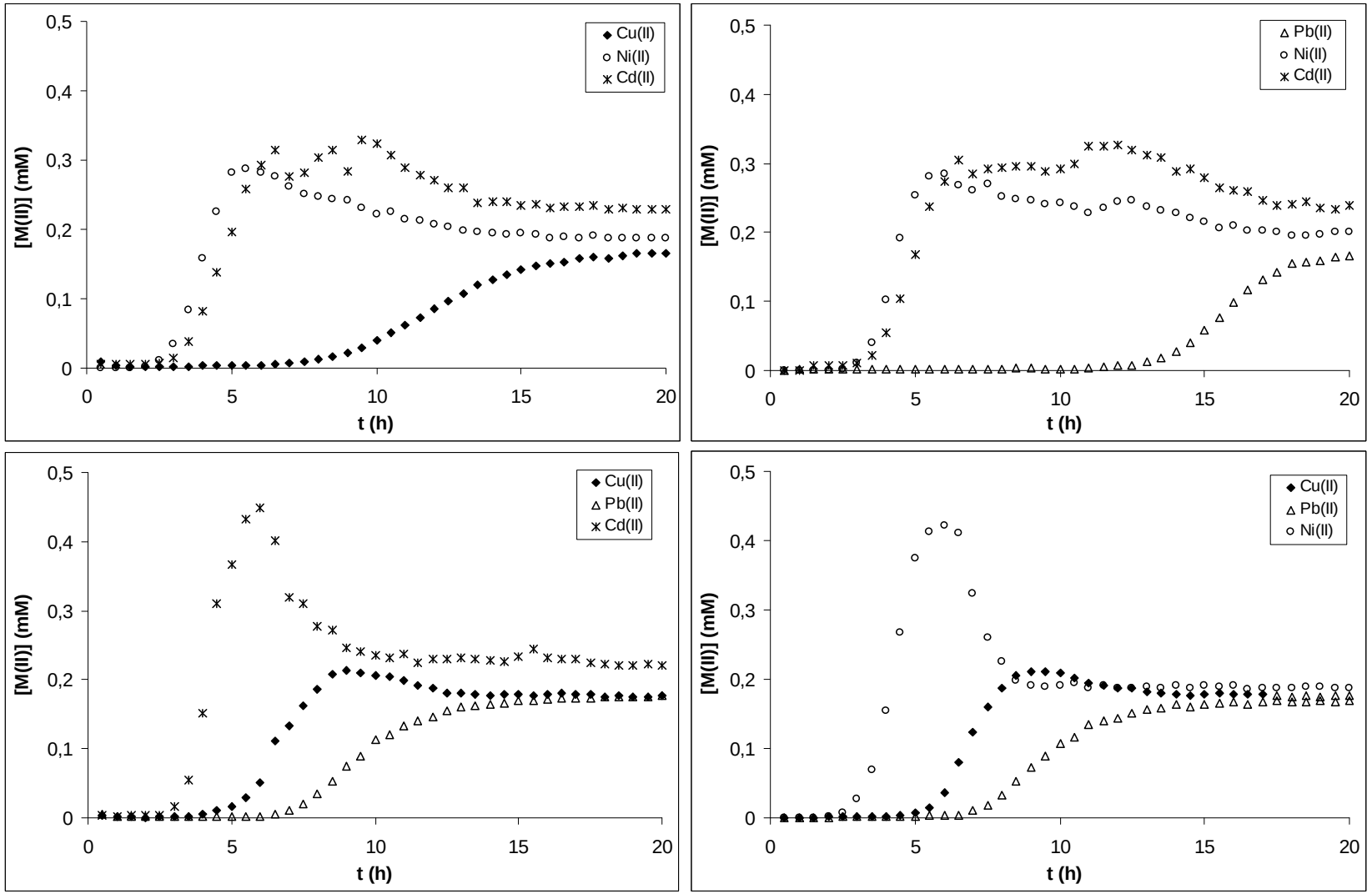

Figure 5: Cu(II), Ni(II), Pb(II) and Cd(II) concentration in solution as a function of time in the different binary mixtures. pH_0: 5.2; $[M(II)]_0 \approx 0.2$ mM; Flow rate≈30 ml·h^{-1}; Sorbent mass≈0.5 g.

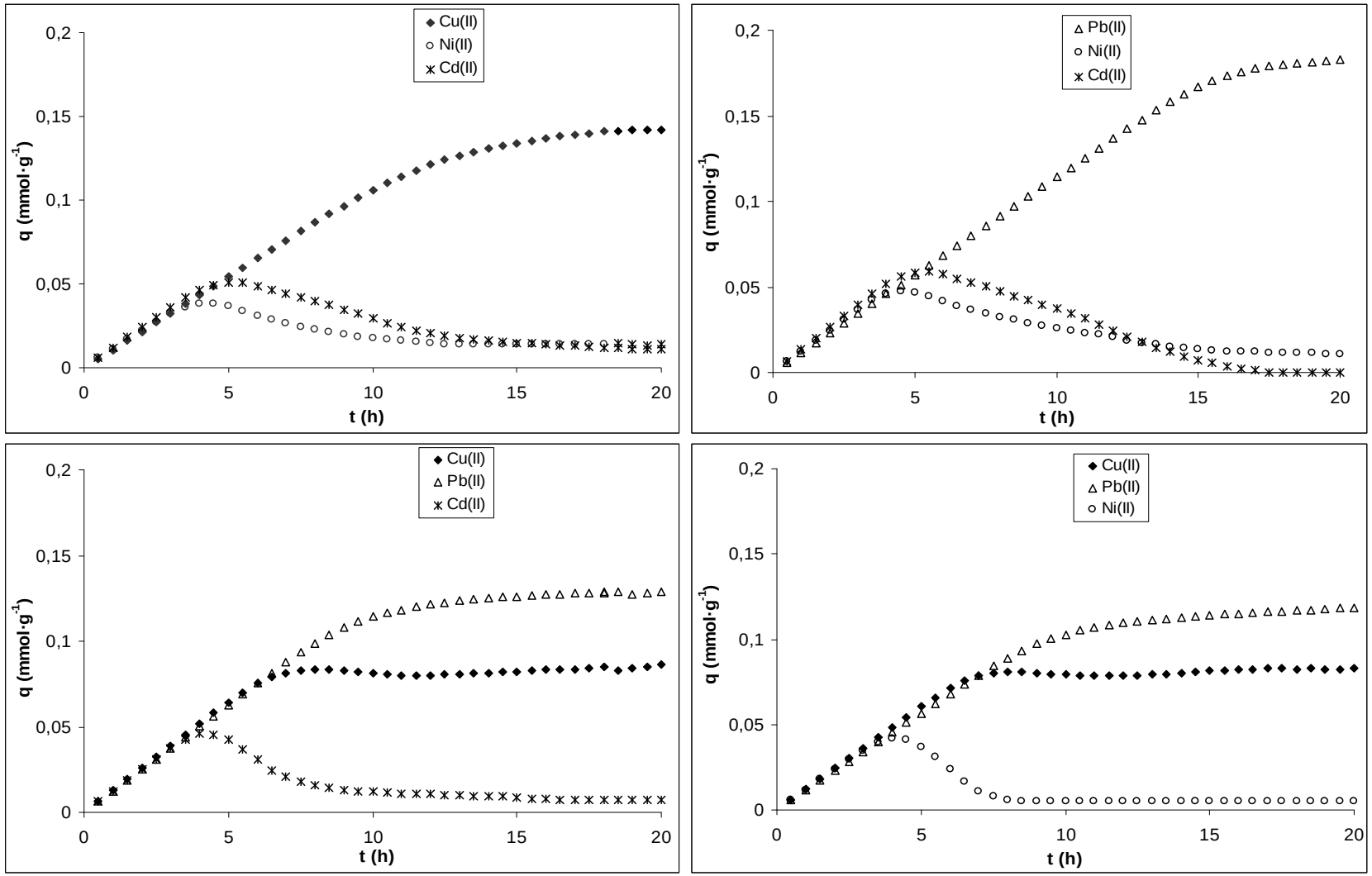

Figure 6: Capacity evolution as a function of time for the adsorption of Cu(II), Ni(II), Pb(II) and Cd(II) in the different ternary mixtures. pH_0: 5.2; $[M(II)]_0 \approx 0.2$ mM; Flow rate≈30 ml·h^{-1}; Sorbent mass≈0.5 g.

As in the case of binary mixtures, the results of both, metal concentration in solution and in the solid phase as a function of time, show quite differenced trends when metal sorption from the different mixtures is compared. In all the systems, always one of the metals is preferently adsorbed, leading to the formation of a typical breakthrough curve, while the other two metals of the mixture exhibit an overconcentration respect to the feeding concentration in the outlet flow (**Figure 5**). As it can be observed, the presence and intensity of overshoots is strongly dependent on the nature of the metals of the ternary mixture. As in the case of the binary mixtures, metal species with lower affinity are pushed off by other species with higher affinity for the sorbent, and the replacement of the first occurs, leading to the observed overconcentration in the outlet flow of the column.

The figures presented here, either as metal concentration in the liquid (**Figure 5**) or in the solid phase (**Figure 6**) as a function of time, clearly demonstrate the sorption competition between the different metals in the continuous bed up-flow sorption process. From the four studied metals, as in the case of the binary solutions, Pb(II) is the only metal that does not suffer an overconcentration in the outlet flow in any of the ternary mixtures. It has to be also remarked that Cu(II) suffers a slight overconcentration only in presence of Pb(II). These facts corroborate the affinity ranking proposed in the case of the binary mixtures, where Pb(II) and Cu(II) were, in this order, the most favourably adsorbed while both, Ni(II) and Cd(II), were displaced by Cu(II) and Pb(II).

In **Figure 5**, it can be observed that the most important metal overconcentration in the outlet effluent occurs when either Ni(II) or Cd(II) coexist in solution with simulatenously Cu(II) and Pb(II). This corroborates that both, Ni(II) and Cd(II) are the metals sorbed with less affinity and that they compete with Cu(II) and Pb(II), that exhibit a greater sorption affinity.

A comparison between metal sorption behaviour in the different ternary mixtures has been carried out according to the parameters exposed in the case of binary mixtures and a summary of these parameters is presented in **Table 3**.

Table 3: Breakthrough parameters for metal sorption in the ternary mixtures.

System	Metal	Overshoot/magnitude	$t_{[M(II)]<0.1\ ppm}$ (h)	$t_{[M(II)]>EU}$ (h)	t_{qmax} (h)	q_{max} (mmol·g^{-1})	q_{eq} (mmol·g^{-1})	CLO (%)	$q_{eq\ (M1+M2)}$ (mmol·g^{-1})
Cu/Ni/Cd	Cu	N	3	9.5	--	--	0.1409	--	0.1659
	Ni	Y/Medium	1.5	1	4.5	0.0382	0.0141	63.1	
	Cd	Y/Intense	0	0	5.0	0.0507	0.0109	78.5	
Cu/Pb/Cd	Cu	Y/Slight	3	5.5	8.0	0.0834	0.0842	0.0	0.2198
	Pb	N	0	0	--	--	0.1287	--	
	Cd	Y/Intense	0	0	4	0.0459	0.0069	84.9	
Cu/Pb/Ni	Cu	Y/Slight	4	6	8	0.0807	0.0831	0.0	0.2090
	Pb	N	2	2	--	--	0.1205	--	
	Ni	Y/Intense	2	1.5	4	0.0419	0.0053	87.4	
Pb/Ni/Cd	Pb	N	0.5	0.5	--	--	0.1841	--	0.1964
	Ni	Y/Intense	2.5	2	5.5	0.0587	0.0115	80.4	
	Cd	Y/Intense	1	1	4.5	0.0476	0	100.0	

* $t_{[M(II)]<0.1\ ppm}$: time from which metal concentration in the outlet flow is >0.1 mg·L^{-1}.
* $t_{[M(II)]>EU}$: time from which metal rises the maximum allowed concentration for drinking water (according to EU criteria).
* t_{qmax}: time to reach maximum capacity for the overshot metal (h).
* q_{max}: maximum metal sorbed amount for the overshot metal (mmol·g^{-1}).
* q_{eq}: metal sorbed amount at equilibrium (mmol·g^{-1}).
* **CLO**: percentage of Capacity Loose from the maximum to the equilibrium value for the Overshot metal (%).
* $q_{eq\ (M1+M2)}$: total divalent metal sorbed amount (mmol·g^{-1}).

In **Table 3**, it has been underlined the time that the process could operate accomplishing the criteria fixed by the EU for the three metals of the mixture simultaneously. The target values fixed by the EU for the maximum allowed metal concentration in solution were presented in the previous section, concerning metal sorption from binary mixtures. As it can be observed, the process does not accomplish the limits for any time in the case of Cu/Ni/Cd and Cu/Pb/Cd mixtures, while in the case of the mixtures Cu/Pb/Ni and Pb/Ni/Cd, this technology could be applied for 1.5 and 0.5 hours respectively.

The effect that the metals provoke on each other sorption can be also evaluated by comparison of the maximum metal capacity (q_{max}) and the achieved at equilibrium (q_{eq}). As it was done in the case of the binary mixture, the decrease on metal sorption capacity is visualized easiear by means of the parameter labelled as CLO (percentage of Capacity Loose from the maximum to the equilibrium value for the Overshot/s metal/s (%)). The values of CLO presented in **Table 3** indicate that the decrease in metal concentration in the solid phase depends on the multimetal environment in which the given metal is present.

The table puts into evidence that high CLO values are the obtained for Ni(II) and Cd(II). For Ni(II), the capacity loose was found to be 63.1% when it was present with Cu(II) and Cd(II), 80.4% when it coexisted with Pb(II) and Cd(II) and the highest capacity decay, 87.4%, when Ni(II) was in solution simultaneously with Cu(II) and Pb(II).

In the case of Cd(II), CLO values ranged from 78.5% when it coexisted with Cu(II) and Ni(II) to 84.9%, with Cu(II) and Pb(II). In the extreme it can be found the total replacement of Cd(II) in the solid phase (CLO value of 100%) when this metal coexisted with Ni(II) and Pb(II).

Despite a slight overshoot is observed for Cu(II) in the ternary mixtures containing Pb(II), the final capacity of the GS for Cu(II) was observed to be almost re-established, obtaining CLO values of 0%. These results are in agreement with the discussion in basis to Metal-GS affinities carried out when studying the particular scenario of the binary mixtures.

The total metal sorption capacity at equilibrium, expressed as the sum of the individual metal sorbed amount, $q_{eq.(M1+M2+M3)}$ (mmol·g^{-1}), was also calculated for the different ternary mixtures and results have been presented in **Table 3**. As in the case of the binary mixtures, this parameter depends on the nature of the ternary solutions that feed the columns. This parameter exhibits a variation ranging from 0.1659 mmol·g^{-1} in the case of the Cu(II)/Ni(II)/Cd mixture to 0.2198 mmol·g^{-1} in the case of the Cu(II)/Pb(II)/Cd(II). In the case of the other two mixtures, the observed values were: 0.2090 in the case of Cu(II)/Pb(II)/Ni(II) and 0.1964 in the case of the Pb(II)/Ni(II)/Cd(II) mixture. As it can be seen, despite for a given metal its individual sorption capacity at equilibrium, (q_{eq}), exhibits an important dependence on the nature of the other metals that form the ternary mixture, the total metal sorption capacity ($q_{eq.(M1+M2+M3)}$), does not differ so much from one mixture to another, reaching always a value close to 0.2 mmol·g^{-1}. Capacity values about 0.2 mmol·g^{-1} had been also obtained for Cu(II), Ni(II), Pb(II) and Cd(II) sorption from single mixtures and also in the case of binary mixtures, in this last case, when sorption was expressed as the sum of the individual contribution of the two metals.

Once analyzed the sorption scenarios from single, binary and ternary metal mixtures, the situation that remains to complete this study would be the treatment of an effluent with the highest polluting load; the corresponding to the sorption from a quaternary Cu(II)/Ni(II)/Pb(II)/Cd(II) mixture. For this situation, both sorptive and desorptive behaviour of the material will be explored by performing the experiments in successive sorption/desorption cycles.

5.4. Cu(II), Ni(II), Pb(II) and Cd(II) sorption/desorption from quaternary mixtures

5.4.1. Sorption/desorption experiments

In this section, copper, nickel, lead and cadmium removal from a quaternary mixture and the possibility of metal recovery by desorption in mild acidic conditions will be evaluated. Feasibility of this process will be evaluated by performing 4 consecutive sorption and desorption cycles.

When metal concentration in solution is plotted as a function of time, breakthrough curves are obtained. In **Figure 7**, the experimental breakthrough curves for the different metals of the quaternary mixture in the different sorption cycles are presented. In the same figure, also pHs of the feeding solution and of the outlet effluent have been included.

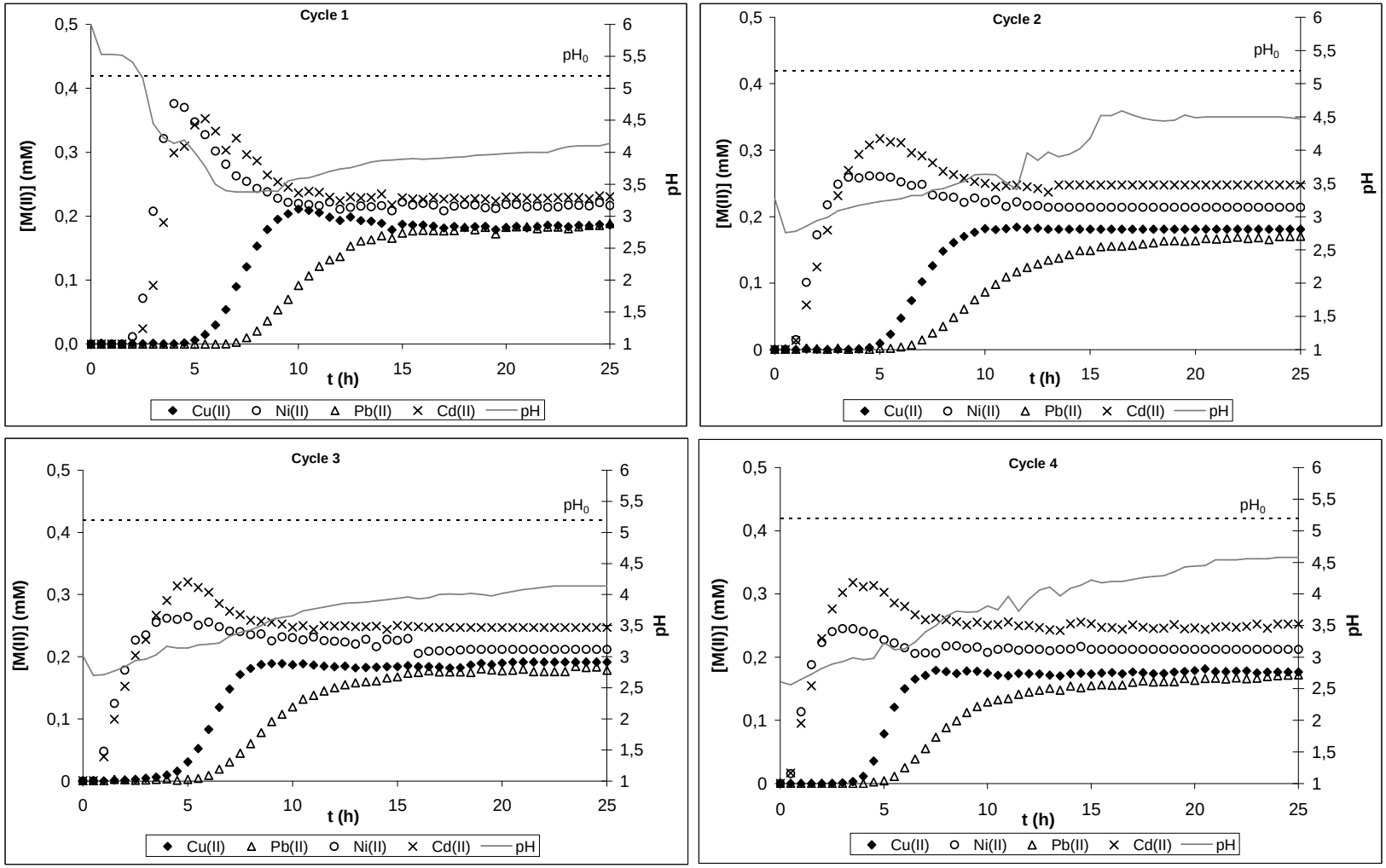

Figure 7: Cu(II), Ni(II), Pb(II) and Cd(II) concentration in solution and pH profile as a function of time for the quaternary mixture in the different sorption cycles. Solid and dotted lines represent outlet and inlet effluent pHs respectively.. pH_0: 5.2; $[M(II)]_0 \approx 0.2$ mM; Flow rate≈30 ml·h^{-1}; Sorbent mass≈0.5 g.

While all these figures clearly indicate that some of the metal ions compete with one another for the material binding sites, it is interesting to emphasize in the fact that Pb(II) binding to GS is almost unaffected by the presence of either Cu(II), Ni(II) or Cd(II). This result is in agreement with the affinity ranking proposed in the study of the sorption from binary mixtures.

As it can be seen in **Figure 7**, a constant shortening of the breakthrough time from cycle to cycle was observed for all the metals, being this shortening the most pronunciated when the first (raw material) and second (after the first acidic desorption and re-conditioning of the bed) sorption cycles are compared. The mass transfer sorption zone broadened with increasing ‘‘age’’ of the biosorbent. The reason for the shortening breakthrough time was apparently not the diminishing equilibrium uptake capacity, as it can be observed in **Table 4**, but rather a slight change in the column overall adsorption rate. This fact is indicating that while sorbent sites of the biomass were still available, they became less accessible after successive sorption/desorption cycles.

In **Figure 7**, also pH evolution as a function of time has been plotted for the different sorption cycles. In all the cycles, the pH decreases from the beginning of the process and then, progressively, increases to reach final values around 4.5. It has to be remarked that, while in the first sorption cycle a minimum pH of 3.5 is achieved in approximately 8 hours, in the case of the 2^{nd}, 3^{rd} and 4^{th} sorption cycles (all carried out after acidic desorption and pH readjustment of the sorbent bed) more acidic pHs, about 2.7, reached in only 1 hour after the beginning of the process, were observed. The profile of pH variation with time demonstrates that H^+ plays a very important role in the sorption mechanism after acidic regeneration of the sorbent bed. It has to be remarked also that light metal release (K^+, Na^+, Mg^{2+} and Ca^{2+}) from the material was analysed in the eluate, and a significant Ca^{2+} release while metal was being sorbed was only observed in the first cycle (data not shown). In all the subsequent sorption cycles no light metal release was observed. The results obtained in this study are indicative of an ion exchange mechanism as metal sorption responsible. In the raw material, sorption might be associated in some extent to a Ca^{2+} and H^+ ion exchange, according to reactions summarized as (1) and (3), while desorption proceeds by protonation of the material and subsequent release of the metal, according to reaction (2).

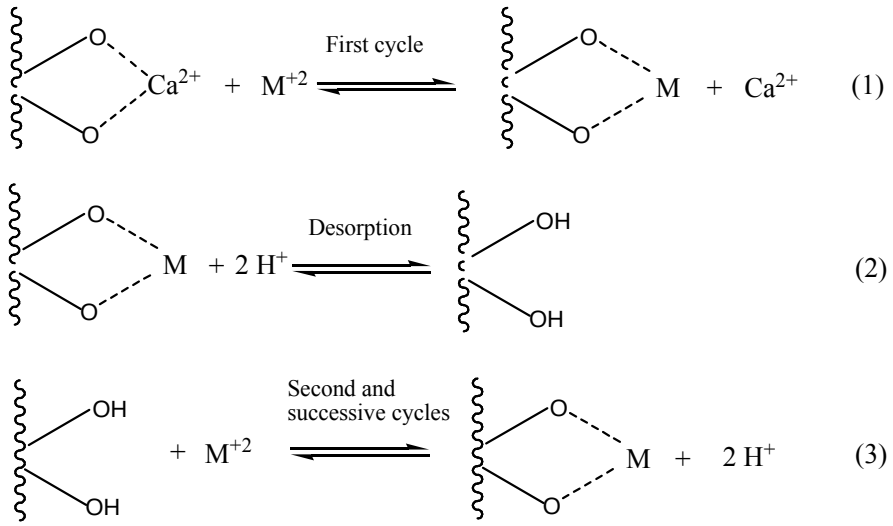

After the first sorption-desorption cycle, all the alkaline and alkaline-earth cations might have been removed from the material and its basic positions must be coordinated to protons, so that sorption proceeds by cation exchange, but only by H^+, according to reaction (3).

As in the case of single, binary and ternary metal mixtures, metal sorption from the quaternary mixture can be also analysed from the point of view of the metal accumulation in the solid phase as a function of time. In **Figure 8** Cu(II), Ni(II), Pb(II) and Cd(II) sorbed amount as a function of time for each sorption cycle is presented. To evaluate the effect of the number of sorption/desorption cycles in the sorptive behaviour of the material through a given metal, sorbed mass as a function of time on each sorption cycle has been plotted separately for Cu(II), Ni(II), Pb(II) and Cd(II). Results are presented in **Figure 9**.

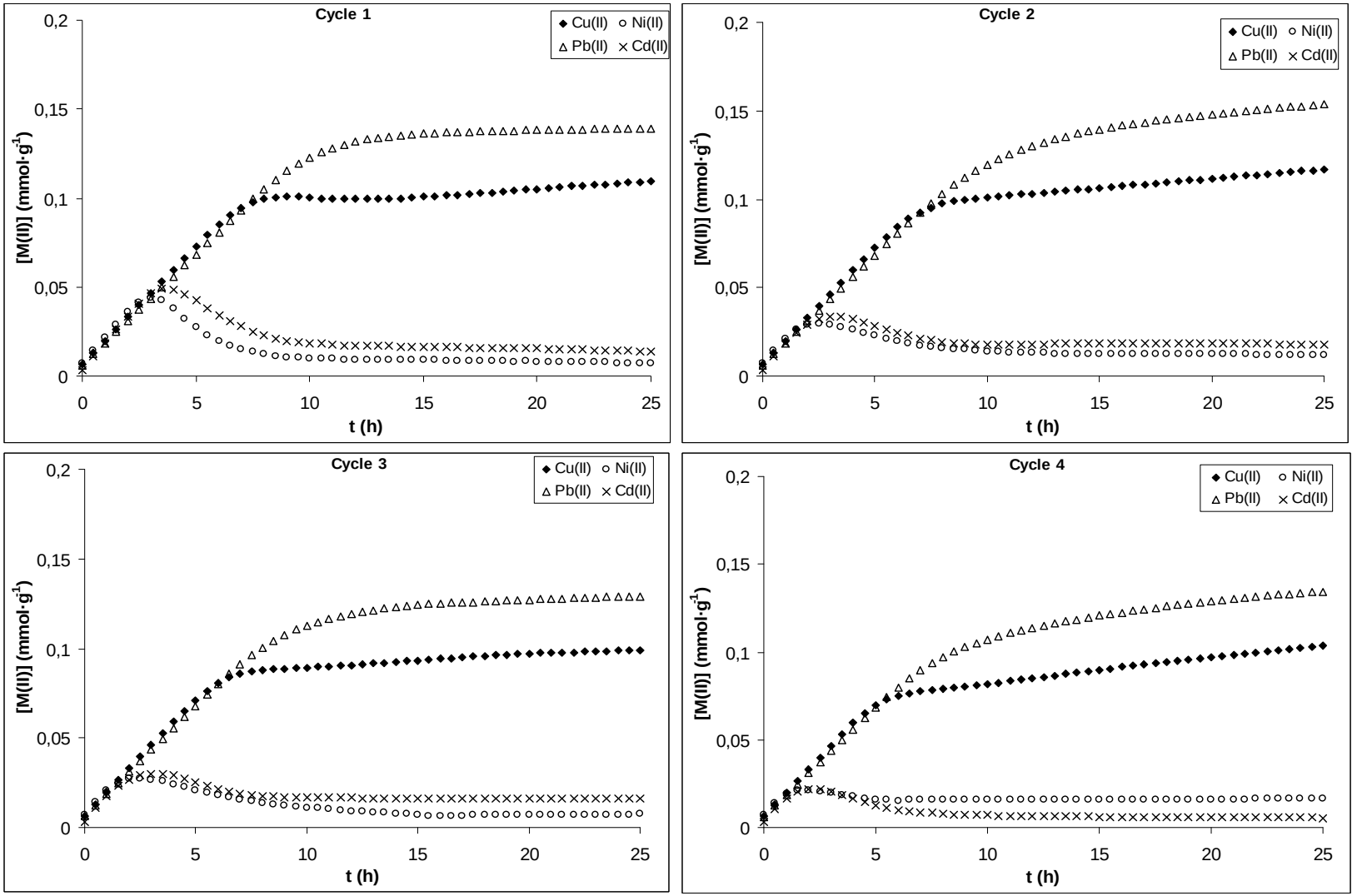

Figure 8: Capacity evolution as a function of time for the adsorption of Cu(II), Ni(II), Pb(II) and Cd(II) in different sorption cycles in the quaternary mixture. pH_0: 5.2; $[M(II)]_0 \approx 0.2$ mM; Flow rate≈30 ml·h^{-1}; Sorbent mass≈0.5 g.

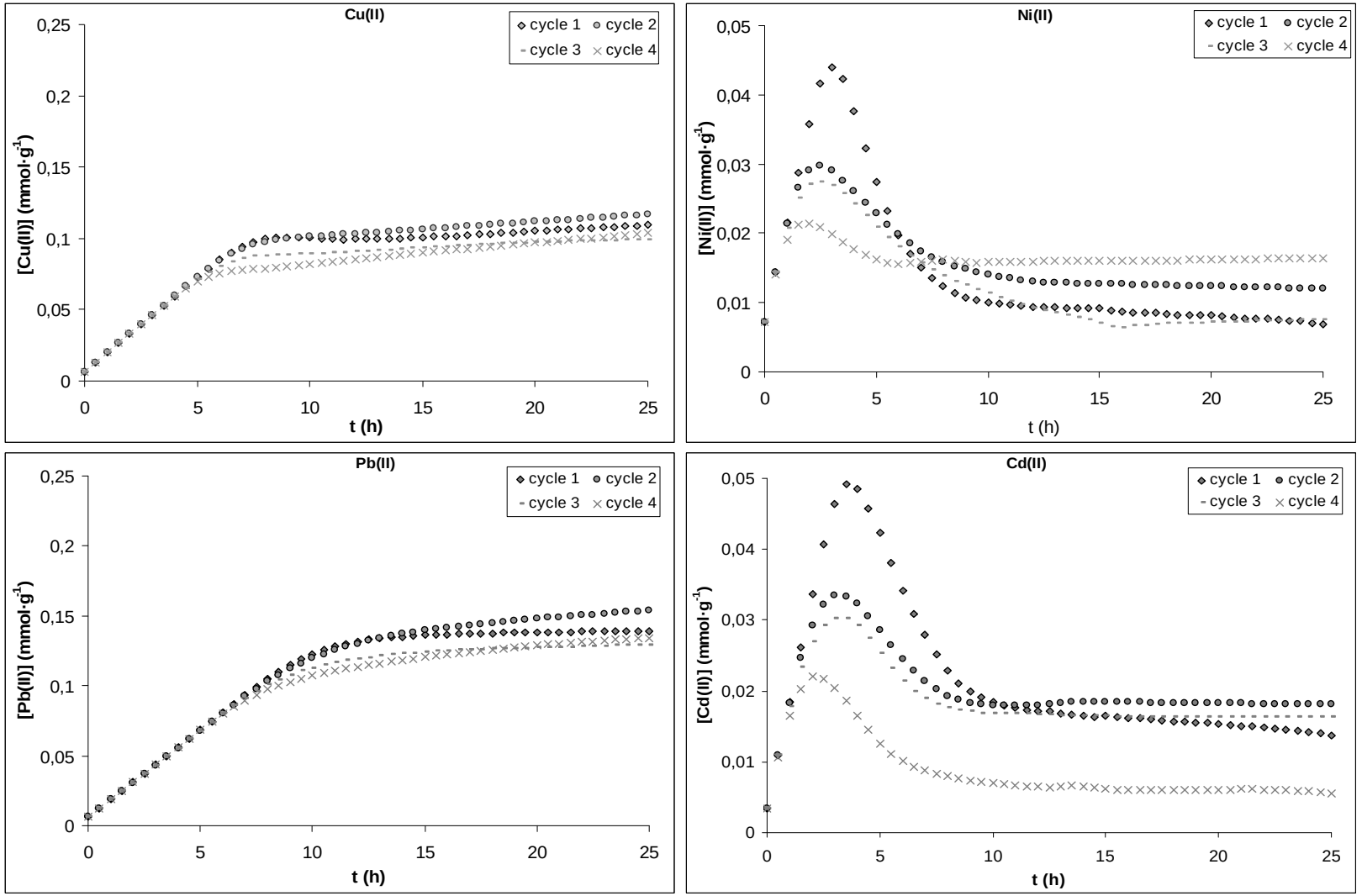

Figure 9: Individual capacity evolution as a function of time for the adsorption of Cu(II), Ni(II), Pb(II) and Cd(II) in the different sorption cycles in the quaternary mixture. pH_0: 5.2; $[M(II)]_0 \approx 0.2$ mM; Flow rate≈30 ml·h^{-1}; Sorbent mass≈0.5 g.

For all the metals in a given sorption cycle or for a given metal in the different cycles (**Figures 8** and **9** respectively), it can be observed that the magnitude of the overshoots for Cu(II), Ni(II) and Cd(II) decreases. In the case of Cu(II), where only a slight overconcentration in the outlet effluent was observed, after the first acidic regeneration of the bed, the overshoot disappears.

For an easier visualization of the effect of the acidic desorption in the equilibrium achieved in the different sorption cycles, in the next table a summary of individual metal capacity ($q_{M(II)}$ (mmol·g^{-1})), total metal capacity (Q_T (mmol·g^{-1})) and percentage of contribution of each metal to the total metal sorbed amount onto the material (R (%)) is presented in the next table. The pamameter R(%) was calculated as $R=(q_{M(II)}/Q_T)*100$.

Table 4: Cu(II), Ni(II), Pb(II) and Cd(II), total divalent metal sorption capacity and relative percentage of each metal sorbed (R) for the different sorption cycles .

	$q_{M(II)}$ (mmol·g^{-1})				Q_T (mmol·g^{-1})	R(%)			
Cycle	**Cu**	**Ni**	**Pb**	**Cd**	**Cu+Ni+Pb+Cd**	**Cu**	**Ni**	**Pb**	**Cd**
1	1.11E-01	5.51E-03	1.39E-01	1.22E-02	2.64E-01	42.09	2.09	52.47	3.36
2	1.21E-01	1.18E-02	1.58E-01	1.82E-02	3.08E-01	39.11	3.82	51.17	5.91
3	1.00E-01	7.80E-03	1.29E-01	1.64E-02	2.86E-01	38.41	3.48	48.43	9.67
4	1.08E-01	1.66E-02	1.38E-01	4.34E-03	3.32E-01	35.31	15.76	44.13	4.80

*$\mathbf{Q_T}$: Total divalent metal sorbed amount: $q_{Cu}+q_{Ni}+q_{Pb}+q_{Cd}$
*$\mathbf{R}$: Relative percentage of Cu(II), Ni(II), Pb(II) and Cd(II) in the solid phase at equilibrium after sorption from the quaternary mixture. $R=(q_{M(II)}/Q_T)*100$

As it can be observed in the table, and discussed previously, the sorption capacity of GS seems not to be clearly modified after the different acidic treatments applied for the metal recovery. In any case, the total sorbent capacity, Q_T (mmol·g^{-1}), obtained as sum of the individual metal capacity, seems to indicate a general increasing trend. It is possible that the successive acidic treatments on the sorbent material lead to the formation of new sorption-active sites that could enhance, particularly for Ni(II), the low initial affinity of GS for this metal.

The values of the parameter R(%) presented in **Table 4** point out that Cu(II) and Pb(II) are the main sorbed metals at equilibrium. The sum of the individual R(%) for these two metals varies from 95.5 in the 1st sorption cycle to approximately 80% in the 4th. On the other hand, Ni(II) and Cd(II) represent only a small fraction of the total sorbed metal

amount. Its contribution, expressed as sum of R(%) for the two metals, varies from about 5.5 to approximately 21% in the 1st and the 4th cycle respectively.

In any case, the low remaining sorbed concentration at equilibrium for Cd(II) and Ni(II) that, in the four sorption cycles is in the order of magnitude of ten times smaller than the capacity observed for Cu(II) and Pb(II), makes difficult an accurate discussion of the effect that the acidic desorption exerts in the sorption of Cd(II) and Ni(II).

In this section, the performance of a GS sorbent bed for the simultaneous removal of Cu(II), Ni(II), Pb(II) and Cd(II) in a quaternary mixture has been discussed. In views of a full application of this technology, if the biosorption process is to be used as an alternative in wastewater treatment, the biosorbent regeneration may be a crucial step to keep low processing costs, turning possible metal ions(s) recovery (Volesky, 2003). In chapter 3, it had been exposed that the most commonly used eluting agents were either acids (Atdor *et al.*, 1995; Ahuja *et al*., 1999; Zhou *et al*., 1998; Hammaini *et al*., 2007) or complexing agents (Gong *et al*., 2005; Hashim *et al*., 2000). Despite complexing agents such as EDTA have been succesfully employed as desorbing agents of different metal cations from different sorbents, the strong chelating activity of these molecules could become an important drawback for a subsequent metal recovery process from the concentrated eluate. In the present work, according to the reasons exposed in the methodology (section 4.2.4.2.), 0.05 M hydrochloric acid will be used for the recovery/regeneration of the sorbent bed.

In **Table 5**, metal concentration in the eluate as a function of time for each desorption cycle is presented.

Table 5: Cu(II), Ni(II), Pb(II) and Cd(II) concentration ($mg \cdot L^{-1}$) as a function of time in the desorption experiments. $[HCl]_0$=0.05 M.

	Cycle 1				Cycle 2				Cycle 3				Cycle 4			
t (min)	**Cu**	**Ni**	**Pb**	**Cd**	**Cu**	**Ni**	**Pb**	**Cd**	**Cu**	**Ni**	**Pb**	**Cd**	**Cu**	**Ni**	**Pb**	**Cd**
0	420.8	36.9	1581.2	77.2	245.2	36.4	903.9	72.8	167.3	25.7	534.2	65.63	213.2	25.5	754.9	65.0
10	227.1	0.4	1122.5	3.4	354.9	3.8	1710.9	11.6	346.1	4.2	1592.3	12.45	360.2	4.4	2324.2	14.1
20	43.3	0.0	254.1	0.0	25.1	0.0	189.3	0.1	49.9	0.3	213.6	0.32	50.0	0.0	162.4	0.0
30	8.3		70.9		1.5		31.9	0.0	2.4	0.0	31.3	0.0	1.0		15.7	
40	1.4		23.6		0.5		16.3		0.3		9.4		0.0		4.3	
50	0.3		12.1		0.2		10.7		0.0		3.6				0.8	
60	0.1		7.2		0.2		7.7				1.9				0.0	
70	0.0		5.6		0.0		6.3				0.2					
80			3.9				5.4				0.0					
90			2.9				4.6									
100			2.5				4.8									
110			1.7				1.3									
120			1.4				0.0									
130			0.8													
140			0.6													
150			0.0													

As it can be seen in **Table 5**, the desorption process is extremely fast, taking place in approximately 40 minutes for all the metals except for Pb(II) in the first and second series, where longer periods, about 120 minutes are required. Fast desorption of several divalent metals in continuous fixed bed processes by passing through the laden sorbent bed diluted acid, has been previously reported by several authors (Volesky *et al*., 2003; Vilar *et al*., 2008; Gupta *et al*., 2008; Pandey *et al*., 2008).

When eluted metal concentration is plotted as a function of time, the desorption curves for the four cycles are obtained. The correspondent profile has been illustrated in **Figure 10**. In this figure, metal concentration has been plotted in $mmol \cdot L^{-1}$ in order to establish an easier comparison between the desorption behaviour of the different metals. Also pH evolution of the eluted effluent during desorption process was followed and results have been included in the same figure.

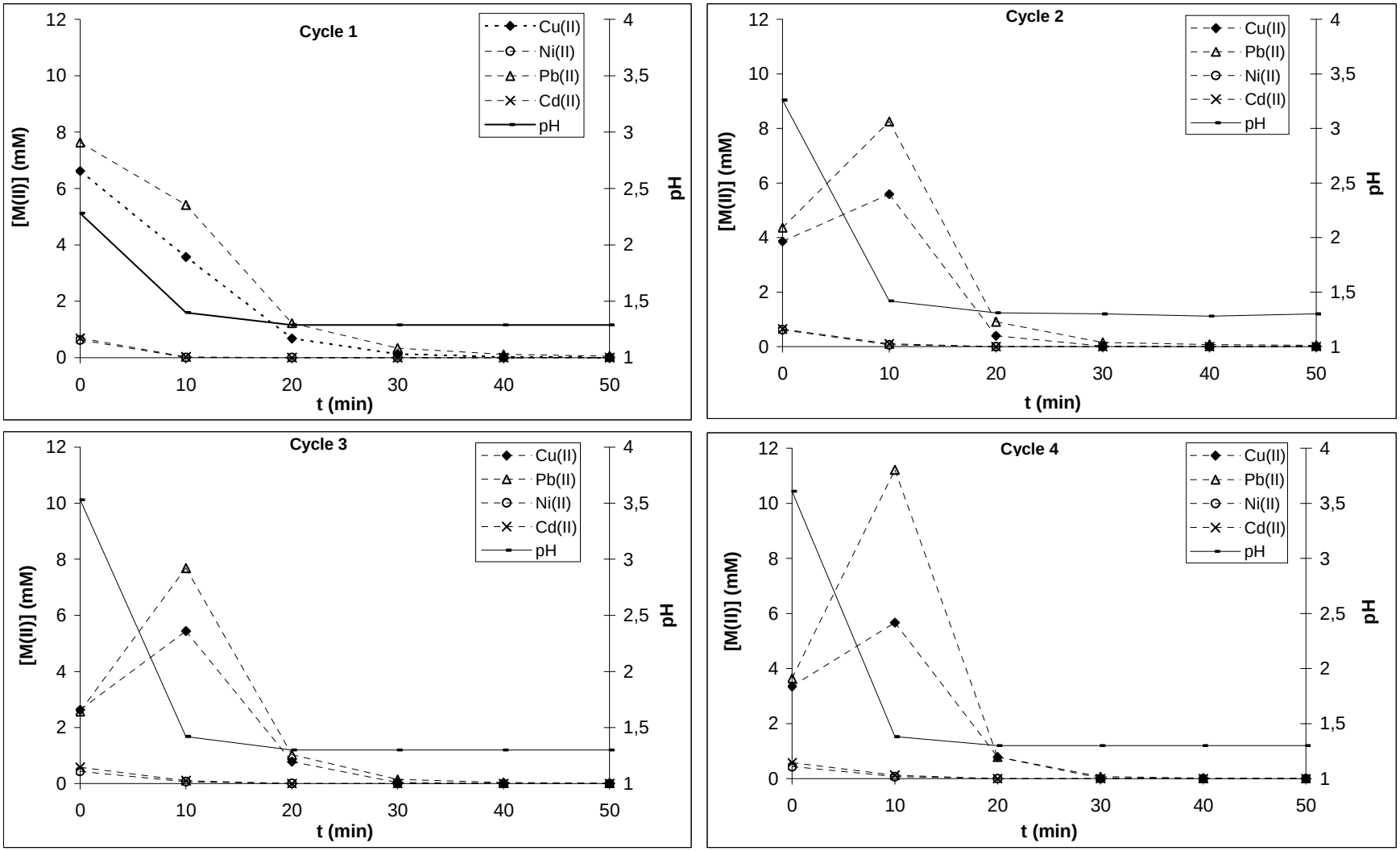

Figure 10: Cu(II), Ni(II), Pb(II) and Cd(II) concentration in solution (mmol·L^{-1}) and pH profile as a function of time for the quaternary mixture in the different desorption cycles. Feeding HCl concentration: 0.05 M (pH_0=1.30); Flow rate≈30 ml·h^{-1}.

Figure 10 puts into evidence that desorption occurs very fast for all the metals. Nevertheless, desorption of the different metals shows different profiles with time: while for Cu(II) and Pb(II) in the 2nd, 3rd and 4th cycles the peak of maximum eluted concentration occurs for the 2nd fraction, corresponding to 10 minutes of process, in the case of Ni(II) and Cd(II), the highest eluted concentration is found in the 1st fraction, corresponding to the first sample eluted from the column. In the first cycle, the desorption profile observed was analogous for the four metals; maximum eluted concentration observed in the first eluted fraction.

In the first step of the desorption process the eluted fraction shows a very important pH increase from the initial value of 1.3 to values ranging from 2.25 to 3.53 from the 1st to the 4th desorption cycle respectively. After this first elution, the pH rapidly decreases in the outlet flow reaching the initial 1.3 values after 20 minutes for all the cycles.

The important pH increase in the desorption process can be explained by the strong proton consumption that takes place when metals bonded to the biomaterial are replaced by H^+.

To evaluate the sorption performance and stability of the material in the different desorption cycles, percentage of metal recovered on each desorption cycle had to be evaluated. The recovery percentage is referred to the individual metal sorbed amount observed on each sorption cycle, $q_{M(II)}$, that had been presented previously in **Table 4**.

The results of metal recovery after the different desorption cycles, expressed in percentage terms, are presented in **Table 6**.

Table 6: Cu(II), Ni(II), Pb(II) and Cd(II) recovery percentage after sorption from the quaternary mixture for the different desorption cycles.

	Recovery (%)			
Cycle	**Cu**	**Ni**	**Pb**	**Cd**
1	111.82	129.40	121.23	66.04
2	92.29	65.61	99.68	46.44
3	99.98	73.80	100.21	48.03
4	102.10	34.59	100.45	100.49

If recovery percentage for the different metals is plotted in the different cycles, the next graphic is obtained.

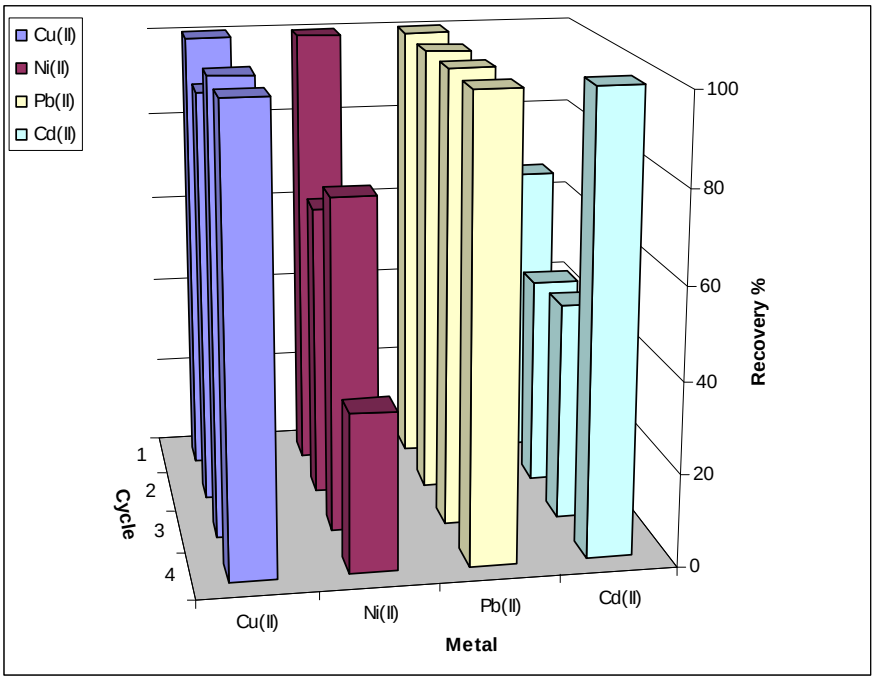

Figure 11: Recovery percentage for Cu(II), Ni(II), Pb(II) and Cd(II) in the different desorption cycles after sorbent loading with the quaternary mixture. $[M(II)]_0 \approx 0.2$ mM; $pH_0=5.20$.

The results obtained in the desorption study indicate that the sorbed Cu(II) and Pb(II) can be quantitatively recovered from the sorbent bed in our mild acidic conditions. **Figure 11** puts into evidence also that the recovery percentage achieved for these two metals is not dependent on the number of sorption/desorption cycles that the sorbent bed has suffered. In the case of Ni(II), a decrease in the efficiency of the recovery process takes place when advancing in the number of desorption cycles. For Cd(II), the recovery percentage seems to exhibit a general increasing trend. The different observed phenomena for Cu(II), Ni(II), Pb(II) and Cd(II) may be caused by changes on the chemistry and of the structure of the biosorbent, as well as by changes of the flow and mass transport conditions within the column. Sorption properties through a given metal may be enhanced or diminished by chemical changes of the structure derived form the acidic treatment, such as activation/deactivation or generation/destruction of specific sorption sites on lignin, which is known to play a major role in biosorption by this kind of materials (Villaescusa *et al.*, 2004).

In any case, if GS sorption behaviour from the quaternary mixture is accepted, taking into account that only Cu(II) and Pb(II) are successfully adsorbed (**Table 4**; Cu(II)+Pb(II) represent about 90 % of the total metal mass sorbed), it can be concluded that the reutilization of the biomaterial for the efficiently separation and recovery of these two metals in this particular multimetal solution is possible. Desorption yields a relatively small volume of highly concentrated metal solutions making possible to eventually recover the metal by conventional electrowinning processes (Volesky, 2003).

5.5. Effect of temperature on Cu(II), Ni(II), Pb(II) and Cd(II) equilibrium

As it had been observed and discussed previously in sections 5.2, 5.3 and 5.4 of the present chapter, divalent cations when present in mixtures, interact in column through competitive ion exchange mechanisms (among others), involving this process that different metals compete for a limited number of binding sites. The degree of mutual inhibition of competing sorbates should be related to the relative size of the molecules being adsorbed, to the relative sorbent affinities towards a metal and to the concentrations of sorbates (Volesky, 2003). In this chapter it has been observed that when the column saturation is approached, species with a lower affinity are pushed off by other species with higher affinity and displacement of the first species occurs. As it had been discussed previously, the condition under which overshoots occur can be formulated as follows: low-affinity species present in the feeding effluent overshoot in the column outlet flow only if the species with the highest affinity in the feed are bound to the biosorbent more strongly than the metals with which the biosorbent had been presaturated.

From the results obtained in the study of metal sorption from the binary mixtures, an apparent affinity ranking according to the overshoots observed was proposed. This grape stalk-divalent metal affinity ranking was, from the metal sorbed with highest affinity to the sorbed with lowest: Pb>Cu>Cd>Ni.

As it had been previously indicated, in our case, the column was always fed with a multimetal solution with a constant equimolar concentration of 0.2 mM on each of the metals, so that the overshoots observed for some of the systems could not be due to a concentration effect, removing thus this variable as a possible explanation of the

overconcentration phenomena and limiting the explanation to the different strength of the interactions sorbent-sorbate.

Despite column experiments provided useful information about the dynamics of divalent metal sorption, amount of metal sorbed as a function of time, maximum capacity and about the sorption incompatibilities of the different metals, no affinity parameters could be derived from these experiments. Furthermore, it had been previously demonstrated that the whole affinity ranking observed in binary mixtures could not be described in basis to the tendency of the metal to form hydrolysed species.

In an attempt to go further in the comprehension of the column overshoot phenomena, the obtention of empirical parameters that could quantify the energy of the interaction metal-sorbate were needed.

In this section, sorption isotherms of Cu(II), Ni(II), Pb(II) and Cd(II) onto GS at different temperature within the range 5 to 60 ºC will be generated. From the experimental sorption equilibrium results, thermodynamic parameters related to the affinity and energy of the sorbent-sorbate interaction will be obtained and discussed in an attempt to give an explanation to the overshoot phenomena observed in the continuous experiments.

5.5.1. Sorption isotherms

Cu(II), Ni(II), Pb(II) and Cd(II) sorption isotherms for the different temperatures were obtained according to the procedure described in the methodology section of the present chapter (section 4.3). In the next table, the results of initial and equilibrium metal concentration in solution are presented.

Table 7: Cu(II), Ni(II), Pb(II) and Cd(II) initial (C_0; mM) and equilibrium (C_e; mM) concentration in solution after contact with GS. Initial pH=5.2; T: 5-60 ºC.

			Cu(II)						**Ni(II)**		
	5 ºC	**20 ºC**	**35 ºC**	**50 ºC**	**60 ºC**		**5 ºC**	**20 ºC**	**35 ºC**	**50 ºC**	**60 ºC**
C_0	C_e	C_e	C_e	C_e	C_e	**C_0**	C_e	C_e	C_e	C_e	C_e
0.09	0.003	0.009	0.006	0.014	0.015	0.083	0.005	0.005	0.006	0.009	0.014
0.15	0.008	0.009	0.011	0.016	0.026	0.183	0.013	0.015	0.017	0.023	0.027
0.46	0.022	0.036	0.045	0.058	0.064	0.524	0.107	0.098	0.115	0.121	0.121
0.80	0.068	0.082	0.107	0.121	0.153	0.770	0.247	0.238	0.243	0.252	0.265
1.62	0.369	0.386	0.427	0.427	0.456	1.561	0.900	0.945	0.962	0.998	0.999
3.38	1.875	1.864	1.907	1.683	1.767	3.879	2.951	2.860	2.831	2.902	2.841
5.11	3.557	3.414	3.589	3.352	3.313	6.226	5.052	5.032	5.009	5.009	5.011
8.26	6.814	6.660	6.621	6.530	6.476	9.800	8.608	8.347	8.542	8.408	8.618
11.65	10.193	10.020	10.143	9.880	9.822	14.373	13.076	12.879	13.061	12.892	13.125
16.89	15.399	15.263	15.383	15.162	15.013	20.750	19.348	19.337	19.513	19.114	19.456
			Pb(II)						**Cd(II)**		
	5 ºC	**20 ºC**	**35 ºC**	**50 ºC**	**60 ºC**		**5 ºC**	**20 ºC**	**35 ºC**	**50 ºC**	**60 ºC**
C_0	C_e	C_e	C_e	C_e	C_e	**C_0**	C_e	C_e	C_e	C_e	C_e
0.006	0.000	0.000	0.000	0.000	0.000	0.047	0.000	0.000	0.000	0.001	0.000
0.038	0.000	0.000	0.000	0.000	0.000	0.099	0.002	0.001	0.002	0.006	0.006
0.130	0.000	0.000	0.000	0.000	0.000	0.325	0.022	0.019	0.020	0.025	0.023
0.218	0.000	0.000	0.000	0.001	0.001	0.511	0.059	0.045	0.048	0.058	0.043
0.458	0.003	0.002	0.001	0.005	0.005	0.966	0.215	0.220	0.185	0.211	0.200
1.103	0.036	0.025	0.037	0.055	0.054	1.975	0.795	0.849	0.809	0.840	0.823
1.546	0.182	0.195	0.190	0.185	0.189	2.948	1.526	1.652	1.618	1.661	1.661
2.432	0.813	0.784	0.807	0.805	0.816	4.786	3.379	3.364	3.331	3.339	3.386
3.401	1.755	1.741	1.639	1.701	1.767	6.940	5.289	5.357	5.317	5.293	5.424
4.783	3.022	3.033	2.993	3.038	2.982	9.548	7.832	7.965	7.864	7.681	8.093

With the data presented in this table, the metal sorbed amount for each temperature and each initial metal concentration was calculated. The results obtained are presented in **Table 8**.

Table 8: Cu(II), Ni(II), Pb(II) and Cd(II) sorbed amount, (q_e; mmol·g^{-1}) as a function of the initial sorbent concentration, (C_0; mM). Initial pH=5.2; T: 5-60 ºC.

	Cu(II)						Ni(II)				
	5 ºC	20 ºC	35 ºC	50 ºC	60 ºC		5 ºC	20 ºC	35 ºC	50 ºC	60 ºC
C_0	q_e	q_e	q_e	q_e	q_e	C_0	q_e	q_e	q_e	q_e	q_e
0.09	0.013	0.012	0.012	0.011	0.011	0.083	0.012	0.012	0.012	0.011	0.010
0.15	0.021	0.021	0.021	0.020	0.019	0.183	0.026	0.025	0.025	0.024	0.023
0.46	0.066	0.064	0.063	0.061	0.060	0.524	0.063	0.064	0.061	0.060	0.060
0.80	0.110	0.107	0.104	0.102	0.097	0.770	0.078	0.080	0.079	0.078	0.076
1.62	0.188	0.185	0.179	0.179	0.175	1.561	0.099	0.092	0.090	0.084	0.084
3.38	0.226	0.228	0.221	0.255	0.242	3.879	0.139	0.153	0.157	0.147	0.156
5.11	0.233	0.254	0.228	0.264	0.269	6.226	0.176	0.179	0.183	0.183	0.182
8.26	0.216	0.239	0.245	0.259	0.267	9.800	0.179	0.218	0.189	0.209	0.177
11.65	0.218	0.244	0.226	0.265	0.274	14.373	0.195	0.224	0.197	0.222	0.187
16.89	0.223	0.243	0.226	0.259	0.281	20.750	0.210	0.212	0.186	0.245	0.194
	Pb(II)						Cd(II)				
	5 ºC	20 ºC	35 ºC	50 ºC	60 ºC		5 ºC	20 ºC	35 ºC	50 ºC	60 ºC
C_0	q_e	q_e	q_e	q_e	q_e	C_0	q_e	q_e	q_e	q_e	q_e
0.006	0.001	0.001	0.001	0.001	0.001	0.047	0.007	0.007	0.007	0.007	0.007
0.038	0.006	0.006	0.006	0.006	0.006	0.099	0.015	0.015	0.014	0.014	0.014
0.130	0.020	0.020	0.020	0.020	0.020	0.325	0.045	0.046	0.046	0.045	0.045
0.218	0.033	0.033	0.033	0.033	0.032	0.511	0.068	0.070	0.069	0.068	0.070
0.458	0.068	0.068	0.069	0.068	0.068	0.966	0.113	0.112	0.117	0.113	0.115
1.103	0.160	0.162	0.160	0.157	0.157	1.975	0.177	0.169	0.175	0.170	0.173
1.546	0.205	0.203	0.203	0.204	0.204	2.948	0.213	0.194	0.200	0.193	0.193
2.432	0.243	0.247	0.244	0.244	0.242	4.786	0.211	0.213	0.218	0.217	0.210
3.401	0.247	0.249	0.264	0.255	0.245	6.940	0.248	0.238	0.243	0.247	0.227
4.783	0.264	0.262	0.269	0.262	0.270	9.548	0.257	0.237	0.253	0.280	0.218

When equilibrium metal concentration in solution (mol·L^{-1}) is plotted as a function of metal concentration in the solid phase (mol·g^{-1}), the sorption isotherms are obtained. Cu(II), Ni(II), Pb(II) and Cd(II) isotherms for the different temperatures are presented in the next figure.

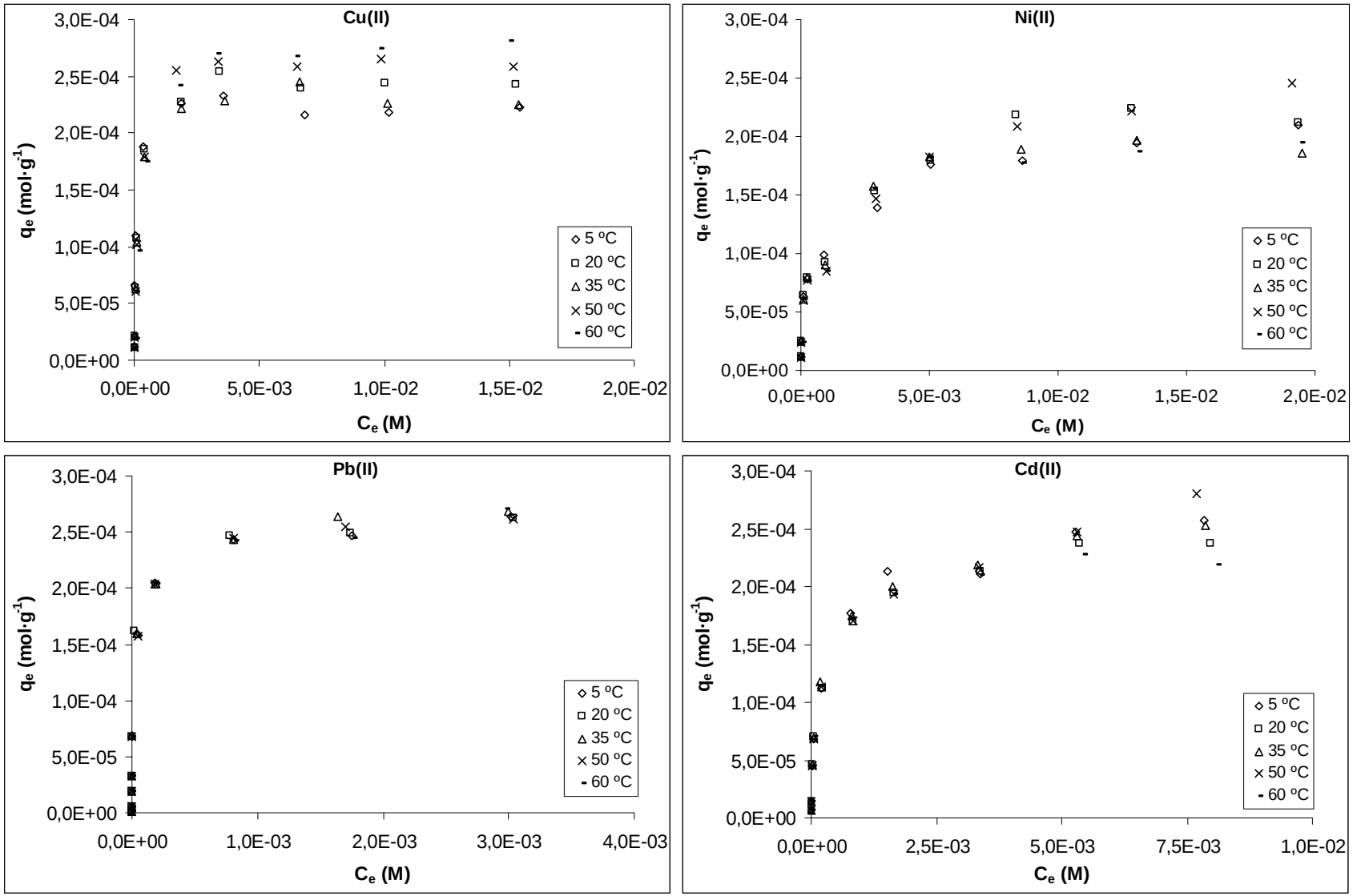

Figure 12: Sorption isotherms of Cu(II), Ni(II), Pb(II) and Cd(II) onto GS. T: 5-60 ºC.

This figure clearly demonstrates that the amount of metal sorbed, Cu(II), Ni(II), Pb(II) or Cd(II), increases until the achievement of a maximum value for all the temperatures studied. Temperature, in our studied range, seems not to have a clear effect on the maximum sorption capacity of GS for any of the divalent metals, except for Cu(II). In this case, the increase of temperature involves an experimental sorption capacity increase at equilibrium from 0.22 $mmol \cdot g^{-1}$ at 5 ºC to 0.28 at 60 ºC.

Experimental Cu(II), Ni(II), Pb(II) and Cd(II) sorption equilibrium results onto GS were modelled. The different models and the results obtained when submitting the experimental sorption data to them, are presented and discussed in the next section.

5.5.2. Calculation of equilibrium parameters of adsorption

The equilibrium adsorption isotherms are one of the most important data to understand the sorption mechanism. Among the different isotherm equations available, three of the most important isotherms have been chosen for this study: Langmuir, Freundlich and Dubinin–Radushkevich (D–R) isotherms.

As it had been previously discussed, in chapter 1, Langmuir model assumes that adsorption occurs at specific homogenous sites within the adsorbent. This treatment is based on the assumption that a maximum adsorption corresponds to a saturated monolayer of solute molecules on the adsorbent surfaces, that the energy of adsorption is constant and that there is no transmigration of adsorbate in the plane of the surface. From this model, the maximum uptake, $q_{max.}$ ($mol \cdot g^{-1}$) and K_L ($L \cdot mol^{-1}$), constant related to energy of adsorption which quantitatively reflects the affinity between the sorbent and the sorbate can be obtained. Thus, the effect of the temperature and of the metal on the different sorption equilibriums can be compared.

By means of the Langmuir constant, the effect of isotherm shape can be discussed with a view to predict whether an adsorption system is favourable or unfavourable. The essential feature of the Langmuir isotherm can be expressed by means of the parameter R_L, a dimensionless constant referred to as separation factor or equilibrium parameter. R_L is calculated using the following equation:

$$R_L = \frac{1}{1 + K_L \cdot C_0} \qquad (2)$$

where K_L is the Langmuir constant in $L \cdot mol^{-1}$ and C_0 is the initial metal concentration expressed in $mol \cdot L^{-1}$. The R_L parameter is considered as more reliable indicator of the adsorption being the next four, the possible situations (Angove *et al*., 1997; Ho *et al*., Özcan *et al*., 2005):

Table 9: The isotherms shape represented by the R_L value

R_L value	**Type of isotherm**
$R_L>1$	Unfavourable
$R_L=1$	Linear
$0<R_L<1$	Favourable
$R_L=0$	Irreversible

The Freundlich isotherm is an empirical equation employed to describe sorption in heterogeneous systems. On its linear form, the Freundlich equation is:

$$\log q_e = \log K_F + \frac{1}{n} \log C_e \qquad (3)$$

where K_F and 1/n are empirical constants indicate of the relative sorption capacity and sorption intensity respectively.

For the treatment of the experimental data of this study, also the Dubinin-Radushkevich (D-R) isotherm model was used because this model is more general than Langmuir and because it does not assume a homogenous surface or a constant adsorption potential. D-R model has been applied by several authors to distinguish between physical and chemical metal adsorption onto different biomaterials (Özcan *et al*., 2005; Benhammou *et al*., 2005) and it follows, on its linear form, the next equation:

$$\ln q_e = \ln q_m - \beta \varepsilon^2 \qquad (4)$$

where β is a constant related to the mean free energy of adsorption per mole of the adsorbate ($mol^2 \cdot J^{-2}$); q_m the theoretical saturation capacity of the monolayer and ε is the Polanyi potential, whose expression is equal to RTln(1+(1/Ce)), being R (8.314 $J \cdot mol^{-1} \cdot K^{-1}$) the gas constant; and T (K), the absolute temperature. Hence, by

plotting $\ln(q_e)$ against ε^2 it is possible to generate the value of q_m ($mol \cdot g^{-1}$) from the intercept, and the value of β from the slope.

The constant β gives an idea about the mean free energy, E ($J \cdot mol^{-1}$) of adsorption per molecule of adsorbate when it is transferred to the surface of the solid from infinity in the solution and can be calculated using the relationship (Hobson, 1969; Hasany and Chaudhary, 1996; Dubey and Gupta, 2005):

$$E = \frac{1}{(2\beta)^{1/2}} \qquad (5)$$

The linear plots of Langmuir, Freundlich and Dubinin-Radushkevich (D–R) adsorption isotherms corresponding to Cu(II), Ni(II), Pb(II) and Cd(II) sorption onto GS for the different temperatures are illustrated in **Figures 13, 14** and **15 respectively**. Also the separation factor (R_L) for the different metals has been plotted and presented in **Figure 16**.

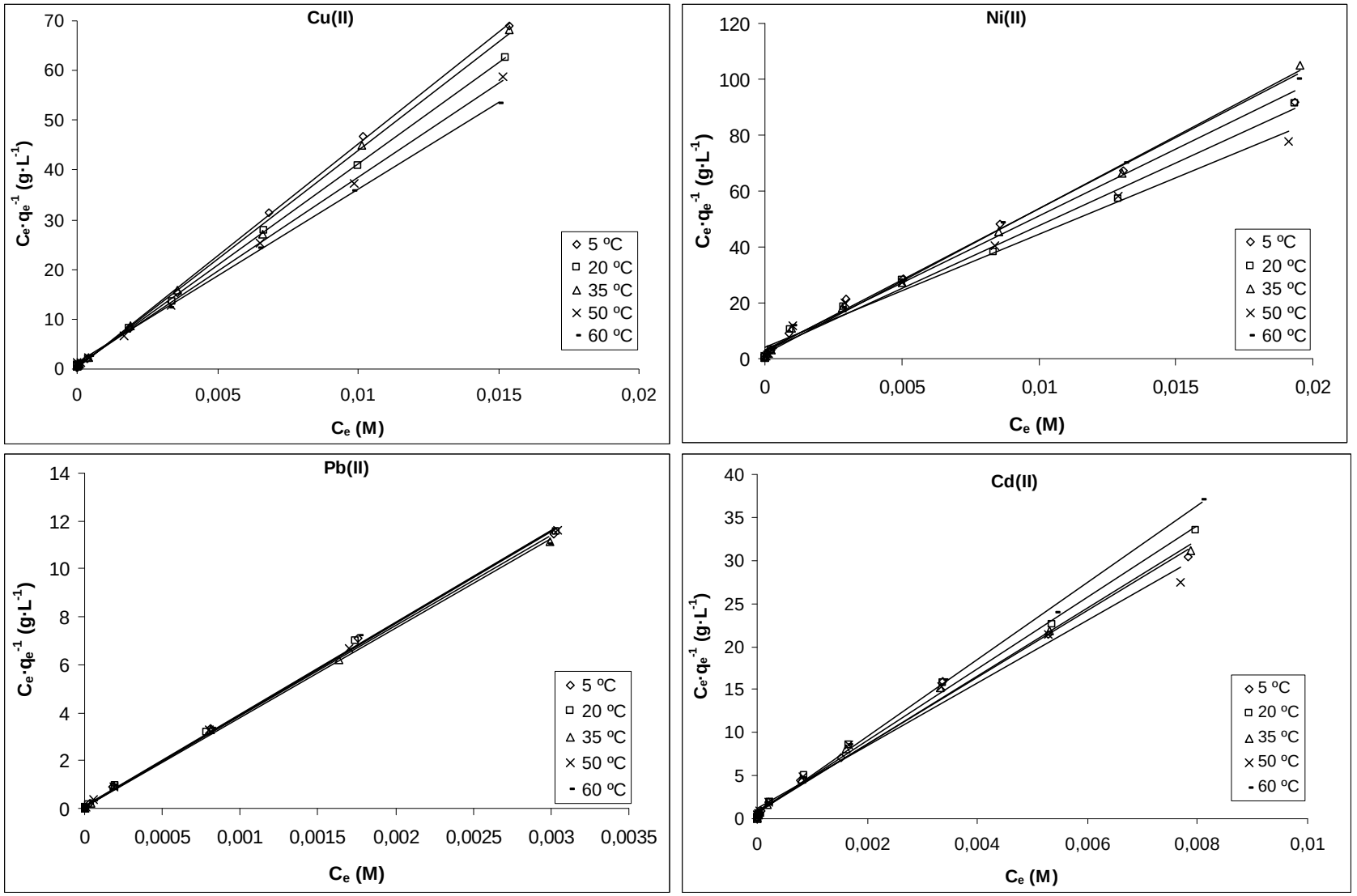

Figure 13: Langmuir model fitting of the experimental Cu(II), Ni(II), Pb(II) and Cd(II) sorption results onto GS. T: 5-60 ºC.

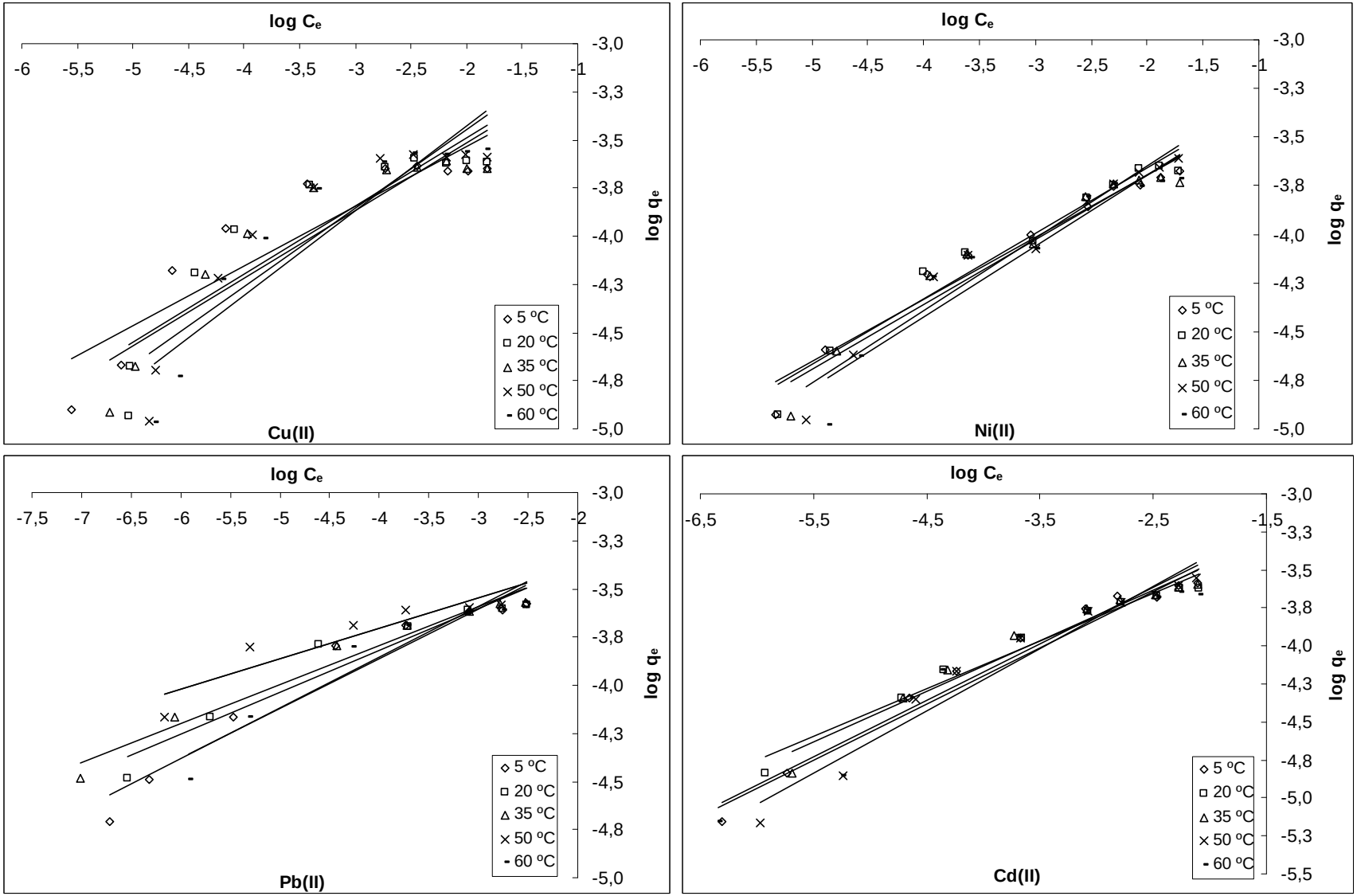

Figure 14: Freundlich model fitting of the experimental Cu(II), Ni(II), Pb(II) and Cd(II) sorption results onto GS. T: 5-60 ºC.

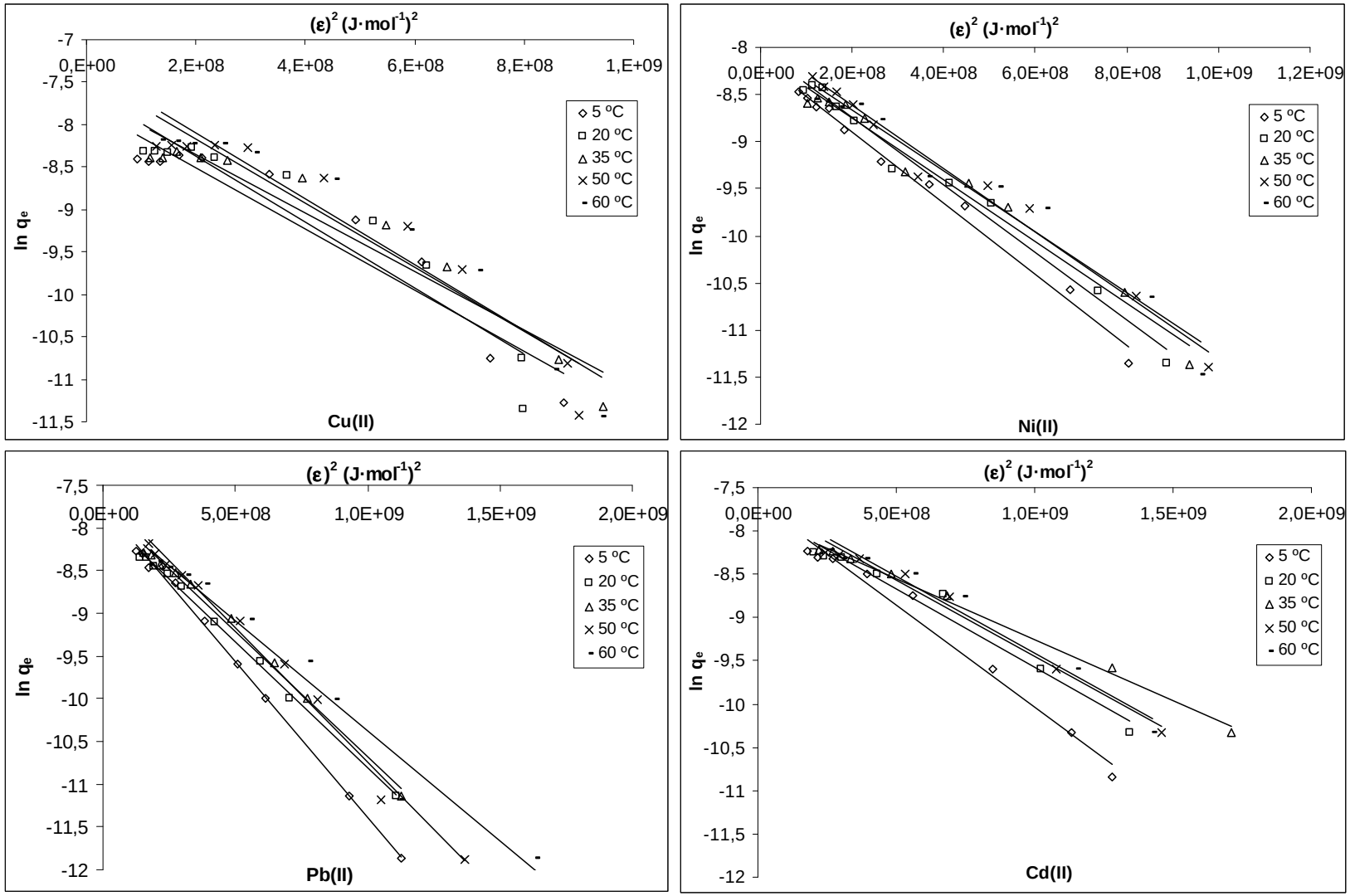

Figure 15: Dubinin-Radushkevich model fitting of the experimental Cu(II), Ni(II), Pb(II) and Cd(II) sorption results onto GS. T: 5-60 ºC.

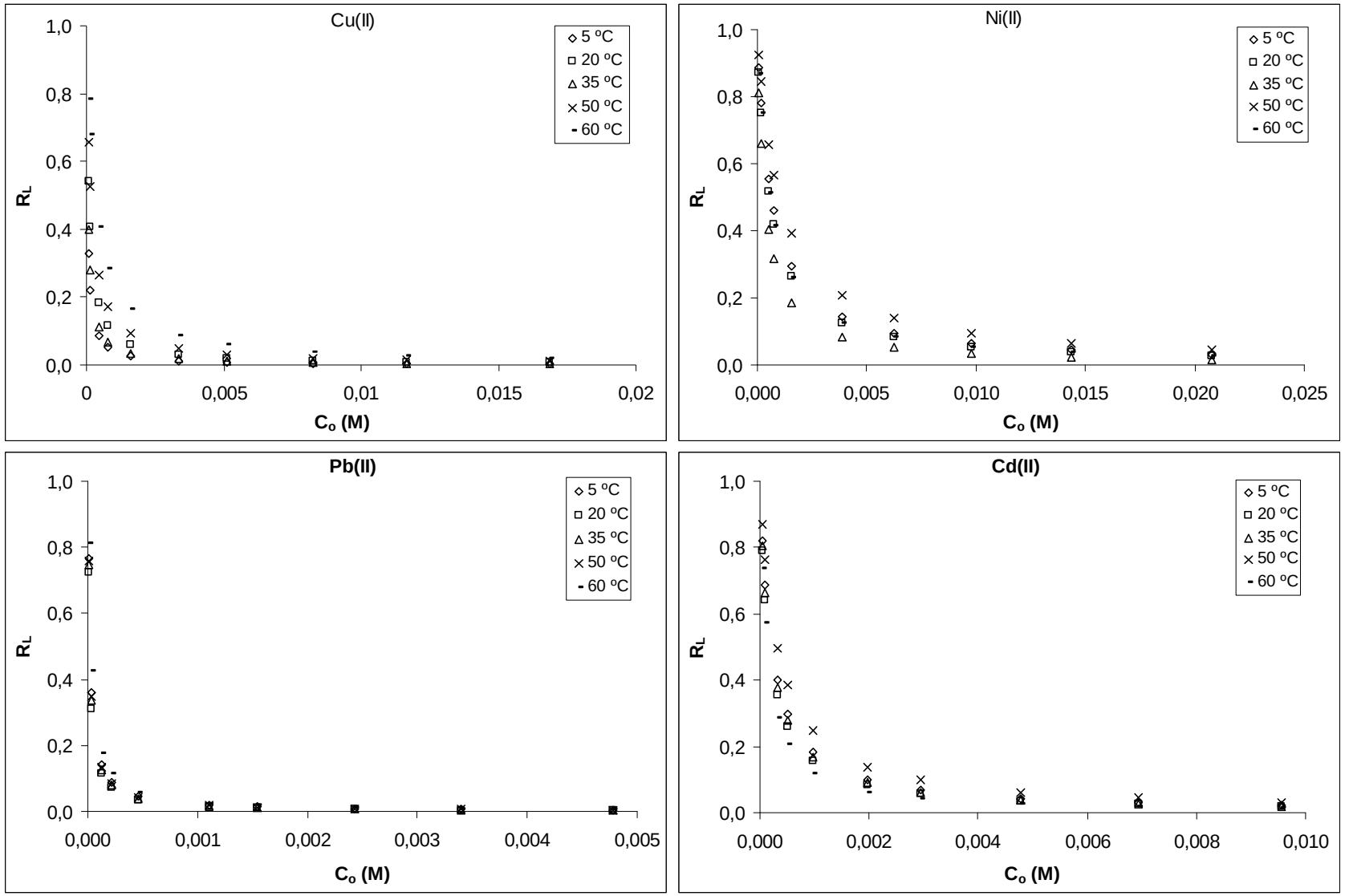

Figure 16: Variation of adsorption intensity (R_L) for Cu(II), Ni(II), Pb(II) and Cd(II) with the initial metal concentration. T: 5-60 ºC.

From the linear plots of the different isotherm models, the characteristic parameters for the adsorption of divalent metal sorption onto GS were calculated and are presented in **Table 10**. The validity of the different equilibrium sorption model was tested by the determination coefficients obtained when submitting experimental results to the different lineal forms of the models.

As it can be observed in **Figure 16**, the profile of the dimensionless separation factor (R_L) with initial metal concentration ($mol \cdot L^{-1}$) for the different M(II)-GS systems and for the different temperatures indicates a decreasing tendency of R_L when increasing metal concentration. The values $0<R_L<1$ obtained for all the systems indicate that Cu(II), Ni(II), Pb(II) and Cd(II) sorption onto GS is a favourable process.

Table 10: Adsorption isotherm constants for the adsorption of Cu(II), Ni(II), Pb(II) and Cd(II) onto GS as a function of temperature.

		Langmuir			Freundlich			Dubinin-Radushkevich			
Metal	**T (ºC)**	**$Q_{max}\cdot10^4$ ($mol\cdot g^{-1}$)**	**$K_L\cdot10^{-4}$ ($L\cdot mol^{-1}$)**	**R^2**	**1/n**	**K_F**	**R^2**	**$Q_{max}\cdot10^4$ ($mol\cdot g^{-1}$)**	**$\beta\cdot10^9$ ($mol^2\cdot kJ^{-2}$)**	**E ($kJ\cdot mol^{-1}$)**	**R^2**
Cu(II)	**5**	2.22	2.34	0.999	0.31	2.04	0.836	4.20	3.61	11.76	0.913
	20	2.46	0.97	0.999	0.36	2.26	0.824	5.04	3.89	11.34	0.895
	35	2.29	1.72	0.998	0.31	2.02	0.858	4.67	3.44	12.06	0.931
	50	2.69	0.60	0.999	0.41	2.55	0.840	6.07	3.78	11.50	0.919
	60	2.85	0.32	0.999	0.44	2.75	0.859	6.64	3.88	11.35	0.926
Ni(II)	**5**	2.09	0.15	0.992	0.32	2.09	0.976	2.93	3.79	11.49	0.913
	20	2.22	0.18	0.993	0.34	2.17	0.958	3.24	3.58	11.82	0.895
	35	1.93	0.28	0.997	0.33	2.16	0.941	3.06	3.28	12.35	0.931
	50	2.45	0.10	0.986	0.37	2.36	0.958	3.55	3.37	12.18	0.919
	60	1.97	0.18	0.997	0.37	2.32	0.914	3.31	3.23	12.44	0.926
Pb(II)	**5**	2.61	4.71	0.999	0.37	2.35	0.972	4.67	2.36	14.55	0.913
	20	2.60	5.86	0.999	0.31	2.06	0.972	4.22	1.81	16.64	0.895
	35	2.68	5.23	0.999	0.33	2.15	0.957	3.92	1.41	18.81	0.931
	50	2.61	4.95	0.994	0.41	2.55	0.957	4.59	1.76	16.84	0.919
	60	2.65	3.55	0.997	0.37	2.34	0.940	4.81	1.77	16.80	0.926
Cd(II)	**5**	2.57	0.46	0.993	0.26	1.83	0.938	4.37	3.66	11.69	0.913
	20	2.40	0.56	0.997	0.22	1.65	0.926	3.84	2.95	13.03	0.895
	35	2.52	0.51	0.995	0.20	1.59	0.966	4.33	2.93	13.06	0.931
	50	2.73	0.31	0.985	0.16	1.44	0.850	5.02	3.15	12.60	0.919
	60	2.24	0.76	0.998	0.26	1.81	0.921	4.12	2.58	13.92	0.926

As it can be seen in the table, the three isotherm models provided acceptable R^2 values despite the best fitting was obtained when results were submitted to Langmuir model. Maximum capacity and M(II)-GS affinity, calculated by means of the Langmuir equation for each metal and temperature presented in **Table 10** indicates that, in general, temperatures in the range 5-60 ºC does not to strongly affect sorption of the studied metals onto GS, except in the case of Cu(II), where the increase on temperature is related to an increase on maximum sorption capacity. When q_{max} is compared for a standard temperature of 20 ºC it can be observed that a very similar capacity, around $2.5 \cdot 10^{-4}$ mol·g^{-1}, is achieved for all the studied metals. Maximum capacity values obtained by means of Langmuir model for copper, nickel, lead and cadmium sorption onto GS at 20 ºC, are in agreement with previously reported data (Martínez *et al*., 2006; Villaescusa *et al*., 2004). The effect of temperature on the strength of the interaction sorbent-sorbate will be explored later by calculating specifically the thermodynamic parameters of the adsorption process.

Modelisation according to the Dubinin–Radushkevich (D–R) equation was able to provide a good fitting of the experimental results. This model allowed us to calculate the mean free energy of adsorption E (kJ·mol^{-1}), according to Eq. (5). This parameter provides useful information to distinguish adsorption mechanism, as chemical ion exchange or physical adsorption. If the magnitude of E is between 8 and 16 kJ·mol^{-1}, the adsorption process follows a chemical ion-exchange (Helfferich, 1962), while for values of E<8 kJ·mol^{-1}, the adsorption process is of a physical nature (Onyango *et al*., 2004; Özcan *et al*., 2005). Values higher than 16 kJ·mol^{-1} would be indicative of more energetic interactions than the corresponding to an ion exchange process. As it can be seen in **Table 10**, values of adsorption mean free energies in the range 8<E(kJ·mol^{-1})<16 were obtained for Cu(II), Ni(II) and Cd(II) sorption at all the temperatures and for Pb(II) at the lowest one, 5 ºC. These results point out that Cu(II), Ni(II) and Cd(II) sorption at all the studied temperatures and Pb(II) sorption at 5 ºC, proceeds mainly via ion exchange. For Pb(II) at temperatures of 20 ºC and higher, values in the range 16.64<E<18.81 would indicate that there exists an extra contribution to ion exchange, based in the formation of stronger Pb(II)-GS bonds.

The study of metal sorption equilibrium as a function of temperature can provide useful information about thermodynamic parameters governing the sorption process, such the

energy and the randomness balance of the sorption process. These thermodynamic data can be used in an attempt to explain the different sorption behaviour of the different metals in continuous. In the next section, calculation on the sorption thermodynamics of Cu(II), Ni(II), Pb(II) and Cd(II) will be carried out and the obtained results will be discussed.

5.5.3. Calculation of thermodynamics parameters of adsorption

Temperature dependence of the sorption process is associated with several thermodynamic parameters and these are necessary to conclude whether the process is spontaneous or not. The Gibbs free energy change, ΔG^0, is an indicative of the spontaneity of a chemical reaction and, therefore, it is an important criterion for spontaneity evaluation. Also, both energetic and entropic factors must be considered in order to determine the Gibbs free energy of the process. Reactions occur spontaneously at a given temperature if ΔG^0 has a negative value. ΔG^0 can be determined from the following equation:

$$\Delta G^0 = -RT \ln K_L \qquad (6)$$

where R is the gas constant (8.314 $J \cdot mo^{-1} \cdot K^{-1}$) and T is the absolute temperature (K). This equation can be linearized as:

$$\Delta G^0 = \Delta H^0 - T\Delta S^0 \qquad (7)$$

The Langmuir equilibrium constant (K_L) can be introduced in the Van Hoff equation to determine the enthalpy (ΔH^0) and the entropy (ΔS^0):

$$\ln K_L = \frac{\Delta S^0}{R} - \frac{\Delta H^0}{RT} \qquad (8)$$

where values of ΔH^0 and ΔS^0 can be determined from the slope and the intercept of the plot of ln K_L versus 1/T. The values of ΔG^0, ΔH^0 and ΔS^0 for the sorption of Cu(II), Ni(II), Pb(II) and Cd(II) onto grape stalk for the different temperatures have been calculated and are presented in **Table 11**.

Table 11: Thermodynamic parameters of Cu(II), Ni(II), Pb(II) and Cd(II) sorption onto GS. T: 5-60 ºC.

Metal	T (ºC)	ΔG^0 (kJ·mol^{-1})	ΔH^0 (kJ·mol^{-1})	ΔS^0 (J·mol^{-1}·K^{-1})
	5	-23.27		
	20	-22.38		
Cu(II)	**35**	-24.98	-17.48	19.99
	50	-23.36		
	60	-22.31		
	5	-16.95		
	20	-18.26		
Ni(II)	**35**	-20.34	-1.30	57.45
	50	-18.54		
	60	-20.79		
	5	-24.88		
	20	-26.76		
Pb(II)	**35**	-27.83	-3.45	78.32
	50	-29.04		
	60	-29.02		
	5	-19.52		
	20	-21.05		
Cd(II)	**35**	-21.87	-5.99	57.34
	50	-21.63		
	60	-24.76		

The negative ΔG^0 values obtained confirm the feasibility of the process and the spontaneous nature of Cu(II), Ni(II), Pb(II) and Cd(II) sorption onto GS.

As it can be observed in this table, negative ΔH^0 values were obtained for the sorption of the four metals, indicating thus that sorption is exothermic. It has to be remarked also that, from the four metals, the sorption of Cu(II) is the process that involves a higher exchange of energy, releasing about 17.5 kJ per mol of sorbed metal. On the contrary, the sorption of all the other metals involves a much lower energy release, varying from about 6 kJ·mol^{-1} in the case of Cd(II) to only 1.30 kJ·mol^{-1} in the case of Ni(II).

The positive values of ΔS^0 observed for Cu(II), Ni(II), Pb(II) and Cd(II) indicates that the randomness at the solid/liquid interface increases during the adsorption of these divalent metal ions onto GS (Özcan *et al*., 2005). A possible explanation to this increase of the disorder of the system can be that the adsorbed water molecules, which are displaced by the adsorbate species when metals are transferred from the liquid to the solid phase, gain more translational energy than the energy lost by the adsorbate ions, thus allowing the increase of randomness in the system (Bulut and Tez, 2007).

For an easier visualization of the effect of temperature on the spontaneity of the sorption process, the values of ΔG^0 obtained for the different metals have been plotted as a function of temperature in the next figure.

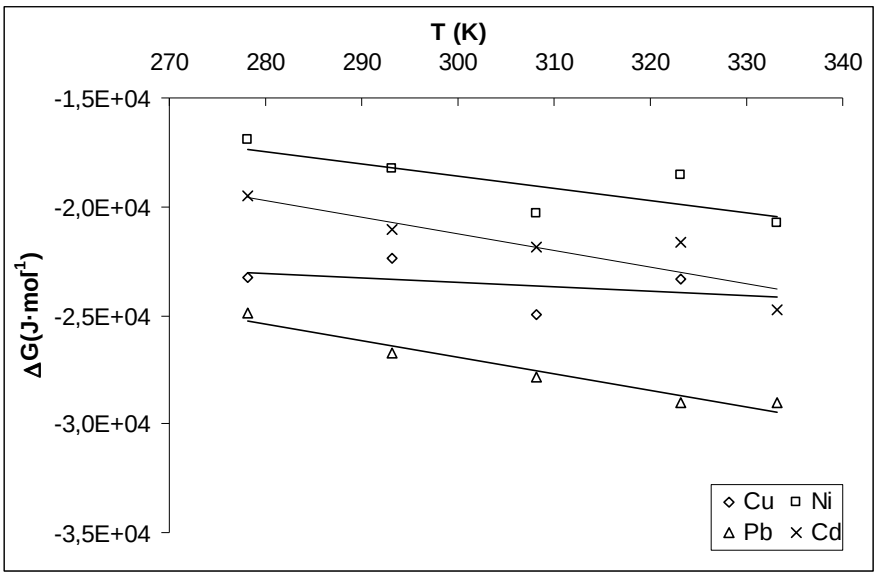

Figure 17: Gibbs free energy variation with temperature for Cu(II), Ni(II), Pb(II) and Cd(II) sorption onto GS.

The figure shows a general decreasing trend on the ΔG^0 when increasing the temperature of the media. This can be summarized with the values of the slopes of this plot for the different metals. The obtained values were: Cu(II): -19.26; Ni(II): -56.01; Pb(II): -76.60 and Cd(II): -76.57. The negative values observed for all the metals indicate that the spontaneity of the sorption process increases when increasing the temperature, being Pb(II) and Cd(II) the most positively affected due to its almost equal and high negative slope values.

When comparing the different values of enthalpy, entropy and variation on Gibbs free energy for the sorption of the different metals, a ranking according to the different thermodynamics parameters can be established. So that, in basis to the energy release when the metal is adsorbed:

$$\Delta H^0: \quad Cu>Cd>Pb>Ni$$

In basis to the increase of randomness that metal sorption provokes in the system:

$$\Delta S^0: \quad Pb>Ni\approx Cd>Cu$$

And finally, in basis to the more general criterion of spontaneity of the sorption process for temperatures within 5 to 50 ºC:

$$\Delta G^0 \text{ (5-50 ºC)}: \text{ Pb>Cu>Cd>Ni}$$

but it has to be remarked that for the highest temperature, 60 ºC, an inversion on the spontaneity of the sorption process takes place between Cd(II) and Cu(II), taking the ranking the next form:

$$\Delta G^0 \text{ (60 ºC)}: \text{ Pb>Cd>Cu>Ni}$$

From all the 16 possible spontaneity sorption ranking combinations, the one predicted by the thermodynamics in the range 5 to 50 ºC is exactly the affinity sequence observed when studying the competence in continuous flow sorption in binary mixtures. Results obtained in this section provide a successful explanation to the sorption competitive process observed in columns: the broad overshoot that Pb(II) provokes in all the other metals, the fact that Cu(II) provokes an overshoot only for Cd(II) and Ni(II) and, finally, that Cd(II) is only able to slightly replace Ni(II). Moreover, the affinity sequence is in agreement with the magnitude of the percentage of Capacity Loose for the Overshot metal (CLO) from the maximum to the equilibrium value observed in binary mixtures and presented previously in **Table 2**. For an easier visualization of this effect, a summary with the metals, difference on Gibbs free energy variation and CLO values is presented in the next table.

Table 12: Difference on the Gibbs free energy variation for the different individual sorption processes onto GS and percentage of Capacity Loose for the Overshot metal (CLO) observed for a temperature of 20 ºC.

M(II) reference	M(II) overshot	$\Delta G^0(\Delta G^0_{Mref} - \Delta G^0_{Mov})$ (kJ·mol^{-1})	CLO (%)
Pb(II)	Cu(II)	-4.38	1.5
	Cd(II)	-5.71	42.7
	Ni(II)	-8.50	93.8
Cu(II)	Cd(II)	-1.33	49.6
	Ni(II)	-4.12	95.5
Cd(II)	Ni(II)	-2.79	0

*ΔG^0_{Mref}: Gibbs free energy variation for the sorption of the reference metal (kJ·mol^{-1})
*ΔG^0_{Mov}: Gibbs free energy variation for the sorption of the overshot metal (kJ·mol^{-1})

As it can be seen in this table, the replacement in the solid phase of the metal overshot for the metal of reference is always a thermodynamically spontaneous process according to the negative values of ΔG^0 obtained.

The further the metals are in the spontaneity ranking, the higher the difference between the ΔG^0 of the sorption process. If the decay from the maximum to the equilibrium amount of metal sorbed for the overshot metals is compared (CLO values), it can be observed that, for a given metal of reference, the higher the difference in ΔG^0, the higher the percentage of capacity loose. These results confirm that in a continuous flow process, metal replacement of the species bonded with the lowest affinities occurs if in the effluent are present species capable of bonding the material with higher affinity. The obtained results point out that the study of the sorption thermodynamics could be successfully applied to the prediction of sorption incompatibilities observed in multimetal mixtures in continuous flow systems.

Thermodynamic sorption results obtained in this study have been compared with those reported by other authors when studying sorption of several heavy metal cations onto different biosorbents. As a summary, results are presented in the next table.

Table 13: Comparison of the thermodynamic parameters of sorption of different materials with the obtained for grape stalk.

Sorbent	Metal	ΔG^0 (kJ·mol^{-1})	ΔH^0 (kJ·mol^{-1})	ΔS^0 (J·mol^{-1})	Reference
Grape stalk	Cu(II)	-22.38	-17.48	19.99	This work
	Ni(II)	-18.26	-1.30	57.45	
	Pb(II)	-27.83	-3.45	78.32	
	Cd(II)	-21.05	-5.99	57.34	
Pseudomonas putida	Pb(II)	-21.20	-18.69	8.4	Uslu and Tanyol, 2006
	Cu(II)	-16.50	23.12	128	
Hazelnut shells	Ni(II)	-15.05	32.49	158.54	Bulut and Tez, 2007
	Pb(II)	-20.94	21.41	142.11	
	Cd(II)	-20.80	12.21	110.73	
Almond shells	Ni(II)	-12.36	47.29	199.00	
	Pb(II)	-21.57	50.55	233.32	
	Cd(II)	-17.45	17.76	118.28	
Capsicum annuum	Cu(II)	-15.93	-7.63	28.35	Özcan *et al*., 2005
Sporopollenin	Cu(II)	-7.54	17.55	85.58	Ünlü and Ersoz, 2006
	Pb(II)	-13.78	31.97	150.98	
	Cd(II)	-8.85	13.99	76.64	
Chitosan	Al(III)	-5.52	-51.03	150.19	Septhum *et al*., 2007

As it can be seen in this table, all the authors reported negative values of ΔG^0 and positive values of ΔS^0. These results point out that sorption is always a spontaneous process that involves an increase of the randomness of the system. On the other hand, reported ΔH^0 values are either positive or negative. Sorption processes showing negative enthalpy values would be the sorption of Cu(II), Ni(II), Pb(II) and Cd(II) onto GS, Pb(II) sorption onto *Pseudomonas putida*, Cu(II) sorption onto *Capsicum annuum* or Al(III) sorption onto chitosan. In contrast, positive enthalpy values have been reported for Cu(II) sorption onto *Pseudomonas putida*, Ni(II), Pb(II) and Cd(II) sorption onto both, hazelnut and almond shells or Cu(II), Pb(II) and Cd(II) sorption onto sporopollenin. These results indicate thus that metal sorption can occur with either release or absorption of energy to or from the system.

6. CONCLUSIONS

When continuous bed up-flow sorption from binary, ternary and quaternary Cu(II), Ni(II), Pb(II) and Cd(II) mixtures is studied, an overconcentration respect to the feeding concentration for some of these metals is observed in the outlet effluent (overshoots). The achievement of a maximum overconcentration produces an inflexion point in the breakthrough curve and, from this point, metal concentration in liquid phase decreases again to approach the concentration of the feeding effluent.

The analysis of the overshoots in binary equimolar mixtures allows proposing the next affinity ranking of the grape stalk for the different divalent metals.

Pb(II)>Cu(II)>Cd(II)>Ni(II).

In the case of sorption from single solutions, for all the metals, always a sorbent capacity about 0.2 $mmol \cdot g^{-1}$ is achieved. In the case of binary and ternary mixtures, despite the individual loading capacity of the sorbent material for a given metal is strongly dependent on the presence of the others, always the total sorption capacity, expressed as the sum of the individual amount of metal sorbed, was about 0.2 $mmol \cdot g^{-1}$, as in the case of the single metal solutions.

In sorption from quaternary Cu(II), Ni(II), Pb(II) and Cd(II) mixtures, only copper and lead can be simultaneously removed. At equilibrium, the sorbed amount of these two metals represents more than 80% of the total sorbed mass in all the sorption cycles.

Metals can be efficiently recovered and the sorbent bed can be regenerated by feeding the column with HCl 0.05 M at the same flow rate of the sorption experiments.

Sorption from the quaternary mixture in the raw material indicates that Ca^{2+} ion exchange mechanism could be the main responsible of metal sorption. After acidic regeneration of the sorbent bed, divalent metal sorption is due to a H^{+} ion exchange.

A constantly shortening breakthrough time from cycle to cycle takes place for all the metals, being the most important shortening the observed when the first (raw material) and second (after the first acidic desorption and re-conditioning of the bed) sorption cycles are compared. The mass transfer sorption zone broadened with increasing ‘‘age’’ of the sorbent. The shortening breakthrough time was apparently not the diminishing equilibrium

uptake capacity, but rather changes in the column overall sorption rate. While sorbent sites of the biomass were still available they seemed to become less accessible.

Cu(II), Ni(II), Pb(II) and Cd(II) sorption equilibrium onto grape stalk follows, for all the temperatures within range 5 to 60 ºC, a Langmuirian sorption trend. Freundlich and Dubinin–Radushkevich models also provide a successful description of the sorption equilibrium. The mean free energy E ($kJ \cdot mol^{-1}$) demonstrated that sorption of Cu(II), Ni(II) and Cd(II) onto grape stalk proceeds mainly via ion exchange. In the case of Pb(II), an extra contribution to the ion exchange and based in the formation of stronger bonds Pb(II)-GS at temperatures higher than 5 ºC might occur.

Cu(II), Ni(II), Pb(II) and Cd(II) sorption onto grape stalk is a spontaneous exothermic process that involves an increase of the randomness of the system.

The thermodynamic parameters of divalent metal sorption onto grape stalk allow establishing different rankings of the metals according to different criteria. In basis to the released energy when metal is being adsorbed: ΔH^0: Cu>Cd>Ni>Pb; to the increase of randomness that metal sorption provokes on the system: ΔS^0: Cd>Pb>Ni>Cu and finally, in basis to a more general criteria of spontaneity of the sorption process: ΔG^0 (5-50 ºC): Pb>Cu>Cd>Ni. From the 16 possible spontaneity sorption ranking combinations, the predicted by the thermodynamics in the range 5 to 50 ºC is exactly the affinity sequence observed when studying the competence in continuous bed up-flow sorption experiments in binary mixtures; ΔG^0 (5-50 ºC): Pb>Cu>Cd>Ni. Thermodynamics of sorption can be used to analyse and predict the overshoots observed in continuous processes.

7. REFERENCES

· Ahuja, P., Gupta, R., Saxena, R.X., Sorption and desorption of cobalt by *Oscilatoria anguistissima*. Current Microbiol. 39 (1999) 49–52.

· Aksu, Z., Determination of the equilibrium, kinetic and thermodynamic parameters of the batch biosorption of nickel(II) ions onto Chlorella vulgaris. Process Biochem. 38 (2002) 89-99.

· Angove, M.J., Johson, J.D., Wells, J.D., Adsorption of cadmium(II) on kaolinite, Colloid Surf. A: Phys. Eng. Aspects 126 (1997) 137-147.

· Antoniadis, V., Tsadilas, C.D., Sorption of cadmium, nickel and zinc in mono- and multimetal systems, Appl. Geochem. 22 (2007) 2375-2380.

· Atdor, I., Fourest, E., Volesky, B., Desorption of cadmium from algal biosorbent. Can. J. Chem. Eng., 73 (1995) 516–522.

· Bulut, Y., Tez, A., Adsorption studies on ground shells of hazelnut and almond, J. Hazard. Mater. (2007), doi. 10.1016/j.jhazmat.2007.03.044

· Chang, J.S., Chen, C.C., Biosorption of lead, copper and cadmium with continuous hollow-fiber microfiltration processes, Sep. Sci. Technol. 34 (1999) 1607-1627.

· Corami, A., Mignardi, S., Ferrini, V., Cadmium removal from single- and multi-metal (Cd+Pb+Zn+Cu) solutions by sorption on hydroxyapatite, J. Coll. Interf. Sci. 317 (2008) 402-408.

· Council Directive 98/83/EC of 3 November 1998 on the quality of water intended for human consumption, Off. J. Eur. Union, 5.12.98.

· Covelo, E.F., Andrade, M.L., Vega, F.A., Heavy metal adsorption by humic umbrisols: selectivity sequences and competitive sorption kinetics, J. Coll. Interf. Sci. 280 (2004) 1-8.

· Dubey, S.S., Gupta, R.K., Removal behaviour of babool bark (*Acacia nilotica*) for submicro concentrations of Hg^{2+} from aqueous solutions: a radiotracer study, Sep. Purif. Technol. 41(1) (2005) 21-28.

· Dursun, A.Y., A comparative study on determination of the equilibrium, kinetic and thermodynamic parameters of biosorption of copper(II) and lead(II) ions ontro pretreated *Aspergillus niger*, Biochem. Eng. J. 28 (2006) 187-195.

· Gong, R., Ding, Y., Lui, H., Chem, Q., Liu, Z., Lead biosorption and desorption by intact and pretreated *Spirula maxima* biomass. Chemosphere 58, (2005) 125–130.

· Gupta, B.S., Curran, M., Hasan, S., Ghosh, T.K., Adsorption characteristics of Cu and Ni on Irish peat moss J. Environ. Manage.

· Hammaini, A., González, F., Ballester, A., Blazquez, M.L., Muñoz, J.A., Biosorption of heavy metals by activated sludge and their desorption characteristics, J. Environ. Manage. 84 (2007) 419-426.

· Hammaini, A., Ballester, A., González, F., Blázquez, M.L., Muñoz, J.A., Activated sludge as biosorbent for heavy metals. Biohydrometallurgy and the environment toward the mining of the 21st century, Part B, Amsterdam: Elsevier (1999) 185-192.

· Hand, D.W., Crittenden, J.C., Thacker, W.E., Simplified models for design of fixed-bed adsorption systems, J. Environ. Eng.-ASCE 110 (1984) 440-456.

· Hasany, S.M., Chaudhary, M.H., Sorption potential of Hare river sand for the removal of antimony from acidic aqueous solution, Appl. Radiat. Isot. 47(4) (1996) 467-471.

· Hashim, M.A., Tan, H.N., Chu, K.H., Immobilized marine algal biomass for multiple cycles of copper adsorption and desorption. Sep. Purif. Technol. 19 (2000) 39–42.

· Helfferich, F., Ion Exchange, McGraw-Hill, New York, 1962.

· Ho, Y.S., Ofomaja, A.E., Biosorption thermodynamics of cadmium on coconut copra meal as biosorbent. Biochem. Eng. J. 30 (2006) 117-123.

· Ho, Y.S., Huang, C.T., Huang, H.W., Equilibrium sorption isotherm for metal ions on tree fern, Process Biochem. 37 (2002) 1421-1430.

· Hobson, J.P., Physical adsorption isotherms extending from ultrahigh vacuum to vapor pressure, J. Phys. Chem. 73(8) (1969) 2720-2727.

· Kratochvil, D., Volesky, B., Advances in the biosorption of heavy metals, Trends Biotechnol. 16 (1998) 291–300.

· Kratochvil, D., Volesky, B., Multicomponent biosorption in fixed beds. Water Res. 34 (2000) 3186-3196.

· Onyango, M.S., Kojima, Y., Aoyi, O., Bernardo, E.C., Matsuda, Y., Adsorption equilibrium modelling and solution chemistry dependence of fluoride removal from water by trivalent cation-exchanged zeolite F-9, J. Colloid Interface Sci. 279 (2) (2004) 341-350.

· Özcan, A., Özcan, A.S., Tunali, S., Akar, T., Kiran, I., Determination of the equilibrium, kinetic and thermodynamic parameters of adsorption of copper(II) ions onto seeds of *Capsicum annuum*, J. Hazard. Mater. B124 (2005) 200-208.

· Pagnanelli, F., Esposito, A., Toro, L., Vegliò, F., Metal speciation and pH effect on Pb, Cu, Zn and Cd biosorption onto *Sphaerolitus natans*: Langmuir-type empirical model, Water Res. 37 (2003) 627-633.

· Pandey, P.K., Verma, Y., Choubey, S., Pandey, M., Chandrasekhar, K., Biosorptive removal of cadmium from contaminated groundwater and industrial effluents, Biores. Technol. 99 (2008) 4420-4427.

· Puranik, P.R., Paknikar, K.M., Influence of co-cations on biosorption of lead and zinc-a comparative evaluation in binary and multimetal systems. Bioresource Technol. 70 (1999) 269-76.

· Rai, L.C., Metal removal from single and multimetallic systems y different biosorbent materials as evaluated by differential pulse anodic stripping voltammetry, Process Biochem. 36 (2000) 175-82.

· Romero-González, J., Peralta-Videa J.R., Rodríguez, E., Ramirez S.L., Gardea-Torresdey J.L. Determination of thermodynamic parameters of Cr(VI) adsorption from aqueous solution onto *Agave lechuguilla* biomass. J. Chem. Thermodynamics 37 (2005) 343–347

· Saeed, A., Iqbala*, M.,* Akhtar, M.W., Removal and recovery of lead(II) from single and multimetal (Cd, Cu,Ni, Zn) solutions by crop milling waste (black gram husk) J. Hazard. Mater. B117 (2005) 65–73.

· Sari, A., Tuzen, M., Citak, D., Soylak, M., Equilibrium, kinetic and thermodynamic studies of adsorption of Pb(II) from aqueous solutions onto Turkish kaolinite clay. J. Hazard. Mater. doi: 10.1016/j.jhazmat.2007.03.078.

· Seco, A., Marzal, P., Gabaldón, C., Adsorption of heavy metals from aqueous solutions onto activated carbon in single and in binary Cu-Ni, Cu-Cd and Cu-Zn systems. J. Chem. Technol. Biotechnol. 68 (1997) 23-30.

· Septhum, C., Rattanaphani, S., Bremner, J.B., Rattanaphani, V., An adsorption study of Al(III) ions onto chitosan, J. Hazard. Mater. 148 (2007) 185-191.

· Smith, R.M., Martell, A.E., Critical stability constants, vol. 4 New York: Plenum Press, 1976.

· Trujillo, E.M., Jeffers, T.H., Ferguson, C., Stevenson, H.Q., Mathematically modeling the removal of heavy metals from a waste water using immobilized biomass, Environ. Sci. Technol. 25 (1991) 1559–1565.

· Ucun, H., Bayhan, Y.K., Kaya, Y., Kinetic and thermodynamic studies of the biosorption of Cr(VI) by Pynus sylvestris Linn. J. Hazard. Mater. doi:10.1016/j.jhazmat.2007.08.018.

· Uslu, G., Tanyol, M., Equilibrium and thermodynamic parameters of single and binary mixture biosorption of lead (II) and copper (II) ions onto *Pseudomonas putida*: Effect of temperature. J. Hazard. Mater. B135 (2006) 87–93.

· Ünlü, N., Ersoz, M., Adsorption characteristics of heavy metal ions onto a low cost biopolymeric sorbent from aqueous solutions, J. Hazard. Mater. 136 (2006) 272-280.

· Vegliò, F., Di Biase, A., Beolchini, F., Pagnanelli, F., Heavy metal biosorption in binary systems: simulation in single- and two-stage UF/MF membrane reactors, Hydrometallurgy, 66 (2002) 107-115.

· Vilar V.J.P., Loureiro, J.M., Botelho, C.M.S., Boaventura, R.A.R., Continuous biosorption of Pb/Cu and Pb/Cd in fixed-bed column using algae *Gelidium* and granulated agar extraction algal waste, J. Hazard. Mater. 154 (2008) 1173-1182.

· Villaescusa, I., Fiol, N., Martínez, M., Miralles, N., Poch J., Serarols, J., Removal of copper and nickel ions from aqueous solutions by grape stalks wastes, Water Res. 38 (2004) 992–1002.

· Volesky, B., Sorption and Biosorption, first ed., BV Sorbex, Inc., Quebec, 2003.

· Volesky, B., Weber, J., Park, J.M., Continuous-flow metal biosorption in a regenerable *Sargassum* column, Water Res. 37 (2003) 297-306.

· Yin, P., Yu, Q., Jin, B., Ling, Z., Biosorption removal of cadmium from aqueous solutions by using pretreated fungal biomass cultured from starch wastewater. Water Res., 33 (1999) 1960-1963.

· Zhou, J.L., Huang, P.L., Lin., R.G., Sorption and desorption of Cu and Cd by macroalgae and microalgae. Environ. Pollut. 101 (1998) 67–75.

Chapter 5. ARSENIC REMOVAL BY A METAL (HYDR)OXIDE WASTE ENTRAPPED IN CALCIUM ALGINATE GEL BEADS

1. INTRODUCTION

Despite industries processing metals, and particularly those concerning electroplating operations, have a very important problem with their aqueous polluted effluents due to the content of hexavalent chromium and metallic cations, it can not be neglected the vast generation of solid waste (muds) after the water detoxification process. As described extensively in the introductory section, currently, the main treatment of the aqueous polluted effluents involved a previous dechromisation step by addition of reducing agents such as Fe(II), followed by a precipitation step in basic media by addition of different reagents such as soda or lime, according to the scheme presented in **Figure 5** of the introduction chapter. As an example, it can be mentioned that, in average, solid wastes from the decontamination processes of these industries (mostly hydroxide muds) represent about 47% of the total waste produced (Cox *et al*., 2006). This material might contain different metallic ions such as iron, copper, nickel, chromium, cadmium, lead or others whose relative concentration in the solid may vary, according to the industrial operation developed in the workshop. In any case, this by-product is a hazardous material itself and it is normally discarded by these industries, involving an important extra economical cost to guarantee its safe management by agreed centres.

Recently, the use of some industrial wastes based on metal oxides or hydroxides, has been reported for the effective removal of arsenic from aqueous solutions. Among others, promising results have been found for arsenic removal using red mud, by-product of the alumina production (Altundogan *et al*., 2000; Altundogan *et al*., 2002); blast furnace slag, from steel plants (Zhang and Itoh, 2005; Ahn *et al*., 2003) and Fe(III)/Cr(III) hydroxide waste, from fertilizer production (Namasivayam and Senthilkumar, 1998).

The arsenic is a ubiquitous metalloid whose presence in dangerous concentrations in natural waters is considered as a worldwide problem, often referred to as a 20th-21st century calamity (Mohan and Pittman, 2007; Smedley and Kinniburgh, 2002; World Health Organisation, 1981; Mandal and Suzuki, 2002). This pollution can be caused by either human activities such as mining, pesticides use, smelting of non-ferrous metals, burning of fossil fuels and timber treatment, but usually the main source of arsenic is geogenic: the Earth's crust is an abundant natural source of arsenic, being present in more

than 200 different minerals. Recently, and not far away from us, a health alarm appeared concerning the presence of arsenic in drinking water on a small village in Spain (Nistal, Castilla y León), whose inhabitants were consuming water with 10 times the maximum arsenic allowed content. Long term drinking water exposure can cause different dysfunctions and diseases as, loss of appetite and nausea, muscular weakness, neurological disorders, and cancers (Kapaj *et al.*, 2006). Consequently, the European standard level in drinking water has been fixed in 10 $\mu g \cdot L^{-1}$ (Directive 98/83/CE).

The chemistry of this element includes the existence of different oxidation states, the most common in natural waters being As(III) in form of $H_3AsO_3^0$ and $H_2AsO_3^-$ and As(V), as $H_2AsO_4^-$ and $HAsO_4^{2-}$, according to the pH of the solution.

For the removal of arsenic, different methods such as oxidation/precipitation, sorption onto different activated carbons, membrane techniques, ion exchange have been used among others (Garelick *et al.*, 2005; Wang and Mulligan, 2006; Mondal *et al.*, 2006) but they are usually expensive. That's why an increasing attention is currently being paid to sorption-based processes (Mohan and Pittman, 2007), where the use of raw materials like natural (Wang and Mulligan, 2006) agricultural (Amin *et al*., 2006) or industrial (Diamadopoulos *et al*., 1993; Zhang and Itoh, 2005; Altundogan *et al*., 2002) wastes is currently developed due to their both local abundance and low cost. Among the different available materials presenting arsenic sorption properties, those containing metals, and specially iron are well known for being very effective sorbent substrates (Shao *et al*., 2008; Deschamps *et al*., 2005; Banerjee *et al*., 2007; Mondal *et al*., 2008; Guo *et al*., 2007; Giménez *et al*., 2007).

2. OBJECTIVES

The main objective of the present chapter is to valorise the waste mud of an electroplating industry as arsenic sorbent. This material is a (hydr)oxide obtained after the precipitation in basic media, coagulation and flocculation of the metals dissolved in the primary polluted effluent.

In this study, the entrapment procedure presented in chapter 1 for grape stalk, will be adapted and optimized for the immobilization of this waste. A basic characterization of the raw and entrapped material including study of the charge distribution as a function of solution pH, obtention of the zero point charge pH (pH_{zpc}), specific surface area and cation exchange capacity will be carried out.

The effect of (hydr)oxide concentration in the gel beads, solution pH, contact time and of arsenic concentration on sorption will be studied and discussed. Furthermore the effect of the gel matrix on both sorption kinetics and equilibrium will be investigated.

Micro- and spectroscopic analysis on the solid phase of the (hydr)oxide before and after arsenic sorption will be carried out in order to obtain information about the chemistry of the interaction between As(III) and As(V) and the sorbent. From this information, a mechanism for arsenite and arsenate sorption by this material will be proposed.

3. MATERIALS AND METHODS

3.1. Reagents

To prepare As(III) and As(V) solutions:

- $NaAsO_2 \cdot 9H_2O$; >99% Fluka
- $Na_2HAsO_4 \cdot 9H_2O$; >98.5% Fluka
- Milli-Q water

To prepare the calcium alginate and calcium alginate containing (hydr)oxide:

- Brown algae sodium alginate Fluka
- $CaCl_2 \cdot 2H_2O$; 99-105% Panreac
- Powdered waste (hydr)oxide (< 250 μm) coming from an electroplating industry from Valencia (Spain)

For pH adjustment:

- HNO_3 (67%) Panreac
- NaOH in pellets Panreac

Standard solutions for Flame Atomic/Emission Spectroscopy calibration:

- $NaAsO_2 \cdot 9H_2O$ in HNO_3 0.5 N (1000 mg/L) Panreac
- $Cr(NO)_3 \cdot 3H_2O$ in HNO_3 0.5 N (1000 mg/L) Panreac
- $Ni(NO_3)_2 \cdot 6H_2O$ in HNO_3 0.5 N (1000 mg/L) Panreac
- $Fe(NO_3)3 \cdot 9H_2O$ in HNO_3 0.5 N (1000 mg/L) Panreac
- $Cu(NO_3)_2 \cdot 3H_2O$ in HNO_3 0.5 N (1000 mg/L) Panreac
- $Ca(NO_3)_2 \cdot 4H_2O$ in HNO_3 0.5 N (1000 mg/L) Panreac

For (hydr)oxide microwave-assisted digestion:

- HNO_3 (65%, Suprapur) Panreac
- HCl (37%, Suprapur) Panreac

For cation exchange capacity determination of the sorbents:

- Cobaltihexammine chloride (Merck)

3.2. Material

General laboratory material
150 mL capacity plastic flasks with cap
Cellulose filters
P Selecta Oven
Orbital shaker (Ikalabortechnik KS 501)
Peristaltic pump (Ismatec Reglo)
Peristaltic pump tubes Tygon R-3603
Chronometers (Berlabo, SA)
pHmeter PHM 250 (Meterlab)
Analytical balance (Metler Toledo)
Sieves (Sulab, S.A.)

3.3. Equipment

· Flame Atomic Absorption/Emission Spectrophotometer Varian SpectrAA 220FS.
· Electron Microscope Zeiss DSM 960 A, with Energy Dispersive X-Ray analyser Link Isis Pentafet (Oxford). For the treatment of the electronic images, Quartz PCI and Picture Gear software was used.
· Fourier transform infrared spectrometer Mattson Satellite, with MKII golden gate reflection ATR system.
· Microwave oven (ETHOS, Milestone)

4. METHODOLOGY

4.1. (Hydr)oxide preparation

The (hydr)oxide mixture was kindly supplied by an electroplating industry from Valencia (Spain). The raw material was washed with distilled water and dried in an oven at 60 ºC until constant weight. Afterwards, it was grinded, powdered and sieved to get a powder (< 250 μm particle size).

4.2. (Hydr)oxide characterization

The content of several metals like Fe, Ni, Cu, Cr and Ca in the (hydr)oxide was determined by dissolving the material in acidic media and analysing the obtained solution by FAAS (Varian Absorption Spectrometer SpectrAA 220FS) to quantify metal concentration. For this purpose, dry waste (hydr)oxide samples (*ca.* 0.3 g) were digested in a microwave oven (ETHOS, Milestone) with 8 mL of HNO_3 and 2 mL of HCl. For the digestion, a 3-step program was carried out. The digestion sequence consisted in a first heating to 90 ºC during 2.5 minutes followed by heating to 130 ºC for 5 minutes and finally to 190 ºC for 13.5 minutes. After this process, samples were allowed to cool to room temperature and were diluted with HPW to a final volume of 100 mL. Metal concentration in this solution was determined by FAAS spectroscopy (Varian Absorption Spectrometer SpectrAA 220FS).

The cation exchange capacity (CEC) of the sorbents was performed according to the norm NF X 31-130 (Afnor, 1997d) by the cobaltihexammine method. In this assay, 2 g of material are contacted with 50 mL of a 0.017 M solution of cobaltihexammine and stirred during 1 h in an orbital shaker (Ikalabortechnik KS 501). Determination of the sorbed amount of cobaltihexammonium cation is carried out by measuring the absorbance at 475 nm of the solutions before and after contact with the samples.. Specific surface area (SSA) of the sorbents was determined by N_2 adsorption according to the Brunauer-Emmet-Teller (BET) protocol on a Micromeritics FlowSorb III equipment. Surface charge distribution as a function of pH and pH_{zpc} was determined from potentiometric titrations of 1 $g \cdot L^{-1}$ solid suspension with 0.01 M NaOH or HNO_3 in 0.01 M $NaNO_3$ medium as supporting

electrolyte and using a PHM 250 (Meterlab) pH meter according to the method proposed by Davranche (Davranche *et al.*, 2003).

4.3. Sorbent gel beads synthesis

Gel beads containing different (hydr)oxide concentrations were prepared according to the scheme shown in **Figure 1** proposed by Fiol (Fiol *et al.*, 2006). The desired amount of (hydr)oxide was added to 100 mL of MilliQ water under strong constant magnetic stirring. When the (hydr)oxide was homogeneously suspended, 1g of sodium alginate was slowly added and the mixture was stirred until total biopolymer dissolution was achieved. A peristaltic pump was used to dispense the suspension in a stirred reservoir containing 200 mL of a chemical "fixing" solution of 0.1 M $CaCl_2$. At the end of the dispensing tube, a micropipette tip was attained and positioned approximately 1 cm above the surface of the fixing solution used for gel formation. The peristaltic pump was programmed to provide a constant flow rate of around 2 drops·s^{-1}. The beads formed (3 mm diameter) were allowed to cure, under continuous stirring, in the same $CaCl_2$ solution for 24 hours and then they were rinsed three times with MilliQ water to ensure the removal of Ca^{2+} ions that don't form part of the hydrogel structure.

When calcium alginate beads were used as a blank, beads were obtained by following the same procedure as before but without the addition of (hydr)oxide. The obtained beads will be named CA (calcium alginate beads) and X% O-CA (beads containing (hydr)oxide). For all the experiments, the non-spherical shape beads were discarded. The gel beads preparation scheme is summarized in the next figure:

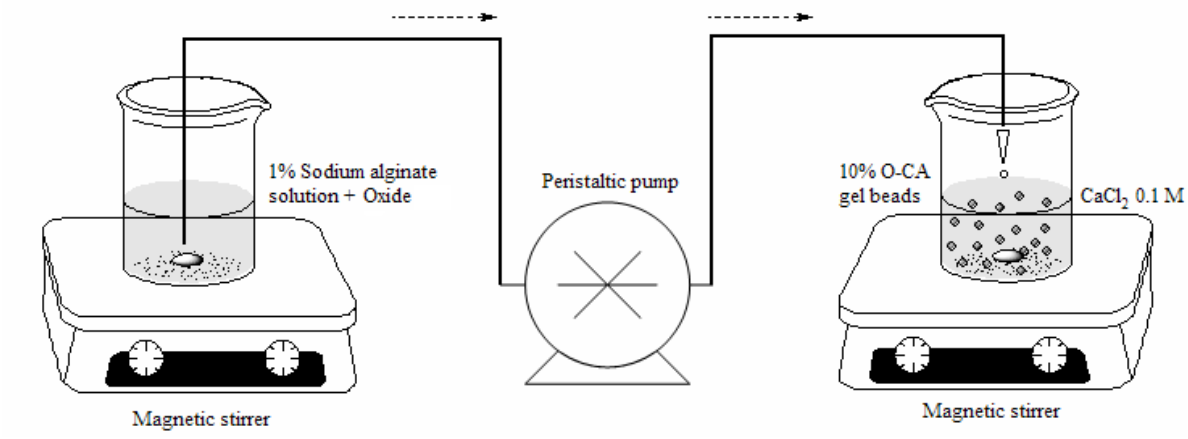

Figure 1: Sorbent preparation scheme.

4.4. General uptake procedure

Batch experiments were carried out separately on As(III) and As(V) solutions at 20±1 ^{o}C in stoppered plastic flasks. The experiments consisted of shaking in an orbital shaker at 200 rpm either a mass of (hydr)oxide mixture (O) or the number of beads of 10% O-CA containing the same mass of (hydr)oxide, with 20 mL of either As(III) or As(V) solutions until equilibrium was reached. After agitation the solid was removed by filtration through a 0.45 μm cellulose filter paper (Millipore Corporation) and solution pH was measured. Initial and final metal concentration in the filtrates before and after sorption, previously acidified, were determined by Flame Atomic Absorption Spectrometry (FAAS) (Varian Absorption Spectrometer SpectrAA 220FS).

Arsenic concentration in the solid phase (q_e) was calculated from the difference between initial, C_i and equilibrium, C_e metal concentration in solution. The following equation was used to compute the specific uptake of the sorbent:

$$q_e = (C_i - C_e)\frac{V}{m} \qquad (1)$$

Where V (expressed in L) is the solution volume and m represents the sorbent mass.

In most of the experiments, As(III) or As(V) concentration was 15 mg·L^{-1} and initial pH was adjusted to 8.0.

4.5. Effect of (hydr)oxide concentration in the beads in As(III) and As(V) removal

The effect of (hydr)oxide content on the sorptive capacity of the sorbent prepared by entrapment in calcium alginate was evaluated. For these experiments, pure CA beads and with (hydr)oxide contents 1, 2, 4, 6, 8, 10 and 12% (w/v) were prepared according to the methodology described previously. The experiments were carried out by shaking in an orbital shaker at 200 rpm, 20 beads with 20 mL of a 15 $mg \cdot L^{-1}$ solution of either As(III) or As(V) for 48 hours. After agitation the sorbent was removed by filtration and the initial and final metal concentration in the filtrates were determined by FAAS.

4.6. pH effect on As(III) and As(V) sorption and sorbent solubilization

The pH is an important parameter in water treatment processes, because proton concentration can strongly modify the redox potential of sorbates and sorbents, as well as chemical speciation of sorbates and surface charge of sorbents.

The effect of initial pH on arsenite and arsenate sorption onto raw and entrapped (hydr)oxide was studied by contacting for 48 hours, either 0.0377 g of raw (hydr)oxide (O) or 20 beads of 10% O-CA (equivalent to a dry (hydr)oxide mass of 0.0377 g), with 20 mL of arsenic solution of initial metal concentration of 15.0 $mg \cdot L^{-1}$. The initial pH was varied within the pH range 2-12.5. The percentage of arsenic removal was computed according to the next equation:

$$\text{Removal}\,\% = \frac{C_i - C_e}{C_i} x\,100 \qquad (2)$$

4.7. Sorption kinetics study

Sorption kinetic experiments were conducted to obtain information on the equilibrium time and on the effect of entrapment gel matrix on the single species sorption rate of As(III) and As(V). Batch experiments were carried out at 20±1 ^{o}C in 1000 mL glass flasks by mixing, at 200 rpm, 1000 mL of 15 $mg \cdot L^{-1}$ As(III) or As(V) solutions with either 1 g of waste (hydr)oxide or the number of 10% O-CA beads equivalent to 1 g of dry waste (hydr)oxide.

Initial pH of the different solutions was adjusted to 8.0 and the pH was allowed to free evolve during the sorption process. At suitable time intervals within the range 0-72 hours, 10 mL samples were withdrawn by using a syringe and filtered. In the filtrates, pH was measured and arsenic concentration was determined. As a blank the same experiment was performed by using 535 CA beads.

4.8. Sorption equilibrium study

Arsenate and arsenite initial concentrations within the range 5-500 mg L^{-1} were used for obtaining the corresponding isotherms. Equilibrium isotherms at 20±1 ^{o}C were determined by contacting for 72 hours either 0.0377 g of raw (hydr)oxide or 20 beads 10% O-CA with 20 mL of different initial arsenic concentration. The initial pH was adjusted to pH 8.0. As a blank, isotherms by using 20 beads of CA beads were also obtained.

4.9. Solid state analysis

Different techniques were used to characterise raw (hydr)oxide mixture and to obtain information about changes on different physicochemical properties of the solid due to arsenic sorption. X ray diffraction (XRD) analysis on a Siemens D5000 diffractometer using filtered copper *K* α 1 radiation were performed in order to ascertain crystalline state on the solid. The 2θ angle was varied in the range 10 to 50º with 2000 steps.

Surface topology and local chemical composition of the sorbent were analysed by Scanning Electron Microscopy (SEM) and Energy Dispersive X-Ray analysis (EDX) respectively.

Infrared spectra with Attenuated Total Reflectance (FTIR-ATR) were obtained by direct measurement on the solid with a Mattson Satellite with MKII golden gate reflection ATR system at 2 cm^{-1} resolution.

For all these analysis, arsenic loaded samples were prepared by contacting 1 g of O or the equivalent number of 10% O-CA beads with 200 mL of either 500 mg L^{-1} solution As(III) or As(V) at pH 8.0 for 48 hours. Before the corresponding analysis, samples were washed with Milli-Q water to remove the non sorbed arsenic and then dried at 105^{o}C until constant weight.

4.10. Hazard classification of the spent sorbent

The US-EPA toxicity characteristic leaching procedure (TCLP) (US Environmental Protection Agency, 1999) was carried out to determine the potential mobility of the metals forming the (hydr)oxide and, thus, to obtain information about the potential hazard of the sorbents before and after arsenic sorption. Samples of sorbents were treated with a standardized extraction fluid (5.7 mL glacial CH_3COOH added to 500 mL of Milli-Q water, plus 64.3 mL of 1 M NaOH and diluted to 1 L, pH 4.9), and agitated on an orbital shaker for 18 h. The solid/liquid ratio was 1:20. The concentrations of extracted metals (Fe, Ni, Cu and Cr) and As were determined by FAAS.

5. RESULTS AND DISCUSSION

5.1. (Hydr)oxide characterization

Raw (hydr)oxide coming directly from the electroplating process was characterized in order to obtain chemical composition information as well as surface properties. The content of the major metals of the raw (hydr)oxide was found to be ($mg.g^{-1}$) Fe(III): 142.3±1.4; Ni(II): 174.4±4.1; Cu(II): 15.4±0.4; Cr(III): 15.1±0.6 and Ca: 12.6±0.4. The absence of Fe(II) and Cr(VI) was checked by means of the colorimetric methods of 1,10-orthophenatroline and 1,5-diphenilcarbazide respectively.

Cation exchange capacity (CEC), pH_{zpc}, specific surface area of the raw (hydr)oxide mixture (O), pure calcium alginate beads (CA) and 10% (w/v) of (hydr)oxide entrapped in calcium alginate beads (10% O-CA) are presented in **Table 1**.

Table 1: Characterization of O, CA and 10% O-CA (CEC, Specific surface and pH_{zpc}).

	CA	O	10% O-CA
CEC ($meq \cdot 100g^{-1}$)	108.39	9.01	22.56
Specific surface ($m^2 \cdot g^{-1}$)	0.24	167.54	23.24
pH_{zpc}	6.47	8.19	8.09

The CEC values provide a quantification of the maximum exchangeable cations of the materials. With the cobaltihexammine method, in the case of calcium alginate that is the material that exhibits the highest CEC, the exchange reaction would be the next.

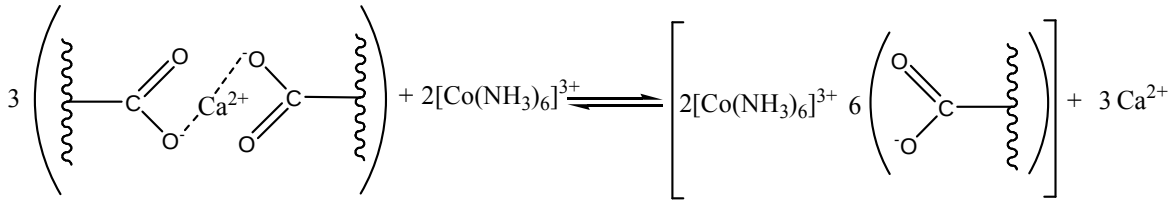

The reaction summarizes the exchange reaction of the calcium ions by the cobaltihexammoniun ions provided by the reagent.

From the values presented in **Table 1**, it is noteworthy the high cation exchange capacity of CA beads, which is about 12 folds the CEC found for O. The high CEC of CA value is supposed to be the responsible of the increase of this parameter when the (hydr)oxide is entrapped in calcium alginate.

On the other hand, the specific surface of the sorbents was observed to be higher in the case of the (hydr)oxide than in the case of pure calcium alginate. For the entrapped material, the specific surface area is higher than in the case of CA but lower than in the case of O.

pH of zero point charge (pH_{zpc}) of O, 10% O-CA and CA beads was also evaluated by plotting the charge per mass unit as a function of solution pH (**Figure 2**).

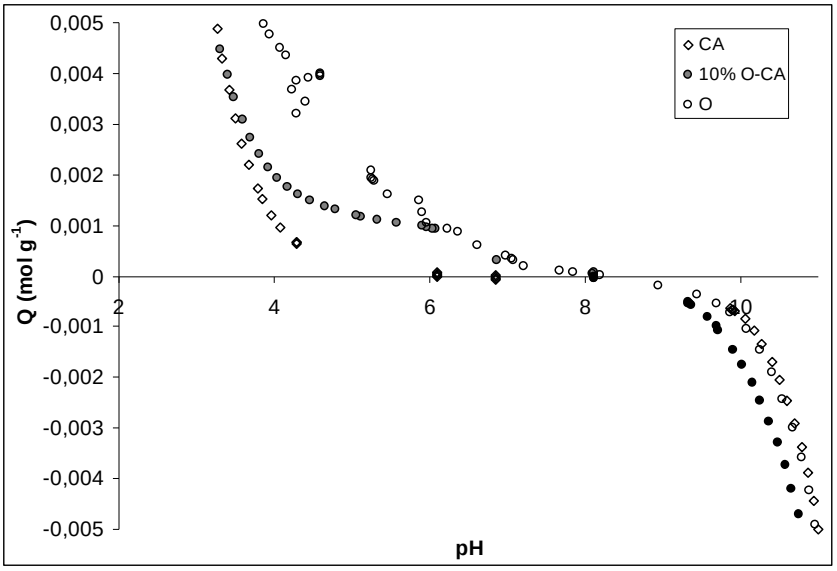

Figure 2: pH_{zpc} determination of CA, O and 10% O-CA.

The results presented in this figure put into evidence that both sorbents (O and 10% O-CA) would remain positively charged until a pH close to 8 while for pHs higher than this value, the surface charge would change to negative. The values of pH_{zpc} obtained in the present study are in agreement with the pH_{zpc} value (8.3) previously reported for a Fe(III)/Cr(III) waste hydroxide mixture (Navasivayam and Senthilkumar, 1998). In the case of pure CA gel beads, a pH_{zpc} of 6.47 was obtained.

5.2. Effect of (hydr)oxide concentration in the beads in As(III) and As(V) removal

In order to optimize arsenic sorption performance of the sorbent prepared by (hydr)oxide entrapment, As(III) and As(V) removal as a function of (hydr)oxide w/v ratio was studied. This ratio corresponds to the amount of (hydr)oxide (g) per 100 mL of alginate solution.
The residual arsenic concentration in solution and the uptake for the different (hydr)oxide contents in the gel beads are presented in **Table 2**.

Table 2: Effect of amount of (hydr)oxide in the alginate gel bead on As(III) and As(V) sorption. $[As]_0$=15.0 mg·L^{-1}; sorbent dose: 1 bead·mL^{-1}, V_{sol}=20 mL, pH_0=8.0, agitation time = 48 h.

	As(III)		As(V)	
O ratio (% w/v)	**[As(IIII)] (mg·L^{-1})**	**q (mg·$bead^{-1}$)·10^3**	**[As(V)] (mg·L^{-1})**	**q (mg·$bead^{-1}$)·10^3**
0	14.88	0.13	14.45	0.67
1	11.41	3.60	8.96	6.16
2	9.48	5.53	6.82	8.30
4	6.55	8.46	4.13	10.99
6	4.42	10.59	1.96	13.16
8	3.35	11.66	1.68	13.44
10	3.02	11.99	1.05	14.07
12	1.99	13.02	0.63	14.49

This table clearly shows an increase of the sorption capacity of the gel beads when the amount of (hydr)oxide is increased on them. If the amount of arsenic uptaken is plotted as a function of w/v ratio of (hydr)oxide in the bead, the next figure is obtained:

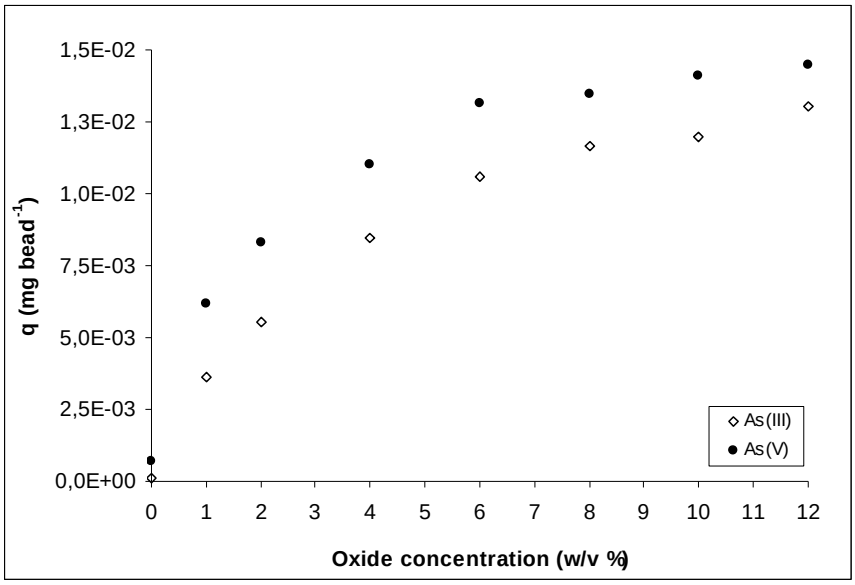

Figure 3: As(III) and As(V) removal percentage as a function of (hydr)oxide concentration in the calcium alginate gel beads. $[As]_0$=15.0 mg·L^{-1}, sorbent dose: 1 bead·mL^{-1}; V_{sol} = 20 mL; pH_0=8.0; agitation time=48 h.

As it can be seen in the figure, both As(III) and As(V) sorption is almost negligible for pure CA beads (corresponding to a 0% w/v ratio of (hydr)oxide). The figure puts into evidence an increase of the sorbed arsenic amount when (hydr)oxide concentration in the bead is increased. It has to be remarked that despite high (hydr)oxide concentrations were observed to adsorb a higher amount of both As(III) and As(V), it was noticed the formation of non-spherical non-homogeneous beads and flow/pumping troubles through the peristaltic tubes for (hydr)oxide w/v ratios higher than 10%. From the results obtained in this section, a 10% (w/v) ratio of (hydr)oxide was chosen to carry out further experiments due to both, a high sorption performance and the absence of troubles during the entrapment procedure.

Once optimized the preparation protocol and chosen a (hydr)oxide concentration on the sorbent bead, the effect of the solution pH on As(III) and As(V) removal and on the chemical stability of the sorbents was explored.

5.3. pH effect on As(III) and As(V) sorption and sorbent solubilization

In this section, pH effect on arsenic sorption by both, (hydr)oxide and 10% O-CA beads is studied. In these experiments, acid/base stability of the sorbents O and 10% O-CA will be also studied and discussed by analyzing the release of metals that form its structures.
In the next table, the results of removal percentage as a function of initial and final pH are presented.

Table 3: Initial and final solution pH and As concentration in solution after contact with raw and entrapped (hydr)oxide. $[As]_0$=15 mg·L^{-1}; sorbent dose: 1.83 g L^{-1}.

		O				10% O-CA	
pH_0	pH_f	[As(III)] (mg·L^{-1})	removal %	pH_0	pH_f	[As(III)] (mg·L^{-1})	removal %
2.01	2.34	7.55	49.09	2.01	2.79	4.62	68.85
3.00	6.30	3.91	73.79	3.00	5.85	2.67	82.10
4.03	6.84	2.97	80.45	4.03	6.67	1.49	90.19
5.01	7.09	2.70	82.33	5.01	6.77	1.40	90.84
6.07	7.18	2.68	82.16	6.07	7.08	1.73	88.48
7.01	7.61	2.75	81.98	7.01	7.29	1.43	90.63
8.03	7.77	2.61	82.87	8.03	7.44	1.51	90.09
8.99	7.95	2.58	82.94	8.99	7.75	1.44	90.48
9.93	8.09	2.56	83.02	9.93	7.34	1.54	89.79
11.02	8.73	2.96	80.49	11.02	8.54	1.83	87.94
12.01	11.87	4.76	68.70	12.01	12.08	2.84	81.33
12.55	12.44	6.45	56.48	12.55	12.49	3.83	74.16

		O				10% O-CA	
pH_0	pH_f	[As(V)] (mg·L^{-1})	removal %	pH_0	pH_f	[As(V)] (mg·L^{-1})	removal %
2.00	2.21	8.72	41.16	2.00	2.61	5.92	60.05
3.01	6.12	5.12	66.14	3.01	5.75	4.67	69.11
4.02	6.65	3.28	78.13	4.02	6.84	2.53	83.13
4.98	7.21	2.18	85.47	4.98	6.91	1.46	90.27
6.02	7.45	1.05	93.00	6.02	7.47	0.87	94.20
7.01	7.62	0.95	93.67	7.01	7.63	0.72	95.20
7.95	7.88	0.92	94.04	7.95	7.81	0.64	95.85
9.01	7.81	0.88	94.13	9.01	8.02	0.73	95.13
10.06	8.12	2.24	85.07	10.06	7.74	1.16	92.27
11.00	9.04	3.87	74.20	11.00	8.81	3.81	74.60
12.00	11.56	6.12	59.20	12.00	11.73	5.81	61.27
12.54	12.41	7.18	52.13	12.54	12.48	6.94	53.73

For both sorbents, an increase of the solution pH was observed for initial pHs lower than 7, indicating thus that some protons are uptaken or hydroxyls are released in the initial pH range 2 to 7. On the other hand, when the initial pH of the solution was higher than 7, an increase on proton concentration in the media occurs, leading to pHs lower than the initial. These results point out a strong buffering capacity of the sorbents, either O or 10% O-CA.
In this experiments it has to be also remarked that no significative differences in final pH were observed respect to a control solution (blank) when either As(III) or As(V) were present in the media.
The removal percentages calculated according Eq. (2) and presented in **Table 3**, indicate that arsenic can be removed by both, O and 10% O-CA. For an easier visualization of the effect that pH exerts on arsenite and arsenate sorption, the removal percentage for both, raw and entrapped (hydr)oxide has been presented in **Figure 4**. Results of sorbed arsenic amount have been plotted as a function of both, initial and final pH.

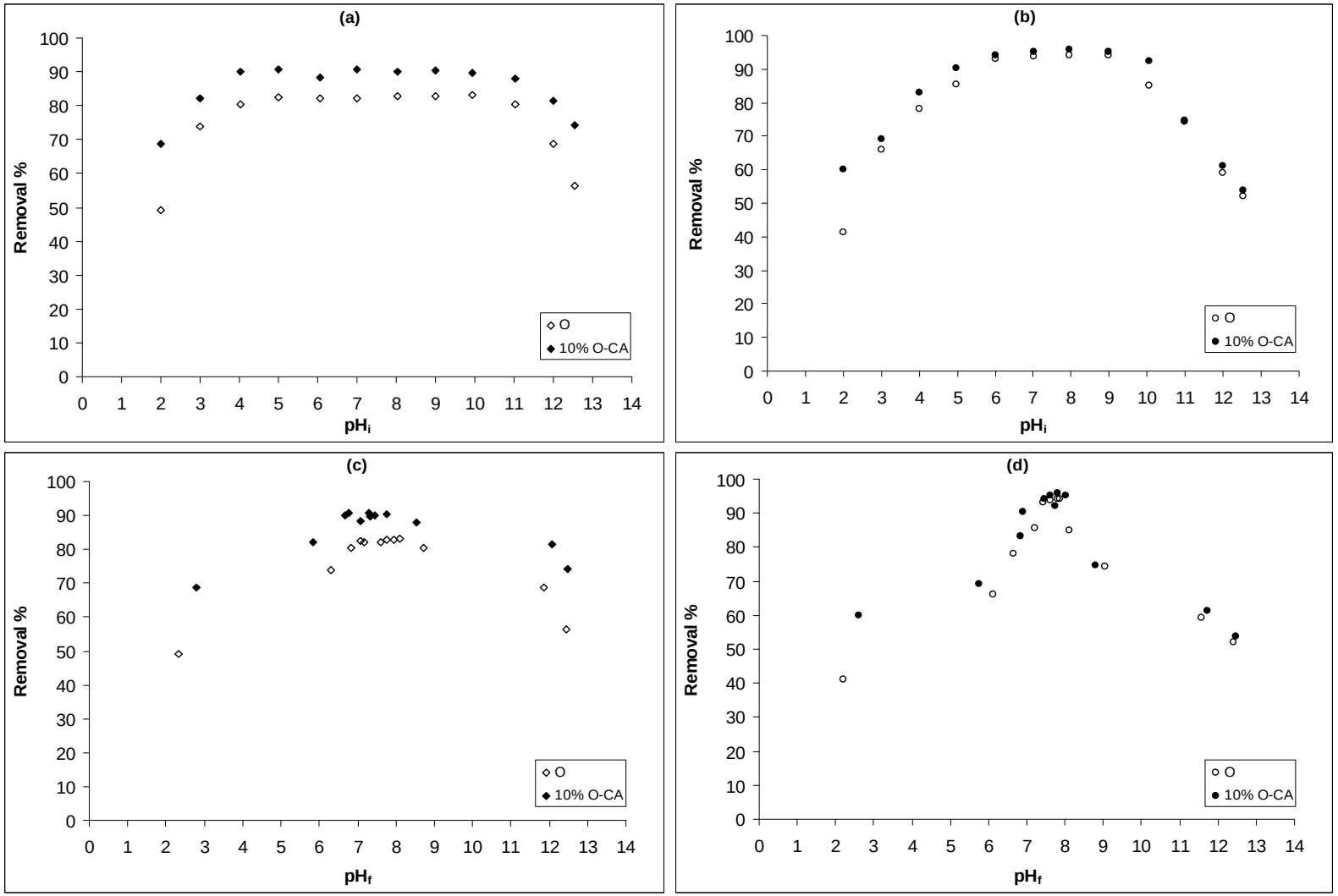

Figure 4: Effect of (a,b) initial and (c,d) final pH on arsenic sorption onto O and 10% O-CA. Rhombus represent As(III) and circles As(V). $[As]_0$=15 mg·L^{-1}; sorbent dose: 1.83 g L^{-1}.

As seen in the **Figure 4 (a)**, As(III) removal percentage achieves a plateau about 81% and 87% for O and 10% O-CA, respectively within the initial pH range of 5-10. In the case of As(V), **Figure 4 (b)** demonstrates that both sorbents achieve 95% removal within a narrower pH range (6-9). It is noticeable that the solid entrapment into the gel matrix seems not to have any influence on As(V) uptake, while a slight favourable effect of the gel entrapment is observed in the case of As(III). It can be also observed that outside the above mentioned pH ranges As(III) and As(V) sorption removal decreases. The decrease on removal percentage that occurs at initial pH≤3 could be due to mass loss by acidic solubilization and/or degradation of the sorbent. On the other hand, the decrease of percentage of arsenic removal observed for pH>10, could be due to the repulsion of the negative charge of the predominant anionic species in solution of arsenite ($H_2AsO_3^-$) and arsenate ($H_2AsO_4^-$ and $HAsO_4^{2-}$), according to the speciation diagrams presented in **Figure 5**, (Puigdomènech, 2007) and the negative surface charge of the sorbents at pH>pH_{zpc}.

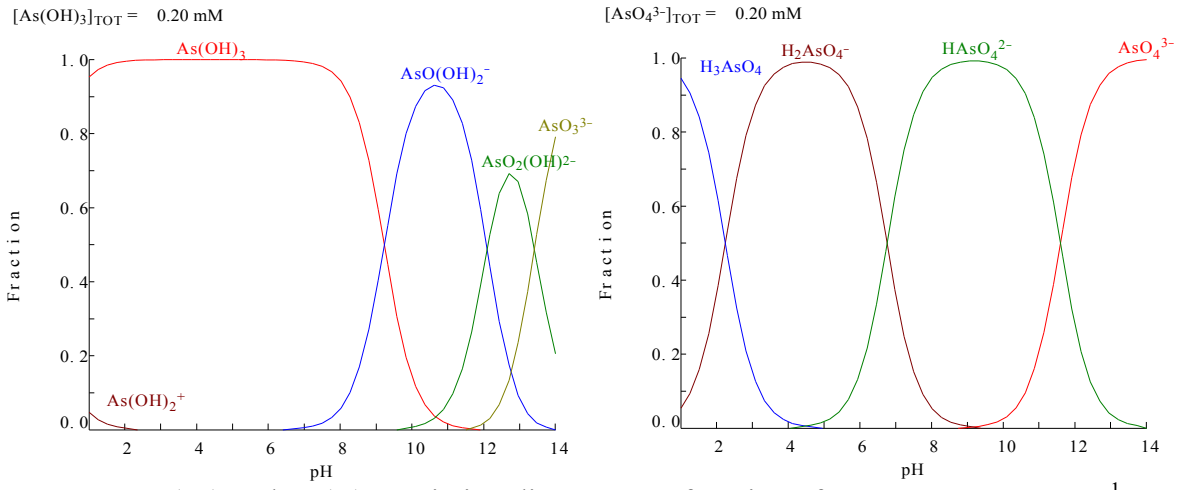

Figure 5: As(III) and As(V) speciation diagram as a function of pH. $[As]_0$=15.0 mg·L^{-1}.

The strong buffering capacity of the sorbents is clearly evidenced in **Figures 4 (c)** and **(d)**, corresponding to the plot of arsenite and arsenate removal percentage respectively, as a function of the final pH. In this figures it can be observed how only the extreme acidic initial pHs (around 2) and the extreme basic (around 12 and 12.5) remain almost unaltered. In contrast, initial pHs within the range 3-11 were found to evolve to final pHs 5.8<pH<9.0.

It must be remarked that after arsenic sorption, pH moved from initial values about 8 to approximately 7.5.

From the results obtained in this study, an initial pH=8.0 was chosen for further experiments. Some considerations about the chosen initial pH must be taken into account when discussing sorption results. At the corresponding equilibrium pH 7.5, the surface of the (hydr)oxide is partially positively charged because the pH is lower than pH_{zpc}; As(III) and As(V) are present in solution as $H_3AsO_3^0$ and $H_2AsO_4^-$ / $HAsO_4^{2-}$, respectively.

As it had been discussed in the Introduction of the present chapter, the (hydr)oxide used as sorbent in this study it's a hazardous materials derived from the precipitation of the metals of the primary polluting effluent of an electroplating industry. In section 5.1 this material had been characterized and demonstrated the high content of mainly Fe and Ni, but also the presence of Cu and Cr. It has to be taken into account thus that, if these ions are mobilized either by the presence of As or by solubilization, the applicability of this sorbent would be very restricted. It was necessary, according to these considerations, the obtention of information concerning the leaching of toxic metals as a function of pH in presence of both As(III) and As(V). It has to be remarked that calcium release, despite not being a toxic metal itself, was also followed in order to check the stability of the solid. Metal leaching from the sorbents was checked by analyzing the iron, nickel, copper, chromium and calcium concentration in the filtrates of the experiments of arsenic sorption as a function of pH. Analysis on the filtrates of assays carried out without arsenic were also performed as a reference blank, for comparison sake. In **Figure 6**, iron, nickel, copper, chromium and calcium release as a function of pH for solutions containing arsenic and for the blank are presented.

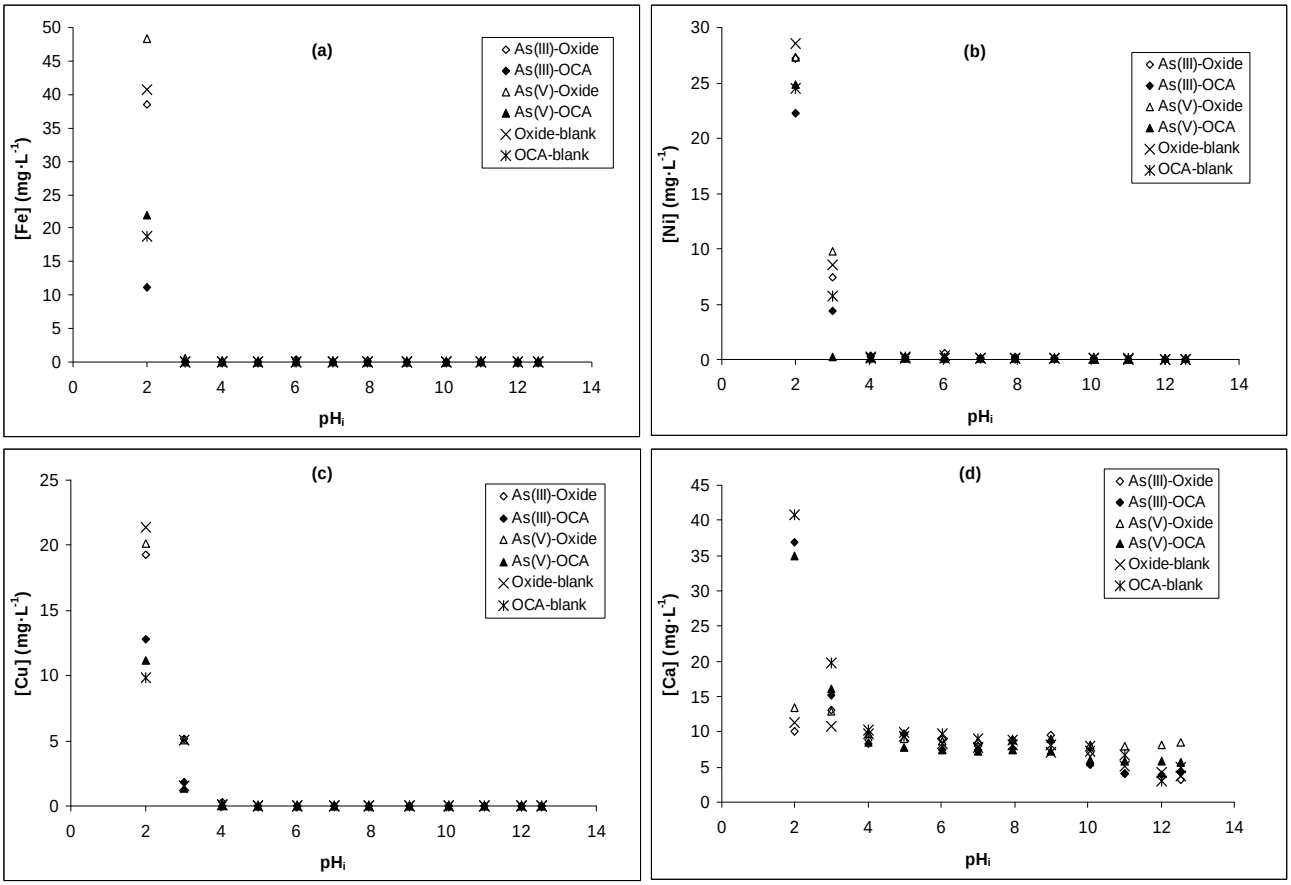

Figure 6: (a) Fe, (b) Ni, (c) Cu and (d) Ca released from the sorbent material a function of initial solution pH for blank, As(III) and As(V) solutions. $[As]_0$=15 mg·L^{-1}; sorbent dose: 1.83 g L^{-1}.

As it can be seen in **Figure 6**, when contacting the sorbents (O and 10% O-CA) with aqueous solutions without arsenic (blank) at different pH there is an important release of some elements such as Fe, Ni, Cu and Ca in acidic medium. This fact indicates that solubilisation of Fe, Ni and Cu (hydr)oxides takes place at pH<3 and would confirm that the loss of sorbent mass by acidic dissolution is the responsible of the removal percentage decay observed and discussed previously. It has to be remarked that no chromium release from the sorbents was observed for any of the initial pHs. This fact could be due to the extremely low solubility of the chromium(III) hydroxide (pKs $Cr(OH)_3$=30.20).

It has to be also remarked that the release of Fe, Ni and Cu is lower when the (hydr)oxide is entrapped in the calcium alginate gel matrix. This observation indicates that calcium alginate acts as a barrier, avoiding the release of these ions from the (hydr)oxide to the solution at acidic pHs. Indeed, it has been reported that calcium ions from the gel can be exchanged by metal cations by the reaction (Apel and Torma, 1993; Aksu *et al.*, 1998; Chen *et al.*, 1997; Chen *et al.*, 2002; Jodra and Mijangos, 2001; Veglio *et al.*, 2002):

$$x\ \{COO\}_2\text{-}Ca + y\ M^{n+} \quad \leftrightarrow \quad y\ \{COO\}_n\text{-}M \ + \ x\ Ca^{2+}$$

If M^{n+} represents the cations of Fe(III), Cu(II) or Ni(II) in solution, this reaction could be assumed to be the responsible of the sequestration of the toxic metal cations leached from the (hydr)oxide that, otherwise, would be released to the fluid.

On the other hand, it is noteworthy that the presence of either As(III) or As(V) at initial pHs 2-3 did not result in an additional release of Fe, Ni, Ca or Cu ions to the media. This fact confirmed that the presence of these ions in solution is not related to the arsenic uptake but to the metal ions mobilisation in acidic media. At pH ≥ 4, Fe, Ni and Cu were not found in solution (metal concentration <0.05 $mg{\cdot}L^{-1}$). Conversely, Ca ions solubilisation was found to take place in all the studied pH range (2-12.5) and to be independent of the presence of either As(III) and As(V) (**Figure 6 (d)**).

Once optimized the sorbent preparation procedure, the pH range to get the best arsenic sorption performance and checked that the sorbent materials would not add toxic metallic ions to the solution to treat, in a further step, arsenic removal rate and effect of the calcium alginate gel matrix will be studied and discussed.

5.4. As(III) and As(V) sorption kinetics onto O and 10% O-CA

In this section sorption behaviour of As(III) and As(V) onto the (hydr)oxide in both, its native and entrapped form, is studied. Kinetic models, as the pseudo-first and pseudo-second order as well as the fractional attainment model, were applied to the experimental data in order to obtain information about the effect of arsenic oxidation state and presence of the calcium alginate matrix in the sorption rate.

In **Table 4** As(III) and As(V) concentration in solution as a function of contact time with either O or 10% O-CA beads is presented.

Table 4: As(III) and As(V) concentration in solution as a function of contact time O and 10% O-CA. $[As]_0$=15 mg·L^{-1}; sorbent dose: 1 g L^{-1}; pH_0=8.0.

	As(III)		As(V)	
t (h)	**O**	**10% O-CA**	**O**	**10% O-CA**
0.	14.93	14.93	15.12	15.12
0.01	13.68	14.41	14.18	14.91
0.02	13.00	14.45	12.25	14.70
0.03	12.49	14.21	10.67	14.68
0.08	11.72	13.71	8.58	14.60
0.17	10.60	13.28	7.10	14.17
0.5	9.47	12.21	5.22	13.59
1	8.86	10.95	4.34	12.51
2	8.33	9.71	3.84	11.60
4	7.86	7.59	3.57	10.14
6	7.75	7.15	3.21	8.79
8	7.71	6.87	2.76	7.56
24	7.08	5.89	1.91	4.20
48	6.41	5.88	1.76	1.82
72	6.16	5.85	1.65	1.55

In the table it can be observed that in all the cases and as it was expected, arsenic concentration in solution progressively decreases when increasing the contact time with the sorbents O and 10% O-CA. When As(III) and As(V) concentration in solution is plotted as a function of contact time, **Figures 7 (a)** and **(b)** are obtained respectively.

(a)

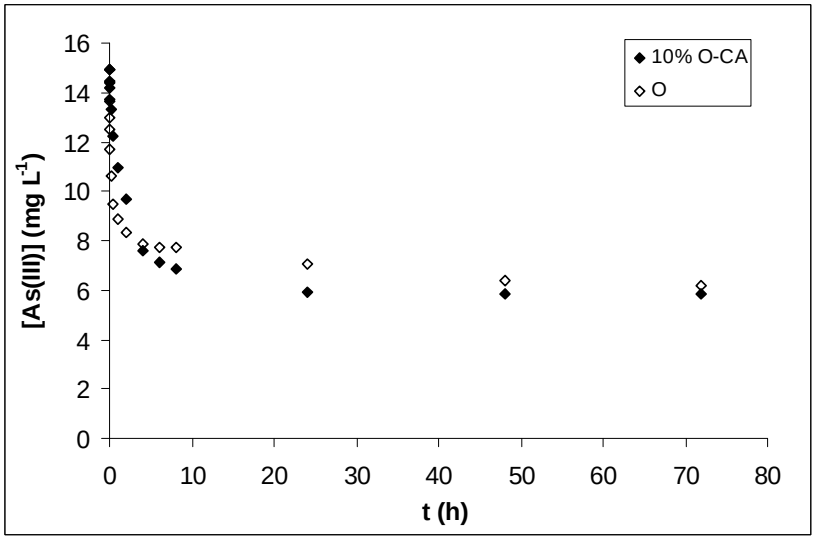

(b)

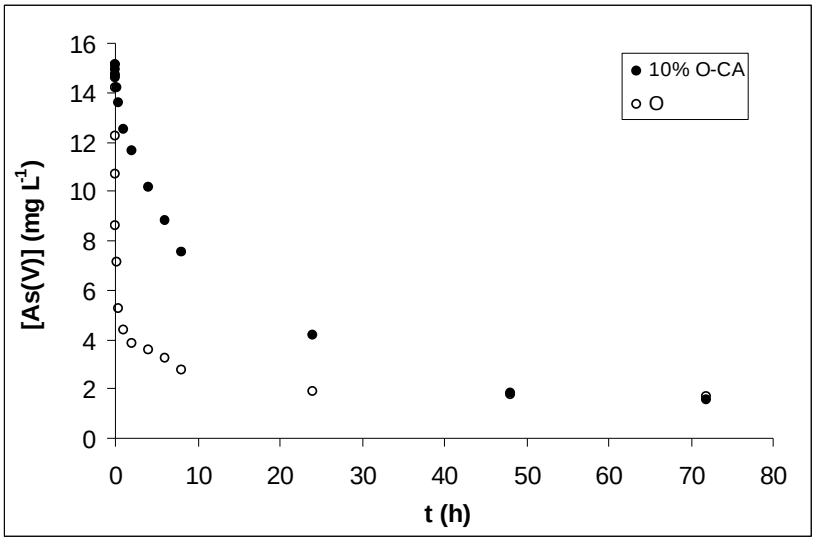

Figure 7: Arsenic concentration in solution as a function of time for (a) As(III) and (b) As(V) sorption onto O and 10% O-CA beads. $[As]_0$=15 mg·L^{-1}; sorbent dose: 1 g·L^{-1}; pH_0=8.0.

Figure 7 (a) puts into evidence that As(III) sorption occurs slightly slower in the case of 10% O-CA than in the case of O. This slightly different kinetics of As(III) sorption onto both sorbents strongly contrast with the observed for As(V), where a very important difference in sorption rate between the entrapped and non-entrapped (hydr)oxide can be observed (**Figure 7 (b)**). The more important slowing down that As(V) suffers when the

(hydr)oxide is entrapped in calcium alginate is indicative of an extra resistance to cross the alginate film that As(III) has not to overcome. In an attempt to give an explanation to this phenomenon, sorption kinetics will be modelled and constant rates for As(III) and As(V) sorption onto both, entrapped and non-entrapped material will be obtained, compared and discussed.

It has to be remarked that, despite of the different arsenic removal rate observed in the case of entrapped and non-entrapped material, almost the same residual concentration in solution was achieved. While in the case of As(III), concentrations of 6.16 and 5.85 $mg \cdot L^{-1}$ were achieved for the raw and entrapped (hydr)oxide, in the case of As(V), remaining concentrations of 1.65 and 1.55 were observed after contact with O and 10% O-CA respectively.

These results indicate that, for the initial arsenic concentration of these studies (15 $mg \cdot L^{-1}$), the calcium alginate seems not to exert any effect on the sorbent capacity.

As can be seen in the figure, both As(III) an As(V) sorption reaches a plateau at approximately 48 hours for both, raw and entrapped (hydr)oxide, therefore, a contact time of 72 hours was used in all subsequent sorption experiments to ensure that equilibrium is achieved. Other authors reported shorter equilibrium times when studying arsenate and arsenite sorption onto different iron(III)-based sorbents. When using ferrihydrite the time needed to reach equilibrium was one hour (Raven *et al.*, 1998) while four hours were needed when goethite and amorphous iron oxide were used (Lenoble *et al.*, 2002). Longer contact times of around 6 and 10 hours in the case of arsenite and arsenate respectively were needed in the case of sorption onto Fe(III)oxyhydroxide-loaded cellulose beads (Guo and Chen, 2005) and 24 hours were needed to reach equilibrium in the case of a Fe(III) loaded lignocellulosic substrate (Dupont *et al.,* 2007).

5.4.1. Sorption kinetics modeling

Arsenic sorption rate was studied by submitting the experimental data to pseudo-first and pseudo-second order kinetics models (McKay *et al.*, 1999). These models had been successfully applied previously for the analysis of hexavalent chromium removal by grape stalk entrapped in calcium alginate and its equations can be found in the chapter 1.

In this study, the models characteristic parameters were determined by non-linear regression analysis of the experimental data by using the computer program Microcal Origin 6.0, and the obtained results are presented in **Table 5**.

Table 5: Pseudo-first and pseudo-second order kinetic parameters for As(III) and As(V) adsorption onto O and 10% O-CA. $[As]_0$=15 mg·L^{-1}; sorbent dose: 1 g·L^{-1}; pH_0=8.0.

	Pseudo-first order model			Pseudo-second order model		
System	**k_1 (h^{-1})**	**q_1 (mg·g^{-1})**	**R^2**	**k_2 (g·mg^{-1}·h^{-1})**	**q_e (mg·g^{-1})**	**R^2**
As(III) O	7.2 ± 1.8	6.9 ± 0.3	0.897	1.4 ± 0.3	7.2 ± 0.2	0.990
As(III) 10% O-CA	0.58 ± 0.09	8.1 ± 0.3	0.976	0.10 ± 0.01	8.7 ± 0.2	0.958
As(V) O	9.9 ± 1.7	11.3 ± 0.4	0.951	1.1 ± 0.2	11.9 ± 0.2	0.981
As(V) 10% O-CA	0.12 ± 0.01	11.7 ± 0.4	0.980	0.018 ± 0.001	13.4 ± 0.0	0.991

In the table k_1 and k_2 represent the rate constants of pseudo-first and pseudo-second order model respectively. In an analogous way, equilibrium sorption capacity calculated from the models has been labelled as q_1 and q_2.

Results presented in this table point out that despite good regression coefficients were obtained when submitting the experimental As(III) and As(V) sorption results to both, pseudo-first and pseudo-second order model, in general, a slightly better fit was achieved when pseudo-second order model was applied.

As shown in the table the values of the rate constants of both models obtained for native (hydr)oxide were always much higher than those obtained for the entrapped material, and this difference in between entrapped and non entrapped material is higher in the case of As(V) than in the case of As(III). These results indicate that the presence of the alginate gel is related to a decrease in sorption rate. It is known that natural hydrocolloid materials, when gelled, form a stable matrix with high porosity and water content. Since the gel forms a quasi-solid structure, however, it would be expected to retard the transport of a solute due to the solute movement through the aqueous regions between the polymer chains (Amsden and Turner, 1999; Scott *et al*., 1989). Moreover, calcium alginate (pH_{zpc}= 6.5), is expected to be partially ionized at 7.5≤pH≤8.0. Therefore, the negative charge on calcium alginate surface could render difficult the diffusion of As(III) (mainly present as $H_3AsO_3^0$) and in a greater extent the diffusion of the negatively-charged As(V) species ($H_2AsO_4^-$) through the gel to reach the sorbent surface of the (hydr)oxide.

According to this, it is clear that As(V) sorption may encounter an additional resistance to reach the solid (hydr)oxide particles than As(III) because of the repulsion that takes place between the anionic matrix and anionic $HAsO_4^{-2}$. This could be the reason of the much lower kinetics of As(V) than As(III) when comparing entrapped and non entrapped (hydr)oxide.

5.4.2. Arsenic diffusion vs. external mass transport modeling onto O and 10% O-CA

In order to determine the actual rate-controlling step involved in As(III) and As(V) sorption process onto both raw and entrapped (hydr)oxide, the sorption data were further analyzed using the kinetic expression given by Boyd (Boyd et al., 1947):

$$F = 1 - \frac{6}{\pi^2}\exp(-Bt) \qquad (3)$$

where F is the fraction of solute adsorbed at different times t and Bt is a mathematical function of F given by:

$$F = \frac{q_t}{q_e} \qquad (4)$$

where q_t and q_e represent the amount adsorbed ($mg \cdot g^{-1}$) at time t and at infinite time. In this work, q_e has been taken from the pseudo-second order kinetic model prediction. Substituting equation (4) into equation (3), the kinetic expression becomes:

$$Bt = -0.4977 - \ln(1 - \frac{q_t}{q_e}) \qquad (5)$$

Thus the value of Bt can be calculated for each value of F using equation (5). The calculated Bt values were plotted against time and results for As(III) and As(V) are presented in **Figures 8 (a)** and **(b)** respectively.

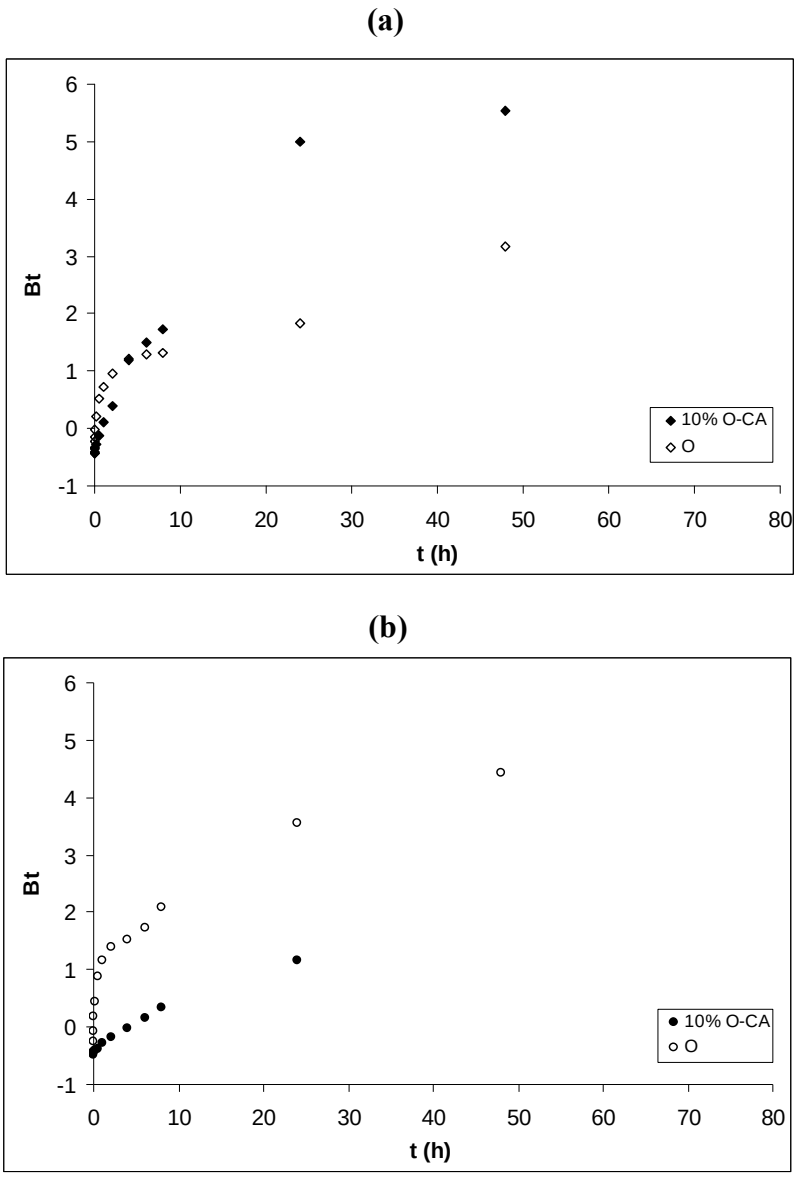

Figure 8: Plots of Bt as a function of time for the diffusion of (a) As(III) and (b) As(V) ions from aqueous solutions on raw and entrapped (hydr)oxide.

The linearity of this plot provides useful information to distinguish between external-transport and intraparticle-transport-controlled rates of adsorption (El-Kamash *et al*., 2005; Mohan and Singh, 2002; Wang *et al*., 2006). If a plot of *Bt* vs. time (having slope *B*) is a straight line passing through the origin, then adsorption is governed by a particle-diffusion mechanism, otherwise it is governed by film diffusion. In this figure, for both arsenic oxidation states sorption onto raw and entrapped (hydr)oxide, it was observed that the plots

were not linear and they did not pass through the origin, indicating that external mass transport mainly governs the rate-limiting process.

5.5. Arsenic sorption equilibrium study onto O and 10% O-CA

In this section the effect of arsenic concentration in solution and of the entrapment on arsenic sorption equilibrium will be studied and discussed.
In the next table, initial arsenic concentration in solution and after contact with the sorbents is shown. Arsenic sorbed amount was calculated according to equation (1) and results have been also included in **Table 6**.

Table 6: Initial arsenic (C_i) and equilibrium (C_e) concentration in solution and sorbed amount (q_e) after contact with O and 10% O-CA gel beads. Sorbent dose: 1 $g \cdot L^{-1}$; pH_0=8.0; Agitation time: 72 h; Temperature: 20±1.

As(III)					As(V)				
	O		10% O-CA			O		10% O-CA	
C_i ($mg \cdot L^{-1}$)	C_e ($mg \cdot L^{-1}$)	q_e ($mg \cdot g^{-1}$)	C_e ($mg \cdot L^{-1}$)	q_e ($mg \cdot g^{-1}$)	C_i ($mg \cdot L^{-1}$)	C_e ($mg \cdot L^{-1}$)	q_e ($mg \cdot g^{-1}$)	C_e ($mg \cdot L^{-1}$)	q_e ($mg \cdot g^{-1}$)
9.61	1.01	4.56	0.86	4.64	10.25	0.31	5.28	0.21	5.33
19.41	3.56	8.41	2.27	9.10	20.21	1.07	10.15	0.49	10.46
29.16	7.39	11.55	4.21	13.23	30.95	3.90	14.35	1.29	15.74
39.22	10.89	15.03	6.85	17.18	40.61	8.32	17.13	2.67	20.13
50.30	15.51	18.45	8.45	22.20	50.71	14.33	19.30	6.05	23.69
61.49	19.80	22.11	11.28	26.63	61.35	22.43	20.65	10.70	26.87
70.43	25.33	23.93	14.42	29.72	70.64	29.44	21.86	16.32	28.82
82.56	30.09	27.84	18.61	33.93	82.80	38.57	23.47	24.17	31.10
91.66	39.63	27.60	23.77	36.02	98.50	54.11	23.55	39.42	31.34
191.88	103.79	46.73	68.95	65.21	201.81	147.52	28.80	123.24	41.68
243.68	141.11	54.41	99.75	76.35	291.83	235.07	30.11	202.08	47.61
378.56	253.75	66.21	189.72	100.18	399.86	339.85	31.83	312.73	46.22
459.09	332.60	67.11	252.05	109.83					

If metal concentration on the solid phase is plotted as a function of metal concentration in solution at equilibrium, sorption isotherms are obtained. Results are presented in **Figure 9 (a)** and **(b)** for As(III) and As(V) respectively:

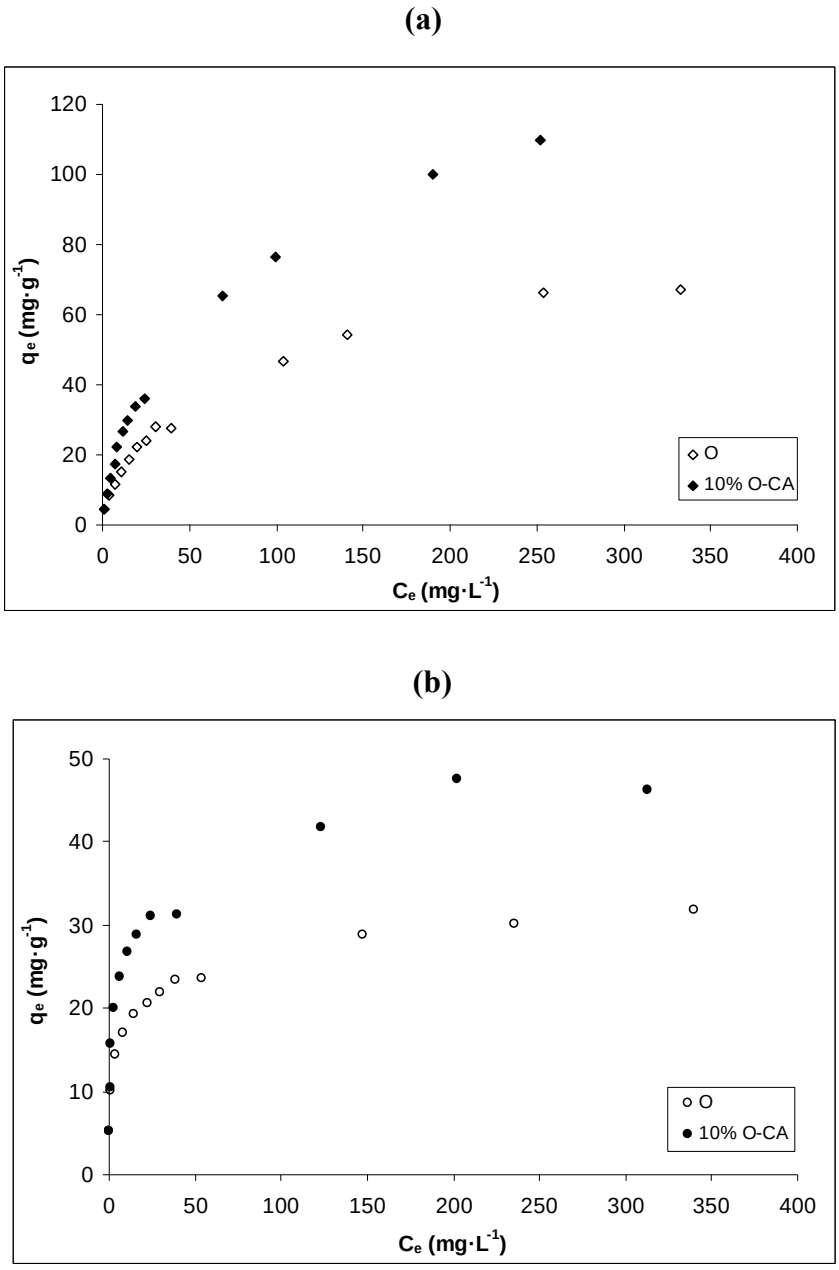

Figure 9: Sorption isotherms of (a) As(III) and (b) As(V) onto O and 10% O-CA. Sorbent dose: 1 $g \cdot L^{-1}$; pH_0=8.0.

In the figure it can be seen the increase on the amount of sorbed arsenic when the equilibrium concentration in solution is raised. The results presented here indicate the different sorption behaviour of O and 10% O-CA. As it can observed, for both As(III) and As(V) always the sorbed amount of arsenic is higher in the case of the entrapped material, being these differences higher as higher is the concentration in solution. These differences

in the sorption behaviour of both sorbents strongly suggest that calcium alginate gel must be playing an important role in the sorption of both, arsenite and arsenate, despite arsenic sorption from an initial concentration about 15 $mg \cdot L^{-1}$ onto pure calcium alginate gel beads was found to be negligible (**Figure 3**).

5.5.1. Sorption equilibrium modeling

The equilibrium experimental data were fitted to Langmuir and Freundlich models and their characteristic parameters were calculated by non-linear analysis of the equilibrium experimental data by using the computer program Microcal Origin 6.0. The obtained results are presented in **Table 7**.

Table 7: Langmuir and Freundlich isotherm constants and maximum uptake (q_{max}) for As(III) and As(V) sorption onto O and 10% O-CA. Initial pH: 8.0; Agitation time: 72 h; Temperature: 20±1.

	Langmuir			Freundlich		
System	q_{max} **(mg·g^{-1})**	K_L **(L·mg^{-1})**	R^2	K_F	*1/n*	R^2
As(III) O	77.4 ± 3.1	0.018 ± 0.002	0.984	6.0 ± 0.6	0.43 ± 0.02	0.985
As(III) 10% O-CA	126.5 ± 5.8	0.019 ± 0.002	0.985	8.1 ± 0.5	0.48 ± 0.01	0.994
As(V) O	26.8 ± 1.0	0.26 ± 0.07	0.905	11.9 ± 0.9	0.16 ± 0.02	0.911
As(V) 10% O-CA	41.6 ± 2.2	0.25 ± 0.07	0.886	15.8 ± 1.2	0.19 ± 0.02	0.946

As it can be seen in the table, despite Freundlich model seems to provide a slightly better fitting, in general, good determination coefficients were obtained with both models, for all the studied systems.

The values of the parameters K_L and *1/n* in Langmuir and Freundlich models respectively are related to the sorbent-sorbate affinity. While in the case of K_L, higher numerical values indicate a more favourable sorption, in the case of *1/n*, lower values are related to a stronger sorbate-surface bond. Results obtained by non-linear adjustment of isothermal data reveal, for a given arsenic oxidation state, a similar affinity of both raw and calcium alginate-entrapped (hydr)oxide. When a comparison of sorption of As(III) and As(V) onto a given sorbent is carried out it was evidenced that, in the experimental conditions of this

work, As(V) sorption was more favourable than As(III), as indicated by the higher K_L and lower *1/n* values.

From the values of q_{max} presented in **Table 7**, an increase of 60% in capacity is evidenced when the solid (hydr)oxide is entrapped. This might be attributed to the presence of calcium alginate but, as said before, As(III) and As(V) sorption by pure calcium alginate beads was found to be negligible in the experimental conditions of in this work. Nevertheless it has been reported that calcium alginate can be activated for arsenate sorption by partial substitution of calcium by ferric ions (Min and Hering, 1998); it may be possible that during the formation of the beads some amount of Fe(III) ions is released from the material and a partial substitution of Ca^{2+} ions takes place that would explain the higher adsorption observed when the (hydr)oxide is in the bead.

The results obtained in this section indicates that despite the affinity of the (hydr)oxide through arsenic is not modified by the presence of the alginate barrier, the gel provokes a positive effect in the sorption capacity.

When model parameters are used to predict the arsenic sorbed mass as a function of the concentration in solution and results are superimposed to experimental sorption data, the next figures are obtained.

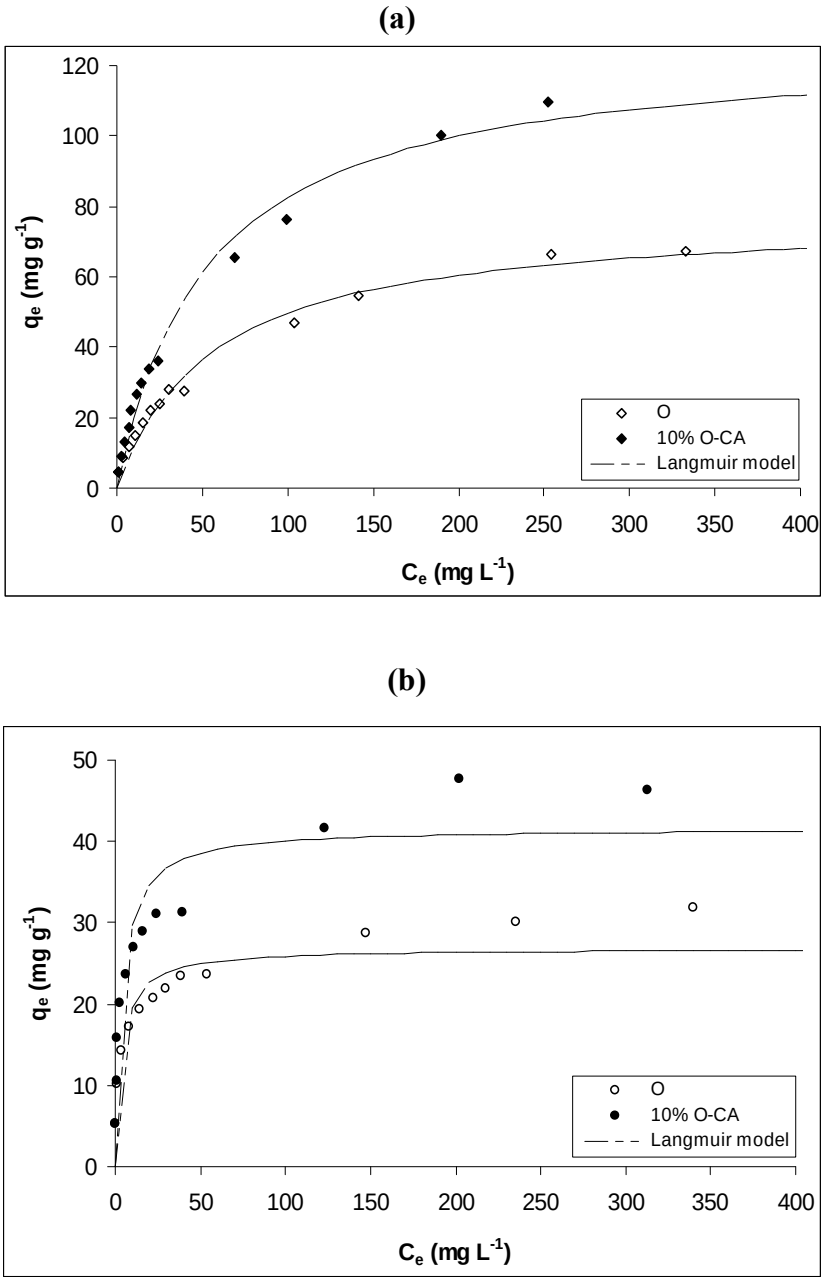

Figure 10: Langmuir model fitting to (a) As(III) and (b) As(V) sorption equilibrium onto both, O and 10% O-CA.

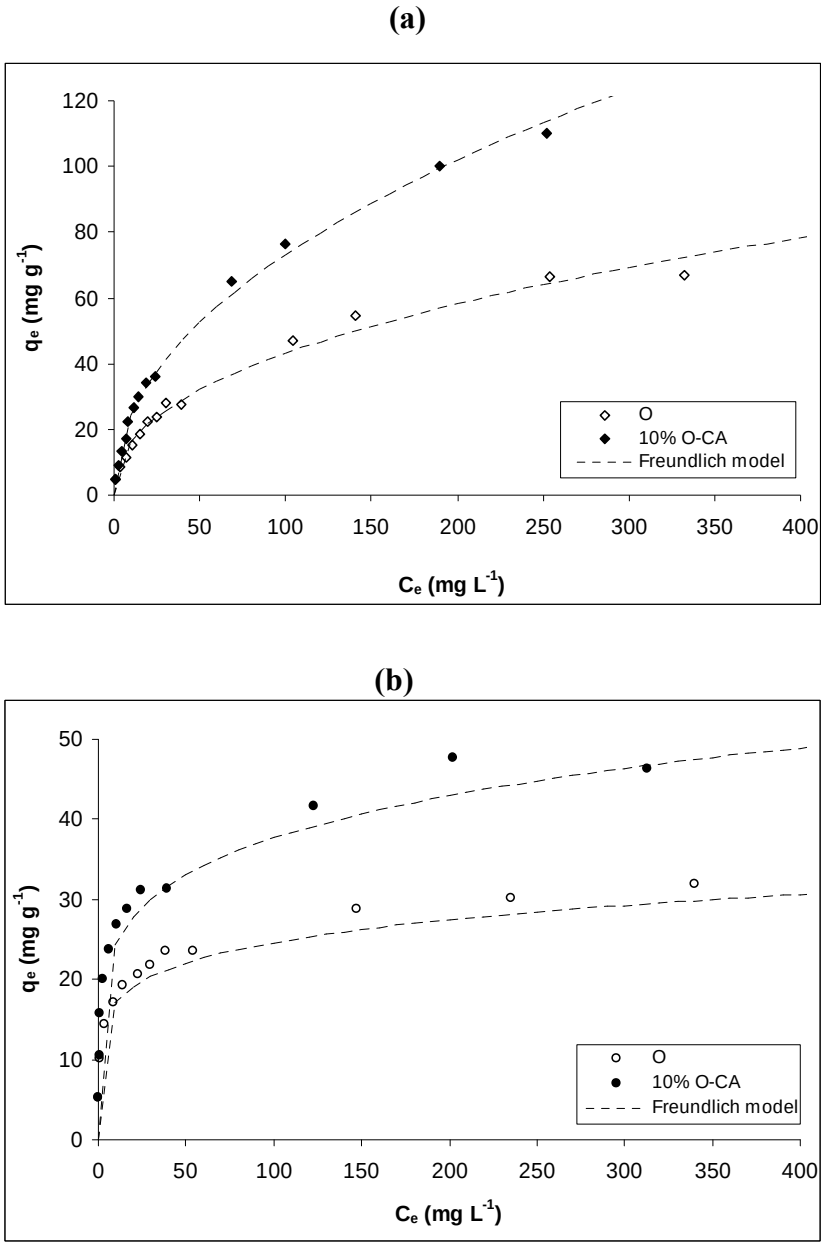

Figure 11: Freundlich model fitting to (a) As(III) and (b) As(V) sorption equilibrium onto both, O and 10% O-CA.

In these figures it can be clearly observed the good agreement between experimental and both, Langmuir and Freundlich models predicted data.

Results obtained in this work have been compared to those obtained by several authors who studied arsenite and arsenate sorption by different Fe(III)-rich minerals or oxide-based materials (**Table 8**).

Table 8: Maximum sorption capacity for arsenic by O and 10% O-CA compared with other adsorbents.

	Capacity ($mg \cdot g^{-1}$)		
Sorbent	**As(III) / *(pH)***	**As(V) / *(pH)***	**Reference**
Raw (hydr)oxide	77.4 / *(8.0)*	26.8 / *(8.0)*	This work
10% O-CA	126.5 / *(8.0)*	41.6 / *(8.0)*	This work
Red mud	0.66 / *(7.25)*	0.52 / *(3.50)*	Altundogan *et al.*, 2002
$FePO_4$ (amorphous)	21 / *(7-9)*	10 / *(6-6.7)*	Lenoble *et al.*, 2005
$FePO_4$ (crystalline)	16 / *(7-9)*	9 / *(6-6.7)*	Lenoble *et al.*, 2005
Goethite	7.5 / *(5.5)*	12.5 / *(5.5)*	Ladeira & Ciminelli, 2004
Ferrihydrite	266.5 /*(8-9)*	111.0 / (8-9)	Raven *et al.*, 1998
Fe(III)-loaded chelating resin	62.9 / (9.0)	55.4 / (3.5)	Matsunaga *et al.*, 1996
Fe(III)-oxide pillared clay	13 / *(<9)*	4 / *(<9)*	Lenoble *et al.*, 2002
Goethite	22 / *(9)*	4 / *(9)*	Lenoble *et al.*, 2002
Hydrous Fe(III)oxide	28 / *(<9)*	7 / *(<9)*	Lenoble *et al.*, 2002
Synthetic mixed Fe-Mn oxide	132.6 / *(4.8)*	71.9 / *(4.8)*	Zhang *et al.*, 2007a
Fe(III)oxyhydroxide-loaded cellulose beads	99.6 / *(7)*	33.2 / *(7)*	Guo & Chen, 2005
Fe(III)oxide-loaded slag	≈ 10 / *(2.5)*	≈ 35 / *(2.5)*	Zhang & Itoh, 2005
Fe(III)-doped lignocellulose	11 / *(6)*	22.5 / *(4)*	Dupont *et al.*, 2007
Fe(III)-loaded resin	11.2 / *(1.7)*	60.0 / *(1.7)*	Rau *et al.*, 2003
Fe(III)-loaded sponge	137 / *(4.5)*	18 / *(9)*	Muñoz *et al.*, 2002
Alginate beads doped with Fe(III) oxide	---	4.75 µg/g / *(7)*	Zouboulis & Katsoyiannis, 2002
Fe(III)oxide-coated alginate beads	---	2.6 µg/g / *(7)*	Zouboulis & Katsoyiannis, 2002
Fe(III)oxide-loaded alginate beads	---	7.2 µg/g / *(7)*	Zouboulis & Katsoyiannis, 2002
NiO	---	≈ 4 / *(8.4)*	Hristovski *et al.*, 2007
Fe(III)oxide/activated carbon composite	---	74.4 / *(5.0)*	Zhang *et al.*, 2007b

As seen, the maximum sorption values obtained for arsenite when using 10% O-CA are comparable to iron-loaded sorbents as synthetic mixed Fe-Mn oxide (Zhang *et al.*, 2007a) and Fe(III)-loaded sponge (Muñoz *et al.*, 2002). In the case of arsenate, the results obtained in this work are similar to those obtained with Fe(III)-loaded chelating resin (Matsunaga *et al.*, 1996) and Fe(III)oxide-loading slag (Zhang & Itoh, 2005).

5.6. Solid state analysis and sorption mechanistic approach

In order to obtain information about the possible/s mechanism/s involved in As(III) and As(V) sorption onto the (hydr)oxide, different spectroscopic and microscopic techniques were used. The possible changes of cristallynity of the sorbent material when loading with arsenic were studied by means of the XRD technique. In a second step, observation of surface topology and analysis of the local chemical composition was carried out by SEM and EDX techniques respectively. Finally, characterization of the surface functional groups of the material and its implication in both, As(III) and As(V) sorption, was carried out by means of FTIR-ATR spectroscopy.

5.6.1. Solid state analysis

In the next figure, the diffractogram of the raw and arsenic-laden material is presented.

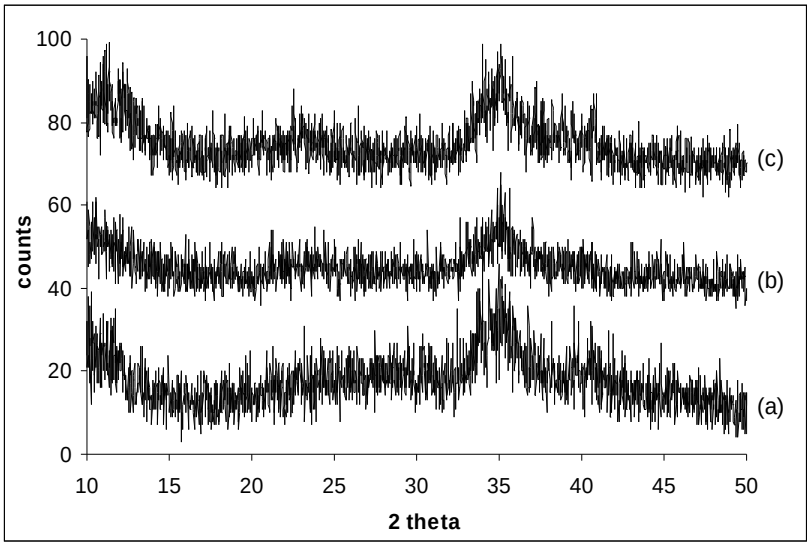

Figure 12: XRD of (hydr)oxide before (a) and after As(III) (b) or As(V) (c) sorption.

According to the XRD pattern of the native (hydr)oxide presented in this figure, this material can be identified as a poorly crystalline iron oxy-hydroxide, similar to 2-lines ferrihydrite (Gautier *et al.*, 2006). The ferrihydrite, of formula $Fe_5(HO)_8 \cdot 4H_2O$ is a poorly crystalline mineral commonly formed as a result of low-temperature geochemical processes at and near the Earth's surface. Both natural and synthetic ferrihydrite occurs in nanoparticulate form, and it is an important adsorbent of minor elements in surface systems

because of its high reactivity and large surface area (Waychunas *et al*., 1993). These particles are the precursors to more stable iron oxide minerals, including goethite and hematite, and the presence of dopants can substantially alter the phase transformations between ferrihydrite and these more stable iron oxides. The almost absence of crystallinity after loading the sample with As(III) and As(V) indicates that there's no crystalline phase transformation after arsenic sorption. Furthermore, despite SEM micrographs reveal an important arsenic surface concentration after treatment with As(III) and As(V) solutions (**Figure 13 (b)** and **(c)** respectively), no significant surface topology changes were evidenced when comparing with the untreated material (**Figure 13 (a)**).

(a)

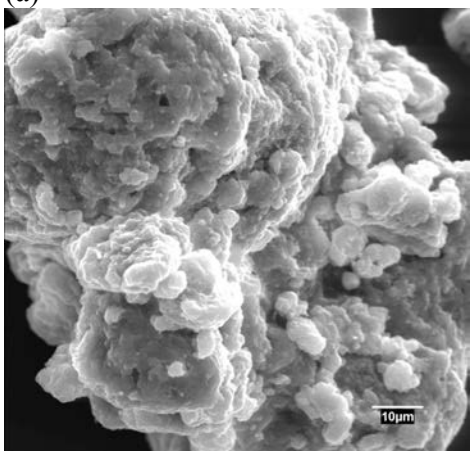

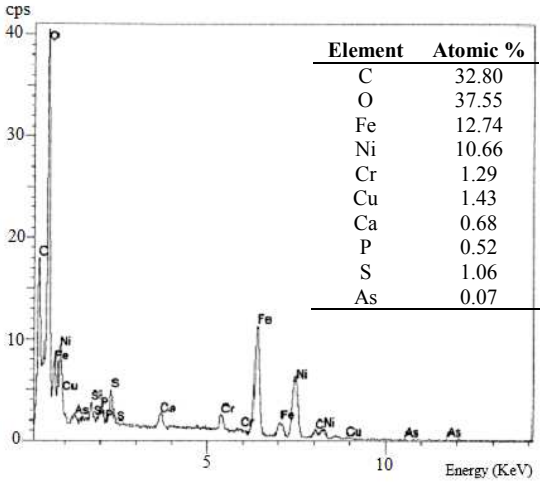

Element	Atomic %
C	32.80
O	37.55
Fe	12.74
Ni	10.66
Cr	1.29
Cu	1.43
Ca	0.68
P	0.52
S	1.06
As	0.07

(b)

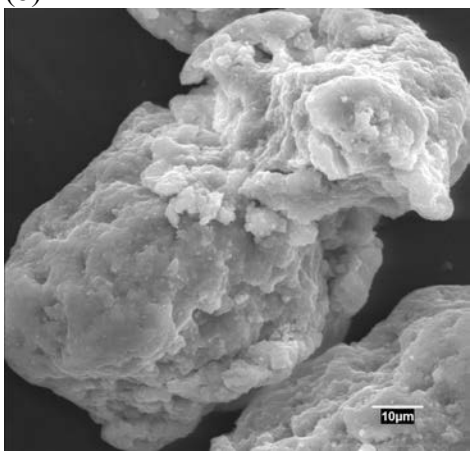

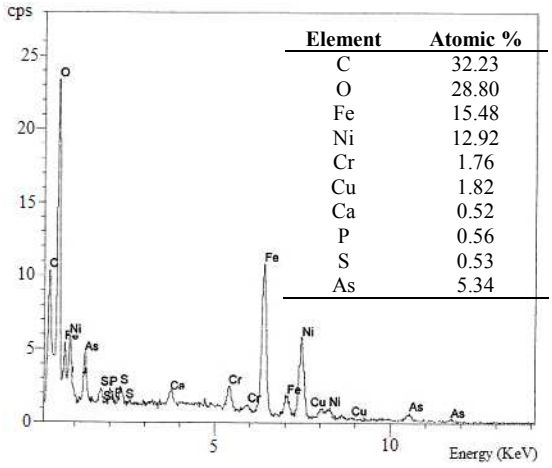

Element	Atomic %
C	32.23
O	28.80
Fe	15.48
Ni	12.92
Cr	1.76
Cu	1.82
Ca	0.52
P	0.56
S	0.53
As	5.34

(c)

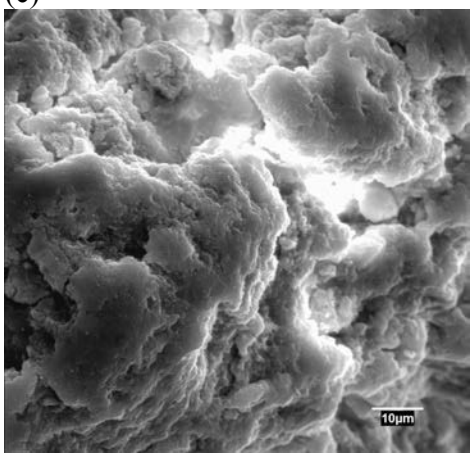

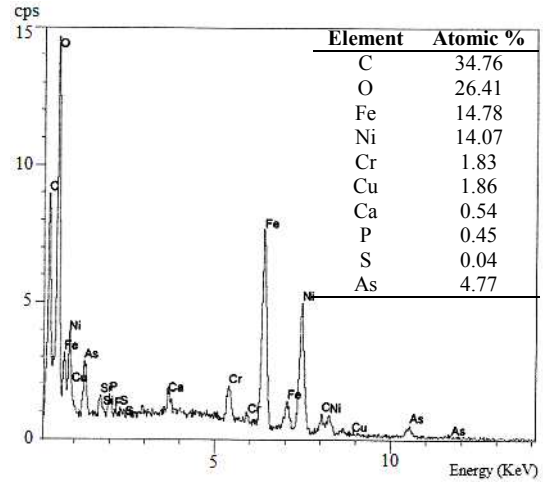

Element	Atomic %
C	34.76
O	26.41
Fe	14.78
Ni	14.07
Cr	1.83
Cu	1.86
Ca	0.54
P	0.45
S	0.04
As	4.77

Figure 13: SEM-EDX analysis of O (a) before and after (b) As(III) and (c) As(V) sorption.

In the next figure the infrared spectra of raw material and after As(III) and As(V) sorption is presented.

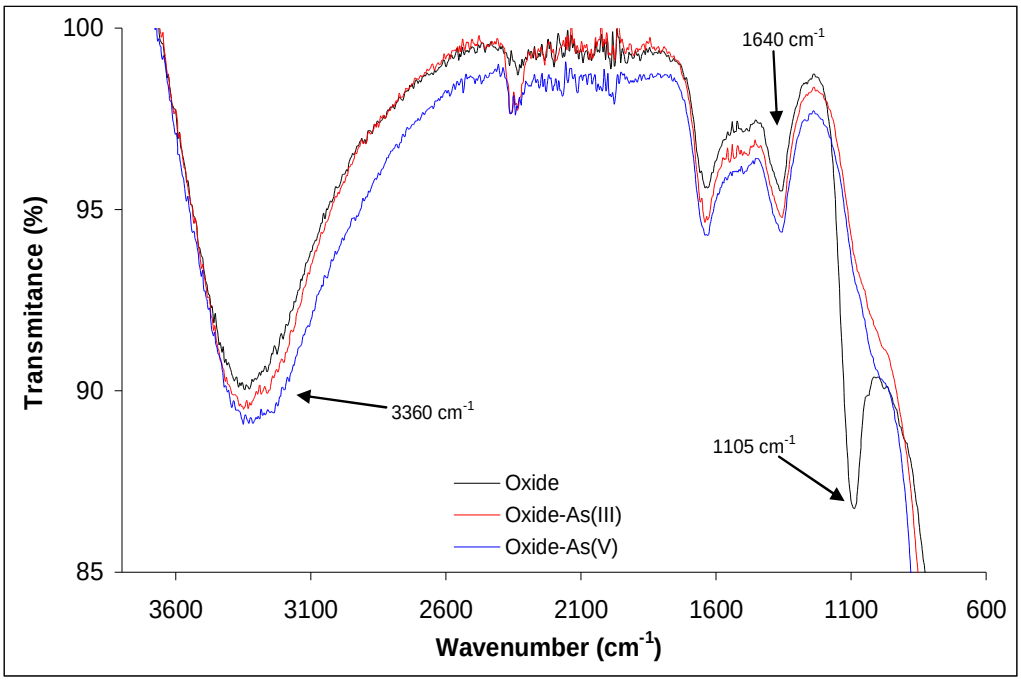

Figure 14: FTIR-ATR spectra of waste (hydr)oxide before and after treatment with As(III) and As(V) solutions.

The FTIR spectra of native dry (hydr)oxide and after treatment with both As(III) and As(V) solutions (**Figure 14**) exhibited a wide band centered at 3360 cm^{-1}, corresponding to bulk OH stretch and free surface OH groups (Arienzo *et al.*, 2002) and another band at 1640 cm^{-1} corresponding to water bending (Zhang *et al.*, 2005). The large width of the 3360 cm^{-1} band confirmed the XRD data for a disordered crystal structure (Arienzo *et al.*, 2002) and the abundance of free hydroxyls of the material.

The band appearing at 1105 cm^{-1}, corresponding to the M-OH bending, almost disappears when loading the sorbent with both As(III) and As(V). This result indicated that substitution of the free hydroxyls coordinated to the metals (M-OH structures) by either As(III) or As(V) species would play an important role in the sorption mechanism (Zhang *et al.*, 2005).

5.6.2. As(III) and As(V) sorption mechanistic approach

Different arsenic sorption mechanisms on various iron(III)-based sorbents have been reported in the literature. Lenoble (Lenoble *et al.*, 2005) proposed As(III) removal mechanisms by Fe(III) derivatives based on the oxidation to As(V) and the precipitation of an Fe(II) arsenate salt like $Fe_3(AsO_4)_2 \cdot 8H_2O$. The process can be summarized by the next reactions:

$$Fe^{3+} + 1e^- \leftrightarrow Fe^{2+}$$
$$H_3AsO_3^0 + 2H_2O \leftrightarrow HAsO_4^{2-} + 4H^+ + 2e^-$$
$$3Fe^{2+} + 2HAsO_4^{2-} \leftrightarrow Fe_3(AsO_4)_2\,(s) + 2H^+$$

In our case, it was checked the absence of iron in solution at pHs within the range 4 to 11, where As(III) sorption is maximum, indicating thus that this mechanism would not be responsible of As(III) removal.

Taking into account (i) the characteristics of our (hydr)oxide solid, (ii) the absence of crystallinity and (iii) the presence of functional groups on the sorbent surface (mainly free hydroxyls) and considering (iv) the nature of arsenic species present in solution at the working pH, we proposed in Figure 8 the mechanisms for As(III) and As(V) sorption onto (hydr)oxide.

For As(III) removal it was supposed that the free hydroxyls of the sorbent interact with the $H_3AsO_3^0$ species according to:

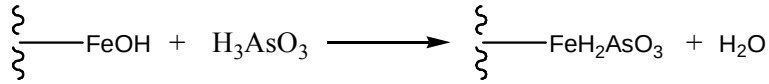

Such a sorption mechanism has been reported in literature, as responsible for arsenite and arsenate sorption onto an aquifer material of complex mixed mineralogical nature (Carrillo and Drever, 1998).

In the case of As(V), two different mechanisms can contribute to sorption: (i) non-specific coulombic interactions between arsenate species and the positively charged functional groups on the sorbent surface and (ii) coordination of arsenate species onto metal (hydr)oxides with the formation of coordination compounds of low solubility, according to:

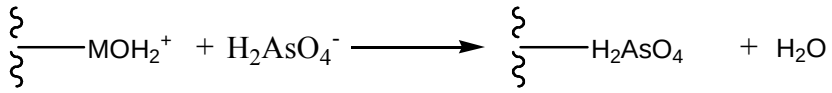

These sorption mechanisms are summarized in **Figure 14**.

A question remains: what can be the effect of co-precipitated metal hydroxides (mainly Ni(II)? Although information from literature is scarce, results reported by Jia and Demopoulos (Jia and Demopoulos, 2008) can be referred. The authors pointed out an enhanced co-precipitation of As(V) with Fe(III) in presence of Ni(II) probably due to co-precipitation of a nickel-ferric hydroxide. Moreover, the As(V) loading capacity of metal-doped goethite decreased in the order: Cu(II)-doped≥Ni(II)-doped≥Co(II)-doped≥pure goethite whatever the pH (Mohapatra *et al*., 2006). Such a doping leaded to an increase in the pH_{zpc} and also in surface area, both phenomena allowing to increase the sorption behaviour.

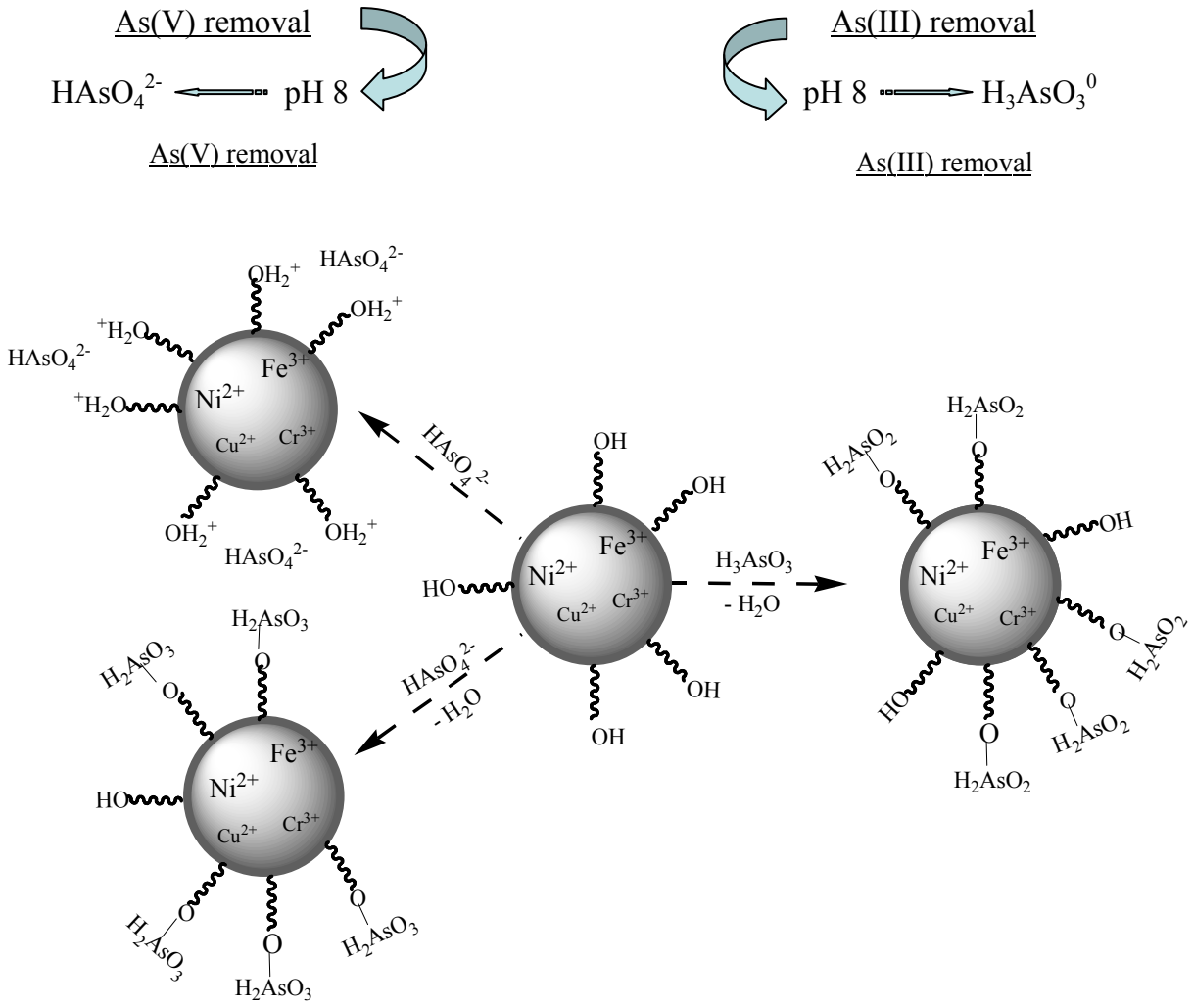

Figure 14: As(III) and As(V) sorption mechanisms onto waste (hydr)oxide.

As summarized in **Figure 14**, while As(III) sorption would be due to the surface complex formation, As(V) sorption would be due to both contributions: surface reactions and also coulombic interactions between the partially positively charged surface and the monohydrogenarsenate species.

5.7. Hazard classification of the spent sorbent

The EPA TCLP Test was applied to the As-loaded sorbent used in sorption experiments to classify this material as inert or hazardous before any disposal (US Environmental Protection Agency, 1999). In an attempt to quantify the hazard, the U.S. EPA established the general guidance that if metal concentrations in the extract do not exceed 100 times the Maximum Contaminant Level (MCL) in drinking water for that metal, the waste would not be considered hazardous. Among the elements in our (hydr)oxide material, only As, Cu and Cr are included in the EPA listing; iron can be found within the national secondary drinking water standards, with a MCL of 0.3 $mg \cdot L^{-1}$. A recent provisional MCL value of 0.1 $mg \cdot L^{-1}$ was given by EPA for nickel in drinking water. Results of the leaching test are presented in **Table 9**.

	Concentration ($mg \cdot L^{-1}$)				
	Fe	**Ni**	**Cu**	**Cr**	**As**
O	0.08	99.8	1.76	0.88	0.12
O-As(III)	0.08	72.59	1.36	0.86	0.09
O-As(V)	0.12	75.16	1.30	0.86	0.15
10% O-CA	0.059	22.3	2.02	1.01	0.13
10% O-CA-As(III)	0.056	23.8	1.88	1.14	0.07
10% O-CA-As(V)	0.052	21.9	1.25	1.03	0.08
*MCL	0.3	0.1	1.3	0.1	0.01
TCLP = 100* MCL	30	10	130	10	1

*MCL: Maximum Contaminant Level

Results of the test put into evidence that neither Fe, Cu, Cr nor As extracted amounts exceeded the criteria of 100 times the MCL set by the U.S. EPA. Only according to the data for nickel, the corresponding waste would have to be managed as a hazardous material. However, it has to be pointed out that this TCLP test is not realistic of common environmental conditions, and that other standardized tests might give different waste classification.

6. CONCLUSIONS

The waste material obtained from the precipitation of the metals present in the wastewater of an electroplating industry can be used as an efficient adsorbent for the removal of As(III) and As(V) from aqueous effluents. This material has a composition, in $mg \cdot g^{-1}$: Fe(III): 142.3±1.4; Ni(II): 174.4±4.1; Cu(II): 15.4±0.4; Cr(III): 15.1±0.6 and Ca: 12.6±0.4 and it is identified as a poorly crystalline iron (hydr)oxide, similar to 2-lines ferrihydrite. The material contains also an important Carbon concentration coming from the use of complexing, flocculating and coagulating agents added in the industrial detoxification process.

For this waste a device based on the entrapment of the dusty raw material in a calcium alginate gel matrix can be successfully implemented for its immobilization. Arsenite and arsenate uptake increases when increasing the (hydr)oxide concentration in the calcium alginate gel beads. A maximum content of 10% weight/volume ratio (hydr)oxide/alginate gel can be easily obtained but the preparation of gel beads with higher (hydr)oxide content is forbidden by the high density and viscosity of the solutions to pump.

As(III) and As(V) sorption onto both entrapped and non-entrapped (hydr)oxide is strongly pH dependent. While arsenite removal onto both sorbents reaches its maximum in the pH range $5 \leq pH \leq 10$, in the case of arsenate, a narrower pH range $6 \leq pH \leq 9$ was observed.

Despite of the high potential toxicity of the material used in this study because of its important content of toxic metal cations, neither acidic solubilisation nor metal release due to the presence of As(III) or As(V) was observed for initial pHs higher than 3. pHs below 3 provokes acidic solubilization of the (hydr)oxide and leaching of the metals to the liquid phase. Under acidic conditions ($pH \leq 3$), calcium alginate acts avoiding partially the leakage of these cations to the fluid.

The presence of the alginate gel provokes a decrease in arsenic sorption rate, being the As(V) the most affected by the entrapment. These fact is explained in basis to the speciation of both, arsenic and alginate gel matrix. While As(III) sorption involves the diffusion of neutral $H_3AsO_3^0$ through the negatively charged alginate matrix (calcium alginate pH_{zpc}: 6.5), in the case of As(V), sorption involves the diffusion of a dianionic

species, $HAsO_4^{-2}$. The negative charge of the alginate and of the $HAsO_4^{-2}$ difficults these species to reach the (hydr)oxide surface.

For an initial arsenic concentration of 15 $mg \cdot L^{-1}$, arsenite and arsenate removal seems to be governed by external mass transport. While the rate of uptake is slower in the case of entrapped material than in the case of the raw (hydr)oxide, a higher maximum capacity is always observed in the case of the entrapped material. Despite calcium alginate does not effectively adsorbs neither arsenite nor arsenate, this material seems to play an important role in the additional arsenic sorption observed in the entrapped material.

For a given arsenic oxidation state, the entrapment in calcium alginate of the waste (hydr)oxide does not seem to affect the sorbent-sorbate affinity. Despite As(V) sorption onto both, entrapped and non-entrapped waste (hydr)oxide, shows a lower affinity than As(III), arsenic sorption on its trivalent oxidation state leads to a higher sorbed amount.

Free hydroxyls on the sorbent material are they key components involved of the sorption process. While As(III) uptake can be attributed to the formation of surface complexes with the free –OH of the material, As(V) removal would have two different contributions: surface complexation reactions and coulombic type interactions in between the partially positively charged surface and the negatively-charged arsenate species. All these modifications take place without crystalline changes in the solid surfaces involved.

7. REFERENCES

· Ahn, J.S., Chon, C.-M, Moon, H.-S., Kim, K.-W., Arsenic removal using steel manufacturing by-products as permeable reactive materials in mine tailing containment systems, Water Res. 37 (10) (2003) 2478–2488.

· Amin, M.N., Kaneco, T., Kitagawa, A., Begum, H., Katsukama, T., Suzuki, T., Ohta, K., Removal of arsenic in aqueous solutions by adsorption onto waste rice husk. Ind. Eng. Chem. Res. 45 (2006) 8105-8110.

· Amsden, B., Turner, N., Diffusion characteristics of calcium alginate gels. Biotechnol. Bioeng. 65 (1999) 605-610.

· Apel, M.L., Torma, E., Determination of kinetics and diffusion coefficients of metal sorption on Ca-alginate beads. Can. J. Chem. Eng. 71 (1993) 652-656.

· Aksu, Z., Egretli, E., Kutsal, T., A comparative study of copper(II) biosorption on Ca-alginate, agarose and immobilized *C. vulgaris* in a packed bed column, Process Biochem. 33 (1998) 393-400.

· Altundogan, H.S., Altundogan, S., Tumen, F., Bildik, M., Arsenic adsorption from aqueous solutions by activated red mud, Waste Manage. 22 (2002) 357–363.

· Altundogan, H.S., Altundogan, S., Tumen, F., Bildik, M., Arsenic removal from aqueous solutions by adsorption on red mud, Waste Manage. 20 (8) (2000) 761–767.

· Arienzo, M., Adamo, P., Chiarenzelli, J., Bianco, M.R., De Martino, A., Retention of arsenic on hydrous ferric oxides generated by electrochemical peroxidation, Chemosphere, 48 (2002) 1009-1018.

· Banerjee, A., Nayak, D., Lahiri, S., Speciation-dependent studies on removal of arsenic by iron-doped calcium alginate beads. Appl. Radiat. Isot. 65 (2007) 769-775

· Boyd, G.E., Adamson, A.W., Mayers, L.S., The exchange adsorption of ions from aqueous solutions by zeolites. II. Kinetics, J. Am. Chem. Soc. 69 (1947) 28–36.

· Carrillo, A., Drever, J.I., Adsorption of arsenic by natural aquifer material in the San Antonio-El Triunfo mining area, Baja California, Mexico, Environ. Geol. 35 (1998) 251-257.

· Chen, J., Hong, L., Wu, S., Wang, L., Elucidation of interactions between metal ions and Ca-alginate based ion-exchange resins by spectroscopic analysis and modelling simulation. Langmuir, 18 (2002) 9413-9421.

· Chen, J., Tendeyong, F., Yiacoumi, S., Equilibrium and kinetic studies of copper ion uptake by calcium alginate, Environ. Sci. Technol. 31 (1997) 1433-1439.

· Davranche, M., Lacour, S., Bordas, F., Bollinger, J.C., An easy determination of the surface chemical properties of simple and natural solids, J. Chem. Educ. 80 (2003) 76-78.

· Deschamps, E., Ciminelli, V.S.T., Höll, W.H. Removal of As(III) and As(V) from water using a natural Fe and Mn enriched sample. Water Res. 39 (2005) 5212-5220.

· Diamadopoulos, E., Loannidis, S., Sakellaropoulos, G.P., As(V) removal from aqueous solutions by fly ash, Water Res. 27 (12) (1993) 1773– 1777.

· Directive 98/83/EC of 3 November 1998 on the quality of water intended for human consumption. Official Journal of the European Union, 5.12.98.

· Dupont, L., Jolly, G., Aplincourt, M., Arsenic adsorption on lignocellulosic substrate loaded with ferric ion. Environ. Chem. Lett. 5 (2007) 125-129.

· Elizalde-González, M.P., Mattusch, J., Einicke, W.D., Wennrich, R., Sorption on natural soils for arsenic removal, Chem. Eng. J. 81 (2001) 187-195.

· El-Kamash, A.M., Kaki, A.A., Abed El Geleel, M., Modelling batch kinetics and thermodynamics of zinc and cadmium, J. Hazard. Mater. B127 (2005) 211-220.

· Fiol, N., Poch, J., Villaescusa, I., Chromium (VI) uptake by grape stalks wastes encapsulated in calcium alginate beads: equilibrium and kinetics studies, Chem. Spec. Bioavailab. 16 (2004) 25-34.

· Garelick, H., Dybowska, A., Valsami-Jones, E., Priest, N.D., Remediation technologies for arsenic contaminated drinking waters. J. Soils Sediments 5 (2005) 182-190.

· Gautier, J., Grosbois, C., Courtin-Nomade, A., Floc'h, J.P., Martin,F., Transformation of natural As-associated ferrihydrite downstream of a remediated mining site, Eur. J. Mineral. 18 (2006) 187-195.

· Giménez, J., Martínez, M., de Pablo, J., Rovira, M., Duro, L., Arsenic sorption onto natural hematite, magnetite and goethite. J. Hazard. Mater. 141 (2007) 575–580.

· Guo, H., Stüben, D., Berner, Z., Removal of arsenic from aqueous solution by natural siderite and hematite. Appl. Geochem. 22 (2007) 1039-1051.

· Guo, X., Chen, F., Removal of arsenic by cellulose beads loaded with iron oxyhydroxide from groundwater. Environ. Sci. Technol. 39 (2005) 6808-6818.

· Hristovski, K., Baumgardner, A., Westerhoff. P., Selecting metal oxide nanomaterials for arsenic removal in fixed bed columns: From nanopowders to aggregated nanoparticle media. J. Hazard. Mater. 147 (2007) 265-274.

· Jia, Y., Demopoulos, G.P., Coprecipitation of arsenate with iron(III) in aqueous sulfate media: Effect of time, lime and co-ions on arsenic retention. Water Res. 42 (2008) 661-668.

· Jodra, Y., Mijangos, F., Ion exchange selectivities of calcium alginate gels for heavy metals, Wat. Sci. Technol. 43 (2001) 237-244.

· Kapaj, S., Peterson, H., Liber, K., Bhattacharya, P., Human health effects from chronic arsenic poisoning – A review. J. Environ. Sci. Health. 41A (2006) 2399-2428.

· Ladeira, A.C.Q., Ciminelli, V.S.T, Adsorption and desorption of arsenic on an oxisol and its constituents, Water Res. 38 (2004) 2087–2094.

· Lenoble, V., Bouras, O., Deluchat, V., Serpaud, B., Bollinger, J.C., Arsenic adsorption onto pillared clays and iron oxides, J. Colloid Interface Sci. 255 (2002) 52-58.

· Lenoble, V., Laclautre, C., Deluchat, V., Serpaud, B., Bollinger, J.C., Arsenic removal by adsorption on iron(III) phosphate, J. Hazard. Mater.123 (2005) 262–268.

· Mandal, B. K., Suzuki, K.T., Arsenic round the world: a review. Talanta, 58 (2002) 201-235.

· Matsunaga, H., Yokoyama, T., Eldridge, R.J., Bolto, B.A., Adsorption characteristics of arsenic(III) and arsenic(V) on iron(III)-loaded chelating resin having lysine-*N*~,*N*~-diacetic acid moiety, React. Polym. 29 (1996) 167–174.

· McKay, G., Ho, Y.S., Ng, J.C.Y. , Biosorption of copper from waste waters: a review, Sep. Purif. Methods 28 (1999) 87-125.

· Min, J.H., Hering, J., Arsenate sorption by Fe(III)-doped alginate gels, Wat. Res. 32 (1998) 1544-1552.

· Mohan D., Pittman Jr. C.U., Arsenic removal from water/wastewater using adsorbents-A critical review, J. Hazard. Mater. 142 (2007) 1-53.

· Mohan D., Singh K.P., Single- and multi-component adsorption of cadmium and zinc using activated carbon derived from bagasse-an agricultural waste, Water Res. 36 (2002) 2304–2318.

· Mondal, P., Majumder, C.B., Mohanty, B., Effects of adsorbent dose, its particle size and initial arsenic concentration on the removal of arsenic, iron and manganese from simulated ground water by Fe^{3+} impregnated activated carbon. J. Hazard. Mater. 150 (2008) 695–702.

· Mohapatra, M., Sahoo, S., Anand, S., Das, R.P., Removal of As(V) by Cu(II)-, Ni(II)-, or Co(II)- doped goethite samples. J. Colloid Interface Sci. 298 (2006) 6-12.
· Mondal, P., Majumder, C.B., Mohanty, B., Laboratory based approaches for arsenic remediation from contaminated water: Recent developments. J. Hazard. Mater. B137 (2006) 464-479.

· Muñoz, J.A., Gonzalo, A., Valiente, M., Arsenic adsorption by Fe(III)-loaded open-celled cellulose sponge. Thermodynamic and selectivity aspects. Environ. Sci. Technol. 36 (2002) 3405-3411.

· Navasivayam, C., Senthilkumar, S., Removal of arsenic(V) from aqueous solutions using industrial solid waste: adsorption rates and equilibrium studies, Ind. Eng. Chem. Res. 37 (1998) 4816-4822.

· Puigdomènech, I., Make Equilibrium Diagrams Using Sophisticated Algorithms (MEDUSA), software version 18 February 2004. Inorganic Chemistry Department, Royal Institute of Technology, Stockholm, Sweden. Available free at http://web.telia.com/~u15651596/, consulted October 05, 2007.

· Rau, I., Gonzalo, A., M. Valiente, M., Arsenic (V) adsorption by immobilized iron mediation. Modeling of the adsorption process and influence of interfering anions. React. Funct. Polym. 54 (2003) 85-94.

· Raven, K.P., Jain, A., Loeppert, R.H., Arsenite and arsenate adsorption on ferrihydrite: kinetics, equilibrium and adsorption envelopes, Environ. Sci. Technol. 32 (1998) 344-349.

· Scott, C.D., Woodward, C.A., Thompson, J.A., Solute diffusion in biocatalyst gel beads containing biocatalysis and other additives. Enzyme Microb. Technol. 11 (1989) 258-263.

· Shao, W., Li, X., Cao, Q., Luo, F., Li, J., Du, Y., Adsorption of arsenate and arsenite anions from aqueous medium by using metal(III)-loaded amberlite resins. Hydrometallurgy 91 (2008) 138-143.

· Smedley, P.L., Kinniburgh, D.G., A review of the source, behaviour and distribution of arsenic in natural waters. Appl. Geochem. 17 (2002) 517-569.

· Usov, A.I., Alginic acids and alginates: analytical methods used for their estimation and characterisation of composition and primary structure, Russ. Chem. Rev. 68 (1999) 957-966.

· Veglio, F., Esposito, A., Reverberi, A.P., Copper adsorption on calcium alginate beads: equilibrium pH-related models, Hydrometallurgy, 65 (2002) 43-57.

· Wang S., Li, H., Xu, L., Application of zeolite MCM-22 for basic dye removal from wastewater, J. Colloid Interface Sci. 295 (2006) 71–78

· Wang, S., Mulligan, C.N., Natural attenuation processes for remediation of arsenic contaminated soils and groundwater. J. Hazard. Mater. B138 (2006) 459-470.

· Waychunas, G.A., Rea, B.A., Fuller, C.C., Davis, J.A., Surface chemistry of ferrihydrite: Part 1. EXAFS studies of the geometry of coprecipitated and adsorbed arsenate. Geochim. Cosmochim. Acta 1993, 57, 2251-2269.

· WHO (World Health Organisation), Environmental Health Criteria, 18: Arsenic, World Health Organisation, Geneva, 1981.

· Zhang, G.S., Qu, J.H., Liu, H.J., Liu, R.P., Li, G.T., Removal mechanism of As(III) by a novel Fe-Mn binary oxide adsorbent: oxidation and sorption. Environ. Sci. Technol. 41 (2007) 4613-4619.

· Zhang, F.S., Itoh, H., Iron oxide-loaded slag for arsenic removal from aqueous system. Chemosphere 60 (2005) 319-325.

· Zhang, Q.L., Lin, Y.C., Chen, X., Gao, N.Y., A method for preparing ferric activated carbon composites adsorbents to remove arsenic from drinking water. J. Hazard. Mater. 148 (2007) 671-678.

· Zhang, Y., Yang, M., Dou, X.M., He, H., Wang, D.S., Arsenate adsorption on an Fe-Ce bimetal oxide adsorbent: role of surface properties, Environ. Sci. Technol. 39 (2005) 7246-7253.

· Zouboulis, A.I., Katsoyiannis, I.A, Arsenic removal using iron oxide loaded alginate beads. Ind. Eng. Chem. Res. 41 (2002) 6149-6155.

Chapter 6. CONCLUSIONS

1. CONCLUSIONS

In the present document, low cost sorption technology has been explored for the removal of Cr(VI), Cr(III), Cu(II), Ni(II), Pb(II), Cd(II), As(V) and As(III). Different sorbents, conditions and environments have been evaluated in an attempt to obtain a broad view of the feasibility of these techniques in the treatment of industrial polluted effluents.

Sorption processes based in the use of low cost material uses biomass raw materials or industrial by-products which are either naturally abundant or because they are wastes of industrial operations. The unique capabilities of certain types of wastes to concentrate and immobilize heavy metals can be more or less effective, dependent to a certain degree on:

- chemical nature and structure of sorbent
- type of metal
- solution environment (multimetal mixtures, presence of additives, pH)
- sorbent preparation
- physico-chemical processes involved

Among the different parameters affecting the detoxification process, it can be remarked by its relevance, the pH of the solution. Along the present document it has been demonstrated the importance of the pH of the effluent in the potential detoxification capacity that the material could achieve. It is well known that the proton concentration in solution strongly influences not only the site dissociation of the sorbent, but also the solution chemistry of the heavy metals: hydrolysis, complexation by organic and/or inorganic ligands, redox reactions, precipitation, the speciation and the availability of the heavy metals for the active sites.

Sorptive capacity of metal cations onto grape stalk and exhausted coffee exhibit an increasing trend with pH. As H^+ competes with metal cations for the active sites of the sorbent, its decrease in solution when pH increases, positively contributes to the removal of the toxic cation. However, too high pH values can cause precipitation of metallic cations, so it must be avoided when sorption experiments are being carried out. In general it has been demonstrated that pHs about 5, lead to the highest sorption performance for heavy metal cations.

On the contrary it can be found the removal of anionic metal species with oxidizing properties, as the hexavalent chromium. In this case, a different trend than in heavy metal cations sorption was observed, indicating thus that proton plays a completely different role.

For the removal of anions, a low pH value is generally favourable sorption. Nevertheless, when biomaterials such as the grape stalk are going to be used as sorbents, too low pH values must be avoided, because degradation of the sorbent by acidic hydrolysis might take place. Optimal removal of Cr(VI) when entrapped grape stalk is employed as sorbent, has been found for an initial solution pH about 3.

In the case of arsenic sorption onto the (hydr)oxide waste material, sorption has been also found to be a process strongly dependent on the pH of the solution and optimal values close to neutrality have been found for both, As(III) and As(V). In this case, also extreme acidic conditions must be avoided due to the solubilization of the sorbent material.

The analysis of the role of H^+ in sorption of the different pollutants in the different sorbents, the study and quantification, when needed, of the possible cation exchange and the application of different instrumental spectroscopic and microcopic techniques, have also contributed to elucidate the possible sorption mechanisms.

In the case of heavy metal cations sorption onto the vegetable biomass, the uptake is governed by a cation exchange mechanism. This exchange might occur with the light metals, such as Ca^{2+} when the raw material is used, or by H^+, if the material has been submitted to a treatment in acidic media. This mechanism is in agreement with the fast sorption kinetics observed, due to the fact that ion exchange is a process that generally occurs with low activation energy.

As radically different was the role of H^+ in Cr(VI) sorption onto grape stalk, completely different is its removal mechanism. In this case, sorption is partially based in the reduction to its trivalent oxidation state, being the extension of this reaction strongly dependent on H^+ concentration in solution. This mechanism was further confirmed by a kinetic model including the hexavalent chromium disappearing by adsorption and by transformation into Cr(III). The proposed model was capable of successfully describe kinetics of the sorption/desorption/reduction processes involved in a stirred tank reactor when fed with Cr(VI) and grape stalk.

Despite of its evident chemical differences, sorption of heavy metal cations and sorption of the oxidizing anion $HCrO_4^-$ onto grape stalk exhibit an important common point; in both cases, lignin seems to be responsible of its removal. This macromolecule provides both, the basic sites necessary for cations removal and the reductive power needed for Cr(VI) reduction.

In the case of As(V) and As(III), an inorganic waste material with (hydr)oxide nature was proposed as sorbent. Due to its dusty shape, an immobilization procedure similar to the employed for the grape stalk, was developed and experiments were carried out for both, raw and entrapped material. Results revealed that the alginate employed as entrapment agent provoked both, a decrease in sorption rate and an increase on maximum sorption capacity when compared to the raw sorbent. With the results obtained in the sorption experiments and those derived from the application of instrumental techniques such as XRD, SEM-EDX and FTIR-ATR, a mechanistical approach was proposed. It can be concluded that for arsenic sorption, the free hydroxyls of the metallic (hydr)oxide are playing the key role. While As(III) sorption takes place by formation of surface complexes with the free –OH of the material, As(V) removal is due to two different contributions: surface complexation and coulombic interactions in between the partially positively charged surface and the negatively-charged arsenate species. These results are also supported by the slow kinetics observed, because mechanisms based in formation of surface complexes, usually involve the net formation and rupture of bonds. Noteworthy is the comparison with the sorption of heavy metal cations onto GS or EC, where the sorption, governed by an ionic exchange was notably faster.

In an attempt to approach to the real sorptive performance in real industrial effluents, in the present document two common scenarios have been simulated; the presence of complexing agents in heavy metal cation sorption and the uptake from multimetal mixtures.

In the case of the study of the effect of complexing agents, EDTA was chosen due to its common presence in many wastewaters of surface treatment industries. The chosen metals were Cu(II) and Ni(II), also present in many of these industries and the sorbents, GS and EC. Results put int evidence that only the non-complexed metal was available for sorption being thus the performance of the sorption treatment strongly dependent on the Metal-EDTA ratio. The explanation to this phenomenon has to be necessary searched in the sorption mechanism involved in the sequestration of heavy metals by these sorbents. As it has been previously exposed, these sorbents effectively adsorb heavy metal cations thanks to its important ion exchange capacity by light metals or protons. It is well known that EDTA forms Cu(II) and Ni(II) complexes with either neutral or anionic charge, depending on the pH of the solution. When the complexing agent is present in the media, the metal is complexed becoming thus an inactive specie through cation exchange and can not be uptaken by the sorbent.

When sorption from multimetal mixtures was studied, GS was chosen as sorbent, due to its excellent sorption performance for Cu(II) and Ni(II). The target metals for this study were Cu(II), Ni(II), Pb(II) and Cd(II), chosen the two first by its industrial recurrence and the last two, because of its particularly important toxicity. The study was carried out in continuous mode to observe the possible sorption competence. The results derived from these assays revealed the existence of an intense competence between metals and allowed us to obtain the next sorption affinity ranking:

Pb(II)>Cu(II)>Cd(II)>Ni(II)

The ranking indicates that the metal sorbed with higher affinity replaces, from its coordinating position in the material, to those sorbed with lower. This replacement produces an overconcentration respect to the feeding metal concentration (overshoot) for the metal that is being displaced. In an attempt to provide an explanation to the observed affinity ranking, sorption thermodynamics was studied for single metal solutions in batch mode. Results put into evidence that the ranking observed in continuous mode follows an increasing order with Gibbs free energy variation, ΔG^0. The lower the ΔG^0 is, the higher the affinity Metal-GS in the continuous flow process. The analysis of sorption thermodynamics allows thus, stablishing predictions on the metals that would suffer an overshoot in continuous processes. Thermodynamics revealed also that Cu(II), Ni(II), Pb(II) and Cd(II) sorption onto grape stalk is a spontaneous exothermic process that takes place with an increase on the randomness of the system.

Some of the sorbents studied in the present document have demonstrated a removal kinetics and equilibrium capacity that provides to them a performance comparable to its closest commercially used competitors, based on polymeric resins. While for the removal of heavy metal cations such as Cu(II), Ni(II), Pb(II) or Cd(II), cationic resins would be required, in the case of hexavalent chromium, anionic resins are needed. Particularly special is the case of the removal of arsenic, where resins containing are the most commonly employed. While commercial resins are rather costly, the sorbents employed in the present document have no adquisition costs. In fact, the waste producer industries that have provided us with the materials used in the present thesis are currently paying for its transport, management and final disposal. The cost-effectiveness of the use of these waste materials or industrial by-products constitutes thus, the main attraction of the detoxification of polluted effluents by means of low cost sorbents.

Additionally, the valorisation of wastes that otherwise would be either sent to incineration plants or landfill (as it is the case of GS and EC) or sent to treatment plants for its special treatment and disposal (as it is the case of the waste (hydr)oxide), is an environmentally-friendly practice and is strongly supported by government policies.

The processing of sorbents, once they loss their removal efficiency or become irreversibly saturated, might not pose an important problem. In the document it has been demonstrated that divalent cations such as Cu(II), Ni(II), Pb(II) and Cd(II) can be efficiently recovered in a concentrated form in mild acidic conditions. The material becomes thus a non-hazardous waste and it can be sent to a landfill, burned in an incinerator or, after neutralization, employed to prepare compost. Alternatively, incineration could be used to produce a metal-rich slag and use it as a secondary source for metallic elements. On the other hand, if the loaded material is going to be disposed in a landfill, its potential hazard, associated to the mobility of its ions, should be previously evaluated. In the present document it has been demonstated that the raw (hydr)oxide employed for the removal of arsenic constitutes a hazardous waste itself due to the important nickel leaching to the liquid phase. The material, independently of its further application for arsenic removal, has to be considered as a hazardous waste and managed by agreed organisms to ensure its harmless disposal.

The use of low cost sorbents based in raw natural materials or in industrial wastes has demonstrated to be a promising alternative for the removal of toxic metals from aqueous effluents. The screening and selection of the most effective low cost sorbents with sufficiently high metal-binding capacity and selectivity for heavy metal ions are prerequisites for a full-scale process. The development and implementation of these sorption processes requires research and development efforts focused in the direction of modelling, regeneration and also of testing of immobilization techniques for potential good sorbents but with either, poor mechanical or hydrodynamical properties.

PUBLISHED ARTICLES

C Escudero, N. Fiol, I. Villaescusa, J.C. Bollinger. “Arsenic removal by a waste metal (hydr)oxide entrapped into calcium alginate beads”. *Journal of Hazardous Materials.* Vol. 164, issue 2-3 (30 may 2009) : p. 533-541

http://dx.doi.org/10.1016/j.jhazmat.2008.08.042

Chemical Engineering Department, Universitat de Girona, Avda. Lluís Santaló, s/n, 17071 Girona, Spain

Université de Limoges, GRESE (Groupement de Recherche Eau - Sol - Environnement), Faculté des Sciences, 123 avenue Albert Thomas, 87060 Limoges, France

Received 28 March 2008; revised 25 july 2008; accepted 11 August 2008; available online 22 august 2008

ABSTRACT

In this work, a solid waste material from an electroplating industrial plant has been investigated for As(III) and As(V) sorption. This sorbent, a mixture of mainly Fe(III) and Ni(II) (hydr)oxides, has been used both in its native form and entrapped in calcium alginate. The effect of sorbent concentration in the gel bead, solution pH, contact time and As(III) and As(V) concentration on sorption has been studied. Furthermore the effect of the gel matrix has been investigated. A 10% (w/v) of (hydr)oxide in the gel beads was found to provide both spherical beads shape and good sorption performance. Solution pH was found to exert a stronger influence in As(V) than in As(III) sorption. The optimum pH range resulted to be within 5–10 for As(III) and within 6–9 for As(V). Taking into account these results, pH 8 was chosen for further sorption experiments. Equilibrium was reached after 48 h contact time for the studied systems. Kinetics data of both As(III) and As(V) onto native (hydr)oxide (O) and entrapped in calcium alginate beads (10% O–CA) were successfully modelled according to pseudo-first and pseudo-second order equations. Sorption equilibrium data were evaluated by the Langmuir isotherm model and the maximum capacity q_{max} were 77.4 and 126.5 mg g^{-1} for As(III) on O and 10% O–CA, and 26.8 and 41.6 mg g^{-1} for As(V) on O and 10% O–CA, respectively. The entrapment of the (hydr)oxide in a calcium alginate gel matrix improved the As(III) and As(V) sorption by 60%.

Keywords: Sorption; Arsenic; Waste (hydr)oxide; Calcium alginate; Iron; Entrapment

C. Escudero, C. Gabaldón, P. Marzal, I. Villaescusa. “Effect of EDTA on divalent metal adsorption onto grape stalk and exhausted coffee wastes”. *Journal of Hazardous Materials.*

http://dx.doi.org/10.1016/j.jhazmat.2007.07.013

Departament d’Enginyeria Química Agrària i Tecnologia Agroalimentària, Universitat de Girona, Escola Politècnica Superior, Av. Lluís Santaló, s/n 17071, Girona, Spain.

[b]Departament d’Enginyeria Química, Universitat de València. Dr. Moliner 50, 46100 Burjassot, València, Spain

Received 13 february 2007; revised 3 july 2007; accepted 4 july 2007; available online 7 july 2007

ABSTRACT

In the present work, two industrial vegetable wastes, grape stalk, coming from a wine producer, and exhausted coffee, coming from a soluble coffee manufacturer, have been investigated for the removal of Cu(II) and Ni(II) from aqueous solutions in presence and in absence of the strongly complexing agent EDTA. Effects of pH and metal–EDTA molar ratio, kinetics as a function of sorbent concentration, and sorption equilibrium for both metals onto both sorbents were evaluated in batch experiments. Metal uptake was dependent of pH, reaching a maximum from pH around 5.5. EDTA was found to dramatically reduce metal adsorption, reaching total uptake inhibition for both metals onto both sorbents at equimolar metal:ligand concentrations.

Kinetic results were successfully modelled by means of the pseudo second order model. Langmuir and Freundlich models were used to describe the sorption equilibrium data.

Grape stalk showed the best performance for Cu(II) and Ni(II) removal in presence and in absence of EDTA, despite exhausted coffee appears as less sensitive to the presence of complexing agent.

The performance of Cu(II) and Ni(II) sorption onto grape stalk in a continuous flow process was evaluated. In solutions containing EDTA, an initial metal concentration in the outlet flow corresponding to the complexed metal fraction was observed from the beginning of the process. A high metal recovery yield (>97%) was achieved by feeding the metal-loaded column with 0.05 M HCl

Keywords: Grape stalk; Exhausted coffee; Adsorption; Heavy metals; EDTA; Batch and column studies